THE UNIVERSITY *of* EDINBURGH

Directed Electrophilic C-H Borylation using Lewis-Base Stabilised Boranes

Emily Noone

A thesis submitted in fulfilment of the requirements

for the degree of Doctor of Philosophy

School of Chemistry

The University of Edinburgh

2024

Declaration

I declare that this thesis and the research work described herein is my own work. Where others have contributed, their contribution is clearly indicated. Previously published journal articles resulting from this research are listed below. This work has not been submitted for any other degree or professional qualification at this or any other institution.

Emily Noone
08/01/2024

Publications

A list of publications associated with this thesis:

1. '*Borylation Directed Borylation of Indoles Using Pyrazabole Electrophiles: A One-Pot Route to C7-Borylated-Indolines*', J. Pahl*, E. Noone*, M. Uzelac, K. Yuan, M. J. Ingleson, *Angew. Chem. Int. Ed.*, 2022, **61**, e2022062, *(* = joint first authors).*
2. '*Synthesis of Electrophiles Derived from Dimeric Aminoboranes and Assessing Their Utility in the Borylation of π Nucleophiles*', C. R. P. Millet, J. Pahl, E. Noone, K. Yuan, G. S. Nichol, M. Uzelac, M. J. Ingleson, *Organometallics*, 2022, **41**, 18, 2638–2647.
3. '*Borylation Directed Borylation of N-Alkyl Anilines using Iodine Activated Pyrazaboles*', C. R. P. Millet, E. Noone, A. V. Schellbach, J. Pahl, J. Łosiewicz, G. S. Nichol, M. J. Ingleson, *Chem. Sci.*, 2023, **14**, 12041-12048.

Abstract

Aryl boranes are widely utilised in a range of applications, including as emissive materials, as active pharmaceuticals and, most commonly, as intermediates in synthetic transformations, with the most notable being the Suzuki-Miyaura cross-coupling reaction. Consequently, there has been considerable interest in the development of efficient methodologies to synthesise aryl boranes. C-H borylation is an atom-economical method to produce aryl boranes by functionalising the (hetero)arene directly, with the use of iridium and cobalt catalysts in these reactions particularly well established. An alternative that avoids expensive / toxic metal catalysts is the use of boron electrophiles, which react in C-H borylation processes via electrophilic aromatic substitution (S_EAr) mechanisms. The application of directing groups in C-H borylation processes enables the regioselective functionalisation of C-H positions that are otherwise unreactive. Directed electrophilic C-H borylation of (hetero)arenes has been demonstrated primarily with trihaloboranes, in contrast the use of Lewis-base stabilised, four-coordinate boranes as electrophiles in such reactions is underdeveloped. Directed electrophilic C-H borylation processes that utilise an E-H unit (E = C, N or O) as the directing group are also underexplored. The results in this thesis seek to address each of these points.

The synthesis of pharmaceutically relevant benzoxaboroles via the directed electrophilic C-H borylation of benzyl alcohols was explored using NHC-boranes (**Chapter 2**). Activation of an NHC-BH_3 complex (to install a good leaving group), followed by addition of the benzyl alcohol generates a three-coordinate borenium cation, with the boron substituents dependent on the stoichiometry of the benzyl alcohol. However, these *in situ* generated borenium cations were demonstrated to be insufficiently electrophilic to enable the *ortho* C-H borylation of benzyl alcohols to form benzoxaboroles. The use of Lewis bases other than NHCs in LB-BH_3 complexes was also ineffective due to the decomplexation of the Lewis base from the borane.

The use of pyrazabole ($[H_2B(\mu\text{-}C_3N_2H_3)]_2$), a readily synthesised diboron compound, as a transient directing group was established and applied to the

'borylation directed borylation' of indoles (**Chapter 3**). Pyrazabole has a B···B separation of ca. 3 Å, so is well suited for the regioselective N/C7-diborylation of indoles/indolines and can be converted to a ditopic electrophile using *bis*-(trifluoromethane sulfonyl) amine ($HNTf_2$). Pyrazabole electrophiles were shown to transform *N*-H indole into an N/C7-diborylated indoline species, with mechanistic studies demonstrating that this proceeds via a hydroboration / protodeboronation / C-H borylation pathway. The pyrazabole unit can be removed at the end of the reaction, generating useful 7-Bpin *N*-H indolines in a one-pot, metal-free process.

Whilst an effective activator of pyrazabole, $HNTf_2$ is expensive and must be handled inside a glovebox. To improve the utility of pyrazabole as a traceless directing group, the use of iodine as an activator was explored (**Chapter 4**). Though the synthesis of 7-Bpin indolines was demonstrated, the yields were lower than the comparative reactions with $HNTf_2$. Analysis of by-products revealed that the degradation of the pyrazabole unit occurs as a competitive side reaction, decreasing the amount of C7-H borylation. This is believed to be the result of the more coordinating iodide group (relative to $[NTf_2]^-$).

In the hope of achieving the C3/C4-diborylation of indoles without C2-C3 hydroboration, synthetic routes to pyrazabole electrophiles that lack B-H bonds were investigated (**Chapter 5**). The synthesis and activation of *di*-halo and *tetra*-halo pyrazaboles was explored using either $HNTf_2$ or $TMSNTf_2$, respectively. The reaction of *tetra*-chloro or -bromo pyrazabole with $TMSNTf_2$ was shown to generate a *mono*-electrophilic pyrazabole derivative, but access to the *di*-electrophile species in large amounts was challenging. The reactivity of the *mono*-electrophile was explored, and whilst the C3-H borylation of *N*-Me indole was possible, C3/C4-diborylation was not achieved via this approach (though some evidence suggested minor C2/C3-diborylation was achieved).

Lay Summary

In the production of complex molecules, e.g. for pharmaceutical or material applications, the joining together of two building blocks can be useful. This process is often described as 'coupling' the two building blocks together, forming a new chemical bond between them. To enable coupling, the individual building blocks generally need to each have a reactive group.

One of the reactive groups chemists can use to enable 'coupling' is a boron-containing group. Building blocks with boron groups are useful because they can be 'coupled' to lots of different building blocks, meaning a diverse range of molecules can be made. Finding new, efficient, and environmentally friendly ways to add boron groups to (or "to borylate") these building blocks is therefore important for these applications. Methods that borylate while avoiding the use of expensive and/or toxic reagents are also desirable. The work discussed in this thesis focuses on developing new approaches that can be used to borylate important and commonly used building blocks (heteroarenes).

In addition, it is important that the boron group is only attached to the heteroarene building block at the position where the new bond should be formed during coupling. This can be challenging if there are lots of similar positions boron can be added to. To control where the boron group is added, 'directing groups' can be used that focus the borylation onto the targeted position. This enables the boron group to be added selectivity at only one position. The work in this thesis also explores new types of directing groups that can be used in the borylation of heteroarenes.

Abbreviations

9-BBN	9-Borabicyclo[3.3.1]nonane
Ar	Aryl
Aq.	Aqueous
Bn	Benzyl
BOC	*tert*-Butyloxycarbonyl
Cat	1,2-dihydroxybenzene (Catechol)
COSY	Correlated Spectroscopy
DBP	2,6-Di-*tert*-butyl-4-methylpyridine
DCE	1,2-Dichloroethane
DCM	Dichloromethane
DG	Directing Group
DIPEA	*N,N*-Diisopropylethylamine (Hünig's base)
DIPP	2,6-Diisopropylphenyl
DMAP	Dimethylamino pyridine
DME	1,2-Dimethoxyethane
DMF	*N,N*-Dimethylformamide
eg	Ethylene glycolato
Eq.	Equivalents
ESI	Electrospray Ionisation
Et	Ethyl
FLP	Frustrated Lewis Pair
HMBC	Heteronuclear Multiple Bond Correlation
HOMO	Highest Occupied Molecular Orbital
HRMS	High-Resolution Mass Spectrometry
HSQC	Heteronuclear Single Quantum Coherence
I^{i}Pr	1,3-Diisopropyl imidazol-2-ylidene
IMe	1,3-Dimethyl imidazol-2-ylidene
IMes	1,3-Dimesityl imidazol-2-ylidene
IPA	2-Propanol
^{i}Pr	Isopropyl
LA	Lewis Acid
LB	Lewis Base
LUMO	Lowest Unoccupied Molecular Orbital

Me	Methyl
Mes	Mesityl
MTBE	Methyl *tert*-butyl ether
NHC	*N*-Heterocyclic Carbene
NMR	Nuclear Magnetic Resonance
***o*-DCB**	1,2-dichlorobenzene
***o*-DFB**	1,2-difluorobenzene
PAH	Polycyclic aromatic hydrocarbon
Pin	Pinacolate
pwhh	Peak Width at Half Height
RT	Room Temperature
S_EAr	Electrophilic Aromatic Substitution
S_NAr	Nucleophilic Aromatic Substitution
^{t}Bu	*tert*-Butyl
Tf	Triflyl
THF	Tetrahydrofuran
TIPS	Triisopropylsilyl
TMS	Trimethylsilyl
Trityl	Triphenylmethyl
xs	Excess

Acknowledgements

I would first like to thank Professor Mike Ingleson for his continued guidance, encouragement, and patience throughout the past four years. Starting a PhD five months before a global pandemic is not ideal, but Mike has been highly supportive throughout all the challenges and has been invaluable as a mentor. I would also like to thank past and present members of the Ingleson group, who have contributed to making my time in Edinburgh so enjoyable. My fellow PhD students (Saqib, Matt, Nojus, Isabel, Justyna, Emily and Anna) have provided motivation, enthusiasm, and a never-depleting snack table, and I am grateful for their friendship. I have also been fortunate enough to work with some fantastic post-docs (Marina, Kang, Jürgen, Sven, Clément, Milan, Shantaram, and Dom) who have also provided an invaluable wealth of knowledge and experience. In addition, Dr Jürgen Pahl, Dr Clément Millet, Adam Allenby and Anna Schellbach have been excellent collaborators for some of the work in this thesis. I must also thank all of the technical staff in the School of Chemistry, including Gary Nichol for the resolution of X-ray crystal structures, Juraj, Lorna, and Richard for their support with NMR spectroscopy, and Logan, Alan, Faye, and Kelly for their assistance with mass spectrometry.

This thesis could not have been written without the endless support of my friends and family, even if they aren't quite sure what my PhD is actually about. My mum, Sue, has never let me believe I couldn't do something. She is my biggest supporter and my best friend, and this thesis is the direct result of her endless reassurance, comfort and, sometimes, tough love too. I'll try and get a real job now, mum. I must also thank my amazing partner, David, for his patience and support during the past four years, especially when I was stressed and grumpy, and for always being up for moving to somewhere new. Finally, I would like to dedicate this thesis to the memories of my grandad, William Peter Harding, who we lost in 2017, and my nanny, Shirley Anne Harding, who passed away in 2023 during the writing of this thesis. I am so lucky to have had such kind and generous grandparents, and I love and miss them both so very much.

Table of Contents

Chapter 1

Introduction

Chapter 1: Introduction

1.1 Organoboranes in Synthetic Chemistry

Organoboranes have a number of applications, including in organic materials,[1–4] and as biologically active molecules.[5–7] Their most common application is as highly versatile synthetic reagents employed in carbon-carbon and carbon-heteroatom bond forming reactions.[8,9] The most notable of these C-B bond transformations is the Suzuki-Miyaura reaction, where an organoborane is coupled to an organohalide (or pseudohalide) in the presence of a catalyst (often palladium) and base to form a new C-C bond (**Figure 1.1**, **top**).[10–12] The Suzuki-Miyaura reaction has been extensively developed and a range of organoboranes have been utilised (**Figure 1.1**, **bottom**), whilst the diversity of the organohalide reagent has also been expanded.[13] The large scope of possible coupling partners, alongside mild and functional group tolerant conditions, means the Suzuki-Miyaura reaction is now one of the most widely used transformations in synthetic chemistry, particularly in the fine-chemical industry.[14–16]

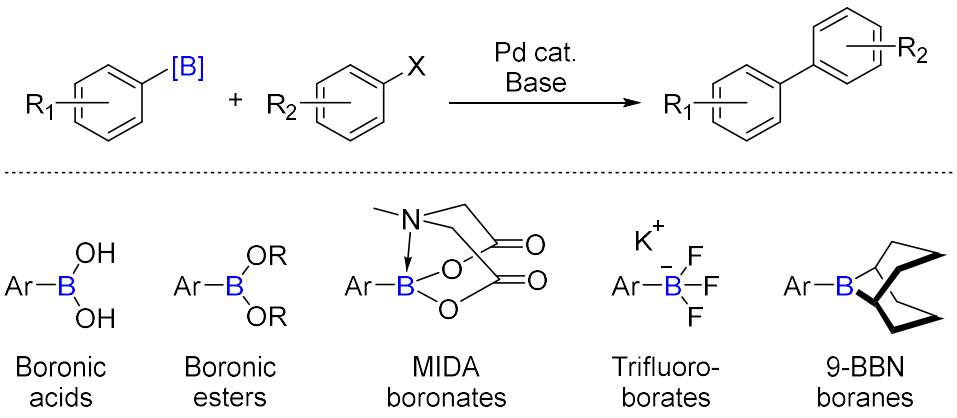

Figure 1.1: A generalised Suzuki-Miyaura reaction (**top**), and common organoborane reagents used in Suzuki-Miyaura reactions (**bottom**).

Several C-B bond transformations use boronic acids (or their ester derivatives) as the organoborane reagent.[9] Many boronic acids are stable under ambient conditions, though they can undergo condensation reactions to form the corresponding anhydrides, and their purification can be challenging due to the propensity of some boronic acids to undergo protodeboronation (the conversion of R-B(OH)$_2$ to R-H under acidic or basic conditions).[17] For convenience boronic

acids are often 'protected' by the substitution of the hydroxyl groups with diols to form the corresponding boronic ester derivatives.[18] Generally, boronic esters (R-B(OR')$_2$) have reduced Lewis acidity compared to their boronic acids (R-B(OH)$_2$) counterparts owing to the σ-donating ability of the alkoxy carbon leading to increased π-donation of the oxygen lone pair into the electron-deficient boron centre.[13] This often improves the stability of the organoborane with respect to protodeboronation.

This stability and ease of handling, coupled with the low toxicity of organoboranes (compared to other organometallic reagents)[19] and the formation of environmentally benign by-products (typically B(OH)$_3$) makes boronic acids/esters ideal synthetic reagents. Therefore, the development of novel and efficient synthetic methods to produce boronic acids/esters is of significant interest, and this will be the focus of this introduction. Of particular relevance is the synthesis of aryl boronic acids/esters, owing to their importance in the synthesis of pharmaceutically relevant biaryl units.[20]

1.2 Electrophilic Trapping of Organometallic Intermediates

One of the earliest reported methods to synthesise aryl boronic acids/esters, and one that is still well utilised today, is the metalation of an aryl halide followed by trapping of the highly nucleophilic organometallic intermediate with a tri-alkyoxyborate electrophile (B(OR)$_3$).[21] This approach was first used in 1909 to prepare phenylboronic acid using Grignard reagents (RMgX) as the organometallic species (**Scheme 1.1**).[22] Addition of phenylmagnesium bromide (prepared via the reaction of bromobenzene and magnesium metal in diethyl ether) to the boron electrophile at -70 °C resulted in the precipitation of the magnesium trialkoxyphenylborate salt.[23] The phenylboronic acid was obtained following aqueous work-up. This procedure has since been optimised, enabling non-cryogenic conditions and the use of other boron sources.[24,25] Grignard reagents have been used in the kilogram-scale preparation of simple aryl boronic acids/esters.[26,27]

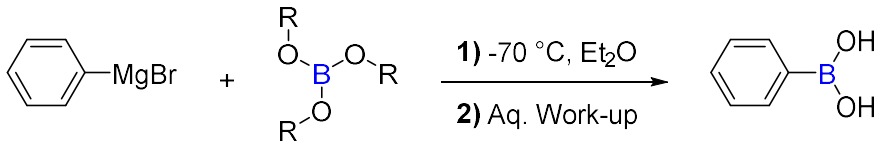

Scheme 1.1: Preparation of phenylboronic acid by the trapping of phenylmagnesium bromide with a borate ester electrophile.

Brown and Cole developed the use of organolithium reagents in place of Grignard reagents.[28] The organolithium intermediates can readily prepared *in situ* via lithium-halogen exchange of the corresponding organohalide with an alkyl lithium base. This approach has been utilised in the synthesis of a range of substituted boronic esters,[29,30] including heterocyclic boronic esters.[31] Organohalide substrates containing acidic hydrogen atoms (e.g. amino groups) are also compatible with this process if they are protected prior to the addition of the highly Brønsted basic lithium reagent (**Scheme 1.2**).[32] This method has been effectively adapted for continuous flow, enabling facile scale-up of the reaction to the kilogram-scale and making it attractive for industrial processes.[33]

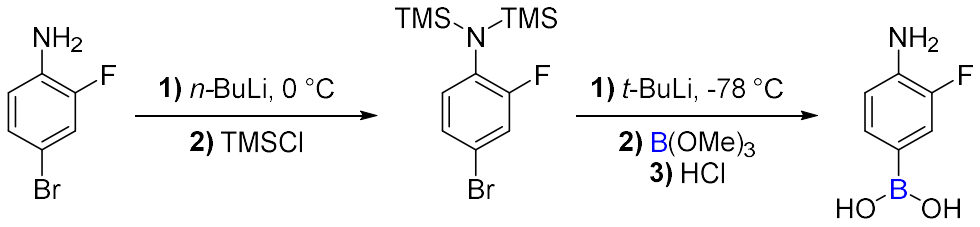

Scheme 1.2: Synthesis of 4-amino 3-fluorophenylboronic acid, via a stepwise protection and 'lithiation-borylation' process.

These two methods have drawbacks that can limit their utility. Both require strongly nucleophilic and Brønsted basic organometallic intermediates (RLi or RMgX), the formation of which can be incompatible with certain functional groups and thus limit the scope of the process.[34,35] The generation of organometallic intermediates can also present safety issues (e.g. requiring the use of *t*-BuLi). Furthermore, the efficiency of the overall process is poor, requiring pre-functionalised precursors and producing a stoichiometric amount of metal waste. This is especially significant for large-scale industrial processes. The commercial availability of the required regioisomer of the starting organohalide (typically iodo- or bromo-substituted) can also limit the scope of these methods.

One way to improve the atom-economy of the metalation route is through the metalation of C-H bonds directly, avoiding the need for pre-functionalised organohalides. This requires deprotonation of the (hetero)arene by a strong alkyl lithium base to generate the desired organometallic intermediate.[36] Trapping this intermediate with a borate electrophile can provide a more efficient route to aryl boronic acids/esters directly from the respective (hetero)arene.[37] The regioselectivity of C-H metalation reactions is largely controlled by the acidity of the (hetero)arene, but sterics can also affect selectivity, with the deprotonation of hindered C-H positions (e.g. *ortho* to other substituents) disfavoured.

To alter the regioselectivity of this process, Lewis basic substituents on the (hetero)arene can be used as directing groups (**Scheme 1.3**).[38,39] Coordination of the alkyl lithium base by the directing group positions it in close proximity to the target *ortho* C-H, enabling selective deprotonation. A variety of Lewis basic moieties have been used in as directing groups, including amines, ethers, amides, and carbamates, whilst a range of electrophiles can be used to trap the *ortho*-metalated intermediates.[40] This method therefore provides a general route to synthesise a variety of 1,2-disubsituted arenes, and has been widely utilised in academia and industry.[36]

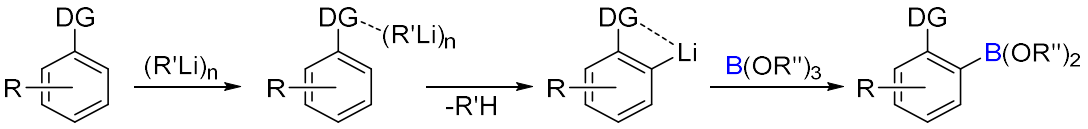

Scheme 1.3: General mechanism of a 'directed *ortho* metalation' reaction with an alkyl lithium base and borate electrophile, where DG = directing group.

In the context of C-B bond formation, directed *ortho* metalation has found applications in the synthesis of *ortho*-substituted aryl boronic acids/esters,[41,42] including in a multi-gram scale production of the anti-hypertensive drug Losartan (**Scheme 1.4**).[43] In this process, lithiation is directed by the Lewis basic tetrazole unit, with the organometallic intermediate then quenched by $B(O^iPr)_3$. This enabled the selective formation of the 2-substituted phenylboronic acid derivative, which was subsequently used in a Suzuki-Miyaura cross coupling to generate the unsymmetrical biaryl unit of Losartan.

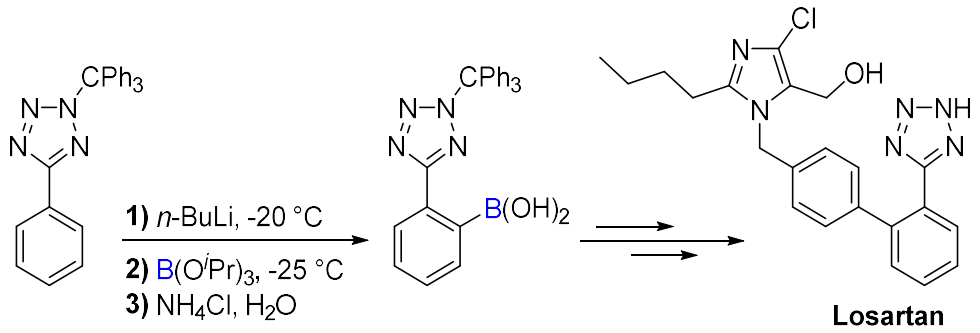

Scheme 1.4: *Ortho*-lithiation and trapping with a borate electrophile, used in the multi-gram synthesis of the pharmaceutical Losartan.

Though some improvements in atom-economy can be made by the direct metalation of C-H bonds, the synthesis of boronic acids/esters via the trapping of organometallic intermediates with boron electrophiles still typically requires cryogenic conditions, generates a stoichiometric amount of metal waste, and requires strongly nucleophilic organometallic reagents that can limit the functional group compatibility. Therefore, it is no surprise that multiple alternative borylation processes have been developed.

1.3 Transition Metal Catalysed Borylation

1.3.1 Catalytic C-X Borylation

Transition metal catalysed borylations can provide more efficient routes to boronic acids/esters by avoiding the need for stoichiometric organometallic reagents. In 1995, Miyaura and co-workers demonstrated the use of palladium catalysis in the cross-coupling of aryl halides with bench-stable diboronyl esters, providing a direct route to aryl boronic esters (**Scheme 1.5**).[44] The reaction requires a weak base, often KOAc, to supress any subsequent reactivity of the boronic ester product, with Suzuki-Miyaura cross coupling to the aryl halide substrate observed if stronger bases (e.g. K_3PO_4) are used. The mild reaction conditions are compatible with a wide range of functional groups, including nitrile and carbonyl groups that would be incompatible with Grignard or alkyl lithium reagents.

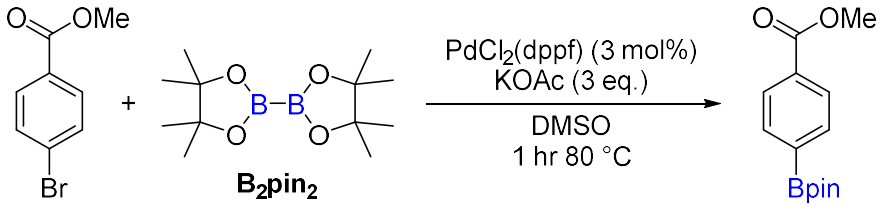

Scheme 1.5: Palladium catalysed cross coupling of aryl halides and diboronyl esters. *(dppf = 1,1'-bis(diphenylphosphino)ferrocene).*

This process typically uses diboron reagents as the nucleophilic coupling partner, with B_2pin_2 commercially available and easy to handle, adding to the overall convenience of the reaction.[45] However, only half of the boron atoms added are converted into the boronic ester product. Work by Masuda and co-workers developed the use of dialkoxyboranes (e.g. HBpin) in this reaction, improving the atom-economy of the overall process.[46] Furthermore, this process is amenable to the borylation of a wide range of substrates, including aryl bromides, iodides and triflates.[47] An attractive feature of this reaction is the ability to combine the C-X borylation step with the Suzuki-Miyaura cross coupling of the boronic ester product, providing a one-pot, two-step route to biaryl units.[48] This has been well utilised in industry due to the improvements in process efficiency and cost.[49]

Due to the low abundance of palladium, and its resultant high costs, the development of more abundant transition metal catalysts for the borylation of aryl halides is an extensive area of research. In particular, nickel and copper catalysts have been demonstrated as capable alternatives to palladium.[50,51] A complete discussion of many developments in transition metal catalysed C-X borylation processes is beyond the scope of this introduction, but the reader is directed towards the several comprehensive reviews of this field.[52–54] However, this approach still requires a pre-functionalised aryl halide. A simpler, more efficient process again would involve the direct transformation of unactivated C-H bonds of the (hetero)arene into the desired C-B bond.

1.3.2 Catalytic C-H Borylation

The functionalisation of a C-H bond, enabled by a transition metal catalyst, is a highly efficient and therefore attractive methodology for the formation of new carbon-carbon or carbon-heteroatom bonds.[55–57] In the context of C-B bond formation, catalytic C-H borylation methodologies can offer improved atom and step-economy over C-X borylation processes.[58] However, controlling the regioselectivity in C-H borylation processes can be challenging if there are multiple similar (in reactivity) C-H positions within the molecule (*vide infra*).[59]

Following reports of stoichiometric C-B bond forming reactions between transition metal-boryl complexes and alkanes/arenes,[60–62] Chen and Hartwig reported the first catalytic C-H borylation of several hydrocarbons, including benzene, under photochemical conditions using manganese or rhenium catalysts.[63] The catalytic C-H borylation of alkanes and arenes was later reported under thermal conditions using rhodium catalysts.[64,65] Iridium complexes were later also demonstrated as highly efficient, functional group tolerant catalysts for the C-H borylation of substituted arenes using B_2pin_2 or HBpin.[58,59] In 2002, Smith and co-workers demonstrated that the addition of chelating phosphine ligands dramatically increased the activity of iridium catalysts, with high yields achieved at low catalytic loadings (**Scheme 1.6a**).[66] Furthermore, this process was shown to be highly selective towards C-H functionalisation: aryl halides underwent C-H borylation without competitive C-X activation (which was previously observed using rhodium catalysts).[65]

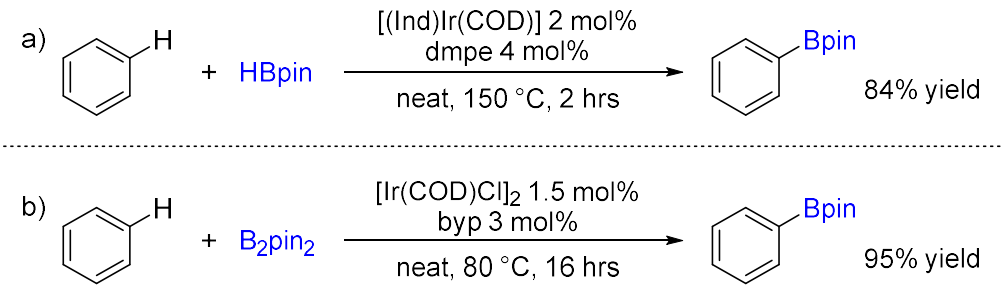

Scheme 1.6: Examples of the iridium catalysed C-H borylation of benzene *(Ind = indenyl, COD = 1,5-cyclooctadiene, dmpe = 1,2-bis(dimethylphosphino)ethane, bpy = 2,2'-bipyridine).*

A concurrent publication by the groups of Miyaura and Hartwig reported the use of a bench-stable iridium catalyst and bipyridine ligand for the C-H borylation of benzene derivatives under more mild conditions (≤80 °C) (**Scheme 1.6b**).[67] Further optimisations of the catalyst/ligand system enabled the C-H borylation of arenes at room temperature.[68] Owing to the mild conditions, good functional group tolerance, high turnover, and stable pre-catalysts, variations of these conditions are among the most commonly used today and have been applied to multiple large-scale industrial processes.[69–71]

Other, more abundant transition metal complexes have also been demonstrated as active catalysts for the C-H borylation of (hetero)arenes, including iron,[72] cobalt,[73] and nickel complexes,[74] with several reviews of this field.[54,75] However, these processes are not as well-developed or as widely applied as iridium-catalysed processes, hence the following section of the introduction focuses specifically on iridium catalysed C-H borylations.

Regioselectivity in Iridium-Catalysed C-H Borylations

In the iridium catalysed C-H borylation of arenes, the regioselectivity is dominated by steric effects, owing to the high sensitivity of iridium catalysts to steric hinderance.[76] As such, the most accessible position is preferentially activated, with the activation of the *ortho*-position generally disfavoured. This is reflected in the scope of the previously discussed work by the groups of Smith, Miyaura, and Hartwig (**Figure 1.2**).[66–68]

The regioselectivity of C-H borylation in substrates with multiple accessible C-H positions is generally poor. For example, for *mono*-substituted arenes (**1.1** and **1.2**), statistical mixtures of the respective *meta*- and *para*-borylated products are obtained with little-to-no *ortho*-substitution. By comparison, 1,3-disubstituted arenes are borylated at the only position not *ortho*- to a substituent (the common *meta*-position), giving a single regioisomer (**1.4**). The borylation of 1,2-disubstituted arenes with identical substituents will yield a single regioisomer (**1.3**), whilst for unsymmetrical 1,2-disubstitued arenes a mixture is typically obtained. For 1,4-disubituted arenes, where there is no unhindered C-H position, *ortho*-borylation can occur if the substituent is moderately sized, albeit with

lower rates and conversions (**1.5**). Note, the electronic effect of many substituents on the regioselectivity of arene C-H borylation is relatively minor, though at lower temperatures the effect can become more significant.[59] Strongly electron-withdrawing substituents can accelerate the rate of *ortho*-borylation,[76] hence for **1.6** the yield is improved (compared to **1.5**).

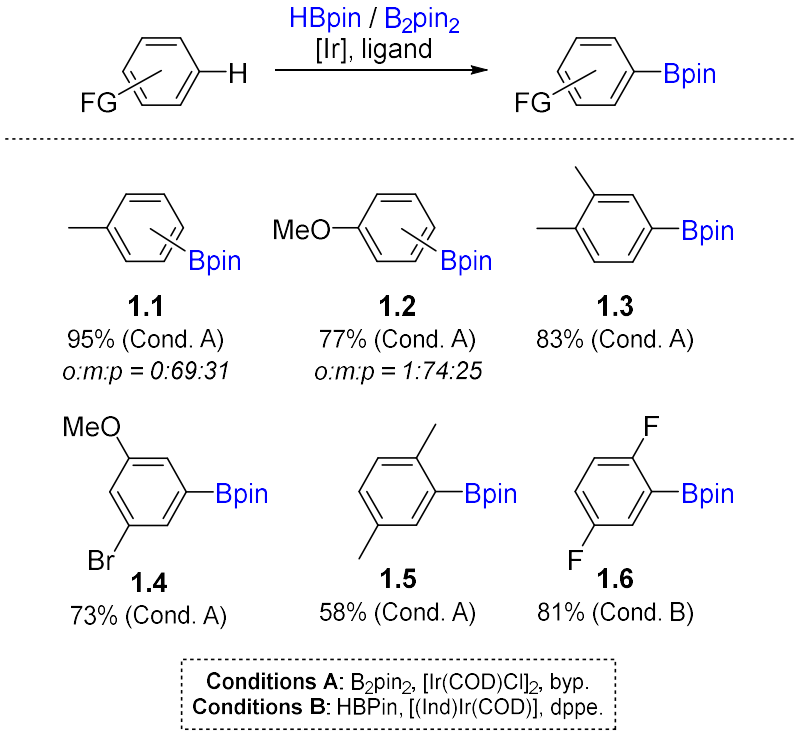

Figure 1.2: Regioselectivity in the iridium catalysed C-H borylation of substituted arenes. *(Ind = indenyl, COD = 1,5-cyclooctadiene, dppe = 1,2-bis(diphenylphosphino)ethane, bpy = 2,2'-bipyridine).*

The iridium catalysed C-H borylation of various heteroarenes using B_2pin_2 or HBpin has also been established under similar conditions.[58] For heteroarenes, the regioselectivity of C-H borylation is controlled by both steric and electronic effects.[59] Miyaura, Hartwig and co-workers demonstrated the iridium catalysed C-H borylation of a range of heteroarenes with B_2pin_2 (**Figure 1.3**).[77] For these substrates, borylation occurs selectively at the 2-position (α to the heteroatom). These substrates react rapidly, hence the partial formation of 2,5-diborylated products is often observed. Heteroarenes generally react faster than arenes, hence in the reactions of benzo-fused heteroarenes, borylation occurs on the 5-

membered heteroarene ring selectively, with no activation of the 6-memebered benzenoid ring observed.

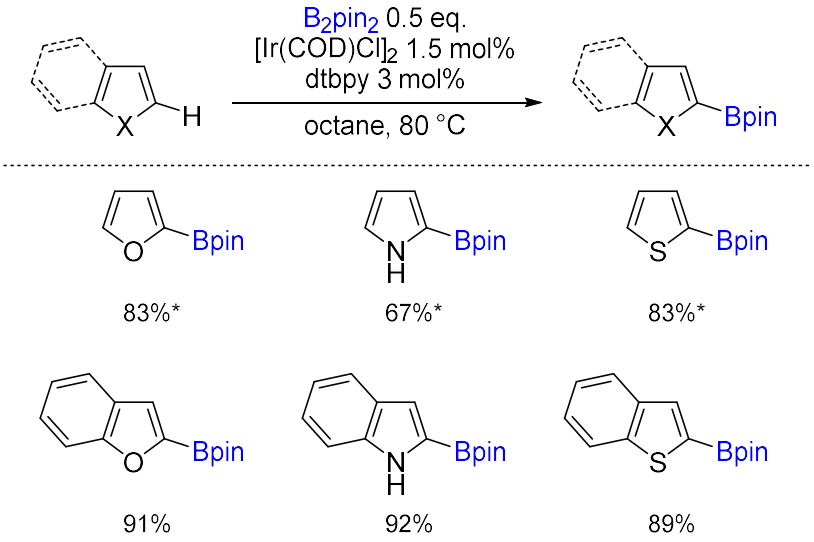

Figure 1.3: Regioselectivity in the iridium catalysed C-H borylation of heteroarenes. ** = Minor 2,5-diborylation observed. (COD = 1,5-cyclooctadiene, dtbpy = 4,4'-di-tert-butyl-2,2'-bipyridine).*

Multiple studies have since explored the intrinsic selectivity in the iridium-catalysed C-H borylation of various heteroarenes.[59,78] Given the content of this thesis, focus will now be on approaches used to achieve regioselectivity during C-H borylation that is distinct to the intrinsic reactivity of that heteroarene.

1.3.3 Altering Regioselectivity in Catalytic C-H Borylation

The Use of Blocking Groups

Bulky substituents can be used as blocking groups to sterically hinder C-H borylation at the respective *ortho*-/C2- position. For example, in the C-H borylation of *N*-TIPS-pyrrole and -indole, C2-H borylation is prevented by the nitrogen-bound triisopropylsilyl group, thus C-H borylation occurs selectively at the C3 position in high yields (**Scheme 1.7a**).[77,79] By comparison, an '*N*-methyl' group is not sufficiently bulky to entirely prevent C2-H borylation, giving a mixture of C2- and C3-borylated products. The C2 blocking effect was also achieved with Boc-protected pyrrole and indole derivatives, with the Boc group removed by thermolysis (at 180 °C) in a subsequent step (**Scheme 1.7b**).[80]

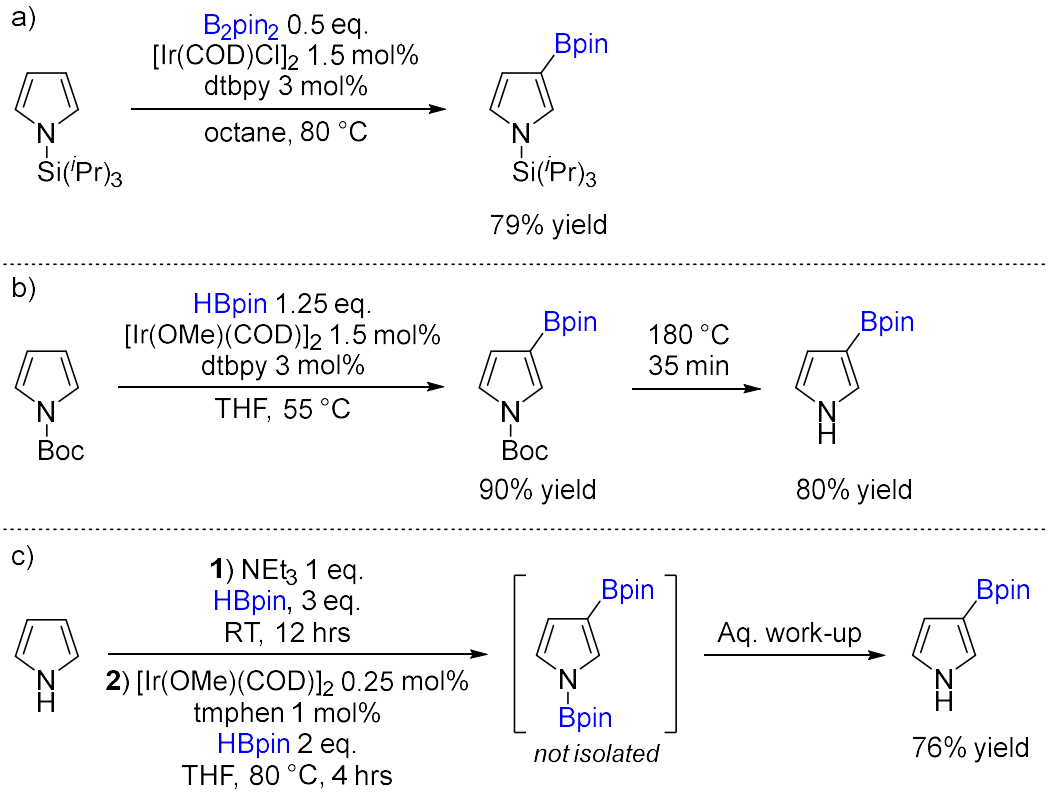

Scheme 1.7: Iridium catalysed C3-H borylation of *N*-substituted pyrrole derivatives *(COD = 1,5-cyclooctadiene, dtbpy = 4,4'-di-tert-butyl-2,2'-bipyridine, tmphen = 3,4,7,8-tetramethyl-1,10-phenanthrene).*

To provide a more efficient and functional-group compatible route to C3-borylated pyrroles/indoles via iridium catalysis, Smith and co-workers developed a 'traceless' approach where a blocking group is installed at nitrogen, C-H borylation proceeds, and the blocking group is removed, all in a one-pot process (**Scheme 1.7c**).[81] In this process, N-H pyrrole (or indole) undergoes an initial *N*-borylation (requiring NEt_3), generating a N-Bpin group. This hinders C2-H activation, thus enabling selective C3-H borylation. The N-Bpin bond is then readily hydrolysed during aqueous work-up, producing 3-Bpin *N*-H pyrrole derivatives in high yields. It should be noted that for substrates containing more acidic N-H bonds (e.g. pyrazoles and azaindoles), *N*-borylation precedes C-H borylation, hence the addition of NEt_3 is not required to enable C3-H borylation. Whilst the use of blocking groups can enable access to other borylated regioisomers, the approach is limited to certain heteroarenes. Other methods have also been developed to alter the regioselectivity of iridium-catalysed C-H borylation processes.

The Use of Selective Protodeboronation

Another approach that has been used to increase the scope of regioisomers accessible by iridium-catalysed C-H borylation processes occurs via a sequence of diborylation and selective protodeboronation of one of the borylated positions. This approach was first demonstrated by Movassaghi and co-workers, where a C3-substitued indole derivative underwent an iridium-catalysed diborylation at the C2 and C7 positions.[82] The higher reactivity of the C2 position (over C7) enabled selective C2-Bpin protodeboronation upon addition of acetic acid, whilst the C7-Bpin bond was maintained (**Scheme 1.8**). Smith and co-workers expanded the scope of this process to other indole derivatives, with bismuth (III) acetate used to facilitate selective protodeboronation.[83] However, this approach has not been widely applied to other (hetero)arenes.

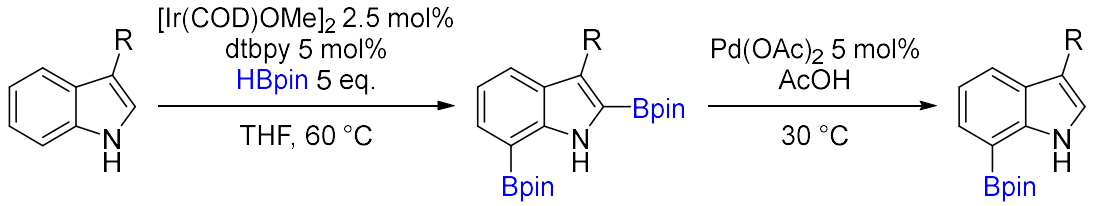

Scheme 1.8: Iridium catalysed C7-H borylation of C3-substituted indole derivatives via selective C2-Bpin protodeboronation.
(COD = 1,5-cyclooctadiene, dtbpy = 4,4'-di-tert-butyl-2,2'-bipyridine).

The Use of Chelating Directing Groups

Directing groups (DGs) installed on the (hetero)arene substrate can be used to alter the regioselectivity of C-H borylation reactions towards C-H positions that are otherwise challenging to functionalise selectively. Directing groups control regioselectivity through interactions with the catalyst, which position the (hetero)arene substrate appropriately to enable site-selective C-H activation.[84] This is distinct from the use of blocking groups which alter regioselectivity through steric hinderance. Directing groups on the substrate can interact with the catalyst in several ways. For example, they can coordinate to the metal centre (*chelating directing groups*) or can interact with ligands on the catalyst through H-bonding or electrostatic interactions (*outer-sphere directed*).

One approach used to direct the regioselectivity of C-H borylations is to use a Lewis basic group on the (hetero)arene substrate that coordinates to the iridium centre and orientates it in close proximity to a specific C-H position, typically the adjacent *ortho* position. This is similar to the previously discussed directed *ortho*-metalation process (*vide supra*, **Scheme 1.3**).[40] Chelating directing groups can enable selective *ortho* C-H borylations that are otherwise challenging to achieve. This approach is sometimes described as an 'inner sphere' type mechanism.[59]

A typical (undirected) iridium-catalysed arene C-H borylation reaction proceeds through the activation of the arene C-H bond by a pentacoordinate 16e$^-$ complex (**Figure 1.4a**).[85] Subsequent reductive elimination produces the borylated arene product, with the catalytically active 16e$^-$ complex regenerated upon oxidative addition of HBpin/B_2pin_2. For a chelate-directed C-H borylation process to proceed with high regioselectivity, an additional vacant coordination site at the iridium centre must be generated (via ligand dissociation) following coordination of the directing group, in order for the subsequent site-selective C-H activation to proceed (**Figure 1.4b**). Consequently, refinement of the catalyst/ligands is essential to achieving the directing effect in a chelate-directed C-H borylation process.[86]

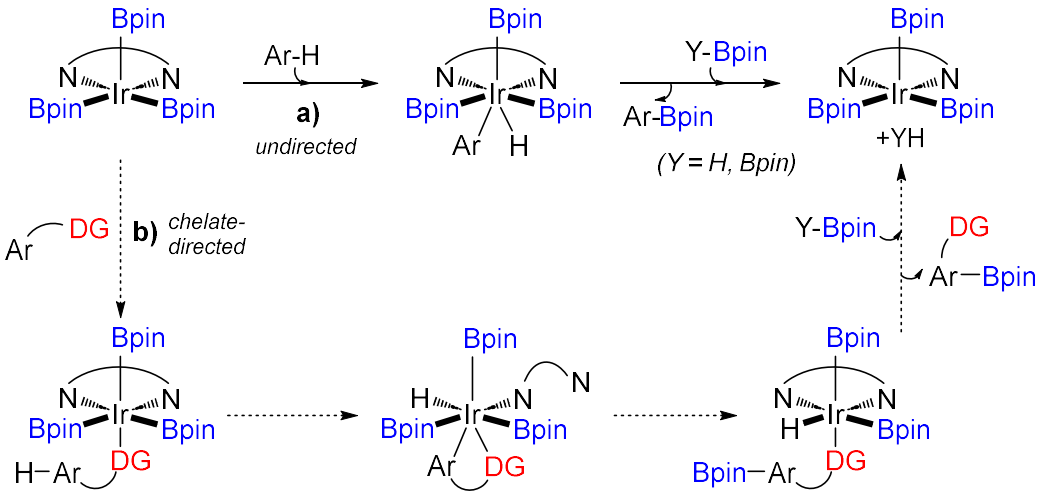

Figure 1.4: Comparison of reaction pathways for the **a)** undirected and **b)** chelate-directed iridium catalysed C-H borylation of arenes.
(DG = directing group).

One example of iridium-catalysed, chelate-directed C-H borylation was developed by Lassaletta and co-workers using hemi-labile *N,N* ligands.[87] These ligands coordinate to iridium reversibly on one side to facilitate the temporary generation of a vacant site, enabling successive directing group coordination and C-H activation. Hemi-labile ligands have been used to enable the nitrogen directed, *ortho*-selective C-H borylation of functionalised aryl pyridines, aromatic *N,N*-dimethyl hydrazones and benzylic amines (**Scheme 1.9**).[87–89] Significant work has been done in this field with a range of substrates,[84] though a comprehensive overview is not appropriate given the content within this thesis.

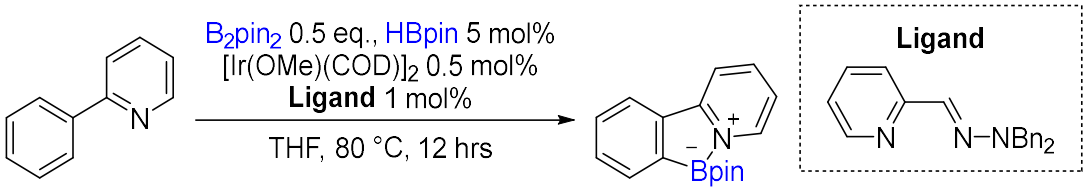

Scheme 1.9: Iridium-catalysed, nitrogen-directed, *ortho*-C-H borylation of 2-phenylpyridine *(COD = 1,5-cyclooctadiene).*

An alternative strategy to enable iridium-catalysed directed C-H borylations that avoids the need for labile bidentate ligands was developed by Hartwig and co-workers for the *ortho* C-H borylation of several benzylic dimethyl silanes (**Scheme 1.10**).[90] In this process (sometimes described as a 'relay-directed' borylation) the *ortho*-directing effect stems from the dialkyl hydrosilyl group on the substrate (rather than a Lewis basic moiety), which reacts with the 16e$^-$ iridium complex via Si-H/Ir-B σ-bond metathesis. This enables the silyl group to bind to the iridium centre and orientate it appropriately, whilst maintaining the vacant coordination site required for subsequent C-H activation and C-B bond formation. The silyl directing group used in this process provides a second versatile functional group for subsequent transformations following C-H borylation, making this a useful method for the synthesis of bifunctional arenes.[91] Further work saw silyl-directing groups applied to the iridium-catalysed C-H borylation of *N*-heterocycles, including indole.[92] This enabled the C7-H borylation of indole, with the benzenoid ring selectively borylated without the need for blocking groups on the 5-membered heteroarene ring. *This work is discussed in more detail in* ***Chapter 3****.*

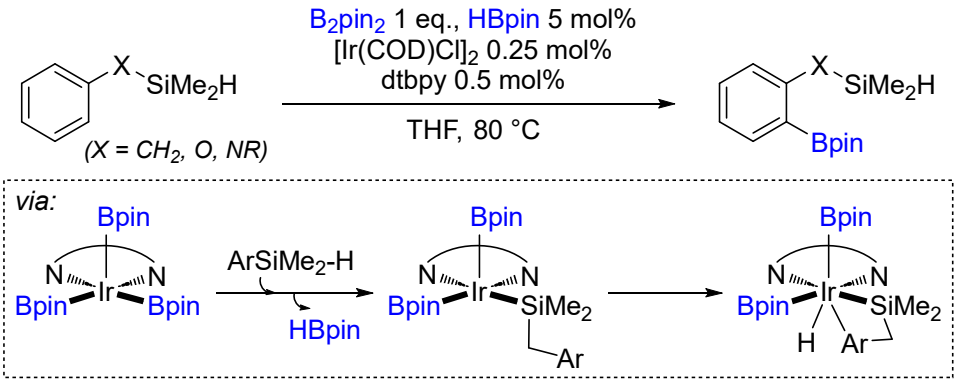

Scheme 1.10: Iridium catalysed, silyl-directed, *ortho*- C-H borylation of benzylic dimethyl silanes
(COD = 1,5-cyclooctadiene, dtbpy = 4,4'-di-tert-butyl-2,2'-bipyridine).

Outer-Sphere Directed C-H Borylation

Outer-sphere direction is an alternative approach that has been applied to iridium-catalysed C-H borylations (and other C-H functionalisation reactions).[93] In these processes, a 'directing' moiety on the substrate interacts with a ligand of the active catalyst, rather than to the metal centre directly. These outer-sphere interactions (typically non-covalent) position the substrate appropriately to enable regioselective C-H activation by the catalyst.

This concept was first applied to iridium-catalysed C-H borylations by Smith and co-workers for the *ortho*-selective C-H borylation of *N*H-Boc anilines (**Scheme 1.11**).[94] The *ortho*-directing effect in this process was attributed to hydrogen bonding between the acidic N-H on the substrate and the boryl ligand on iridium. By comparison, the iridium-catalysed C-H borylation of the corresponding *N*-Boc$_2$ aniline derivatives yielded *meta*/*para*-borylated products, with regioselectivity under steric control. Later work enabled the 'traceless' hydrogen-bond directed *ortho* C-H borylation of unsubstituted (NH$_2$-)anilines via the *in situ* formation and removal of a 'transient' *N*H-Bpin group.[81,95] Multiple groups have since made use of outer-sphere directing effects to enable *ortho*-selective iridium catalysed C-H borylations of (hetero)arenes.[96–98]

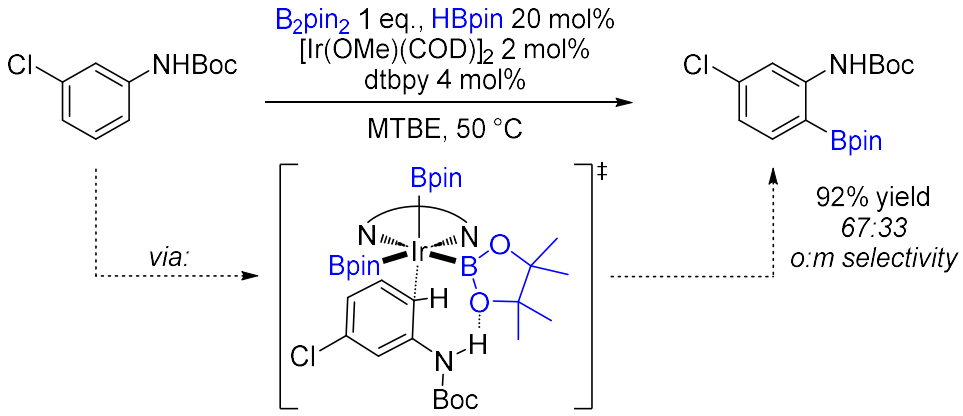

Scheme 1.11: Outer-sphere H-bond directed, iridium catalysed *ortho* C-H borylation of *N*H-Boc aniline derivatives
(COD = 1,5-cyclooctadiene, dtbpy = 4,4'-di-tert-butyl-2,2'-bipyridine).

The most notable feature of this approach is in enabling selective C-H borylation at positions not adjacent to the directing moiety on the substrate, e.g. the *meta*- or *para*-positions, by modification of the 'interacting' ligand to control the positioning of the substrate for C-H activation. The first application of this concept in iridium-catalysed C-H borylation enabled the 'remote' *meta*-selective borylation of arenes.[99] Here, regioselectivity was controlled by a hydrogen bond interaction between a pendant urea group on the bipyridine ligand and a carbonyl functionality on the substrate, thus positioning the iridium centre in close proximity to the *meta* C-H bond (**Figure 1.5**).

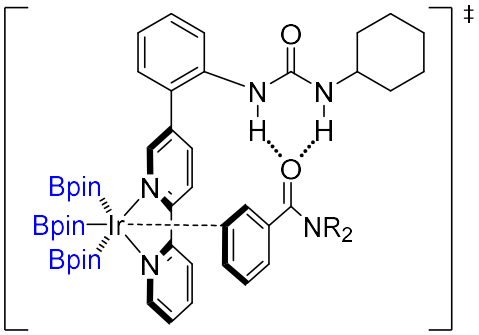

Figure 1.5: Proposed transition state for the *meta*-selective C-H borylation of *N*-alkyl benzamide derivatives, showing the hydrogen bonding interactions between the ligand and substrate.

The use of charged ligands/substrates to control regioselectivity via electrostatic ion pairing has also been developed to enable *meta*- and *para*- selective C-H

borylation processes.[100–102] This is beyond the scope of this introduction, but the interested reader is directed towards the recent reviews of this field.[103–105]

This section demonstrates that iridium catalysed C-H borylation has become a powerful methodology for the synthesis of a wide array of aryl boronic acids/esters under mild and functional group tolerant conditions. Several strategies have been developed to alter the regioselectivity of C-H borylation, enabling a range of regioisomers to be produced in high yields. However, these methodologies remain limited by their use of precious metals, which can result in high costs for large-scale processes. For the synthesis of pharmaceutical compounds, this also necessitates extensive purification steps to remove potentially toxic (and therefore tightly controlled) metallic impurities. Thus, processes that enable transition-metal free C-H borylation reactions are of significant interest. The following section considers the application of electrophilic C-H borylation processes as an alternative, metal-free route to aryl boronic acids/esters.

1.4 Electrophilic C-H Borylation

In recent years, electrophilic C-H borylation has been demonstrated as simple and often inexpensive method to produce a range of (hetero)aromatic boronic acids/esters without transition metals.[106] One attractive feature of electrophilic C-H borylation is that it can be used to access complementary regioselectivity to iridium-catalysed C-H borylation processes (*vide infra*).

1.4.1 Early Studies on Electrophilic C-H Borylation

Electrophilic borylation of arenes was first reported in 1948, where heating benzene with diborane gas at 100 °C resulted in the formation of phenylboronic acid upon aqueous work-up.[107] Following this, boron-analogues of the Friedel-Crafts reaction were developed, with arenes undergoing borylation with BX_3 (X = Cl, Br, I) following activation by AlX_3 (**Scheme 1.12**).[108,109] For these reactions, removal of the Brønsted acidic by-product (HX) was essential to prevent protodeboronation of the products. This was achieved via loss of gaseous HX from an open vessel, or via the irreversible reaction of HX with Al to form H_2.

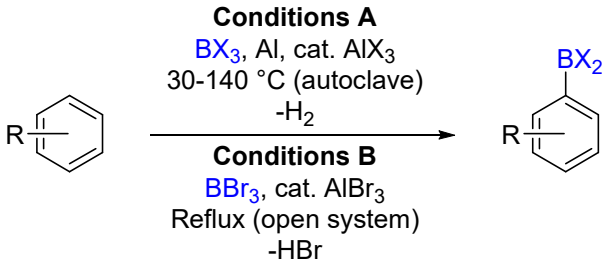

Scheme 1.12: Synthesis of aryl dihaloboranes via the boron Friedel-Crafts reactions of arenes with BX_3 and catalytic AlX_3.

Muetterties proposed that these reactions proceeded via the abstraction of a halide from a solvated arene-BX_3 intermediate by AlX_3, generating [arene·BX_2][AlX_4] *in situ*.[110] An alternative activation mode was proposed by Olah, where coordination of AlX_3 to BX_3 generates a halide bridged [BX_2-(μ-X)-AlX_3] intermediate.[111] Both activation modes would lead to increased electrophilicity at boron (compared to the parent BX_3 compound), forming highly reactive 'super-electrophiles' which enable arene C-H borylation.

Whilst this process was effective for the electrophilic borylation of simple arenes, the highly Brønsted and Lewis acidic reagents meant the process was not compatible with many functional groups or acid-sensitive heteroarenes (e.g. thiophenes), resulting in substrate decomposition. To expand the scope of electrophilic C-H borylation, less reactive (than BX_3-$AlCl_3$) boron electrophiles are required along with more efficient proton scavenging. To this end, borocations have been explored over the past 15 years to enable the electrophilic C-H of a wide scope of (hetero)arenes.[112]

1.4.2 Borocations in Electrophilic C-H Borylation

The terminology for borocations, defined by Köelle and Nöth, is dependent on the coordination number at boron: 2-coordinate *borinium* ions, 3-coordinate *borenium* ions, and 4-coordinate *boronium* ions (**Figure 1.6**).[113]

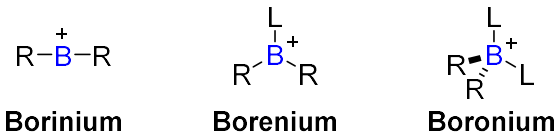

Figure 1.6: Terminology for borocations of varying coordination number, where L is a neutral Lewis base, and R is a *mono*-anionic substituent.

The reactivity of these borocations is dominated by their electrophilicity at boron. For electrophilic C-H borylation, the majority of examples proceed via 3-coordinate borenium ions, which possess considerable electrophilicity and can be generated via relatively facile activation methods.[114] Whilst borinium ions are known, they are generally too unstable to be useful synthetic reagents.[115] Boronium ions can be useful electrophiles if the Lewis base at the fourth coordination site can be readily displaced by an incoming nucleophile (e.g. an aryl π-system). In addition, formally neutral, 4-coordinate Lewis acid-base adducts ($L\text{-}BH_2X$) containing a weakly-bound anionic substituent (e.g. X = NTf_2) can also be utilised as boron electrophiles in C-H borylation processes. These two types of 4-coordinate species can be considered as more synthetic equivalents of borenium ions (sometimes described as 'masked' borenium ions).[114]

Borenium Ions

Borenium ions (and borenium ion equivalents) are often generated from neutral Lewis acid-base complexes (L-BR_2Y) by halide or hydride abstraction (B-Y heterolysis, **Figure 1.7**). This can be achieved via addition of an 'activator', such as a trityl ($[Ph_3C]^+$) salt, a strong Brønsted acid (e.g. $HNTf_2$) or a neutral Lewis acid (e.g. $AlCl_3$).[113] It should be noted that in some cases, borenium ion formation can be reversible, leading to complex equilibria between neutral and cationic species, complicating both reactivity and analysis.[116]

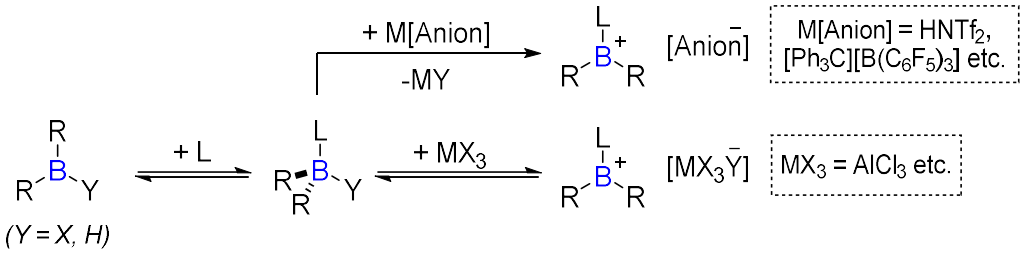

Figure 1.7: The generation of borenium ions via B-X/B-H heterolysis, where L is a neutral Lewis base, and R is a *mono*-anionic substituent.

In order to access borenium ions it is important that the Lewis base coordinates sufficiently strongly at boron, otherwise dissociation and competitive coordination (e.g. to the stronger Lewis acid, $AlCl_3$), or protonation (e.g. by $HNTf_2$) of the Lewis base can occur.[112] The coordinating Lewis base also needs to provide sufficient stabilisation to the boron centre via steric crowding and/or π-donation to enable activation of the Lewis acid-base complex (by B-Y heterolysis). To meet these requirements, nucleophilic and/or sterically demanding amines, phosphines and *N*-heterocyclic carbenes (NHCs) are commonly used Lewis bases, particularly for the generation of observable (by NMR spectroscopy) borenium ions. When weaker bases are used, borenium ions can still be formed and effect C-H borylation, but their formation is endergonic. Furthermore, the anion used must be robust and weakly coordinating. For example, the use of fluorinated anions (e.g. $[BF_4]^-$) can result in fluoride abstraction,[117] whilst relatively coordinating anions (e.g. $[OTf]^-$) can interact strongly with the boron centre in the absence of significant steric/electronic stabilisation, supressing Lewis acidity.[114] Weak interactions between a borenium cation and anion (e.g. $[NTf_2]^-$) can be

tolerated in borylation chemistry and can be used to generate 4-coordinate borenium ion equivalents (*vide infra*).

Chloride abstraction by $AlCl_3$ was used to generate the first example of a borenium ion characterised by NMR spectroscopy.[118] Addition of 2 equiv. $AlCl_3$ to [4-picoline]·BCl_3 resulted in reversible borenium ion formation (**1.7**, **Scheme 1.13**). This was characterised by ^{11}B NMR spectroscopy which showed a significant downfield shift, indicating a change from 4 to 3-coordinate boron. Addition of a Lewis base to the borenium salt (**1.7**) generated a 4-coordinate boronium salt (**1.8**), whilst the neutral adduct did not react with the Lewis base to form a boronium ion in the absence of $AlCl_3$.

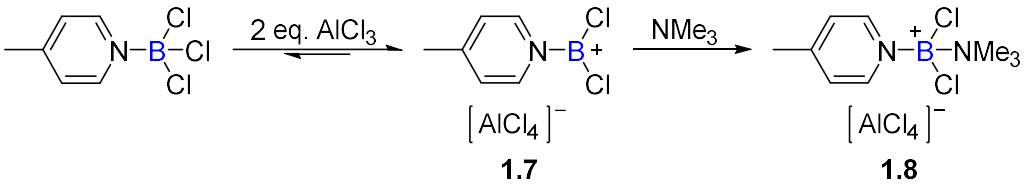

1.7 **1.8**

Scheme 1.13: Halide abstraction from a 4-coordinate borane results in the reversible formation of a borenium salt, which can be 'trapped' as a boronium salt upon addition of a Lewis base.

Borenium ions can also be generated by the addition of a Lewis base to a neutral 3-coordinate borane, provided the borane contains a suitable leaving group and there is sufficient steric congestion around boron to disfavour the formation of a 4-coordinate adduct. The Lewis base used is important, as demonstrated in the reactivity of 9-BBN-OTf (**Scheme 1.14**). Addition of pyridine generated 4-coordinate adduct **1.9**, whilst more sterically demanding 2,6-lutidine was able to displace the triflate group and generate the 3-coordinate borenium ion **1.10**.[119]

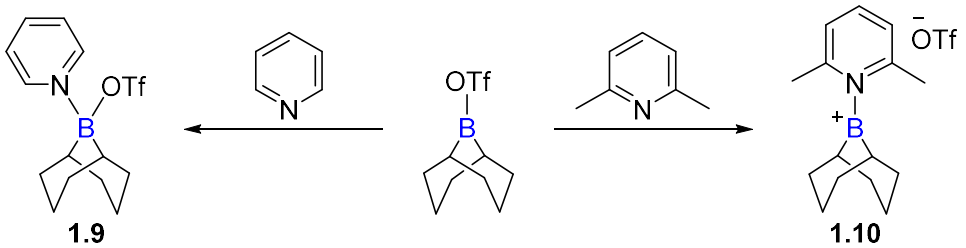

1.9 **1.10**

Scheme 1.14: Reactions of 9-BBN-OTf with pyridine bases, forming either Lewis acid-base adducts (LHS) or borenium salts (RHS).

A detailed overview of the many developments in the generation of borenium ions, their structures and their Lewis acidity is beyond the scope of this introduction but is presented in the reviews of this field.[112–115]

'Masked' Borenium Ions Equivalents

Borenium ions can form more stable boronium ions by the coordination of a Lewis basic moiety.[120] Boronium ions ([L-BR_2-L]$^+$) can used in electrophilic C-H borylation reactions as 'masked' borenium ion equivalents if the second Lewis base is readily displaced by an incoming nucleophile.[114] In a similar manner, neutral Lewis base-borane adducts can behave as 'masked' borenium ion equivalents if they contain a good leaving group at boron (L-BH_2X, where X = the leaving group). These complexes are often accessible via substitution reactions of L-BH_3 complexes. For example, Curran and co-workers demonstrated that NHC-BH_2X electrophiles could be generated from bench-stable NHC-borane complexes following activation with strong acids or halogens (**Scheme 1.15**).[121]

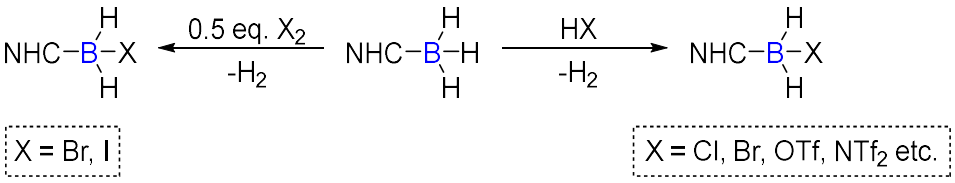

Scheme 1.15: Substitution reactions of NHC-BH_3 complexes.

The electrophilicity of these 'L-BH_2X' complexes is dependent on the coordinating ability of the anionic leaving group, X^-. If X^- is strongly coordinating (e.g. chloride), a tightly bound L-BH_2X complex will be produced and X^- will not be displaced except by the strongest nucleophiles, thereby preventing most nucleophilic substitutions at boron. Less strongly coordinating anions (e.g. iodide) will be displaced by a wider range of nucleophiles, hence can be viewed as synthetic equivalents of borenium ions, where the anion is instead coordinated at boron.[122] If the anion is very weakly coordinating, it can be displaced by the starting L-BH_3 complex to form a boronium ion. This was observed by Vedejs and co-workers, where hydride abstraction of a benzylamine-borane adduct (**1.11**) by [Ph_3C][$B(C_6F_5)_4$] at -20 °C led to the observation of a 3c2e$^-$ hydride bridged boronium ion, **1.13**, formed via the rapid coordination of the B-H σ-bond of the

starting borane to the non-stabilised borenium ion **1.12** (**Scheme 1.16**).[123] Upon warming to RT, the neutral borane (**1.11**) is displaced from **1.13** by the aryl C-H, and intramolecular C-H borylation proceeds *(with this process discussed in more detail in a subsequent section).* Therefore, **1.13** can be considered as an *in situ* source of the borenium ion **1.12**.

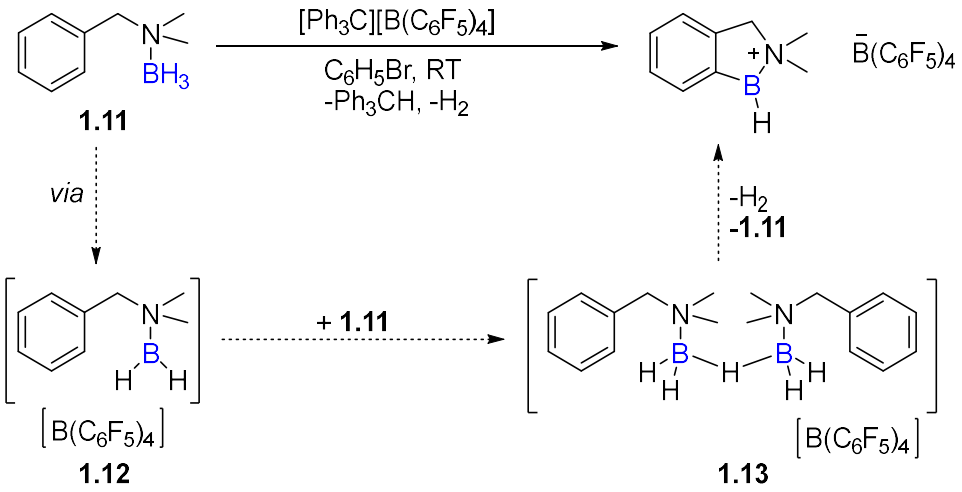

Scheme 1.16: Intramolecular C-H borylation of benzyl amines via an *in situ* generated borenium ion equivalent.

The above has shown select examples, but a range of highly electrophilic borenium ions (or their synthetic equivalents) have been produced from neutral boranes. These cations generally react with (hetero)arene nucleophiles via S_EAr-type mechanisms (stepwise or concerted), hence show higher reactivity with electron-rich arenes.[106,112] The following sections considers intermolecular and intramolecular electrophilic C-H borylation reactions that proceed through borenium ions (or their synthetic equivalents), with a focus on routes that can be used to generate synthetically useful aryl boronic acids/esters (directly, or via subsequent transformations). This largely excludes the significant work on generating boron-containing organic materials via electrophilic C-H borylation, but readers are directed to reviews of this important field.[124,125]

1.4.3 Intermolecular Electrophilic C-H Borylation via Borenium Ions

The generation of highly electrophilic borenium ions (or their synthetic equivalents) can enable the intermolecular C-H borylation of (hetero)arenes. However, as demonstrated in the early examples of electrophilic arene C-H borylation with BX_3 (*vide supra*, **Scheme 1.12**),[109] the Brønsted acidic by-product formed during the reaction can cause decomposition of acid-sensitive substrates and/or protodeboronation of the borylated products, unless it is effectively removed. To expand electrophilic C-H borylation to a wider range of substrates, Ingleson and co-workers utilised catechol-ligated borenium ions ($[CatB\text{-}L]^+$), where release of the coordinated Lewis base during C-H borylation irreversibly sequesters the Brønsted acidic by-product (**Scheme 1.17**).[116] The borenium ion, **1.14**, was generated *in situ* by the addition of $AlCl_3$ to an amine·CatBCl adduct, generating an equilibrium between the neutral species and **1.14** (which was observed by ^{11}B NMR spectroscopy). Addition of the arene substrate led to *para*-selective arene C-H borylation, alongside the formation of [amine-H][$AlCl_4$].

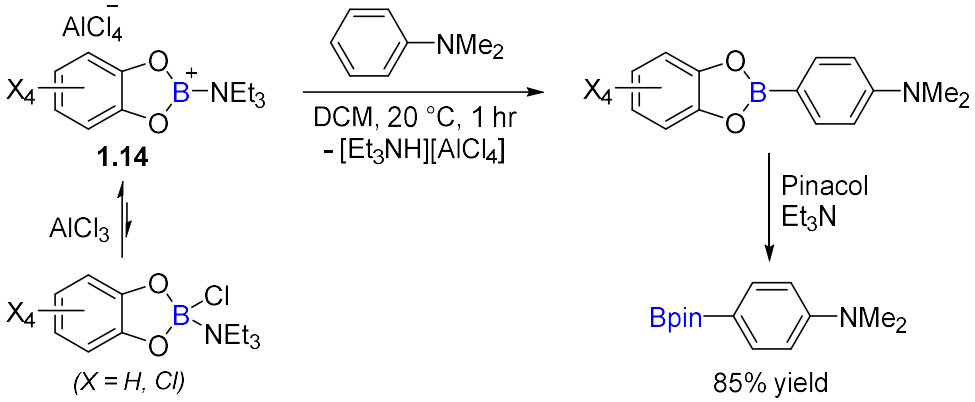

Scheme 1.17: Electrophilic C-H borylation of arenes via an *in situ* generated borenium ion, where dissociated NEt_3 acts as a protic scavenger.

It should be noted that the corresponding pinacolato-ligated borenium ion, $[PinB\text{-}L]^+$, was insufficiently electrophilic to borylate even highly activated (hetero)arenes, owing to the more donating pinacol unit. In comparison, the use of a less donating diol, tetrachlorocatecholato, resulted in a more electrophilic borenium ion ($[Cl_4\text{-}CatB\text{-}L]^+$), enabling faster arene C-H borylation. Following arene C-H borylation, transesterification of the B-catechol moiety (which can be

sensitive to protodeboronation) with pinacol enabled isolation of synthetically useful aryl boronic esters. The reaction was compatible with halide and ether groups and was applied to the C-H borylation of a range of electron-rich (hetero)arenes, including indoles, pyrroles and thiophenes. The regioselectivity of this process is largely controlled by the electronics of the (hetero)arenes, with borylation proceeding at the most activated, non-sterically hindered position.[124] For example, *N*-*N*-dimethyl anilines reacted at the *para*- position, whilst indoles reacted at C3. This therefore provides complementary selectivity to iridium-catalysed processes, which operate under steric control or by heteroatom direction (*vide supra*).[59] This difference in selectivity is most clearly demonstrated with 3-bromo-*N,N*-dimethylaniline, with the electrophilic C-H borylation process yielding the C4-borylated product. By comparison, 1,3-disubstituted arenes borylate exclusively at the C5-position in iridium-catalysed reactions, owing to the sensitivity of the iridium catalyst to steric hinderance.[58]

At the same time, Vedejs and co-workers used a similar approach to generate a reactive boronium ion that could be used in electrophilic arene C-H borylation (**Scheme 1.18**).[126] The addition of 1,8-*bis*(dimethylamine)naphthalene to 9-BBN-NTf_2 generated the boronium ion **1.15** which, upon addition of activated heteroarenes (indoles and pyrroles), reacts as a masked borenium ion via amine dissociation, thus enabling heteroarene C-H borylation. However, this process was limited in scope, and the conversion of the 9-BBN moiety into synthetically useful boronic acids/esters was challenging.

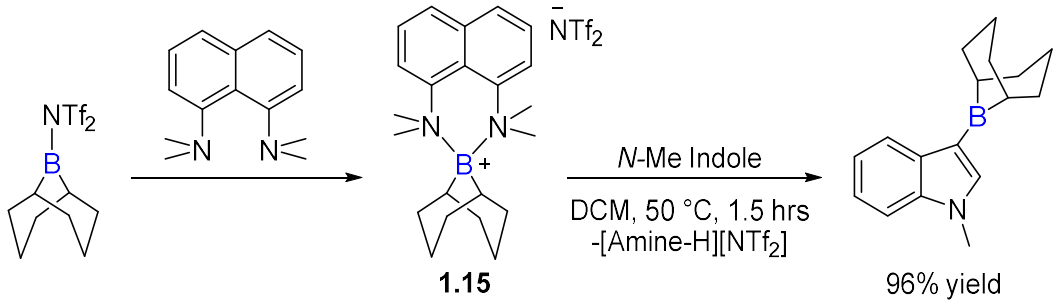

Scheme 1.18: Electrophilic C-H borylation of *N*-methyl indole via an *in situ* generated boronium ion, reacting as a masked borenium ion equivalent.

In the hope of expanding the scope of electrophilic C-H borylation to a wider range of (hetero)arenes, Ingleson and co-workers reported several borenium cations containing weaker π-donors (than catechol) to increase electrophilicity at boron.[127] For example, dichloride borenium ions, $[Cl_2B\text{-}L]^+$, were shown to have increased electrophilicity over $[CatB\text{-}L]^+$ owing to the reduced π-donating ability of the chloride anions.[128] Dichloride borenium ions are readily generated by mixing equimolar BCl_3, $AlCl_3$ and an amine, forming **1.16** (though the process is in dynamic equilibrium, **Scheme 1.19**). The increased electrophilicity of **1.16** enabled the C-H borylation of an extensive scope of (hetero)arenes at room temperature.[128–130] Less activated arenes (e.g. naphthalene, benzothiophene etc.) are also capable of undergoing C-H borylation at increased temperatures (80-150 °C). Conveniently, the use of **1.16** produces (hetero)aryl-BCl_2 products, which are versatile intermediates that can be converted into boronic acids, pinacol esters, or quaternized MIDA-boronates within a one-pot process.

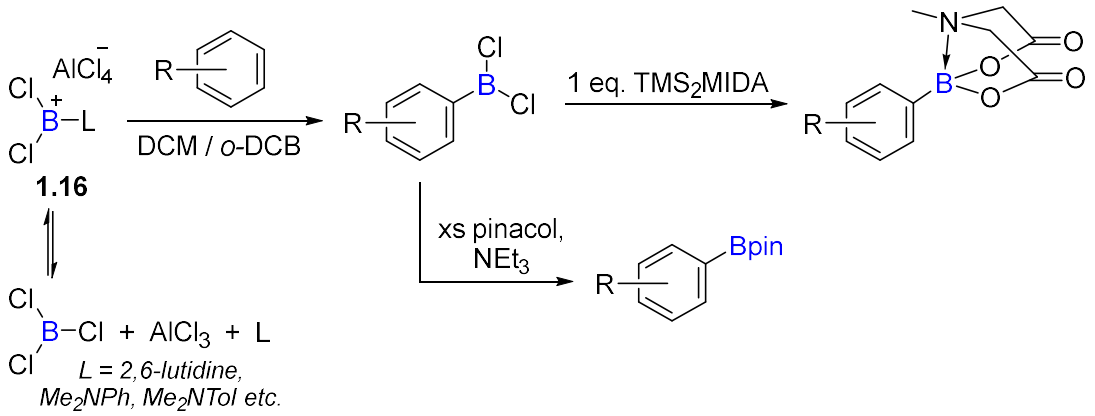

Scheme 1.19: Amine-mediated electrophilic C-H borylation of (hetero)arenes, with subsequent diversification to aryl-Bpin and aryl-B(MIDA) products.

The higher Lewis acidity of BBr_3 over BCl_3 can enable the electrophilic C-H borylation of (hetero)arenes and terminal alkenes to proceed without the need for an exogenous activator (e.g. AlX_3). Hattori and co-workers demonstrated that BBr_3 and 2,6-lutidine could be used for the room temperature C-H borylation of *N*-methyl indole, yielding the C3-borylated product exclusively in high yields.[131] Mechanistic studies suggested that the reaction proceeded through the *in situ* formation of $[Br_2B\text{-}L][BBr_4]$, although the formation of this borenium ion is calculated to be endergonic and it is not observed by NMR spectroscopy.

Therefore, the generation of novel and highly electrophilic borenium ions has enabled electrophilic C-H borylation reactions to be applied to a wide range of (hetero)arenes, often under relatively mild conditions, with several examples proceeding at room temperature.[106] The development of efficient strategies to sequester the Brønsted acid by-product has also enabled reactions of acid-sensitive functional groups / heteroarenes. The regioselectivity of electrophilic C-H borylation is largely controlled by arene electronics, hence it can be complementary to steric-controlled iridium catalysed processes.[124]

Despite these advantages, these processes often require stoichiometric amounts of the activator to generate the reactive boron electrophile. There is significant interest in the development of processes that are catalytic in activator and can be applied to a wide scope of substrates.[132] One notable example of this was initially reported by Oestreich and co-workers, where $B(C_6F_5)_3$ is used as a catalytic activator of the H-B bond in HBCat. This generates borenium ion **1.17** (or its synthetic equivalent) *in situ* and facilitates the C-H borylation of several electron-rich arenes (**Scheme 1.20**).[133] The key turnover step of this process is the combination of Brønsted acid by-product ($[L\text{-}H]^+$) with the B-H moiety of H(L)BCat, forming H_2 and regenerating the active electrophile **1.17**.

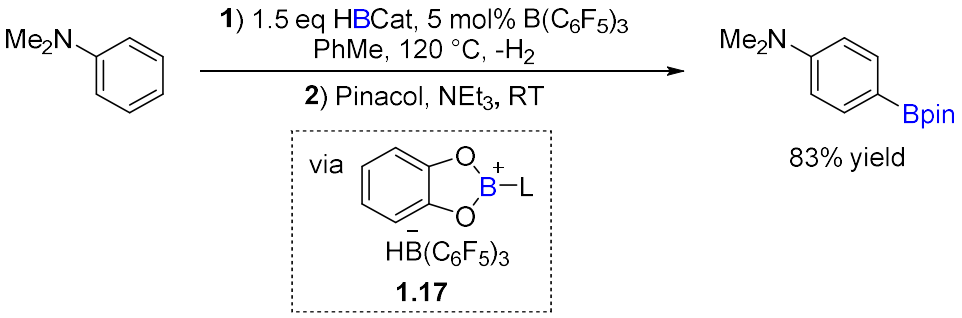

Scheme 1.20: $B(C_6F_5)_3$ catalysed electrophilic C-H borylation of anilines, where L = the substrate, *N,N*-dimethylaniline.

Neutral intramolecular frustrated Lewis pairs (FLPs) have also found applications as ambiphilic catalysts (able to react as both the active electrophile and amine base) for the electrophilic C-H borylation of heteroarenes, with turnover enabled by a dehydrocoupling step (evolving H_2).[134,135] However, as they do not involve borenium ions (or their synthetic equivalents) they are not

discussed in depth in this introduction. It should be noted, however that these reactions proceed via a concerted S_EAr mechanism, compared to the stepwise S_EAr mechanism of borenium-ion mediated C-H borylation.

1.4.4 Directed (Intramolecular) Electrophilic C-H Borylation

With intermolecular electrophilic C-H borylation, the regioselectivity is largely directed by the (hetero)arenes electronic effects combined with sterics.[106] Substrates containing strongly electron-donating substituents can give high regioselectivity. For example, *N,N*-dimethyl aniline undergoes electrophilic C-H borylation at the *para*-position only. For substrates where there is not a significant electronic directing effect, a mixture of regioisomers are formed.[124]

As with iridium-catalysed C-H borylation reactions, directing groups (DGs) can be used to alter the regioselectivity of C-H borylation to positions that are otherwise challenging to borylate selectively – for example, the *ortho*-position of aniline derivatives. Directed electrophilic C-H borylation proceeds via the initial coordination of the boron electrophile to a Lewis basic directing group (E or E-H) on the (hetero)arene, forming a dative or covalent E-B bond (with deprotonation of E in the latter case). This positions the electrophile in close proximity to the target C-H position (typically *ortho*- to the Lewis basic moiety).[125] Intramolecular C-H borylation can then proceed, forming a boracyclic ring (**Scheme 1.21**).

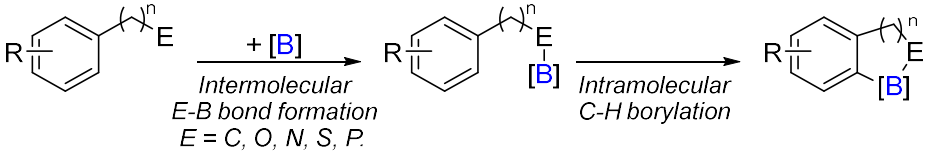

Scheme 1.21: General procedure for 'E'-directed electrophilic C-H borylation.

The directing groups used in electrophilic C-H borylation can categorised as: (a) 'built in' directing groups, where the Lewis basic moiety is already present in the target molecule and remains following C-H borylation, (b) 'removable' directing groups, which are pre-installed onto the target molecule prior to C-H borylation, then removed in subsequent steps, and (c) 'transient' directing groups, which are installed *in situ*, used to direct C-H borylation, then removed all in a one-pot

process.[124] The following section presents selected examples of the application of these three directing groups classes in electrophilic C-H borylation reactions.

'Built In' Directing Groups

A range of Lewis basic moieties that are already present in a (hetero)arene substrate can be used to direct C-H borylation to the respective *ortho*-position. The earliest examples of this approach were developed by Dewar and co-workers, with several N-directed electrophilic C-H borylation processes reported using BCl_3 and catalytic $AlCl_3$.[136,137] In one example, the addition of BCl_3 to 2-NH_2 biphenyl derivatives formed aryl-N(H)BCl_2 intermediates (**1.18**) upon heating (**Scheme 1.22**). The significant B-N double bond character of these intermediates reduces Lewis acidity at boron, hence catalytic $AlCl_3$ is required to generate sufficiently reactive boron electrophiles to effect intramolecular C-H borylation and form 6-membered B-N boracycles. Initial reports of this process required forcing conditions; it has since been demonstrated in refluxing benzene.[138]

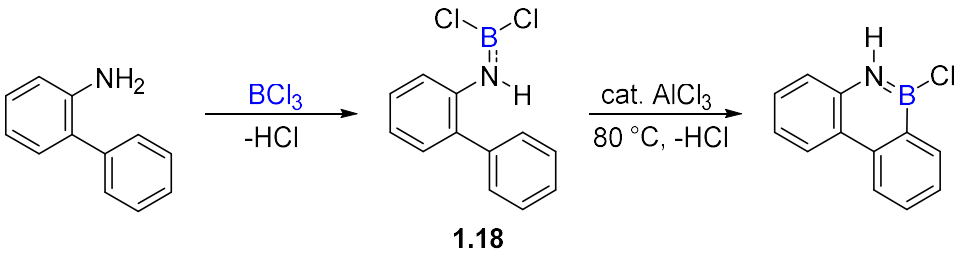

Scheme 1.22: N-directed intramolecular arene C-H borylation using BCl_3 and catalytic $AlCl_3$.

This approach was later applied to 2-OH and 2-SH biphenyl derivatives, where addition of BCl_3 generated the corresponding aryl-E-BCl_2 intermediates (E = O, S) alongside loss of HCl.[139,140] Notably, subsequent intramolecular arene C-H borylation (catalysed by $AlCl_3$) proceeds at lower temperatures for these substrates compared to 2-NH_2 biphenyl: 60 °C for 2-OH biphenyl, and 20 °C for 2-SH biphenyl. This correlates with the π-donating ability of the heteroatom bonded to boron (S < O < N). Significant π-donation decreases the Lewis acidity of the boron centre; hence the reaction of 2-SH biphenyl generates the most reactive boron electrophile of the series, and thus arene C-H borylation occurs at room temperature. *This work is discussed in more detail in* ***Chapter 2****.*

In a similar approach, Murakami and co-workers used a pyridine ring to enable the directed C-H borylation of 2-phenyl pyridine with BBr_3 and an external base (**Scheme 1.23**).[141] It was proposed that initial N-B coordination enables the formation of a $[Br_2B\text{-}L]^+$ borenium ion **1.19**, which undergoes C-H borylation at room temperature to form a robust pyridine-dibromo borane complex (**1.20**). In this example, borenium ion formation is endergonic, but is energetically accessible according to calculations. The bromides of **1.20** can be substituted in subsequent reactions, whilst the 5-membered pyridine-borane ring is maintained; hence this process has since become invaluable in the synthesis of a wide range of functionalised pyridine-borane complexes that are especially useful in the production of boron-doped organic materials.[142]

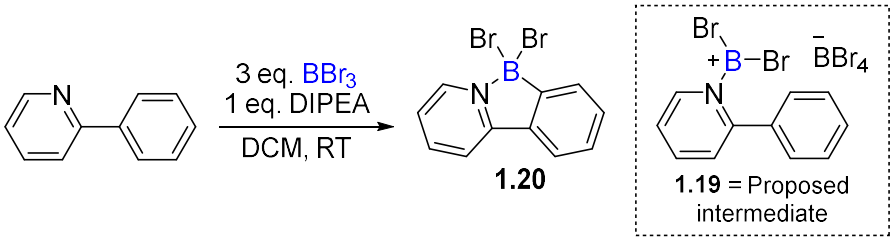

Scheme 1.23: N-directed electrophilic C-H borylation of 2-phenylpyridine.

Other examples of intramolecular (hetero)arene C-H borylation processes have utilised quinolines,[143] thiazoles,[144] and other *N*-heterocycles as directing groups,[125] which proceed via similar mechanisms. The previously discussed example of amine-directed intramolecular C-H borylation of benzyl amines, developed by Vedejs and co-workers (*vide supra,* **Scheme 1.16**), is another example of using a 'built in' directing group that remains in the final product.[123] Therefore, Lewis base directed electrophilic C-H borylation can be a useful technique if boracyclic products containing the directing group and boron are the targets, with many examples of this. However, the inability to remove the directing groups from the product limits this approach in terms of accessing boronic acids/esters for subsequent transformations. As such, the development of directing groups that can be transformed into new functional groups (or removed entirely) following C-H borylation is an ongoing area of research.

Removable Directing Groups

Removable directing groups can enable the products generated from directed electrophilic C-H borylation reactions to undergo a wide range of subsequent transformations.[124] These processes typically proceed via installation of the directing group into the substrate (often with isolation and purification required) prior to addition of the borylating reagent. The directing group then effects electrophilic C-H borylation at the *ortho* position, and is subsequently removed from the borylated product. It is important that the directing group is removed under conditions that are compatible with the newly generated C-B bond, and do not result in protodeboronation (or other decomposition side reactions). In some examples, functionalisation of the C-B bond is carried out prior to the removal of the directing group, thereby avoiding potential issues with decomposition.[145,146]

In one example of removable directing groups in electrophilic C-H borylation processes, Vedejs and co-workers utilised a diisopropylphosphine directing group, with the phosphine-borane complex **1.21** isolated and purified prior to the reaction.[147] Addition of $HNTf_2$ to **1.21** facilitated intramolecular arene C-H borylation upon heating, generating boracyclic intermediate **1.22** (**Scheme 1.24**). Addition of KHF_2 following borylation converted the product to the corresponding potassium trifluoroborate salt, **1.23**, with concomitant removal of the phosphine directing group in a one-pot process. The trifluoroborate salts were subsequently shown to be useful coupling partners in Suzuki-Miyaura cross coupling reactions.

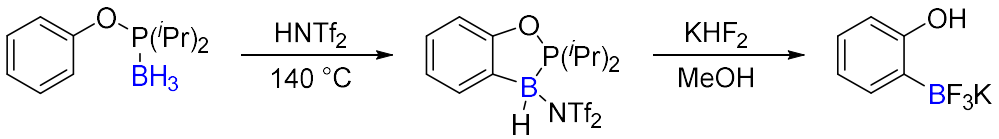

1.21 **1.22** *not isolated* **1.23**

Scheme 1.24: Directed electrophilic C-H borylation of phenol derivatives using a removable phosphorus directing group.

More recently, the groups of Shi, Houk, and Ingleson concurrently developed the use of acyl directing groups for electrophilic C-H borylation.[148,149] This process was used to enable the *ortho* C-H borylation of anilines and indoles using BBr_3,

following prior installation of a pivaloyl directing group (requiring column purification). Subsequent C-H borylation, pinacol protection and pivaloyl deprotection could all be done in a stepwise, one-pot process without the need to isolate or purify intermediate **1.24** (**Scheme 1.25**). Notably, in the C-H borylation of indoles the regioselectivity of C-H borylation could be altered by changing the site of pivaloyl installation prior the reaction, with C4 and C7-borylated indoles formed via this approach. *This work is discussed more extensively in* ***Chapter 3****.*

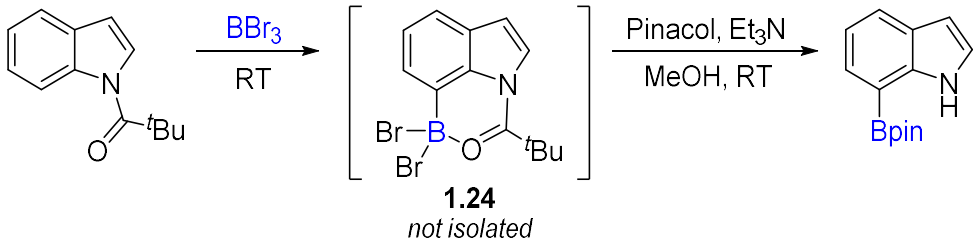

Scheme 1.25: Pivaloyl directed C7-H borylation of indoles using BBr_3.

The ability to remove directing groups within the same-one pot process as C-H borylation improves the efficiency of directed electrophilic C-H borylation to some degree; however a transient directing group approach is preferable as this does not require prior installation of the directing group and subsequent purification.

Transient Directing Groups

The use of transient directing groups, that are installed onto the (hetero)arene substrate, used to direct the boron electrophile for C-H borylation and readily removed all within a one-pot process, is highly desirable owing to the improvements in reaction efficiency.[150,151]

Examples of transient directing groups applied to electrophilic C-H borylation reactions are extremely limited, with only one example that was published during the completion of work reported in this thesis. Rej and Chatani reported the *ortho* C-H borylation of benzaldehyde by transformation of the carbonyl functional group into an imine *in situ*. The intermediate, **1.25**, was concentrated *in vacuo* to remove solvent/excess amine, with subsequent redissolution and addition of BBr_3 enabling *ortho* C-H borylation (**Scheme 1.26**).[152] The carbonyl moiety was

regenerated during the subsequent pinacol protection, enabling the direct synthesis of 2-Bpin benzaldehydes within a one-pot process. *This work is discussed in more detail in* ***Chapter 3****.*

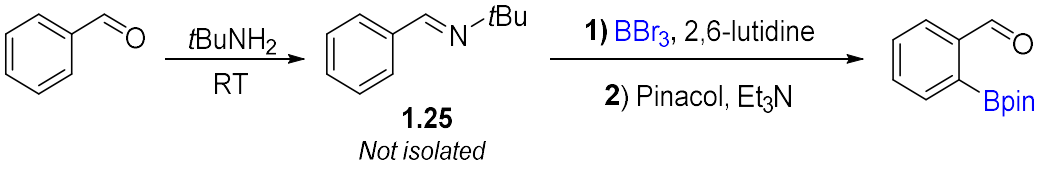

Scheme 1.26: *Ortho* C-H borylation of benzaldehyde via a transient imine directing group.

1.5 Thesis Aims

The versatility of aryl boronic acids/esters has led to considerable efforts to develop more efficient methods to synthesise them. Whilst iridium-catalysed C-H borylation is a powerful methodology, electrophilic C-H borylation can provide complementary regioselectivity in transition metal-free processes. Furthermore, the use of directing groups is a powerful method used to alter the regioselectivity of electrophilic C-H borylation reactions towards C-H positions that are otherwise challenging to borylate selectively.

An analysis of the field of directed electrophilic C-H borylation at the start of the work discussed within this thesis revealed two areas where there was virtually no precedence:

(i) **The use of O-H as a directing group**: Previously this had been limited to just one example by Dewar and co-workers: using 2-OH-biphenyl in the reaction with BCl_3 and catalytic $AlCl_3$. This contrasts to the application of N-H as a directing group, which has been well utilised. Therefore, one aim of this thesis was to explore the feasibility of using O-H as a directing group in electrophilic C-H borylation. If feasible, this would provide an efficient and metal-free route to B-O containing boracycles that are of increasing interest in medicinal chemistry. *This study is reported in* ***Chapter 2***.

(ii) **The use of transient directing groups**: The application of transient directing groups, which are installed, used to direct C-H borylation, and removed all in a one pot process, in electrophilic C-H borylation processes is significantly underdeveloped, with only one example reported during the development of the work within this thesis. Addressing this would provide significant improvements to the efficiency of directed electrophilic C-H borylation.
Studies towards this are discussed in ***Chapters 3***, ***4*** *and* ***5***.

1.6 References

1 F. Jäkle, *Chem. Rev.*, 2010, **110**, 3985–4022.

2 D. Li, H. Zhang and Y. Wang, *Chem. Soc. Rev.*, 2013, **42**, 8416–8433.

3 E. von Grotthuss, A. John, T. Kaese and M. Wagner, *Asian J. Org. Chem.*, 2018, **7**, 37–53.

4 S. K. Mellerup and S. Wang, *Chem. Soc. Rev.*, 2019, **48**, 3537–3549.

5 S. J. Baker, C. Z. Ding, T. Akama, Y.-K. Zhang, V. Hernandez and Y. Xia, *Future Med Chem.*, 2009, **1**, 1275–1288.

6 D. B. Diaz and A. K. Yudin, *Nature Chem.*, 2017, **9**, 731–742.

7 F. Yang, M. Zhu, J. Zhang and H. Zhou, *Med. Chem. Commun.*, 2018, **9**, 201–211.

8 J. X. Qiao and P. Y. S. Lam, *Synthesis*, 2011, **2011**, 829–856.

9 C. Sandford and V. K. Aggarwal, *Chem. Commun.*, 2017, **53**, 5481–5494.

10 N. Miyaura and A. Suzuki, *J. Chem. Soc., Chem. Commun.*, 1979, 866–867.

11 N. Miyaura, K. Yamada and A. Suzuki, *Tetrahedron Lett.*, 1979, **20**, 3437–3440.

12 N. Miyaura and A. Suzuki, *Chem. Rev.*, 1995, **95**, 2457–2483.

13 A. J. J. Lennox and G. C. Lloyd-Jones, *Chem. Soc. Rev.*, 2013, **43**, 412–443.

14 C. Torborg and M. Beller, *Adv. Synth. Catal.*, 2009, **351**, 3027–3043.

15 J. Magano and J. R. Dunetz, *Chem. Rev.*, 2011, **111**, 2177–2250.

16 D. G. Brown and J. Boström, *J. Med. Chem.*, 2016, **59**, 4443–4458.

17 H. G. Kuivila and K. V. Nahabedian, *J. Am. Chem. Soc.*, 1961, **83**, 2164–2166.

18 H. G. Kuivila, A. H. Keough and E. J. Soboczenski, *J. Org. Chem.*, 1954, **19**, 780–783.

19 E. D. Farfán-García, N. T. Castillo-Mendieta, F. J. Ciprés-Flores, I. I. Padilla-Martínez, J. G. Trujillo-Ferrara and M. A. Soriano-Ursúa, *Toxicol. Lett.*, 2016, **258**, 115–125.

20 K. C. Nicolaou, P. G. Bulger and D. Sarlah, *Angew. Chem. Int. Ed.*, 2005, **44**, 4442–4489.

21 S. M. Berger, M. Ferger and T. B. Marder, *Chem. Eur. J.*, 2021, **27**, 7043–7058.

22 E. Khotinsky and M. Melamed, *Ber. Dtsch. Chem. Ges.*, 1909, **42**, 3090–3096.

23 William. Seaman and J. R. Johnson, *J. Am. Chem. Soc.*, 1931, **53**, 711–723.

24 X. Wang, X. Sun, L. Zhang, Y. Xu, D. Krishnamurthy and C. H. Senanayake, *Org. Lett.*, 2006, **8**, 305–307.

25 T. Leermann, F. R. Leroux and F. Colobert, *Org. Lett.*, 2011, **13**, 4479–4481.

26 P. C. Ruenitz, C. S. Bourne, K. J. Sullivan and S. A. Moore, *J. Med. Chem.*, 1996, **39**, 4853–4859.

27 D. E. Cladingboel, *Org. Process Res. Dev.*, 2000, **4**, 153–155.

28 H. C. Brown and T. E. Cole, *Organometallics*, 1983, **2**, 1316–1319.

29 V. V. Zhdankin, P. J. Persichini, L. Zhang, S. Fix and P. Kiprof, *Tetrahedron Lett.*, 1999, **40**, 6705–6708.

30 W. Li, D. P. Nelson, M. S. Jensen, R. S. Hoerrner, D. Cai, R. D. Larsen and P. J. Reider, *J. Org. Chem.*, 2002, **67**, 5394–5397.

31 N. K. Garg, R. Sarpong and B. M. Stoltz, *J. Am. Chem. Soc.*, 2002, **124**, 13179–13184.

32 S. Das, V. L. Alexeev, A. C. Sharma, S. J. Geib and S. A. Asher, *Tetrahedron Lett.*, 2003, **44**, 7719–7722.

33 H. Usutani and D. G. Cork, *Org. Process Res. Dev.*, 2018, **22**, 741–746.

34 C. Najera and M. Yus, *Curr. Org. Chem.*, 2003, **7**, 867–926.

35 T. Klatt, J. T. Markiewicz, C. Sämann and P. Knochel, *J. Org. Chem.*, 2014, **79**, 4253–4269.

36 J. Clayden, *Organolithiums: selectivity for synthesis*, Pergamon, Oxford, 1st ed., 2002.

37 N. Primas, A. Bouillon and S. Rault, *Tetrahedron*, 2010, **66**, 8121–8136.

38 H. Gilman, W. Langham and A. L. Jacoby, *J. Am. Chem. Soc.*, 1939, **61**, 106–109.

39 G. Wittig and G. Fuhrmann, *Ber. Dtsch. Chem. Ges.*, 1940, **73**, 1197–1218.

40 V. Snieckus, *Chem. Rev.*, 1990, **90**, 879–933.

41 M. Lauer and G. Wulff, *J. Organomet. Chem.*, 1983, **256**, 1–9.

42 M. J. Sharp and V. Snieckus, *Tetrahedron Lett.*, 1985, **26**, 5997–6000.

43 R. D. Larsen, A. O. King, C. Y. Chen, E. G. Corley, B. S. Foster, F. E. Roberts, C. Yang, D. R. Lieberman, R. A. Reamer, D. M. Tschaen, T. R. Verhoeven, P. J. Reider, Y. S. Lo, L. T. Rossano, A. S. Brookes, D. Meloni, J. R. Moore and J. F. Arnett, *J. Org. Chem.*, 1994, **59**, 6391–6394.

44 T. Ishiyama, M. Murata and N. Miyaura, *J. Org. Chem.*, 1995, **60**, 7508–7510.

45 E. C. Neeve, S. J. Geier, I. A. I. Mkhalid, S. A. Westcott and T. B. Marder, *Chem. Rev.*, 2016, **116**, 9091–9161.

46 M. Murata, S. Watanabe and Y. Masuda, *J. Org. Chem.*, 1997, **62**, 6458–6459.

47 M. Murata, T. Oyama, S. Watanabe and Y. Masuda, *J. Org. Chem.*, 2000, **65**, 164–168.

48 G. A. Molander, S. L. J. Trice and S. M. Kennedy, *J. Org. Chem.*, 2012, **77**, 8678–8688.

49 F. St-Jean, T. Remarchuk, R. Angelaud, D. E. Carrera, D. Beaudry, S. Malhotra, A. McClory, A. Kumar, G. Ohlenbusch, A. M. Schuster and F. Gosselin, *Org. Process Res. Dev.*, 2019, **23**, 783–793.

50 D. A. Wilson, C. J. Wilson, B. M. Rosen and V. Percec, *Org. Lett.*, 2008, **10**, 4879–4882.

51 C. Kleeberg, L. Dang, Z. Lin and T. B. Marder, *Angew. Chem. Int. Ed.*, 2009, **48**, 5350–5354.

52 W. K. Chow, O. Y. Yuen, P. Y. Choy, C. M. So, C. P. Lau, W. T. Wong and F. Y. Kwong, *RSC Adv.*, 2013, **3**, 12518–12539.

53 K. Kubota, H. Iwamoto and H. Ito, *Org. Biomol. Chem.*, 2017, **15**, 285–300.

54 S. K. Bose, L. Mao, L. Kuehn, U. Radius, J. Nekvinda, W. L. Santos, S. A. Westcott, P. G. Steel and T. B. Marder, *Chem. Rev.*, 2021, **121**, 13238–13341.

55 J. A. Labinger and J. E. Bercaw, *Nature*, 2002, **417**, 507–514.

56 K. Godula and D. Sames, *Science*, 2006, **312**, 67–72.

57 R. de Jesus, K. Hiesinger and M. van Gemmeren, *Angew. Chem. Int. Ed.*, 2023, e202306659.

58 I. A. I. Mkhalid, J. H. Barnard, T. B. Marder, J. M. Murphy and J. F. Hartwig, *Chem. Rev.*, 2010, **110**, 890–931.

59 J. S. Wright, P. J. H. Scott and P. G. Steel, *Angew. Chem. Int. Ed.*, 2021, **60**, 2796–2821.

60 P. Nguyen, H. P. Blom, S. A. Westcott, N. J. Taylor and T. B. Marder, *J. Am. Chem. Soc.*, 1993, **115**, 9329–9330.

61 K. M. Waltz, X. He, C. Muhoro and J. F. Hartwig, *J. Am. Chem. Soc.*, 1995, **117**, 11357–11358.

62 K. M. Waltz and J. F. Hartwig, *Science*, 1997, **277**, 211–213.

63 H. Chen and J. F. Hartwig, *Angew. Chem. Int. Ed.*, 1999, **38**, 3391–3393.

64 H. Chen, S. Schlecht, T. C. Semple and J. F. Hartwig, *Science*, 2000, **287**, 1995–1997.

65 J.-Y. Cho, C. N. Iverson and M. R. Smith III, *J. Am. Chem. Soc.*, 2000, **122**, 12868–12869.

66 J.-Y. Cho, M. K. Tse, D. Holmes, R. E. Maleczka and M. R. Smith, *Science*, 2002, **295**, 305–308.

67 T. Ishiyama, J. Takagi, K. Ishida, N. Miyaura, N. R. Anastasi and J. F. Hartwig, *J. Am. Chem. Soc.*, 2002, **124**, 390–391.

68 T. Ishiyama, J. Takagi, J. F. Hartwig and N. Miyaura, *Angew. Chem. Int. Ed.*, 2002, **41**, 3056–3058.

69 L.-C. Campeau, Q. Chen, D. Gauvreau, M. Girardin, K. Belyk, P. Maligres, G. Zhou, C. Gu, W. Zhang, L. Tan and P. D. O'Shea, *Org. Process Res. Dev.*, 2016, **20**, 1476–1481.

70 J. J. Douglas, B. W. V. Adams, H. Benson, K. Broberg, P. M. Gillespie, O. Hoult, A. K. Ibraheem, S. Janbon, G. Janin, C. D. Parsons, R. C. Sigerson and D. J. Klauber, *Org. Process Res. Dev.*, 2019, **23**, 62–68.

71 K. Arrington, G. A. Barcan, N. A. Calandra, G. A. Erickson, L. Li, L. Liu, M. G. Nilson, I. I. Strambeanu, K. F. VanGelder, J. L. Woodard, S. Xie, C. L. Allen, J. A. Kowalski and D. C. Leitch, *J. Org. Chem.*, 2019, **84**, 4680–4694.

72 L. Britton, J. H. Docherty, G. S. Nichol, A. P. Dominey and S. P. Thomas, *Chin. J. Chem.*, 2022, **40**, 2875–2881.

73 J. V. Obligacion, S. P. Semproni and P. J. Chirik, *J. Am. Chem. Soc.*, 2014, **136**, 4133–4136.

74 Y.-M. Tian, X.-N. Guo, Z. Wu, A. Friedrich, S. A. Westcott, H. Braunschweig, U. Radius and T. B. Marder, *J. Am. Chem. Soc.*, 2020, **142**, 13136–13144.

75 L. Xu, G. Wang, S. Zhang, H. Wang, L. Wang, L. Liu, J. Jiao and P. Li, *Tetrahedron*, 2017, **73**, 7123–7157.

76 T. Ishiyama and N. Miyaura, in *Boronic acids: preparation and applications in organic synthesis, medicine and materials*, ed. D. G. Hall, Wiley-VCH, Weinheim, 2nd edn., 2011.

77 J. Takagi, K. Sato, J. F. Hartwig, T. Ishiyama and N. Miyaura, *Tetrahedron Lett.*, 2002, **43**, 5649–5651.

78 M. A. Larsen and J. F. Hartwig, *J. Am. Chem. Soc.*, 2014, **136**, 4287–4299.

79 M. K. Tse, J.-Y. Cho and M. R. Smith III, *Org. Lett.*, 2001, **3**, 2831–2833.

80 V. A. Kallepalli, F. Shi, S. Paul, E. N. Onyeozili, R. E. Maleczka Jr. and M. R. Smith III, *J. Org. Chem.*, 2009, **74**, 9199–9201.

81 S. M. Preshlock, D. L. Plattner, P. E. Maligres, S. W. Krska, R. E. Maleczka Jr. and M. R. Smith III, *Angew. Chem. Int. Ed.*, 2013, **52**, 12915–12919.

82 R. P. Loach, O. S. Fenton, K. Amaike, D. S. Siegel, E. Ozkal and M. Movassaghi, *J. Org. Chem.*, 2014, **79**, 11254–11263.

83 F. Shen, S. Tyagarajan, D. Perera, S. W. Krska, P. E. Maligres, M. R. Smith III and R. E. Maleczka Jr., *Org. Lett.*, 2016, **18**, 1554–1557.

84 A. Ros, R. Fernández and J. M. Lassaletta, *Chem. Soc. Rev.*, 2014, **43**, 3229–3243.

85 T. M. Boller, J. M. Murphy, M. Hapke, T. Ishiyama, N. Miyaura and J. F. Hartwig, *J. Am. Chem. Soc.*, 2005, **127**, 14263–14278.

86 T. Ishiyama, H. Isou, T. Kikuchi and N. Miyaura, *Chem. Commun.*, 2010, **46**, 159–161.

87 A. Ros, B. Estepa, R. López-Rodríguez, E. Álvarez, R. Fernández and J. M. Lassaletta, *Angew. Chem. Int. Ed.*, 2011, **50**, 11724–11728.

88 R. López-Rodríguez, A. Ros, R. Fernández and J. M. Lassaletta, *J. Org. Chem.*, 2012, **77**, 9915–9920.

89 A. J. Roering, L. V. A. Hale, P. A. Squier, M. A. Ringgold, E. R. Wiederspan and T. B. Clark, *Org. Lett.*, 2012, **14**, 3558–3561.

90 T. A. Boebel and John. F. Hartwig, *J. Am. Chem. Soc.*, 2008, **130**, 7534–7535.

91 B. Su and J. F. Hartwig, *Angew. Chem. Int. Ed.*, 2018, **57**, 10163–10167.

92 D. W. Robbins, T. A. Boebel and J. F. Hartwig, *J. Am. Chem. Soc.*, 2010, **132**, 4068–4069.

93 J. Trouvé and R. Gramage-Doria, *Chem. Soc. Rev.*, 2021, **50**, 3565–3584.

94 P. C. Roosen, V. A. Kallepalli, B. Chattopadhyay, D. A. Singleton, R. E. Jr. Maleczka and M. R. I. Smith, *J. Am. Chem. Soc.*, 2012, **134**, 11350–11353.

95 M. R. Smith III, R. Bisht, C. Haldar, G. Pandey, J. E. Dannatt, B. Ghaffari, R. E. Maleczka Jr. and B. Chattopadhyay, *ACS Catal.*, 2018, **8**, 6216–6223.

96 H. L. Li, Y. Kuninobu and M. Kanai, *Angew. Chem. Int. Ed.*, 2017, **56**, 1495–1499.

97 B. Chattopadhyay, J. E. Dannatt, I. L. Andujar-De Sanctis, K. A. Gore, R. E. Jr. Maleczka, D. A. Singleton and M. R. I. Smith, *J. Am. Chem. Soc.*, 2017, **139**, 7864–7871.

98 S.-T. Bai, C. B. Bheeter and J. N. H. Reek, *Angew. Chem. Int. Ed.*, 2019, **58**, 13039–13043.

99 Y. Kuninobu, H. Ida, M. Nishi and M. Kanai, *Nature Chem*, 2015, **7**, 712–717.

100 H. J. Davis, M. T. Mihai and R. J. Phipps, *J. Am. Chem. Soc.*, 2016, **138**, 12759–12762.

101 M. E. Hoque, R. Bisht, C. Haldar and B. Chattopadhyay, *J. Am. Chem. Soc.*, 2017, **139**, 7745–7748.

102 H. J. Davis, G. R. Genov and R. J. Phipps, *Angew. Chem. Int. Ed.*, 2017, **56**, 13351–13355.

103 C. Haldar, M. Emdadul Hoque, R. Bisht and B. Chattopadhyay, *Tetrahedron Letters*, 2018, **59**, 1269–1277.

104 Y. Kuroda and Y. Nakao, *Chem. Lett.*, 2019, **48**, 1092–1100.

105 R. Bisht, C. Haldar, M. M. M. Hassan, M. E. Hoque, J. Chaturvedi and B. Chattopadhyay, *Chem. Soc. Rev.*, 2022, **51**, 5042–5100.

106 M. J. Ingleson, *Synlett*, 2012, **23**, 1411–1415.

107 D. T. Hurd, *J. Am. Chem. Soc.*, 1948, **70**, 2053–2055.

108 E. L. Muetterties, *J. Am. Chem. Soc.*, 1959, **81**, 2597–2597.

109 E. L. Muetterties, *J. Am. Chem. Soc.*, 1960, **82**, 4163–4166.

110 E. L. Muetterties and F. N. Tebbe, *Inorg. Chem.*, 1968, **7**, 2663–2664.

111 G. A. Olah, *Angew. Chem. Int. Ed.*, 1993, **32**, 767–788.

112 M. J. Ingleson, in *Synthesis and Application of Organoboron Compounds*, eds. E. Fernández and A. Whiting, Springer, Heidelberg, 2015.

113 P. Köelle and H. Nöth, *Chem. Rev.*, 1985, **85**, 399–418.

114 T. S. De Vries, A. Prokofjevs and E. Vedejs, *Chem. Rev.*, 2012, **112**, 4246–4282.

115 W. E. Piers, S. C. Bourke and K. D. Conroy, *Angew. Chem. Int. Ed.*, 2005, **44**, 5016–5036.

116 A. Del Grosso, P. J. Singleton, C. A. Muryn and M. J. Ingleson, *Angew. Chem. Int. Ed.*, 2011, **50**, 2102–2106.

117 E. Vedejs, T. Nguyen, D. R. Powell and M. R. Schrimpf, *Chem. Commun.*, 1996, 2721–2722.

118 G. E. Ryschkewitsch and J. W. Wiggins, *J. Am. Chem. Soc.*, 1970, **92**, 1790–1791.

119 C. K. Narula and H. Nöth, *Inorg. Chem.*, 1985, **24**, 2532–2539.

120 A. Prokofjevs, J. W. Kampf, A. Solovyev, D. P. Curran and E. Vedejs, *J. Am. Chem. Soc.*, 2013, **135**, 15686–15689.

121 A. Solovyev, Q. Chu, S. J. Geib, L. Fensterbank, M. Malacria, E. Lacôte and D. P. Curran, *J. Am. Chem. Soc.*, 2010, **132**, 15072–15080.

122 A. Prokofjevs, A. Boussonnière, L. Li, H. Bonin, E. Lacôte, D. P. Curran and E. Vedejs, *J. Am. Chem. Soc.*, 2012, **134**, 12281–12288.

123 T. S. De Vries, A. Prokofjevs, J. N. Harvey and E. Vedejs, *J. Am. Chem. Soc.*, 2009, **131**, 14679–14687.

124 S. Rej and N. Chatani, *Angew. Chem. Int. Ed.*, 2022, **61**, e202209539.

125 S. A. Iqbal, J. Pahl, K. Yuan and M. J. Ingleson, *Chem. Soc. Rev.*, 2020, **49**, 4564–4591.

126 A. Prokofjevs, J. W. Kampf and E. Vedejs, *Angew. Chem. Int. Ed.*, 2011, **50**, 2098–2101.

127 S. A. Solomon, A. Del Grosso, E. R. Clark, V. Bagutski, J. J. W. McDouall and M. J. Ingleson, *Organometallics*, 2012, **31**, 1908–1916.

128 A. D. Grosso, M. D. Helm, S. A. Solomon, D. Caras-Quintero and M. J. Ingleson, *Chem. Commun.*, 2011, **47**, 12459–12461.

129 V. Bagutski, A. Del Grosso, J. A. Carrillo, I. A. Cade, M. D. Helm, J. R. Lawson, P. J. Singleton, S. A. Solomon, T. Marcelli and M. J. Ingleson, *J. Am. Chem. Soc.*, 2013, **135**, 474–487.

130 A. D. Grosso, J. A. Carrillo and M. J. Ingleson, *Chem. Commun.*, 2015, **51**, 2878–2881.

131 S. Tanaka, Y. Saito, T. Yamamoto and T. Hattori, *Org. Lett.*, 2018, **20**, 1828–1831.

132 X. Tan and H. Wang, *Chem. Soc. Rev.*, 2022, **51**, 2583–2600.

133 Q. Yin, H. F. T. Klare and M. Oestreich, *Angew. Chem. Int. Ed.*, 2017, **56**, 3712–3717.

134 M.-A. Légaré, M.-A. Courtemanche, É. Rochette and F.-G. Fontaine, *Science*, 2015, **349**, 513–516.

135 É. Rochette, V. Desrosiers, Y. Soltani and F.-G. Fontaine, *J. Am. Chem. Soc.*, 2019, **141**, 12305–12311.

136 M. J. S. Dewar, V. P. Kubba and R. Pettit, *J. Chem. Soc.*, 1958, 3073–3076.

137 M. J. S. Dewar and W. H. Poesche, *J. Org. Chem.*, 1964, **29**, 1757–1762.

138 Q. J. Zhou, K. Worm and R. E. Dolle, *J. Org. Chem.*, 2004, **69**, 5147–5149.

139 M. J. S. Dewar and R. Dietz, *Tetrahedron Lett.*, 1959, **1**, 21–23.

140 F. A. Davis and M. J. S. Dewar, *J. Am. Chem. Soc.*, 1968, **90**, 3511–3515.

141 N. Ishida, T. Moriya, T. Goya and M. Murakami, *J. Org. Chem.*, 2010, **75**, 8709–8712.

142 M. Yusuf, K. Liu, F. Guo, R. A. Lalancette and F. Jäkle, *Dalton Trans.*, 2016, **45**, 4580–4587.

143 A. C. Shaikh, D. S. Ranade, S. Thorat, A. Maity, P. P. Kulkarni, R. G. Gonnade, P. Munshi and N. T. Patil, *Chem. Commun.*, 2015, **51**, 16115–16118.

144 S. A. Iqbal, K. Yuan, J. Cid, J. Pahl and M. J. Ingleson, *Org. Biomol. Chem.*, 2021, **19**, 2949–2958.

145 L. Niu, H. Yang, R. Wang and H. Fu, *Org. Lett.*, 2012, **14**, 2618–2621.

146 S. Rej, A. Das and N. Chatani, *Chem. Sci.*, 2021, **12**, 11447–11454.

147 C. Cazorla, T. S. De Vries and E. Vedejs, *Org. Lett.*, 2013, **15**, 984–987.

148 S. A. Iqbal, J. Cid, R. J. Procter, M. Uzelac, K. Yuan and M. J. Ingleson, *Angew. Chem. Int. Ed.*, 2019, **58**, 15381–15385.

149 J. Lv, X. Chen, X.-S. Xue, B. Zhao, Y. Liang, M. Wang, L. Jin, Y. Yuan, Y. Han, Y. Zhao, Y. Lu, J. Zhao, W.-Y. Sun, Kendall. N. Houk and Z. Shi, *Nature*, 2019, **575**, 336–340.

150 F. Zhang and D. R. Spring, *Chem. Soc. Rev.*, 2014, **43**, 6906–6919.

151 G. Rani, V. Luxami and K. Paul, *Chem. Commun.*, 2020, **56**, 12479–12521.

152 S. Rej and N. Chatani, *J. Am. Chem. Soc.*, 2021, **143**, 2920–2929.

Chapter 2

Attempted Synthesis of Benzoxaboroles via O-Directed Electrophilic Borylation

Chapter 2: Attempted Synthesis of Benzoxaboroles via O-Directed Electrophilic Borylation

2.1 Introduction

In recent years, there has been increasing attention into the therapeutic potential of numerous boron-containing compounds.[1–4] In particular, benzoxaboroles (5-membered cyclic aryl boronic esters, **Figure 2.1**) have been recognised as an important class of compounds in medicinal chemistry, showing various biological activities including anti-fungal, anti-viral, anti-bacterial, and anti-inflammatory properties.[5,6] In addition, benzoxaboroles possess desirable physiochemical properties for pharmaceutical applications, including improved solubility and resistance to hydrolysis at physiological pH (compared to their acyclic aryl boronic acid counterparts) along with low biotoxicity.[7,8] At the time of writing, two benzoxaborole-based pharmaceuticals have been fully approved by the U.S. Food and Drug Administration (FDA): Tavaborole, a topical anti-fungal treatment against onychomycosis,[9,10] and Crisaborole, an anti-inflammatory medication for treatment of atopic dermatitis (**Figure 2.1**).[11] Several benzoxaborole derivatives are also candidates in ongoing clinical studies,[12] including GSK8175 (an inhibitor of hepatitis C virus),[13] and GSK656 (a treatment for pulmonary tuberculosis).[14] Benzoxaboroles have wider applications in several other areas, including molecular recognition and supramolecular chemistry.[8]

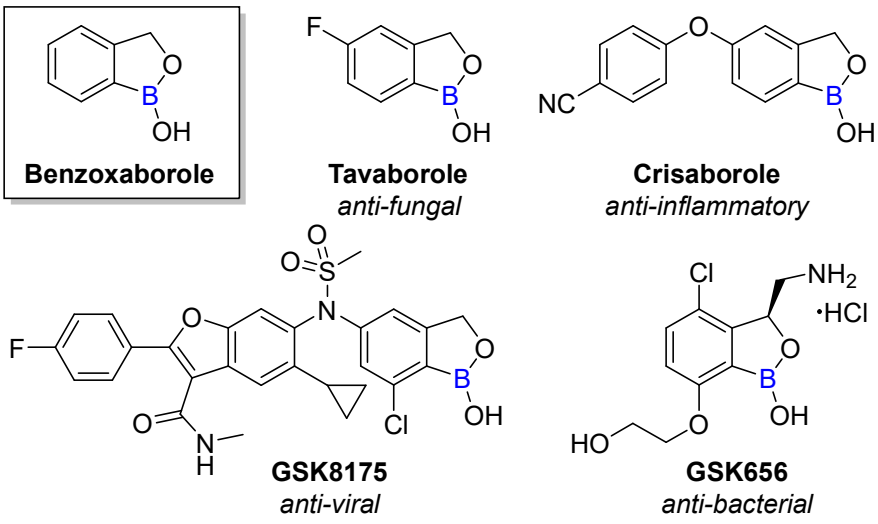

Figure 2.1: Select benzoxaborole-containing pharmaceutical compounds.

Benzoxaboroles are commonly prepared from the corresponding *ortho*-halide benzyl alcohols, where the boronic acid group is installed via an initial C-X borylation step, followed by intramolecular esterification to generate the 5-membered oxaborole ring.[15] One method used to install the boronic acid group is the metalation of *ortho*-halo benzyl alcohol derivatives using an alkyl lithium, followed by trapping of the organometallic intermediate with a borate electrophile (**Scheme 2.1**).[16] Whilst this method can tolerate hydroxy groups, two equivalents of the alkyl lithium are then required.[17] Therefore, the hydroxy group is often protected with an acid-labile group (e.g. tetrahydropyranyl (THP) or methoxymethyl (MOM) groups) during C-X borylation, with both alcohol deprotection and subsequent benzoxaborole formation occurring upon acidic work-up.[18] This protocol was utilised in the early development of Crisaborole.[11]

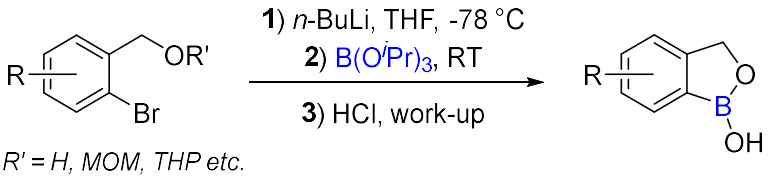

Scheme 2.1: Synthesis of benzoxaboroles via the lithiation and borate trapping of *ortho*-bromide benzyl alcohol derivatives.

Alternatively, the boronic acid group can be installed via a palladium-catalysed Miyaura borylation of the *ortho*-halide benzyl alcohol derivatives using B_2pin_2 and a weak base (**Scheme 2.2a**).[19] This process avoids the production of stoichiometric metal waste, and benefits from more mild conditions and improved tolerance of functional groups on the aryl halide substrate (compared to the lithiation/borylation route). Thus this approach is often used in the synthesis of highly functionalised benzoxaboroles for screening of potential biological activity.[13,20] Furthermore, this process is amenable to the C-X borylation of *ortho*-halide benzaldehydes, generating *ortho*-Bpin benzaldehyde derivatives. Subsequent carbonyl reduction and intramolecular esterification then generates benzoxaboroles.[21–23] Whilst these methods are effective and have been applied to the synthesis of highly functionalised benzoxaboroles, they use stoichiometric or catalytic quantities of potentially hazardous and/or expensive metal reagents. To this end, photo-induced C-X borylation methodologies have

also been applied to the synthesis of benzoxaboroles, providing a metal free alternative, though the scope of this is less established (**Scheme 2.2b**).[24,25]

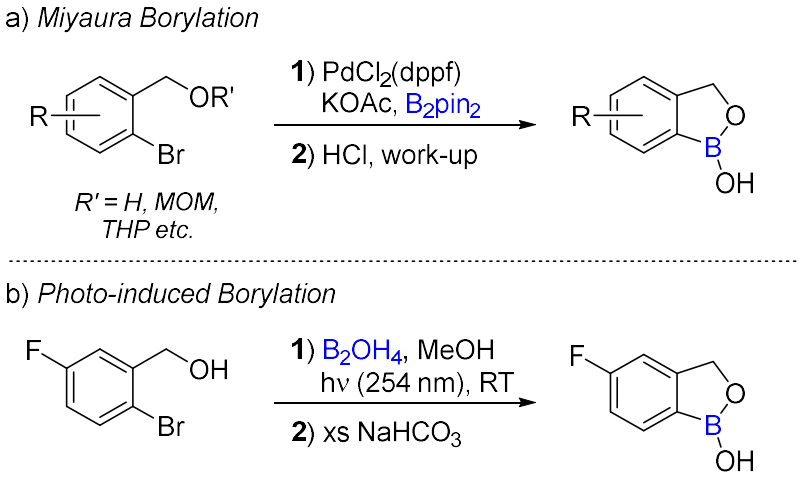

Scheme 2.2: Synthesis of benzoxaboroles via **a)** the palladium-catalysed Miyaura borylation of *ortho*-bromide benzyl alcohol derivatives and **b)** photo-induced C-X borylation.

However, these methodologies all require pre-functionalised, *ortho*-halide substituted starting materials, reducing the overall atom-economy of the process. A simpler, more efficient route to benzoxaboroles would see the transformation of the unactivated *ortho* C-H bond of a benzyl alcohol derivative into a C-B bond. Intramolecular esterification would then generate the benzoxaborole. The C-H borylation of (hetero)arenes has been achieved through transition metal catalysis (typically iridium) or using boron electrophiles (via a Friedel Crafts-type mechanism). For transition metal catalysed processes, the regioselectivity of C-H borylation is generally dominated by steric effects,[26,27] whilst the regioselectivity of electrophilic C-H borylation is controlled by both steric and electronic factors *(this is discussed in more detail in **Chapter 1**).*[28] This sensitivity to steric effects means these approaches generally do not result in C-H borylation at positions *ortho*- to other substituents (as would be required for benzoxaborole formation). Instead, directing groups on the substrate are necessary to enable *ortho* C-H borylation.[29,30]

These approaches could potentially be applied to the synthesis of benzoxaboroles if the benzyl alcohol '-OH' moiety could be utilised as an oxygen-based directing

group. Whilst oxygen-based directing groups previously have been utilised in *ortho*-selective iridium-catalysed C-H borylation processes,[29] at the time of writing there had been no reported examples of the use of '-OH' directing groups for this approach. By comparison, the use of chelating carbonyl moieties as directing groups is more prevalent.[31–33]

Directed electrophilic C-H borylation can also be used to generate *ortho*-substituted aryl boronic esters, with the additional benefit of avoiding expensive transition metal catalysts.[30] These reactions proceed via an initial E-B bond forming step between the boron electrophile and the directing moiety (where E is typically = N(H)R), followed by intramolecular C-H borylation. The use of oxygen-based directing groups, proceeding via initial O-B bond formation, is much less established. In notable early work, Dewar and co-workers reported the '-OH' directed C-H borylation of 2-OH biphenyl with BCl_3 and catalytic $AlCl_3$ to generate a 6-membered boracycle upon heating to 60 °C (**Scheme 2.3**).[34] By comparison, the 2-NH_2 biphenyl derivative required heating to 80 °C to enable C-H borylation.[35] This difference in reaction conditions correlates with the π-donating ability of the heteroatom (N vs. O). With 2-OH biphenyl, the weaker π-donating ability of oxygen increases the electrophilicity of intermediate **2.I**, enabling C-H borylation to proceed at lower temperature.

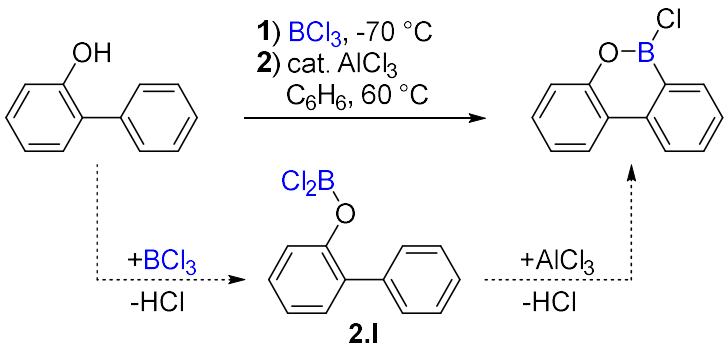

Scheme 2.3: Oxygen-directed electrophilic C-H borylation of 2-OH biphenyl.

Whilst reports of 'OH' as a directing group for electrophilic C-H borylation have been very limited, a 2017 patent described the oxygen-directed C-H borylation of 3-fluorobenzyl alcohol with BCl_3 as a method to generate the commercialised pharmaceutical Tavaborole (**Scheme 2.4**).[36] The experimental details in this

patent report were limited, but it described the addition of BCl_3 to the benzyl alcohol at low temperatures, with C-H borylation proceeding upon refluxing the mixture. Aqueous work-up then reportedly generated Tavaborole in a 35% isolated yield, with reported analytical data matching the literature.

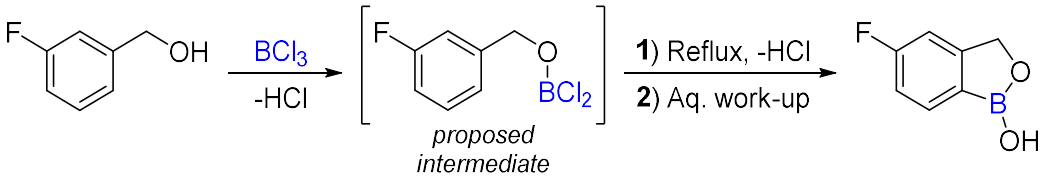

Scheme 2.4: Reported route to Tavaborole via the oxygen-directed electrophilic C-H borylation of 3-fluorobenzyl alcohol.

This approach is similar in concept to work by Nagy and co-workers,[37] where benzazaborole derivatives (**2.III**, **Scheme 2.5a**) were prepared by the addition of $PhBCl_2$ to *N*-methyl benzylamines, generating N-borylated intermediate **2.II**. Subsequent room-temperature activation by Al_2Cl_6 increased the electrophilicity of **2.II**, enabling intramolecular arene C-H borylation at the *ortho* C-H position.

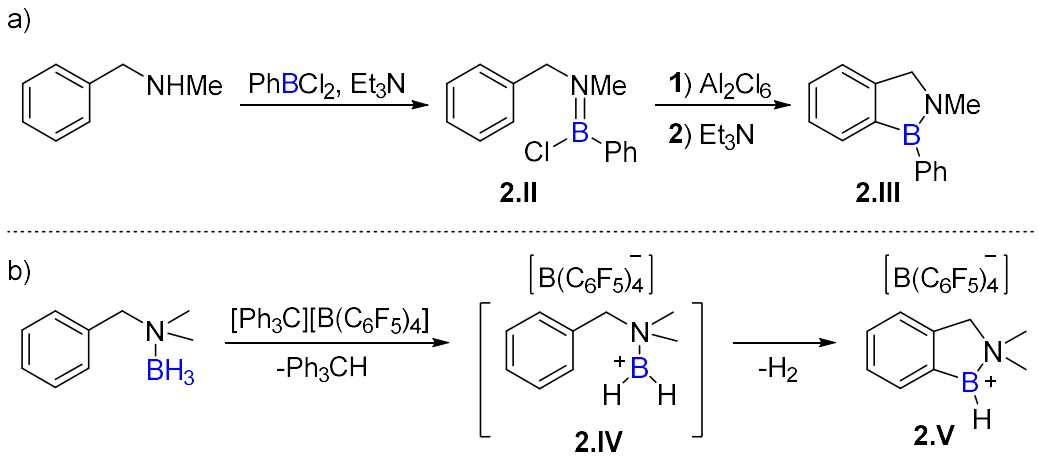

Scheme 2.5: Examples of N-directed electrophilic C-H borylation of benzylamine derivatives by **a)** Nagy and co-workers and **b)** Vedejs and co-workers.

In another related example, the Vedejs group reported the N-directed electrophilic C-H borylation of a benzylamine-borane adduct, where the abstraction of a hydride generated a borenium ion equivalent (**2.IV**, **Scheme 2.5b**).[38] This highly electrophilic intermediate enabled intramolecular C-H

borylation, generating a 5-membered benzazaborole ring (**2.V**). Note, the arene C-H borylation step proceeds via a four-membered transition state, evolving H_2.

Going back to the oxygen-directed C-H borylation process discussed in the patent, it is interesting that the reaction reportedly proceeds without the need for an activator (e.g. $AlCl_3$, as in Dewar's work with 2-OH biphenyl,[34] and the example by Nagy and co-workers).[37] This would suggest that a sufficiently electrophilic boron intermediate is formed following coordination of BCl_3 to the benzyl alcohol. Therefore, confirming the results of the patent could enable further extensions to the scope of oxygen-directed electrophilic C-H borylation processes, and this is the focus of this chapter.

It should be noted that after the commencement of the work discussed herein, Rej and Chatani reported a transient imine directing group for the *ortho* C-H borylation of benzaldehydes using BBr_3 and an exogenous base (**Scheme 2.6**).[39] In the initial reaction using benzaldehyde, coordination of BBr_3 to oxygen was observed, but no intramolecular C-H borylation then occurred. Conversion of the aldehyde into a more electron-donating imine (**2.VI**) increased the accessibility of the respective borenium cation, hence upon addition of BBr_3 *ortho* C-H borylation was achieved (to form **2.VII**). The -BBr_2 unit could be converted into Bpin within the same pot, and the carbonyl moiety then regenerated upon work-up to yield 2-Bpin benzaldehydes in a one-pot process. The authors subsequently demonstrated several transformations of the 2-Bpin benzaldehyde products, including the generation of substituted benzoxaboroles via addition of a Grignard reagent. Therefore, this process represents a transition metal free route to medicinally relevant benzoxaboroles under relatively mild conditions.

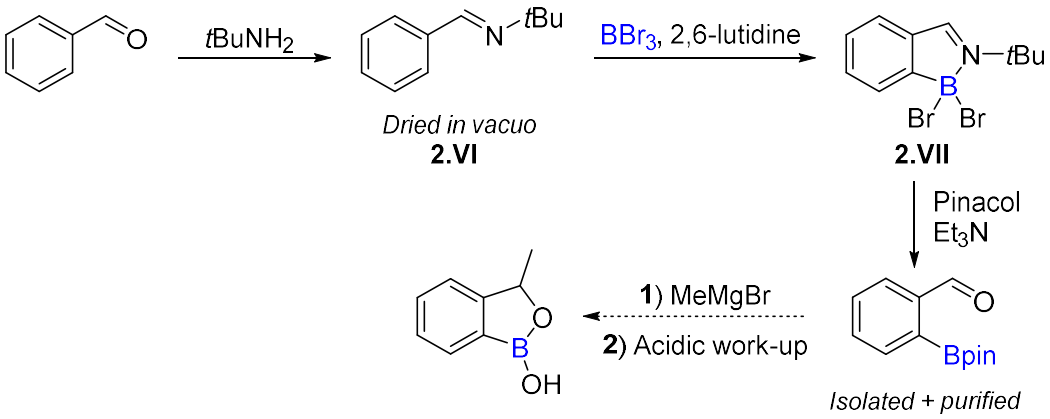

Scheme 2.6: One-pot electrophilic C-H borylation of benzaldehyde via *in situ* formation of a transient imine directing group, with the subsequent transformation into a benzoxaborole derivative.

2.2 Project Aims

Considering the wide scope of applications for benzoxaboroles, the development of efficient synthetic methods to prepare these organoboranes is of considerable interest. The electrophilic *ortho* C-H borylation of benzyl alcohols, directed by the hydroxy group, could provide an alternative to the use of expensive and/or potentially hazardous metal reagents. However, hydroxy groups have not yet been widely applied as directing groups in electrophilic C-H borylation processes.

Therefore, the work described in this chapter investigated the feasibility of hydroxy-directed electrophilic C-H borylation of benzyl alcohols, initially as described in a recent patent.[36] The patent report provided little experimental information or mechanistic investigation; hence the initial goal of this project was to replicate the synthesis of Tavaborole via this method. It was hoped that, if successful, this method could then be applied to the synthesis of other benzoxaboroles.

2.3 Results and Discussion

To investigate the validity of the patented process, the reaction of 3-fluorobenzyl alcohol with BCl_3 was first evaluated to see if C-H borylation could be achieved, and if the hydroxy group was able to act as an *ortho* directing group.

2.3.1 Reactivity with Haloboranes *(Replicating Patented Work)*

For the electrophilic C-H borylation of 3-fluorobenzyl alcohol to proceed, it is important that the Brønsted acidic by-product from O/C-H borylation, HCl, is efficiently removed from the reaction to prevent potential issues such as protodeboronation of the borylated products.[28] In previous examples of electrophilic C-H borylation this has been achieved by running the reaction in an open system, or by the addition of an exogenous base to sequester the acidic by-product. Therefore, in the initial reaction of 3-fluorobenzyl alcohol with BCl_3, the reaction was heated to reflux under a dynamic flow of nitrogen (**Scheme 2.7**).

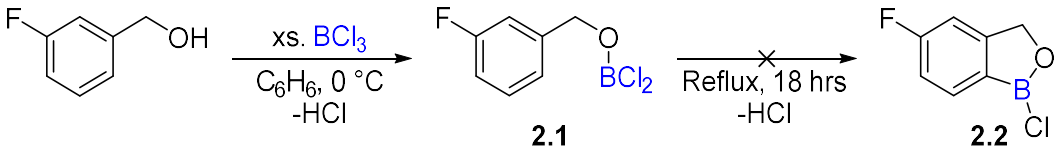

Scheme 2.7: Initial conditions used for the attempted oxygen-directed C-H borylation of 3-fluorobenzyl alcohol with BCl_3.

The low-temperature addition of BCl_3 to 3-fluorobenzyl alcohol led to the complete consumption of the starting alcohol and the formation of several new benzyl species (**Figure 2.2a**), whilst the ^{11}B NMR spectrum showed a new resonance at 31 ppm. This is consistent with a [RO-BCl_2] species,[40] therefore the major benzyl species (δ_{1H} = 4.57 ppm) was assumed to be the O-borylated benzyl intermediate **2.1**. Upon heating, the $^{1}H/^{11}B$ resonances assigned to **2.1** were consumed, with two benzyl species now observed in the ^{1}H NMR spectrum (**Figure 2.2b**). The ^{11}B NMR spectrum showed several new broad resonances between 19-16 ppm, consistent with multiple $B(OR)_3$ species,[41] rather than the expected product from arene C-H borylation (**2.2**).

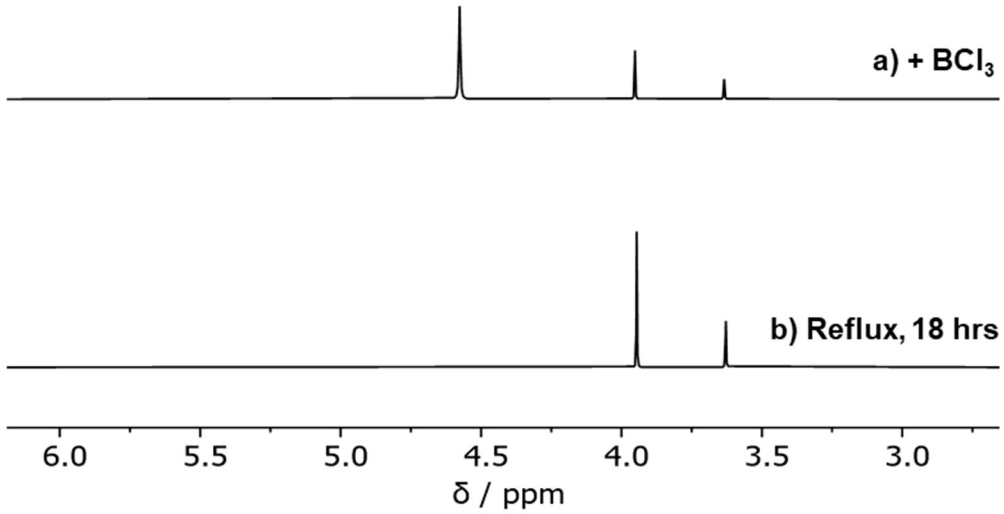

Figure 2.2: Stacked ^{1}H NMR spectra of 3-fluorobenzyl alcohol following **a)** addition of BCl_3, and **b)** after 18 hours at reflux.
(Solvent = C_6D_6, NMR temperature = 300 K).

To determine whether arene C-H borylation had proceeded, the reaction was quenched and concentrated *in vacuo*. The two benzyl products were isolated and purified by column chromatography but could not be separated. NMR spectroscopy revealed that these benzyl products were not borylated, with no ^{11}B resonances observed post-chromatography. The major benzyl product was identified as 3-fluorobenzyl chloride,[42] indicating cleavage of the benzyl-oxygen bond during the reaction. This could proceed via the nucleophilic substitution of the O-borylated intermediate **2.1** (or a derivative thereof) by Cl^-, with a potential leaving group being a π-stabilised oxoborane anion (**Scheme 2.8**). Oxoborane anions have been previously reported, thus the $[Cl_2BO]^-$ anion is a feasible short-lived leaving group.[43,44] The minor product was identified as 1-benzyl-3-fluorobenzene,[45] presumably formed via nucleophilic substitution of **2.1** (or a derivative thereof) by the solvent.

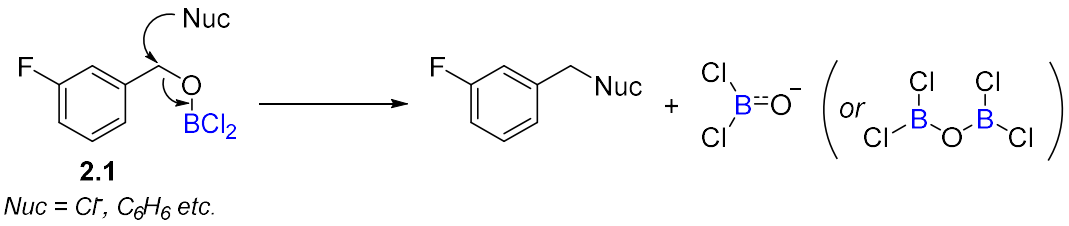

Scheme 2.8: Nucleophilic substitution of the O-borylated benzyl intermediate would generate the observed benzyl side-products.

This indicates that **2.1** (or a derivative thereof) is highly vulnerable to benzyl cleavage via nucleophilic substitution under these conditions, and this reaction outcompetes arene C-H borylation. Benzyl cleavage was also reported as a minor side reaction by DeVries during the development of the N-directed electrophilic C-H borylation of benzylamines (*vide supra*, see **Scheme 2.5**).[38,46] The N-borylated intermediate was believed to undergo nucleophilic substitution with Ph_3CH (the by-product from borane activation), cleaving the benzyl-nitrogen bond and generating Ph-CH_2-Ph (**Scheme 2.9**). This side reaction was prevented by limiting the activator stoichiometry and shortening the reaction time.

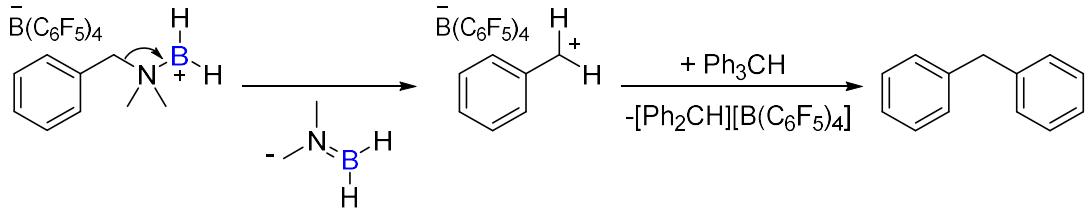

Scheme 2.9: Reported nucleophilic substitution reaction of a N-borylated benzylamine, forming Ph-CH_2-Ph, as described by DeVries.

For the reaction of benzyl alcohols, it was hypothesised that HCl was not being effectively removed from the solution and could be catalysing benzyl chloride formation (e.g. by protonation of **2.1**). Thus, by finding conditions to remove HCl from the reaction more efficiently, nucleophilic substitution of an O-borylated intermediate (such as **2.1**) by Cl^- could be prevented. To this end, the reaction of 3-fluorobenzyl alcohol and BCl_3 was repeated in the presence of 2 equiv. of a non-coordinating base, 2,6-(*t*Bu)$_2$-4-methyl pyridine (DBP), to sequester HCl. However, whilst the partial protonation of DBP was observed during the reaction, it was not sufficient to prevent the formation of the benzyl

chloride side product upon heating, indicating some source of Cl^- was still present in solution along with a sufficiently reactive benzyl electrophile.

Further modification of reaction conditions, including reducing the excess of BCl_3 added and increasing the time stirring at room temperature before heating, were also ineffective at preventing conversion to 3-fluorobenzyl chloride upon heating, and no evidence of arene C-H borylation was observed. The addition of $AlCl_3$ to the reaction was also explored, in the hope that this would increase the electrophilicity of the O-borylated intermediate **2.1** (by coordinating to oxygen/chlorine) and therefore enable arene C-H borylation. However, this too was unsuccessful and led to no change in reaction outcome. Finally, the reaction of 3-fluorobenzyl alcohol with BBr_3 was also tested to see if the increased electrophilicity of the benzyl-O-BBr_2 intermediate would favour intramolecular C-H borylation (over the intermolecular reaction to form the benzyl bromide). However, conversion to 3-fluorobenzyl bromide was observed at room temperature.[47] Again, there was no indication that arene C-H borylation had occurred. Therefore, replication of the patented borylation reaction of 3-fluorobenzyl alcohol with BCl_3 was unsuccessful, and arene C-H borylation to generate the benzoxaborole derivative **2.2** could not be achieved via this route.

The reactivity of the corresponding benzaldehyde was also evaluated, to see if the required O-borylated intermediate (**2.1**) could be generated via hydroboration of the aldehyde with $HBCl_2$, therefore avoiding the production of HCl that may induce nucleophilic substitution and lead to 3-fluorobenzyl chloride. It was hoped that this would enable **2.1** to then undergo arene C-H borylation (**Scheme 2.10**). The reaction of 3-fluorobenzaldehyde with $HBCl_2$ in the presence of DBP did result in aldehyde hydroboration (indicated by the absence of the C(H)=O resonance in the ^1H NMR spectrum) but a complex mixture of O-borylated benzyl intermediates (of the type $[(RO)_nB(Cl)_{3-n}]$) were generated. Upon heating, these intermediates converged to form 3-fluorobenzyl chloride as the only product. The same result was obtained when the reaction was left at room temperature, with complete conversion to 3-fluorobenzyl chloride after 5 days.

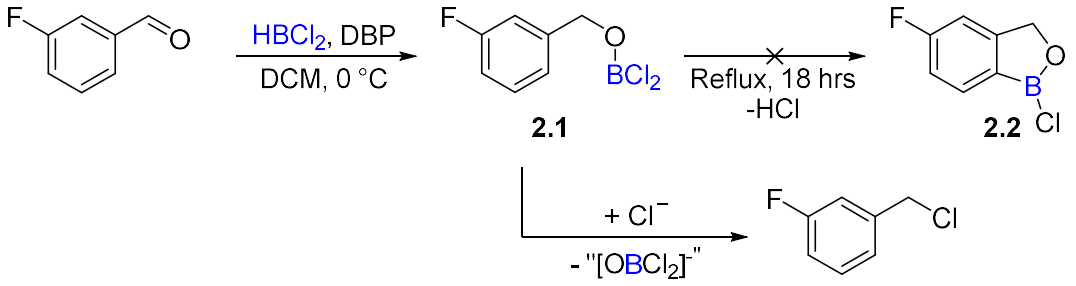

Scheme 2.10: Attempted hydroboration/C-H borylation of 3-fluorobenzyl alcohol with $HBCl_2$, leading to 3-fluorobenzyl chloride and no evidence of arene C-H borylation.

The reactions thus far with 3-fluorobenzyl alcohol / benzaldehyde indicate that the O-borylated arene intermediate **2.1** (or a derivative thereof) is highly susceptible to nucleophilic attack, with the benzyl-oxygen bond cleaved during substitution reactions. The proposed oxoborane leaving group is stabilised by π-donation by oxygen into the boron p_z orbital, thus facilitating the substitution process. If this is correct, possible ways to disfavour the nucleophilic substitution of the O-borylated intermediate could be to (a) avoid the presence of any halides; (b) use a Lewis base stabilised 4-coordinate boron electrophile that can undergo O-H borylation (e.g. **2.3**, **Scheme 2.11**). The corresponding O-borylated intermediate **2.4** would therefore feature a 4-coordinate boron unit, which could subsequently react in an S_N2-type process at boron to yield the desired C-H borylated product **2.5**. Nucleophilic attack of the benzyl CH_2 unit of **2.4** would hopefully be disfavoured due to the absence of any good nucleophiles and no π-stabilisation (B=O formation) in the anionic oxoborane leaving group.

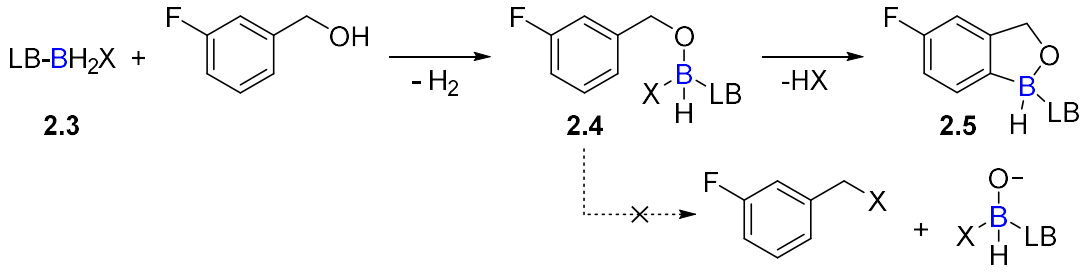

Scheme 2.11: Proposed reaction of 3-fluorobenzyl alcohol with a 4-coordinate boron electrophile, enabling C-H borylation without competitive nucleophilic substitution *(LB = Lewis Base).*

The Lewis base used needs to strongly coordinate to boron so to not be displaced during the initial O-B bond forming step, but should still be removable after C-H borylation. The addition of *N*-heterocyclic carbenes (NHCs) to boranes has been previously demonstrated to generate very robust Lewis acid-base adducts.[48] NHC-BH_3 complexes are readily synthesised, are typically bench stable and can be purified via column chromatography,[49] but can react as synthetic equivalents of borenium ions when activated with strong acids, halogens, or hydride abstracting agents.[50] This results in the substitution of a hydride for a weakly coordinating anion that is readily displaced by stronger incoming nucleophiles (e.g. an aryl π-system).

The activation of NHC-BH_3 complexes with *bis*-(trifluoromethane sulfonyl) amine ($HNTf_2$) has been shown to produce highly electrophilic NHC-BH_2NTf_2 intermediates capable of reacting with a range of π-nucleophiles.[51] The NHC-borylated products can then be readily transformed at the end of the reaction.[52,53] Therefore, NHC-BH_2NTf_2 complexes could be suitable electrophiles to enable the desired oxygen-directed C-H borylation of benzyl alcohols. The use of the weakly coordinating $[NTf_2]^-$ anion should also avoid any potential nucleophilic substitution of the benzyl CH_2 (with benzyl-NTf_2 formation being disfavoured relative to benzyl halides) Therefore, the subsequent goal of this project was to explore the reactivity of 3-fluorobenzyl alcohol with NHC-BH_2NTf_2, to see if this system could be used to generate Tavaborole (or its derivatives).

2.3.2 Reactivity with NHC-Boranes

Initial Studies with $IMeBH_3$

Reactivity was first explored with the 'simplest' NHC-borane, 1,3-dimethyl imidazol-2-ylidene borane, $IMeBH_3$ (**2.6**, **Scheme 2.12**). This species reacted rapidly with $HNTf_2$ at room temperature, resulting in H_2 evolution and the complete conversion to $IMeBH_2NTf_2$ (**2.7**), as previously reported.[51]

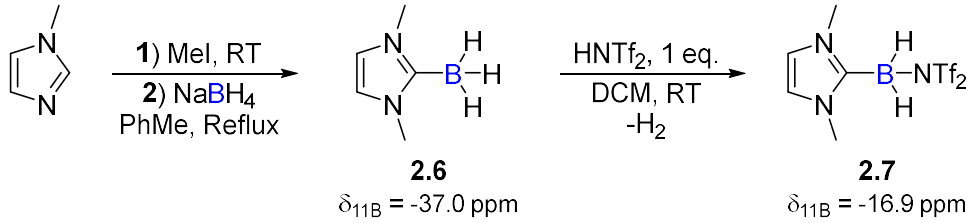

Scheme 2.12: Synthesis of $IMeBH_3$, followed by activation with $HNTf_2$ to generate $IMeBH_2NTf_2$.

The 1:1 addition of 3-fluorobenzyl alcohol to **2.7** in DCM resulted in further H_2 evolution. The *in situ* ^1H NMR spectrum showed the full conversion of 3-fluorobenzyl alcohol, along with the formation of two new benzyl species and two new sets of 'IMe' resonances. The major benzyl CH_2 resonance was in a relative 4:6 ratio to the corresponding IMe 'CH_3' resonance, whilst the minor benzyl species showed a relative 2:6 ratio. This indicated the major product contained two benzoxy units per NHC, whilst the minor product contained one benzoxy unit per NHC. Furthermore, ^1H-^{13}C HSQC / HMBC NMR spectra also revealed that in each product, the benzoxy units contained intact –(C_6H_4F) ring(s), with no evidence of C-H borylation on the arene.

Further information was provided by the ^{11}B NMR spectrum (**Figure 2.3**). This showed only partial consumption of $IMeBH_2NTf_2$, indicating this was not reacting with 3-fluorobenzyl alcohol in the desired 1:1 ratio. Two new ^{11}B resonances were also observed – the major resonance at 22.4 ppm showed no B-H coupling, whilst the minor resonance at 36.5 ppm did show B-H coupling (based on the difference in peak width at half height (pwhh) in the ^{11}B and $^{11}B\{^1H\}$ NMR spectra, though the resonance was too broad to distinguish the coupling constant/multiplicity). After 18 hours at room, the minor product disappeared

from the NMR spectra, with no significant new species formed (suggesting this product may have degraded over time).

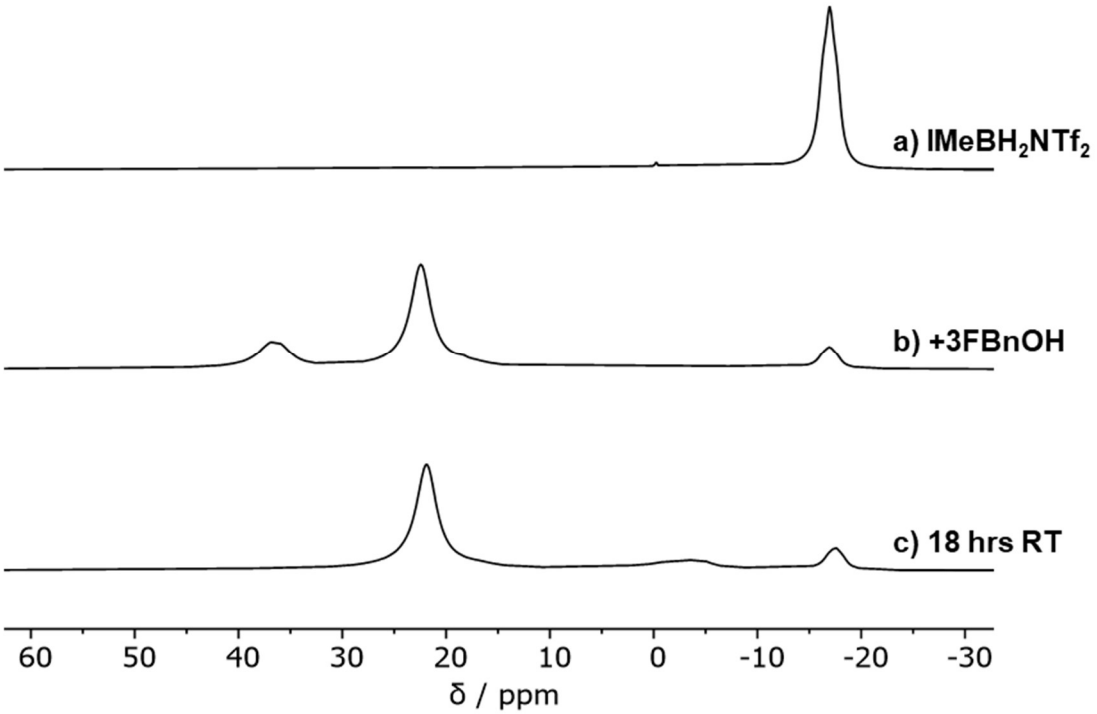

Figure 2.3: Stacked *in situ* ^{11}B NMR spectra for the reaction of $IMeBH_2NTf_2$ with 3-fluorobenzyl alcohol at room temperature.
(Solvent = CH_2Cl_2, NMR temperature = 300 K).

Based on this combined data, it was hypothesised that the major benzyl product (δ_{11B} = 24.4 ppm) was a 3-coordinate NHC-borenium ion containing two benzoxy substituents at boron (**2.8**, **Figure 2.4**). The ^{11}B resonance of this product is close to the reported resonances of structurally similar amine-BCat borenium ions (δ_{11B} = 25-28 ppm), further supporting this assignment.[54]

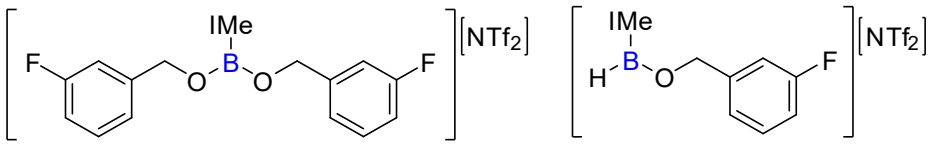

Figure 2.4: Assumed structures of the two benzyl products observed in the reaction of $IMeBH_2NTf_2$ and 3-fluorobenzyl alcohol.

For the minor benzyl product (δ_{11B} = 36.5 ppm), this is assumed to also be a 3-coordinate borenium ion, with one hydride and one benzoxy substituent (**2.9**). Examples of B-H containing NHC-borenium ions are limited, though Erker and co-workers reported the generation of highly electrophilic [NHC-BH(C_6F_5)]$^+$ borenium ions, where δ_{11B} ca. 52 ppm.[55] The significantly more upfield ^{11}B resonance of **2.9** could be the result of π-donation by oxygen into the vacant p_z orbital, reducing boron's Lewis acidity. However, this borenium ion is stabilised to a lesser extent than the di-benzoxy borenium ion **2.8**, which may explain why this species was not stable in solution. Further support for the assignment of **2.9** came from calculating its predicted ^{11}B NMR chemical shift, which indicated a δ_{11B} = 35.5 ppm, close to the observed resonance. Calculations were performed by Dr Kang Yuan at the ωB97XD/aug-cc-pvDZ // PCM (CH_3Cl) level of theory. Calculations at this level on well-defined borenium cations gave good matches between calculated and reported δ_{11B}.

The ratio of benzyl addition products formed was shown to be dependent on the stoichiometry of 3-fluorobenzyl alcohol. The reaction with 1 equiv. of the benzyl alcohol resulted in a mixture of the single addition product (**2.9**) and the double addition product (**2.8**), suggesting that the second addition of benzyl alcohol to **2.9** is faster than the first addition, hence IMeBH_2NTf_2 is not fully consumed. Reducing the addition temperature and/or slow addition of the benzyl alcohol slowly was not sufficient to prevent competitive formation of **2.8**, hence **2.9** could not be formed selectively with this NHC-borane (*vide infra*). Furthermore, **2.9** readily decomposed at room temperature to form a complex mixture with no evidence of intramolecular arene C-H borylation observed. This also prevented *in situ* characterisation of **2.9** by NMR/mass spectrometry. Calculations performed by Dr Kang Yuan (at the ωB97XD/aug-cc-pvDZ//PCM (CH_3Cl) level of theory) indicated that the intramolecular arene C-H borylation of **2.9**, leading to H_2 evolution, was thermodynamically favoured at room temperature (**Scheme 2.13**). The absence of C-H borylation could therefore be attributed to a significant kinetic barrier to borylation.

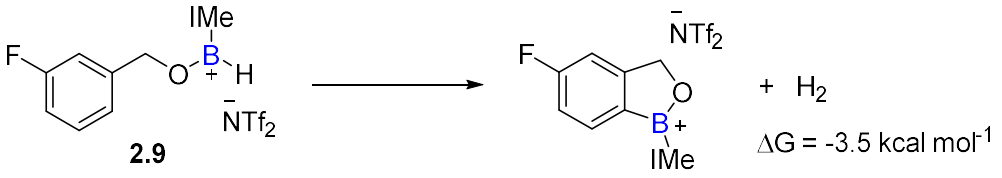

Scheme 2.13: Calculated Gibbs free energy for the intramolecular arene C-H borylation of [IMeBH(OBn-F)][NTf_2].

The double addition product, **2.8**, could be synthesised selectively by addition of 2 equiv. of 3-fluorobenzyl alcohol, leading to complete conversion of $IMeBH_2NTf_2$. This borenium ion was characterised *in situ* by NMR spectroscopy and the cation was observed by mass spectrometry, however attempts to purify / crystallise **2.8** were unsuccessful (*vide infra*), with this species shown to be highly sensitive to hydrolysis. The addition of ≥2 equiv. of the benzyl alcohol to $IMeBH_2NTf_2$ led to the partial formation of a third borylated species (δ_{11B} = 18.6 ppm), with this species generated cleanly in the reaction of 4 equiv. of the benzyl alcohol. This product was isolated, purified and characterised as $B(OBn\text{-}F)_3$ (**2.10**), generated by the triple addition of 3-fluorobenzyl alcohol to $IMeBH_2NTf_2$. This also resulted in the protonation of the NHC to form [IMeH][NTf_2]. A proposed pathway for the sequential addition of 3-fluorobenzyl alcohol to the activated NHC-borane derivative is depicted in **Scheme 2.14**.

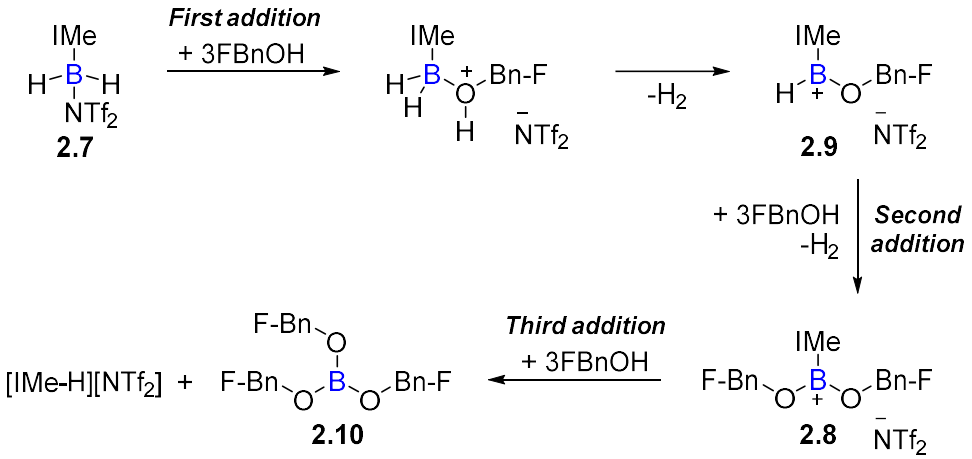

Scheme 2.14: Proposed mechanistic pathway for the addition of 3-fluorobenzyl alcohol to IMe-BH_2NTf_2, generating three borylated benzyl products depending on stoichiometry *(Bn-F = 3-fluorobenzyl)*.

Owing to the observed challenges in producing the single addition product, **2.9**, selectively in large amounts, the reactivity of the second addition product, **2.8**, was investigated to see if this borenium ion was sufficiently electrophilic to undergo an intramolecular C-H borylation of one of the substituent arene rings in the presence of an appropriate exogenous base (to facilitate deprotonation of the arenium intermediate in the S_EAr process). Although the reaction of 1 equiv. 3-fluorobenzyl alcohol with 1 equiv. $IMeBH_2NTf_2$ resulted in a mixture of **2.8** and **2.9**, the presence of unreacted $IMeBH_2NTf_2$ could lead to side reactions. Hence **2.8** was formed selectively with 2 equiv. 3-fluorobenzyl alcohol, and its reactivity was subsequently explored.

Inducing Intramolecular Arene C-H Borylation

Compound **2.8** (δ_{11B} = 24.4 ppm) was stable in a solution of dichloromethane at room temperature with no further reactivity/decomposition observed after 5 days. This is consistent with the absence of an exogenous base precluding C-H borylation, as previously observed in examples of arene C-H borylation using other borenium cations.[56] The addition of an exogenous base was explored next to see if this could facilitate deprotonation of the arenium intermediate during arene C-H borylation. To prevent irreversible coordination to the Lewis acidic borenium ions, a sterically hindered base, 2,6-(*t*Bu)$_2$-4-methyl pyridine (DBP), was added to **2.8** to see if this enabled the desired intramolecular arene C-H borylation to proceed (**Scheme 2.15**).

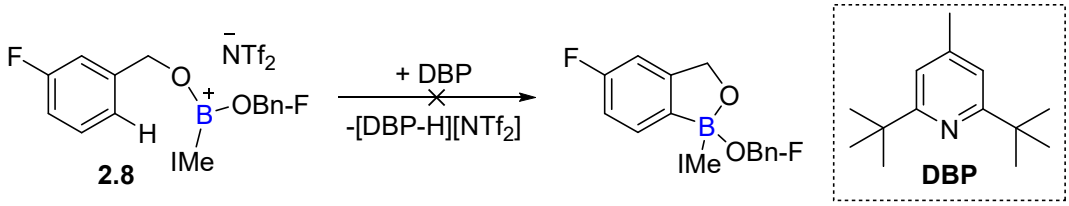

Scheme 2.15: Attempted intramolecular arene C-H borylation of $[IMe(OBn\text{-}F)_2][NTf_2]$, facilitated by the addition of an exogenous base *(Bn-F = 3-fluorobenzyl)*.

The room temperature addition of 1 equiv. DBP to an *in situ* generated sample of **2.8** resulted in the immediate loss of **2.8** from the ^{11}B NMR spectrum of the

homogeneous sample, alongside the formation of $B(OBn\text{-}F)_3$ **2.10** and two sharp singlet resonances at 0.3 and -1.2 ppm (**Figure 2.5**).

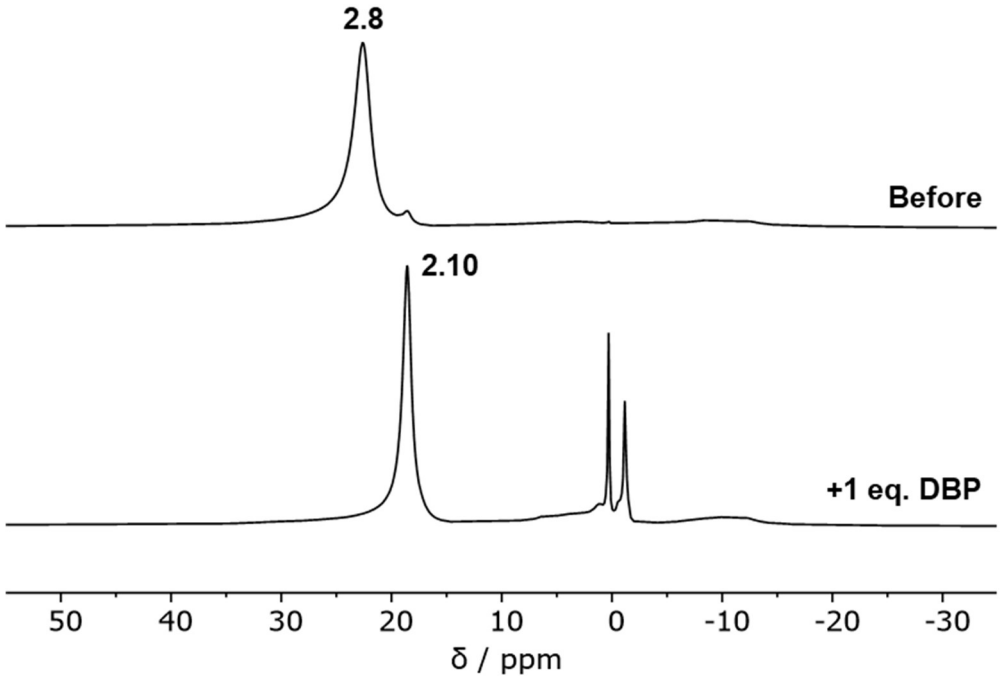

Figure 2.5: Stacked *in situ* ^{11}B NMR spectra of the reaction of $[IMeB(OBn\text{-}F)_2][NTf_2]$ before and after addition of 1 equiv. DBP at RT. *(Solvent = CD_2Cl_2, NMR temperature = 300 K).*

The ^1H NMR spectrum also showed the loss of the benzyl CH_2 resonance of **2.8** (**Figure 2.6**), with the formation of **2.10** observed as the only significant benzyl-containing species in the ^1H and ^{13}C NMR spectra and only one 'Ar-F' resonance in the ^{19}F NMR spectrum (two would have been observed if there had been any significant C-H borylation). The ^1H NMR spectrum showed multiple NHC resonances, including $[IMe\text{-}H][NTf_2]$. In addition, a small amount of protonated DBP was also observed, though the majority was left unprotonated. No further changes to the NMR spectra were observed upon mixing the reaction at room temperature or heating to 60 °C. The observation of protonated base (both IMe and DBP) provides some indication that arene C-H borylation may have occurred, as there are no other proton sources in the reaction mixture. However, no other significant benzyl resonances that could correspond to the C-H borylated product were observed in any of the NMR spectra. The majority of the benzyl alcohol

substrate appeared to have been converted to B(OBn-F)$_3$ **2.10**, hence the potential amount of C-H borylated product present would only be very minor.

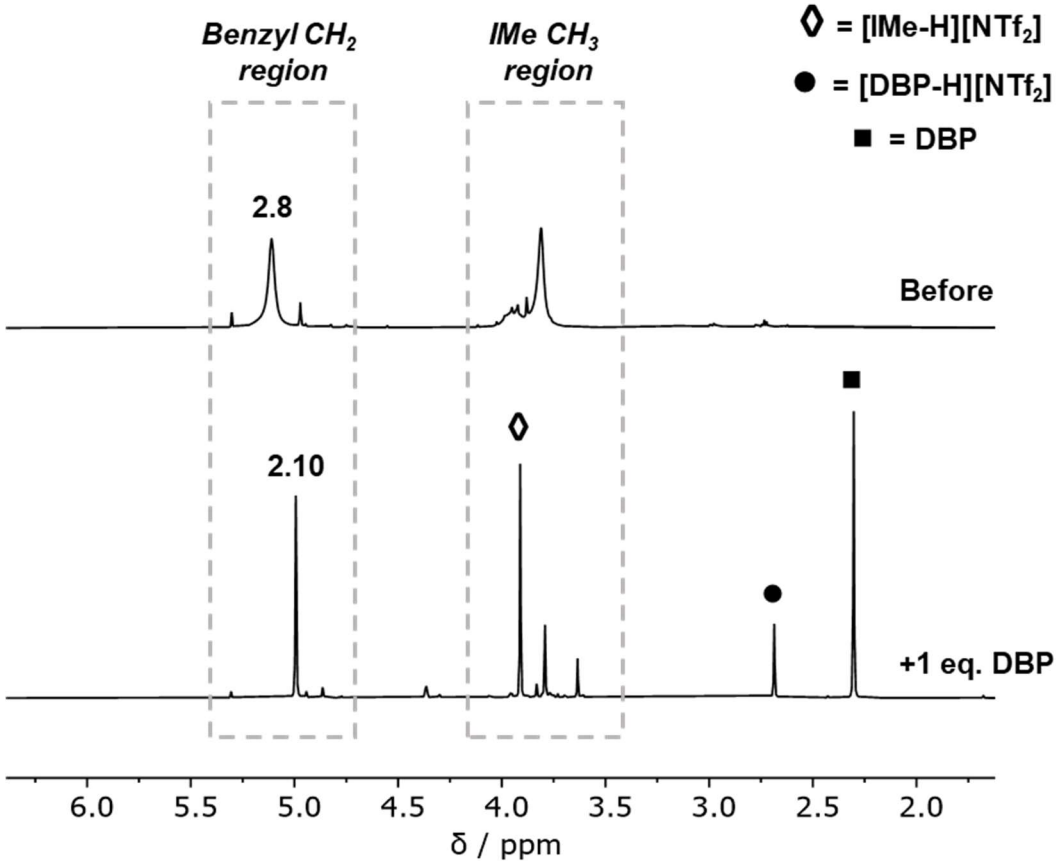

Figure 2.6: Stacked *in situ* ^{1}H NMR spectra of the reaction of [IMeB(OBn-F)$_2$][NTf$_2$] before and after addition of 1 equiv. DBP at RT. *(Solvent = CD_2Cl_2, NMR temperature = 300 K).*

Attempts were made to purify this sample by extracting into pentane (to remove the protonated bases), but only B(OBn-F)$_3$ **2.10** was isolated, and the leftover polar residue did not feature any benzyl resonances. It was therefore concluded that for this reaction, the desired arene C-H borylation of **2.8** is only proceeding in very low yields (if at all). It is hypothesised that a small degree of C-H borylation of **2.8** to form the benzoxaborole product could lead to release of the NHC (with the reversible binding of NHCs to aryl-B(OR)$_2$ reported).[57] Thus, this free NHC may catalyse substituent redistribution of the remaining **2.8**, leading to the formation of B(OBn-F)$_3$ **2.10**. However, without identification of the remaining mass balance further conjecture is not warranted.

The reactivity of **2.8** was also explored using an alternative exogenous base, *N,N*-diisopropylethylamine (DIPEA). The *in situ* NMR spectra showed the loss of **2.8** following addition of the base, but this was slower than with DBP, requiring 24 hours at room temperature for **2.8** to be fully consumed. The resulting spectra were very similar to the reactions with DBP, showing the formation of $B(OBn\text{-}F)_3$ **2.10** and a sharp singlet resonance at 0.3 ppm in the ^{11}B NMR spectrum, with no other significant benzyl species in the $^{1}H/^{13}C$ NMR spectra. Protonated bases (IMe and DIPEA) were also observed. Therefore the same undesirable reactivity appears to occur with both bases, forming $B(OBn\text{-}F)_3$ **2.10** as the major benzyl-O containing product. However, it is not clear how **2.10** is formed in solution.

One possible way to favour intramolecular arene C-H borylation (over the formation of **2.10**) is to increase the nucleophilicity of the arene. Therefore, the reactivity of unsubstituted benzyl alcohol was also explored, as the absence of an electronegative fluorine atom slightly increases the nucleophilicity of the arene (F σ_{para} = 0.06)[58] and hence may increase the rate of C-H borylation. The reaction of 2 equiv. benzyl alcohol with $IMeBH_2NTf_2$ **2.7** led to the complete conversion of **2.7**, with a new ^{11}B resonance observed at 22.8 ppm. This was assumed to be the corresponding double addition product $[IMeB(OBn)_2][NTf_2]$, based on its similar chemical shift to **2.8**. Addition of 1 equiv. DBP to the sample at room temperature resulted in the conversion of this species to the respective triple addition product, $B(OBn)_3$ (δ_{11B} = 18.7 ppm).[59] The ^{11}B NMR spectrum also showed two sharp singlets at 0.3 and -1.2 ppm, identical to the resonances observed in the reactions with 3-fluorobenzyl alcohol. As seen previously, some protonated base was formed but no other significant benzyl species were observed in the NMR spectra. Therefore, it was concluded that the change in substrate has made little difference to the reaction outcome, with the respective tri-benzoxy boronate ester still the major product.

An alternative approach to facilitate arene C-H borylation could be to increase the electrophilicity of boron in the O-borylated intermediate. The single addition product **2.9** should be more electrophilic at boron due to the reduced π-donation into the vacant p_z orbital (relative to **2.8**), and therefore more likely to undergo

subsequent intramolecular arene C-H borylation. However, the reactions of benzyl alcohols with IMeBH$_2$NTf$_2$ have thus far not formed **2.9** in significant amounts. Therefore, the use of larger NHCs was explored to see if these would provide sufficient steric protection to stabilise the respective single addition product whilst slowing the rate of over-addition. It was hoped that this would enable the respective single addition product to be formed selectively, and its subsequent reactivity towards intramolecular arene C-H borylation to be explored.

Using Larger NHC-boranes

The addition of 3-fluorobenzyl to other HNTf$_2$-activated NHC-boranes with more sterically demanding NHCs was explored (**Scheme 2.16**).

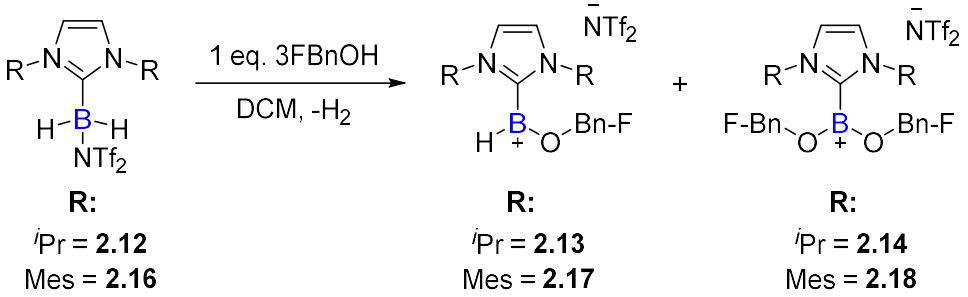

Scheme 2.16: Reaction of HNTf$_2$-activated NHC-boranes with 3-fluorobenzyl alcohol. *(Bn-F = 3-fluorobenzyl)*.

A sample of 1,3-diisopropylimidazol-2-ylidene borane, I^{i}PrBH$_3$ (**2.11**), was activated by the addition of HNTf$_2$, forming I^{i}PrBH$_2$NTf$_2$ (**2.12**) *in situ*. The addition of 1 equiv. 3-fluorobenzyl alcohol at room temperature resulted in H$_2$ evolution, however the selectivity was poor, forming a mixture of the three addition products. The double addition product (**2.14**, δ_{11B} = 24.0 ppm) was observed as the major product (**Figure 2.7b**). Only minor amounts of the corresponding single addition product (**2.13**, δ_{11B} = 36.8 ppm) were observed, and a small resonance for the triple addition product, B(OBn-F)$_3$ **2.10**, was also observed (δ_{11B} = 18.5 ppm). The selectivity of benzyl alcohol addition was very similar to the reaction with IMeBH$_3$ (**Figure 2.7a**), indicating there is little effect on selectivity from replacing *N*-methyl with *N*-isopropyl groups.

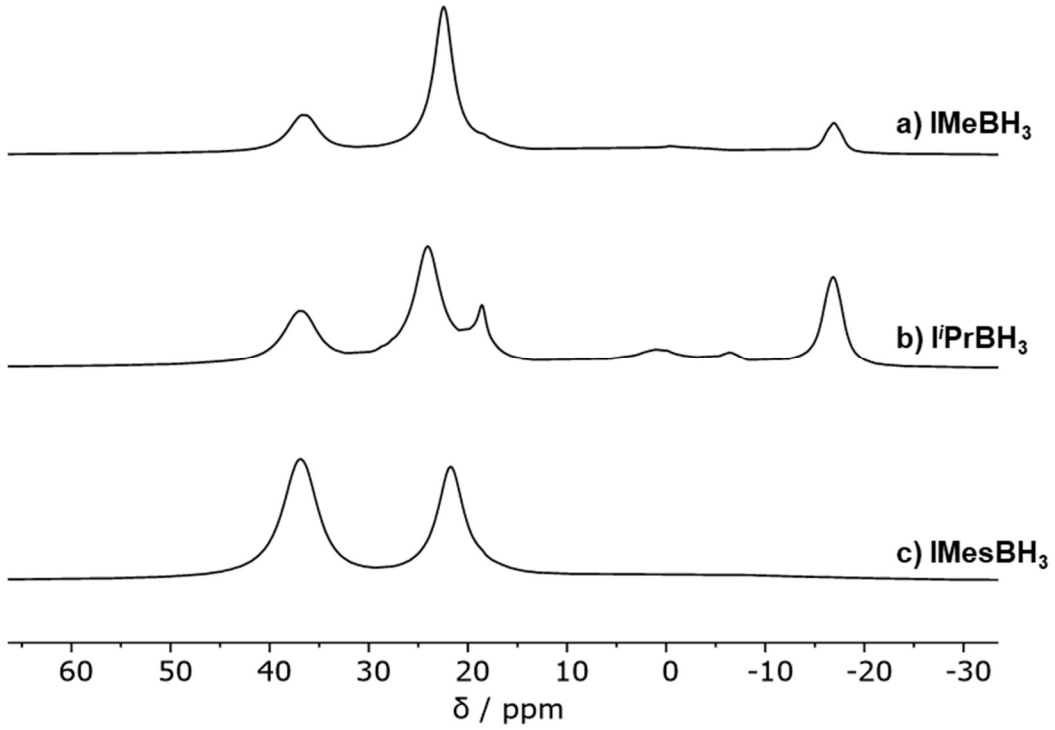

Figure 2.7: Stacked *in situ* ^{11}B NMR spectra comparing the reactions of **a)** $IMeBH_3$, **b)** I^iPrBH_3, and **c)** $IMesBH_3$, all following activation with 1 equiv. $HNTf_2$ and addition of 1 equiv. 3-fluorobenzyl alcohol at RT. *(Solvent = CD_2Cl_2, NMR temperature = 300 K).*

The reactivity with 1,3-di(2,4,6-trimethylphenyl)imidazol-2-ylidene borane, $IMesBH_3$ (**2.15**), was subsequently investigated. Activation with $HNTf_2$ generated $IMesBH_2NTf_2$ (**2.16**) *in situ*, with 1 equiv. 3-fluorobenzyl alcohol then added at room temperature. For this NHC, the respective single addition product (**2.17**, δ_{11B} = 36.9 ppm) was a significant species in the ^{11}B NMR spectrum (**Figure 2.7c**), showing clear improvement in the addition selectivity compared to $IMeBH_3$ and I^iPrBH_3. This is assumedly due to the steric bulk of the NHC mesityl substituents, hindering the addition of 3-fluorobenzyl alcohol to [IMesBH(OBn-F)][NTf_2] **2.17**. The reaction was not entirely selective, however, with a considerable resonance corresponding to the respective double addition product, **2.18**, also observed (δ_{11B} = 21.7 ppm). The larger NHC also improved the stability of the borenium ions (compared to IMe), with **2.17** stable at room temperature, with no change to the NMR spectra after 4 days.

To try to improve selectivity towards **2.17**, a solution of 3-fluorobenzyl alcohol (1 equiv.) was added dropwise to $IMesBH_2NTf_2$ **2.16** at 0 °C. The reaction was left at 0 °C for 30 minutes, with H_2 evolution observed, then warmed to room temperature. The ^{11}B NMR spectrum showed that lowering the addition temperature improved selectivity, with **2.17** formed as the major product (**Figure 2.8a**). However, a significant amount of **2.16** remained unreacted. To try and form **2.17** cleanly, a further 0.2 equiv. 3-fluorobenzyl alcohol was added under the same conditions. This enabled the full consumption of **2.16** with reasonably selective formation of **2.17**, and only minor double addition to form **2.18** (**Figure 2.8b**). The $^{1}H\{^{11}B\}$ NMR spectrum showed a broad B-H resonance at 4.6 ppm, supporting the proposed structure of a B-H containing borenium ion. However, attempts to characterise **2.17** by mass spectrometry were unsuccessful, and crystals suitable for X-ray diffraction could not be formed.

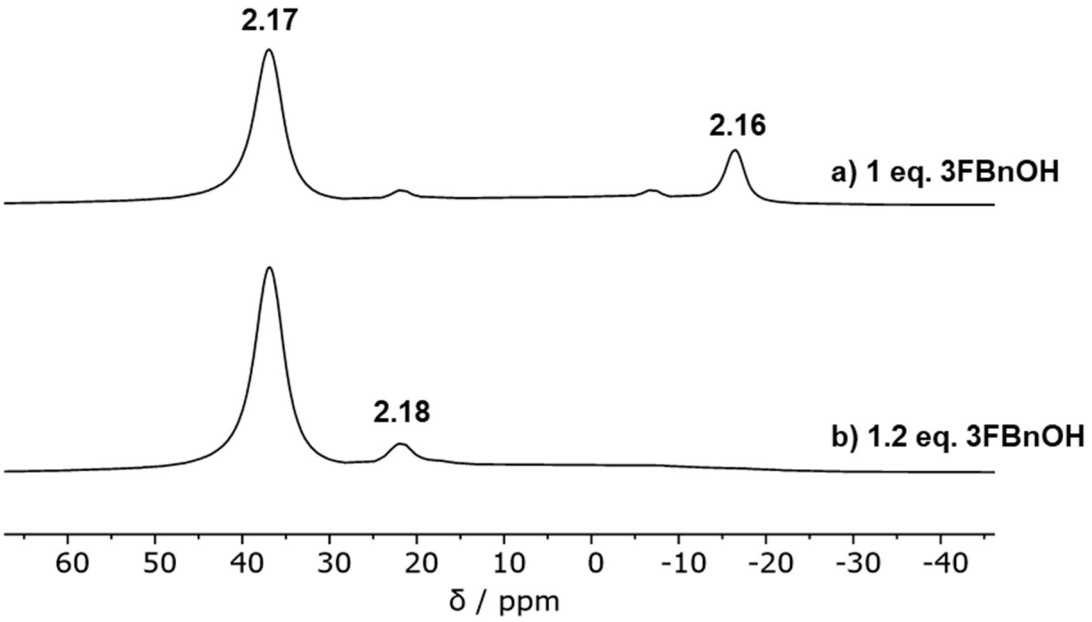

Figure 2.8: Stacked ^{11}B NMR spectra of the reactions of $IMesBH_2NTf_2$ with **a)** 1 equiv. and **b)** 1.2 equiv. 3-fluorobenzyl alcohol, with addition at 0 °C. *(Solvent = CD_2Cl_2, NMR temperature = 300 K).*

When this process was repeated under (assumedly) identical conditions, the same selectivity could not be replicated, and significant amounts of **2.18** were formed with considerable $IMesBH_2NTf_2$ left unreacted. Further attempts saw the addition temperature dropped to -20 °C, the rate of addition of 3-fluorobenzyl

alcohol slowed, and/or the time spent at low temperature following addition increased. However, these measures were not effective at improving the selectivity towards **2.17**, and no explanation for this change in reaction outcome could be established. There was no evidence of the degradation of any **2.17** that had been formed. Therefore, the reactivity of **2.17** towards intramolecular arene C-H borylation could not be investigated, and it was concluded that the single addition borenium ion, **2.17**, could not be selectively synthesised in a reproducible process.

By comparison, the double addition product, **2.18**, could be selectively synthesised via the dropwise addition of 2 equiv. 3-fluorobenzyl alcohol to $IMesBH_2NTf_2$ at 0 °C, with no over-addition to $B(OBn\text{-}F)_3$ **2.10** observed. This process was reproducible, and the borenium ion was characterised by NMR spectroscopy, with single crystals suitable for X-ray diffraction formed from chlorobenzene / pentane (**Figure 2.9**). The crystal structure confirmed the initial assignment as a planar three-coordinate NHC-borenium ion with two benzoxy substituents, with the combined angles of the substituents around boron equal to 360°. The NHC-B distance of **2.18** (1.599(6) Å) is comparable that reported for a similar NHC-borenium ions, including [IDipp-$B(OH)_2$][OTf] (NHC-B = 1.591(6) Å, where IDipp = 1,3-di(2,6-diisopropylphenyl) imidazol-2-ylidene).[60] The two B-O bonds in **2.18** (both 1.343(6) Å) are longer than those in [IDipp-$B(OH)_2$][OTf] (1.310(6), 1.307(7) Å), but shorter than the B-O bonds in another borenium ion, [Et_3N-$B(CatCl_4)$][$AlCl_4$] (1.364(3) and 1.370(3) Å) which is reactive towards arene C-H borylation.[61] This is indicative of significant π-donation from the two benzoxy substituents into the vacant p_z orbital in **2.18**. This O-B double bond character reduces the Lewis acidity at boron in **2.18**, contributing to the observed lack of reactivity towards arene C-H borylation.

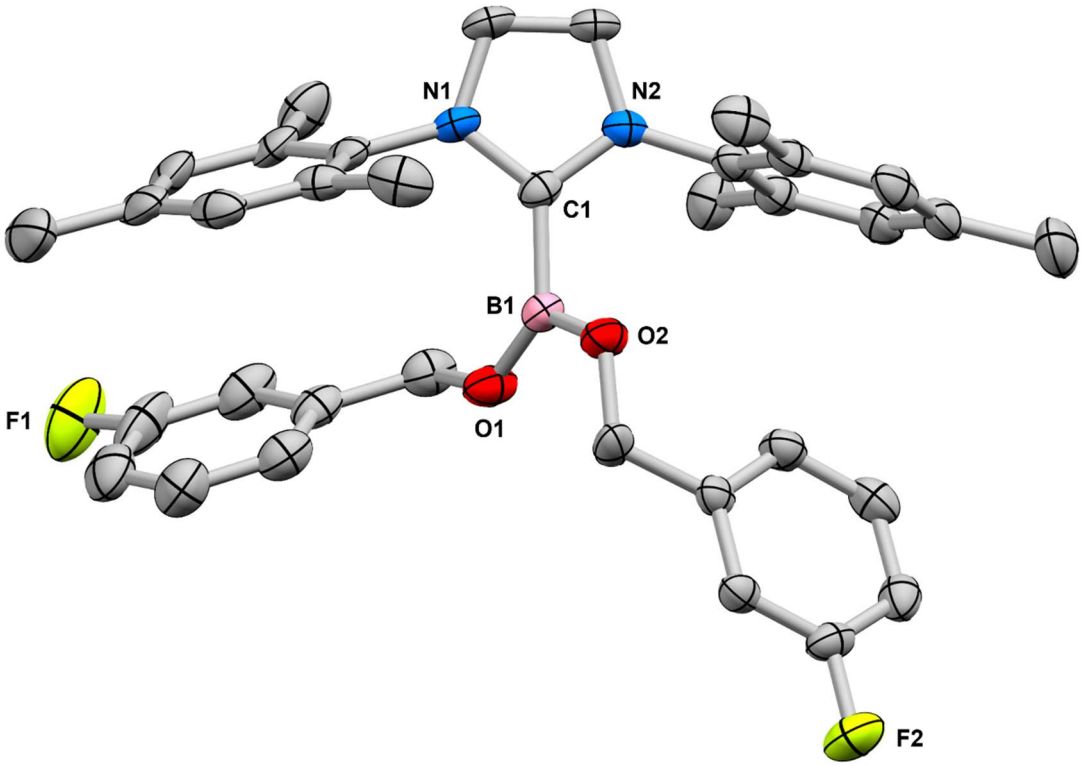

Figure 2.9: Solid-state structure of the cationic portion of **2.18** *(measured by Dr Marina Uzelac, solved by Dr Gary Nichol)*.
Ellipsoids at the 50% probability level. Hydrogen atoms removed for clarity.
Note: The anion, NTf_2, is disordered and also omitted for clarity.
Selected distances (Å) and angles (°): C1-B1 1.599(6), B1-O1 1.343(6), B1-O2 1.343(6); O1-B1-O2 120.8(4), O1-B1-C1 125.0(4), C1-B1-O2 114.2(4).

The reactivity of **2.18** could potentially be explored, but it is likely even less reactive than the IMe-equivalent, **2.8**, owing to increased steric bulk from the NHC which will disfavour 4-coordinate transition states/intermediates during the intramolecular C-H borylation process. This would increase the barrier to arene C-H borylation. When characterising this borenium ion, an attempt was made to probe its Lewis acidity using the established Gutmann-Beckett method.[62] This was unsuccessful, as addition of the Lewis base, Et_3PO, to a sample of **2.18** resulted in substituent exchange and the formation of $B(OBn\text{-}F)_3$ **2.10** (as observed in the previous reactions of **2.8** with DBP, where it was proposed that free NHC was catalysing substituent scrambling). Therefore, it was concluded that the potential reactivity of this borenium ion (**2.18**) towards intramolecular arene C-H borylation was unfeasible, hence this project was not pursued any further.

It remained notable that the double addition borenium ions, of the general formula [NHC-B(OBn)$_2$][NTf$_2$], did not exhibit any intramolecular arene C-H borylation, which is in contrast to the reactivity of other reported borenium ions. For example, [Et$_3$N-BCat][AlCl$_4$] (derived from CatBCl, Et$_3$N and AlCl$_3$) was shown to undergo intermolecular (hetero)arene C-H borylation at room temperature.[61] To better understand this difference in reactivity, the effect of NHCs on the Lewis acidity of borenium cations was explored by calculating the relative hydride ion affinity (HIA) of [IMe-BCat]$^+$. Calculations were performed by Professor Michael J. Ingleson at the M06-2X/6-311G(d,p), PCM (CH_2Cl_2) level of theory. This level enabled direct comparison to previously calculated HIAs for other [LB-BCat]$^+$ borenium cations,[54] hence the effect of the NHC could be evaluated (**Figure 2.10**).

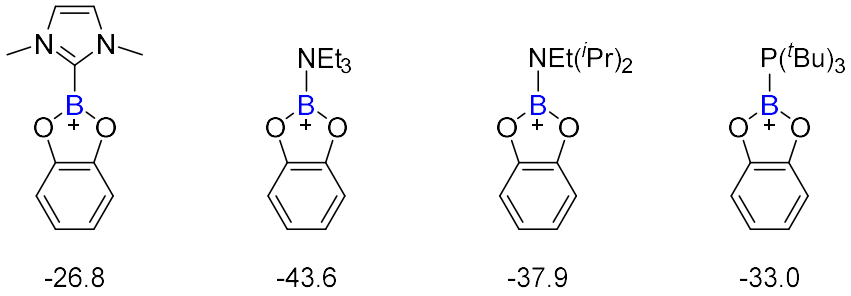

Figure 2.10: Calculated hydride ion affinities (ΔG/ kcal mol^{-1}, relative to BEt$_3$).

The calculated HIA of [IMe-BCat]$^+$ is significantly lower than for other [LB-BCat]$^+$ borenium cations with amine and phosphorus Lewis bases. This therefore demonstrates that the strongly σ-donating ability of the NHC reduces electrophilicity at boron, hence borenium ions with NHCs are less reactive towards nucleophiles (e.g. aryl π-systems) than their counterparts with other bases. These calculations support the observations from this work, with **2.8** unreactive towards intramolecular arene C-H borylation.

2.4 Conclusions

The reactivity of 3-fluorobenzyl alcohol with two types of boron electrophile has been investigated, in the hope that the oxygen-directed *ortho* C-H borylation could be achieved to provide a metal-free route to benzoxaboroles. Initially the reactivity with haloboranes (largely boron trichloride) was investigated. It was found that whilst these haloborane electrophiles did react at oxygen, the resulting intermediates were highly susceptible to nucleophilic substitution, cleaving the benzyl-oxygen bond and forming benzyl chloride. Attempts to prevent this unwanted reaction were unsuccessful, and benzoxaboroles could not be produced via this approach. Thus, it is unclear how Tavaborole was synthesised via electrophilic C-H borylation with BCl_3 in the published patent.

Subsequently, the reactivity of benzyl alcohols with $HNTf_2$-activated NHC-boranes was explored. It was found that benzyl alcohols added to these boron electrophiles via a dehydrocoupling process, evolving H_2. If the stoichiometry of the benzyl alcohol was not controlled, double and triple addition of the benzyl alcohol dominated. The single addition product, [NHC-BH(OBn-F)][NTf_2], was the most suitable for arene C-H borylation based on its expected higher electrophilicity. However, this borenium ion was highly challenging to synthesise selectively due to overreaction with further equivalents of benzyl alcohol. The double addition product, [NHC-B(OBn-F)$_2$][NTf_2] could be selectively synthesised. However, this species did not undergo intramolecular C-H borylation, instead forming B(OBn-F)$_3$ upon addition of a Lewis base. This, combined with HIA calculations, indicated that the boron centre is not electrophilic enough to undergo intramolecular arene C-H borylation. The low electrophilicity of these borenium ions is the result of significant electron donation by the NHC, reducing Lewis acidity. No direct evidence of intramolecular arene C-H borylation from these borenium ions was observed, indicating that this is not an effective method to synthesise benzoxaboroles.

It should be noted that reactivity of activated amine-boranes with benzyl alcohols was also investigated by an undergraduate student, Adam Allenby, in the Ingleson group.[63] It was hoped that the reduced σ-donation from this Lewis base would

increase the electrophilicity of the respective borenium ions formed upon addition of benzyl alcohol, therefore favouring intramolecular arene C-H borylation. Allenby studied the reactivity of Et_3N-BH_2NTf_2 with benzyl alcohols under a range of conditions, but this led to the formation of $B(OBn)_3$, $HB(OBn)_2$ and $[Et_3NH][NTf_2]$ as the major products due to the more labile Et_3N-B bond. Identical outcomes were observed using DIPEA in place of Et_3N.

Therefore, a suitable method for the synthesis of benzoxaboroles via oxygen-directed electrophilic C-H borylation has not been identified. A major challenge here is the generation of reactive, but stable (to benzyl cleavage) electrophiles following the initial O-B bond formation. The significant double bond character of the O-B bond reduces Lewis acidity at boron and can also improve the leaving group ability of the O-BX_2 moiety, leading to benzyl cleavage in the presence of suitable nucleophiles (e.g. chloride). By comparison, the approach developed by Rej and Chatani, published after the work in this chapter was performed, converts the C=O of benzaldehyde to a transient imine, therefore enabling intramolecular arene C-H borylation to proceed.[39] The authors also noted that benzaldehyde was not reactive towards electrophilic C-H borylation. Therefore, the approach of Rej and Chatani is more suited to the metal-free synthesis of benzoxaboroles and has effectively solved this challenge.

2.5 Experimental

2.5.1 General Considerations

The following applies to all experimental work described in Chapters 2-5.

All reactions were performed under an inert atmosphere using standard Schlenk techniques (N_2 atmosphere), or in an MBraun Unilab glovebox (Ar atmosphere, <0.1 ppm H_2O/O_2), unless otherwise stated. All chemicals were purchased from commercial sources and used as received, unless otherwise stated. Solutions of $BH_3{\cdot}SMe_2$, BCl_3 and BBr_3 were transferred to ampules fitted with J. Young's valves prior to use. Dry solvents were obtained from a Solvent Purification System (*Inert PureSolv MD5 SPS*) and stored over 3 Å molecular sieves. Chlorobenzene, 1,2-difluorobenzene and 1,2-dichlorobenzene were dried over CaH_2, distilled, and stored over 3 Å molecular sieves. Column chromatography was performed using a *Teledyne Isco CombiFlash® NextGen 300+ Autocolumn* instrument.

NMR spectra were recorded on *Bruker Avance III 400 MHz, Bruker Avance III 500 MHz,* or *Bruker PRO 500 MHz* spectrometers. Unless otherwise stated, NMR spectra were recorded at 20 °C. Chemical shifts (δ) are quoted in parts per million (ppm), spin-spin (*J)* coupling constants are given in hertz (Hz) to the nearest 0.5 Hz, and as positive vales regardless of their real individual signs. ^{1}H and $^{13}C\{^{1}H\}$ shifts are referenced to the appropriate residual solvent peak while ^{11}B and ^{19}F shifts are referenced relative to external $BF_3{\cdot}Et_2O$ and C_6F_6, respectively. Abbreviations used are s (singlet), d (doublet), t (triplet), q (quartet), p (pentet), dd (doublet of doublets), dt (doublet of triplets), m (multiplet), and br (broad). The $^{13}C\{^{1}H\}$ resonances of carbon atoms directly bonded to boron atoms were not always observed due to the quadrupolar relaxation effects. The observation of very broad signals at ca. 0 ppm in ^{11}B NMR spectra owes to the use of borosilicate glass NMR tubes and boron-containing parts in the NMR cavity. Mass spectrometry was performed by the *Scottish Instrumentation and Resource Centre for Advanced Mass Spectrometry* (SIRCAMS) at the University of Edinburgh using electron impact (EI) or electrospray ionisation (ESI) techniques. Elemental analysis was conducted at Elemental Microanalysis Ltd.

2.5.2 Reactivity with Haloboranes

The NMR spectra for all reactions can be found in the appendix of this thesis.

Attempted C-H Borylation of 3-Fluorobenzyl Alcohol with BCl_3

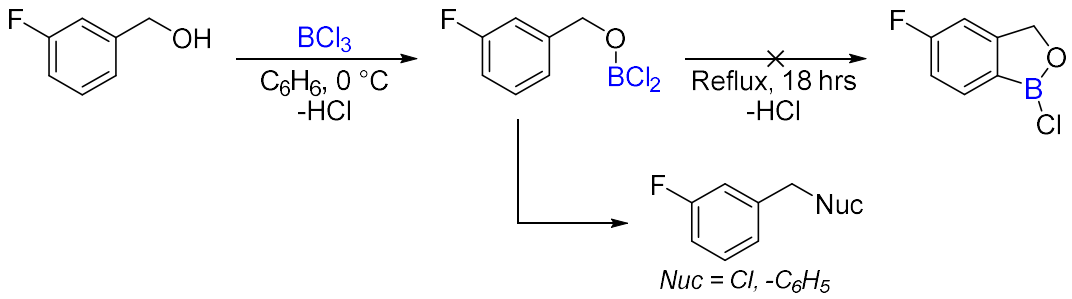

BCl_3 (1 M in hexanes, 1.8 mL, 1.8 mmol, 3 equiv.) was added dropwise to a solution of 3-fluorobenzyl alcohol (0.65 mL, 0.6 mmol) in C_6H_6 (3 mL) at 0 °C. The reaction was warmed to room temperature and stirred for 1 hour. The reaction was refluxed (open flask with fitted condenser) for 18 hours, after which an aliquot was taken for analysis by NMR spectroscopy. The residual BCl_3 / HCl was quenched by addition of THF (3 mL), and the reaction was concentrated *in vacuo* to yield an off white solid. The two benzyl products were purified via column chromatography (hexane/EtOAc) and characterised as 3-fluorobenzyl chloride (major product),[42] and 1-benzyl-3-fluorobenzene (minor product),[45] with analytical data in accordance with literature values. *In situ NMR studies revealed the same outcome, thus no major products are lost during chromatography.*

Attempted Hydroboration/C-H Borylation of Benzaldehyde with $HBCl_2$

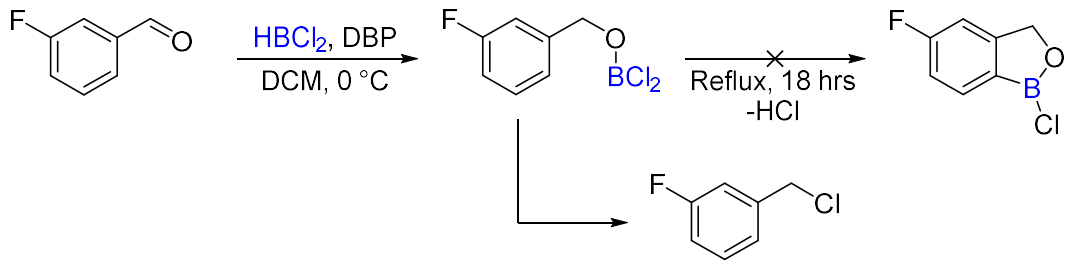

$HBCl_2$ (Dioxane complex, 3 M in DCM, 1.8 mL, 0.6 mmol, 2 equiv.) was added dropwise to a solution of 3-fluorobenzaldehyde (0.032 mL, 0.3 mmol) and 2,6-(*t*Bu)$_2$-4-methyl pyridine (0.123 g, 0.6 mmol, 2 equiv.) in DCM (0.3 mL) at 0 °C. The reaction was mixed by inversion (approx. 1 rotation / s) at room

temperature and analysed by *in situ* NMR spectroscopy at regular time points. Samples were heated in a heating block (up to 60 °C) without inversion / external mixing. After 5 days at room temperature (or 18 hours 60 °C) the complete conversion to 3-fluorobenzyl chloride was observed, with analytical data in accordance with literature values.[42]

2.5.3 Synthesis of NHC-boranes

1,3-Dimethylimidazol-2-ylidene borane, $IMeBH_3$ – 2.6

This is a modified route based on reports by the groups of Curran and Ingleson.[49,53]

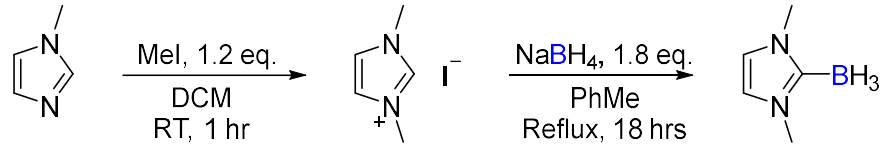

Methyl iodide (3.74 mL, 60 mmol, 1.2 equiv.) was added dropwise to a solution of *N*-methyl imidazole (4.0 mL, 50 mmol) in DCM (10 mL) at 0 °C. The solution was warmed to room temperature and stirred for 1 hour. All volatiles were subsequently removed *in vacuo*, yielding an off-white solid. To the solid was added toluene (50 mL) and sodium borohydride (3.40 g, 90 mmol, 1.8 equiv.), and the resulting suspension was heated at reflux for 18 hours, during which time an insoluble residue was formed. The reaction was filtered whilst hot, with further product extracted from the residue by washing with toluene (2 x 40 mL). The filtrate and washings were combined and concentrated *in vacuo*. The crude product was purified by recrystallisation from boiling water (55 mL) to yield the title product as needle-shaped colourless crystals in 17% yield (0.96 g, 8.73 mmol). Analytical data are in accordance with literature values.[49,53]

^{1}H NMR (500 MHz, $CDCl_3$) δ 6.79 (s, 2H), 3.73 (s, 6H), 1.01 (1:1:1:1 q, $^{1}J_{BH}$ = 86.5 Hz, 3H);

^{11}B NMR (161 MHz, $CDCl_3$) δ -37.5 (q, $^{1}J_{BH}$ = 86.5 Hz);

^{13}C{^{1}H} NMR (126 MHz, $CDCl_3$) δ 120.03, 36.08 ppm (*C-B was not visible even via ^{1}H-^{13}C HMBC*).

1,3-Diisopropylimidazol-2-ylidene borane, I^{i}PrBH$_3$ – 2.11

This is a modified route based on reports by the groups of Curran and Ingleson.[49,53]

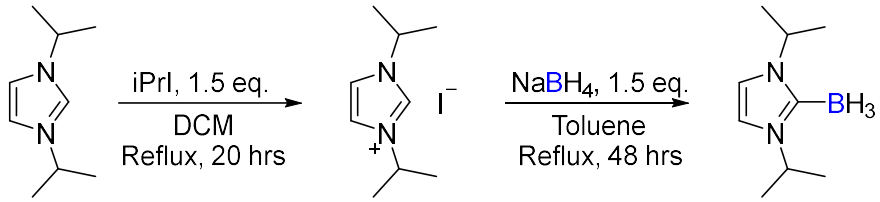

Isopropyl iodide (4.54 mL, 45 mmol, 1.5 equiv.) was added dropwise to a solution of *N*-isopropyl imidazole (3.44 mL, 30 mmol) in DCM (6 mL) at 0 °C. The solution was then heated at reflux for 20 hours. All volatiles were subsequently removed *in vacuo*, yielding a yellow oil. Addition of diethyl ether (50 mL) and rapid stirring resulted in the precipitation of a white solid, with the diethyl ether then removed *in vacuo*. To the solid was then added toluene (30 mL) and sodium borohydride (0.80 g, 22.5 mmol, 0.75 equiv.) and the resulting suspension was heated at reflux for 24 hours, after which time a second portion of sodium borohydride (0.80 g, 22.5 mmol, 0.75 equiv.) was added, and the reaction was heated at reflux for a further 24 hours. The reaction was filtered whilst hot, with further product extracted from the residue by washing with toluene (2 x 20 mL). The filtrate and washings were combined and concentrated *in vacuo*. The crude product was purified via column chromatography (Pet. Ether/EtOAc) to yield the title product as a pale-yellow solid in 9% yield (0.42 g, 2.65 mmol). Analytical data are in accordance with literature values.[49,53]

^{1}H NMR (500 MHz, $CDCl_3$) δ 6.91 (s, 2H), 5.13 (sept., $^{3}J_{HH}$ = 5 Hz, 2H), 1.39 (d, $^{3}J_{HH}$ = 5 Hz, 12H), 1.07 (1:1:1:1 q, $^{1}J_{BH}$ = 85 Hz, 3H);

^{11}B NMR (161 MHz, $CDCl_3$) δ -37.3 (q, $^{1}J_{BH}$ = 85 Hz);

^{13}C{^{1}H} NMR (126 MHz, $CDCl_3$) δ 115.07, 49.30, 22.84 ppm (*C-B was not visible even via ^{1}H-^{13}C HMBC*).

1,3-Di(2,4,6-trimethylphenyl)imidazol-2-ylidene borane, IMesBH$_3$ – 2.15

This modified procedure is based on a previous report by Lindsay and McArthur.[64]

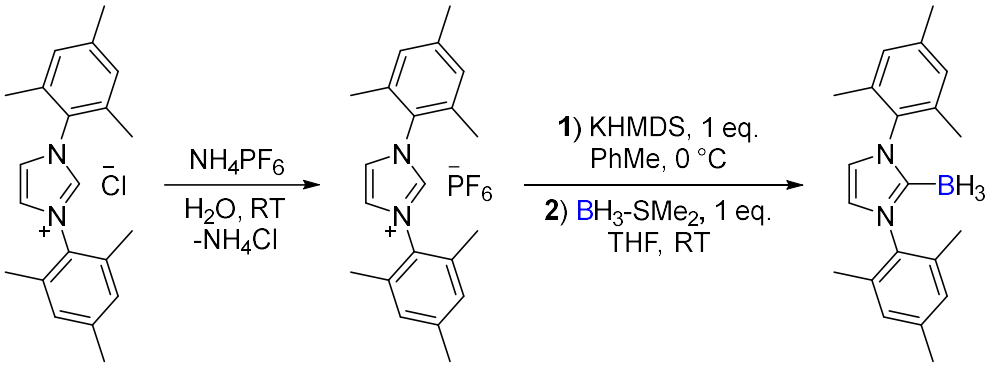

Synthesis of IMes·PF$_6$: To a saturated aqueous solution of IMes·HCl (1.02 g, 3 mmol) was added a saturated aqueous solution of NH_4PF_6 (0.49 g, 3 mmol, 1 equiv.), resulting in the precipitation of a white solid. The suspension was stirred at room temperature for 30 minutes, and the precipitate was filtered and concentrated *in vacuo*. The crude product was purified by recrystallisation from DCM/hexane to yield the title product as a white crystalline solid in 75% yield (1.02 g, 2.26 mmol). Analytical data are in accordance with literature values.[64]

Synthesis of IMesBH$_3$: A solution of KHMDS (0.42 g, 2.10 mmol, 1 equiv.) in toluene (4 mL) was added dropwise to a solution of IMes·PF$_6$ (0.95 g, 2.10 mmol) in THF (30 mL) at 0 °C. The reaction was then stirred at 0 °C for 30 minutes, after which time a solution of BH_3-SMe_2 (2 M in THF, 1.05 mL, 2.10 mmol, 1 equiv.) was added dropwise. The reaction was stirred at 0 °C for a further 30 minutes, then warmed to room temperature and stirred for 2 hours. The reaction was concentrated *in vacuo* to give a white solid, which was triturated with minimal DCM and filtered. The filtrate was concentrated *in vacuo*, and the crude product was purified via a silica plug (eluting with DCM) to yield the title product as a white solid in 78 % yield (0.53 g, 1.67 mmol). Analytical data are in accordance with literature values.[64]

^{1}H NMR (400 MHz, $CDCl_3$) δ 6.99 (s, 4H), 6.97 (s, 2H), 2.34 (s, 6H), 2.07 (s, 12H), 0.53 (1:1:1:1 q, $^1J_{BH}$ = 88.5 Hz, 3H);

^{11}B NMR (128 MHz, $CDCl_3$) δ -37.5 (q, $^1J_{BH}$ = 88.5 Hz);

^{13}C{^{1}H} NMR (100 MHz, $CDCl_3$) δ 139.25, 135.02, 134.67, 129.23, 120.60, 21.27, 17.72 ppm (*C-B was not visible even via ^{1}H-^{13}C HMBC*).

2.5.4 Characterising Addition Products: 3-Fluorobenzyl Alcohol and NHC-Boranes

General Procedure 2.1: Addition of 3-Fluorobenzyl Alcohol to NHC-BH_2NTf_2

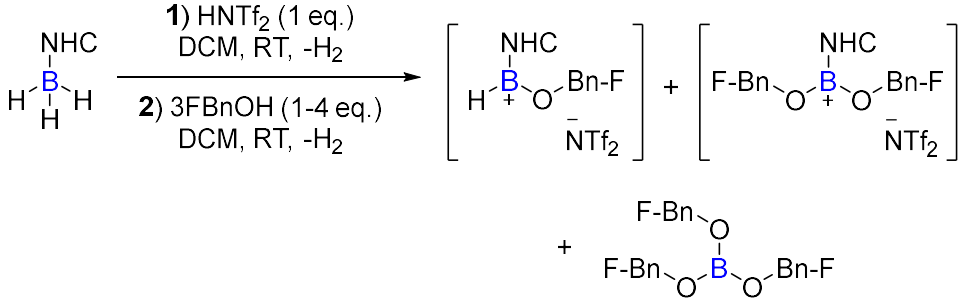

To a J. Young's NMR tube was added NHC-BH_3 (NHC = IMe, I^{i}Pr or IMes, 0.3 mmol), $HNTf_2$ (0.084 g, 0.3 mmol, 1 equiv.), and CH_2Cl_2/CD_2Cl_2 (0.5 mL), resulting in H_2 evolution. The sample was left at room temperature until gas evolution had ceased. To the sample was added 3-fluorobenzyl alcohol (1-4 equiv.), resulting in H_2 evolution. The sample was left at room temperature until gas evolution had ceased, before being analysed by *in situ* NMR spectroscopy. The ratio of the three borylated benzyl products formed was dependent on the equivalents of 3-fluorobenzyl alcohol added.

[IMeB(OBn-F)$_2$][NTf_2] – 2.8

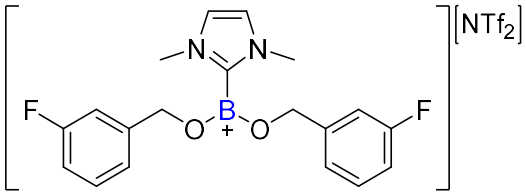

Compound **2.8** was prepared following **General Procedure 2.1** with $IMeBH_3$ (0.033 g, 0.3 mmol) and 2 equiv. 3-fluorobenzyl alcohol (0.065 mL, 0.6 mmol) in CH_2Cl_2 (0.5 mL). The title product was formed as the major product in solution and was directly characterised by NMR spectroscopy *in situ* without further purification. *(Note: a small amount of **2.10** and [IMeH][NTf_2] were also observed in this sample).*

^{1}H NMR (500 MHz, CH_2Cl_2) δ 7.38 (m, 2H, ArC*H*), 7.33 (s, 2H, N-C*H*), 7.15 (m, 2H, ArC*H*), 7.06 (m, 4H, ArC*H*), 5.15 (s, 4H, CH_2), 3.83 (s, 6H, N-CH_3);

^{11}B NMR (160 MHz, CH_2Cl_2) δ 22.5 (s, NHC-*B*$(OR)_2^+$);

^{13}C{^{1}H} NMR (126 MHz, CH_2Cl_2) δ 162.93 (d, J_{CF} = 246 Hz), 139.86 (d, J_{CF} = 7.5 Hz), 130.55 (d, J_{CF} = 8.5 Hz), 125.43, 122.82 (d, J_{CF} = 3 Hz), 119.76 (q, $^1J_{CF}$ = 321 Hz, S*C*F_3), 115.18 (d, J_{CF} = 21 Hz), 113.94 (d, J_{CF} = 22 Hz), 67.25, 37.35;

^{19}F NMR (471 MHz, CH_2Cl_2) δ -79.39 (s, SC*F*$_3$), -113.23 (m, Ar-*F*) ppm.

HRMS (ESI^+) *m/z* calcd for $C_{19}H_{20}BF_2N_2O_2^+$: 357.15858 $[M]^+$, found 357.1608.

Tri-(3-fluorobenzyl)borate ester – 2.10

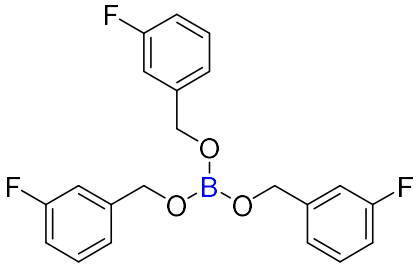

Compound **2.10** was prepared following **General Procedure 2.1** with $IMeBH_3$ (0.033 g, 0.3 mmol) and 4 equiv. 3-fluorobenzyl alcohol (0.13 mL, 1.2 mmol) in CD_2Cl_2 (0.5 mL). The sample was mixed by inversion (approx. 1 rotation / s) at room temperature for 24 hours. The crude product was extracted with pentane (0.9 mL) and the sample was concentrated *in vacuo* at 40 °C for 4 hours to remove excess 3-fluorobenzyl alcohol. The title product was isolated as a colourless oil.

^{1}H NMR (500 MHz, CD_2Cl_2) δ 7.31 (m, 3H, ArC*H*), 7.11 (m, 3H, ArC*H*), 7.05 (m, 3H, ArC*H*), 6.98 (m, 3H, ArC*H*), 5.00 (s, 6H, C*H*$_2$);

^{11}B NMR (160 MHz, CD_2Cl_2) δ 18.5 (s, *B*$(OR)_3$);

^{13}C{^{1}H} NMR (126 MHz, CD_2Cl_2) δ 163.41 (d, J_{CF} = 245 Hz), 143.0 (d, J_{CF} = 7 Hz), 130.34 (d, J_{CF} = 8 Hz), 122.51 (d, J_{CF} = 3 Hz), 114.52 (d, J_{CF} = 21.5 Hz), 113.75 (d, J_{CF} = 22 Hz), 65.27 (d, $^4J_{CF}$ = 2 Hz);

^{19}F NMR (471 MHz, CD_2Cl_2) δ -114.04 (m, Ar-*F*) ppm.

HRMS (EI^+) *m/z* calcd for $C_{21}H_{18}BF_3O_3^{\cdot+}$: 386.12956 $[M]^+$, found 386.12940.

[IMesBH(OBn-F)][NTf$_2$] – 2.17

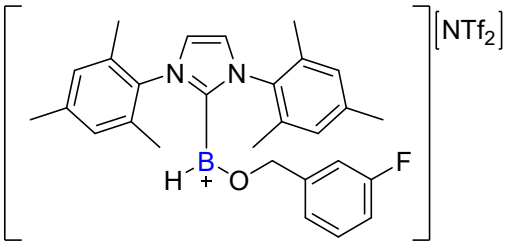

Compound **2.17** was prepared following an adapted version of **General Procedure 2.1**: To an ampule was added IMesBH$_3$ (0.095 g, 0.3 mmol), HNTf$_2$ (0.084 g, 0.3 mmol, 1 equiv.), and CD_2Cl_2 (0.5 mL), resulting in H_2 evolution. The reaction was stirred at room temperature until gas evolution had ceased. The ampule was cooled to 0 °C, and a solution of 3-fluorobenzyl alcohol (0.033 mL, 0.3 mmol, 1 equiv.) in CD_2Cl_2 (0.25 mL) was added dropwise. The reaction was stirred at 0 °C for 30 minutes, then warmed to room temperature. An aliquot was taken from the ampule for analysis by NMR spectroscopy, showing the partial formation of **2.17** with some unreacted IMesBH$_2$NTf$_2$. The aliquot was returned to the ampule, which was subsequently cooled to 0 °C again. A solution of 3-fluorobenzyl alcohol (0.007 mL, 0.06 mmol, 0.2 equiv.,) in CD_2Cl_2 (0.05 mL) was added dropwise. The reaction was stirred at 0 °C for 30 minutes, then warmed to room temperature. The title product was formed as the major product in solution and directly characterised by NMR spectroscopy *in situ* without further purification. *Note: a small amount of **2.18** was also observed in this sample. It should also be noted that subsequent attempts to replicate the results of this process (to probe the reactivity of **2.17**) led to varying proportions of **2.17** and **2.18**.*

^{1}H NMR (500 MHz, CD_2Cl_2) δ 7.73 (s, 2H, N-C*H*), 7.27 (m, 1H, ArC*H*), 7.10 (s, 4H, Mes-*H*), 7.01 (m, 1H, ArC*H*), 6.67 (m, 1H, ArC*H*), 6.40 (m, 1H, ArC*H*), 5.04 (s, 2H, C*H*$_2$), 2.41 (s, 6H, Mes(*p*-C*H*$_3$)), 2.05 (s, 12H, Mes(*o*-CH$_3$));

^{1}H{^{11}B} NMR (500 MHz, CD_2Cl_2) δ 7.73 (s, 2H, N-C*H*), 7.27 (m, 1H, ArC*H*), 7.10 (s, 4H, Mes-*H*), 7.01 (m, 1H, ArC*H*), 6.67 (m, 1H, ArC*H*), 6.40 (m, 1H, ArC*H*), 5.04 (s, 2H, C*H*$_2$), 4.64 (br, 1H, B-*H*), 2.41 (s, 6H, Mes(*p*-C*H*$_3$)), 2.05 (s, 12H, Mes(*o*-CH$_3$));

^{11}B NMR (160 MHz, CD_2Cl_2) δ 36.9 (br, NHC-*B*H(OR)$^+$);

^{11}B{^{1}H} NMR (160 MHz, CD_2Cl_2) δ 36.9 (s, NHC-*B*H(OR)$^+$);

^{13}C{^{1}H} NMR (126 MHz, CD_2Cl_2) δ 163.07 (d, $J_{C\text{-}F}$ = 248 Hz), 144.60 (br, *C*-B), 142.07, 138.91 (d, $J_{C\text{-}F}$ = 7.5 Hz), 134.25, 131.87, 130.51 (d, $J_{C\text{-}F}$ = 8 Hz), 130.15,

128.27, 123.0k (d, J_{C-F} = 3 Hz), 120.21 (q, $^{1}J_{C-F}$ = 320 Hz, S<u>*C*</u>F_3), 115.61 (d, J_{C-F} = 20 Hz), 114.17 (d, J_{C-F} = 23 Hz), 76.42 (d, $^{4}J_{C-F}$ = 2 Hz), 21.20, 17.31;

^{19}F NMR (471 MHz, CD_2Cl_2) δ -79.30 (s, SC<u>*F*</u>$_3$), -113.26 (m, Ar-<u>*F*</u>) ppm.

The title compound was not observed via mass spectrometry (both ESI and EI).

[IMesB(OBn-F)$_2$][NTf$_2$] – 2.18

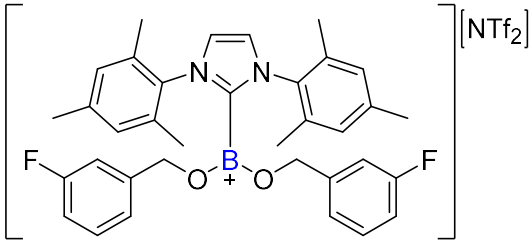

Compound **2.18** was prepared following an adapted version of **General Procedure 2.1**: To an ampule was added $IMesBH_3$ (0.191 g, 0.6 mmol), $HNTf_2$ (0.168 g, 0.6 mmol, 1 equiv.), and CD_2Cl_2 (1 mL), resulting in H_2 evolution. The reaction was stirred at room temperature until gas evolution had ceased. The ampule was cooled to 0 °C, and a solution of 3-fluorobenzyl alcohol (0.13 mL, 1.2 mmol, 2 equiv.) in CD_2Cl_2 (2 mL) was added dropwise. The reaction was stirred at 0 °C for 30 minutes, then warmed to room temperature. The title product was formed as the major product in solution and directly characterised by NMR spectroscopy *in situ* without further purification. Crystals suitable for X-ray diffraction were formed by layering a sample of **2.18** in chlorobenzene with pentane at room temperature.

^{1}H NMR (500 MHz, CD_2Cl_2) δ 7.60 (s, 2H, N-C<u>*H*</u>), 7.24 (m, 2H, ArC<u>*H*</u>), 7.00 (m, 2H, ArC<u>*H*</u>), 6.95 (s, 4H, Mes-<u>*H*</u>), 6.67 (m, 2H, ArC<u>*H*</u>), 6.44 (m, 2H, ArC<u>*H*</u>), 4.82 (s, 4H, C<u>*H*</u>$_2$), 2.35 (s, 6H, Mes(*p*-C<u>*H*</u>$_3$)), 2.05 (s, 12H, Mes(*o*-CH_3));

^{11}B NMR (160 MHz, CD_2Cl_2) δ 21.8 (s, NHC-<u>*B*</u>$(OR)_2^+$);

^{13}C{^{1}H} NMR (126 MHz, CD_2Cl_2) δ 163.07 (d, J_{C-F} = 246.5 Hz), 145.04 (br, <u>*C*</u>-B), 142.18, 138.93 (d, J_{C-F} = 7.5 Hz), 134.25, 131.53, 130.58 (d, J_{C-F} = 8.5 Hz), 130.38, 127.01, 122.69 (d, J_{C-F} = 3 Hz), 112.21 (q, $^{1}J_{C-F}$ = 321 Hz, S<u>*C*</u>F_3), 115.43 (d, J_{C-F} = 21 Hz), 113.73 (d, J_{C-F} = 22 Hz), 68.11 (d, $^{4}J_{C-F}$ = 2 Hz), 21.13, 17.45;

^{19}F NMR (471 MHz, CD_2Cl_2) δ -79.36 (s, SC<u>*F*</u>$_3$), -112.95 (m, Ar-<u>*F*</u>) ppm.

The title compound was not observed via mass spectrometry (both ESI and EI).

2.5.5 Attempts to Induce Intramolecular Arene C-H Borylation

General Procedure 2.2: Reactivity of 2.8 with Exogenous Bases

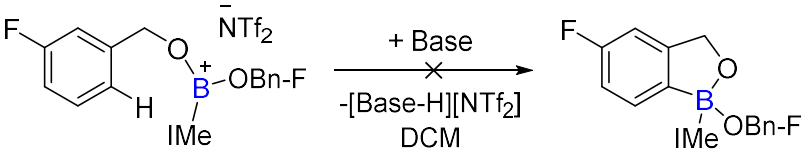

In a J. Young's NMR tube, **2.8** was initially prepared following **General Procedure 2.1** with $IMeBH_3$ (0.033 g, 0.3 mmol) and 2 equiv. 3-fluorobenzyl alcohol (0.065 mL, 0.6 mmol) in CD_2Cl_2 (0.5 mL).

To the sample was added exogenous base (DBP or DIPEA, 0.3 mmol, 1 equiv.). The sample was mixed by inversion (approx. 1 rotation / s) at room temperature or heated to 60 °C in a heating block without inversion / external mixing, with analysis by *in situ* NMR spectroscopy at regular time points.

The reactivity of benzyl alcohol was also explored following **General Procedure 2.2**, with $IMeBH_3$ (0.033 g, 0.3 mmol), benzyl alcohol (0.031 mL, 0.6 mmol, 1 equiv.) and DBP (0.061 g, 0.3 mmol, 1 equiv.).

2.5.6 X-Ray Crystallography

[IMesB(OBn-F)$_2$][NTf$_2$] – 2.18

Experimental: Single colourless block-shaped crystals of **2.18** were recrystallised from a mixture of pentane and chlorobenzene. A suitable crystal with dimensions 0.34 × 0.22 × 0.20 mm^3 was selected and mounted on a MITIGEN holder in Paratone oil on a Rigaku Oxford Diffraction XCalibur diffractometer. The crystal was kept at a steady T = 120.0 K during data collection. The structure was solved with the ShelXT[65] solution program using dual methods and by using Olex2 1.5-beta[66] as the graphical interface. The model was refined with ShelXL 2018/3[67] using full matrix least squares minimisation on F^2.

Crystal Data:

Formula	$C_{37}H_{36}BF_8N_3O_6S_2$
$D_{calc.}$ / g cm^{-3}	1.460
μ /mm^{-1}	0.227
Formula Weight	845.62
Colour	Colourless
Shape	Block-Shaped
Size/ mm^3	0.34 × 0.22 × 0.20
T/ K	120.00
Crystal System	Orthorhombic
Space Group	*Pbca*
a /Å	11.4679(2)
b /Å	15.9115(4)
c /Å	42.1622(9)
α /°	90
β /°	90
γ /°	90
V / Å^3	7693.4(3)
Z	8
Z'	1
Wavelength / Å	0.71073
Radiation type	Mo K_α
Θ_{min} /°	3.261
Θ_{max} /°	25.350
Measured Refl's.	139611
Indep't Refl's	7027
Refl's I≥2 σ(I)	6063
R_{int}	0.1125
Parameters	668
Restraints	588
Largest Peak	0.805
Deepest Hole	-0.845
GooF	1.120
wR_2 (all data)	0.2268
wR_2	0.21.99
R_1 (all data)	0.1090
R_1	0.0978

2.6 References

1 S. J. Baker, C. Z. Ding, T. Akama, Y.-K. Zhang, V. Hernandez and Y. Xia, *Future Med Chem.*, 2009, **1**, 1275–1288.

2 B. C. Das, P. Thapa, R. Karki, C. Schinke, S. Das, S. Kambhampati, S. K. Banerjee, P. Van Veldhuizen, A. Verma, L. M. Weiss and T. Evans, *Future Med Chem.*, 2013, **5**, 653–676.

3 D. B. Diaz and A. K. Yudin, *Nature Chem.*, 2017, **9**, 731–742.

4 M. P. Silva, L. Saraiva, M. Pinto and M. E. Sousa, *Molecules*, 2020, **25**, 4323.

5 A. Adamczyk-Woźniak, K. M. Borys and A. Sporzyński, *Chem. Rev.*, 2015, **115**, 5224–5247.

6 G. F. S. Fernandes, W. A. Denny and J. L. Dos Santos, *Eur. J. Med. Chem.*, 2019, **179**, 791–804.

7 A. Adamczyk-Woźniak, M. K. Cyrański, A. Żubrowska and A. Sporzyński, *J. Organomet. Chem.*, 2009, **694**, 3533–3541.

8 C. T. Liu, J. W. Tomsho and S. J. Benkovic, *Bioorg. Med. Chem.*, 2014, **22**, 4462–4473.

9 S. J. Baker, Y.-K. Zhang, T. Akama, A. Lau, H. Zhou, V. Hernandez, W. Mao, M. R. K. Alley, V. Sanders and J. J. Plattner, *J. Med. Chem.*, 2006, **49**, 4447–4450.

10 F. L. Rock, W. Mao, A. Yaremchuk, M. Tukalo, T. Crépin, H. Zhou, Y.-K. Zhang, V. Hernandez, T. Akama, S. J. Baker, J. J. Plattner, L. Shapiro, S. A. Martinis, S. J. Benkovic, S. Cusack and M. R. K. Alley, *Science*, 2007, **316**, 1759–1761.

11 T. Akama, S. J. Baker, Y.-K. Zhang, V. Hernandez, H. Zhou, V. Sanders, Y. Freund, R. Kimura, K. R. Maples and J. J. Plattner, *Bioorg. Med. Chem. Lett.*, 2009, **19**, 2129–2132.

12 B. C. Das, M. Adil Shareef, S. Das, N. K. Nandwana, Y. Das, M. Saito and L. M. Weiss, *Bioorg. Med. Chem.*, 2022, **63**, 116748.

13 P. Y. Chong, J. B. Shotwell, J. Miller, D. J. Price, A. Maynard, C. Voitenleitner, A. Mathis, S. Williams, J. J. Pouliot, K. Creech, F. Wang, J. Fang, H. Zhang, V. W.-F. Tai, E. Turner, K. M. Kahler, R. Crosby and A. J. Peat, *J. Med. Chem.*, 2019, **62**, 3254–3267.

14 X. Li, V. Hernandez, F. L. Rock, W. Choi, Y. S. L. Mak, M. Mohan, W. Mao, Y. Zhou, E. E. Easom, J. J. Plattner, W. Zou, E. Pérez-Herrán, I. Giordano, A. Mendoza-Losana, C. Alemparte, J. Rullas, I. Angulo-Barturen, S. Crouch, F. Ortega, D. Barros and M. R. K. Alley, *J. Med. Chem.*, 2017, **60**, 8011–8026.

15 J. Zhang, M. Zhu, Y. Lin and H. Zhou, *Sci. China Chem.*, 2013, **56**, 1372–1381.

16 G. R. Mereddy, A. Chakradhar, R. M. Rutkoski and S. C. Jonnalagadda, *J. Organomet. Chem.*, 2018, **865**, 12–22.

17 V. V. Zhdankin, P. J. Persichini, L. Zhang, S. Fix and P. Kiprof, *Tetrahedron Lett.*, 1999, **40**, 6705–6708.

18 L. Ye, D. Ding, Y. Feng, D. Xie, P. Wu, H. Guo, Q. Meng and H. Zhou, *Tetrahedron*, 2009, **65**, 8738–8744.

19 T. Ishiyama, M. Murata and N. Miyaura, *J. Org. Chem.*, 1995, **60**, 7508–7510.

20 Y.-K. Zhang, J. J. Plattner, Y. R. Freund, E. E. Easom, Y. Zhou, J. Gut, P. J. Rosenthal, D. Waterson, F.-J. Gamo, I. Angulo-Barturen, M. Ge, Z. Li, L. Li, Y. Jian, H. Cui, H. Wang and J. Yang, *Bioorg. Med. Chem. Lett.*, 2011, **21**, 644–651.

21 Y.-K. Zhang, J. J. Plattner, T. Akama, S. J. Baker, V. S. Hernandez, V. Sanders, Y. Freund, R. Kimura, W. Bu, K. M. Hold and X.-S. Lu, *Bioorg. Med. Chem. Lett.*, 2010, **20**, 2270–2274.

22 D. Ding, Y. Zhao, Q. Meng, D. Xie, B. Nare, D. Chen, C. J. Bacchi, N. Yarlett, Y.-K. Zhang, V. Hernandez, Y. Xia, Y. Freund, M. Abdulla, K.-H. Ang, J. Ratnam, J. H. McKerrow, R. T. Jacobs, H. Zhou and J. J. Plattner, *ACS Med. Chem. Lett.*, 2010, **1**, 165–169.

23 Y.-K. Zhang, J. J. Plattner, Y. R. Freund, E. E. Easom, Y. Zhou, L. Ye, H. Zhou, D. Waterson, F.-J. Gamo, L. M. Sanz, M. Ge, Z. Li, L. Li, H. Wang and H. Cui, *Bioorg. Med. Chem. Lett.*, 2012, **22**, 1299–1307.

24 A. M. Mfuh, J. D. Doyle, B. Chhetri, H. D. Arman and O. V. Larionov, *J. Am. Chem. Soc.*, 2016, **138**, 2985–2988.

25 J. Luo, X. Jia, Y. Hu, J. Chen and T. Sun, *Org. Biomol. Chem.*, 2021, **19**, 10455–10459.

26 I. A. I. Mkhalid, J. H. Barnard, T. B. Marder, J. M. Murphy and J. F. Hartwig, *Chem. Rev.*, 2010, **110**, 890–931.

27 J. S. Wright, P. J. H. Scott and P. G. Steel, *Angew. Chem. Int. Ed.*, 2021, **60**, 2796–2821.

28 M. J. Ingleson, *Synlett*, 2012, **23**, 1411–1415.

29 A. Ros, R. Fernández and J. M. Lassaletta, *Chem. Soc. Rev.*, 2014, **43**, 3229–3243.

30 S. A. Iqbal, J. Pahl, K. Yuan and M. J. Ingleson, *Chem. Soc. Rev.*, 2020, **49**, 4564–4591.

31 T. Ishiyama, H. Isou, T. Kikuchi and N. Miyaura, *Chem. Commun.*, 2010, **46**, 159–161.

32 H. Itoh, T. Kikuchi, T. Ishiyama and N. Miyaura, *Chem. Lett.*, 2011, **40**, 1007–1008.

33 I. Sasaki, H. Doi, T. Hashimoto, T. Kikuchi, H. Ito and T. Ishiyama, *Chem. Commun.*, 2013, **49**, 7546–7548.

34 M. J. S. Dewar and R. Dietz, *Tetrahedron Lett.*, 1959, **1**, 21–23.

35 Q. J. Zhou, K. Worm and R. E. Dolle, *J. Org. Chem.*, 2004, **69**, 5147–5149.

36 W. Di and C. Liu, *Preparation Method for Tavaborole, Faming Zhuanli Shenqing*, CN106467557, 2017.

37 A. M. Genaev, G. E. Salnikov, V. G. Shubin and S. M. Nagy, *Chem. Commun.*, 2000, 1587–1588.

38 T. S. De Vries, A. Prokofjevs, J. N. Harvey and E. Vedejs, *J. Am. Chem. Soc.*, 2009, **131**, 14679–14687.

39 S. Rej and N. Chatani, *J. Am. Chem. Soc.*, 2021, **143**, 2920–2929.

40 C. D. Good and D. M. Ritter, *J. Am. Chem. Soc.*, 1962, **84**, 1162–1166.

41 W. D. Phillips, H. C. Miller and E. L. Muetterties, *J. Am. Chem. Soc.*, 1959, **81**, 4496–4500.

42 P. V. Ramachandran, A. A. Alawaed and H. J. Hamann, *Org. Lett.*, 2023, **25**, 4650–4655.

43 I. Bernal, J. Cetrullo, J. Cai, R. A. Geanangel and J. H. Worrell, *J. Chem. Soc., Dalton Trans.*, 1995, 99–104.

44 M. Bao, Y. Dai, C. Liu and Y. Su, *Inorg. Chem.*, 2022, **61**, 11137–11142.

45 S. Pal, S. Chowdhury, E. Rozwadowski, A. Auffrant and C. Gosmini, *Adv. Synth. Catal.*, 2016, **358**, 2431–2435.

46 T. S. De Vries, PhD Thesis, The University of Michigan, 2008.

47 L. Pan, K.-M. Lee, Y.-Y. Chan, Z. Ke and Y.-Y. Yeung, *Org. Lett.*, 2023, **25**, 53–57.

48 D. P. Curran, A. Solovyev, M. Makhlouf Brahmi, L. Fensterbank, M. Malacria and E. Lacôte, *Angew. Chem. Int. Ed.*, 2011, **50**, 10294–10317.

49 S. Gardner, T. Kawamoto and D. P. Curran, *J. Org. Chem.*, 2015, **80**, 9794–9797.

50 A. Solovyev, Q. Chu, S. J. Geib, L. Fensterbank, M. Malacria, E. Lacôte and D. P. Curran, *J. Am. Chem. Soc.*, 2010, **132**, 15072–15080.

51 A. Prokofjevs, A. Boussonnière, L. Li, H. Bonin, E. Lacôte, D. P. Curran and E. Vedejs, *J. Am. Chem. Soc.*, 2012, **134**, 12281–12288.

52 S. Nerkar and D. P. Curran, *Org. Lett.*, 2015, **17**, 3394–3397.

53 J. E. Radcliffe, V. Fasano, R. W. Adams, P. You and M. J. Ingleson, *Chem. Sci.*, 2019, **10**, 1434–1441.

54 E. R. Clark, A. Del Grosso and M. J. Ingleson, *Chem. Eur. J.*, 2013, **19**, 2462–2466.

55 C. Chen, J. Li, C. G. Daniliuc, C. Mück-Lichtenfeld, G. Kehr and G. Erker, *Angew. Chem. Int. Ed.*, 2020, **59**, 21460–21464.

56 I. A. Cade and M. J. Ingleson, *Chem. Eur. J.*, 2014, **20**, 12874–12880.

57 A. F. Eichhorn, S. Fuchs, M. Flock, T. B. Marder and U. Radius, *Angew. Chem. Int. Ed.*, 2017, **56**, 10209–10213.

58 D. H. McDaniel and H. C. Brown, *J. Org. Chem.*, 1958, **23**, 420–427.

59 K. Bourumeau, A.-C. Gaumont and J.-M. Denis, *J. Organomet. Chem.*, 1997, **529**, 205–213.

60 A. Solovyev, S. J. Geib, E. Lacôte and D. P. Curran, *Organometallics*, 2012, **31**, 54–56.

61 A. Del Grosso, P. J. Singleton, C. A. Muryn and M. J. Ingleson, *Angew. Chem. Int. Ed.*, 2011, **50**, 2102–2106.

62 P. Erdmann and L. Greb, *Angew. Chem. Int. Ed.*, 2022, **61**, e202114550.

63 A. Allenby, MChem Thesis, The University of Edinburgh, 2022.

64 D. M. Lindsay and D. McArthur, *Chem. Commun.*, 2010, **46**, 2474–2476.

65 G. M. Sheldrick, *Acta Cryst C*, 2015, **71**, 3–8.

66 O. V. Dolomanov, L. J. Bourhis, R. J. Gildea, J. a. K. Howard and H. Puschmann, *J. Appl. Cryst.*, 2009, **42**, 339–341.

67 G. M. Sheldrick, *Acta Cryst. A*, 2015, **71**, 3–8.

Chapter 3

'Borylation Directed Borylation' of Indoles using Pyrazabole Electrophiles

Chapter 3: 'Borylation Directed Borylation' of Indoles using Pyrazabole Electrophiles

3.1 Introduction

Indole is a ubiquitous heterocycle widely found in natural products and biologically active compounds (**Figure 3.1a**).[1] Tryptophan, a 3-substituted indole derivative, is an essential amino acid and a component in most proteins, whilst serotonin is a vital neurotransmitter in the central nervous system.[2] Owing to their abundance in nature, indoles are extensively utilised as structural motifs in pharmaceuticals (**Figure 3.1b**).[3] Substituted indoles have been previously described as "privileged structures", capable of binding to several biological receptors with high affinity.[4,5] For example, psilocin and LSD are non-selective serotonin receptor agonists which cause potent hallucinogenic effects. Other indole-containing pharmaceutical compounds include the nonsteroidal anti-inflammatory drug Etodolac and the erectile dysfunction medication Tadalafil.[6]

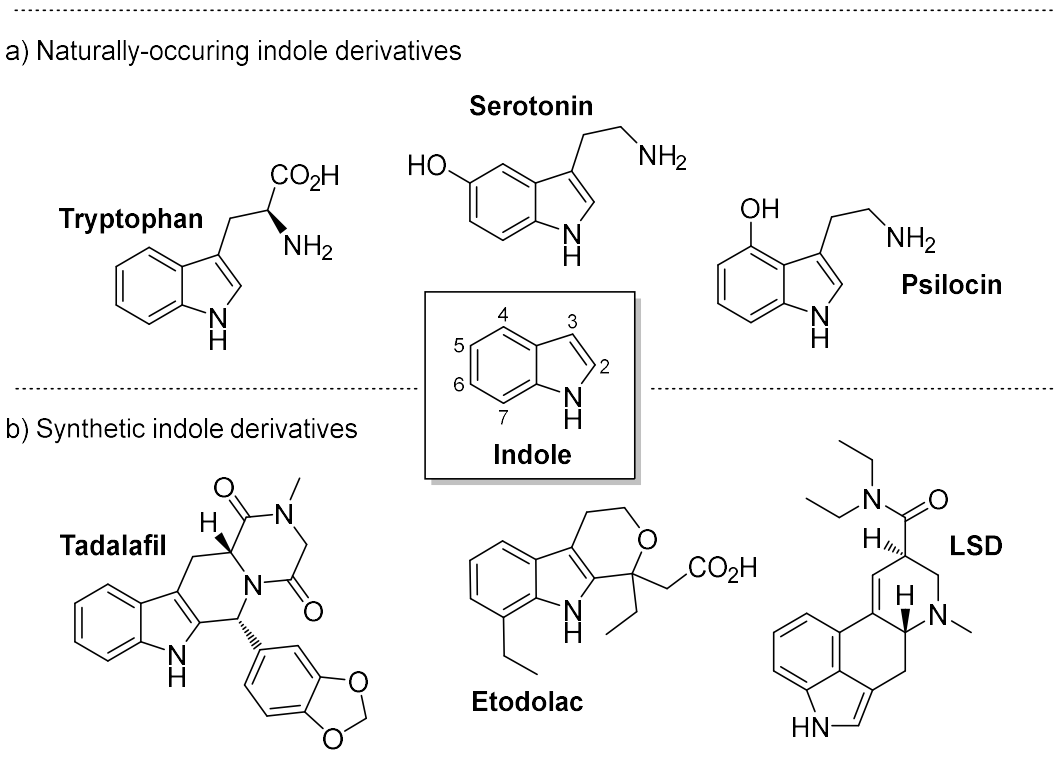

Figure 3.1: Examples of **a)** naturally occurring indole derivatives and **b)** synthetic indole derivatives.

Indoline is closely related to indole, where the C2-3 bond is instead saturated (**Figure 3.2**). The indoline moiety also is present in numerous biologically active natural products,[7,8] such as physostigmine, which is used as an antidote in atropine poisoning.[9,10] It is also found in several drug candidates.[11–13] Substituted indolines are commonly prepared through reduction of the more commercially available parent indoles, with several well-established methods for this.[14,15]

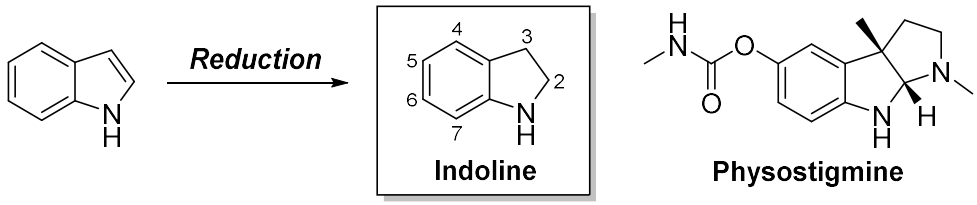

Figure 3.2: Synthesis of indolines via the reduction of the respective parent indole, and physostigmine, an indoline-containing natural product with useful medicinal applications.

C-H Functionalisation of Indoles

Considering the synthetic importance of both indole and indoline compounds, the development of new routes to substituted indoles is an important area of research for synthetic organic chemists. Short, atom-economical routes from the parent indole are desirable, with C-H functionalisation a powerful methodology to produce complex indole scaffolds with a range of functionalities and substitution patterns.[16,17] Examples of C-H functionalisation at the C2- and 3-positions of indole are much more prevalent than at the C4-/5-/6-/7- positions, owing to the higher reactivity of the enamine unit over the benzenoid ring.[18,19]

Focusing on C-H borylation specifically, transition metal (mostly iridium) catalysed C-H borylation of indoles largely occurs at the more acidic C2, though this electronic directing effect can be overridden by steric factors (*vide infra*).[20–23] Alternative methods of indole C-H borylation include lithiation/borylation, where deprotonation followed by trapping again yields 2-borylated indoles,[24] and electrophilic C-H borylation, where regioselectivity is controlled by the heteroarene's electronics. This leads to C3-borylation for indole,[25,26] and with the use of excess reagent resulting in C3, C5-diborylation.[27]

Regioselective C-H borylation onto indole's benzenoid unit at C4, C6 and C7 therefore remains a challenge for both metal and metal-free systems.

Directed C-H Borylation of Indoles

One approach used to direct the selectivity of C-H borylation towards the benzenoid C-H positions is to use substrates with substituents at C2 and/or C3, thereby preventing reactivity at these sites.[28,29] This approach limits the scope of substrates that can be used, however, hence will not be discussed any further.

A more generally applicable alternative is the use of directing groups to enable C-H borylation at positions that are otherwise challenging to functionalise.[30,31] For the regioselective C-H borylation of indole's benzenoid ring, a directing group can be installed onto the indole scaffold, which is capable of coordinating to the borylation catalyst / borylating reagent and positioning it in close spatial proximity to the target C-H. The directing group can then be removed or modified at the end of the reaction.

One example of the use of directing groups to achieve indole C-H borylation at C7 was reported by Hartwig and co-workers (**Scheme 3.1**).[32] In this one-pot protocol, a ruthenium catalyst first installs a hydrosilyl group at the indole nitrogen atom. This hydrosilyl group then directs the iridium catalyst to functionalise the C7-H, enabling regioselective C-H borylation. The N-silyl bond is then hydrolysed, yielding 7-Bpin *N*-H indoles.

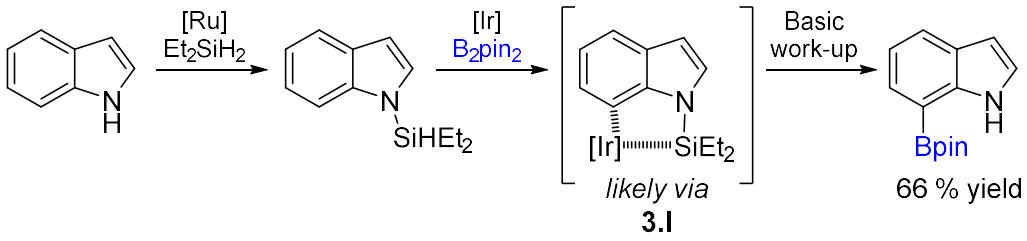

Scheme 3.1: Silyl-directed, iridium catalysed C7-H borylation of indoles.

The C7 selectivity of this process is attributed to the *in situ* formation of a 5-membered metallocycle (**3.I**, **Scheme 3.1**), containing the iridium catalyst and the hydrosilyl group, which is energetically favoured over the 4-membered metallocycle that would be formed from C2-functionalisation. A limitation of this

approach, however, is the use of two expensive precious metal catalysts used at appreciable loadings (1 and 0.5 mol% for Ru and Ir, respectively).

Directing groups have also been used to target indole C7-borylation in metal-free approaches using boron electrophiles (which would otherwise react at C3/C5).[25,26] Work by the groups of Shi and Houk,[33,34] and Ingleson,[35] employed a pivaloyl moiety as a directing group to enable regioselective borylations of indole at C7 using boron tribromide (BBr_3). Prior installation of the pivaloyl group at the indole nitrogen (to form **3.II**, **Scheme 3.2**), followed by addition of BBr_3 enabled C-H borylation at C7. The -BBr_2 moiety could then be transformed into the synthetically versatile Bpin, with the N-pivaloyl moiety also removed in the same step, producing 7-Bpin *N*-H indoles. The pivaloyl group in **3.II** acts as a 'removable', or 'traceless' directing group, as it can be removed in the same one-pot process as the C-H borylation step.[36,37]

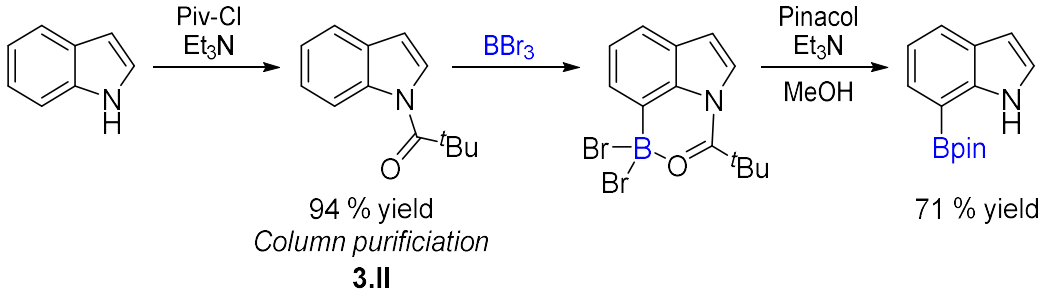

Scheme 3.2: Pivaloyl-directed electrophilic C7-H borylation of indole.

The work by Shi and Houk also reported the challenging C4-H borylation by installation of the pivaloyl directing group at C3, followed by protection of the nitrogen with tosyl chloride (to form **3.III**, **Scheme 3.3**). Addition of BBr_3, with subsequent pinacol protection led to the 4-borylated products, but the pivaloyl directing group and the nitrogen protecting group could not be removed.[33]

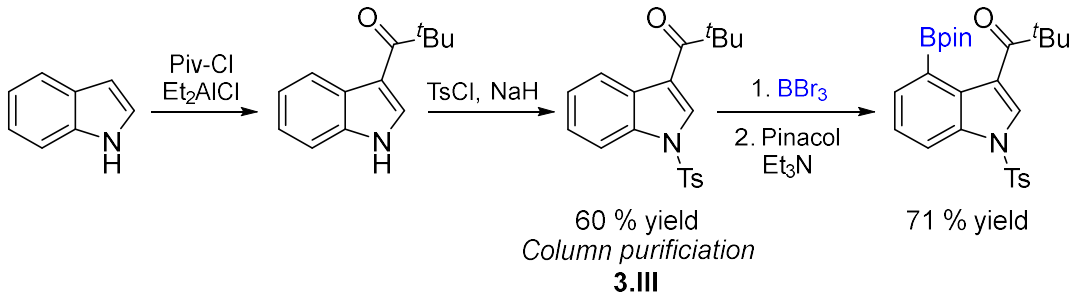

Scheme 3.3: Pivaloyl-directed electrophilic C4-H borylation of indole.

The limitation of these processes, and of directing groups in general, is the extra steps and compatibility problems created by the installation and/or removal of the directing groups (which can require forcing conditions that other functional groups may not tolerate).[36,37] In the examples by Shi, Houk and Ingleson, column chromatography is required after directing group installation (compounds **3.II** and **3.III**), reducing the overall efficiency of the processes.[33–35] Further loss in efficiency may be incurred through removal (or modification) of the directing group (as per the C3-acyl directed C4-H borylation process in **Scheme 3.3**). In particular, indole C7-Bpin groups are sensitive to protodeboronation and so the conditions required for directing group removal may result in decomposition of the borylated compound.[38] Overall, these limitations may hinder the practical applications of this approach.

Transient Directing Groups in C-H Borylation

A more efficient alternative to the use of preinstalled directing groups on the indole scaffold is to use 'transient' directing groups which are installed onto the (hetero)arene, used to direct C-H borylation, and removed (or transformed into a new useful functionality) all in a one-pot process without requiring the isolation/purification of intermediates.[36] The use of transient directing groups is well established in transition metal catalysed C-H activation reactions, enabling highly regioselective C-H activation at otherwise unreactive C-H bonds, whilst improving the overall step-efficiency, atom economy and functional group compatibility of the process.[37]

Transient directing groups also have been utilised in transition metal-catalysed C-H borylation reactions. For example, in the iridium catalysed *ortho* borylation

of anilines reported by Smith and co-workers.[39] In this process 'B_2eg_2' (eg = ethylene glycolate) is used as the borylating reagent, which acts as a transient directing group by hydrogen-bonding to the aniline N-H whilst coordinating to the iridium catalyst, thereby positioning the catalyst for the *ortho* C-H functionalisation of aniline (**3.IV**, **Scheme 3.4**). Addition of pinacol and work-up cleaves the N-Beg unit and generates 2-Bpin anilines within a one-pot process.

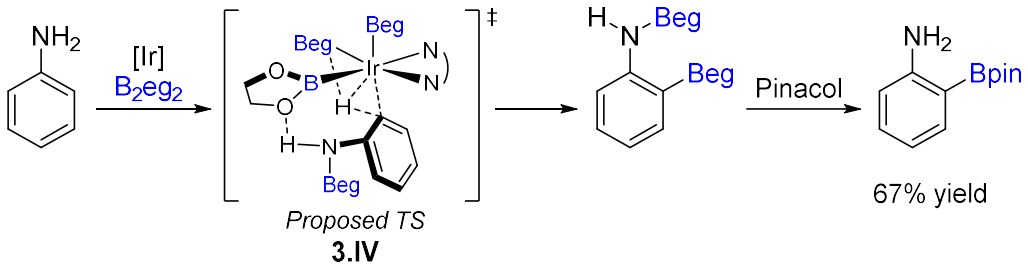

Scheme 3.4: The iridium-catalysed *ortho*-borylation of anilines using B_2eg_2, which acts as a transient directing group.

For the C-H borylation of indoles, there have been reports on the application of bulky blocking groups that are installed onto indole's nitrogen *in situ* and enable the metal-catalysed C3-H borylation (by sterically hindering C-H borylation at C2).[40,41] These blocking groups can subsequently be removed in the one-pot processes, hence are often described as 'traceless'. However, since these blocking groups do not coordinate to the metal catalyst and so do not 'direct' C-H borylation, they will not be discussed any further.

The application of transient directing groups in electrophilic C-H borylation methodologies is underdeveloped. One example is the *ortho* C-H borylation of benzaldehyde derivatives using BBr_3, with regioselectivity controlled by a 'transient' imine (**Scheme 3.5**).[42,43] In this work the electron-deficient benzaldehyde starting material is initially unreactive towards electrophilic C-H borylation. By transformation of the carbonyl functional group into an electronically activating imine moiety *in situ* (intermediate **3.V**), a transient directing group is formed which, upon addition of BBr_3, enables regioselective *ortho* C-H borylation. It should be noted, however, that this process requires drying *in vacuo* after imine formation to remove excess amine and H_2O, prior to addition of BBr_3.

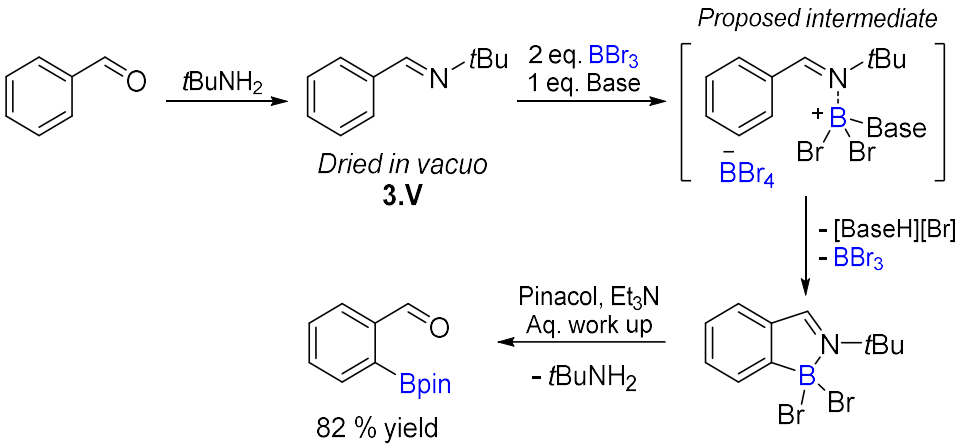

Scheme 3.5: Electrophilic C-H borylation of benzaldehyde yields *ortho*-Bpin benzaldehyde via *in situ* formation of a transient imine directing group.

The -BBr_2 moiety could be converted to the more synthetically familiar Bpin within the same one-pot process and the imine moiety was converted back to a carbonyl group during aqueous work-up, yielding 2-Bpin benzaldehydes in excellent yields.

Diboron Compounds as Transient Directing Groups

A transient directing group strategy could be applied to the electrophilic C-H borylation of indole to target reactivity towards the less reactive benzenoid positions without the issue of directing group installation / removal in separate steps. One novel approach to achieve this would be to incorporate the boron electrophile and the directing group into one molecule. This could be achieved using a diboron compound that behaves as a bidentate directing group in a 'borylation directed borylation' approach.[44] In theory, one boron unit of the diboron compound could act as the transient directing group and initially borylate the more reactive C3 or N positions on the 5-membered ring of indole (**Scheme 3.6a** and **b,** respectively). If the diboron compound has a fixed B···B distance similar to the C3-H···C4-H (ca. 2.7 Å)[45] or N-H···C7-H (ca. 3.1 Å)[33] distance in indole, this would position the second boron unit in close spatial proximity to C4-H or C7-H, respectively, enabling regioselective C-H borylation. The more reactive C3-B / N-B bond could then be protodeboronated during work-up,[46,47] generating C4-borylated or C7-borylated indoles that are otherwise challenging to synthesise.

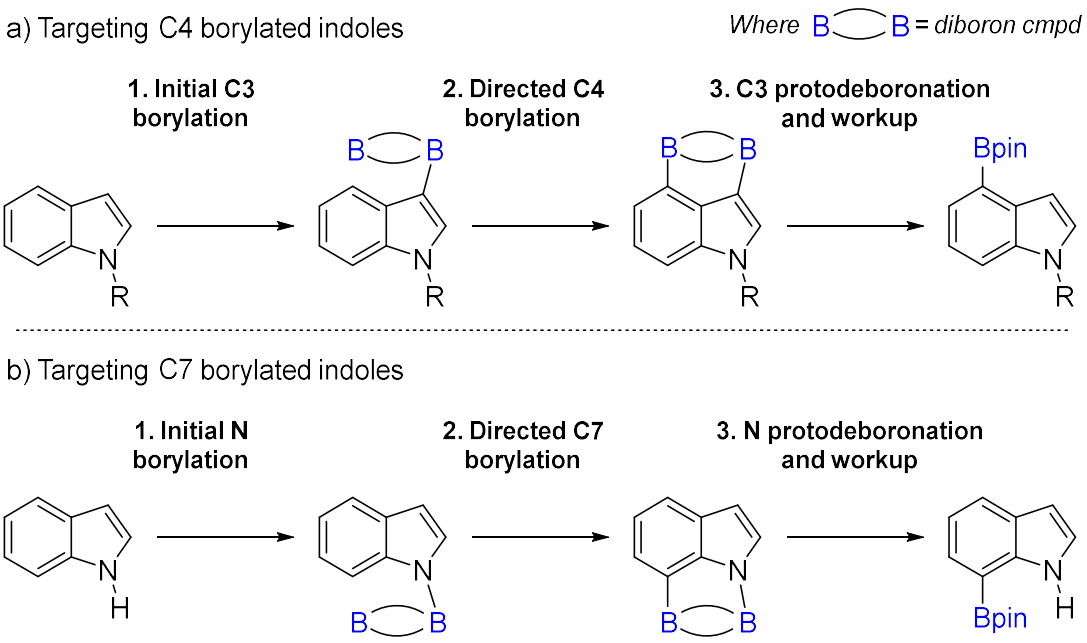

Scheme 3.6: Proposed **a)** C4-borylation and **b)** C7-borylation of indoles using a transient diboron directing group.

To enable this proposed reactivity, the diboron compound must have a robust structure with a fixed B···B distance. If the B···B distance is not fixed or the structure breaks apart easily, the templating effect that provides the regioselectivity would be lost. In addition, the B···B distance in the diboron compound must be close to the C3-H···C4-H distance or N-H···C7-H distance in indole, otherwise there will likely be too much strain on the indole scaffold to enable diborylation. Furthermore, the diboron compound must be able to perform double electrophilic borylation. Finally, in order to be 'transient' the diboron group must be readily cleaved / transformed into a synthetically useful boronic acid / ester moiety (e.g. Bpin) to enable the wide range of subsequent transformations possible with organoboranes.[48,49]

One relevant example of the use of diboron compounds in double electrophilic C-H borylation was reported by Wagner and co-workers.[50,51] In this work, an *in situ* generated diboron compound (**3.VI**, **Scheme 3.7**) undergoes vicinal diborylation on a range of arene moieties to generate doubly boron-doped polycyclic aromatic hydrocarbons (B-PAHs). One boron unit in the diboron compound undergoes an initial borylation at the most reactive C-H position, thereby positioning the second boron unit in close proximity to the vicinal C-H,

enabling double borylation. Whilst this is a useful technique for accessing B-PAHs, the diborylated products cannot be transformed into boronic esters to enable further synthetic diversification, limiting the utility of this reaction.

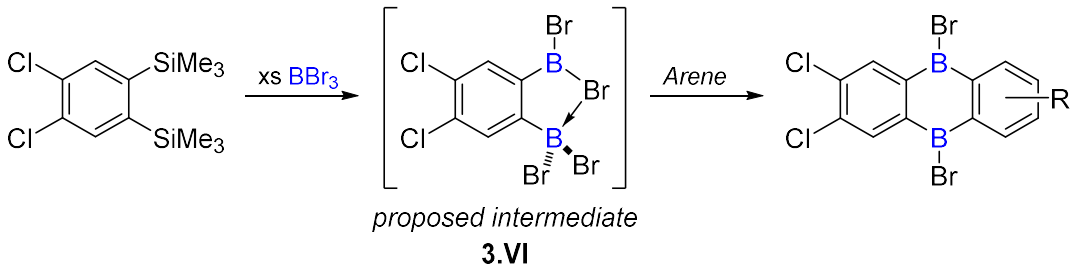

Scheme 3.7: Vicinal double electrophilic C-H borylation of arenes using an *in situ* generated diboron compound.

A diboron compound with an appropriate B···B distance is pyrazabole, a well-studied diboron compound with established reactivity and applications.[52–56] Pyrazabole has a B···B distance of ca. 2.9 Å,[57] meaning it is well suited for the C3/C4 or N/C7 borylation of indoles. Pyrazabole is easily synthesised from pyrazole and $BH_3{\cdot}SMe_2$ and is air/moisture stable (**Scheme 3.8**).[58] The B-H bonds of pyrazabole undergo facile activation via substitution reactions, with the B_2N_4 core remaining intact throughout.[59–61] The B_2N_4 core of pyrazabole is relatively flexible and can adopt a planar, chair and boat conformations, which may help lower barriers in borylation directed borylation processes and reduce strain in the diborylated indole products.[62]

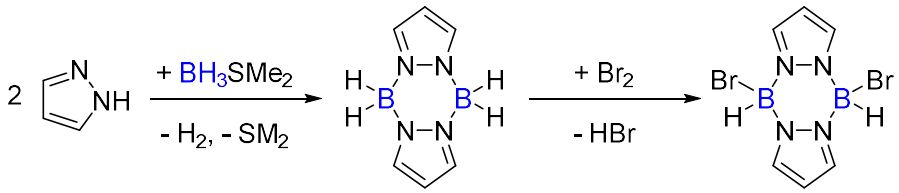

Scheme 3.8: Synthesis of pyrazabole, and activation of the B-H bonds via a double substitution reaction.

Furthermore, the dissociation of pyrazabole into its respective monomers was previously shown to be endergonic (**Scheme 3.9a**), so it should be robust enough under the reaction conditions to have the desired directing effect.[63] This was calculated to be significantly more endergonic than the dissociation of an

amidoborane dimer, an alternative diboron species with a shorter B···B distance (**Scheme 3.9b**).[64]

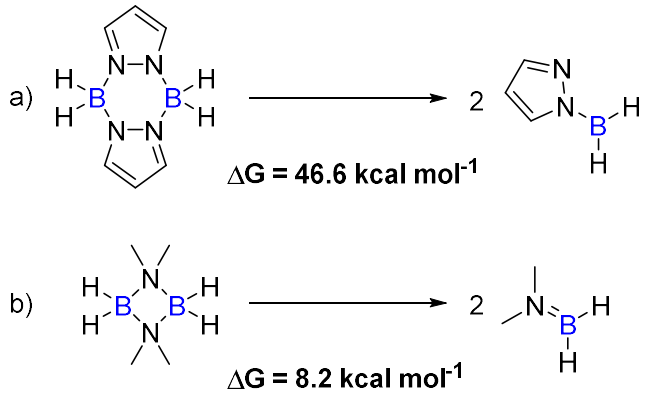

Scheme 3.9: Calculated energy changes during the dissociation of **a)** pyrazabole into its pyrazole-borane monomer and **b)** amidoborane dimer $[Me_2NBH_2]_2$ into its monomer $Me_2N{=}BH_2$.

Based on this, pyrazabole was deemed to be a suitable candidate for a diboron directing group to be used in the C3/C4 or N/C7 diborylation of indoles. First, a suitable activator to generate sufficient electrophilicity at boron needed to be identified, so that the reactivity with indoles could be evaluated.

3.2 Preliminary Studies

The initial work described in this section was completed by Dr Jürgen Pahl (unless otherwise stated) prior to the author's work on this project and is discussed in more detail in the publication of this work.[65]

Activation of Pyrazabole to Mono- or Di-topic Electrophiles

There is considerable literature precedence for the use of *bis*-(trifluoromethane sulfonyl) amine ($HNTf_2$) in the activation of LB-BH_3 complexes (e.g. NHC-boranes) to form electrophilic borenium ion equivalents able to functionalise π-nucleophiles.[66–69] Hence, $HNTf_2$ was chosen for initial studies in the activation of pyrazabole to a mono- / di-electrophile.

The addition of 2 equiv. of $HNTf_2$ to pyrazabole (**3.1**) resulted in immediate evolution of H_2 gas and precipitation of a white solid (**Scheme 3.10**). *Di*-NTf_2 pyrazabole (**3.2**) could be directly isolated without the need for further purification. It is poorly soluble in non-coordinating / halocarbon solvents, which prevented complete characterisation by NMR spectroscopy. However, it showed some solubility in *o*-DFB with δ_{11B} = -3 ppm, shifted downfield compared to unactivated pyrazabole (δ_{11B} = -8.3 ppm).

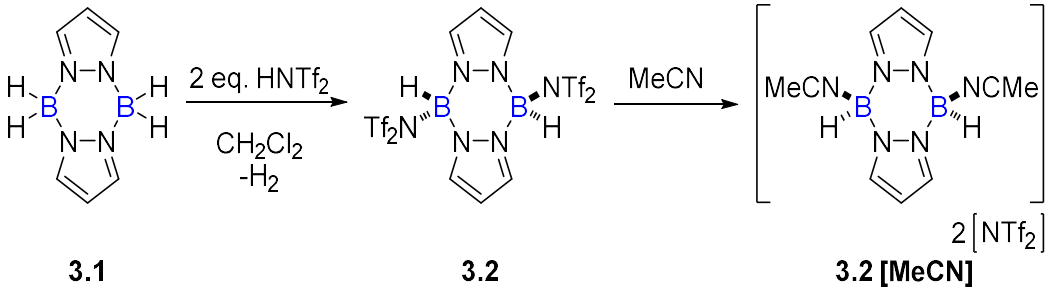

Scheme 3.10: Activation of pyrazabole to *di*-NTf_2 pyrazabole, followed by formation of *di*-MeCN pyrazabole.

The solid-state structure of **3.2** showed the substitution of two B-H bonds by $HNTf_2$, with the two NTf_2 units in a *trans*- arrangement. With a B···B distance of 3.126(2) Å, **3.2** is well suited for the C3/C4 or N/C7 diborylation of indoles.[33,45] The two NTf_2 units can be displaced from **3.2** by the addition of excess MeCN. This demonstrates that *di*-NTf_2 pyrazabole **3.3** reacts as a double boron electrophile.[67]

The salt, **3.2 [MeCN]**, crystallises as the *cis*-isomer, showing that the formation of *di*-NTf_2 pyrazabole **3.2** does not fix the *trans*- configuration. This is important as the product from indole double borylation would have a *cis*- configuration.

When pyrazabole was reacted with 1 equiv. of $HNTf_2$, 0.5 equiv. was left unreacted, whilst 0.5 equiv. of **3.2** was formed. NMR spectroscopy of 1:1 mixtures of **3.1** and **3.2** showed broadening of peaks in the ^{1}H NMR spectrum, whilst the ^{11}B NMR spectrum showed new broad resonances between -1 and -5 ppm. This suggests an exchange process occurs between **3.1** and **3.2** in solution, giving access to the mono-electrophile, *mono*-NTf_2 pyrazabole (**3.3**, **Scheme 3.11**). Attempts to isolate **3.3** from the reaction were unsuccessful and just yielded an equimolar mixture of **3.1** and **3.2**.

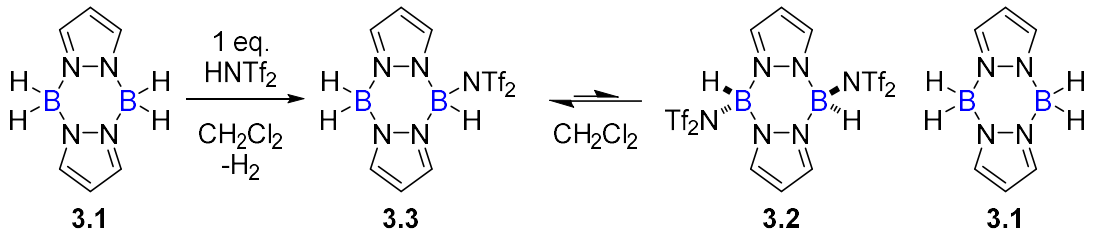

Scheme 3.11: Proposed formation of *mono*-NTf_2 pyrazabole *in situ*, by activation of **3.1** with 1 equiv. $HNTf_2$ or by substituent exchange between equimolar **3.1** and **3.2** in solution.

Reactivity with *N*-Methyl Indole

Reactivity studies with *N*-Me indole and *mono*-NTf_2 pyrazabole (**3.3**, formed *in situ* from the reaction of **3.1** and 1 equiv. $HNTf_2$), revealed consumption of *N*-Me indole along with the formation of a new species. This was fully characterised as the product from the hydroboration of *N*-Me indole at the C2=C3 bond, (**3.4**, **Scheme 3.12**), resulting in one boron unit of the pyrazabole bonded at C3 and the second coordinated at N. The reaction did not proceed any further, even upon heating. It should be noted that no hydroboration of *N*-methyl indole (or *N*-H indole, *vide supra*) occurred when the unactivated pyrazabole **3.1** was used. Swapping the pyrazabole for an NHC-borane, $IMeBH_2NTf_2$, was also unsuccessful and no hydroboration was observed. This implies that the rapid hydroboration

of *N*-methyl indole with *mono*-NTf_2 pyrazabole may be related to the *bis*-hydroborane structure of **3.3**.

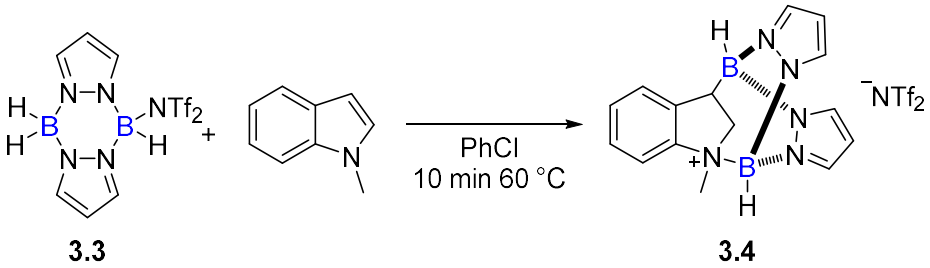

3.3 **3.4**

Scheme 3.12: Hydroboration of *N*-methyl indole with **3.3** to form **3.4**.

Reactivity with *N*-SiMe$_3$ Indole

Preventing / weakening the coordination of boron at nitrogen could potentially lead to that boron unit undergoing C-H borylation at C4, resulting in C3/C4-borylated indolines. It was hypothesised that increasing the steric bulk at nitrogen could disfavour coordination of the second boron unit at nitrogen following hydroboration.

The reactions of **3.3** with *N*-trimethylsilyl indole (*N*-TMS indole) still resulted in hydroboration and N-B bond formation, with the formation of **3.5** observed (**Scheme 3.13**). However, heating the reaction mixture containing **3.5** to 100 °C led to the formation of a new species. This was identified as the double-borylated indoline derivative **3.6**, with one pyrazabole unit bound at N and C7.

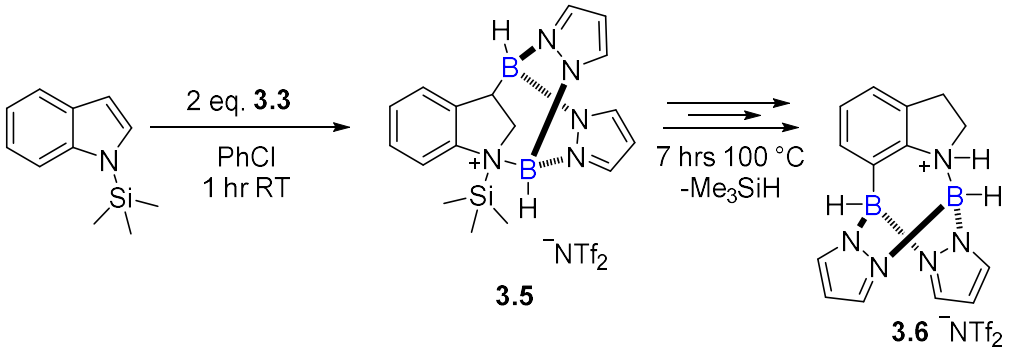

3.5 **3.6**

Scheme 3.13: Hydroboration of *N*-trimethylsilyl indole with **3.3** to form **3.5**, which upon heating is converted to **3.6**.

The N-TMS bond had been cleaved and converted to a N-H, with Me_3SiH observed as the major silane by-product (presumably formed by abstraction of a hydride

from a pyrazabole B-H unit by a silane electrophile).[70] The yield of **3.6** was significantly improved by increasing the loading of **3.3** to 2 equiv. Based on these observations, a reaction pathway was proposed (**Scheme 3.14**). In this pathway, C7-H borylation occurs alongside protodeboronation of the C3-B bond.

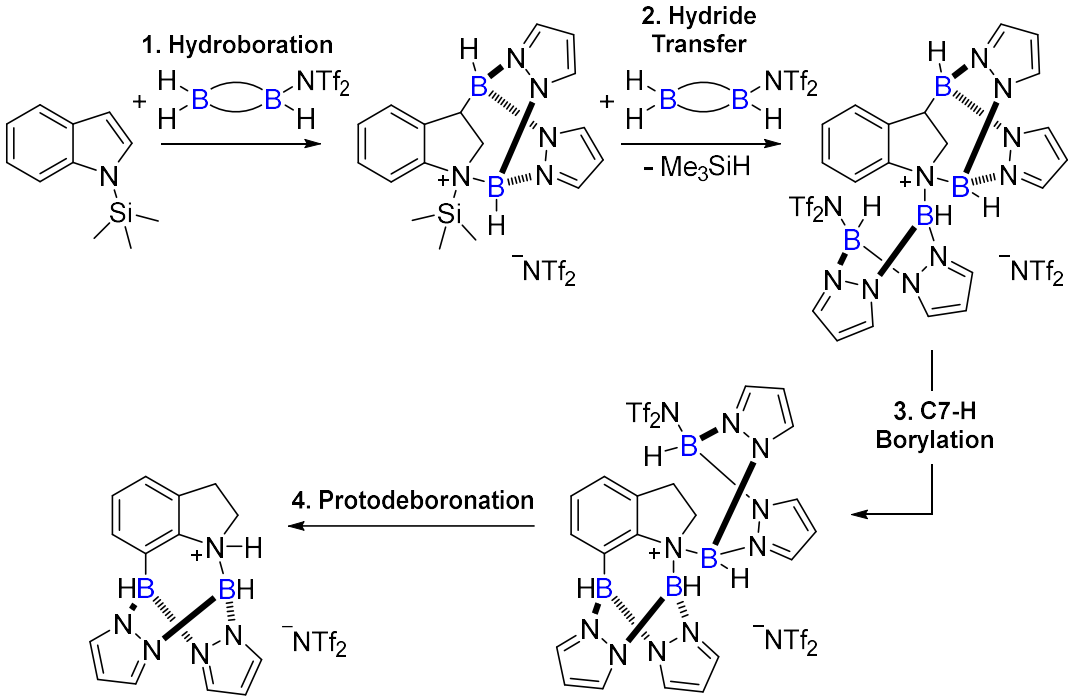

Scheme 3.14: Proposed reaction pathway for the reactivity of *N*-SiMe$_3$ indole, showing how **3.6** could be formed in the reaction with **3.3**.

The observation that the N-SiMe$_3$ bond was broken over the N-B coordination suggested that achieving C3/C4 diborylation via this approach was unlikely to be successful. Therefore, focus was shifted to developing the reduction and N/C7 diborylation of *N*-H indoles to yield C7-borylated indolines.

Reactivity with *N*-H Indole

Applying the reaction conditions established for *N*-TMS indole, the reaction of *N*-H indole and 2 equiv. of **3.3** (hereby always formed *in situ* from a 1:1 mixture of pyrazabole and *di*-NTf_2 pyrazabole) gave complete conversion to the N/C7-borylated product (**3.6**, **Figure 3.3**), after 18 hours at 100 °C.

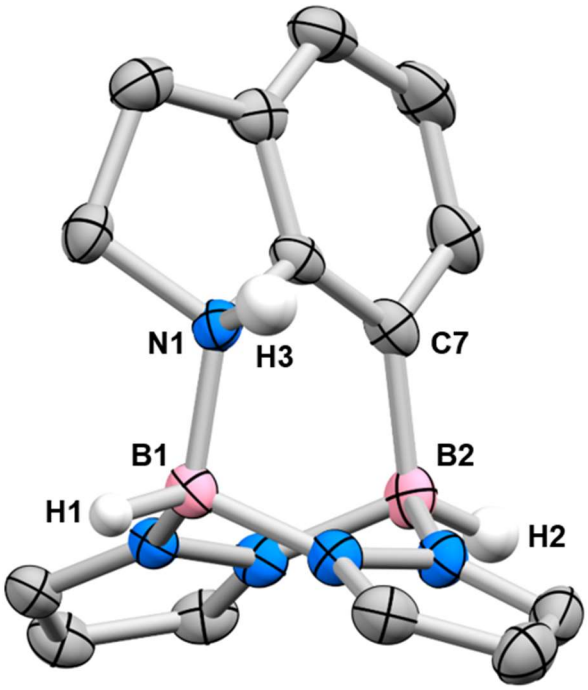

Figure 3.3: Solid-state structure of the cationic portion of **3.6** *(measured and solved by Dr Marina Uzelac).* Ellipsoids at the 50% probability level. Hydrogen atoms (except H1, H2, H3) removed for clarity.
Selected distances (Å): N1-B1 1.578(3), C7-B2 1.602(4), B1···B2 2.858(4).

It should be noted that the reaction of *N*-H indole with 2 equiv. of *di*-NTf_2 pyrazabole, **3.2**, led to no observable N/C7-H borylation, with significant indole leftover after 18 hours at 100 °C. Addition of a hindered base, 2,6-(tBu)$_2$-4-methyl pyridine (DBP), to the reaction resulted in C2-C3 reduction and N/C7-borylation to form **3.6,** as observed with **3.3**. These 'alternative' reaction conditions gave the same outcome, but are less atom efficient than using just **3.3**, so were not used for further scoping / optimisations.

Going back to the reaction of *N*-H indole with **3.3**, the pyrazabole unit of **3.6** was then converted *in situ* to the more synthetically useful pinacol boronate ester by refluxing the sample for 18 hours in an aqueous/DCM solution with excess

pinacol and K_2CO_3. This process cleaved the more reactive N-B bond, but maintained the C7-B bond, giving 7-Bpin indoline (**3.7**, **Scheme 3.15**). Extraction of the Bpin product into pentane, followed by multiple aqueous washes to remove pyrazabole-based impurities gave **3.7** in a 71% isolated yield.

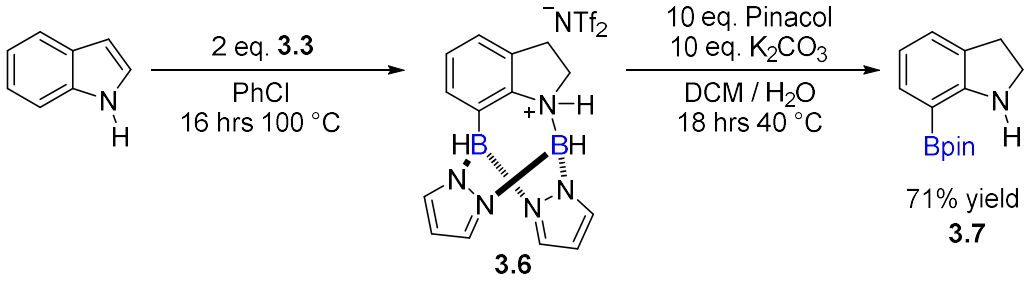

Scheme 3.15: Formation of 7-Bpin indoline by reaction of *N*-H indole with **3.3**.

3.3 Project Aims

The initial work by Dr Jürgen Pahl, discussed in **Section 3.2**, established that *mono*-NTf_2 pyrazabole, **3.3**, can be used to convert *N*-H indole to 7-Bpin indolines through a 'borylation directed borylation' process. Though not the original target of this work, C7-functionalised indolines are of significant interest in medicinal chemistry and beyond (*vide infra*, and see **Section 2.1***)*.[7–13] Therefore, the work described in this chapter aimed to develop and optimise this process and then assess the substrate scope.

The conditions used thus far, depicted in **Scheme 3.15**, had several areas where further optimisation was needed to improve the utility of the overall process:

a) An excess of *mono*-NTf_2 pyrazabole was used, resulting in a stoichiometric amount of pyrazabole waste and a poor atom-economy. This was particularly important to address as it led to several pyrazabole-based impurities that then needed to be removed when isolating / purifying the final product.
b) Large excesses of pinacol and K_2CO_3 were required to form to the Ar-Bpin product, along with relatively harsh conditions (compared to other "pinacol protection" methods).[71]
c) The 7-Bpin indoline products are highly sensitive to protodeboronation, and so are challenging to purify with silica chromatography.[39] Therefore, the development of an alternative purification method was necessary.

Furthermore, this project sought to develop an understanding of the reduction / C7-borylation mechanism. Doing so could potentially support further process optimisation, help to identify compatible substrates, and potentially help to establish whether the C3/C4 diborylation of indoles or indolines is possible using this approach.

3.4 Results and Discussion

3.4.1 Initial Substrate Scoping

Using the initial N/C7-borylation conditions (**Scheme 3.15**), the reactivity of substituted (*N*-H) indoles with *mono*-NTf_2 pyrazabole, **3.3**, were studied and compared to the reactivity of *N*-H indole.

Methyl-Substituted *N*-H Indoles

By comparing the reactivity of indoles with methyl substituents in the 2-, 3-, 5- or 6- positions, the compatibility of a substituent at different positions was explored. 5-methyl indole underwent N/C7-borylation under the same conditions as indole (**Scheme 3.16**). The pinacol protection step also proceeded smoothly, yielding 5-methyl 7-Bpin indoline, **3.8**, in a 73% isolated yield following extraction into pentane and aqueous washing, without the need for any further purification.

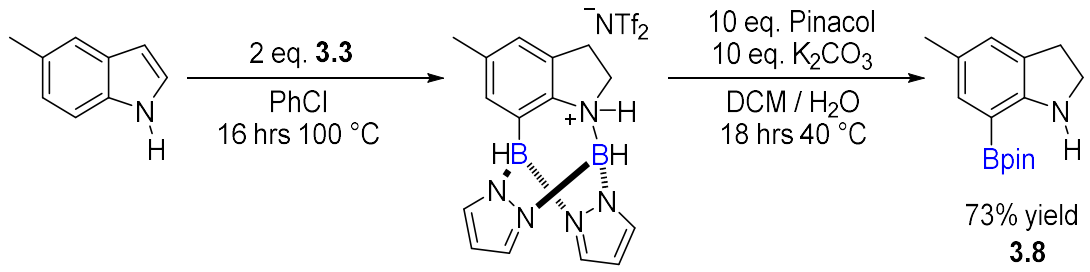

Scheme 3.16: Formation of 5-methyl 7-Bpin indoline by reaction of 5-methyl indole with **3.3**.

For the reaction of 2-methyl indole, heating for 16 hours at 100 °C gave complete consumption of the starting material, but following pinacol protection a minor by-product was observed alongside 2-methyl 7-Bpin indoline (**3.9**). This was identified as 2-methyl 7-Bpin indole (**3.10**) by NMR spectroscopy, where the C2/C3 bond has not been reduced (**Scheme 3.17**). It was hypothesised that having some steric bulk around C2 bond slows down hydride delivery to C2 during hydroboration, and so a small amount of starting material undergoes N/C7-borylation directly, giving the N/C7-borylated indole by-product.

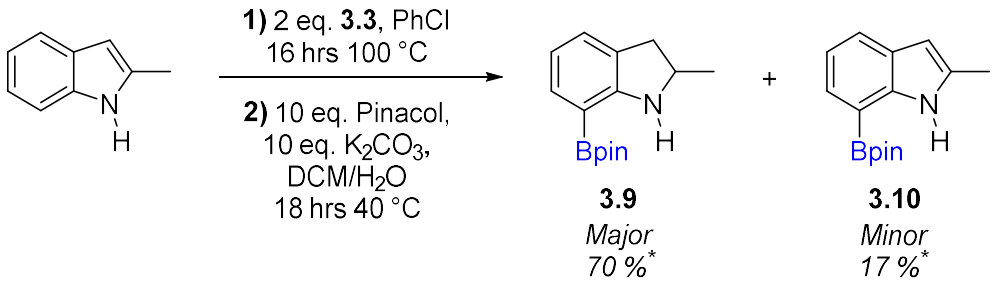

Scheme 3.17: The reaction of 2-methyl indole with **3.3** gave 2-methyl 7-Bpin indoline as the major product, and 2-methyl 7-Bpin indole as the minor product. **(% Yields are NMR yields following work-up, relative to an internal standard).*

Attempts to increase the formation of the **3.10** (as this would be another desirable product) were unsuccessful; however, its formation could be completely prevented (thereby giving **3.9** as the only Bpin product after work-up) by stirring the reaction at room temperature for 1 hour prior to heating to 100 °C. This assumedly gives enough time for the slower hydroboration step to go to completion prior to C7-borylation upon heating.

When reacting 3-methyl indole under the initially established conditions, there was no evidence (via NMR spectroscopy) for the formation of 3-methyl 7-Bpin indole as a by-product (**Scheme 3.18**). This indicates, therefore, that substituents in the 3-position do not hinder the initial hydroboration step to the same extent as substituents in the 2-position, supporting the assumption that it is the hydride delivery to C2 that is slowed down with 2-methyl indole. After 16 hours at 100 °C, there was full consumption of 3-methyl indole, and the N/C7-borylated product was converted into 3-methyl 7-Bpin indoline (**3.11**) without issue.

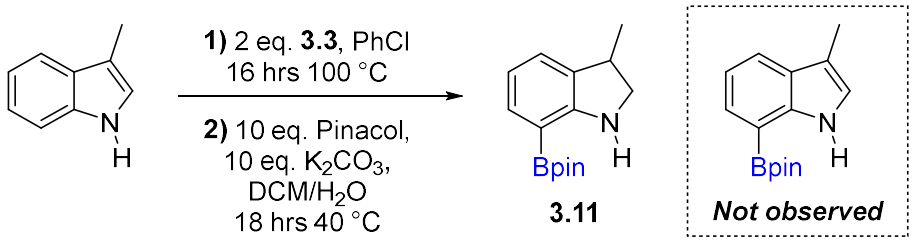

Scheme 3.18: The reaction of 3-methyl indole with **3.3** gave 3-methyl 7-Bpin indoline only, no 3-methyl 7-Bpin indole was observed.

Though 2- and 3-methyl 7-Bpin indoline were the only indoline / Bpin products in their respective reactions, a large amount of pyrazabole impurities were present in both samples that were not removed during the work-up procedure. Several attempts were then made to try to purify the 2-/3-methyl 7-Bpin indoline products without causing protodeboronation of the C7-B bond (which would result in the respective C7-H indoline species).

Heating a crude sample of 3-methyl 7-Bpin indoline (**3.11**) to 40 °C under vacuum (4 x 10^{-2} mbar) for 18 hours was effective at removing most of the leftover unactivated pyrazabole (**3.1**) via sublimation. However, other pyrazabole-based impurities were not removed by this method, and some partial protodeboronation of the C7-B bond was also observed (**Figure 3.4**).

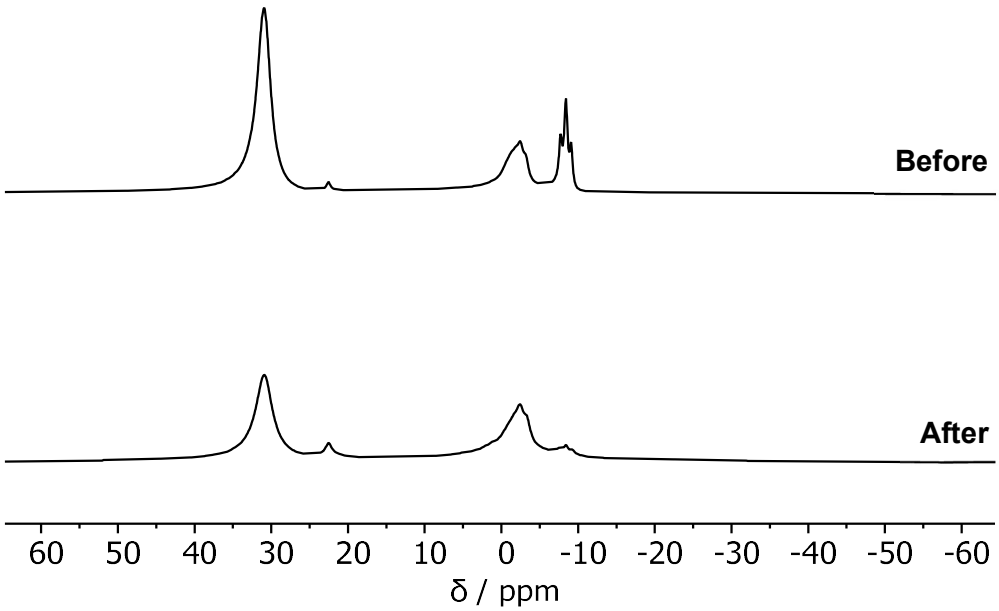

Figure 3.4: Stacked ^{11}B NMR spectra of a crude sample of **3.11** (δ_{11B} = 31 ppm) before and after heating under vacuum at 40 °C for 18 hours, resulting in removal of **3.1** (δ_{11B} = -8 ppm). *(Solvent = $CDCl_3$, NMR temperature = 300 K).*

The 7-Bpin indoline products also underwent protodeboronation when loaded onto silica for chromatography, or if rapidly flushed through a short plug of silica. Treating the silica with a triethylamine solution prior to addition of crude product prevented protodeboronation, but the separation from the pyrazabole-

based impurities was poor and neither 2- nor 3-methyl 7-Bpin indoline could be isolated cleanly via this approach. Reverse phase chromatography (using a C18 column and methanol as the eluent, *see* ***Section 3.6.2*** *for further details*) was compatible: the 7-Bpin indoline products did not undergo protodeboronation and could be separated from the pyrazabole-based impurities. However, the yields were low: for 2-methyl 7-Bpin indoline (**3.9**), the isolated yield was 26%. The origin for this low yield is not clear.

The reactivity of 6-methyl indole under the initial reaction conditions was also evaluated. The N/C7 diborylation proceeded after 18 hours at 100 °C, with full consumption of the starting material and no evidence of issues arising from the increased steric bulk close to C7. Conversion to the 'Bpin' product, however, was more challenging than for other substrates. Using the established conditions (18 hours at 40 °C), two products were observed after work-up in a 7:3 ratio. ^{1}H NMR spectroscopy showed two sets of triplet resonances for each product in the aliphatic region, indicating both products are non-diastereotopic indoline derivatives with non-chiral, 3-coordinate nitrogen (thus are not the 6-methyl analogues of the N/C7-borylated product **3.6**). The minor product was characterised as 6-methyl 7-Bpin indoline (**3.12**, **Scheme 3.19**).

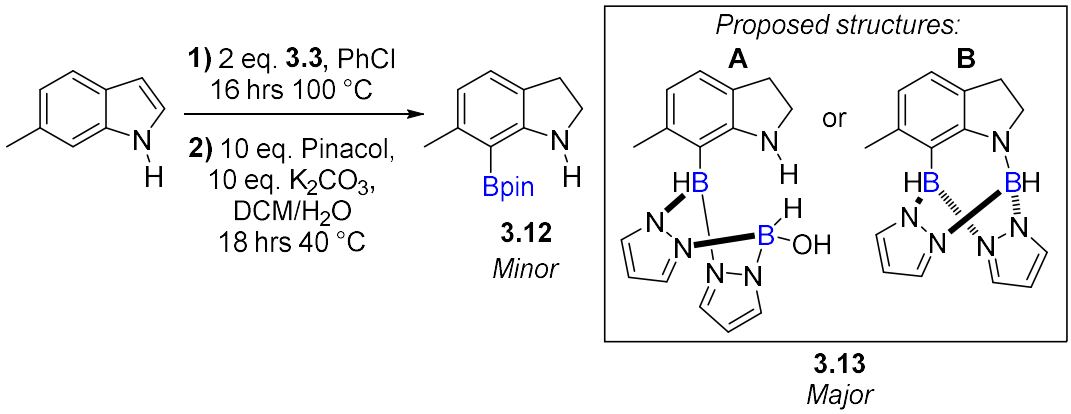

Scheme 3.19: The reaction of 6-methyl indole with **3.3** gave 6-methyl 7-Bpin indoline as the minor product. The major product could not be isolated but was proposed to be either **3.13 A** or **B** based on NMR spectroscopy data.

For the major product, two possible structures were proposed based on the observed $^{1}H/^{13}C$ NMR resonances. One possibility is **3.13A**, with a pyrazabole unit still bonded at C7 but not at nitrogen. Another possible structure, **3.13B**, is the N/C7-borylated product after deprotonation at nitrogen. The major product could not be isolated, and the exact structure could not be confirmed. It was clear, however, that the pyrazabole unit at C7 had not reacted with pinacol. It was hypothesised that the formation of the desired Bpin product, **3.12**, is slower for this substrate due to the increased steric hindrance at C6, and the majority of the N/C7-borylated product forms **3.13A/B** and does not react further. Using more forcing conditions (80 °C) during the pinacol protection step did improve the yield of **3.12** but it remained lower than for other substituted indoles (e.g. 5-methyl indole). In addition, purification was challenging and a clean sample of **3.12** could not be isolated using these reaction conditions.

The reaction of several substituted indoles with **3.3** gave the respective 7-Bpin indoline products, with minor variations needed from the initially established conditions. However, the high-sensitivity of the 7-Bpin indoline products and the number of persistent pyrazabole-based impurities made purification challenging. Though reverse-phase chromatography was a suitable purification method, at this point only a few 7-Bpin indolines were isolated cleanly, and in low yields. Therefore, more work was needed to optimise the procedure so the 7-Bpin indoline products could be obtained in both high purity and yield (*vide infra*).

Halogen-Substituted *N*-H Indoles

The reactivity of halogen-substituted *N*-H indoles was also explored to see if the reaction tolerated less nucleophilic substrates.

The reaction of 5-chloro indole with 2 equiv. **3.3** gave a single product (by *in situ* NMR spectroscopy) after 16 hours 100 °C. Pinacol protection and work-up yielded a single product, but this was not the expected 5-chloro 7-Bpin indoline (**3.14**, **Scheme 3.20**). The ^{1}H NMR spectrum showed an additional resonance in the aromatic region, and the resonances matched 7-Bpin indoline (**3.7**). At some point during the reaction, the C-Cl bond had been converted to C-H.

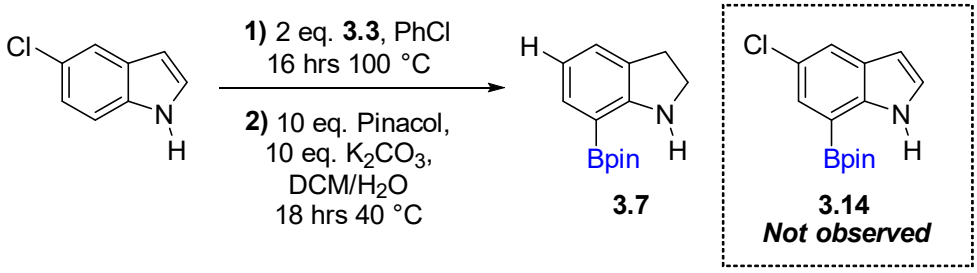

Scheme 3.20: The reaction of 5-chloro indole with **3.3** yielded 7-Bpin indoline. The expected product, 5-chloro 7-Bpin indoline, was not observed.

Monitoring the reaction by *in situ* NMR spectroscopy revealed that after 1 hour at 100 °C most of the starting material had been consumed, and a N/C7-borylated product was observed, characterised by 4 distinctive diastereotopic indoline resonances (**Figure 3.5**, **top**). Upon further heating, this initial product disappeared, and a new species was observed (at similar or overlapping δ).

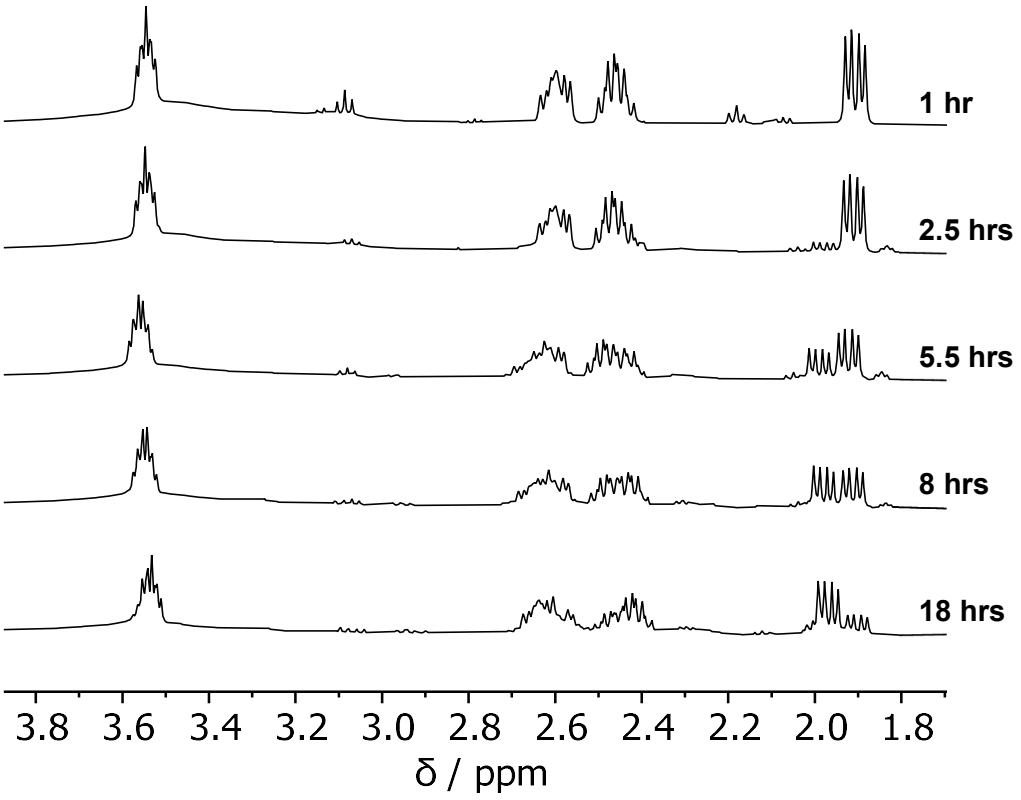

Figure 3.5: Stacked *in situ* ^{1}H NMR spectra for the reaction of 5-chloro indole with **3.3** at 100 °C. *(Solvent = C_6D_5Br, NMR temperature = 300 K).*

Based on this, it is believed that N/C7-borylation of 5-chloro indole proceeds as expected, giving **3.15** as the initial product (**Scheme 3.21**), but this reacts further and undergoes a hydrodehalogenation reaction with a hydride source, resulting in formation of **3.6** after 18 hours (as seen in **Figure 3.5**, **bottom**) This species then undergoes pinacol protection, yielding **3.7** as the only Bpin product.

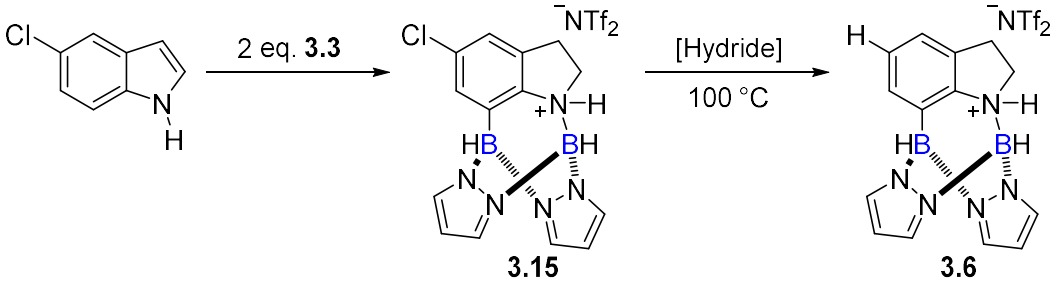

Scheme 3.21: The reaction of 5-chloro indole with **3.3** initially forms **3.15**, but upon extended heating at 100 °C **3.15** reacts with a hydride source to give **3.6**.

The spectra in **Figure 3.5** suggest the formation of **3.6** could be prevented by not overheating. Heating to 100 °C for 1 hour gave mostly **3.15** but some 5-chloro indole remained and small amounts of **3.6** were observed. Better results were achieved by reducing the reaction temperature. Heating to 60 °C for 18 hours resulted in full consumption of starting material and formation of **3.15**. No **3.6** was observed. After pinacol protection, **3.14** was the only indoline species present (**Scheme 3.22**). As before, several pyrazabole-based impurities were not removed during work-up and subsequent purification was challenging. Reverse-phase chromatography gave clean **3.14** in a 33% isolated yield.

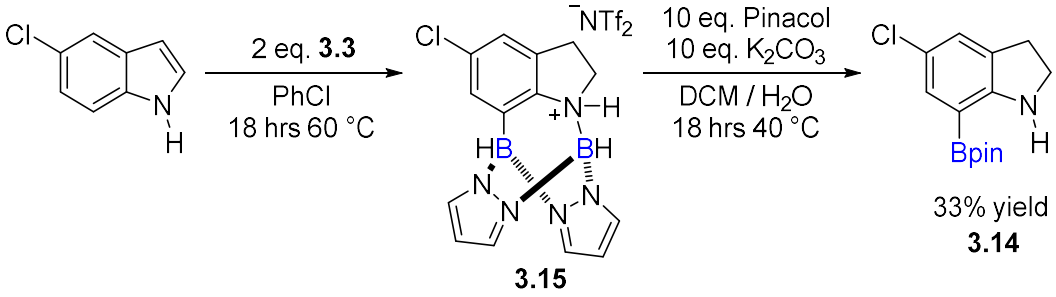

Scheme 3.22: The reaction of 5-chloro indole and **3.3** at 60 °C gave 5-chloro 7-Bpin indoline, with no hydrodehalogenation of the C5-Cl bond observed.

The reactivity of 6-chloro indole was then compared to the 5-chloro. This substrate could be heated to 100 °C for 3 hours, with full conversion of the starting material to the respective N/C7-borylated product (**3.16**, **Scheme 3.23**) with no evidence of hydrodehalogenation of the C6-Cl bond. Extended heating did partially convert **3.16** into a new species, but the reaction was not clean, and the incoming product could not be formed in large enough amounts to confirm its assumed identity as the hydrodehalogenated analogue **3.6**. This implies that changing the position of the chloro-substituent (the leaving group) from the *para* position (relative to the electron-withdrawing indolinium N^+) to the *meta* position slows hydrodehalogenation. This supports the theory that the hydrodehalogenation reaction is proceeding via a nucleophilic aromatic substitution mechanism.[72,73] Further work to understand the mechanism and synthetic utility of hydrodehalogenation of 5-chloro indole and other halo-substituted indoles is discussed in **Section 3.4.5**.

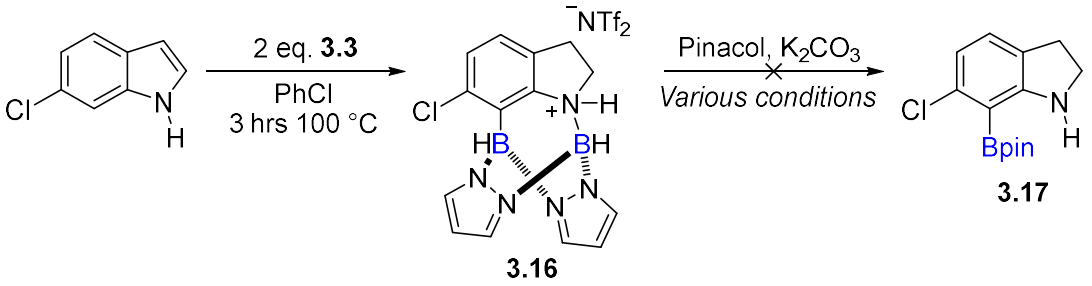

Scheme 3.23: The N/C7-borylation of 6-chloro indole proceeded without C6-Cl hydrodehalogenation, but 6-chloro 7-Bpin indoline could not be formed.

Though the N/C7-borylation of 6-chloro indole could be achieved without competitive hydrodehalogenation of the C6-Cl bond, converting **3.16** to 6-chloro 7-Bpin indoline (**3.17**) was highly challenging. Very little **3.17** could be formed (and what was formed was not isolated cleanly), even when more forcing conditions (up to 70 °C) were used. This supports observations from the N/C7-borylation and pinacol protection of 6-methyl indole (*vide supra*), where the increased steric bulk at C6 did not affect C7-H borylation significantly but did hinder the subsequent pinacol protection. Based on this, the reactivity of 6-chloro indole was not studied any further.

Following this, the reactivity of 5-fluoro, 5-bromo and 5-iodo indole were tested to see if N/C7-borylation was possible, and whether hydrodehalogenation occurs with other halogen leaving groups. For 5-fluoro indole, complete N/C7-borylation had occurred after 2 hours at 100 °C, with no hydrodehalogenation observed. Heating for a further 25 hours gave minor amounts of a side-product, though this could not be characterised. Therefore, it is assumed that hydrodehalogenation of this substrate occurs very slowly, if at all. With 5-bromo indole the results resembled 5-chloro indole: after 2 hours at 100 °C, partial N/C7-borylation had occurred, but the starting material had not been fully consumed and formation of the hydrodehalogenated product, **3.6**, was observed. This indicates that, as with 5-chloro indole, lower reaction temperatures would be needed to prevent hydrodehalogenation with this substrate. Finally, 5-iodo indole was fully consumed after 2 hours at 100 °C, with only one N/C7-borylated product observed. This was shown to be the hydrodehalogenated product, **3.6**, showing that with iodine as the leaving group hydrodehalogenation is very quick, and hence the 5-iodo N/C7-borylated product is not observed at all. Further work to understand the rates of hydrodehalogenation is discussed in **Section 3.4.5**.

These initial studies demonstrate that halogen-substituted indoles are suitable substrates for the N/C7-borylation of indoles using the initially established conditions, but that hydrodehalogenation of C-X bonds can occur, likely via transfer of a hydride from one of the pyrazabole species. The rate of hydrodehalogenation appeared to be related to the leaving group, with F < Cl < Br < I (consistent with a concerted S_NAr reaction, *vide infra*).[73] Decreasing the reaction temperature was sufficient at preventing hydrodehalogenation with 5-chloro indole, though it had not been tested with other halogens. As with methyl-substituted indoles, however, removal of pyrazabole-based impurities from the Bpin products was problematic, meaning only low isolated yields were obtained.

3.4.2 Reaction Profiling and Mechanistic Studies

Studies so far have demonstrated that although several substituted indoles are compatible in the reaction with two equiv. of *mono*-NTf_2 pyrazabole **3.3**, the biggest challenge was purifying the 7-Bpin indoline products and removing the persistent pyrazabole-based impurities. Therefore, further *in situ* NMR spectroscopy was used to profile the N/C7-diborylation reaction to try to develop a better understanding of the mechanism, in the hope that this would enable further optimisation of the conditions. Doing so could potentially reduce the number of impurities / side-products present, simplifying the purification (and therefore improving the isolated yields) of the 7-Bpin indoline products.

Studies with 5-Chloro Indole

Considering the reaction pathway that was proposed by Dr Jürgen Pahl for the reactivity of *N*-$SiMe_3$ indole (*vide supra*, **Scheme 3.14**), if *N*-H indoles react via an analogous reaction pathway this would result in loss of H_2 gas (in place of $HSiMe_3$) by reaction of the indole's N-H with a B-H bond in **3.3**. This would enable a second equivalent of **3.3** to coordinate to indole's nitrogen and subsequently undergo C7-H borylation. However, when monitoring the hydrodehalogenation side reaction of 5-chloro indole by *in situ* ^1H NMR spectroscopy, no resonances for H_2 were observed,[74] and no pressure build up / gas release was observed when the J. Young's NMR tubes were later opened. From these observations, it appears that the mechanism proposed for *N*-$SiMe_3$ indole is not applicable to the reactivity of 5-chloro indole (and potentially other *N*-H indoles).

An alternative reaction pathway that does not proceed with loss of H_2 is proposed in **Scheme 3.24**. Following hydroboration of 5-chloro indole (to form **3.18**), protodeboronation of the C3-B bond can occur, forming **3.19** where pyrazabole is bound at indole's nitrogen only. Consequently, the second boron unit in **3.19** is able to undergo electrophilic C7-H borylation, yielding the N/C7-borylated product **3.15**. With this alternative reaction pathway, only 1 equiv. of **3.3** would be required for complete N/C7-diborylation of 5-chloro indole.

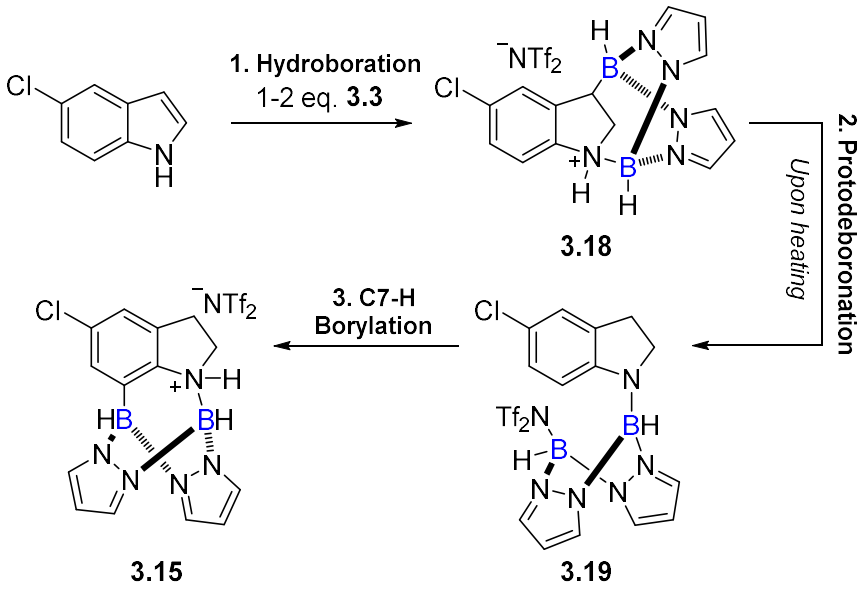

Scheme 3.24: Proposed alternative reaction pathway for the reaction of 1-2 equiv. *mono*-NTf_2 pyrazabole **3.3** and 5-chloro indole.

To test this hypothesis, the reaction of 5-chloro indole with 1.1 equiv. of **3.3** was studied (1.1 equiv. of **3.3** was used due to potential loss of boron electrophile to minor protic impurities). Heating for 2 hours at 100 °C resulted in the formation of the N/C7-borylated product **3.15** in high conversion. Repeating the reaction on a larger scale (with improved stirring) enabled complete formation and characterisation of **3.15**, demonstrating that the reactions with 1.1 or 2 equiv. of **3.3** give the same N/C7-borylated product (**Figure 3.6**). This supports the pathway proposed in **Scheme 3.24**.

The pinacol protection of **3.15** (formed using 1.1 equiv. of **3.3**) was then performed using the previously established conditions, giving 5-chloro 7-Bpin indoline (**3.14**) in a 65% yield (*NMR yield following work-up, relative to an internal standard*). The yield being >50% confirms that the reaction is not limited by only 1.1 equiv. of **3.3** being used. It should be noted here that no hydrodehalogenation of **3.15** was observed when using 1.1 equiv. of **3.3**, even upon extended heating at 100 °C (this is further discussed in **Section 3.4.5**).

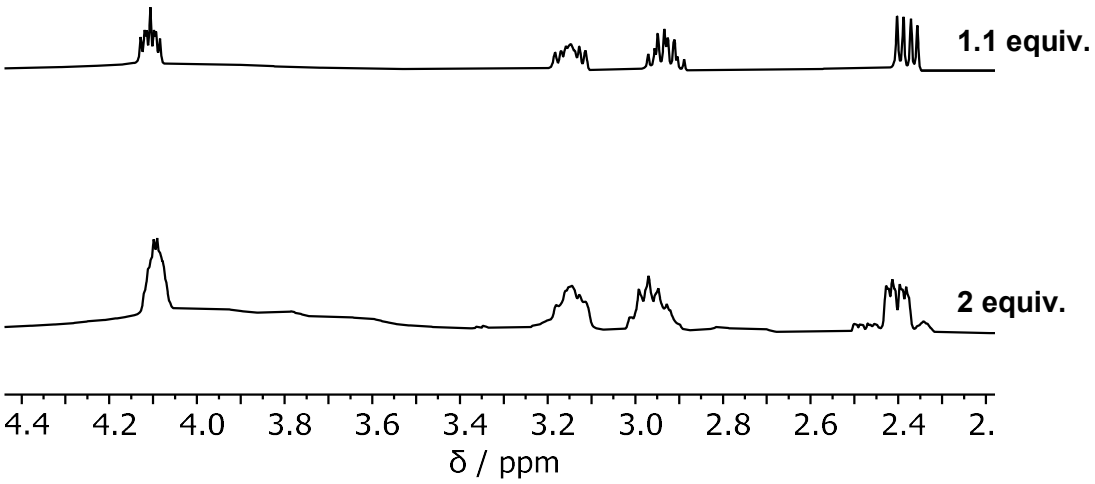

Figure 3.6: Stacked ^{1}H NMR spectra for the formation of **3.15** in the reactions of 5-chloro indole with 1.1 / 2 equiv. **3.3** after 2 hours at 100 °C. *Note: partial hydrodehalogenation of **3.15** had occurred in the reaction with 2 equiv. **3.3**, hence resonances are broadened. (Solvent = C_6H_5Cl, NMR temperature = 300 K).*

The reaction of 5-chloro indole and 1.1 equiv. of **3.3** at room temperature (RT) was then also studied using *in situ* NMR spectroscopy, to see if any supporting evidence for the proposed hydroboration/protodeboronation process could be observed (**Figure 3.7**). One practical difficulty was the poor solubility of **3.2** (0.55 equiv. of pyrazabole **3.1** and *di*-NTf_2 pyrazabole **3.2** are added to form 1.1 equiv. *mono*-NTf_2 pyrazabole **3.3** *in situ*) at low temperatures.

Hydroboration of 5-chloro indole by **3.3** occurred at room temperature. After 3 hours, 5-chloro indole had fully reacted, and multiple diastereotopic ^{1}H resonances were observed between 2.0 - 3.8 ppm. Coupled with ^{13}C NMR spectra, this indicated the presence of two indoline species, with at least one of these having a 4-coordinate nitrogen, indicative of boron binding at C3 and N (i.e. the hydroborated intermediate, **3.18**, **Scheme 3.24**).

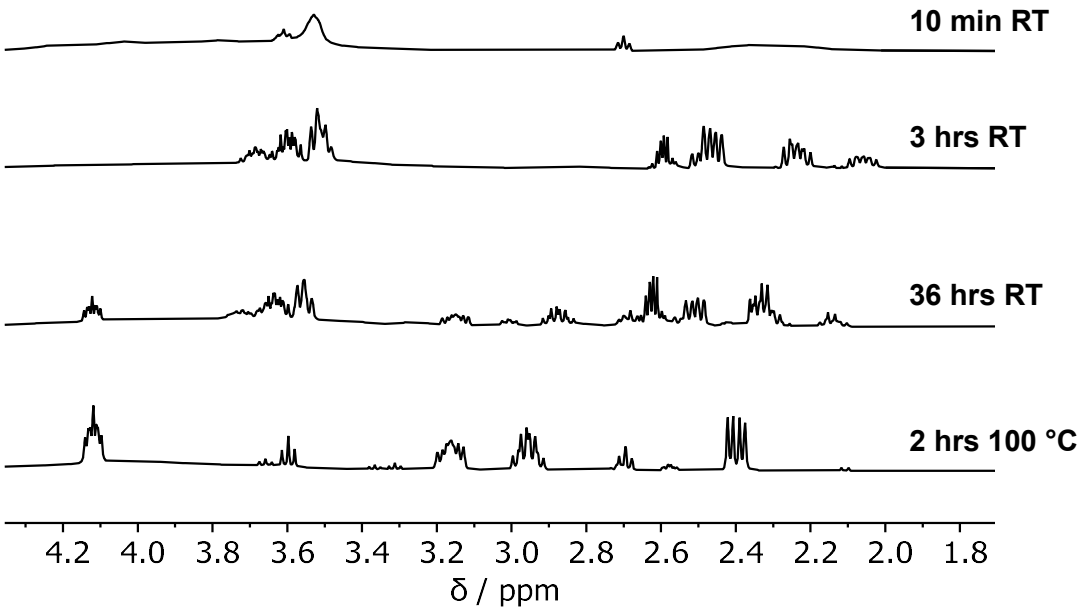

Figure 3.7: Stacked *in situ* ^{1}H NMR spectra for the reaction of 5-chloro indole with 1.1 equiv. **3.3** at RT, then upon heating to 100 °C.
(Solvent = C_6H_5Cl, NMR temperature = 300 K).

After 36 hours at room temperature, indolinium resonances were still present, but the partial formation of the N/C7-borylated product, **3.15**, was observed. The initial species disappeared after heating to 100 °C, with **3.15** now the major product. After two hours at 100 °C, two minor triplet resonances were also observed at 3.6 and 2.7 ppm. These could correspond to the protodeboronated species **3.19**, but the resonances are very minor. They could also correspond to the deprotonated version of **3.15**, hence cannot be confidently assigned as **3.19**.

Whilst this time-profile provided some insight into the hydroboration step and the formation of **3.18**, it provided little information on the assumed protodeboronation step and formation of **3.19**. Further studies to produce the hydroborated species **3.18** or the protodeboronated species **3.19** cleanly enough for characterisation (or assignment of resonances) were unsuccessful, with a complex mixture always obtained.

Studies with Indole

Following the observations with 5-chloro indole, the reactivity of indole with 1.1 equiv. of *mono*-NTf_2 pyrazabole **3.3** was compared to see if the N/C7-diborylation also went to completion. After 18 hours at 100 °C, complete formation of the N/C7-borylated product, **3.6**, was observed, with isolation and characterisation confirming that this is the same product as in the reaction with 2 equiv. of **3.3**. Based on these studies, it was concluded that more than 1 equiv. of **3.3** is not necessary for *N*-H indoles, unlike for *N*-$SiMe_3$ indole.

The ^{1}H NMR spectrum of **3.6** shows 4 resonances for the diastereotopic protons at C2 and C3 (**Figure 3.8**), which are inequivalent due to the adjacent chiral, four-coordinate nitrogen. Addition of 1 equiv. *N*,*N*-diisopropylethylamine (DIPEA), an exogenous base, deprotonated the *N*-H of **3.6** to give **3.20** (**Scheme 3.25**), simplifying the ^{1}H NMR spectrum to two triplets for the C2 and C3 protons.

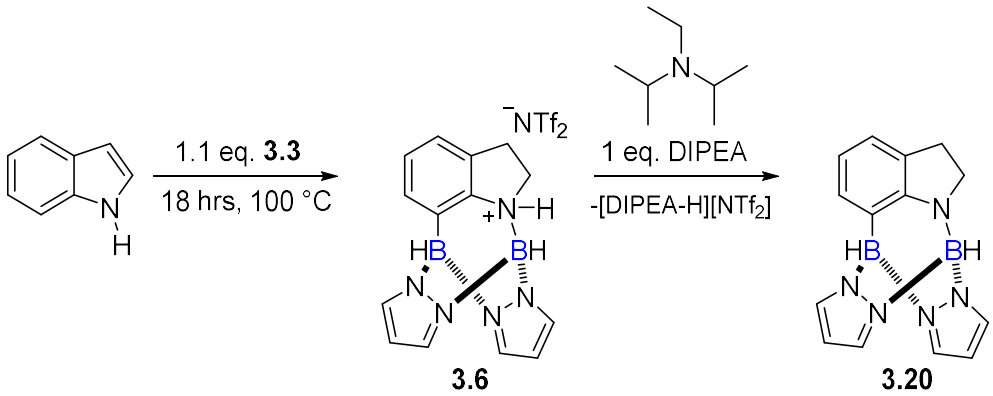

Scheme 3.25: The reaction of indole with 1.1 equiv. of **3.3** yields the N/C7-borylated product **3.6**, which can be deprotonated by addition of exogenous base to form **3.20**.

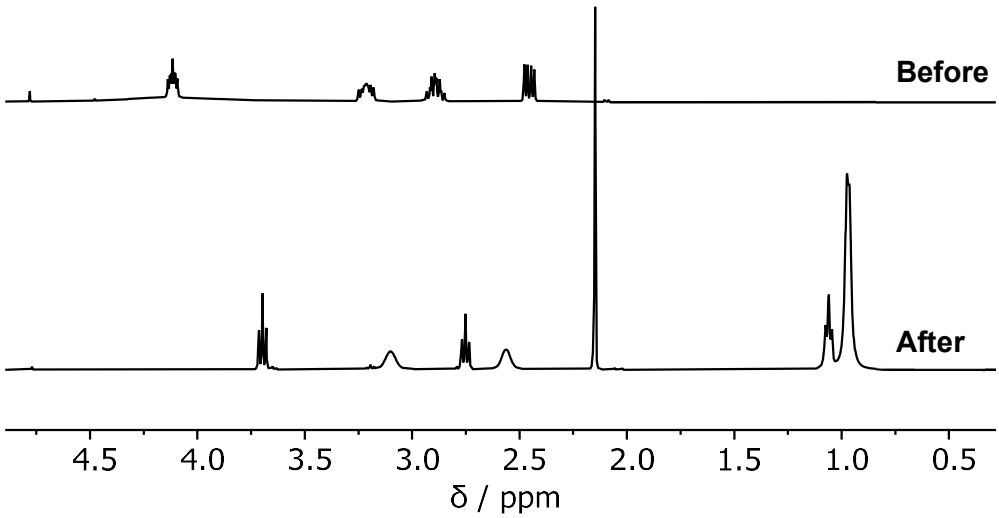

Figure 3.8: Stacked ^{1}H NMR spectra of a sample of **3.6** before (**top**) and after (**bottom**) addition of 1 equiv. of DIPEA to form **3.20**. *Note: the peak at 2.29 ppm is due to 1,3,5- trimethylbenzene (added as internal standard), whilst the peaks at 3.10, 2.56, 1.06 and 0.98 ppm correspond to [DIPEA-H][NTf_2].*
(Solvent = C_6H_5Cl, NMR temperature = 300 K).

The reactivity at lower temperatures was again studied by *in situ* NMR spectroscopy (**Figure 3.9**). The ^{1}H and ^{13}C NMR spectra looked similar to the reaction of 5-chloro indole, with hydroboration occurring rapidly at room temperature leading to one major indoline species with 3 diastereotopic proton resonances. This matches the expected resonances of the hydroborated species, **3.21** (**Scheme 3.26**), where pyrazabole is bonded to indole at C3 and N. The reaction did not appear to go any further at room temperature so was heated to 40 °C in the hope of pushing the reaction towards the C7-borylated species. The initially formed indoline species decreased, and partial formation of the N/C7 borylated species, **3.6**, was observed. Heating to 100 °C led to complete formation of **3.6**. Again, clean synthesis / isolation of any of the reaction intermediates (such as **3.21** and **3.22**) could not be realised, with a mixture was always obtained.

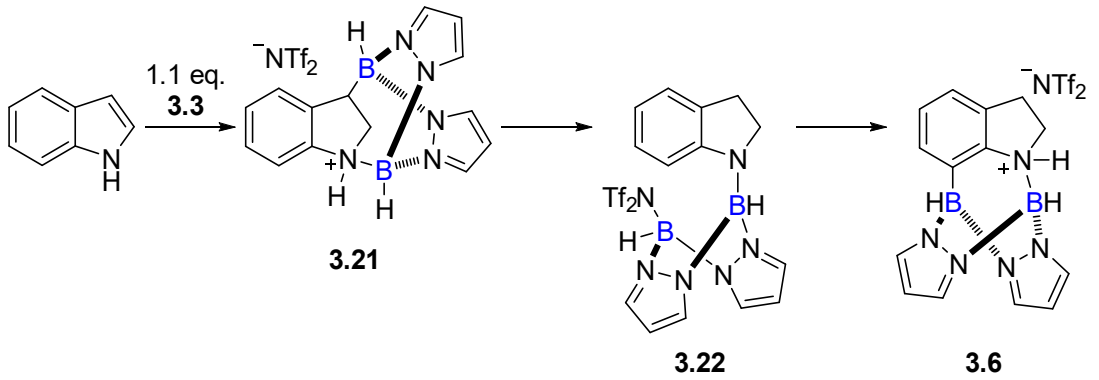

Scheme 3.26: Proposed intermediate species in the reaction of 1.1 equiv. *mono*-NTf_2 pyrazabole **3.3** and *N*-H indole.

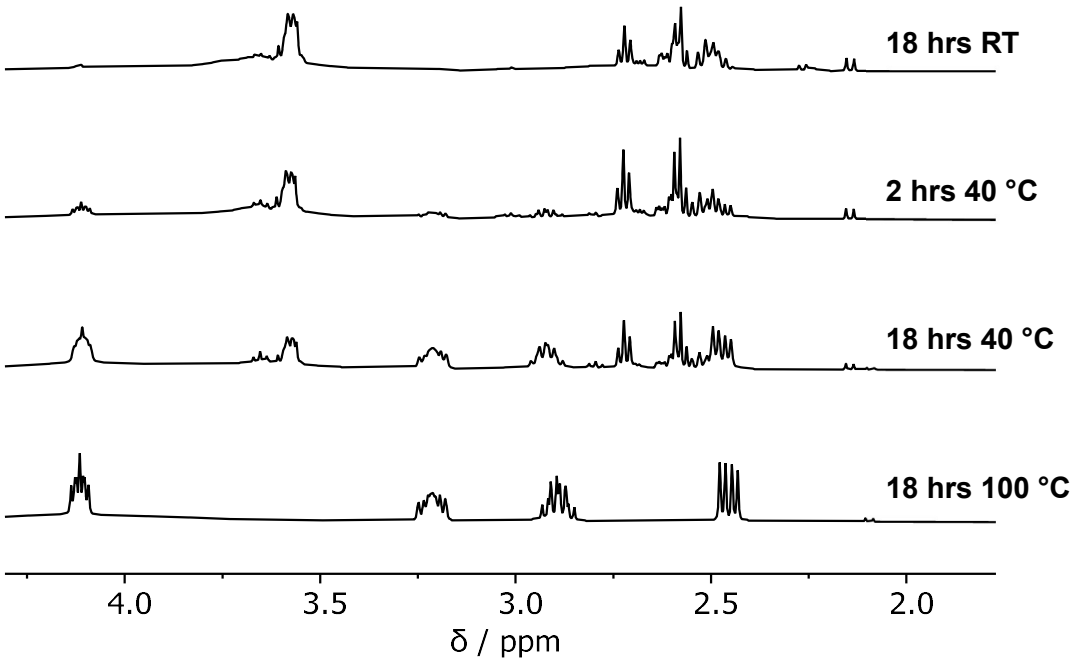

Figure 3.9: Stacked *in situ* ^{1}H NMR spectra for the reaction of indole with 1.1 equiv. **3.3** at RT, then upon heating to 40 °C, then to 100 °C.
(Solvent = C_6H_5Cl, NMR temperature = 300 K).

From the *in situ* NMR spectra of the reactions of indole / 5-chloro indole and **3.3**, it was not known if the N-H observed in the respective N/C7-borylated product was the initial N-H in the starting material. In the reaction pathway proposed in **Scheme 3.24** / **Scheme 3.26**, the initial N-H bond is broken during hydroboration / protodeboronation, and later a new N-H bond is formed which is observed in the N/C7-borylated product. To understand this process, *N*-D

indole was synthesised and reacted with 1.1 equiv. of **3.3** and monitored by *in situ* NMR spectroscopy.

As in **Figure 3.9**, hydroboration was shown to occur at room temperature, with complete consumption of indole observed by ^{1}H NMR spectroscopy. However, the ^{2}H NMR spectrum showed the partial decrease of the N-D resonance at 7.82 ppm, with a broad incoming resonance at 2.5 ppm (**Figure 3.10**). The broad resonance at 2.5 ppm is postulated to be the result of the reversible coordination of *mono*-NTf_2 pyrazabole, **3.3**, to the nitrogen of *N*-D indole (**Scheme 3.27**, **top**). Subsequent tautomerisation to the 3-deutero N-B iminium form would, upon N-B bond cleavage, produce very minor amounts of 3-deutero indole that was not present prior to addition of **3.3**. Hydroboration of this minor species would result in the ^{2}H resonance observed at 2.5 ppm.

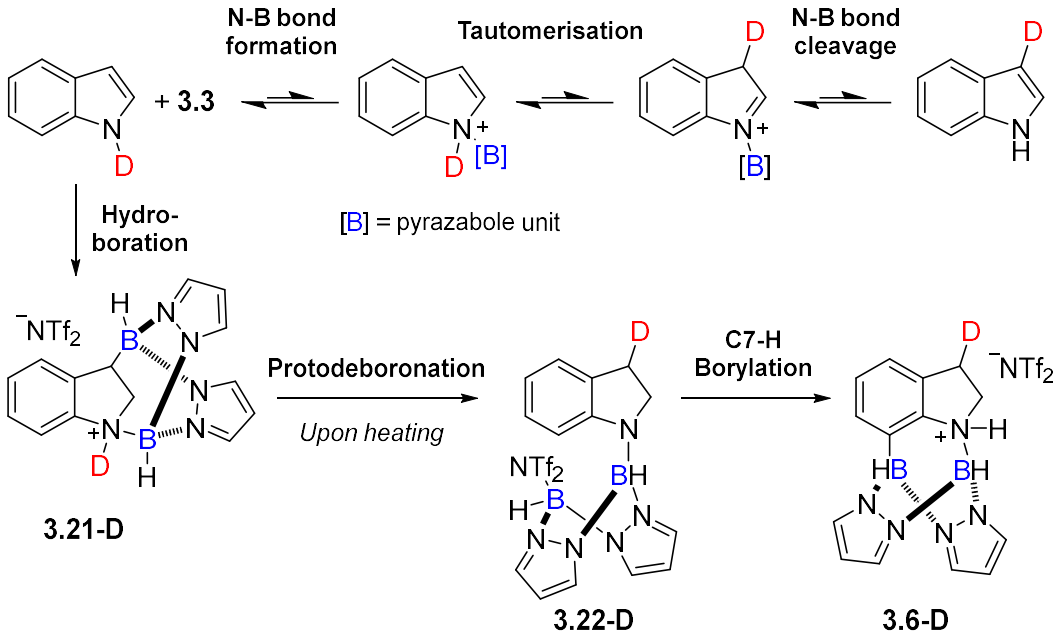

Scheme 3.27: Proposed reaction pathway for the reaction of *mono*-NTf_2 pyrazabole **3.3** and *N*-D indole, where reversible N-B bond formation and tautomerisation (top) could result in the minor species observed at RT.

This initial N-B bond formation is likely to be reversible since there is no exogenous base present to deprotonate the iminium species and trap it as 3-deutero N-B indole. Formation of the C3-B bond is irreversible after hydride

delivery to C2 (**Scheme 3.27**, **bottom**), hence the hydroborated species (**3.21-D**) is the major observed species at room temperature.

Heating to 100 °C led to the ^{2}H peak at 7.82 ppm disappearing, and a sharp new resonance at 2.77 ppm. This supports the hypothesis that protodeboronation of the C3-B bond is slower (than hydroboration) and occurs upon heating. The deuterium is abstracted from nitrogen and forms a C-D bond at C3 (initially forming **3.22-D**). Protodeboronation is followed by C7-H borylation to yield **3.6-D**, with the C3-D bond remaining after C7-H borylation.

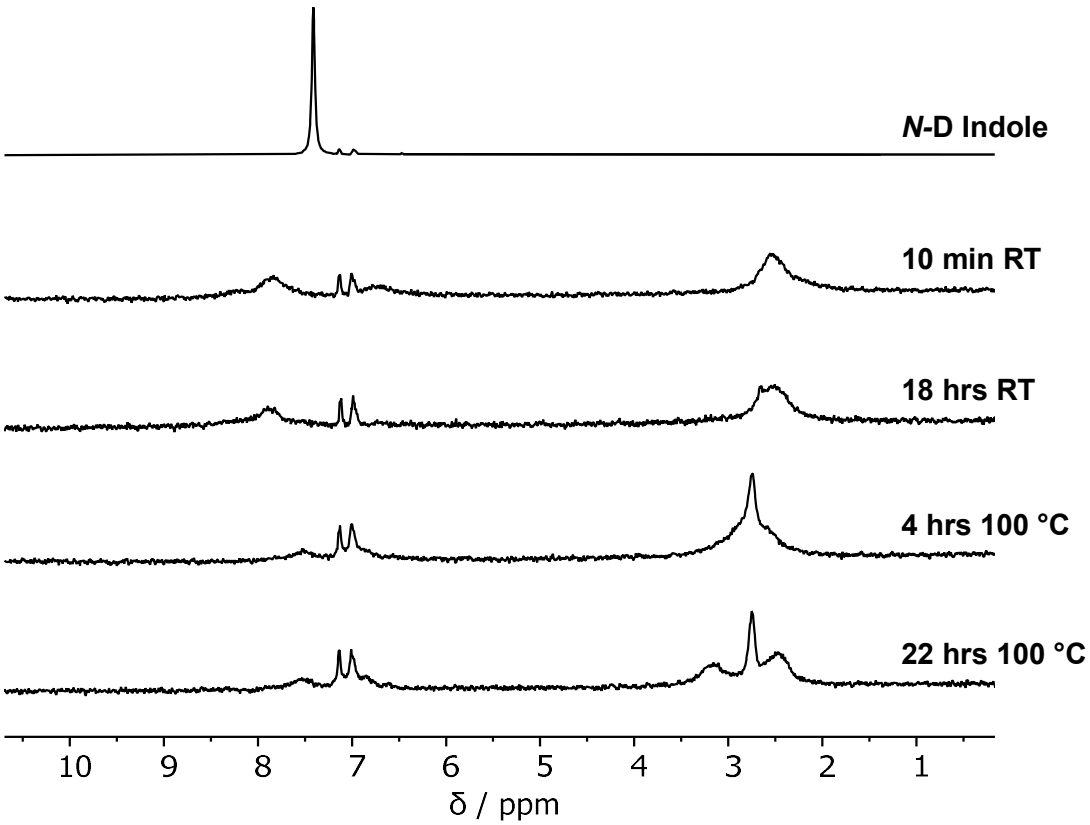

Figure 3.10: Stacked *in situ* ^{2}H NMR spectra for the reaction of *N*-D indole with 1.1 equiv. **3.3** at RT, then heating to 100 °C. *Note: The resonances at 7.13 and 6.98 ppm are due to trace C_6D_5Cl. (Solvent = C_6H_5Cl, NMR temperature = 300 K).*

Scale up of the reaction of *N*-D indole enabled isolation and characterisation of 3-deutero 7-Bpin indoline (**3.7-D**, **Scheme 3.28**), further demonstrating that there is no further hydride / deuterium exchange after protodeboronation.

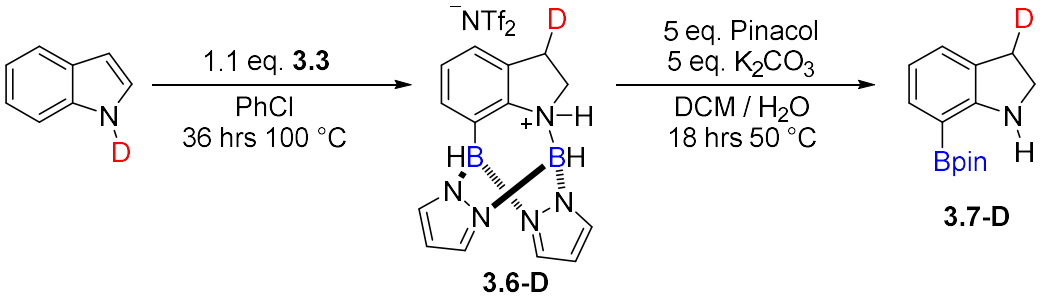

Scheme 3.28: Formation of 3-deuteo 7-Bpin indoline by reaction of *N*-D indole with **3.3**.

Proposed Mechanism

Following studies with indole and 5-chloro indole, a mechanism for the reduction and N/C7 diborylation of indoles was proposed. It is assumed that the reacting pyrazabole species is the *mono*-activated electrophile **3.3**, as reactions using *di*-NTf_2 pyrazabole **3.2** (*performed by Dr Jürgen Pahl, see* ***Section 3.2***) did not proceed without an exogenous base (unlike the reactivity observed with **3.3**). Previous work by Fontaine et al. reported the hydrogenation of *N*-H indoles using LB-BH_3 sources.[75,76] In this system, C2=C3 hydroboration can occur with the hydride and boron moiety installed at the 2- and 3-positions, respectively, followed by C3-B protodeboronation with the N-H, which transfers the boron moiety to nitrogen. A similar mechanism is proposed in this system, supported by the deuterium-labelling studies with indole and *in situ* NMR monitoring. Hydroboration across the C2-C3 system yields the hydroborated product with both C3 and nitrogen coordinated to boron (**Scheme 3.29**).

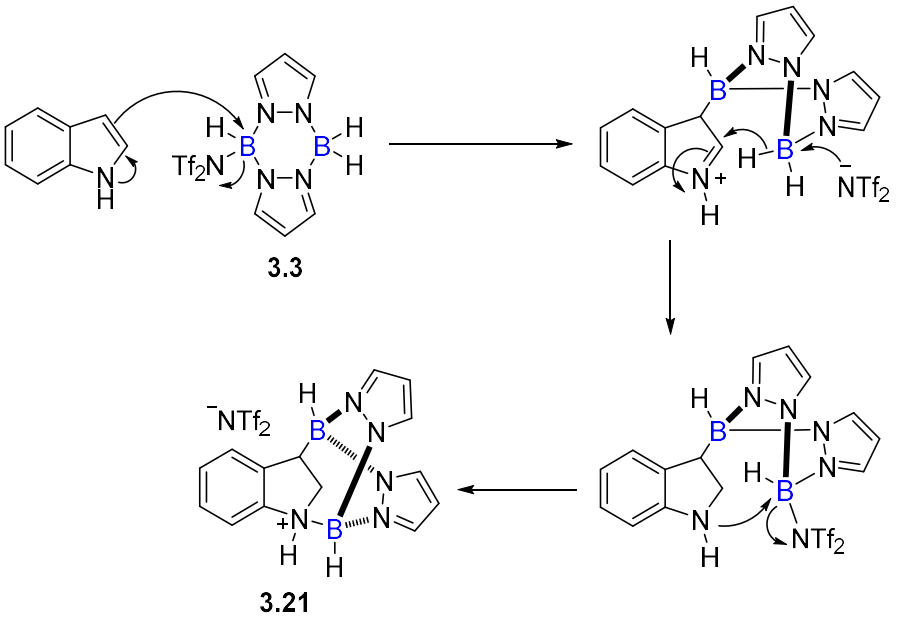

Scheme 3.29: Proposed mechanism for the hydroboration of indole with **3.3**.

Subsequent deprotonation of N-H and cleavage of the C3-B bond via protodeboronation results in the transfer of the H (or D, for *N*-D indole) to the aliphatic C3 position (**Scheme 3.30**). This produces intermediate **3.22**, where the second boron unit of the pyrazabole unit (which contains a regenerated reactive -$BH(NTf_2)$ moiety) is positioned towards C7, enabling regioselective C-H

borylation. The indoline nitrogen acts as an internal base for the C-H borylation, forming the N/C7-borylated indolinium cation **3.6**, with a quaternized nitrogen, that was fully characterised by NMR spectroscopy and crystallography *(by Dr Jürgen Pahl, see **Figure 3.3**)*.

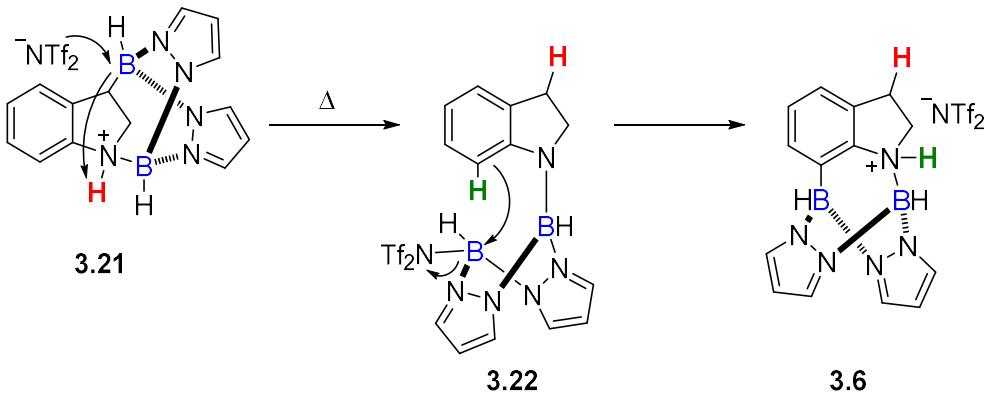

Scheme 3.30: Proposed mechanism for the protodeboronation and C7-H borylation process in the reaction of indole with **3.3**.

Attempted Catalytic Reactivity

The final part of the optimisation of this process was to investigate whether the reaction could be performed with catalytic amounts of the activator, $HNTf_2$. Achieving turnover, via activating the *mono*-NTf_2 pyrazabole *in situ* would likely require a dehydrocoupling step, where the N-H in the N/C7-borylated indolinium cation **3.6** reacts with the B-H of unactivated pyrazabole to release H_2 and form an equivalent of *mono*-NTf_2 pyrazabole that goes onto react with more indole / indoline (**Scheme 3.31**).

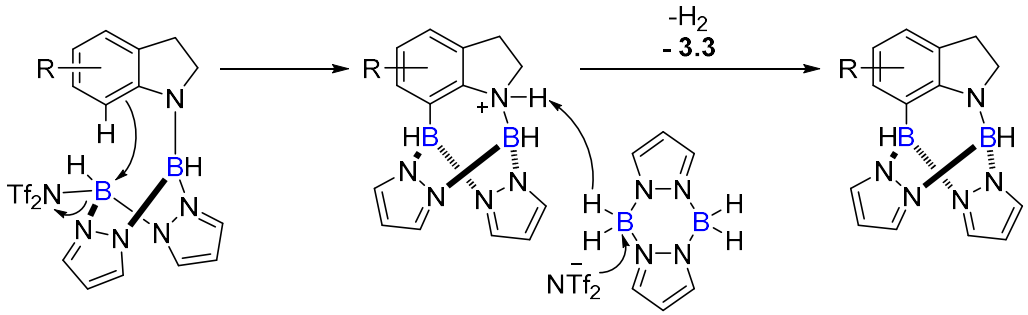

Scheme 3.31: Proposed mechanism to achieve C7-H borylation that is catalytic in $HNTf_2$, by regenerating **3.3** in *situ* using a dehydrocoupling step.

The reaction of 5-chloro indole (chosen for its faster reaction rate, *vide infra*) with 1 equiv. of pyrazabole **3.1**, and 20 mol% $HNTf_2$ was monitored by *in situ* NMR spectroscopy. After 3 hours at 100 °C, reduction of the C2-C3 bond to form two to three indoline species had occurred, with multiple triplet resonances in the ^1H NMR spectrum. Little C7-H borylation (internal yield of **3.15** = <10%) was observed. Based on these observations, it is hypothesised that whilst hydroboration and protodeboronation can occur, the protodeboronated indoline intermediate, **3.19**, quickly undergoes pyrazabole substituent scrambling with the unactivated **3.1** (**Scheme 3.32**). Whilst this regenerates **3.3** (which can then reduce the remaining 5-chloro indole) it converts **3.19** into a species (**3.23**) unreactive towards C7-H borylation, hence why most of the reaction only undergoes indole reduction and very little **3.15** is formed. This was therefore not studied any further, though could be a potential area for future studies.

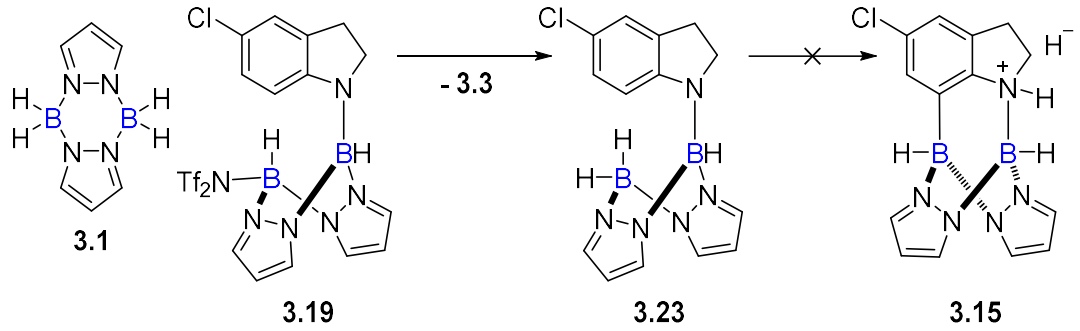

Scheme 3.32: Based on *in situ* ^1H NMR spectroscopy, it is proposed that the majority of the protodeboronated intermediate **3.19** reacts with unactivated pyrazabole **3.1**, forming a by-product (**3.23**) unable to undergo C7-H borylation.

3.4.3 Evaluating the Substrate Scope using Optimised Conditions

Having demonstrated that the directed N/C7-borylation of *N*-H indoles only requires 1.1 equiv. of **3.3**, the overall process was re-optimised with these new conditions and the substrate scope of the reaction was established (**Table 3.1**). For the second step in the one-pot process, reducing the amount of pinacol and K_2CO_3 from 10 to 5 equiv., and increasing the temperature to 50 °C was shown to give equally efficient installation of the pinacol group, whilst reducing the number of by-products present after work-up. Thus, the majority of 7-Bpin indoline products could be isolated in high purity (>95%) without the need for purification by reverse-phase column chromatography.

Table 3.1: Substrate Scope for the Directed C7-H Borylation of *N*-H Indoles

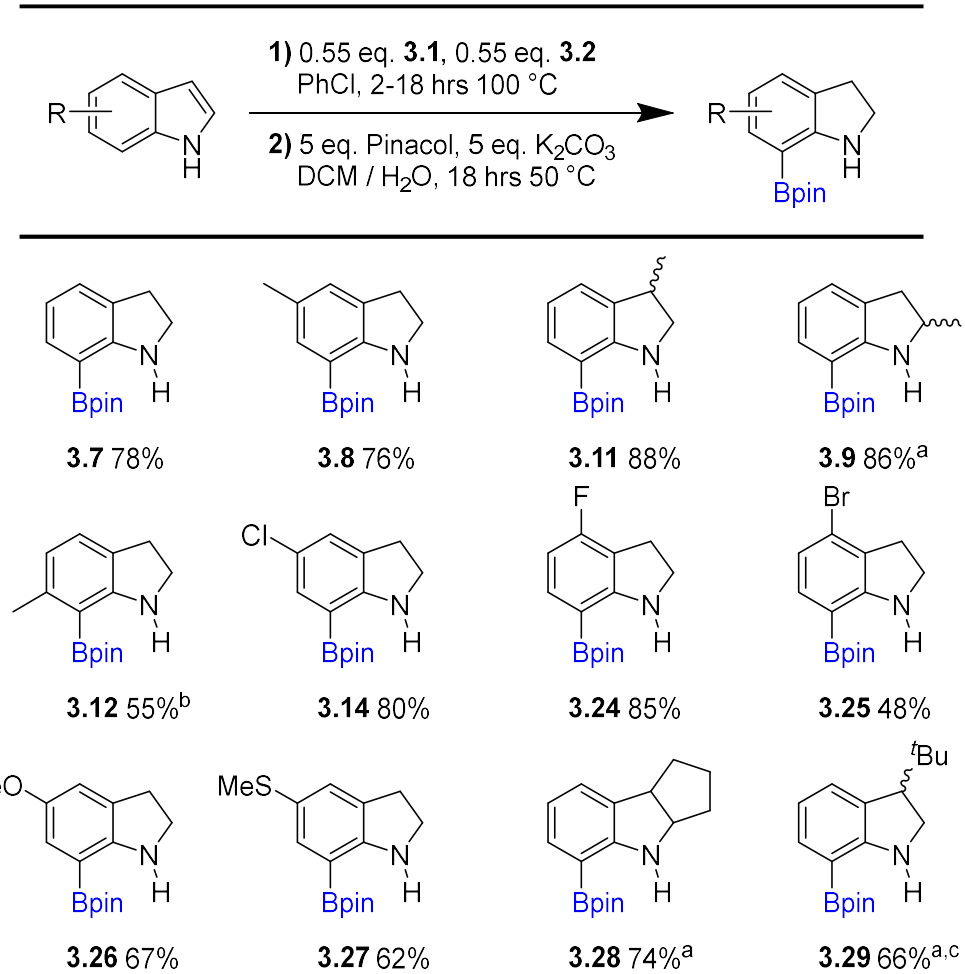

(**a**) = Reaction stirred at RT for 1 hour prior to heating to 100 °C
(**b**) = Pinacol protection heated to 80 °C for 18 hrs (+ PhCl instead of DCM)
(**c**) = Reaction and isolation performed by Dr Kang Yuan

The N/C7-borylation of indole, 5-methyl indole and 3-methyl indole all proceeded to complete conversion in 18 hours at 100 °C and yielded **3.7**, **3.8** and **3.11** respectively after pinacol protection, in excellent yields. For 2-methyl indole, leaving the reaction stirring at room temperature for 1 hour prior to heating to 100 °C for 18 hours prevented the formation of the indole by-product (*vide supra, see* ***Scheme 3.17***) and **3.9** was isolated cleanly in excellent yield. For 6-methyl indole, N/C7-borylation was complete after 18 hours at 100 °C and increasing the pinacol protection temperature to 80 °C (with DCM swapped for the higher boiling PhCl) enabled **3.12** to be isolated cleanly, albeit in a lower yield than other substrates.

The reactions of 5-chloro indole, 4-fluoro indole and 4-bromo indole gave **3.14**, **3.24** and **3.25** respectively and were noticeably faster than the methyl-substituted substrates, with N/C7-borylation complete after 2 hours at 100 °C. One feasible explanation for the increased rate of reaction is that the presence of an electron-withdrawing substituent decreases the pK_a of the hydroborated indolinium intermediate (e.g. **3.18** for 5-chloro indole) and therefore increases the rate of protodeboronation, where a proton is transferred from N to C3.[77–79] It should be noted, however, that a thorough analysis of the effect of indole substituents on reaction rates was not performed.

No hydrodehalogenation was observed for these substrates under these conditions. Excellent yields of **3.14** and **3.24** were obtained with no further purification necessary, but reverse-phase chromatography was required to purify **3.25**, resulting in a somewhat decreased yield. The reaction of 5-iodo indole still resulted in competitive hydrodehalogenation, however, despite the use of just 1.1 equiv. of **3.3**, suggesting that the rate of hydrodehalogenation of the 5-iodo N/C7-borylated intermediate outcompetes the rate of C7-H borylation. The clean formation of 5-iodo 7-Bpin indoline could not be realised.

The process tolerated methoxy (OMe) and thioether (SMe) functional groups, with **3.26** and **3.27** both formed in good yields without further purification. Again, the N/C7-borylation step was complete after 2 hours at 100 °C. The process also tolerated substituents with increased sterics at C2 and/or C3. A

C2/C3 disubstituted indole, 1,2,3,4-tetrahydrocyclopent[*b*] indole, reacted to give **3.28** in high yield after purification via reverse-phase chromatography, and **3.29** was formed from 3-*tert*-butyl indole in good yield with no chromatography required (*reaction and isolation performed by Dr Kang Yuan*). For both these substrates, the reaction was stirred at room temperature for 1 hour (as established with 2-methyl indole) to ensure hydroboration occurred prior to C7-H borylation.

The reaction of 5-trifluoromethyl (CF_3) indole with **3.3** appeared successful, with complete conversion to the N/C7-borylated indoline intermediate observed by *in situ* ^{1}H NMR spectroscopy after 1 hour at 100 °C (assigned by the 4 diastereotopic protons, but not isolated), The CF_3 group was still intact and there was no evidence of C-F bond activation (by ^{19}F NMR spectroscopy).[80] The shorter reaction time supports the hypothesis that electron-withdrawing substituents increase the rate of protodeboronation.[77–79] However, conversion of this intermediate to the 7-Bpin indoline product was extremely slow (**Scheme 3.33**). Very little 5-CF_3 7-Bpin indoline was formed, even with prolonged heating at increased temperatures (80 °C). One reasonable explanation for this result is that electron-withdrawing CF_3 group *meta* to the C7-B bond enhances the Lewis acidity of boron, increasing the B-N(Pyrz) bond strength.[81] This results in a higher barrier to pinacol protection.

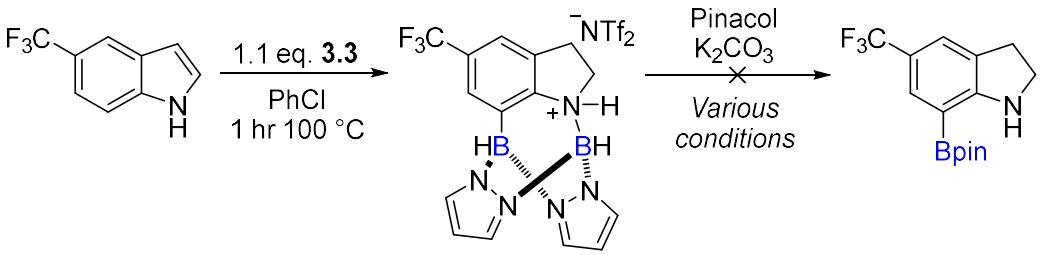

Scheme 3.33: N/C7-borylation of 5-trifluromethyl indole with **3.3** was successful, but the pinacol protection could not be achieved.

Nitro (NO_2) groups were incompatible with the reaction. The reaction of 5-nitro indole resulted in a dark black mixture, with only very weak resonances observed during *in situ* ^{1}H NMR spectroscopy. Groups prone to hydroboration were also not compatible with the reaction. In the reaction of 5-methyoxycarbonyl

(COOMe) indole, hydroboration of the ester functionality was observed by *in situ* ^{1}H NMR spectroscopy, with no evidence of C7-H borylation. Therefore, these substrates were not studied any further.

The reaction of indole was shown to work on x5 larger scale (1.5 mmol), with an improved isolated yield of **3.7** (**Scheme 3.34a**). As before, no further purification was required after work-up. The Suzuki-Miyaura cross coupling of 7-Bpin indoline **3.7** with bromobenzene was also demonstrated, yielding 7-phenyl indoline in 57% isolated yield (**Scheme 3.34b**).

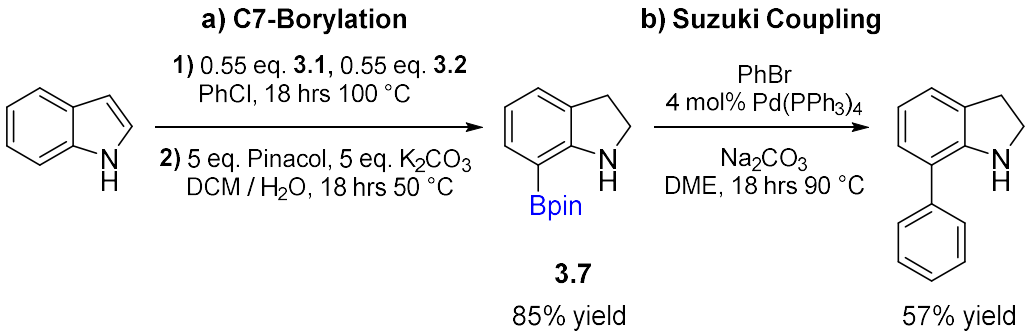

Scheme 3.34: a) Synthesis and **b)** Suzuki-Miyaura cross coupling of 7-Bpin indoline.

3.4.4 Directed *Ortho* C-H Borylation of Indoline and Aniline Derivatives

The process could also be adapted to use *N*-H indolines, rather than indoles, as the substrates. When using indoline, there are no hydroboration and protodeboronation steps, meaning that when using the *mono*-activated pyrazabole, **3.3**, the second boron unit cannot be activated *in situ*. For this reason, the *di*-NTf_2 pyrazabole, **3.2**, is required. Furthermore, the lack of protodeboronation step means the initial N-H of indoline is preserved and the nitrogen cannot act as an internal base for the C7-H borylation step. For this reason, an equivalent of exogenous base is required. The hindered base 2,6-(^{t}Bu)$_2$-4-methyl pyridine (DBP) was initially used.

The reaction of indoline with 1.1 equiv. **3.2** and 1 equiv. DBP resulted in clean formation of the N/C7-borylated product **3.6**, matching (by NMR spectroscopy) the species formed in the analogous reaction with indole. This could be converted to the Bpin product in an identical manner to the reaction with indole, yielding 7-Bpin indoline **3.7** in a 64% yield (*NMR yield following work-up, relative to an internal standard*). Some leftover DBP base was not removed during work-up.

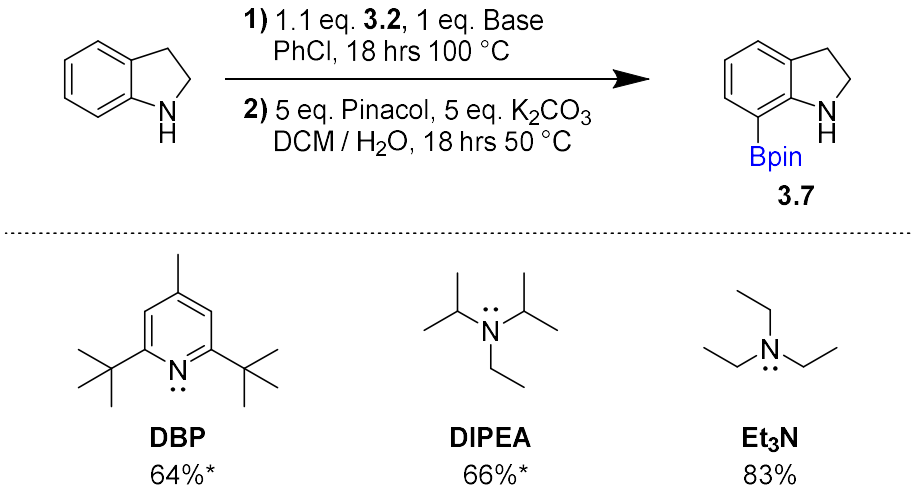

Figure 3.11: Screening of exogenous bases for the C7-H borylation of indoline. *(%*Yields are NMR yields following work-up, relative to an internal standard).*

The use of cheaper, but less bulky bases was explored (**Figure 3.11**). The reaction with *N,N*-diisopropylethylamine (DIPEA) in place of DBP proceeded smoothly without any issues arising from coordination of the base to the pyrazabole

electrophile. The yield of **3.7** was slightly improved to 66% (*NMR yield following work-up, relative to an internal standard*). Again, a small amount of residual DIPEA was challenging to remove. Finally, triethylamine (Et_3N) could be used as the base, giving **3.7** in a significantly improved 83% isolated yield. The low boiling point of Et_3N meant any leftover was removed *in vacuo*.

These optimised conditions could be applied to the *ortho* C-H borylation of other substrates. Tetrahydroquinoline underwent *ortho* C-H borylation with 1.1 equiv. of **3.2** and 1 equiv. of Et_3N to yield 8-Bpin tetrahydroquinoline, **3.30**, in a 71% isolated yield (**Scheme 3.35**). Subsequent work by Dr Clément Millet expanded this methodology to the directed *ortho* C-H borylation of *N*-methyl aniline.[82]

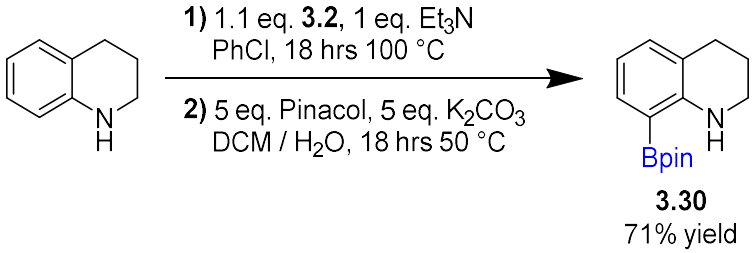

Scheme 3.35: The directed *ortho* C-H Borylation of tetrahydroquinoline using **3.2** and Et_3N.

3.4.5 Further Studies into Hydrodehalogenation Side Reactions

The hydrodehalogenation of halogen-substituted indoles was identified as a side reaction in **Section 3.4.1**. In the reaction of 5-chloro indole with 2 equiv. of **3.3**, the desired N/C7-borylated intermediate, **3.15**, was initially formed but upon extended heating the 5-Cl bond was replaced with 5-H (to form **3.6**). It was shown that reducing the reaction temperature to 60 °C prevented hydrodehalogenation.

It was later shown that hydrodehalogenation of 5-chloro indole does not occur if only 1.1 equiv. of **3.3** is used, as **3.3** is fully consumed in the faster N/C7-diborylation process. This indicates that one of the pyrazabole species present in solution reacts as a hydride source towards the N/C7-borylated indolinium species, and this may be proceeding via a nucleophilic aromatic substitution (S_NAr) mechanism, where an electron poor arene (e.g. the anilinium in **3.15**) is

attacked by an nucleophile, followed by elimination of a leaving group (often a halogen).[72] The majority of S_NAr reactions proceed via a stepwise 'addition-elimination' mechanism.[83] Nucleophilic addition dearomatises the system, forming a carbanion (Meisenheimer) intermediate. Subsequent elimination of the leaving group rearomatises the arene. In such reactions, the rate is often proportional to the electronegativity of the leaving group X, where I < Br < Cl < F.[84] This is because C-X bond cleavage is not the rate-determining step, and so the increased electronegativity of X activates the arene towards nucleophilic attack.

In this observed hydrodehalogenation reaction, however, reactivity follows the trend F < Cl < Br < I, with the N/C7-borylated product formed from 5-iodo indole undergoing hydrodehalogenation fastest and still being competitive even when only 1.1 equiv. of **3.3** is used. This implies that the hydrodehalogenation is instead proceeding via a concerted S_NAr mechanism.[73] Concerted S_NAr reactions do not form Meisenheimer intermediates, instead the C-Nuc bond is formed and C-X bond is broken within a single transition state (**Scheme 3.36**).[85] Reaction rates follow the inverse trend for leaving groups, where F < Cl < Br < I. This is because the rate determining step now involves cleavage of the C-X bond, so is proportional to C-X bond strength.[72] There are other examples on the use of hydrides as nucleophiles in hydrodehalogenation reactions, which also proceed via concerted S_NAr mechanisms.[86,87]

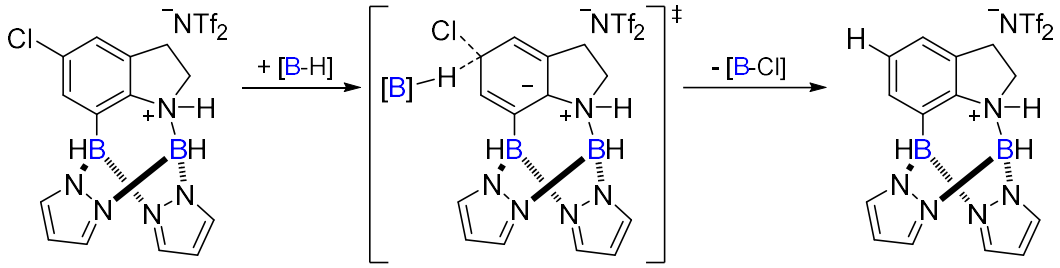

Scheme 3.36: Proposed concerted S_NAr mechanism for the observed hydrodehalogenation of **3.15** with a pyrazabole-based hydride source.

Furthermore, in this system, the N/C7-borylated product formed from 5-chloro indole (**3.15**) was shown to undergo hydrodehalogenation faster than the N/C7-borylated product from 6-chloro indole (**3.16**). This is because the strongly

electron withdrawing indolinium nitrogen in **3.15/3.16** increases the electrophilicity of the *ortho*/*para* carbon positions, meaning the C-X position is more susceptible to nucleophilic attack. The *meta* carbon position is activated to a lesser extent.[72] Hence, the *para* C5-Cl bond undergoes hydrodehalogenation faster than the *meta* C6-Cl bond.

Probing the Active Borohydride Species

To gain more information on the nature of the pyrazabole acting as a hydride source, a sample of **3.15** was first prepared using the optimised conditions, and then charged with either unactivated pyrazabole **3.1**, *mono*-NTf_2 pyrazabole **3.3** or *di*-NTf_2 pyrazabole **3.2** (**Scheme 3.37**).

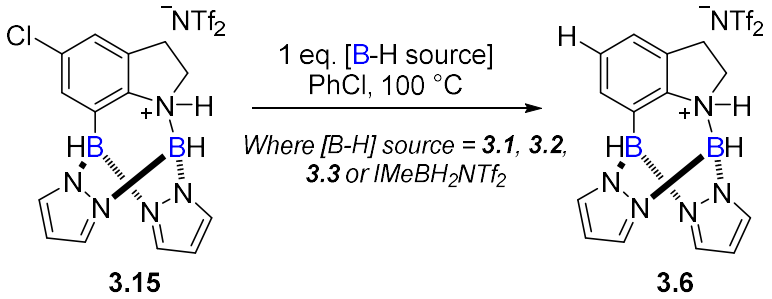

Scheme 3.37: Studies into the identity of the hydride source in the hydrodehalogenation of **3.15** to **3.6**.

Hydrodehalogenation to form **3.6** was only observed with the activated pyrazaboles **3.3** and **3.2**. Furthermore, a $HNTf_2$-activated NHC-borane, $IMeBH_2NTf_2$, was also not capable of hydrodehalogenation. Overall this demonstrates that a diboron scaffold, with at least one electrophilic boron unit, may be critical to reactivity. From these observations, it is proposed that the electrophilic [-BH-NTf_2] unit of the activated pyrazabole interacts with the halide, thereby weakening the C-X bond, whilst the other [-BH_2] (or [-BH-NTf_2] for **3.2**) unit provides the hydride nucleophile (**Figure 3.12**).

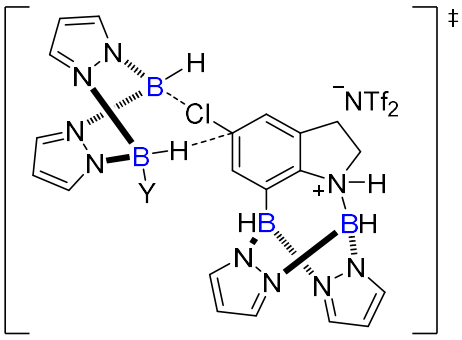

Figure 3.12: Proposed transition state for the interaction between the diboron scaffold of **3.2**/**3.3** and **3.15**, which enables the concerted S_NAr reaction to form **3.6**. *(Y = H for **3.3**, and NTf_2 for **3.2**)*

Attempted Hydrodehalogenation of 4-Nitrochlorobenzene

Finally, to see if NTf_2-activated pyrazaboles could be utilised as hydride sources in the hydrodehalogenation of other electron-deficient arenes, the hydrodehalogenation of 4-nitrochlorobenzene was attempted using *mono*-NTf_2 pyrazabole **3.3** (**Scheme 3.38**). Halogen-substituted nitrobenzenes are commonly utilised as substrates in nucleophilic aromatic substitution reactions, with the electron withdrawing nitro group generating sufficient electrophilicity at the *ortho* or *para* carbons.[88]

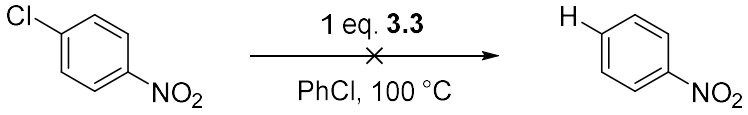

Scheme 3.38: Attempted hydrodehalogenation of 4-nitrochlorobenzene.

When the sample was heated to 100 °C, no consumption of the starting material was observed, even upon extended heating. No incoming resonances for the formation of nitrobenzene were detected either. Therefore, hydrodehalogenation reactions using activated pyrazabole species are so far just limited to the niche example, where the indolinium nitrogen acts as a strongly electron-withdrawing group and activates **3.15** towards S_NAr. Given this observation and the fact that there are other, more effective hydrodehalogenation methods using much simpler hydroboranes (e.g. $NaBH_4$),[89] this reaction was not pursued any further.

3.5 Conclusions

Activated pyrazaboles are capable of reacting as transient directing groups. Pyrazabole is a suitable diboron compound for this reactivity because of its robust B_2N_4 core, and a B···B separation that makes it ideal for the directed N/C7 diborylation of indole. Upon activation of pyrazabole with $HNTf_2$, either a mono- or di-topic electrophile is generated. These electrophiles initially reduce indole to indoline, but then are able to direct C-H borylation towards C7. This process provides access to C7-Bpin indolines in a one-pot, metal-free process without the need to preinstall a directing group or use forcing conditions in its removal.

Whilst 7-Bpin indolines can be synthesised using the pivaloyl directed methodologies developed by the groups of Shi, Houk and Ingleson,[33–35] this requires prior installation of the pivaloyl onto the nitrogen of indoline, and column chromatography to purify these intermediates. The use of activated pyrazaboles as transient directing groups in this work improves the overall efficiency of the C-H borylation process. In addition, the pyrazabole electrophiles used are compatible with methoxy- and thioether- functional groups that are not compatible with BBr_3 (due to competitive ether cleavage), widening the substrate scope. It is likely that with further modification of the reaction conditions (e.g. lower reaction temperatures) the process may be able to tolerate iodo-substituted indoles without competitive hydrodehalogenation. The development of alternative pinacol protection conditions (or transformation into a different boron moiety) may also enable the scope to be expanded to trifluoromethyl-substituted indoles, a synthetically valuable functional group. The use of stoichiometric $HNTf_2$ as the activator is problematic, however, due to its high cost and moisture sensitivity. The use of an alternative activator of pyrazabole could improve the atom economy and synthetic utility of this process.

The use of activated pyrazaboles results in rapid and unavoidable reduction of indoles to the respective indolines, however, meaning the 7-Bpin indole analogues cannot be formed directly in this reaction (unlike the pivaloyl directed methodologies). Achieving C-H borylation without C2=C3 reduction would require an alternative pyrazabole species that is less hydric. One approach to this

would be to remove the hydride substituents from pyrazabole completely. This could potentially enable the C3/C4 (or N/C7-) diborylation of indoles without reduction of C2=C3. The use of pyrazaboles in the directed C-H borylation of other (hetero)arenes is also underexplored and warrants further studies.

3.6 Experimental

*For general experimental considerations, see **Chapter 2**.*

*The preliminary studies with N-Me indole and N-TMS indole (including the characterisation of **3.4**) were performed by Dr Jürgen Pahl. This work is described in the publication of this work and not included below.*[65]

3.6.1 Synthesis and Activation of Pyrazabole

The NMR spectra of the synthesised pyrazaboles can be found in the publication of this work and are not included below.[65]

Pyrazabole – 3.1

This modified procedure is based on a previous report by Trofimenko.[58]

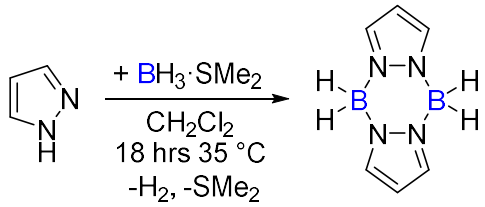

Neat $BH_3{\cdot}SMe_2$ (4.0 ml, 42.2 mmol) was slowly added to a solution of pyrazole (2.87 g, 42.2 mmol, 1 equiv.) in DCM (20 ml) at 0 °C. After the initial gas evolution had stopped the reaction was heated for 18 hrs at 35 °C in an open system. All volatiles were removed *in vacuo* and the remaining white solid was sublimed (120 °C, 4 x 10^{-2} mbar) to yield the title product as a white powder in 68% yield (2.29 g, 14.32 mmol). Analytical data are in accordance with literature values.[58]

^{1}H NMR (500 MHz, $CDCl_3$) δ 7.61 (d, $^{3}J_{HH}$ = 2 Hz, 4H), 6.31 (t, $^{3}J_{HH}$ = 2 Hz, 2H), 3.61 (1:1:1:1 q, $^{1}J_{BH}$ = 101 Hz, 4H);

^{11}B NMR (161 MHz, $CDCl_3$) δ -8.5 (t, $^{1}J_{BH}$ = 101 Hz);

^{13}C{^{1}H} NMR (126 MHz, $CDCl_3$) δ 135.08, 105.54 ppm.

Di-NTf_2 Pyrazabole – 3.2

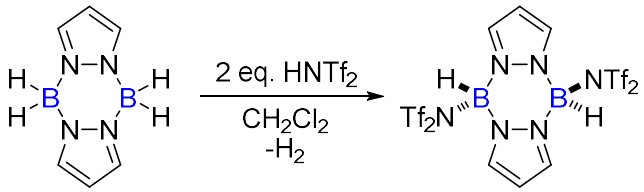

A solution of $HNTf_2$ (5.62 g, 20 mmol, 2 equiv.) in DCM (30 ml) was added dropwise to a solution of pyrazabole **3.1** (1.60 g, 10 mmol) in DCM (1 ml) leading to gas evolution and precipitation of a white solid. The suspension was filtered after stirring at room temperature for 16 hours. The obtained white solid was washed with DCM (3 x 5 ml) and dried *in vacuo*. The title product was obtained as a white powder in 74% yield (5.294 g, 7.37 mmol). The product is highly air/moisture sensitive and must be kept under inert gas in the glovebox or a sealed ampule. Very low solubility of **3.2** in weakly-coordinating solvents (e.g. 1,2-difluorobenzene) resulted in poor NMR data (see below). Better NMR data could be obtained using MeCN-d_3, but this formed **3.2 [MeCN]**.[65]

^{11}B NMR (160 MHz, $C_6H_4F_2$) δ -3.4 (d, $^1J_{BH}$ = 86 Hz, *B*H);

^{11}B{^{1}H} NMR (160 MHz, $C_6H_4F_2$) δ -3.6 (s, *B*H) ppm.

HRMS (ESI+) *m/z* calculated for $C_{10}H_7B_2F_{12}N_6O_8S_4^+$: 716.92215 $[M-(H^-)]^+$; found 716.91972.

Formation of *mono*-NTf_2 Pyrazabole (3.3) *in situ*

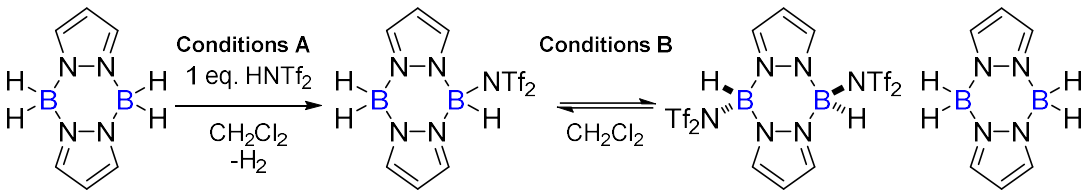

Conditions A: Pyrazabole **3.1** (0.053 g, 0.33 mmol) and $HNTf_2$ (0.093 g, 0.033 mmol, 1 equiv.) were suspended in PhCl (2 mL), leading to immediate gas evolution. Attempts to isolate **3.3** from the reaction solution resulted in precipitation of equimolar **3.1** and **3.2**.

Conditions B: Pyrazabole **3.1** (0.005 g, 0.03 mmol) and *di*-NTf_2 pyrazabole **3.2** (0.023 g, 0.03 mmol, 1 equiv.) were suspended in CD_2Cl_2 (0.55 ml) and stirred at room temperature for 10 minutes.

With both **Conditions A** and **B**, *in situ* NMR spectra showed very broad resonances in the NMR spectra and no resonances for **3.1** For *in situ* NMR spectra resulting from **Conditions B**, see the publication of this work.[65]

3.6.2 Directed C7-H Borylation of *N*-H Indoles

*The NMR spectra of the synthesised 7-Bpin indolines, and the synthesis of 3-tert-Butyl 7-Bpin Indoline **3.29** (performed by Dr Kang Yuan), can be found in the publication of this work and are not included below.*[65]

General Procedure 3.1: The Synthesis of 7-Bpin Indolines

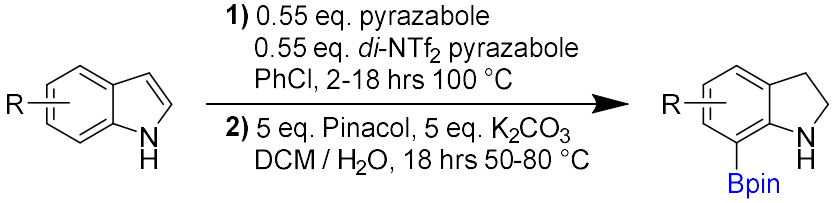

Pyrazabole **3.1** (0.026 g, 0.165 mmol, 0.55 equiv.), *di*-NTf_2 pyrazabole **3.2** (0.118 g, 0.165 mmol, 0.55 equiv.) and the corresponding indole (0.3 mmol, 1 equiv.) were suspended in chlorobenzene (2 mL) and heated to 100 °C in a sealed ampule for 2-18 hours. Upon cooling, pinacol (0.177 g, 1.5 mmol, 5 equiv.), K_2CO_3 (0.207 g, 1.5 mmol, 5 equiv.), DCM (4 mL) and water (4 mL) were added sequentially, and the ampule was sealed and heated to 50 °C (or 80 °C) for 18 hours, with rapid stirring to mix the resulting biphasic mixture. Upon returning to room temperature, the 7-BPin indoline product was extracted with pentane (4 x 10 mL). The combined organic phases were washed with water (4 x 10 mL), dried over $MgSO_4$, and filtered. Concentration *in vacuo* yielded the desired product. *Further purification was enabled by reverse phase chromatography (4 g C18 silanised silica (30 μm) column, MeOH eluent, celite dry load) where required.*

7-Bpin Indoline – 3.7

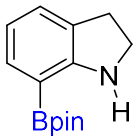

Compound **3.7** was prepared following **General Procedure 3.1** with indole (0.035 g). Reaction was heated to 100 °C for 18 hours to effect C7-borylation, then to 50 °C for 18 hours to convert to the BPin product. The product was isolated as a white solid (0.057 g, 0.233 mmol, 78 %) with no further purification necessary.

^{1}H NMR (500 MHz, $CDCl_3$) δ 7.38 (d, $^{3}J_{HH}$ = 7 Hz, 1H, ArC*H*), 7.15 (d, $^{3}J_{HH}$ = 7 Hz, 1H, ArC*H*), 6.61 (t, $^{3}J_{HH}$ = 7 Hz, 1H, ArC*H*), 5.02 (br, 1H, N*H*), 3.60 (t, $^{3}J_{HH}$ = 8.5 Hz, 2H, H_2C-C*H*$_2$-N), 3.00 (t, $^{3}J_{HH}$ = 8.5 Hz, 2H, *H*$_2$C-CH_2-N), 1.33 (s, 12H, O-C(C*H*$_3$)$_2$);

^{11}B NMR (160 MHz, $CDCl_3$) δ 31.0 (s, Ar*B*Pin);

^{13}C{^{1}H} NMR (126 MHz, $CDCl_3$) δ 158.74, 133.67, 128.52, 127.65, 117.03, 106.23 (br, *C*-B, *only detectable via ^{1}H ^{13}C HMBC*), 83.53, 47.09, 29.30, 25.10 ppm.

HRMS (ESI+) *m/z* calcd for $C_{14}H_{21}BNO_2^+$: 246.1660 $[M+H]^+$, found 246.1659.

5-Methyl 7-Bpin Indoline – 3.8

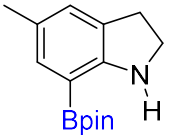

Compound **3.8** was prepared following **General Procedure 3.1** with 5-methylindole (0.039 g). Reaction was heated to 100 °C for 18 hours to effect C7-borylation, then to 50 °C for 18 hours to convert to the BPin product. The product was isolated as a yellow solid (0.059 g, 0.228 mmol, 76 %) with no further purification necessary.

^{1}H NMR (500 MHz, $CDCl_3$) δ 7.19 (s, 1H, ArC*H*), 7.00 (s, 1H, ArC*H*), 4.87 (br, 1H, N*H*), 3.57 (t, $^{3}J_{HH}$ = 8.5 Hz, 2H, H_2C-C*H*$_2$-N), 2.96 (t, $^{3}J_{HH}$ = 8.5 Hz, *H*$_2$C-CH_2-N), 2.22 (s, 3H, ArC-C*H*$_3$), 1.33 (s, 12H, O-C(C*H*$_3$)$_2$);

^{11}B NMR (160 MHz, $CDCl_3$) δ 31.0 (s, Ar*B*Pin);

^{13}C{^{1}H} NMR (126 MHz, $CDCl_3$) δ 156.63, 133.33, 129.04, 128.88, 126.27, 106.45 (br, *C*-B, *only detectable via ^{1}H ^{13}C HMBC*), 83.52, 47.40, 29.39, 25.09, 20.69 ppm.

HRMS (ESI+) *m/z* calcd for $C_{15}H_{23}BNO_2^+$: 260.1816 $[M+H]^+$, found 260.1825.

3-Methyl 7-Bpin Indoline – 3.11

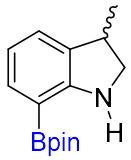

Compound **3.11** was prepared following **General Procedure 3.1** with 3-methylindole (0.039 g). Reaction was heated to 100 °C for 18 hours to effect C7-borylation, then to 50 °C for 18 hours to convert to the BPin product. The product was isolated as a colourless oil (0.068 g, 0.262 mmol, 88 %) with no further purification necessary.

^{1}H NMR (500 MHz, $CDCl_3$) δ 7.40 (dt, $^{4}J_{HH}$ = 1 Hz, $^{3}J_{HH}$ = 7.5 Hz, 1H, ArC*H*), 7.13 (dt, $^{4}J_{HH}$ = 1 Hz, $^{3}J_{HH}$ = 7.5 Hz, 1H, ArC*H*), 6.65 (t, $^{3}J_{HH}$ = 7.5 Hz, 1H, ArC*H*), 4.93 (br, 1H, N*H*), 3.76 (dd, $^{3}J_{HH}$ = 8.5 Hz, 1H, $(H_3C)CH$-C*H*$_2$-N), 3.35 (m, 1H, $(H_3C)C$*H*-CH_2-N), 3.17 (dd, $^{3}J_{HH}$ = 8.5 Hz, 1H, $(H_3C)CH$-C*H*$_2$-N), 1.34 (s, 12H, O-C(C*H*$_3$)$_2$), 1.33 (d, $^{3}J_{HH}$ = 7 Hz, 3H, (*H*$_3$C)CH-CH_2-N);

^{11}B NMR (160 MHz, $CDCl_3$) δ 30.9 (s, Ar*B*Pin);

^{13}C{^{1}H} NMR (126 MHz, $CDCl_3$) δ 158.31, 133.76, 133.52, 126.42, 117.06, 106.46 (br, *C*-B, *only detectable via ^{1}H ^{13}C HMBC*), 83.49, 55.18, 36.06, 25.11, 25.04 (inequivalent pinacol *C*H$_3$ resonances), 18.87 ppm.

HRMS (ESI+) *m/z* calcd for $C_{15}H_{23}BNO_2^+$: 260.1816 $[M+H]^+$, found 260.1826.

2-Methyl 7-Bpin Indoline – 3.9

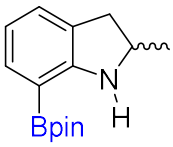

Compound **3.9** was prepared following **General Procedure 3.1** with 2-methylindole (0.039 g). Reaction was stirred at room temperature for 1 hour (*hydroboration step is slower for 2-substituted indoles*), heated to 100 °C for 18 hours to effect C7-borylation, then to 50 °C for 18 hours to convert to the BPin product. The product was isolated as a yellow oil (0.067 g, 0.259 mmol, 86 %) with no further purification necessary.

^{1}H NMR (500 MHz, $CDCl_3$) δ 7.40 (d, $^{3}J_{HH}$ = 7.5 Hz, 1H, ArC*H*), 7.13 (d, $^{3}J_{HH}$ = 7.5 Hz, 1H, ArC*H*), 6.62 (dd, $^{3}J_{HH}$ = 7.5 Hz, 1H, ArC*H*), 5.05 (br, 1H, N*H*), 4.05 (m, 1H, H_2C-C*H*(CH_3)-N), 3.13 (dd, J_{HH} = 16 Hz, 8.5 Hz, 1H, *H*$_2$C-CH(CH_3)-N), 2.63 (dd, J_{HH} = 16 Hz, 8.5 Hz, 1H, *H*$_2$C-CH(CH_3)-N), 1.36 (s, 6H, O-C(CH_3)$_2$), 1.35 (s, 6H, O-C(CH_3)$_2$), 1.33 (d, $^{3}J_{HH}$ = 6 Hz, 3H, H_2C-CH(CH_3)-N);

11B NMR (160 MHz, $CDCl_3$) δ 31.0 (s, Ar*B*Pin);

^{13}C{^{1}H} NMR (126 MHz, $CDCl_3$) δ 158.0, 133.68, 128.10, 127.67, 116.89, 105.96 (br, *C*-B, *only detectable via ^{1}H ^{13}C HMBC*), 83.44, 54.97, 37.32, 25.12, 25.0 (inequivalent pinacol *C*H_3 resonances), 22.39 ppm.

HRMS (ESI+) *m/z* calcd for $C_{15}H_{23}BNO_2^+$: 260.1816 [M+H]$^+$, found 260.1827.

6-Methyl 7-Bpin Indoline – 3.12

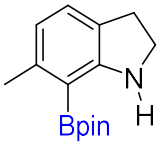

Compound **3.12** was prepared following **General Procedure 3.1** with 6-methylindole (0.039 g). Reaction was heated to 100 °C for 18 hours to effect C7-borylation, then to 80 °C for 18 hours (with PhCl in place of DCM) to convert to the BPin product. The product was isolated as a yellow oil (0.043 g, 0.166 mmol, 55 %) with no further purification necessary.

^{1}H NMR (500 MHz, $CDCl_3$) δ 7.00 (d, $^{3}J_{HH}$ = 7 Hz, ArC*H*) 6.43 (d, $^{3}J_{HH}$ = 7 Hz, ArC*H*) 5.34 (br, 1H, N*H*), 3.57 (t, $^{3}J_{HH}$ = 8 Hz, 2H, H_2C-C*H*$_2$-N), 2.95 (t, $^{3}J_{HH}$ = 8 Hz, 2H, *H*$_2$C-CH_2-N), 2.44 (s, 3H, Ar-C*H*$_3$), 1.33 (s, 12H, O-C(CH_3)$_2$);

^{11}B NMR (160 MHz, $CDCl_3$) δ 31.1 (s, Ar*B*Pin);

^{13}C{^{1}H} NMR (126 MHz, $CDCl_3$) δ 160.10, 144.46, 126.87, 125.93, 119.05, 106.30 (*C*-B), 82.95, 47.19, 29.05, 25.12, 22.77 ppm.

HRMS (ESI+) *m/z* calcd for $C_{15}H_{23}BNO_2^+$: 260.1816 [M+H]$^+$, found 260.1820.

5-Chloro 7-Bpin Indoline – 3.14

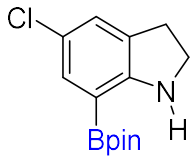

Compound **3.14** was prepared following **General Procedure 3.1** with 5-chloroindole (0.045 g). Reaction was heated to 100 °C for 2 hours to effect C7-borylation, then to 50 °C for 18 hours to convert to the BPin product. The product was isolated as an orange oil (0.067 g, 0.240 mmol, 80 %) with no further purification necessary. *Note: the broad N-H resonance was not observed for this substrate in the ^{1}H NMR spectrum.*

^{1}H NMR (500 MHz, $CDCl_3$) δ 7.32 (d, $^{4}J_{HH}$ = 2 Hz, 1H, ArC*H*), 7.08 (d, $^{4}J_{HH}$ = 2 Hz, 1H, ArC*H*), 3.62 (t, $^{3}J_{HH}$ = 8 Hz, 2H, H_2C-C*H*$_2$-N), 2.99 (t, $^{3}J_{HH}$ = 8 Hz, 2H, *H*$_2$C-CH_2-N), 1.32 (s, 12H, O-C(C*H*$_3$)$_2$);

^{11}B NMR (160 MHz, $CDCl_3$) δ 30.6 (s, Ar*B*Pin);

^{13}C{^{1}H} NMR (126 MHz, $CDCl_3$) δ 157.22, 132.60, 130.79, 127.74, 121.68, 105.59 (*C*-B), 83.86, 47.34, 29.16, 25.07 ppm.

HRMS (ESI+) *m/z* calcd for $C_{14}H_{20}BNO_2Cl^+$: 280.1270 $[M+H]^+$, found 280.1274.

4-Fluoro 7-Bpin Indoline – 3.24

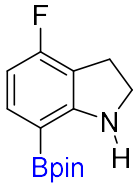

Compound **3.24** was prepared following **General Procedure 3.1** with 4-fluoroindole (0.041 g). Reaction was heated to 100 °C for 2 hours to effect C7-borylation, then to 50 °C for 18 hours to convert to the BPin product. The product was isolated as a colourless oil (0.067 g, 0.255 mmol, 85 %) with no further purification necessary.

^{1}H NMR (500 MHz, $CDCl_3$) δ 7.35 (dd, $^{4}J_{HF}$ = 6.5 Hz, $^{3}J_{HH}$ = 8.5 Hz, 1H, ArC*H*), 6.31 (dd, $^{3}J_{HF}$ = 8.5 Hz, $^{3}J_{HH}$ = 8.5 Hz, 1H, ArC*H*), 5.12 (br, 1H, N*H*), 3.66 (t, $^{3}J_{HH}$ = 8.5 Hz, 2H, H_2C-C*H*$_2$-N), 3.04 (t, $^{3}J_{HH}$ = 8.5 Hz, 2H, *H*$_2$C-CH_2-N), 1.33 (s, 12H, O-C(C*H*$_3$)$_2$);

^{11}B NMR (160 MHz, $CDCl_3$) δ 30.5 (s, Ar*B*Pin);

^{19}F NMR (471 MHz, $CDCl_3$) δ -114.59 (dd, $^{4}J_{HF}$ = 6.5 Hz, $^{3}J_{HF}$ = 8.5 Hz, ArC*F*);

$^{13}C\{^{1}H\}$ NMR (126 MHz, $CDCl_3$) δ 162.65 (d, $^{1}J_{CF}$ = 163 Hz), 161.62 (d, $^{3}J_{CF}$ = 74 Hz), 136.32 (d, $^{3}J_{CF}$ = 9 Hz), 113.17 (d, $^{2}J_{CF}$ = 20 Hz), 104.88 (d, $^{2}J_{CF}$ = 20 Hz), 102.31 (br, *C*-B, *only detectable via ^{1}H ^{13}C HMBC*), 83.55, 47.31, 25.54, 25.06 ppm.

HRMS (ESI+) *m/z* calcd for $C_{14}H_{20}BFNO_2^+$: 264.1566 $[M+H]^+$, found 264.1569.

4-Bromo 7-Bpin Indoline – 3.25

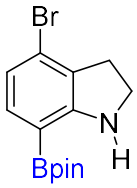

Compound **3.25** was prepared following **General Procedure 3.1** with 4-bromoindole (0.059 g, 0.038 mL). Reaction was heated to 100 °C for 2 hours to effect C7-borylation, then to 50 °C for 18 hours to convert to the BPin product. The crude product was purified via reverse phase chromatography to yield the product as a white solid (0.047 g, 0.145 mmol, 48%).

^{1}H NMR (500 MHz, $CDCl_3$) δ 7.20 (d, $^{3}J_{HH}$ = 8 Hz, 1H, ArC*H*), 6.71 (d, $^{3}J_{HH}$ = 8 Hz, 1H, ArC*H*), 5.16 (br, 1H, N*H*), 3.64 (t, $^{3}J_{HH}$ = 8.5 Hz, 2H, H_2C-C*H*$_2$-N), 3.02 (t, $^{3}J_{HH}$ = 8.5 Hz, 2H, *H*$_2$C-CH_2-N), 1.32 (s, 12H, O-C(C*H*$_3$)$_2$);

^{11}B NMR (160 MHz, $CDCl_3$) δ 30.8 (s, Ar*B*Pin);

$^{13}C\{^{1}H\}$ NMR (126 MHz, $CDCl_3$) δ159.46, 135.32, 128.87, 123.62, 119.86, 105.59 (*C*-B), 83.71, 46.09, 30.64, 25.07 ppm.

HRMS (ESI+) *m/z* calcd for $C_{14}H_{20}BNO_2Br^+$: 324.0765 $[M+H]^+$, found 324.0765.

5-Methoxy 7-Bpin Indoline – 3.26

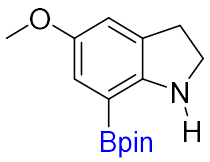

Compound **3.26** was prepared following **General Procedure 3.1** with 5-(methoxy) indole (0.044 g). Reaction was heated to 100 °C for 2 hours to effect C7-borylation, then to 50 °C for 18 hours to convert to the BPin product. The product was isolated as a yellow oil (0.055 g, 0.200 mmol, 67 %) with no further purification necessary. *Note: the broad N-H resonance is not observed for this substrate in the ^{1}H NMR spectrum.*

^{1}H NMR (500 MHz, $CDCl_3$) δ 6.88 (m, 1H, ArC*H*), 6.84 (m, 1H, ArC*H*), 3.76 (s, 3H, Ar-OC*H*$_3$), 3.57 (t, $^{3}J_{HH}$ = 8.5 Hz, 2H, H_2C-C*H*$_2$-N), 2.97 (t, $^{3}J_{HH}$ = 8.5 Hz, 2H, *H*$_2$C-CH_2-N), 1.33 (s, 12H, O-C(C*H*$_3$)$_2$);

^{11}B NMR (160 MHz, $CDCl_3$) δ 30.8 (s, Ar*B*Pin);

^{13}C{^{1}H} NMR (126 MHz, $CDCl_3$) δ 153.32, 152.25, 130.82, 117.06, 115.46, 105.48 (br, *C*-B, *only detectable via ^{1}H ^{13}C HMBC*), 83.61, 56.29, 47.64, 29.64, 25.07 ppm.

HRMS (ESI+) *m/z* calcd for $C_{15}H_{23}BNO_3^+$: 276.1766 $[M+H]^+$, found 276.1767.

5-Methylthio 7-Bpin Indoline – 3.27

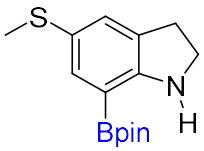

Compound **3.27** was prepared following **General Procedure 3.1** with 5-(methylthio) indole (0.049 g, 0.040 mL). Reaction was heated to 100 °C for 2 hours to effect C7-borylation, then to 50 °C for 18 hours to convert to the BPin product. The product was isolated as a brown oil (0.054 g, 0.185 mmol, 62 %) with no further purification necessary.

^{1}H NMR (500 MHz, $CDCl_3$) δ 7.45 (m, 1H, ArC*H*), 7.21 (m, 1H, ArC*H*), 5.29 (br, 1H, N*H*), 3.63 (t, $^{3}J_{HH}$ = 8.5 Hz, 2H, H_2C-C*H*$_2$-N), 3.00 (t, $^{3}J_{HH}$ = 8.5 Hz, *H*$_2$C-CH_2-N), 2.40 (s, 3H, Ar-SC*H*$_3$), 1.32 (s, 12H, O-C(C*H*$_3$)$_2$);

^{11}B NMR (160 MHz, $CDCl_3$) δ 30.6 (s, Ar*B*Pin);

^{13}C{^{1}H} NMR (126 MHz, $CDCl_3$) δ 156.79, 136.10, 130.27, 130.16, 124.69, 107.89 (br, *C*-B, *only detectable via ^{1}H ^{13}C HMBC*), 83.78, 47.16, 29.04, 25.06, 19.63 ppm.

HRMS (ESI+) *m/z* calcd for $C_{15}H_{23}BNO_2S^+$: 292.1537 $[M+H]^+$, found 292.1538.

2,3-Tetrahydrocyclopentyl 7-BPin Indoline – 3.28

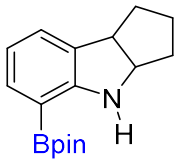

Compound **3.28** was prepared following **General Procedure 3.1** with 1,2,3,4-tetrahydrocyclopent[*b*] indole (0.047 g). Reaction was stirred at room temperature for 1 hour (*hydroboration step is slower for 2-substituted indoles*), heated to 100 °C for 18 hours to effect C7-borylation, then to 50 °C for 18 hours to convert to the BPin product. The crude product was purified via reverse phase chromatography to yield the product as a colourless oil (0.063 g, 0.221 mmol, 74%).

^{1}H NMR (500 MHz, $CDCl_3$) δ 7.36 (d, $^{3}J_{HH}$ = 7.5 Hz, 1H, ArC*H*), 7.08 (d, $^{3}J_{HH}$ = 7.0 Hz, 1H, ArC*H*), 6.56 (dd, $^{3}J_{HH}$ = 7.5, 7.0 Hz, 1H, ArC*H*), 5.03 (br, 1H, N*H*), 4.43 (br, 1H, HC-$(CH_2)_3$-C*H*-N), 3.73 (br, 1H, *H*C-$(CH_2)_3$-CH-N), 2.00-1.54 (m, 6H, HC-$(CH_2)_3$-CH-N), 1.35 (s, 12H, O-C$(CH_3)_2$);

^{11}B NMR (160 MHz, $CDCl_3$) δ 30.9 (s, Ar*B*Pin);

^{13}C{^{1}H} NMR (126 MHz, $CDCl_3$) δ 158.34, 133.85, 132.24, 127.50, 116.05, 104.24 (br, *C*-B, *only detectable via ^{1}H ^{13}C HMBC*), 83.33, 63.14, 46.43, 36.82, 35.15, 25.17, 24.55, 24.55 ppm.

HRMS (ESI+) *m/z* calcd for $C_{17}H_{25}BNO_2^+$: 286.1973 $[M+H]^+$, found 286.1979.

Scaled-up Synthesis of 7-Bpin Indoline 3.7

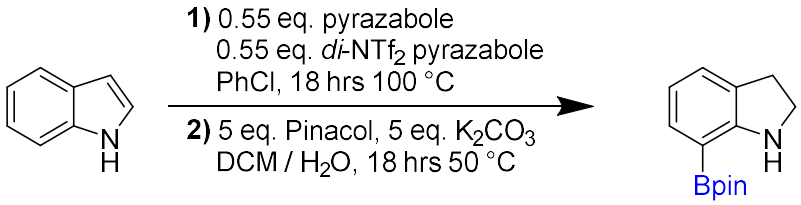

Pyrazabole **3.1** (0.132 g, 0.825 mmol, 0.55 equiv.), *di*-NTf_2 pyrazabole **3.2** (0.592 g, 0.825 mmol, 0.55 equiv.) and *N*-H indole (0.175 g, 1.5 mmol, 1 equiv.) were suspended in chlorobenzene (10 mL) and heated to 100 °C in a sealed ampule for 18 hours. Upon cooling, pinacol (0.886 g, 7.5 mmol, 5 equiv.), K_2CO_3 (1.036 g, 7.5 mmol, 5 equiv.), DCM (20 mL) and water (20 mL) were added sequentially, and the ampule was sealed and heated to 50 °C for 18 hours, with

rapid stirring to mix the resulting biphasic mixture. Upon returning to room temperature, the 7-BPin indoline product was extracted with pentane (4 x 30 mL). The combined organic phases were washed with water (4 x 30 mL), dried over $MgSO_4$, and filtered. Concentration *in vacuo* yielded the desired product, **3.7**, as a white solid (0.314 g, 1.28 mmol, 85 %) with no further purification necessary. Analytical data matched the sample of **3.7** synthesised using **General Procedure 3.1**. *The NMR spectra of this reaction can be found in the appendix of this thesis.*

Reactivity of 7-Bpin Indoline: Suzuki-Miyaura Cross-Coupling

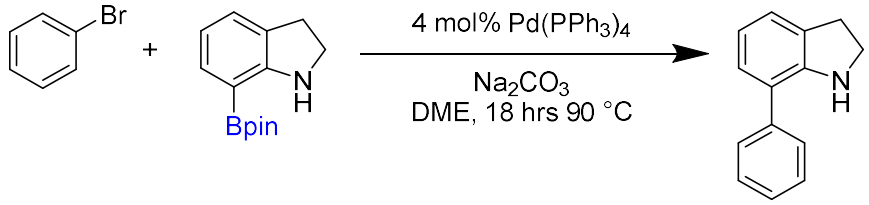

A round-bottom flask was charged with $Pd(PPh_3)_4$ (20 mg, 0.016 mmol, 0.04 equiv.). A degassed solution of bromobenzene (0.043 mL, 0.41 mmol, 1 equiv.) in dimethoxyethane (DME) (3 mL) was added to the flask and the reaction stirred for 15 minutes at room temperature. A degassed solution of **3.7** (*prepared following **General Procedure 3.1**, 100 mg, 0.41 mmol*) in DME (5 mL) was added to the flask and the reaction stirred for 15 minutes at room temperature, followed by addition of a degassed solution of Na_2CO_3 (173 mg, 0.82 mmol, 2 equiv.) in water (2 mL). The reaction was heated to 90 °C and refluxed for 18 hours. The product was extracted with ethyl acetate (4 x 15 mL). The combined organic phases were washed with brine (2 x 20 mL), dried over $MgSO_4$, and purified by column chromatography on silica gel (EtOAc : Hexane) to yield the desired product as a dark orange solid (0.045 g, 0.230 mmol, 57 %). Analytical data are in accordance with literature values.[90] *The NMR spectra of this reaction can be found in the appendix of this thesis.*

^{1}H NMR (500 MHz, $CDCl_3$) δ 7.59-7.56 (m, 2H), 7.47-7.43 (m, 2H), 7.35-7.30 (m, 1H),7.15-7.10 (m, 2H), 6.83 (t, $^{3}J_{HH}$ = 7.5 Hz, 1H), 4.08 (br, 1H, N*H*), 3.55 (t, $^{3}J_{HH}$ = 8.5 Hz, 2H), 3.13 (t, $^{3}J_{HH}$ = 8.5 Hz, 2H);

^{13}C{^{1}H} NMR (126 MHz, $CDCl_3$) δ 149.22, 139.71, 129.82, 128.84, 128.12, 127.50, 126.92, 123.86, 123.13, 119.10, 47.48, 30.19 ppm.

HRMS (ESI+) *m/z* calcd for $C_{14}H_{13}NNa^{+}$: 218.09402 [M+Na]$^{+}$, found 218.0946.

3.6.3 Directed *Ortho* C-H Borylation of Indoline and Aniline Derivatives

*The NMR spectra of the N/C7-borylated indoline intermediate **3.6** (starting from indoline) 7-Bpin indoline, **3.7**, (starting from indoline) and 8-Bpin tetrahydroquinoline, **3.30**, can be found in the appendix of this thesis.*

General Procedure 3.2: Directed *Ortho* C-H Borylation of Indoline and Tetrahydroquinoline

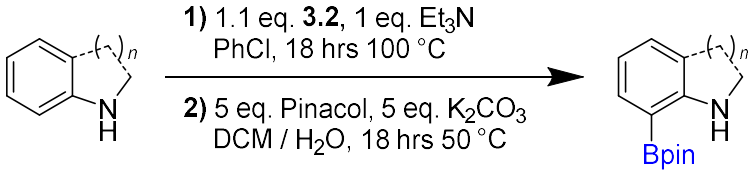

Di-NTf_2 pyrazabole **3.2** (0.237 g, 0.33 mmol, 1.1 equiv.), and the corresponding indoline (*n=1*) / tetrahydroquinoline (*n=2*) (0.3 mmol, 1 equiv.) were suspended in chlorobenzene (2 mL) and stirred at room temperature for 30 minutes. Triethylamine (0.042 mL, 0.3 mmol, 1 equiv.) was added, and the reaction was stirred again for 30 minutes at room temperature before being heated to 100 °C in a sealed ampule for 18 hours. Upon cooling, pinacol (0.177 g, 1.5 mmol, 5 equiv.), K_2CO_3 (0.207 g, 1.5 mmol, 5 equiv.), DCM (4 mL) and water (4 mL) were added sequentially, and the ampule was sealed and heated to 50 °C for 18 hours, with rapid stirring to mix the resulting biphasic mixture. Upon returning to room temperature, the BPin product was extracted with pentane (4 x 10 mL). The combined organic phases were washed with water (4 x 10 mL), dried over $MgSO_4$, and filtered. Concentration, and removal of excess triethylamine *in vacuo* yielded the desired product cleanly without the need for further purification.

7-Bpin Indoline (3.7) from Indoline

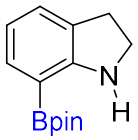

Compound **3.7** was prepared following **General Procedure 3.2** with *N*-H indoline (0.034 mL). The product was isolated as a white solid (0.061 g, 0.249 mmol, 83 %). Analytical data matched the sample of **3.7** synthesised using **General Procedure 3.1** starting from *N*-H indole.

8-Bpin Tetrahydroquinoline – 3.30

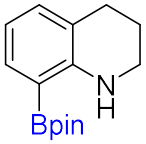

Compound **3.30** was prepared following **General Procedure 3.2** with *N*-H tetrahydroquinoline (0.038 mL). The product was isolated as a yellow oil (0.055 g, 0.212 mmol, 71 %). Analytical data are in accordance with literature values.[32]

^{1}H NMR (500 MHz, $CDCl_3$) δ 7.47 (d, $^{3}J_{HH}$ = 7.5 Hz, 1H, ArC*H*), 7.01 (d, $^{3}J_{HH}$ = 7.5 Hz, 1H, ArC*H*), 6.52 (t, $^{3}J_{HH}$ = 7 Hz, 1H, ArC*H*), 5.86 (br, 1H, N*H*), 3.39-3.36 (m, $^{3}J_{HH}$ 2H, CH_2-CH_2-C*H*$_2$-N), 2.77 (t, $^{3}J_{HH}$ = 6.5 Hz, 2H, CH_2-C*H*$_2$-CH_2-N), 1.95-1.90 (m, $^{3}J_{HH}$ 2H, C*H*$_2$-CH_2-CH_2-N), 1.35 (s, 12H, O-C(C*H*$_3$)$_2$);

^{11}B NMR (160 MHz, $CDCl_3$) δ 31.1 (s, Ar*B*Pin);

^{13}C{^{1}H} NMR (126 MHz, $CDCl_3$) δ 151.46, 135.08, 132.97, 120.29, 115.02, 109.65 (br, *C*-B, *only detectable via ^{1}H ^{13}C HMBC*), 83.47, 41.77, 27.79, 25.01, 21.72 ppm.

HRMS (ESI+) *m/z* calcd for $C_{15}H_{23}BNO_2^+$: 260.18164 $[M+H]^+$, found 260.1822.

3.6.4 Characterisation of N/C7-Borylated Indoline Intermediates

The NMR spectra of the synthesised N/C7-borylated indolines intermediates can be found in the publication of this work and are not included below.[65]

General Procedure 3.3: N/C7 Borylation of Indole

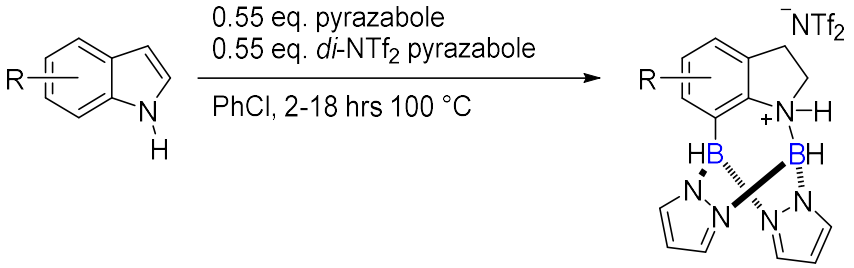

Pyrazabole **3.1** (0.018 g, 0.11 mmol, 0.55 equiv.), *di*-NTf_2 pyrazabole **3.2** (0.079 g, 0.11 mmol, 0.55 equiv.) and the corresponding indole (0.1 mmol, 1 equiv.), were added to an ampule and suspended in chlorobenzene (1.5 mL). The reaction was heated to 100 °C in a sealed ampule for 2-18 hours. The reaction was then concentrated, and the solvent replaced with $CDCl_3$ for NMR characterisation.

N/C7-Borylated Indoline Intermediate – 3.6

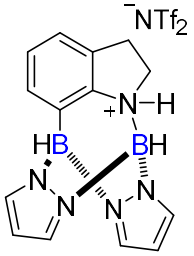

Compound **3.6** was prepared following **General Procedure 3.3** with indole (0.023 g). Reaction was heated to 100 °C for 18 hours to effect C7-borylation then concentrated, and the solvent replaced with $CDCl_3$ for NMR characterisation.

^{1}H NMR (500 MHz, $CDCl_3$) δ 8.14 (d, $^3J_{HH}$ = 3 Hz, 1H, N=C*H*-CH), 7.95 (d, $^3J_{HH}$ = 3 Hz, 1H, N=C*H*-CH), 7.92 (d, $^3J_{HH}$ = 3 Hz, 1H, N=C*H*-CH), 7.77 (d, $^3J_{HH}$ = 3 Hz, 1H, N=C*H*-CH), 7.7 (br, s, 1H N-*H*), 7.46 (d, $^3J_{HH}$ = 7 Hz, 1H, ArC*H*), 7.31 (t, $^3J_{HH}$ = 7 Hz, 1H, ArC*H*), 7.22 (d, $^3J_{HH}$ = 7 Hz, 1H, ArC*H*), 6.53 (dd, $^3J_{HH}$ = 3 Hz, 3 Hz, 1H, N=CH-C*H*), 6.45 (dd, $^3J_{HH}$ = 3 Hz, 3 Hz, 1H, N=CH-C*H*), 4.29 (m, 1H, N-C*H*$_2$-CH$_2$), 3.38 (m, 1H, N-CH$_2$-C*H*$_2$), 3.25 (m, 1H, N-C*H*$_2$-CH$_2$), 2.89 (m, 1H, N-CH$_2$-C*H*$_2$);

^{1}H{^{11}B} NMR (500 MHz, $CDCl_3$) δ 8.14 (d, $^{3}J_{HH}$ = 3 Hz, 1H, N=C*H*-CH), 7.95 (d, $^{3}J_{HH}$ = 3 Hz, 1H, N=C*H*-CH), 7.92 (d, $^{3}J_{HH}$ = 3 Hz, 1H, N=C*H*-CH), 7.77 (d, $^{3}J_{HH}$ = 3 Hz, 1H, N=C*H*-CH), 7.7 (br, s, 1H N-*H*), 7.46 (d, $^{3}J_{HH}$ = 7 Hz, 1H, ArC*H*), 7.31 (t, $^{3}J_{HH}$ = 7 Hz, 1H, ArC*H*), 7.22 (d, $^{3}J_{HH}$ = 7 Hz, 1H, ArC*H*), 6.53 (dd, $^{3}J_{HH}$ = 3 Hz, 3 Hz, 1H, N=CH-C*H*), 6.45 (dd, $^{3}J_{HH}$ = 3 Hz, 3 Hz, 1H, N=CH-C*H*), 4.35 (br, 2H, B*H*), 4.29 (m, 1H, N-C*H*$_2$-CH$_2$), 3.38 (m, 1H, N-CH$_2$-C*H*$_2$), 3.25 (m, 1H, N-C*H*$_2$-CH$_2$), 2.89 (m, 1H, N-CH$_2$-C*H*$_2$);

^{11}B NMR (160 MHz, $CDCl_3$) δ -4.0 (br, C7-*B*(Pyrz), N-*B*(Pyrz));

^{11}B{^{1}H} NMR (160 MHz, $CDCl_3$) δ -3.6 (s, C7-*B*(Pyrz)), -5.2 (s, N-*B*(Pyrz));

^{13}C{^{1}H} NMR (126 MHz, $CDCl_3$) δ 141.93, 139.76, 139.67, 138.86, 137.97, 135.77, 133.20, 129.30, 125.37 119.92 (q, $^{1}J_{CF}$ = 321 Hz, S*C*F$_3$), 108.07, 107.98, 53.67, 28.79 (*C-B was not visible even via ^{1}H ^{13}C HMBC*);

^{19}F NMR (471 MHz, $CDCl_3$) δ -78.61 (s, SC*F*$_3$) ppm.

HRMS (ESI+) *m/z* calcd for $C_{14}H_{16}B_2N_5^+$: 276.1586 $[M]^+$, found 276.1596.

N/C7-Borylated 5-Chloro Indoline Intermediate – 3.15

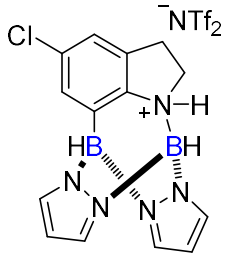

Compound **3.15** was prepared following **General Procedure 3.3** with 5-chloro indole (0.030 g). Reaction was heated to 100 °C for 2 hours to effect C7-borylation then concentrated, and the solvent replaced with $CDCl_3$ for NMR characterisation. *Note: the broad N-H resonance that was observed for **3.6** is not observed in the spectra of this congener, but all other data are closely comparable to **3.6** supporting the characterisation of this species as **3.15**.*

^{1}H NMR (500 MHz, $CDCl_3$) δ 8.12 (d, $^{3}J_{HH}$ = 2.5 Hz, 1H, N=C*H*-CH), 7.94 (d, $^{3}J_{HH}$ = 2.5 Hz, 1H, N=C*H*-CH), 7.92 (d, $^{3}J_{HH}$ = 2.5 Hz, 1H, N=C*H*-CH), 7.77 (d, $^{3}J_{HH}$ = 2.5 Hz, 1H, N=C*H*-CH), 7.41 (d, $^{4}J_{HH}$ = 1.5 Hz, 1H, ArC*H*), 7.17 (d, $^{4}J_{HH}$ = 1.5 Hz, 1H, ArC*H*), 6.55 (dd, $^{3}J_{HH}$ = 2.5 Hz, 2.5 Hz, 1H, N=CH-C*H*), 6.46 (dd, $^{3}J_{HH}$ = 2.5 Hz, 2.5 Hz, 1H, N=CH-C*H*), 4.29 (m , 1H, N-C*H*$_2$-CH$_2$), 3.36 (m , 1H, N-CH$_2$-C*H*$_2$), 3.26 (m , 1H, N-C*H*$_2$-CH$_2$), 2.88 (m , 1H, N-CH$_2$-C*H*$_2$);

^{1}H{^{11}B} NMR (500 MHz, $CDCl_3$) δ 8.12 (d, $^{3}J_{HH}$ = 2.5 Hz, 1H, N=C*H*-CH), 7.94 (d, $^{3}J_{HH}$ = 2.5 Hz, 1H, N=C*H*-CH), 7.92 (d, $^{3}J_{HH}$ = 2.5 Hz, 1H, N=C*H*-CH), 7.77 (d, $^{3}J_{HH}$ = 2.5 Hz, 1H, N=C*H*CH), 7.41 (d, ^{4}JHH = 1.5 Hz, 1H, ArC*H*), 7.17 (d, $^{4}J_{HH}$ = 1.5 Hz, 1H, ArC*H*), 6.55 (dd, $^{3}J_{HH}$ = 2.5 Hz, 2.5 Hz, 1H, N=CH-C*H*), 6.46 (dd, $^{3}J_{HH}$ = 2.5 Hz, 2.5 Hz, 1H, N=CH-C*H*), 4.31 (br, 2H, B*H*), 4.29 (m , 1H, N-C*H*$_2$-CH_2), 3.36 (m , 1H, N-CH_2-C*H*$_2$), 3.26 (m , 1H, N-C*H*$_2$-CH_2), 2.88 (m , 1H, N-CH_2-C*H*$_2$);

^{11}B NMR (160 MHz, $CDCl_3$) δ -4.1 (br, C7-*B*(Pyrz), N-*B*(Pyrz));

^{11}B{^{1}H} NMR (160 MHz, $CDCl_3$) δ -3.8 (s, C7-*B*(Pyrz)), -5.2 (s, N-*B*(Pyrz));

^{13}C{^{1}H} NMR (126 MHz, $CDCl_3$) δ 140.43, 139.96, 139.92, 139.11, 138.20, 138.02, 135.15, 133.00, 125.38, 119.84 (q, $^{1}J_{CF}$ = 321 Hz, S*C*F_3), 108.28, 108.20, 53.94, 28.72 (*C-B was not visible even via ^{1}H ^{13}C HMBC*);

^{19}F NMR (471 MHz, $CDCl_3$) δ -78.70 (s, SC*F*$_3$) ppm.

HRMS (ESI+) *m/z* calcd for $C_{14}H_{15}B_2N_5Cl^+$: 310.1197 [M]$^+$, found 310.1198.

Addition of Exogenous Base to N/C7-Borylated Indoline Intermediate 3.6

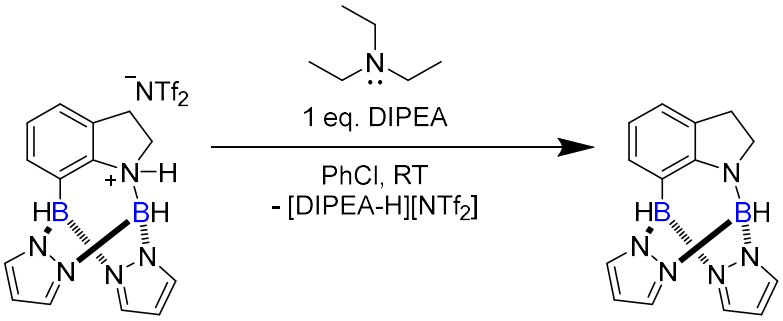

To a sample of **3.6** (0.1 mmol, 0.056 g) in chlorobenzene (0.5 mL) was added *N,N*-Diisopropylethylamine (1 equiv., 0.017 mL). NMR spectra were recorded after 15 minutes at room temperature.

3.6.5 Reaction Profiling using *in situ* NMR Spectroscopy

The full NMR spectra of these reactions can be found in the appendix of this thesis.

General Procedure 3.4: Profiling the Reactions of Indole / 5-Chloro Indole

To a J. Young's NMR tube was added the corresponding indole (0.1 mmol), pyrazabole **3.1** (0.009 g, 0.055 mmol, 0.55 equiv.), *di*-NTf_2 pyrazabole **3.2** (0.039 g, 0.055 mmol, 0.55 equiv.) and chlorobenzene (0.5 mL). This was mixed by inversion (approx. 1 rotation / s) at room temperature and analysed by NMR spectroscopy at regular time points. Samples were heated in a heating block without inversion / external mixing.

Attempted Catalytic Reaction of 5-Chloro Indole

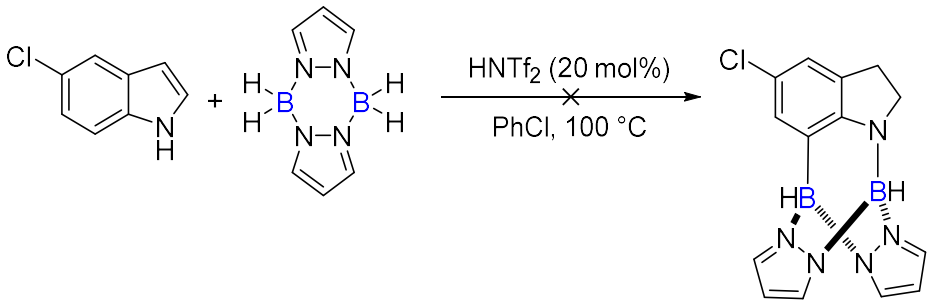

To a J. Young's NMR tube was added pyrazabole **3.1** (0.016 g, 0.1 mmol, 1 equiv.), $HNTf_2$ (0.006 g, 0.020 mmol, 0.20 equiv.) and chlorobenzene (0.5 mL). This was mixed by inversion (approx. 1 rotation / s) at room temperature for 30 minutes. 5-chloro indole (0.015 g, 0.1 mmol, 1 equiv.) was added and the sample was heated to 100 °C in a heating block without inversion / external mixing. The sample was analysed by NMR spectroscopy at regular time points.

3.6.6 Deuterium-Labelling Experiments

The NMR spectra of the synthesised compounds and the profiled reaction reported below can be found in the appendix of this thesis.

Synthesis of *N*-D Indole

This procedure is based on a previous report by Liu et al.[91]

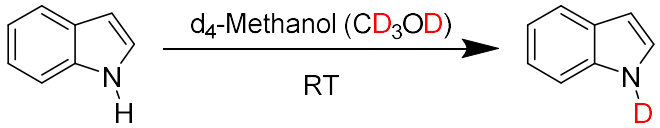

N-H Indole (1.0 g, 8.53 mmol) was added to an ampule and suspended in d_4-methanol (6 mL). The reaction was stirred at room temperature for 4 hours. Concentration *in vacuo* yielded an off-white solid. The solid was redissolved in d_4-methanol (6 mL) and stirred at room temperature for 18 hours. Concentration *in vacuo* yielded the title product as a yellow solid (0.902 g, 7.63 mmol, 89 %) with 81% D incorporation. Analytical data are in accordance with literature values.[91]
Note: A small amount of N-H indole is present (19%) and can be seen as a minor species in the ^{13}C NMR spectrum, and a minor N-H resonance in the ^{1}H NMR spectrum.

^{1}H NMR (500 MHz, $CDCl_3$) δ 7.67 (t, J_{HH} = 8.5 Hz, 1H), 7.41 (d, J_{HH} = 8.5 Hz, 1H), 7.23-7.19 (m, 2H), 7.15 (q, J_{HH} = 7 Hz, 1H), 6.58 (t, J_{HH} = 3 Hz, 1H);

^{2}H NMR (77 MHz, $CHCl_3$) δ 8.17 (br s, N-*D*);

^{13}C{^{1}H} NMR (126 MHz, $CDCl_3$) δ 135.78, 127.99, 124.08, 122.13, 120.88, 119.95, 111.09 (d, J_{CD} = 2.5 Hz), 102.74ppm.

Monitoring the Reaction of *N*-D Indole with *mono*-NTf_2 pyrazabole

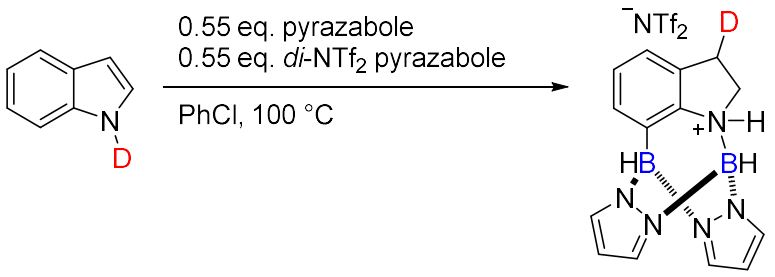

To a J. Young's NMR tube was added *N*-D indole (0.012g, 0.1 mmol), pyrazabole **3.1** (0.009 g, 0.055 mmol, 0.55 equiv.), *di*-NTf_2 pyrazabole **3.2** (0.039 g, 0.055 mmol, 0.55 equiv.) and chlorobenzene (0.5 mL). This was mixed by inversion (approx. 1 rotation / s) at room temperature and analysed by NMR spectroscopy at regular time points. The sample was heated in a heating block without inversion / external mixing.

Synthesis of 3-Deutero 7-Bpin Indoline – 3.7-D

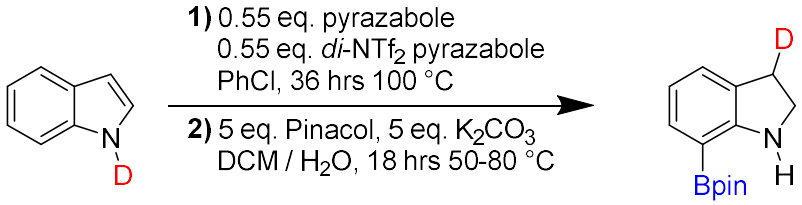

Compound **3.7-D** was prepared following **General Procedure 3.1** with *N*-D indole (0.035 g). Reaction was heated to 100 °C for 18 hours to effect C7-borylation, then to 50 °C for 18 hours to convert to the BPin product. The product was isolated as a white solid (0.028 g, 0.119 mmol, 51 %). *Note: A small amount of 3-H 7-Bpin indoline (**3.7**) is observed in the NMR spectra, due to the presence of minor N-H indole in the starting material. There is also a small amount of 3-D indoline, due to protodeboronation of the C7-B bond.*

^{1}H NMR (500 MHz, $CDCl_3$) δ 7.38 (d, $^3J_{HH}$ = 7 Hz, 1H, ArC*H*), 7.15 (d, $^3J_{HH}$ = 7 Hz, 1H, ArC*H*), 6.61 (t, $^3J_{HH}$ = 7 Hz, 1H, ArC*H*), 3.60 (t, $^3J_{HH}$ = 8.5 Hz, 2H, H_2C-C*H*$_2$-N), 3.01 (t, $^3J_{HH}$ = 8.5 Hz, 2H, *H*$_2$C-CH_2-N), 1.33 (s, 12H, O-C(C*H*$_3$)$_2$);

^{2}H NMR (77 MHz, $CHCl_3$) δ 3.41 (br s, C-*D*);

^{11}B NMR (160 MHz, $CDCl_3$) δ 30.89 (s, Ar*B*Pin);

$^{13}C\{^{1}H\}$ NMR (126 MHz, $CDCl_3$) δ 158.74 (d, J_{CD} = 3 Hz), 133.66 (d, J_{CD} = 1 Hz), 128.52, 127.65 (d, J_{CD} = 3 Hz), 117.01, 83.53, 47.02 (d, J_{CD} = 10 Hz), 29.28, 25.09 ppm (*C-B was not visible even via ^{1}H ^{13}C HMBC*).

HRMS (ESI+) *m/z* calcd for $C14H_{20}DBNO_2^+$: 247.17226 $[M+H]^+$, found 247.1726.

3.6.7 Hydrodehalogenation Studies

The NMR spectra of these reactions can be found in the appendix of this thesis.

General Procedure 3.5: N/C7-Borylation and Hydrodehalogenation

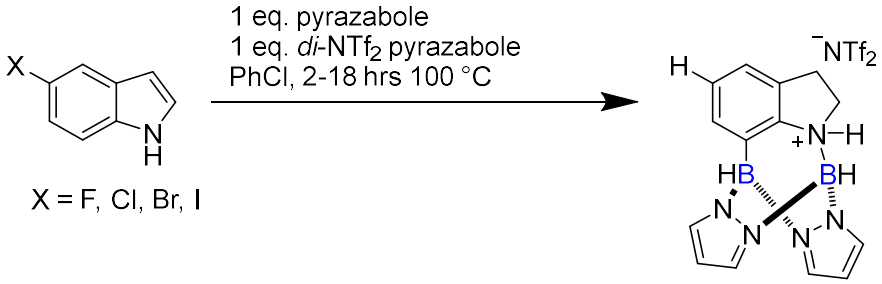

To a J. Young's NMR tube was added the corresponding 5-halo indole (0.1 mmol), pyrazabole **3.1** (0.016 g, 0.1 mmol, 1 equiv.), *di*-NTf_2 pyrazabole **3.2** (0.072 g, 0.1 mmol, 1 equiv.) and chlorobenzene (0.5 mL). Samples were heated to 100 °C in a heating block without inversion / external mixing and analysed by NMR spectroscopy at regular time points.

General Procedure 3.6: Hydrodehalogenation of Indolinium Cations

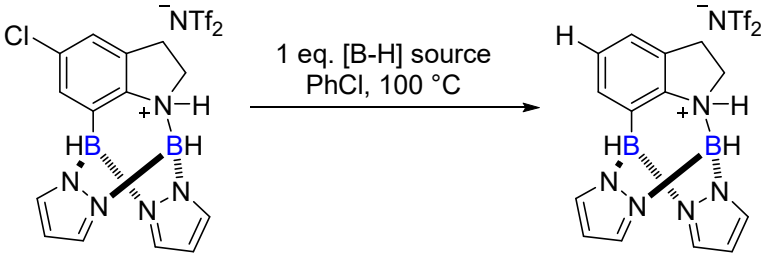

A sample of 5-chloro N/C7-borylated indoline intermediate **3.15** was prepared following **General Procedure 3.3** with 5-chloro indole (0.030 g). Reaction was heated to 100 °C for 2 hours to effect C7-borylation. Following this, 1.1 equiv. of [B-H] source was added. Samples were heated to 100 °C in a heating block without inversion / external mixing and analysed by NMR spectroscopy at regular time points.

[B-H] sources tested:

- Pyrazabole **3.1**: 0.018 g
- *Mono*-NTf_2 pyrazabole **3.3**: Made *in situ* via addition of 0.55 equiv. pyrazabole (0.009 g) and 0.55 equiv. *di*-NTf_2 pyrazabole (0.039 g).
- *Di*-NTf_2 pyrazabole **3.2**: 0.079 g
- $IMeBH_2NTf_2$: Made *in situ* via addition of 1.1 equiv. $IMeBH_3$ (0.012 g) and 1.1 equiv. $HNTf_2$ (0.031 g), based on a reported procedure.[67]

Attempted Hydrodehalogenation of 4-Nitrochlorobenzene

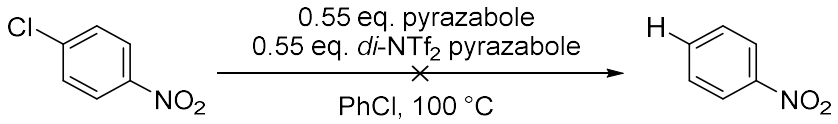

To a J. Young's NMR tube was added pyrazabole **3.1** (0.009 g, 0.055 mmol, 0.55 equiv.), *di*-NTf_2 pyrazabole **3.2** (0.039 g, 0.055 mmol, 0.55 equiv.) and chlorobenzene (0.5 mL). This was mixed by inversion (approx. 1 rotation / s) at room temperature for 1 hour. 4-nitrochlorobenzene (0.012 mL, 0.1 mmol). The sample was heated to 100 °C in a heating block without inversion / external mixing and analysed by NMR spectroscopy at regular time points, which showed no reactivity.

3.7 References

1 G. R. Humphrey and J. T. Kuethe, *Chem. Rev.*, 2006, **106**, 2875–2911.

2 J. A. Joule and K. Mills, *Heterocyclic chemistry*, Blackwell Science, Oxford, 4th ed., 2000.

3 R. D. Taylor, M. MacCoss and A. D. G. Lawson, *J. Med. Chem.*, 2014, **57**, 5845–5859.

4 B. E. Evans, K. E. Rittle, M. G. Bock, R. M. DiPardo, R. M. Freidinger, W. L. Whitter, G. F. Lundell, D. F. Veber, P. S. Anderson, R. S. L. Chang, V. J. Lotti, D. J. Cerino, T. B. Chen, P. J. Kling, K. A. Kunkel, J. P. Springer and J. Hirshfield, *J. Med. Chem.*, 1988, **31**, 2235–2246.

5 D. A. Horton, G. T. Bourne and M. L. Smythe, *Chem. Rev.*, 2003, **103**, 893–930.

6 M. Baumann, I. R. Baxendale, S. V. Ley and N. Nikbin, *Beilstein J. Org. Chem.*, 2011, **7**, 442–495.

7 K.-H. Lim, O. Hiraku, K. Komiyama and T.-S. Kam, *J. Nat. Prod.*, 2008, **71**, 1591–1594.

8 J. T. Ndongo, J. N. Mbing, M. F. Tala, A. Monteillier, D. E. Pegnyemb, M. Cuendet and H. Laatsch, *Phytochemistry*, 2017, **144**, 189–196.

9 P. L. Julian and J. Pikl, *J. Am. Chem. Soc.*, 1935, **57**, 755–757.

10 P. W. Moore, J. J. Rasimas and J. W. Donovan, *J. Med. Toxicol.*, 2015, **11**, 159–160.

11 J. E. Wilson, R. Kurukulasuriya, M. Reibarkh, M. Reiter, A. Zwicker, K. Zhao, F. Zhang, R. Anand, V. J. Colandrea, A.-M. Cumiskey, A. Crespo, R. A. Duffy, B. A. Murphy, K. Mitra, D. G. Johns, J. L. Duffy and P. Vachal, *ACS Med. Chem. Lett.*, 2016, **7**, 261–265.

12 S. Zeeli, T. Weill, E. Finkin-Groner, C. Bejar, M. Melamed, S. Furman, M. Zhenin, A. Nudelman and M. Weinstock, *J. Med. Chem.*, 2018, **61**, 4004–4019.

13 A. Thakur, A. Singh, N. Kaur, R. Ojha and K. Nepali, *Bioorg. Chem.*, 2020, **94**, 103436.

14 T. S. Silva, M. T. Rodrigues, H. Santos, L. A. Zeoly, W. P. Almeida, R. C. Barcelos, R. C. Gomes, F. S. Fernandes and F. Coelho, *Tetrahedron*, 2019, **75**, 2063–2097.

15 H. Wei, B. Li, N. Wang, Y. Ma, J. Yu, X. Wang, J. Su and D. Liu, *ChemistryOpen*, 2023, **12**, e202200235.

16 R. Rossi, F. Bellina, M. Lessi and C. Manzini, *Adv. Synth. Catal.*, 2014, **356**, 17–117.

17 A. H. Sandtorv, *Adv. Synth. Catal.*, 2015, **357**, 2403–2435.

18 J. A. Leitch, Y. Bhonoah and C. G. Frost, *ACS Catal.*, 2017, **7**, 5618–5627.

19 J. Wen and Z. Shi, *Acc. Chem. Res.*, 2021, **54**, 1723–1736.

20 J. Takagi, K. Sato, J. F. Hartwig, T. Ishiyama and N. Miyaura, *Tetrahedron Lett.*, 2002, **43**, 5649–5651.

21 I. A. I. Mkhalid, J. H. Barnard, T. B. Marder, J. M. Murphy and J. F. Hartwig, *Chem. Rev.*, 2010, **110**, 890–931.

22 J. S. Wright, P. J. H. Scott and P. G. Steel, *Angew. Chem. Int. Ed.*, 2021, **60**, 2796–2821.

23 B. A. Vanchura II, S. M. Preshlock, P. C. Roosen, V. A. Kallepalli, R. J. Staples, R. E. Maleczka Jr., D. A. Singleton and M. R. Smith III, *Chem. Commun.*, 2010, **46**, 7724–7726.

24 G. W. Rewcastle and A. R. Katritzky, in *Advances in Heterocyclic Chemistry*, ed. A. R. Katritzky, Academic Press, Cambridge, Massachusetts, 1993, vol. 56, pp. 155–302.

25 A. D. Grosso, M. D. Helm, S. A. Solomon, D. Caras-Quintero and M. J. Ingleson, *Chem. Commun.*, 2011, **47**, 12459–12461.

26 M. J. Ingleson, *Synlett*, 2012, **23**, 1411–1415.

27 S. Zhang, Y. Han, J. He and Y. Zhang, *J. Org. Chem.*, 2018, **83**, 1377–1386.

28 C. G. Hartung, A. Fecher, B. Chapell and V. Snieckus, *Org. Lett.*, 2003, **5**, 1899–1902.

29 S. Paul, G. A. Chotana, D. Holmes, R. C. Reichle, R. E. Maleczka and M. R. Smith III, *J. Am. Chem. Soc.*, 2006, **128**, 15552–15553.

30 S. A. Iqbal, J. Pahl, K. Yuan and M. J. Ingleson, *Chem. Soc. Rev.*, 2020, **49**, 4564–4591.

31 A. Ros, R. Fernández and J. M. Lassaletta, *Chem. Soc. Rev.*, 2014, **43**, 3229–3243.

32 D. W. Robbins, T. A. Boebel and J. F. Hartwig, *J. Am. Chem. Soc.*, 2010, **132**, 4068–4069.

33 J. Lv, X. Chen, X.-S. Xue, B. Zhao, Y. Liang, M. Wang, L. Jin, Y. Yuan, Y. Han, Y. Zhao, Y. Lu, J. Zhao, W.-Y. Sun, Kendall. N. Houk and Z. Shi, *Nature*, 2019, **575**, 336–340.

34 J. Lv, B. Zhao, Y. Yuan, Y. Han and Z. Shi, *Nat. Commun.*, 2020, **11**, 1316.

35 S. A. Iqbal, J. Cid, R. J. Procter, M. Uzelac, K. Yuan and M. J. Ingleson, *Angew. Chem. Int. Ed.*, 2019, **58**, 15381–15385.

36 F. Zhang and D. R. Spring, *Chem. Soc. Rev.*, 2014, **43**, 6906–6919.

37 G. Rani, V. Luxami and K. Paul, *Chem. Commun.*, 2020, **56**, 12479–12521.

38 V. A. Kallepalli, F. Shi, S. Paul, E. N. Onyeozili, R. E. Maleczka Jr. and M. R. Smith III, *J. Org. Chem.*, 2009, **74**, 9199–9201.

39 M. R. Smith III, R. Bisht, C. Haldar, G. Pandey, J. E. Dannatt, B. Ghaffari, R. E. Maleczka Jr. and B. Chattopadhyay, *ACS Catal.*, 2018, **8**, 6216–6223.

40 S. M. Preshlock, D. L. Plattner, P. E. Maligres, S. W. Krska, R. E. Maleczka Jr. and M. R. Smith III, *Angew. Chem. Int. Ed.*, 2013, **52**, 12915–12919.

41 Y.-M. Tian, X.-N. Guo, Z. Wu, A. Friedrich, S. A. Westcott, H. Braunschweig, U. Radius and T. B. Marder, *J. Am. Chem. Soc.*, 2020, **142**, 13136–13144.

42 S. Rej and N. Chatani, *J. Am. Chem. Soc.*, 2021, **143**, 2920–2929.

43 K. Yamazaki, S. Rej, Y. Ano and N. Chatani, *Org. Lett.*, 2022, **24**, 213–217.

44 G. Rouquet and N. Chatani, *Angew. Chem. Int. Ed.*, 2013, **52**, 11726–11743.

45 A. Escande, D. L. Crossley, J. Cid, I. A. Cade, I. Vitorica-Yrezabal and M. J. Ingleson, *Dalton Trans.*, 2016, **45**, 17160–17167.

46 F. Shen, S. Tyagarajan, D. Perera, S. W. Krska, P. E. Maligres, M. R. Smith III and R. E. Maleczka Jr., *Org. Lett.*, 2016, **18**, 1554–1557.

47 R. P. Loach, O. S. Fenton, K. Amaike, D. S. Siegel, E. Ozkal and M. Movassaghi, *J. Org. Chem.*, 2014, **79**, 11254–11263.

48 D. G. Hall, *Boronic acids: preparation and applications in organic synthesis, medicine and materials*, Wiley-VCH, Weinheim, 2nd edn., 2011.

49 C. Sandford and V. K. Aggarwal, *Chem. Commun.*, 2017, **53**, 5481–5494.

50 C. Reus, S. Weidlich, M. Bolte, H.-W. Lerner and M. Wagner, *J. Am. Chem. Soc.*, 2013, **135**, 12892–12907.

51 A. John, M. Bolte, H.-W. Lerner and M. Wagner, *Angew. Chem. Int. Ed.*, 2017, **56**, 5588–5592.

52 S. Trofimenko, *J. Am. Chem. Soc.*, 1966, **88**, 1842–1844.

53 K. Niedenzu and S. Trofimenko, in *Structural Chemistry of Boron and Silicon*, Springer, Berlin, Heidelberg, 1986, pp. 1–37.

54 M.-A. Tehfe, S. Schweizer, A.-C. Chany, C. Ysacco, J.-L. Clément, D. Gigmes, F. Morlet-Savary, J.-P. Fouassier, M. Neuburger, T. Tschamber, N. Blanchard and J. Lalevée, *Chem. Eur. J.*, 2014, **20**, 5054–5063.

55 M. Henkelmann, A. Omlor, M. Bolte, V. Schünemann, H.-W. Lerner, J. Noga, P. Hrobárik and M. Wagner, *Chem. Sci.*, 2022, **13**, 1608–1617.

56 C. I. Nieto, D. Sanz, R. M. Claramunt, I. Alkorta and J. Elguero, *Coord. Chem. Rev.*, 2022, **473**, 214812.

57 E. Hanecker, T. G. Hodgkins, K. Niedenzu and H. Noeth, *Inorg. Chem.*, 1985, **24**, 459–462.

58 S. Trofimenko, *J. Am. Chem. Soc.*, 1967, **89**, 3165–3170.

59 S. Trofimenko, *J. Am. Chem. Soc.*, 1967, **89**, 4948–4952.

60 K. Niedenzu and H. Nöth, *Chem. Ber.*, 1983, **116**, 1132–1153.

61 C. M. Clarke, M. K. Das, E. Hanecker, J. F. Mariategui, K. Niedenzu, P. M. Niedenzu, H. Noeth and K. R. Warner, *Inorg. Chem.*, 1987, **26**, 2310–2317.

62 E. Cavero, R. Giménez, S. Uriel, E. Beltrán, J. L. Serrano, I. Alkorta and J. Elguero, *Crystal Growth & Design*, 2008, **8**, 838–847.

63 C. R. P. Millet, J. Pahl, E. Noone, K. Yuan, G. S. Nichol, M. Uzelac and M. J. Ingleson, *Organometallics*, 2022, **41**, 2638–2647.

64 C. A. Jaska, K. Temple, A. J. Lough and I. Manners, *J. Am. Chem. Soc.*, 2003, **125**, 9424–9434.

65 J. Pahl, E. Noone, M. Uzelac, K. Yuan and M. J. Ingleson, *Angew. Chem. Int. Ed.*, 2022, **61**, e202206230.

66 W. Zhao and J. Sun, *Chem. Rev.*, 2018, **118**, 10349–10392.

67 A. Prokofjevs, A. Boussonnière, L. Li, H. Bonin, E. Lacôte, D. P. Curran and E. Vedejs, *J. Am. Chem. Soc.*, 2012, **134**, 12281–12288.

68 A. Boussonnière, X. Pan, S. J. Geib and D. P. Curran, *Organometallics*, 2013, **32**, 7445–7450.

69 T. S. De Vries, A. Prokofjevs and E. Vedejs, *Chem. Rev.*, 2012, **112**, 4246–4282.

70 E. von Grotthuss, S. E. Prey, M. Bolte, H.-W. Lerner and M. Wagner, *J. Am. Chem. Soc.*, 2019, **141**, 6082–6091.

71 S. Tanaka, Y. Saito, T. Yamamoto and T. Hattori, *Org. Lett.*, 2018, **20**, 1828–1831.

72 M. R. Crampton, in *Arene Chemistry*, John Wiley & Sons, Ltd, 2015, pp. 131–173.

73 S. Rohrbach, A. J. Smith, J. H. Pang, D. L. Poole, T. Tuttle, S. Chiba and J. A. Murphy, *Angew. Chem. Int. Ed.*, 2019, **58**, 16368–16388.

74 G. R. Fulmer, A. J. M. Miller, N. H. Sherden, H. E. Gottlieb, A. Nudelman, B. M. Stoltz, J. E. Bercaw and K. I. Goldberg, *Organometallics*, 2010, **29**, 2176–2179.

75 A. Jayaraman, L. C. M. Castro, V. Desrosiers and F.-G. Fontaine, *Chem. Sci.*, 2018, **9**, 5057–5063.

76 A. Jayaraman, H. Powell-Davies and F.-G. Fontaine, *Tetrahedron*, 2019, **75**, 2118–2127.

77 D. H. McDaniel and H. C. Brown, *J. Org. Chem.*, 1958, **23**, 420–427.

78 C. Hansch and A. Leo, *Substituent constants for correlation analysis in chemistry and biology*, Wiley, New York, 1979.

79 Q. Yang, Y. Li, J.-D. Yang, Y. Liu, L. Zhang, S. Luo and J.-P. Cheng, *Angew. Chem. Int. Ed.*, 2020, **59**, 19282–19291.

80 T. Stahl, H. F. T. Klare and M. Oestreich, *J. Am. Chem. Soc.*, 2013, **135**, 1248–1251.

81 J. A. Plumley and J. D. Evanseck, *J. Phys. Chem. A*, 2009, **113**, 5985–5992.

82 C. R. P. Millet, E. Noone, A. V. Schellbach, J. Pahl, J. Łosiewicz, G. S. Nichol and M. J. Ingleson, *Chem. Sci.*, 2023, **14**, 12041–12048.

83 F. Terrier, *Modern nucleophilic aromatic substitution*, Wiley-VCH, Weinheim, 1st ed., 2013.

84 G. Bartoli and P. E. Todesco, *Acc. Chem. Res.*, 1977, **10**, 125–132.

85 E. E. Kwan, Y. Zeng, H. A. Besser and E. N. Jacobsen, *Nature Chem.*, 2018, **10**, 917–923.

86 H. Handel, M. A. Pasquini and J. L. Pierre, *Tetrahedron*, 1980, **36**, 3205–3208.

87 K. Kikushima, M. Grellier, M. Ohashi and S. Ogoshi, *Angew. Chem. Int. Ed.*, 2017, **56**, 16191–16196.

88 M. Mąkosza, *ChemTexts*, 2019, **5**, 10.

89 T. D. Schoch, M. Mondal and J. D. Weaver, *Org. Lett.*, 2021, **23**, 1588–1593.

90 V. Kanchupalli, D. Joseph and S. Katukojvala, *Org. Lett.*, 2015, **17**, 5878–5881.

91 H. Zhang, H.-Y. Wang, Y. Luo, C. Chen, Y. Cao, P. Chen, Y.-L. Guo, Y. Lan and G. Liu, *ACS Catal.*, 2018, **8**, 2173–2180.

Chapter 4

Reactivity of Iodine-Activated Pyrazaboles

Chapter 4: Reactivity of Iodine-Activated Pyrazaboles

4.1 Introduction

The work in **Chapter 3** demonstrated how an electrophilic pyrazabole derivative can be used as a transient directing group in the electrophilic C-H borylation of indoles via a process we have termed 'borylation directed borylation'.[1] The activation of pyrazabole using *bis*-(trifluoromethane sulfonyl) amine ($HNTf_2$) generates a *mono*-electrophile *in situ*, which is key to enabling the reduction and N/C7-diborylation of indoles. Subsequent transformation of the pyrazabole derived borylation product enables the isolation of 7-Bpin indolines in a metal-free, one-pot process without the need to preinstall a directing group or remove one in a separate step (**Scheme 4.1**).

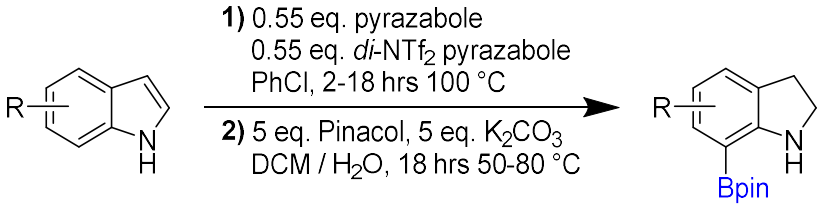

Scheme 4.1: The synthesis of 7-Bpin indolines via the 'borylation directed borylation' of indoles using *mono*-NTf_2 pyrazabole.

Though $HNTf_2$ provides access to highly reactive pyrazabole electrophiles, this requires stoichiometric amounts of the activator which has a high molecular mass and is relatively expensive.[2] Furthermore, $HNTf_2$ and NTf_2-pyrazabole electrophiles are highly moisture-sensitive and have to be handed within a glovebox, reducing the convenience of the methodology.[3] The substitution of $HNTf_2$ for a cheaper and easier to handle activator would improve the efficiency and synthetic utility of the borylation-directed borylation strategy.

From evaluation of compounds previously used to activate Lewis base (LB) borane complexes,[4,5] iodine is an attractive option that generates reactive boron electrophiles of the general formula LB-BH_2I.[6] Iodine is inexpensive,[7] can be stored/handled in air, and LB-BH_2I species have been shown have similar reactivity to Lewis Base-borane electrophiles generated by $HNTf_2$ activation (i.e. LB-BH_2NTf_2 species).[8,9] For example, Curran, Vedejs and co-workers reported the

room temperature hydroboration of alkenes using an NHC-borane ($IMeBH_3$) activated by catalytic $HNTf_2$ (**Scheme 4.2a**).[8] Upon addition of the alkene, the NTf_2-activated NHC-boranes rapidly performed *di*-hydroboration, leading to NHC-dialkylboranes.

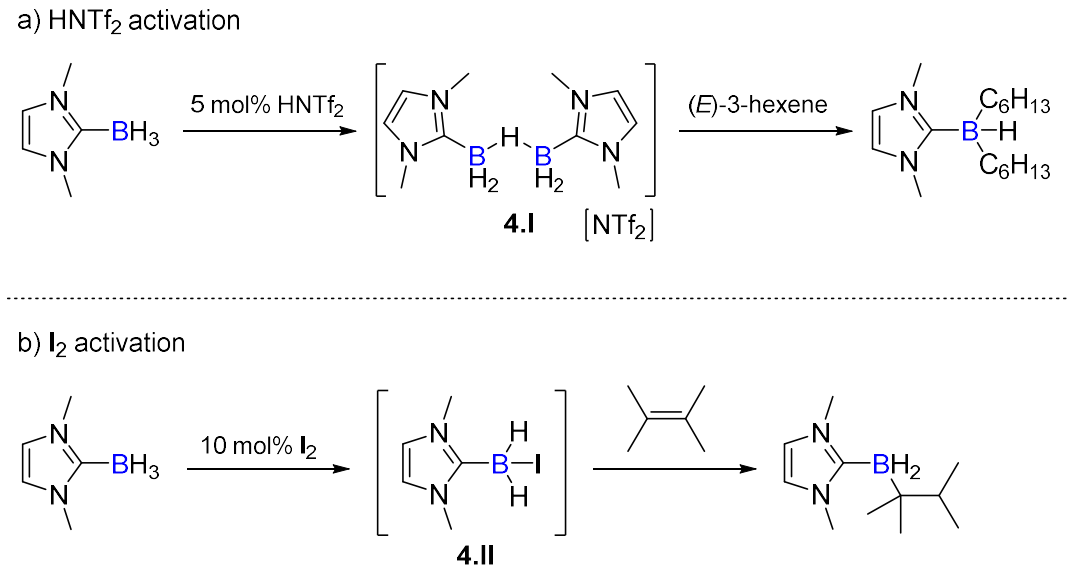

Scheme 4.2: Hydroboration of alkenes using IMe-BH_3 and either **a)** catalytic $HNTf_2$, forming boron electrophile **4.I** *in situ*, or **b)** catalytic iodine, forming boron electrophile **4.II** *in situ*.

Curran and co-workers later modified the process to use catalytic iodine in place of $HNTf_2$ (**Scheme 4.2b**).[9] The use of iodine as the activator expanded the scope and improved the convenience of the overall process. For some alkenes, the loading of iodine needed to be increased, and the reaction often stopped at the *mono*-hydroborated NHC-alkylboranes. These observations demonstrate that iodine-activation leads to boranes that are slightly less reactive than that from $HNTf_2$ activation. NMR spectroscopy revealed that the two activators generate significantly different electrophilic boron species *in situ* in these catalytic reactions. The reaction of $IMeBH_3$ with catalytic amounts of $HNTf_2$ was shown to form intermediate **4.I**, where the initially formed B-NTf_2 bond is displaced by the B-H bond of the remaining unactivated $IMeBH_3$, forming a hydride bridged species.[4] The [H-BH_2-IMe] unit is then displaced upon addition of a stronger nucleophile, e.g. the alkene. In contrast, the activation of $IMeBH_3$ with catalytic amounts of I_2 forms **4.II**, with the B-I bond not displaced by excess $IMeBH_3$.[5] This

demonstrates the more coordinating nature of iodide versus NTf_2, meaning it is less easily substituted by incoming nucleophiles.

The use of iodine to activate NHC-boranes can also lead to reactivity not observed with other activators. Ingleson and co-workers reported the *trans*-hydroboration of alkynes using a borenium cation generated by activation of an NHC-borane with catalytic $B(C_6F_5)_3$ (**Scheme 4.3a**).[10]

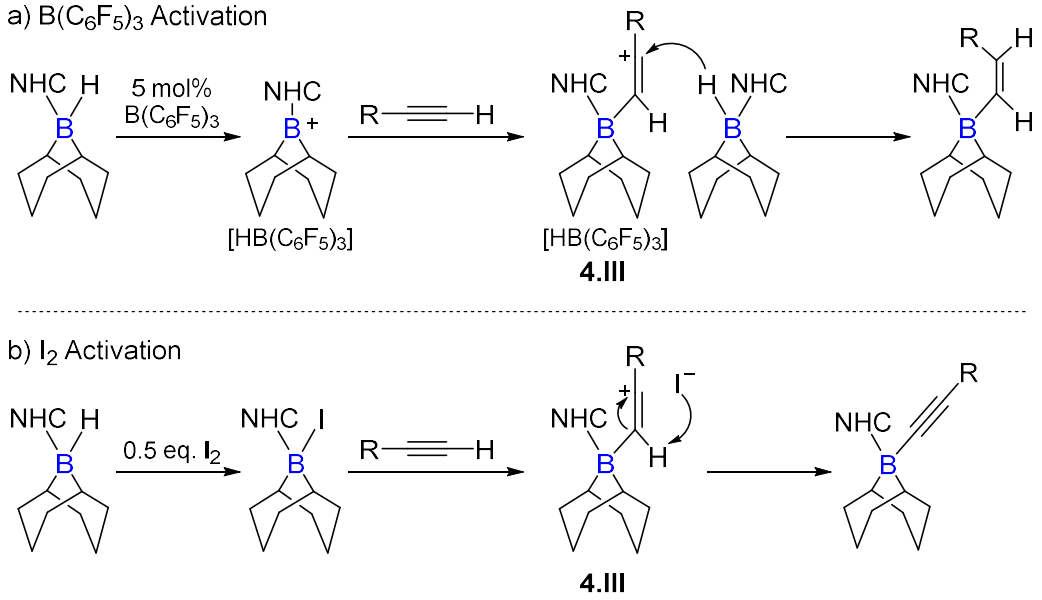

Scheme 4.3: The reaction of NHC-boranes with alkynes results in either **a)** *trans*-hydroboration, when using $B(C_6F_5)_3$ as the activator, or **b)** dehydroboration / C-H borylation, when using iodine as the activator.

Following activation of the alkyne and C-B bond formation to form intermediate **4.III,** intermolecular hydride transfer from an equivalent of NHC-borane forms the *trans*-hydroborated alkene product whilst regenerating the boron electrophile. In contrast, activation of the NHC borane using iodine results in a different reaction pathway (**Scheme 4.3b**). Following alkyne activation, the resulting iodide counterion is sufficiently Brønsted basic to deprotonate intermediate **4.III**, resulting in dehydroboration to form the C-H borylated alkyne product.

The Brønsted basicity of an iodide counterion was also utilised to enable the electrophilic C-H borylation of indoles at C2.[11] Electrophilic C-H borylation of indole typically occurs at the more nucleophilic C3.[12] In this process, the iodine-activated NHC-borane initially reacts with indole at C3, but in the absence of an exogenous base (and therefore, rapid deprotonation of the arenium cation) the migration of the boron moiety from C3 to C2 occurs (**Scheme 4.4**). The arenium cation (**4.IV**) is then deprotonated by the iodide counterion, yielding C2-borylated indoles. Deprotonation by I^- produces HI, which activates further NHC-borane, enabling the process to be catalytic in activator and producing H_2 as the only by-product. In contrast, no significant C-H borylation was observed using $HNTf_2$ in place of I_2, presumably due to the low basicity of $[NTf_2]^-$.

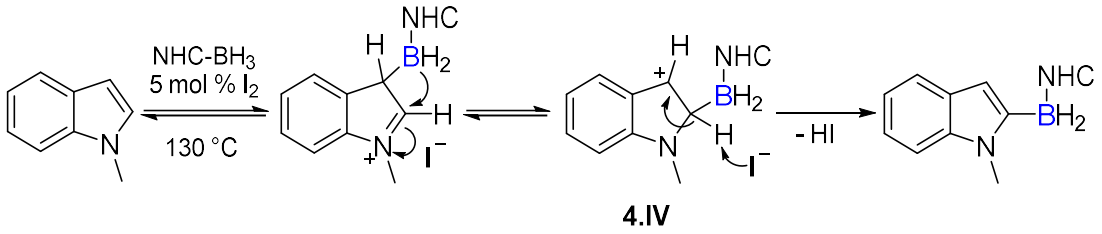

Scheme 4.4: Electrophilic C-H borylation of indoles using NHC-boranes and catalytic I_2 gives C2-borylated indoles, not C3.

These examples highlight that reactive boron electrophiles can still be accessed by replacing $HNTf_2$ for iodine. However, due to differences in the coordinating ability and basicity of the respective counterions (I^-, $[NTf_2]^-$), distinct reactivity patterns are observed.

4.2 Project Aims

Improving the efficiency and synthetic utility of the use of pyrazabole electrophiles as transient directing groups requires the substitution of the $HNTf_2$ activator for an alternative that is less expensive and easier to handle. Iodine is a feasible substitute that meets these requirements, and iodine-activated boron electrophiles have been demonstrated to react with a range of π-nucleophiles.[8,9] Furthermore, iodine-activated pyrazaboles are desirable boron electrophiles, as iodine is less coordinating to boron than the lighter halogens. This was confirmed for a series of NHC-BX_2Ar compounds (X = halide). The reactions of the iodide- and bromide- congeners with water was shown to be much faster than the reactions of the fluoride- and chloride- analogues.[13] Whilst bromide- and chloride- substituted pyrazaboles have been previously described, no iodide-substituted pyrazaboles had been isolated at the time of writing.[14–16]

The work described in this chapter aimed to investigate the activation of pyrazaboles with iodine, and subsequently develop the reactivity of iodine-activated pyrazaboles as transient directing groups. It was hoped that iodine-activated pyrazaboles would have similar reactivity to $HNTf_2$-activated pyrazaboles and so could be used for the reduction and N/C7-diborylation of indoles, providing a more convenient and economical route to 7-Bpin indolines. Establishing conditions that avoided the use of gloveboxes was also desirable.

4.3 Results and Discussion

4.3.1 Synthesis of Iodine-Activated Pyrazaboles

The stepwise bromination of pyrazabole was reported by Nöth and co-workers, using either Br_2 or BBr_3 as the bromine source.[14] To selectively synthesise *di*-bromo pyrazabole, the bromine source stoichiometry must be controlled to prevent overreaction to the *tri*- or *tetra*- bromo pyrazabole species. The synthesis of *di*-iodo pyrazabole was attempted using via a similar approach.

Addition of 1 equiv. of I_2 to a solution of pyrazabole, **4.1**, resulted in the evolution of hydrogen gas and the precipitation of yelllow solid. Following extraction and washing of the precipitate, *di*-iodo pyrazabole, **4.2**, was isolated (**Scheme 4.5**). The isolated solid of **4.2** has improved solubility compared to the insoluble *di*-NTf_2 pyrazabole, enabling full characterisation by NMR spectroscopy.

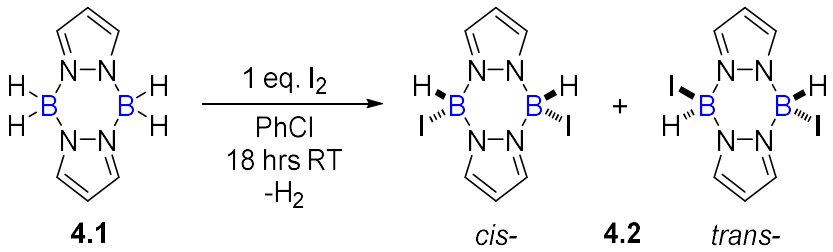

Scheme 4.5: Activation of pyrazabole to *di*-iodo pyrazabole, which forms a ca. 1:1 mixture of the *cis*- and *trans*- isomers.

The NMR spectra of **4.2** in $CDCl_3$ showed a ca. 1:1 mixture of two species, with two doublets observed in the ^{11}B NMR spectrum (δ_{11B} = -13.5, -15.2 ppm) and two sets of pyrazole resonances (two peaks of 2:1 relative integral) in the ^{1}H NMR spectrum. Together, this is consistent with two symmetrically substituted pyrazaboles, each with two -BHI units. The two species are assigned as the *cis*- and *trans*- isomers of **4.2**. The formation of *cis*- and *trans*- isomers of the lighter *di*-halo pyrazaboles has been previously reported.[17] Layering a solution of **4.2** in DCM with hexane formed single crystals of the *cis*-isomer that were suitable for X-ray diffraction studies (**Figure 4.1**, *crystals grown by Dr Jürgen Pahl*). The B···B distance of 3.031(8) Å demonstrates that **4.2** is still well suited to the N/C7- (or C3/C4-) diborylation of indoles.[18,19]

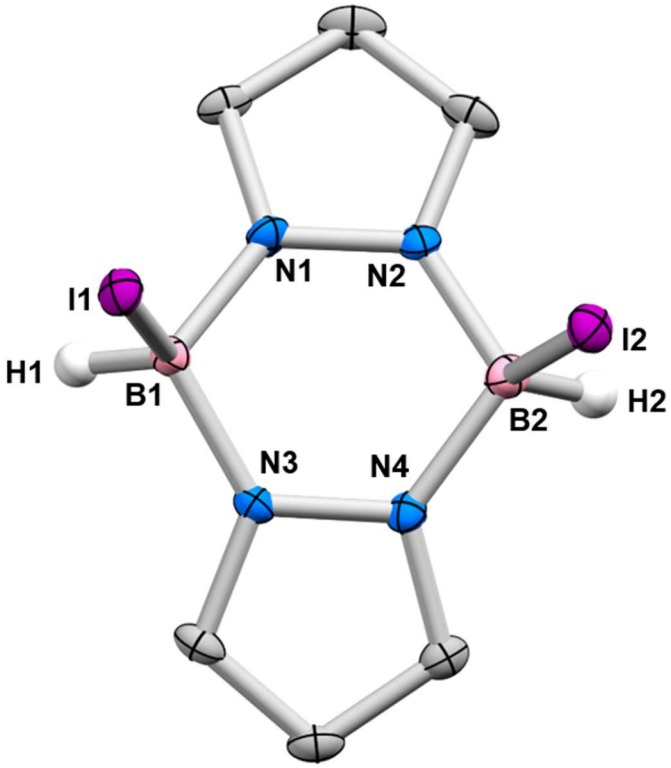

Figure 4.1: Solid-state structure of *cis*-**4.2** *(measured and solved by Dr Gary Nichol)*. Ellipsoids at the 50% probability level.
Hydrogen atoms (except H1 and H2) removed for clarity.
Selected distances (Å): B1-I1 2.286(7), B2-I2 2.302(7), B1···B2 3.031(8).

The *mono*-iodo pyrazabole, **4.3**, could be generated *in situ* by the addition of 0.5 equiv. I_2 to a solution of pyrazabole (**Scheme 4.6a**). After 2 hours at room temperature, the partial formation of a new pyrazabole species was observed by NMR spectroscopy. The ^{11}B NMR spectrum in chlorobenzene (PhCl) showed two new resonances of equal integral, with δ_{11B} = -8.3 ppm (triplet) and -14.5 ppm (doublet) corresponding to the -BH_2 and -BHI units of **4.3**, respectively. It should be noted that partial overreaction to **4.2** was observed, and consequently some leftover **4.1** was also present in the ^{11}B NMR spectrum.

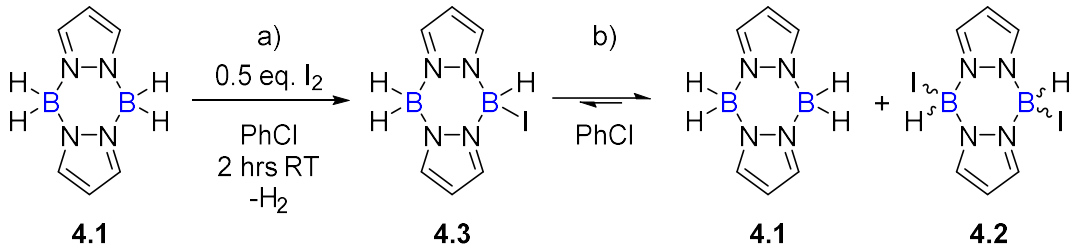

Scheme 4.6: *Mono*-iodo pyrazabole can be formed *in situ* by either **a)** activation of pyrazabole with 0.5 equiv. I_2, or **b)** substituent exchange between equimolar pyrazabole and *di*-iodo pyrazabole in solution.

As previously observed with $HNTf_2$-activated pyrazaboles, *mono*-iodo pyrazabole **4.3** could also be formed in solution at ambient temperatures by mixing equimolar **4.1** and **4.2** (**Scheme 4.6b**), demonstrating that intermolecular H/I exchange can occur. Though the formation of **4.3** could be observed in solution (by NMR spectroscopy), attempts at isolation always yielded an equimolar mixture of **4.1** and **4.2**. A similar issue was encountered when trying to isolate *mono*-NTf_2 pyrazabole and is attributed to the lower solubility of the double-activated pyrazaboles.

Solutions of *mono*- and *di*-iodo pyrazabole could be heated to high temperatures without significant decomposition, demonstrating the thermal stability of the pyrazabole scaffold. For example, heating a sample of **4.2** to 100 °C for 7 days led to <5% degradation. It should be noted, however, that iodine-activated pyrazabole species are not compatible with CH_2Cl_2 (DCM), as they can undergo halogen exchange with the solvent, forming B-Cl bonds and CH_2ClI. This has also been observed with iodine-activated NHC-boranes.[20]

4.3.2 Reactivity with Indole

With a method to activate pyrazabole to a *mono*- or *di*-topic electrophile using iodine established, the reactivity of iodine-activated pyrazaboles with indole was studied and compared to the reactivity of $HNTf_2$-activated pyrazaboles.[1] Using the conditions optimised for *mono*-NTf_2 pyrazabole, the synthesis of 7-Bpin indoline was attempted using *mono*-iodo pyrazabole **4.3** (**Scheme 4.7**). As with *mono*-NTf_2 pyrazabole, **4.3** was generated *in situ* via addition of 0.55 equiv. pyrazabole **4.1** and 0.55 equiv. *di*-iodo pyrazabole **4.2**. The reaction was heated for 18 hours, by which time a white precipitate had crashed out. The precipitate was initially thought to be the N/C7-diborylated product, **4.4**, with the I^- counterion assumed to decrease the solubility of the salt compared to the weakly coordinating $[NTf_2]^-$ counterion *(vide infra).*

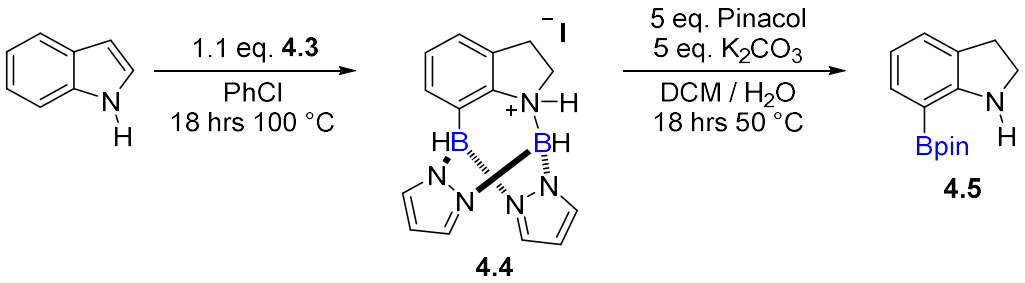

Scheme 4.7: Attempted synthesis of 7-Bpin indoline via the reaction of indole and *mono*-iodo pyrazabole using the conditions previously established with *mono*-NTf_2 pyrazabole.

Pinacol protection via the previously optimised conditions resulted in the formation of **4.5** as the only 'Bpin' species, but in very minor amounts. The major product was *N*-H indoline. Based on this, it was hypothesised that reduction of indole occurs as observed for the $HNTf_2$ system, but the C7-H borylation of the indoline intermediate **4.6** (**Scheme 4.8**) is slower due to the more coordinating nature of iodide relative to $[NTf_2]^-$. Cleavage of the N-B bond in the unreacted **4.6** under the pinacol protection conditions would then yield the observed *N*-H indoline.

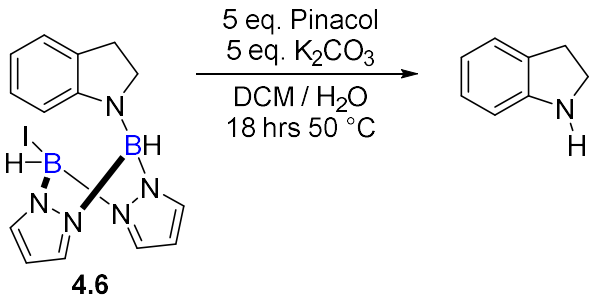

Scheme 4.8: Proposed reaction for the formation of *N*-H indoline via the N-B cleavage of the indoline intermediate **4.6** under pinacol protection conditions.

Several attempts were made to optimise this reaction and push the C7-H borylation step to completion. The reaction temperature was increased to 130 °C, then 150 °C (the solvent was changed to *o*-DCB for these reactions), but this did not increase the amount of **4.5** present after pinacol protection and *N*-H indoline was still the major product. Increasing the time heating also had no beneficial effect. This indicates that the poor reactivity is not simply due to the increased kinetic barrier in the C7-H borylation of **4.6**. Addition of an exogenous base (DBP) to the reaction (to facilitate the deprotonation of an arenium intermediate during C7-H borylation) was also unsuccessful in improving the reaction outcome. Finally, generating the *mono*-iodo pyrazabole **4.3** directly in solution (by addition of 0.5 equiv. I_2 to pyrazabole prior to addition of indole) did not have any effect on the reaction outcome and so this process was used from here on, as it avoided the use of *di*-iodo pyrazabole which is moisture-sensitive.

Despite these efforts to optimise the reaction, the highest yield of 7-Bpin indoline obtained in the reaction of *mono*-iodo pyrazabole **4.3** with indole was 10% (NMR yield after work-up, relative to an internal standard, **Scheme 4.9a**). The equivalent reaction with *mono*-NTf_2 pyrazabole gave 7-Bpin indoline in a 78% isolated yield.[1] The reaction was also attempted using *di*-iodo pyrazabole **4.2** and 1 equiv. base (conditions established with *di*-NTf_2 pyrazabole and indole) but this made no significant difference to the reaction outcome and 7-Bpin indoline was formed in a 9% yield (NMR yield after work-up, relative to an internal standard, **Scheme 4.9b**).

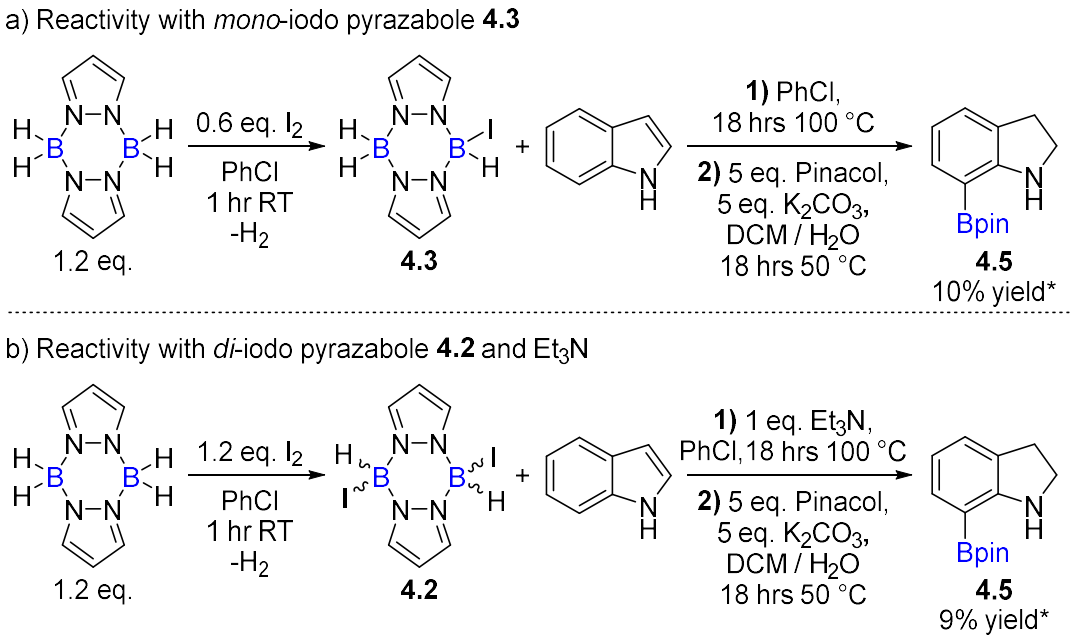

Scheme 4.9: Synthesis of 7-Bpin indoline via the reaction of indole with **a)** *mono*-iodo pyrazabole, or **b)** *di*-iodo pyrazabole and Et_3N.
**(% Yields are NMR yields following work-up, relative to an internal standard).*

To try to understand why the yields of 7-Bpin indoline were repeatedly so low, *in situ* NMR spectroscopy was used to analyse the reaction of indole and *mono*-iodo pyrazabole **4.3** prior to the addition of pinacol. After 18 hours at 100 °C, a complex mixture was observed in the ^{1}H NMR spectrum, with all indole consumed. The minor formation of the N/C7-diborylated indoline species **4.4** could be identified, with four diastereotopic indoline 'CH_2' resonances (**Figure 4.2**) along with a new set of pyrazabole resonances. In addition, the ^{11}B NMR spectrum showed a new broad resonance at -2.9 ppm (in C_6H_5Cl), very close in chemical shift to the fully characterised analogue of **4.4** with $[NTf_2]^-$ as the counterion. Analysis of the ^{11}B NMR spectrum showed that a significant amount of *mono*-iodo pyrazabole **4.3** was still present, indicating that it was not reacting in the expected 1:1 ratio with indole, hence **4.3** had not been fully consumed. The major product in the ^{1}H NMR spectrum was an unknown indoline species, with two triplets (of equal integral) in the aliphatic region (**Figure 4.2**), indicating that the nitrogen of this species is three-coordinate (non-chiral).

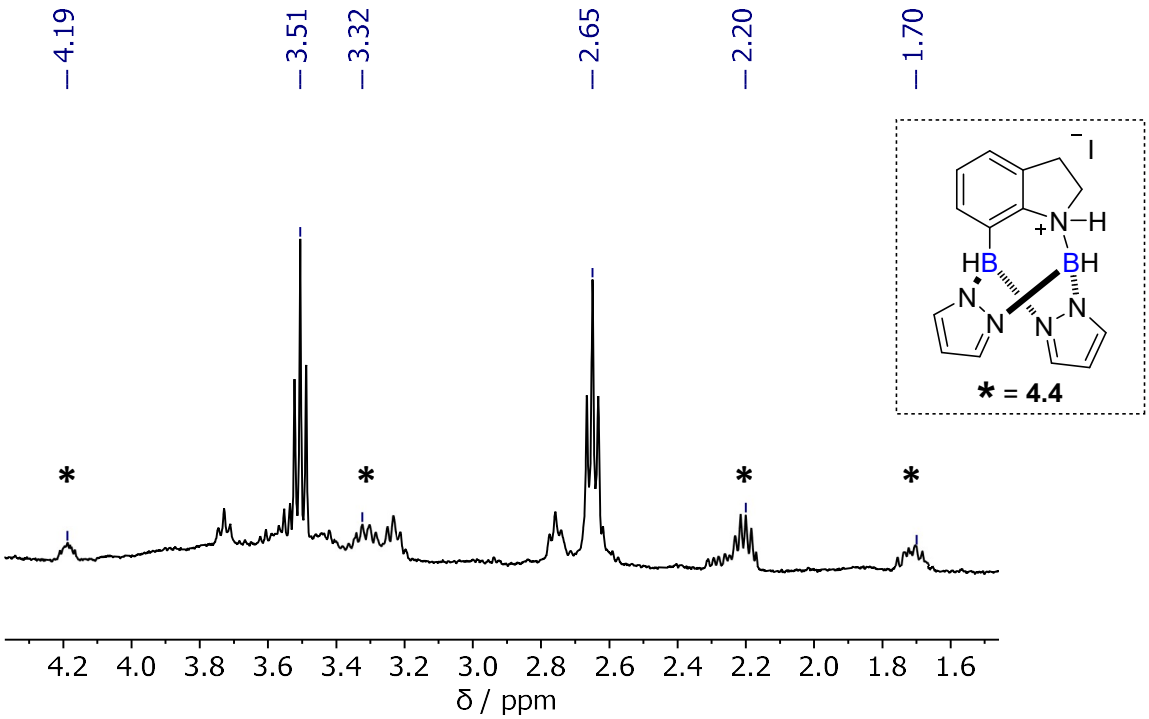

Figure 4.2: *In situ* ^{1}H NMR spectrum for the reaction of indole with **4.3** after 18 hours at 100 °C. *Note: Due to the presence of other overlapping resonances, the integrals of the four diastereotopic resonances of **4.4** cannot be determined. (Solvent = C_6H_5Cl, NMR temperature = 300 K).*

Further heating did not lead to the consumption of this unknown species, and no new products were formed. Together this indicates that while the hydroboration of indole may proceed as expected, the formation of this unreactive indoline side product competes with the formation of **4.4**. The identity of this unknown indoline species is proposed to be (Indoline)$_2$-BH (**4.7**, **Scheme 4.10**), with a broad downfield resonance (δ_{11B} = 25.1 ppm) observed in the NMR spectrum matching previous reports.[21,22] This side product is assumed to be the source of *N*-H indoline observed after pinacol protection and work-up. Attempts to isolate and fully characterise **4.7** were unsuccessful.

The white solid that precipitated during the reaction was filtered, washed with PhCl, and dissolved in $CDCl_3$. The ^{11}B NMR spectrum showed one doublet (δ_{11B} = -5.3, $^{1}J_{B\text{-}H}$ = 117 Hz), and the ^{1}H NMR showed this to be a symmetrical pyrazabole species. No other ^{1}H resonances were observed, suggesting that this precipitate is formed of three pyrazole rings and two B-H units (**4.8**, **Scheme**

4.10). This assignment was later confirmed by the independent synthesis and crystallisation of **4.8** (*by Dr Clément Millet, vide infra*).[23]

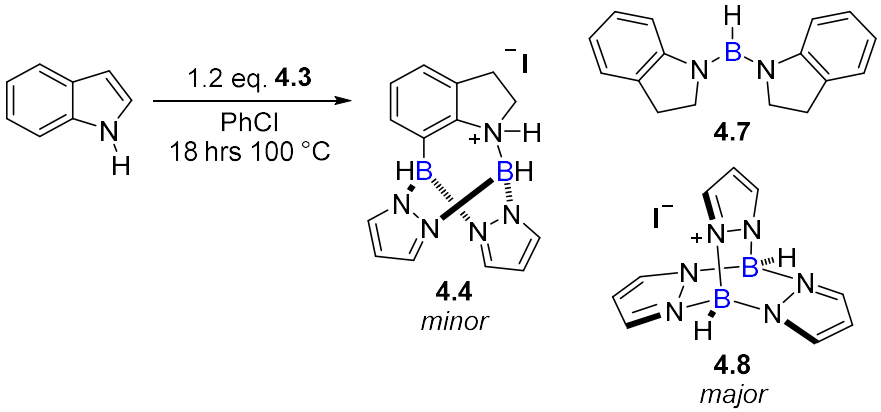

Scheme 4.10: The reaction of indole with **4.3** at 100 °C results in the minor formation of N/C7-diborylated indoline **4.4**, but the major species present are **4.7** and **4.8**, believed to be from the decomposition of the pyrazabole unit.

The formation of **4.7** and **4.8** suggests that the pyrazabole core is breaking apart during the reaction, forming species that are non-productive for C7-H borylation (to form **4.4**). These by-products were not observed in the reactions with $HNTf_2$ activation.[1] However, it is not known if the decomposition of the pyrazabole unit occurs as a side reaction during the indole reduction step, or during the C7-H borylation step. To probe this, and to explore the reactivity of iodine-activated pyrazaboles in a simpler system, the *ortho* C7-H borylation of indoline was studied to compare to indole.

4.3.3 Reactivity with Indoline

The reaction of *N*-H indoline with *di*-iodo pyrazabole **4.2**, and 1 equiv. of DBP (a non-coordinating exogenous base) was studied. *Di*-iodo pyrazabole **4.2** was generated *in situ* by the addition of 1 equiv. I_2 to a solution of pyrazabole. After pinacol protection of the *ortho* C7-H borylated product, 7-Bpin indoline **4.5** was formed in a 20% yield (*NMR yield following work-up, relative to an internal standard*). The major species present, however, was *N*-H indoline.

The reactivity with two other exogenous bases, DIPEA and Et_3N, was evaluated and compared, with the use of Et_3N providing some minor improvement in the yield of **4.5** (**Figure 4.3**). Switching the order of addition for the indoline and base was shown to have no significant effect on yield. Though slightly higher than the reactions of indole and **4.3**, the yields of **4.5** were significantly lower compared to the equivalent reactions using $HNTf_2$-activated pyrazaboles.

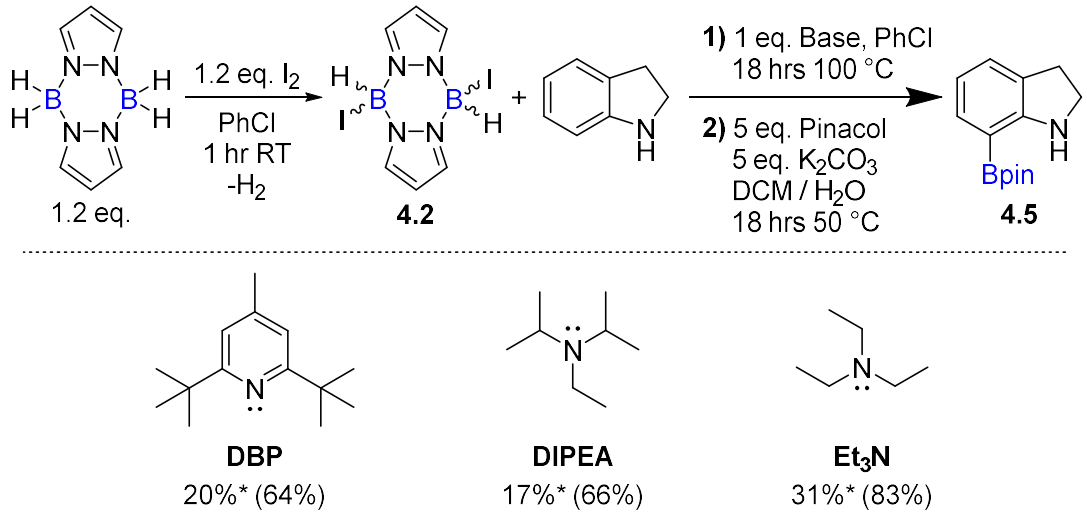

Figure 4.3: Screening of exogenous bases for the C7-H borylation of indoline using *di*-iodo pyrazabole **4.2**. (**Yields are NMR yields following work-up, relative to an internal standard). (The yield of **4.5** for the equivalent reaction with di-NTf_2 pyrazabole are shown in brackets, for comparison).*

Analysis of the reaction of *di*-iodo pyrazabole **4.2**, indoline and Et_3N after 18 hours at 100 °C (prior to the addition of pinacol) by *in situ* NMR spectroscopy revealed a similar outcome to the reaction of indole and *mono*-iodo pyrazabole **4.3**. The ^1H NMR spectrum showed the minor formation of the N/C7-diborylated indoline species **4.4**. The major product observed was the same indoline side

product, **4.7**, with two triplet resonances observed at identical chemical shift (**Figure 4.4**). Note that these resonances are not due to the deprotonated version of **4.4**, which has two triplet resonances at 3.70 and 2.75 ppm (in C_6H_5Cl).

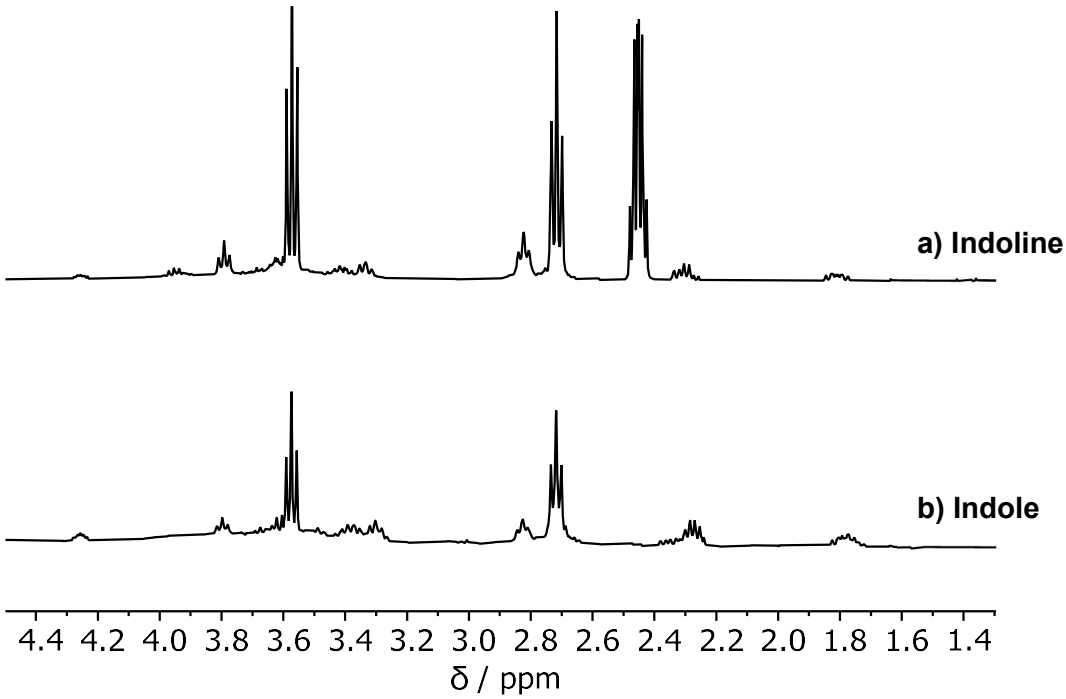

Figure 4.4: Stacked *in situ* ^{1}H NMR spectra for the reactions of **a)** indoline with *di*-iodo pyrazabole **4.2** and Et_3N, or **b)** indole with *mono*-iodo pyrazabole **4.3**, both after 18 hours at 100 °C. *Note: The resonance at 2.49 ppm corresponds to the CH_2 of $[Et_3NH][I]$. (Solvent = C_6H_5Cl, NMR temperature = 300 K).*

As in the indole reaction, the ^{11}B NMR spectrum showed significant iodine-activated pyrazabole (both **4.2** and **4.3**) remaining, and the broad downfield resonance at 25 ppm, assigned to **4.7**, was again observed (**Figure 4.5**). The precipitation of **4.8** (along with some $[Et_3NH][I]$) was also observed, matching the solid isolated from the reaction with indole and **4.3**.

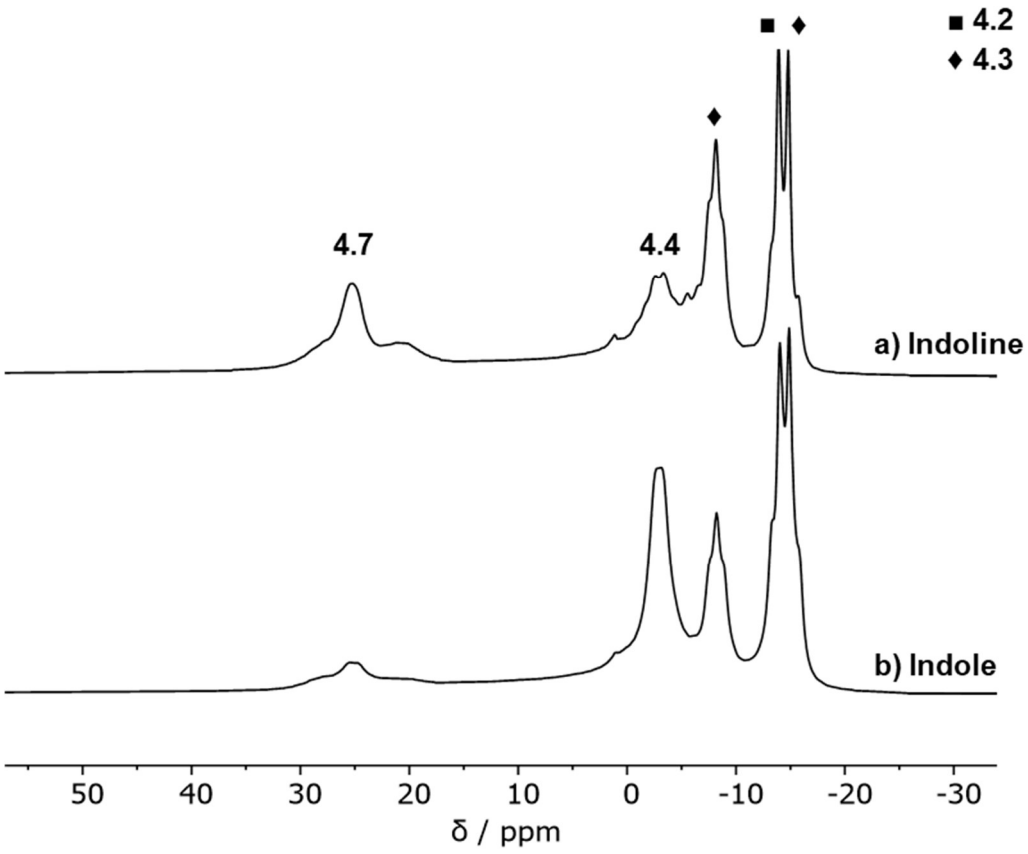

Figure 4.5: Stacked *in situ* ^{11}B NMR spectra for the reactions of **a)** indoline with *di*-iodo pyrazabole **4.2** and Et_3N, or **b)** indole with *mono*-iodo pyrazabole **4.3**, both after 18 hours at 100 °C. *(Solvent = C_6H_5Cl, NMR temperature = 300 K).*

Together, this indicates that the decomposition side reaction that is leading to the breaking apart of the pyrazabole unit (and the formation of **4.7** and **4.8**) is occurring from an indoline species. With indoles, the intermediates in the hydroboration and protodeboronations steps do not appear to be forming these side products, although this does not explain why the yields are ~20% lower for the reactions of indole than indoline.

4.3.4 Understanding the Decomposition Side-Reaction

*The discussion in this section is supported by work done in parallel by Dr Clément Millet on the ortho C-H borylation of N-methyl aniline using di-iodo pyrazabole **4.2**. This is discussed in more detail in the publication of that work.*[23]

The reactions of indole and indoline with *mono*- and *di*-iodo pyrazabole, respectively, were shown to give consistently lower yields of 7-Bpin indoline **4.5** than the $HNTf_2$-activated equivalent reactions. With both of these substrates the competitive (to C7-H borylation) formation of unreactive side products **4.7** and **4.8** via the decomposition of the pyrazabole core was observed.

The same side reaction was observed in the *ortho* C-H borylation of *N*-methyl aniline (*by Dr Clément Millet*). In this reaction, the yield of 2-Bpin *N*-methyl aniline (**4.10**) was higher than the reaction with indoline, but it was also lower than the $HNTf_2$-activated equivalent (**Scheme 4.11**). The formation of **4.8** and $(Ph(Me)N)_2$-BH was observed prior to addition of pinacol, indicating that the same competitive side reaction occurs with this substrate too.

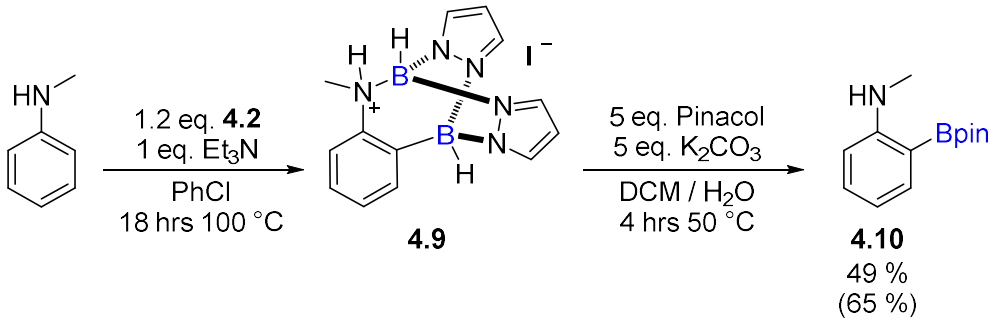

Scheme 4.11: Optimised conditions for the *ortho* C-H borylation of *N*-methyl aniline using *di*-iodo pyrazabole **4.2,** performed by Dr Clément Millet. *(The yield of **4.10** for the reaction using di-NTf_2 pyrazabole is shown in brackets).*

To understand these differences in reaction outcome, the *ortho* C-H borylation of *N*-methyl aniline with *di*-NTf_2 pyrazabole **4.11** was first analysed by Dr Clément Millet. The reaction of **4.11** with Et_3N, followed by *N*-methyl aniline gave the rapid and clean formation of a new species at room temperature (**Scheme 4.12a**). This was characterised as **4.12**, a dicationic dimer of the intermediate following N-B bond formation between **4.11** and *N*-methyl aniline. The same species could

also be generated *in situ* by the combination of **4.11** and *di*-(*N*-methyl anilide) pyrazabole **4.13**, **Scheme 4.12b**. (**4.13** was synthesised directly through the room temperature reaction of 2 equiv. *N*-methyl aniline with 1 equiv. *di*-NTf_2 pyrazabole **4.11** and Et_3N).[23] The formation of **4.12** at room temperature demonstrates how rapidly $[NTf_2]^-$ is displaced from boron by *N*-methyl aniline. Heating the sample of **4.12** is proposed to lead to dimer dissociation and *ortho*-borylation to form **4.9**, with no pyrazabole decomposition or other side reactions observed by $^1H/^{11}B$ NMR spectroscopy.

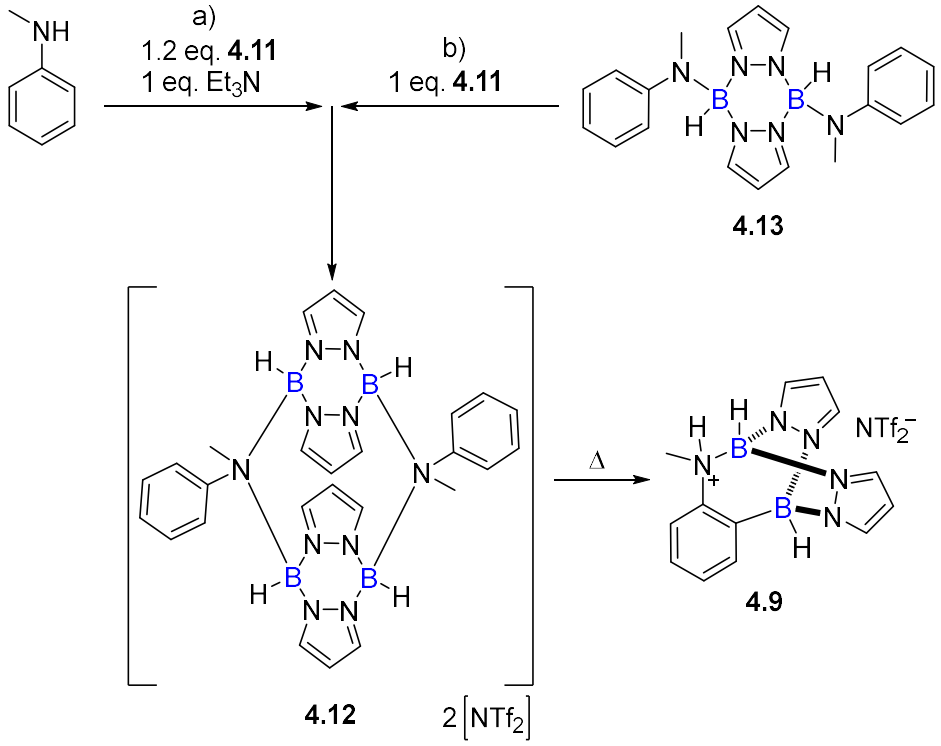

Scheme 4.12: Proposed pathway for the reaction of *N*-Me aniline with *di*-NTf_2 pyrazabole **4.11**. The reaction proceeds by the formation of dimer **4.12**, which dissociates upon heating and undergoes C-H borylation to form **4.9**.
Work by Dr Clément Millet.

By comparison, when the reaction of *di*-iodo pyrazabole **4.2** with *N*-methyl aniline and Et_3N was monitored, the formation of the analogous dicationic dimer **4.12** (with I^- as the counterions) was not observed. Instead, the reaction at room temperature gave a complex mixture, with *di*-(*N*-methyl anilide) pyrazabole **4.13** observed as the major new species by *in situ* ^1H NMR spectroscopy. Heating the reaction then led to the partial formation of **4.9**, alongside $(Ph(Me)N)_2$-BH and

4.8. These observations indicate that the formation of **4.9** in the reaction is hindered by the more coordinating iodide (compared to $[NTf_2]^-$), which slows the exchange reaction between the initially formed **4.13** and *di*-iodo pyrazabole **4.2**, which is needed to form a species capable of undergoing C-H borylation (i.e. the dimer **4.12**). Consequently, this enables the competitive decomposition of the pyrazabole unit (**Scheme 4.13**). This would explain why a significant amount of *di*-iodo pyrazabole **4.2** is observed at the end of the reaction.

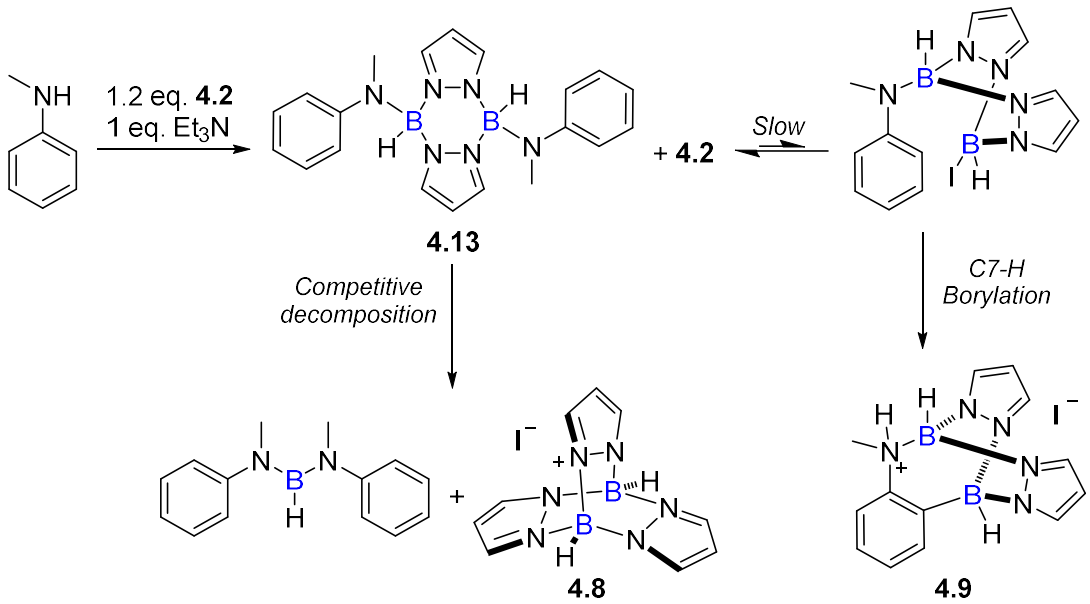

Scheme 4.13: Proposed pathway for the reaction of *N*-Me aniline with *di*-iodo pyrazabole **4.2**. The formation of the intermediate that undergoes C-H borylation is slowed by the more coordinating iodide in **4.2**, which facilitates the competitive decomposition of the pyrazabole. *Work by Dr Clément Millet*.

Monitoring the reaction of *N*-H indoline, *di*-iodo pyrazabole **4.2** and Et_3N at room temperature by *in situ* ^1H NMR spectroscopy gave a complex reaction mixture with several overlapping indoline resonances observed, making assignments challenging. Attempts were made to independently synthesis *di*-indolide pyrazabole (using the conditions established for the synthesis of **4.13**, *vide supra*), however this was unsuccessful and *di*-indolide pyrazabole could not be cleanly formed, and so the formation of *di*-indolide pyrazabole in the *in situ* monitored reactions could not be confirmed. Heating the reactions to 100 °C for 1 hour resulted in the formation of the side-products **4.7** and **4.8**, alongside minor **4.4**, demonstrating how rapidly the decomposition reaction occurs upon heating.

Therefore, it is assumed that the reaction of indoline with **4.2** occurs via the same mechanistic pathway proposed by Dr Clément Millet (**Scheme 4.13**), with decomposition occurring rapidly with indoline (*vide infra*), making it challenging to observe the *in situ* formation of *di*-indolide pyrazabole. It should be noted that the same challenges in assigning the intermediate species in the *in situ* ^{1}H NMR spectra also occurred when monitoring the reaction of indole with **4.3**, with a complex mixture of indoline species observed at room temperature.

4.3.5 Differences in Reactivity Between Indoline and *N*-Methyl Aniline

Despite presumably proceeding via the same mechanistic pathway, the *ortho* C-H borylation of indolines using *di*-iodo pyrazabole **4.2** gave consistently lower yields than the equivalent reactions of *N*-methyl aniline under identical conditions (**Scheme 4.14**).

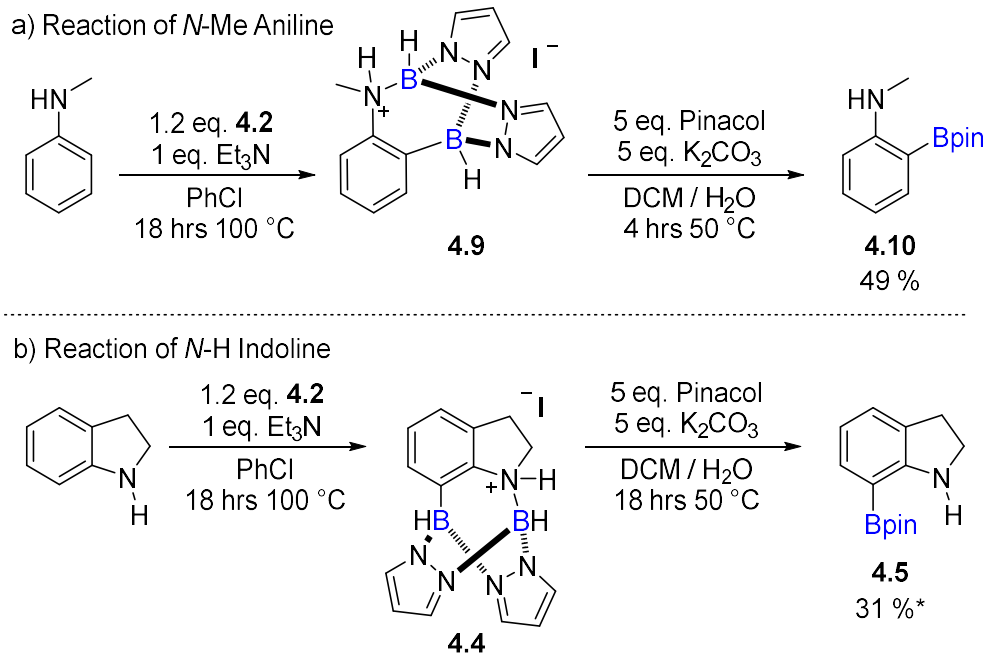

Scheme 4.14: Yields for the *ortho* C-H borylation of **a)** *N*-methyl aniline or **b)** *N*-H indoline, both using *di*-iodo pyrazabole **4.2** and Et_3N.
**(% Yields are NMR yields following work-up, relative to an internal standard).*

One hypothesis for why the reactions with indoline gave consistently poorer yields was that the 5-membered ring of indoline (and indole) orientates the

indoline nitrogen in a way that increases the distance/angle between the N-R and C7-R substituents. This could potentially result in increased distortion energy in the key transition states for C7-H borylation, and thus increase the energy of the transition state in the formation of **4.4**. By comparison, the nitrogen in *N*-methyl aniline is not constrained in a ring, meaning there will more flexibility (lower distortion energy) during C7-H borylation. The decreased transition state energy in the formation of **4.9** would explain the higher yields of **4.10** under identical conditions.

To probe this, the reactivity of tetrahydroquinoline was studied. In this substrate, the nitrogen is part of a 6-membered ring, therefore the separation between the N-R and C8-R substituents is decreased (relative to the N/C7-subsitutents in indoline). This would, in theory, reduce the amount of distortion energy during diborylation to form the N/C8-diborylated species, and thereby increase the yield of *ortho*-borylation similar to what is observed with *N*-methyl aniline. The *ortho* C-H borylation of tetrahydroquinoline using *di*-iodo pyrazabole **4.2** was tested with 3 different exogenous bases (**Figure 4.6**). The yields of 8-Bpin tetrahydroquinoline (**4.14**) were consistently higher with all three bases compared to their equivalent reactions with indoline, with the yields matching the reaction of *N*-methyl aniline.

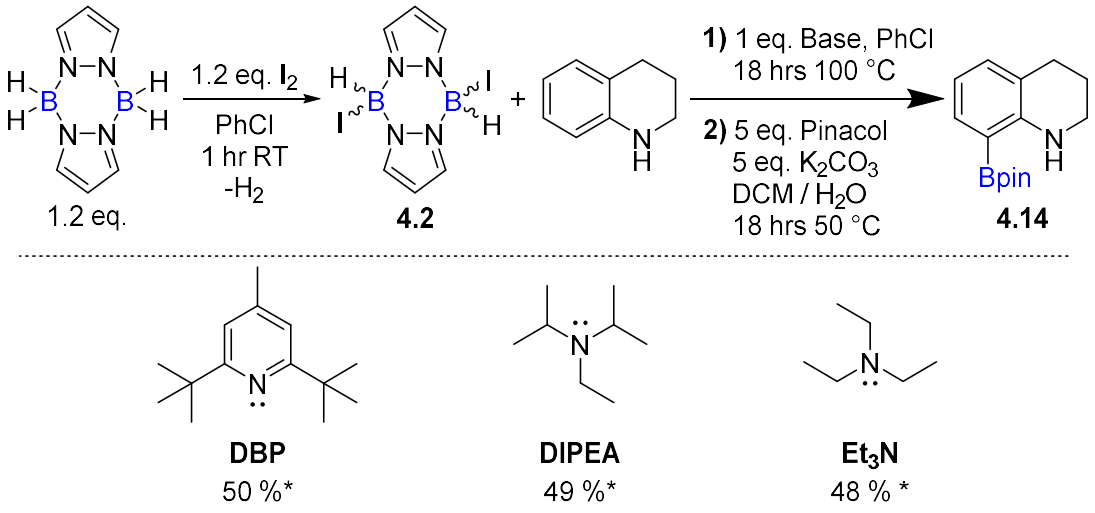

Figure 4.6: Screening of exogenous bases for the C8-H borylation of tetrahydroquinoline using *di*-iodo pyrazabole **4.2**.
**(Yields are NMR yields following work-up, relative to an internal standard).*

These observations support the hypothesis that change in the orientation of the N-R substituent in indoline (due to nitrogen's incorporation in a 5-membered ring) results in decreased yields (compared to *N*-methyl aniline) and may favour the competitive decomposition side-reaction. As the iodine-activated pyrazaboles were very poor at the N/C7-diborylation of indoles (the key objective), this project was not continued further.

4.4 Conclusions

Iodine-activated pyrazabole electrophiles can be easily generated *in situ* from the addition of iodine to pyrazabole, which avoids the need for gloveboxes. Iodine is a cheaper and easier to handle activator compared to $HNTf_2$, but the more coordinating nature of iodide versus $[NTf_2]^-$ has a significant effect on the reactivity of the pyrazabole electrophiles, particularly towards indoles.

The synthesis of 7-Bpin indolines via the reaction of either indole or indoline with iodine-activated pyrazaboles has been demonstrated, but there is a higher barrier to the C7-H borylation of the indoline intermediate when using iodine-activated pyrazaboles, which leads to the break-up of the pyrazabole unit to form by-products being the dominant outcome – as these species are unproductive for the desired reactivity the yields of C7-H borylation are low. Attempts to optimise the reactions to minimise this side-reaction and favour C7-H borylation have been largely unsuccessful. In addition, the C7-H borylation of indole/indoline was shown to be more challenging compared to *N*-methyl aniline and tetrahydroquinoline, further decreasing yields. Therefore, whilst the use of iodine-activated pyrazaboles is more desirable, the reactions using $HNTf_2$-activated pyrazaboles are cleaner (no side reactions) and are significantly higher yielding. The use of iodine-activated pyrazaboles over $HNTf_2$-activated pyrazaboles is not a viable alternative in the synthesis of 7-Bpin indolines.

It should be noted that subsequent work by Dr Clément Millet combined the benefits of each activator into one system using an anion exchange process that converted iodo-pyrazaboles into the more reactive NTf_2-pyrazaboles *in situ*.[23] The *ortho* C-H borylation of several *N*-methyl aniline derivatives, including indoline and tetrahydroquinoline, was achieved using 1 equiv. of *di*-iodo pyrazabole and 0.2 equiv. of $[Et_3NH][NTf_2]$ (**Scheme 4.15**).

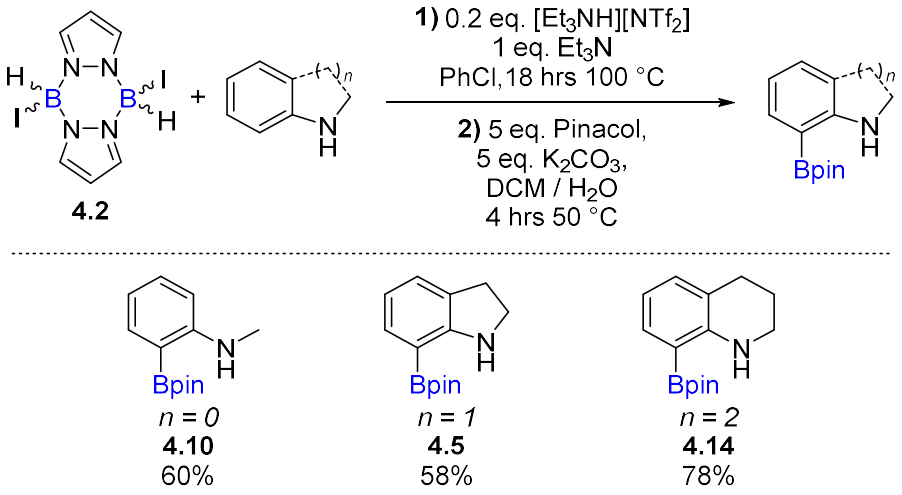

Scheme 4.15: Isolated yields for the *ortho* C-H borylation of *N*-methyl aniline, *N*-H indoline and *N*-H tetrahydroquinoline using *di*-iodo pyrazabole and 0.2 equiv. $[Et_3NH][NTf_2]$. *Work by Dr Clement Millet.*[23]

The anion exchange process is likely driven by the precipitation of the $[Et_3NH][I]$ salt. This led to a significant enhancement in yield (compared to using just the iodine-activated pyrazabole system), and no decomposition of the pyrazabole unit was observed. This enabled high yielding, clean reactions, without requiring the use of a glovebox or stoichiometric amounts of $HNTf_2$.

4.5 Experimental

*For general experimental considerations, see **Chapter 2**.*

4.5.1 Synthesis of Iodine Activated Pyrazaboles

*The synthesis of pyrazabole (**4.1**) is reported in **Chapter 3**. The NMR spectra of the isolated di-iodo pyrazabole (**4.2**), and the formation mono-iodo pyrazabole (**4.3**) in situ can be found in the appendix of this thesis. Crystallographic data for the structure of **4.2** (by Dr Jürgen Pahl) can be found in the publication of this work.*[23]

_Di_-Iodo Pyrazabole – 4.2

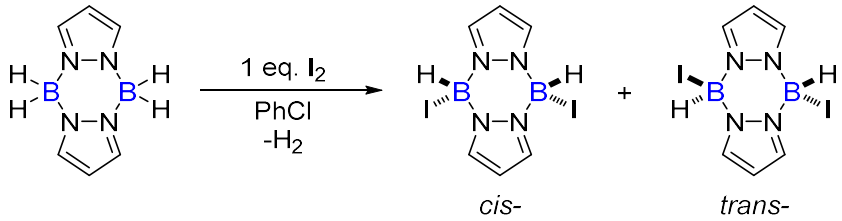

A solution of iodine (1.588 g, 6.26 mmol, 1 equiv.) in PhCl (50 mL) was added dropwise to a solution of pyrazabole **4.1** (1.0 g, 6.26 mmol) in PhCl (10 mL) at 0 °C, leading to gas evolution. Following addition, the reaction was warmed to room temperature and stirred for 18 hours, during which time a white solid precipitated. The suspension was filtered, and the precipitate was washed with PhCl (3 x 5 mL). The PhCl filtered fractions were combined, concentrated *in vacuo* until saturated, then cooled to 0 °C. A precipitate formed, which was filtered and dried *in vacuo* to afford the title product as a pale yellow solid in a 75% yield (1.934 g, 4.70 mmol), as a 1:1 mixture of the *cis*- and *trans*- isomers. The NMR data below is for this mixture of isomers.

^{1}H NMR (500 MHz, $CDCl_3$) δ 8.20 (d, $^{3}J_{HH}$ = 2.5 Hz, 4H, N=C*H*-CH), 8.02 (d, $^{3}J_{HH}$ = 2.5 Hz, 4H, N=C*H*-CH), 6.70 (t, $^{3}J_{HH}$ = 2.5 Hz, 2H, N=CH-C*H*), 6.64 (t, $^{3}J_{HH}$ = 2.5 Hz, 2H, N=CH-C*H*), 6.15-5.02 (m br, 4H, B*H*I);

^{1}H{^{11}B} NMR (500 MHz, $CDCl_3$) δ 8.20 (d, $^{3}J_{HH}$ = 2.5 Hz, 4H, N=C*H*-CH), 8.02 (d, $^{3}J_{HH}$ = 2.5 Hz, 4H, N=C*H*-CH), 6.70 (t, $^{3}J_{HH}$ = 2.5 Hz, 2H, N=CH-C*H*), 6.64 (t, $^{3}J_{HH}$ = 2.5 Hz, 2H, N=CH-C*H*), 5.74 (s br, 2H, B*H*I), 5.45 (s br, 2H, B*H*I);

^{11}B NMR (160 MHz, $CDCl_3$) δ -13.5 (d, $^{1}J_{BH}$ = 150 Hz, *B*HI) -15.2 (d, $^{1}J_{BH}$ = 150 Hz, *B*HI);

^{11}B {^{1}H} NMR (160 MHz, $CDCl_3$) δ -13.5 (s, *B*HI) -15.2 (s, *B*HI);

$^{13}C\{^{1}H\}$ NMR (126 MHz, $CDCl_3$) δ 140.17, 138.60, 109.39, 108.61 ppm.
HRMS (ESI$^+$) m/z calcd for $C_6H_7B_2I_2N_4^+$: 410.89409 [M-H]$^+$, found 410.89235.

Formation of *mono*-Iodo Pyrazabole (4.3) *in situ*

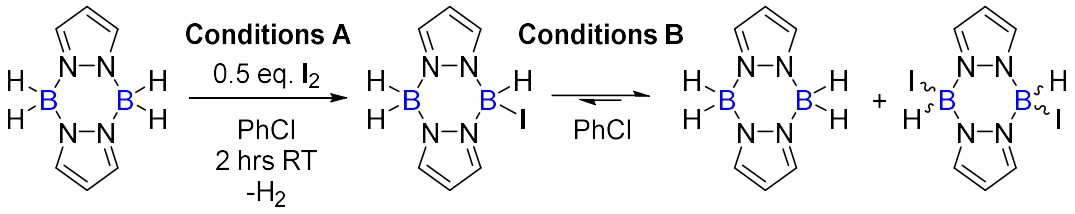

Conditions A: A solution of iodine (0.019 g, 0.075 mmol, 0.5 equiv.) in PhCl (0.5 mL) was added to a solution of pyrazabole **4.1** (0.024 g, 0.15 mmol) in PhCl (0.5 mL), leading to gas evolution. After 2 hours stirring at room temperature, *in situ* ^{11}B NMR spectroscopy showed partial formation of a new pyrazabole species (though some overreaction to **4.2** occurred, and consequently some leftover **4.1** is observed in the NMR spectra).

Conditions B: Pyrazabole **4.1** (0.016 g, 0.1 mmol) and *di*-iodo pyrazabole **4.2** (0.042 g, 0.1 mmol) were suspended in PhCl (0.5 mL). After 30 minutes stirring at room temperature, *in situ* ^{11}B NMR spectroscopy showed partial formation of a new pyrazabole species. However, the poor solubility of **4.2** at room temperature means that some unreacted **4.1** remained and is observed in the NMR spectra. Better quality data was collected after heating the reaction for 1 hour at 100 °C, ensuring **4.2** had fully dissolved and **4.3** was the major species present.

With both **Conditions A** and **B**, attempts to isolate **4.3** from the reaction solution resulted in the formation of equimolar **4.1** and **4.2** due to the precipitation of **4.2**.

4.5.2 Directed C7-H Borylation of *N-H* Indoles

*The characterisation of 7-Bpin indoline (**4.5**) can be found in **Chapter 3**. The NMR spectra of these reactions (after work-up) can be found in the appendix of this thesis.*

General Procedure 4.1: Reactivity with *Mono*-Iodo Pyrazabole

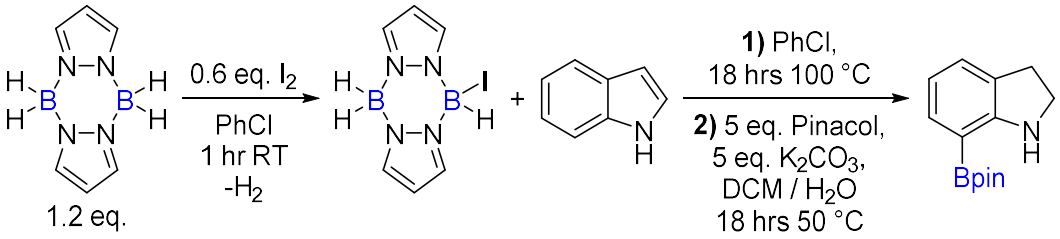

Pyrazabole **4.1** (0.058 g, 0.36 mmol, 1.2 equiv.) and iodine (0.046 g, 0.18 mmol, 0.6 equiv.) were suspended in chlorobenzene (2 mL), leading to gas evolution. After stirring at room temperature for 1 hour, *N*-H indole (0.035 g, 0.3 mmol) was added, and the reaction was heated to 100 °C in a sealed ampule for 18 hours. Upon cooling, pinacol (0.177 g, 1.5 mmol, 5 equiv.), K_2CO_3 (0.207 g, 1.5 mmol, 5 equiv.), DCM (4 mL) and water (4 mL) were added sequentially, and the ampule was sealed and heated to 50 °C for 18 hours, with rapid stirring to mix the resulting biphasic mixture. Upon returning to room temperature, the product was extracted with pentane (4 x 10 mL). The combined organic phases were washed with water (4 x 10 mL), dried over $MgSO_4$, filtered, and concentrated *in vacuo* to yield an oily residue.

The residue was dissolved in $CDCl_3$ (0.5 mL), and yields were determined by integration of diagnostic ^1H resonances against 1,3,5-trimethylbenzene (0.015 mL, 0.108 mmol) added as an internal standard. The NMR yield of 7-Bpin indoline **4.5** was calculated to be 10% (0.007 g, 0.028 mmol), with analytical data in accordance with a sample of **4.5** synthesised from the reaction with *mono*-NTf_2 pyrazabole.[1]

General Procedure 4.2: Reactivity with *Di*-Iodo Pyrazabole

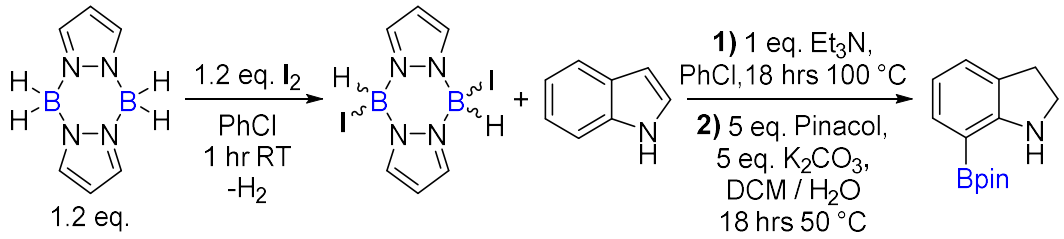

Pyrazabole **4.1** (0.058 g, 0.36 mmol, 1.2 equiv.) and iodine (0.091 g, 0.36 mmol, 1.2 equiv.) were dissolved in chlorobenzene (2 mL), leading to gas evolution. After stirring at room temperature for 1 hour, *N*-H indole (0.035 g, 0.3 mmol) was added and the reaction was stirred at room temperature for 30 minutes, after which time triethylamine (0.041 mL, 0.3 mmol, 1 equiv.) was added and the reaction was again stirred at room temperature for 30 minutes. The reaction was then heated to 100 °C in a sealed ampule for 18 hours. Upon cooling, pinacol (0.177 g, 1.5 mmol, 5 equiv.), K_2CO_3 (0.207 g, 1.5 mmol, 5 equiv.), DCM (4 mL) and water (4 mL) were added sequentially, and the ampule was sealed and heated to 50 °C for 18 hours, with rapid stirring to mix the resulting biphasic mixture. Upon returning to room temperature, the product was extracted with pentane (4 x 10 mL). The combined organic phases were washed with water (4 x 10 mL), dried over $MgSO_4$, filtered, and concentrated *in vacuo* to yield an oily residue.

The residue was dissolved in $CDCl_3$ (0.5 mL), and yields were determined by integration of diagnostic ^1H resonances against 1,3,5-trimethylbenzene (0.015 mL, 0.108 mmol) added as an internal standard. The NMR yield of 7-Bpin indoline **4.5** was calculated to be 9% (0.006 g, 0.026 mmol), with analytical data in accordance with a sample of **4.5** synthesised from the reaction with *mono*-NTf_2 pyrazabole.[1]

4.5.3 Directed C-H Borylation of Indoline and Tetrahydroquinoline

*The characterisation of 7-Bpin indoline (**4.5**) and 8-Bpin tetrahydroquinoline (**4.14**) can be found in **Chapter 3**. The NMR spectra of these reactions (after work-up) can be found in the appendix of this thesis.*

General Procedure 4.3: Reactivity with *Di*-Iodo Pyrazabole

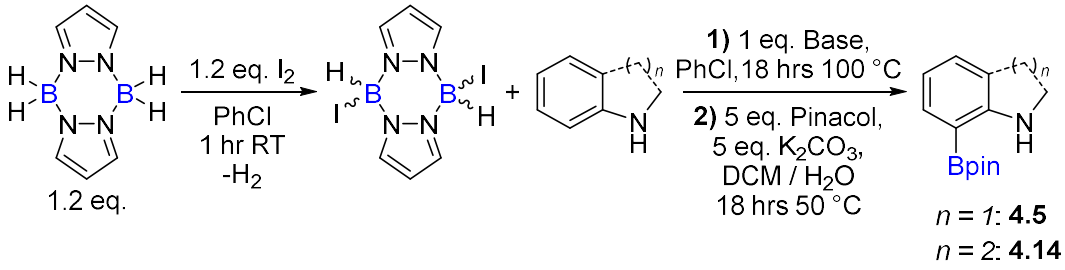

Pyrazabole **4.1** (0.058 g, 0.36 mmol, 1.2 equiv.) and iodine (0.091 g, 0.36 mmol, 1.2 equiv.) were dissolved in chlorobenzene (2 mL), leading to gas evolution. After stirring at room temperature for 1 hour, indoline (*n=1*) or tetrahydroquinoline (*n=2*) (0.3 mmol, 1 equiv.) was added and the reaction was stirred at room temperature for 30 minutes, after which time the corresponding base (0.3 mmol, 1 equiv.) was added and the reaction was again stirred at room temperature for 30 minutes. The reaction was then heated to 100 °C in a sealed ampule for 18 hours. Upon cooling, pinacol (0.177 g, 1.5 mmol, 5 equiv.), K_2CO_3 (0.207 g, 1.5 mmol, 5 equiv.), DCM (4 mL) and water (4 mL) were added sequentially, and the ampule was sealed and heated to 50 °C for 18 hours, with rapid stirring to mix the resulting biphasic mixture. Upon returning to room temperature, the product was extracted with pentane (4 x 10 mL). The combined organic phases were washed with water (4 x 10 mL), dried over $MgSO_4$, filtered, and concentrated *in vacuo* to yield an oily residue.

The residue was dissolved in $CDCl_3$ (0.5 mL), and yields were determined by integration of diagnostic ^1H resonances against 1,3,5-trimethylbenzene (0.015 mL, 0.108 mmol) added as an internal standard. Analytical data for **4.5 / 4.14** are in accordance with samples synthesised from the reaction with *mono*-NTf_2 pyrazabole *(see **Chapter 3**).*

Table 2: Screening the exogenous base for the reactivity of indoline / tetrahydroquinoline, following **General Procedure 4.3**.
Highest yielding conditions are highlighted.

Entry	Substrate	Product	Base	Variation(s)	Yield*
1	Indoline	**4.5**	DBP	**-**	20%
2	Indoline	**4.5**	DIPEA	**-**	17%
3	Indoline	**4.5**	Et_3N	**-**	31%
4	Indoline	**4.5**	Et_3N	A	28%
5	Indoline	**4.5**	Et_3N	B	19%
6	Tetrahydroquinoline	**4.14**	DBP	-	50%
7	Tetrahydroquinoline	**4.14**	DIPEA	-	49%
8	Tetrahydroquinoline	**4.14**	Et_3N	-	48%
9	Tetrahydroquinoline	**4.14**	Et_3N	A	49%
10	Tetrahydroquinoline	**4.14**	Et_3N	C	36%

Variation(s):

A. *Order of addition switched*: Following activation of pyrazabole, base was added first, followed by substrate.

B. Base and substrate added simultaneously as a solution in PhCl.

C. *Stepwise activation of pyrazabole*: During activation step, *mono*-iodo pyrazabole was formed *in situ* using 0.5 equiv. I_2. Following addition of substrate, followed by base, a further 0.5 equiv. of I_2 was added in an attempt to regenerate the pyrazabole electrophile *in situ*.

% Yields of **4.5/4.14 are NMR yields following work-up, relative to an internal standard*.

4.5.4 Reaction Profiling using *in situ* NMR Spectroscopy

The full NMR spectra of these reactions can be found in the appendix of this thesis.

General Procedure 4.4: Monitoring the Reaction of Indole

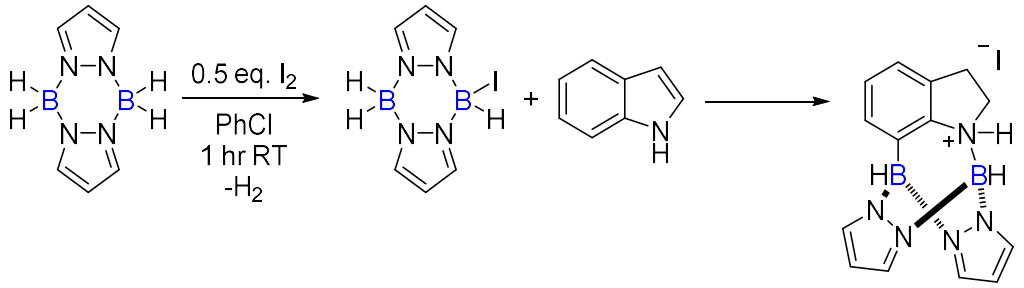

To a J. Young's NMR tube was added pyrazabole **4.1** (0.016 g, 0.1 mmol, 1 equiv.) and chlorobenzene (0.5 mL). Iodine (0.013 g, 0.05 mmol, 0.5 equiv.) was added, causing gas evolution. The tube was left open (to nitrogen flow) until gas evolution had stopped (1 hour), and the sample was sealed and analysed by NMR spectroscopy to check for formation of *mono*-iodo pyrazabole **4.3**. Subsequently, indole (0.012 g, 0.1 mmol, 1 equiv.) was added. The sample was mixed by inversion (approx. 1 rotation / s) at room temperature and analysed by NMR spectroscopy at regular time points. The sample was heated in a heating block without inversion / external mixing.

General Procedure 4.5: Monitoring the Reaction of Indoline

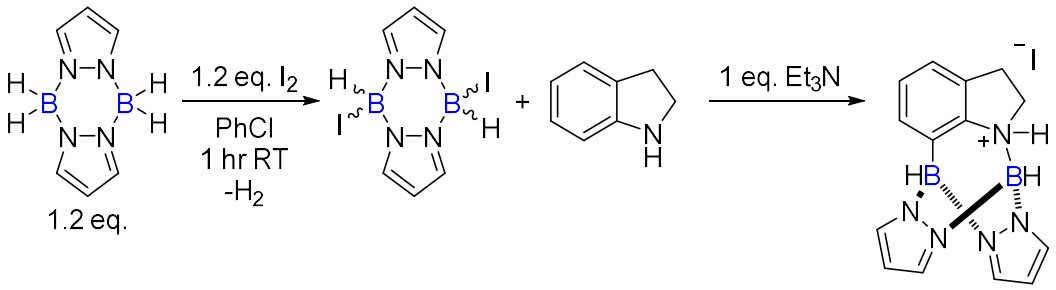

To a J. Young's NMR tube was added pyrazabole **4.1** (0.016 g, 0.12 mmol, 1.2 equiv.) and chlorobenzene (0.5 mL). Iodine (0.030 g, 0.12 mmol, 1.2 equiv.) was added, causing gas evolution. The tube was left open (to nitrogen flow) until gas evolution had stopped (1 hour), and the sample was sealed and analysed by NMR spectroscopy to check for formation of *di*-iodo pyrazabole **4.2**. Subsequently, indoline (0.011 mL, 0.1 mmol, 1 equiv.) was added, followed by Et_3N (0.014 mL,

0.1 mmol, 1 equiv.). The sample was mixed by inversion (approx. 1 rotation / s) at room temperature and analysed by NMR spectroscopy at regular time points. The sample was heated in a heating block without inversion / external mixing.

4.5.5 Characterisation of Decomposition By-Products

*The full NMR spectra used to characterise these by-products can be found in the appendix of this thesis. Note: (Indoline)$_2$-BH (**4.7**) is assigned by comparison to literature.*[21,22]

[HB-(Pyrazole)$_3$-BH][I] – 4.8

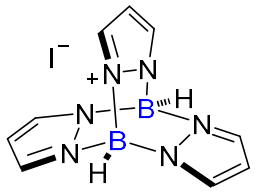

Following the reaction of indole (0.3 mmol) via **General Procedure 4.4**, a white precipitate was filtered by cannula, washed with PhCl (2 x 2 mL) and dried *in vacuo.* The precipitate was dissolved in $CDCl_3$ (0.5 mL) for NMR characterisation. Analytical data are in accordance with a sample of **4.8** independently synthesised and crystallised *(by Dr Clément Millet).*[23]

^{1}H NMR (500 MHz, $CDCl_3$) δ 8.23 (d, $^3J_{HH}$ = 2.5 Hz, 6H, N=C*H*-CH), 6.50 (t, $^3J_{HH}$ = 2.5 Hz, 3H, N=CH-C*H*), 5.00 (1:1:1:1 q, $^1J_{BH}$ = 130 Hz, 2H, B-*H*);

^{11}B NMR (160 MHz, $CDCl_3$) δ -5.31 (d, $^1J_{BH}$ = 130 Hz, *B*-H);

^{11}B{^{1}H} NMR (160 MHz, $CDCl_3$) δ -5.31 (s, *B*-H);

^{13}C{^{1}H} NMR (126 MHz, CDCl3) δ 138.41, 108.30 ppm.

4.6 References

1 J. Pahl, E. Noone, M. Uzelac, K. Yuan and M. J. Ingleson, *Angew. Chem. Int. Ed.*, 2022, **61**, e202206230.

2 A search carried out on 11/10/2023 found > 99% purity *bis-(*trifluoromethanesulfonyl)imide (product number B2541) was available for £44 for 5 g (= £2.47 per mmol) via TCI Chemicals.

3 W. Zhao and J. Sun, *Chem. Rev.*, 2018, **118**, 10349–10392.

4 T. S. De Vries, A. Prokofjevs and E. Vedejs, *Chem. Rev.*, 2012, **112**, 4246–4282.

5 A. Solovyev, Q. Chu, S. J. Geib, L. Fensterbank, M. Malacria, E. Lacôte and D. P. Curran, *J. Am. Chem. Soc.*, 2010, **132**, 15072–15080.

6 J. M. Clay and E. Vedejs, *J. Am. Chem. Soc.*, 2005, **127**, 5766–5767.

7 A search carried out on 11/10/2023 found > 99% purity Iodine (product number I0604) was available for £16 for 25 g (= £0.16 per mmol) via TCI Chemicals.

8 A. Prokofjevs, A. Boussonnière, L. Li, H. Bonin, E. Lacôte, D. P. Curran and E. Vedejs, *J. Am. Chem. Soc.*, 2012, **134**, 12281–12288.

9 X. Pan, A. Boussonnière and D. P. Curran, *J. Am. Chem. Soc.*, 2013, **135**, 14433–14437.

10 J. S. McGough, S. M. Butler, I. A. Cade and M. J. Ingleson, *Chem. Sci.*, 2016, **7**, 3384–3389.

11 J. S. McGough, J. Cid and M. J. Ingleson, *Chem. Eur. J.*, 2017, **23**, 8180–8184.

12 M. J. Ingleson, *Synlett*, 2012, **23**, 1411–1415.

13 S. Nerkar and D. P. Curran, *Org. Lett.*, 2015, **17**, 3394–3397.

14 E. Hanecker, T. G. Hodgkins, K. Niedenzu and H. Noeth, *Inorg. Chem.*, 1985, **24**, 459–462.

15 C. M. Clarke, M. K. Das, E. Hanecker, J. F. Mariategui, K. Niedenzu, P. M. Niedenzu, H. Noeth and K. R. Warner, *Inorg. Chem.*, 1987, **26**, 2310–2317.

16 C. I. Nieto, D. Sanz, R. M. Claramunt, I. Alkorta and J. Elguero, *Coord. Chem. Rev.*, 2022, **473**, 214812.

17 K. Niedenzu and H. Nöth, *Chem. Ber.*, 1983, **116**, 1132–1153.

18 J. Lv, X. Chen, X.-S. Xue, B. Zhao, Y. Liang, M. Wang, L. Jin, Y. Yuan, Y. Han, Y. Zhao, Y. Lu, J. Zhao, W.-Y. Sun, Kendall. N. Houk and Z. Shi, *Nature*, 2019, **575**, 336–340.

19 A. Escande, D. L. Crossley, J. Cid, I. A. Cade, I. Vitorica-Yrezabal and M. J. Ingleson, *Dalton Trans.*, 2016, **45**, 17160–17167.

20 J. McGough, PhD Thesis, The University of Manchester, 2017.

21 D. Wechsler, B. Davis and P. G. Jessop, *Can. J. Chem.*, 2010, **88**, 548–555.

22 A. Jayaraman, H. Powell-Davies and F.-G. Fontaine, *Tetrahedron*, 2019, **75**, 2118–2127.

23 C. R. P. Millet, E. Noone, A. V. Schellbach, J. Pahl, J. Łosiewicz, G. S. Nichol and M. J. Ingleson, *Chem. Sci.*, 2023, **14**, 12041–12048.

Chapter 5

Targeting C3/C4-Diborylation of Indoles

Chapter 5: Targeting C3/C4-Diborylation of Indoles

5.1 Introduction

As outlined in **Chapter 3**, the second target reaction utilising pyrazabole electrophiles as transient directing groups was the C3/C4-diborylation of indoles. C4-functionalised indoles are well utilised motifs in biological and medicinal chemistry, and in material sciences.[1,2] A metal-free and 'traceless' route to C4-borylated indoles would therefore be synthetically useful, and significantly expand the scope of the 'borylation directed borylation' approach.

Studies thus far with $HNTf_2$- or iodine-activated pyrazaboles have yielded C7-borylated indolines as a result of the initial hydroboration of indole.[3,4] Subsequent C3-B protodeboronation transfers the pyrazabole directing group to the nitrogen atom, from which C7-H borylation occurs. To prevent indole hydroboration, and thus ensure the pyrazabole directing group remains at the C3 position, hydride transfer to the intermediate following C3-B bond formation, **5.I**, must be prevented (**Scheme 5.1**). One possible solution would be to replace the hydride substituents for an alternative, 'E', that is not readily transferred in the respective 'elementoboration' process. Preventing elementoboration would then, in theory, enable the deprotonation of **5.I** by an exogenous base to form the C3-H borylated intermediate **5.II**. This species would have the second boron unit positioned in close proximity to C4, hopefully enabling C4-H borylation to form the diborylated indole **5.III**. Pinacol protection and work-up would then cleave the more reactive C3-B bond to yield C4-Bpin indoles.[3]

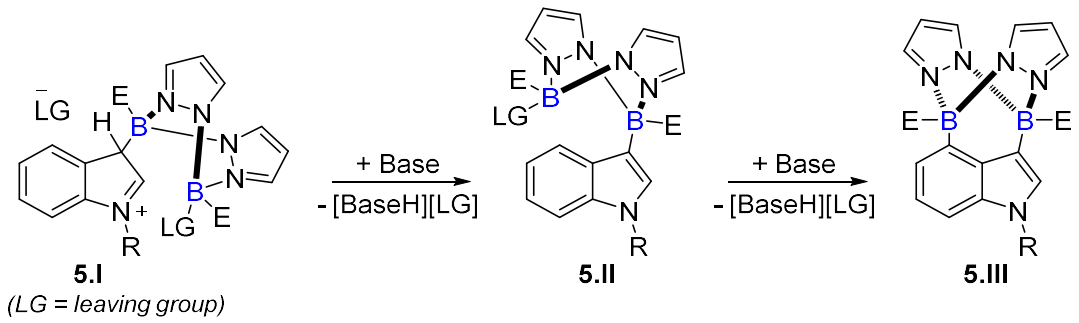

Scheme 5.1: A proposed method to achieve the C3/C4-diborylation of *N*-R indoles, using an alternative *di*-electrophilic pyrazabole directing group *(E = non-transferrable substituent).*

One potential challenge with this proposed reaction would be ensuring that the process is selective for C4-H borylation from intermediate **5.II**, over C2-H borylation. Competitive C2/C3-diborylation could be disfavoured by the use of a large, bulky (but removable) substituent 'R' at nitrogen, which would act as a blocking group to prevent C2-H borylation. Examples of nitrogen blocking groups previously used to prevent indole C2-H borylation include Boc, TIPS and Bpin.[5–7]

One option for the substituent 'E' would be a halogen. Haloboration, the addition of a B-X bond across an unsaturated moiety, is much less utilised than hydroboration.[8,9] Though the haloboration of (terminal) alkynes is a useful and established method to produce various *di*-functionalised alkenes, the haloboration of alkenes is significantly more limited.[10] Computational studies by Wang and Uchiyama showed haloboration of alkenes to be a thermodynamically unfavourable process.[11] The chloroboration of propyne with BCl_3 was calculated to be exergonic at 293 K (ΔG = -1.5 kcal mol^{-1}, **Scheme 5.2a**), whilst the analogous reaction of propene was calculated to be endergonic (ΔG = 9.4 kcal mol^{-1}, **Scheme 5.2b**), consistent with the lack of observed reactivity between BCl_3 and alkenes.

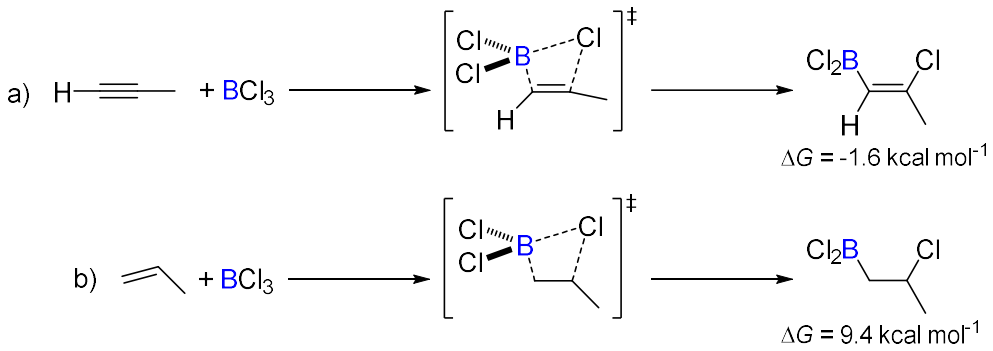

Scheme 5.2: Reaction pathway and calculated Gibbs free energy for the chloroboration of **a)** propyne and **b)** propene using BCl_3.

Furthermore, there have been no previous reports of the haloboration of the enamine unit in indoles by B-X containing boron electrophiles (to the best of our knowledge). Based on this, halo-substituted pyrazabole derivatives could be suitable traceless directing groups for the C3/C4-diborylation of indoles.

Halo-substituted pyrazaboles can be readily synthesised from the parent 'BH_2' pyrazabole. The substitution of the B-H bonds in pyrazaboles to B-X bonds was first reported by Trofimenko in 1967, using excess X_2 (X = Cl, Br) to form the respective *tetra*-halo substituted pyrazabole derivatives (**Scheme 5.3**).[12] Substitution of the B-H bonds occurred without halogenation of the pyrazole ring. *Tetra*-fluoro pyrazabole was synthesised directly by refluxing a mixture of pyrazole and Me_3N-BF_3 in toluene, albeit in lower yields. The stability of the *tetra*-halo pyrazabole species was reported to be dependent on the strength of the B-X bond (F > Cl > Br).[13]

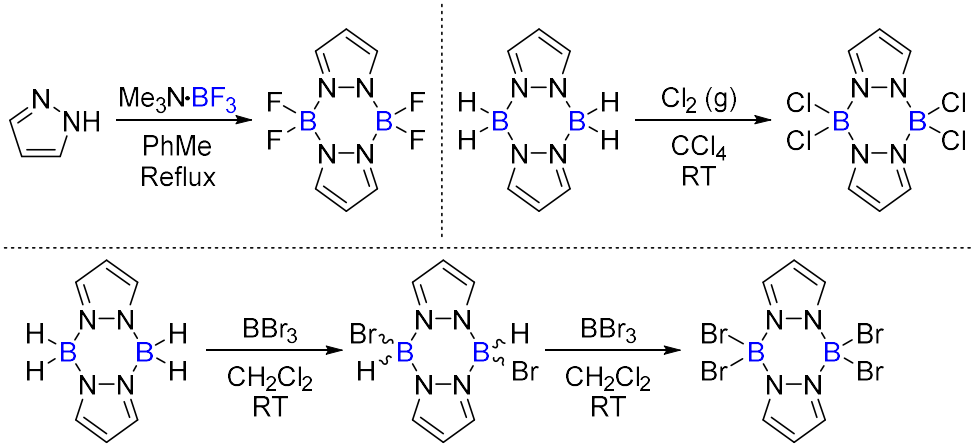

Scheme 5.3: Reported synthetic routes to fluoro-, chloro- and bromo-substituted pyrazaboles.

Subsequent work by Nöth and co-workers developed the use of BBr_3 as an alternative source of bromide.[14,15] This enabled the selective synthesis of *di*-bromo pyrazabole if the stoichiometry of BBr_3 was controlled, as the addition of >0.67 equiv. BBr_3 resulted in partial overreaction to *tetra*-bromo pyrazabole (**Scheme 5.3**). The *in situ* formation of *mono*- and *tri*-bromo pyrazabole was also reported, however these unsymmetrical pyrazabole species underwent disproportionation to form the symmetrical halo-pyrazabole equivalents. It should be noted that the synthesis of *di*-chloro pyrazabole using BCl_3 has not been reported, though the synthesis of several other fluoro, chloro- and bromo-substituted pyrazabole derivatives have been reported via similar approaches, with various substitution patterns on the pyrazole backbone.[16–18]

In assessing which halo-substituted pyrazabole would be the most appropriate for use as traceless directing groups, chloro- and bromo-substituted pyrazaboles are believed to be the optimal choices. Iodo-substituted pyrazaboles were studied in **Chapter 4**, where it was shown that the labile B-I bond is substituted by incoming nucleophiles.[4] Iodide would therefore not be a suitable choice for a substituent that needs to not be displaced by the nucleophiles present in the target reaction (e.g. indole, bases etc.). By comparison, fluoro-substituted pyrazaboles would be an ideal choice in terms of inertness, as the strength of the B-F bond would prevent substitution by incoming nucleophiles.[12] However, this stability could also be detrimental to a) the activation step (by B-F cleavage) to make the required *di*-electrophilic pyrazabole species and b) the transformation of the pyrazabole directing group into a synthetically useful organoborane (e.g. R-Bpin) at the end of the reaction.[19] For these reasons, chloro and bromo-substituted pyrazaboles were selected.

To probe whether chloro- and bromo-substituted pyrazaboles could generate boron electrophiles that are sufficiently reactive for the C3/C4-diborylation of indoles, DFT was used to calculate the relative hydride ion affinities (HIAs) of the respective pyrazabole-based borenium cations (**Figure 5.1**). Calculations were performed by Professor Michael J. Ingleson at the M06-2X/6-311G(d,p), PCM (CH_2Cl_2) level of theory. This level enabled direct comparison to previously calculated HIAs for other reactive borenium cations used in C-H borylation reactions (e.g. **5.VII** and **5.VIII**).[20]

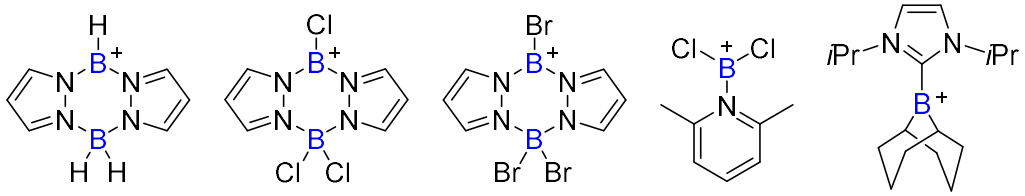

Figure 5.1: Calculated hydride ion affinities (ΔG/ kcal mol^{-1}, relative to BEt_3).

Based on these calculated values, chloro- and bromo-substituted borenium cations **5.V** and **5.VI** are significantly more electrophilic than the hydride-

substituted equivalent, **5.IV**. Considering that N/C7-diborylation of indoline was achieved using *mono*-NTf_2 pyrazabole (a 'masked' borenium ion equivalent of **5.IV**), this indicates that **5.V** and **5.VI** should be sufficiently reactive to enable C3/C4-diborylation of indole. The HIAs of **5.V** and **5.VI** are also higher than for the reported borenium cations **5.VII** and **5.VIII**, which have both been previously employed in the functionalisation of π-nucleophiles and as the Lewis acidic component in FLPs that enable the heterolytic activation of H_2.[20,21] It should be noted, however, that the HIAs of **5.IV**, **5.V** and **5.VI** are for the three-coordinate borenium cations. These values do not consider the energy change associated with the loss of the leaving group from the neutral four-coordinate pyrazabole species, which will depend upon the coordinating nature of the leaving group.

5.2 Project Aims

In order to target the C3/C4-diborylation of indoles, the synthesis of chloro- or bromo-substituted pyrazabole electrophiles was sought. For these halo-substituted pyrazaboles to be sufficiently electrophilic, activation is required. This could be achieved through the abstraction of a substituent to form the respective three-coordinate borenium cations (such as **5.V** and **5.VI**, **Figure 5.1**) or via the installation of a readily displaced leaving group, which would generate a four-coordinate 'masked' borenium ion (such as *di*-NTf_2 pyrazabole, **Chapter 3**).[3] Since the reactivity of B-NTf_2 bonds with indole nucleophiles was reasonably well understood following **Chapter 3**, activation methods that form NTf_2-susbstituted pyrazabole electrophiles were explored. Two routes to form the target halo-substituted pyrazabole electrophiles were proposed (**Scheme 5.4**).

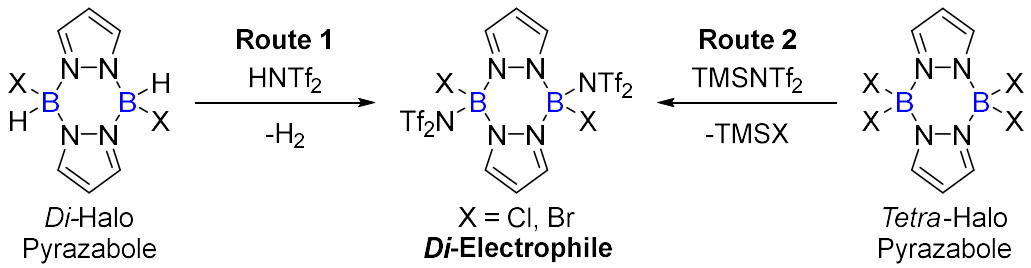

Scheme 5.4: Two possible routes to form the desired ditopic chloro- or bromo-substituted pyrazabole electrophiles.

'**Route 1**' starts from the *di*-halo substituted pyrazaboles, where activation using $HNTf_2$ would form the desired *di*-electrophiles. It was proposed that the selectivity for the substitution of the B-H bonds over the B-X bonds would be due to the formation of H_2 as a by-product over HBr, providing an enthalpic and entropic driving force. Alternatively, '**Route 2**' starts from the *tetra*-halo substituted pyrazaboles. For this starting pyrazabole species, it was proposed that TMS-NTf_2 could be used to abstract the halide substituents and form the desired *di*-electrophiles, with the formation of TMS-X providing sufficient driving force to enable the activation. This reagent, generated via the protodesilylation of PhTMS with $HNTf_2$, has been previously used to abstract bromide from [H_2(R)N-BBr_3] adducts.[22]

Therefore, the work described in this chapter aimed to evaluate these two synthetic routes to determine whether the desired halo-substituted pyrazabole electrophiles could be cleanly formed. Once formed, the reactivity with *N*-methyl indole could then be explored, with the goal of achieving the traceless C3/C4-diborylation of indoles. It should be noted that C2/C3-diborylation was also a feasible outcome, though it was hoped that this could be disfavoured (*vide supra*).

5.3 Results and Discussion

Since '**Route 1**' was the more atom-efficient of the two proposed routes to the halo-substituted pyrazabole electrophiles of interest, the synthesis and reactivity of *di*-halo pyrazaboles (Cl and Br) was explored first.

5.3.1 Synthesis of *Di*-Halo Pyrazaboles

As previously described by Nöth and co-workers,[14,15] the room-temperature bromination of pyrazabole **5.1** using BBr_3 yielded *di*-bromo pyrazabole **5.2**, which was isolated in an 88% yield (**Scheme 5.5**). Quenching the gaseous diborane by-products in-line was achieved by bubbling the nitrogen outflow through methanol, and this was shown to have a beneficial effect on the yield of **5.2**, presumably by removing the B-H containing by-products and thus driving the B-H/B-Br exchange equilibrium forward.

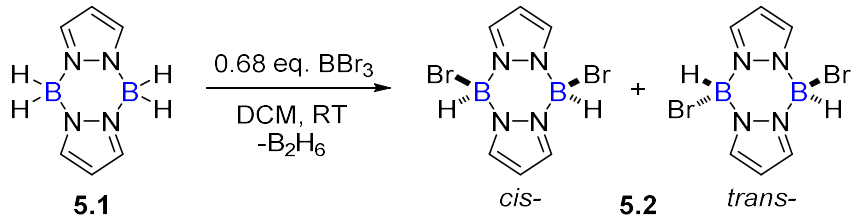

Scheme 5.5: Bromination of pyrazabole to *di*-bromo pyrazabole, which isomerises in solution to form a 1:1 mixture of the *cis*- and *trans*- isomers.

The ^{1}H NMR spectrum of **5.2** in $CDCl_3$, recorded 5 minutes after dissolution, showed two symmetrical pyrazabole species in a ratio of 11:1 (**Figure 5.2**). After two hours at room temperature, this ratio was ca. 1:1. The ^{11}B NMR spectra also showed the formation of two (overlapping) doublets at -5.7 and -6.7 ppm, with the proportion of the downfield resonance increasing over time and a 1:1 ratio reached after 2 hours at room temperature. These two pyrazabole species are assigned as the *cis*- and *trans*- isomers of **5.2** (in line with previous reports).[14–16] This indicates that one isomer may be favoured in the solid state, but upon dissolution in solvent the isomerisation of **5.2** occurs, eventually forming a roughly equimolar mixture of the two stereoisomers after approximately two hours at room temperature.

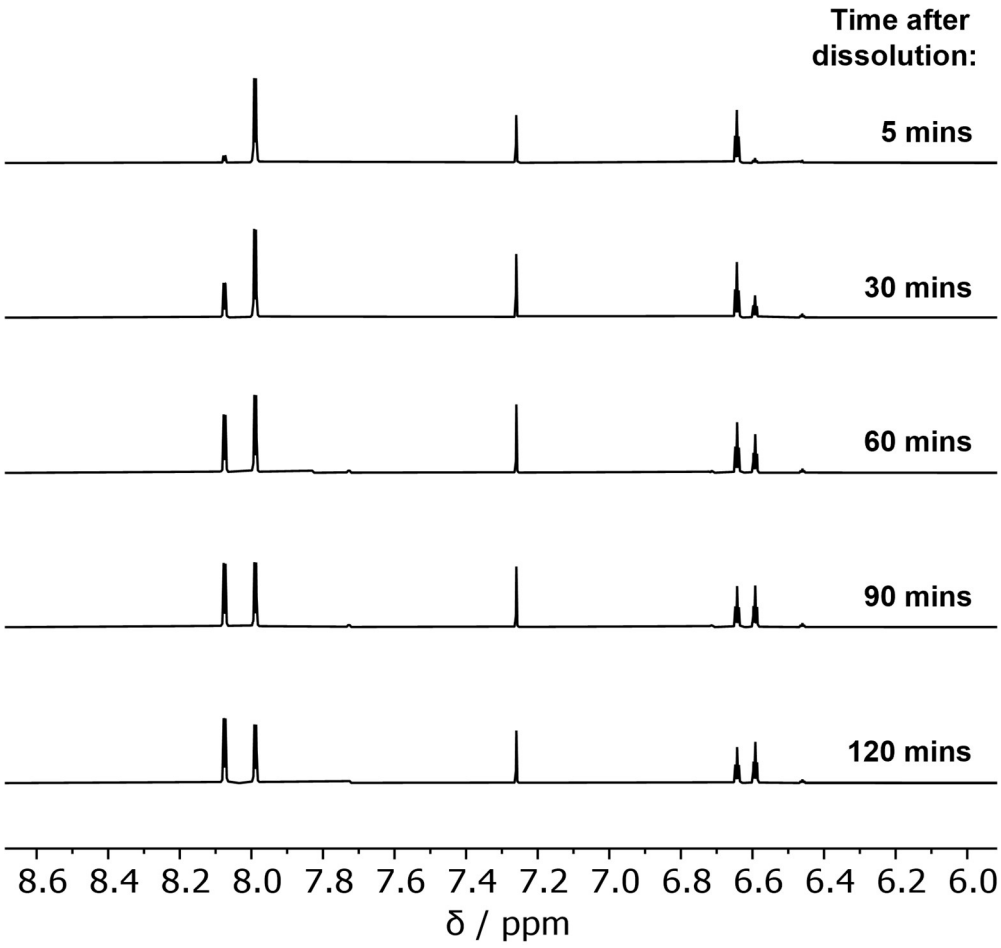

Figure 5.2: Stacked ^{1}H NMR spectra showing the isomerisation of *di*-bromo pyrazabole following dissolution in $CDCl_3$ at room temperature.
(Solvent = $CDCl_3$, NMR temperature = 300 K)

Attempts to form single crystals of **5.2** for X-ray diffraction studies were unsuccessful, but the reported crystal structure of a similar *di*-bromo substituted pyrazabole species (using 3-chloro pyrazole in place of pyrazole), showed the two bromide substituents in a *cis*- configuration.[14] Based on this and the crystal structures of *di*-iodo pyrazabole,[4] and *di*-chloro pyrazabole (*vide infra*), it is assumed that the major isomer of **5.2** immediately after dissolution is the *cis*-isomer, which isomerises to form the *trans*- isomer.

The formation of *cis*- and *trans*- isomers was also observed with *di*-iodo pyrazabole (**Chapter 4**), but the ^{1}H NMR spectrum showed a 1:1 mixture of the two isomers just 10 minutes after dissolution in $CDCl_3$, indicating a faster rate of isomerisation. The observation that the rates of isomerisation appear inversely

proportional to the B-X bond strengths suggests that the isomerisation mechanism likely proceeds through via loss of the halide substituent, rather than via cleavage of the pyrazole N-B bond and opening of the B_2N_4 core.

The synthesis of *di*-chloro pyrazabole, **5.3**, was achieved via the equivalent reaction of pyrazabole **5.1** and BCl_3, with **5.3** cleanly isolated in a 56% yield (**Scheme 5.6**). For this species, the ^1H / ^{11}B NMR spectra in $CDCl_3$ showed one symmetrical pyrazabole species (δ_{11B} = -2.8, doublet), with no isomerisation observed at room temperature or upon heating to 100 °C. This indicates that the more coordinating nature of chloride to boron, and thus the higher B-Cl bond strength (compared to B-Br),[13] prevents the isomerisation of **5.3**.

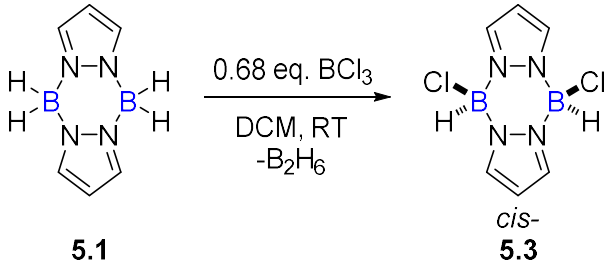

Scheme 5.6: Chlorination of pyrazabole to *di*-chloro pyrazabole, where only the *cis*-isomer is observed in solution.

Single crystals of *di*-chloro pyrazabole **5.3** suitable for X-ray diffraction studies were formed via DCM / hexane vapour diffusion. The crystal structure of **5.3** showed the two chloride substituents in a *cis*- configuration (**Figure 5.3**). The B···B distance of 3.039(13) Å is slightly increased compared to *di*-iodo pyrazabole (3.031(8) Å),[4] but is still suited for the C3/C4-diborylation of indoles.[23]

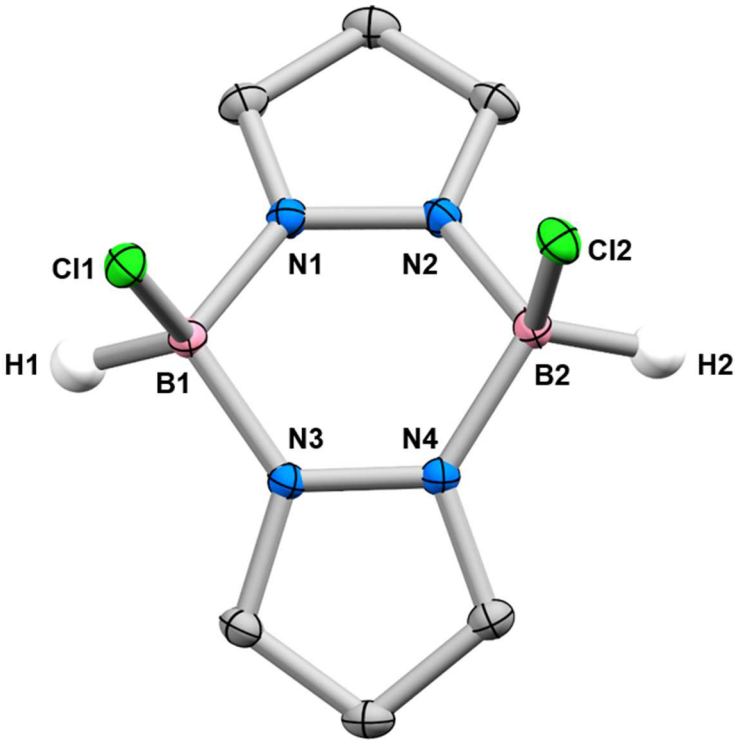

Figure 5.3: Solid-state structure of *cis*-**5.3** *(measured and solved by Dr Gary Nichol).* Ellipsoids at the 50% probability level. Hydrogen atoms (except H1 and H2) removed for clarity. Selected distances (Å): B1-Cl1 1.8776(5), B2-Cl2 1.8803(5), B1···B2 3.039(13).

To begin investigations into the activation of these *di*-halo pyrazaboles, samples of **5.2** and **5.3** were heated alongside *N*-methyl indole and 2 equiv. DBP. Heating to 100 °C for up to three days did not provide any evidence of C-H borylation, nor any other indications of reactivity (such as the consumption of *N*-methyl indole or the protonation of DBP). As expected, the increased B-X bond strength in these *di*-halo pyrazabole species (compared to *di*-NTf_2 / *di*-iodo pyrazabole) means the halide substituent is not displaced by incoming nucleophiles, as desired.

5.3.2 Reactivity of *Di*-Halo Pyrazaboles with $HNTf_2$: 'Route 1'

To investigate the feasibility of '**Route 1**' as a route to the desired halo-substituted pyrazabole electrophiles, the activation of *di*-bromo pyrazabole **5.2** with $HNTf_2$ was first investigated, with the aim of forming *di*-bromo *di*-NTf_2 pyrazabole **5.4** (**Scheme 5.7**). The synthesis of *di*-bromo pyrazabole **5.2** had been previously reported,[15] hence it was synthesised before *di*-chloro pyrazabole **5.3**, and so its reactivity with $HNTf_2$ was studied first.

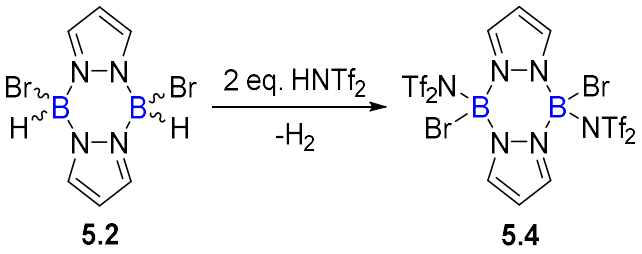

5.2 **5.4**

Scheme 5.7: Proposed reaction between *di*-bromo pyrazabole and $HNTf_2$, selectively activating the B-H bonds to form *di*-bromo *di*-NTf_2 pyrazabole.

Initial Studies: Activation of *Di*-Bromo Pyrazabole

Addition of 2 equiv. $HNTf_2$ to **5.2** in DCM resulted in very little observed reactivity at room temperature. Heating to 45 °C resulted in minor H_2 evolution, suggesting activation had partially occurred. However, NMR spectroscopy showed Br/Cl halogen exchange between **5.2** (or **5.4**) and the solvent, evidenced by multiple new resonances between 1 and -2 ppm in the ^{11}B NMR spectrum (consistent with the δ_{11B} of chloro-pyrazaboles).[14] Repeating the reaction in chlorobenzene resulted in the full consumption of **5.2** after 18 hours at 100 °C. During this time a white solid precipitated. Cooling the reaction flask to -20 °C facilitated further precipitation of the solid, which was filtered, washed with pentane, and dried *in vacuo*. The solid was poorly soluble in many weakly coordinating organic solvents, but ^1H NMR spectroscopy following partial dissolution in dry $CDCl_3$ showed the formation of one symmetrical pyrazabole species with two resonances in 2:1 relative integral (**Figure 5.4a**), whilst the ^{11}B NMR spectrum showed a single singlet resonance at -6.9 ppm (**Figure 5.4b**). This characterisation data, alongside the observation of H_2 evolution, led to the tentative initial assignment of this product as the desired species **5.4**.

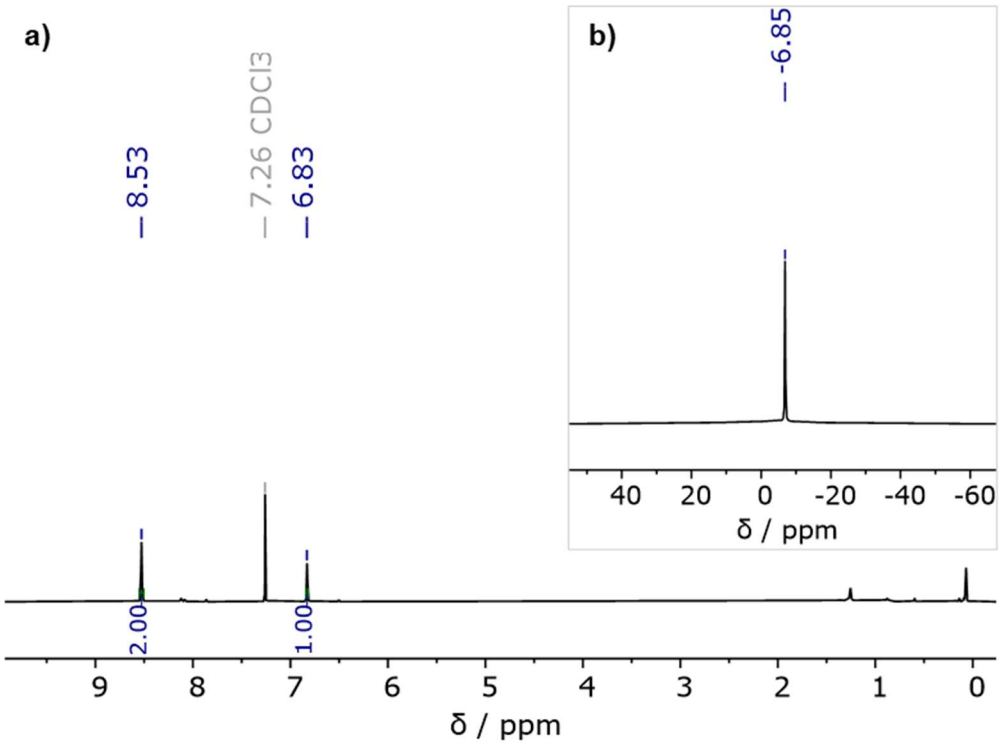

Figure 5.4: **a)** ^{1}H NMR and **b)** ^{11}B NMR spectra of the precipitate isolated from the reaction of *di*-bromo pyrazabole and $HNTf_2$, initially assigned as *di*-bromo *di*-NTf_2 pyrazabole. *(Solvent = $CDCl_3$, NMR temperature = 300 K).*

The poor solubility of "**5.4**" was not unexpected, considering that the solubility of *di*-NTf_2 (*di*-H) pyrazabole is also extremely poor. It should be noted that when a sample was taken directly from the reaction after 18 hours at 100 °C and analysed by NMR spectroscopy, the same weak resonances for "**5.4**" were observed as the only pyrazabole species in solution.

Reactivity with *N*-Methyl Indole

Fully characterising "**5.4**" was challenging due to its poor solubility in suitable low reactivity solvents. Whilst attempts were made to recrystallise the precipitate to confirm its identity, the reactivity of *in situ* generated "**5.4**" with *N*-methyl indole was studied concurrently. To do this, experiments were conducted in J. Young's NMR tubes, in which *di*-bromo pyrazabole **5.2** and 2 equiv. $HNTf_2$ were heated to 100 °C for 18 hours. The *in situ* $^{1}H/^{11}B$ NMR spectra showed the formation of "**5.4**", with a white solid precipitating as before. Subsequently, 2 equiv. DBP and 1 equiv. *N*-methyl indole were added, with the goal of achieving the C3/C4-diborylation of *N*-methyl indole (**Scheme 5.8**).

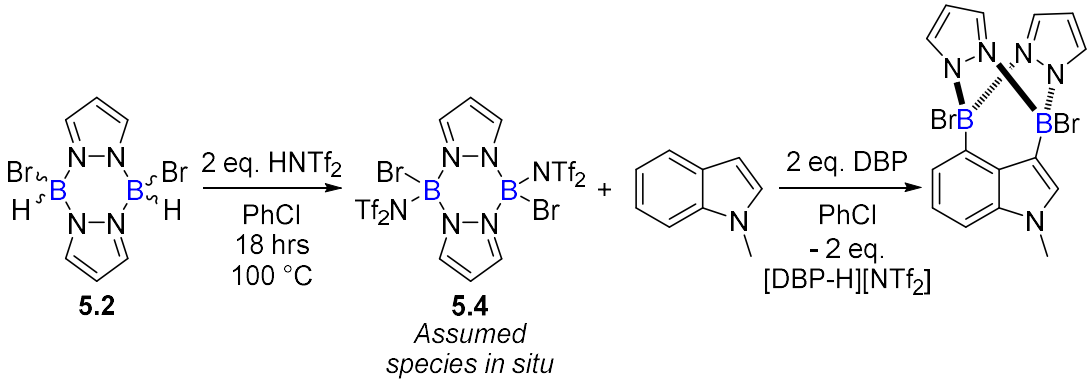

Scheme 5.8: Proposed reactivity between "*di*-bromo *di*-NTf_2 pyrazabole" (generated *in situ*) and *N*-methyl indole, resulting in C3/C4-diborylation.

In situ NMR spectra recorded approximately 15 minutes after the addition of *N*-methyl indole (at room temperature) showed that all of the DBP present in solution was now protonated, an indicator that C-H borylation may have occurred (**Figure 5.5a**). In addition, several new '*N*-methyl' resonances (3.61-3.55 ppm, **Figure 5.5b**) were observed alongside some unreacted *N*-methyl indole (3.32 ppm), suggesting the partial conversion of the substrate. No aliphatic C2/C3 resonances were observed in the $^{1}H/^{13}C$ NMR spectra, implying that these new '*N*-methyl' species were indole derivatives, rather than indoline derivatives. Furthermore, the ^{11}B NMR spectrum showed the formation of a new broad peak (1.72 to -3.69 ppm), made up of overlapping resonances (**Figure 5.5c**). This, alongside the observation of several new methyl resonances in the ^{1}H NMR spectrum, suggests an unselective reaction had occurred, partially forming several borylated indole species. Some leftover "**5.4**" (-6.8 ppm) was also observed in the ^{11}B NMR spectrum. The minor peak at -7.3 ppm was possibly the unreacted [B-Br(NTf_2)] unit of a pyrazabole species that has only reacted with *N*-methyl indole once.

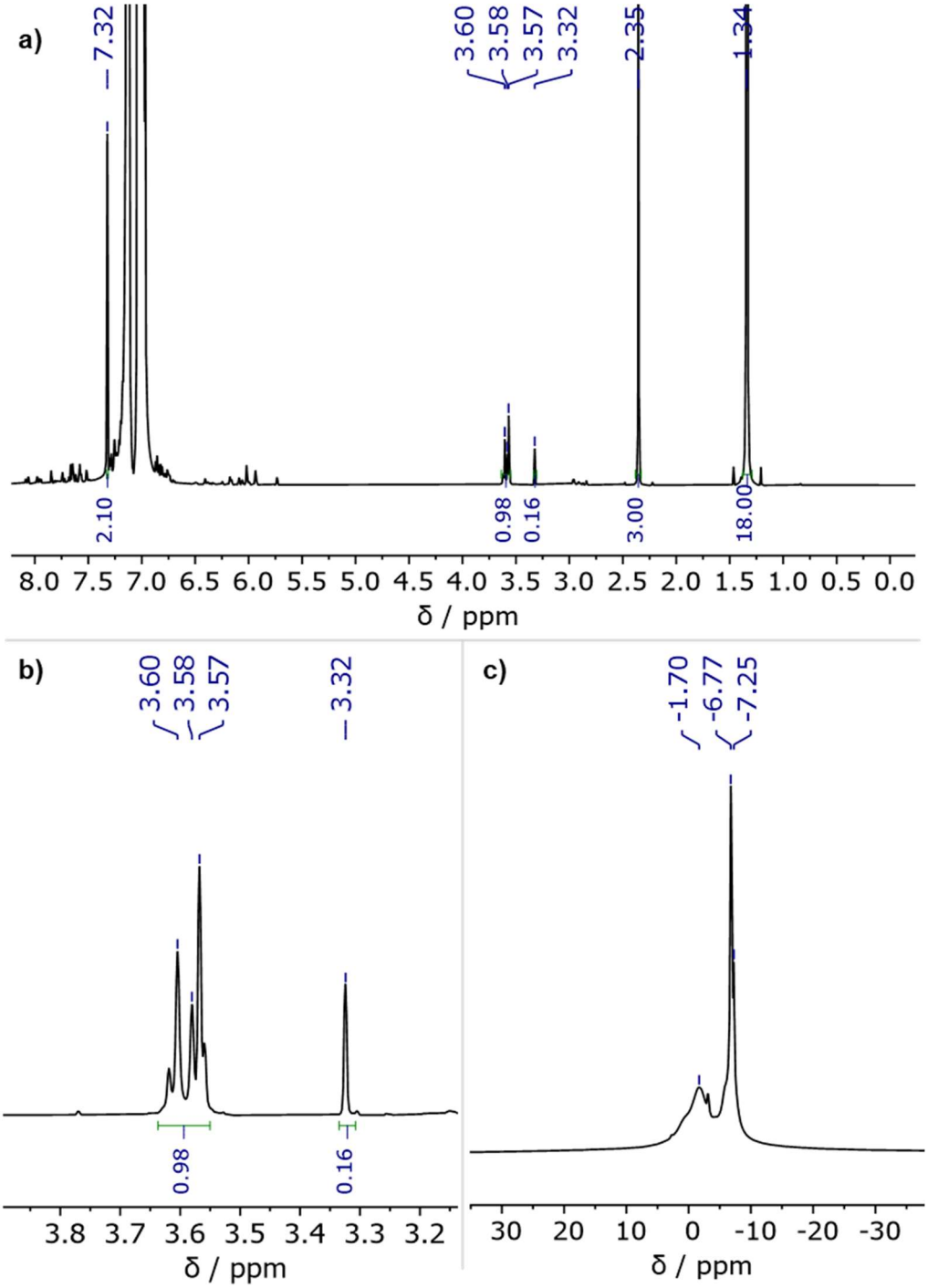

Figure 5.5: **a)** ^{1}H NMR spectrum, **b)** 'Methyl' region of the ^{1}H NMR spectrum, and **c)** ^{11}B NMR spectrum, of the reaction of *in situ* generated "*di*-bromo *di*-NTf_2 pyrazabole", DBP and *N*-methyl indole, after 15 minutes at room temperature. *Note: The ^{1}H resonances at 1.34, 2.35, 7.32 ppm correspond to [DBP-H][NTf_2], with the N-H resonating at 10.77 ppm. (Solvent = C_6H_5Cl, NMR temperature = 300 K).*

The reaction was left at room temperature for 18 hours, and heated to 100 °C for 18 hours in attempts to react the leftover *N*-methyl indole. No further reactivity was observed by *in situ* NMR spectroscopy, however. This was potentially as DBP was fully protonated which could prevent further C-H borylation.

To determine whether C-H borylation had occurred, pinacol, K_2CO_3, DCM and water were added, and the reaction was heated to 50 °C for 18 hours. This would convert any C-B(Pyrz) bonds into C-Bpin, enabling identification. The reaction was not worked up due to the small scale and potential for protodeboronation. The ^{11}B NMR spectrum of a sample taken directly from the reaction mixture showed a mixture of boron species (**Figure 5.6**). Of note, however, is the broad resonance at 30 ppm, which appears to be formed of two overlapping singlets at 30.3 ppm and 28.6 ppm. These chemical shifts are characteristic of 'ArBpin' species, and match the reported ^{11}B NMR resonances for 3-Bpin *N*-methyl indole and 2-Bpin *N*-methyl indole, respectively.[24]

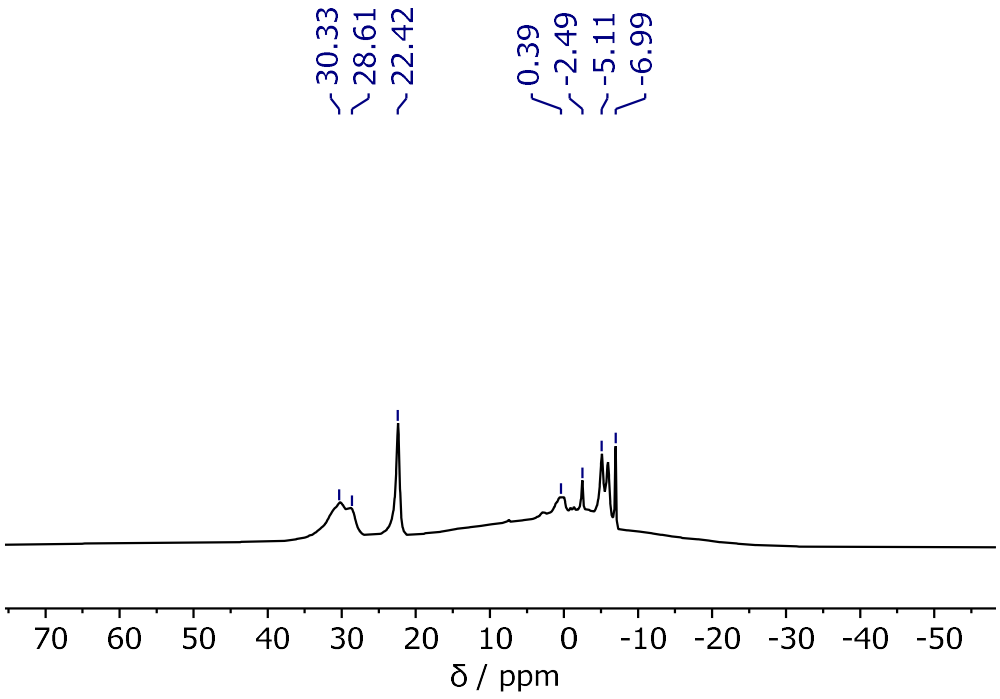

Figure 5.6: ^{11}B NMR spectrum following the 'pinacol protection' of the reaction between *in situ* generated "*di*-bromo *di*-NTf_2 pyrazabole", DBP and *N*-methyl indole. *(Solvent = CH_2Cl_2, NMR temperature = 300 K).*

The observation of these characteristic 'indolyl-Bpin' resonances provides some evidence that C2/C3-diborylation may have occurred, though not cleanly or in high yields (**Scheme 5.9**). Based on this result, and given that *mono*-boron electrophiles only give C3- and C5-H borylation of *N*-methyl indole,[25] it became important to fully characterise the reactive species formed in the initial activation of *di*-bromo pyrazabole **5.2** (assumed to be **5.4**), before pursuing this further.

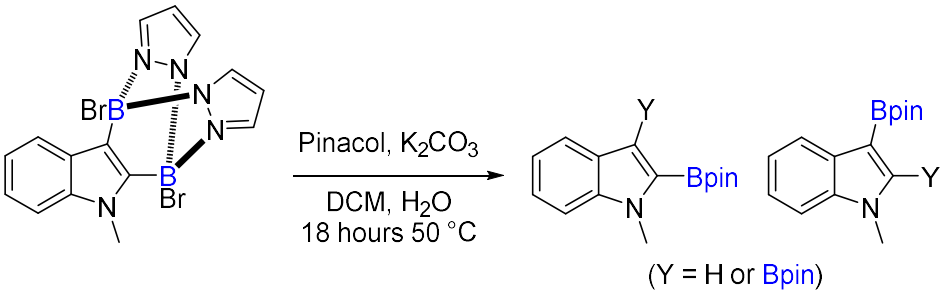

Scheme 5.9: The observation of 2-Bpin *N*-methyl indole and 3-Bpin *N*-methyl indole indicates that C2/C3-diborylation of *N*-methyl indole may have occurred.

Characterising The Active Electrophile(s)

Following the "activation" of *di*-bromo pyrazabole **5.2** with 2 equiv. $HNTf_2$ at 100 °C, the precipitate was isolated from the reaction and partially dissolved in chlorobenzene at 80 °C. The saturated solution was filtered whilst hot and then allowed to cool down slowly. Single crystals were isolated and analysed by X-ray diffraction, however the unit cell parameters matched the reported data for *di*-NTf_2 (*di*-H) pyrazabole (**5.5**).[3] This would be consistent with the *di*-bromo pyrazabole **5.2** reacting with $HNTf_2$ at the B-Br bonds, forming *di*-NTf_2 pyrazabole **5.5** (with HBr as the by-product), rather than reacting at the B-H bonds to form the desired *di*-bromo *di*-NTf_2 pyrazabole **5.4** (**Scheme 5.10**).

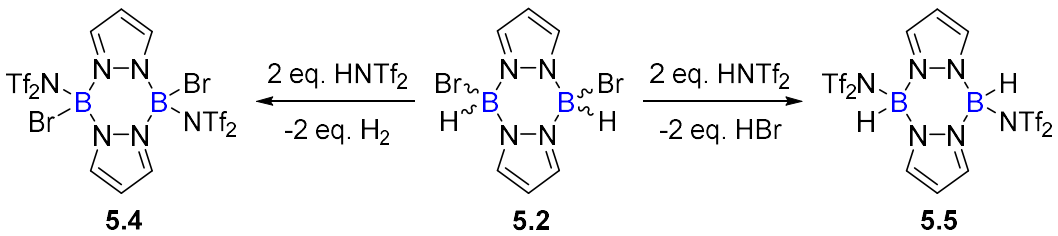

Scheme 5.10: *Di*-bromo pyrazabole could react with $HNTf_2$ at either the B-H bonds, forming *di*-bromo *di*-NTf_2 pyrazabole and H_2, or the B-Br bonds, forming *di*-NTf_2 pyrazabole and HBr.

This outcome, however, does not explain the observed H_2 formation, or the pyrazabole species seen by NMR spectroscopy (see **Figure 5.4**), as *di*-NTf_2 pyrazabole **5.5** is insoluble in $CDCl_3$ at room temperature. This therefore suggests that a second pyrazabole species is also formed in addition to **5.5**. This was confirmed by suspending the precipitate isolated from the reaction of **5.2** and 2 equiv. $HNTf_2$ in dry d_3-MeCN, and stirring for 2 hours at room temperature until the precipitate had fully dissolved. The ^{11}B NMR spectrum now showed two resonances, corresponding to two pyrazabole species (**Figure 5.7**).

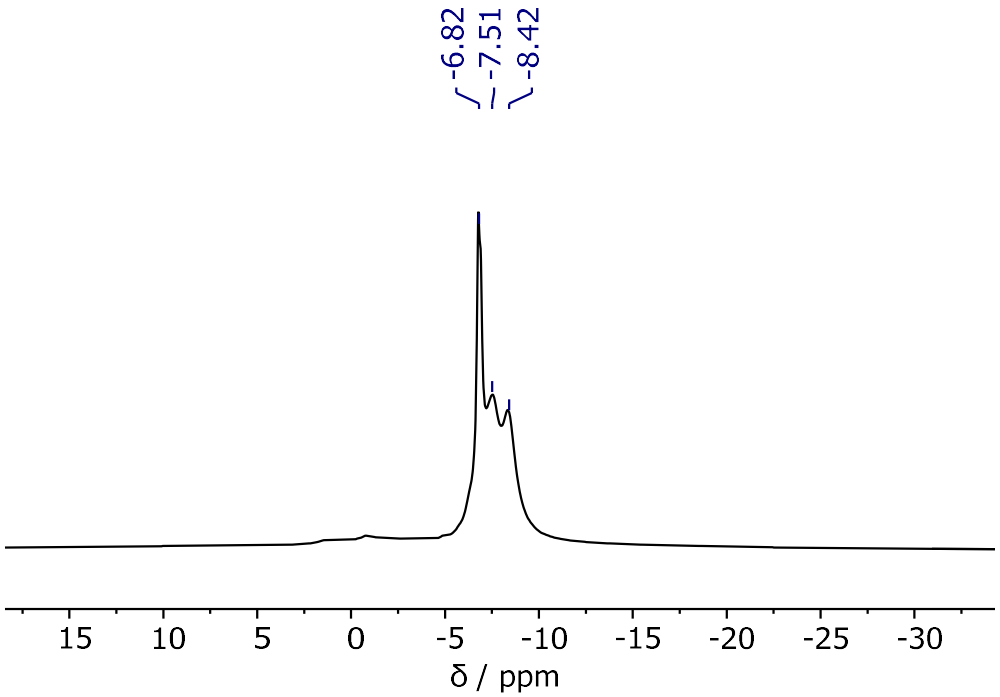

Figure 5.7: ^{11}B NMR spectrum of the precipitate isolated from the reaction of *di*-bromo pyrazabole and 2 equiv. $HNTf_2$ (18 hours 100 °C).
(Solvent = CD_3CN, NMR temperature = 300 K).

One species, appearing as a doublet at -7.9 ppm, was identified as [*di*-MeCN pyrazabole][NTf_2]$_2$ (**5.5[MeCN]**) a dicationic pyrazabole species previously formed when characterising *di*-NTf_2 pyrazabole **5.5** in d_3-MeCN (see **Chapter 3**).[3] This therefore confirms the formation of **5.5** in the activation reaction. The second pyrazabole species corresponded to a singlet at -6.8 ppm. This was hypothesised to be *tetra*-bromo pyrazabole (**5.6**), with this assignment confirmed by the independent synthesis of *tetra*-bromo pyrazabole (*vide infra*).[15] The NMR data for the synthesised *tetra*-bromo pyrazabole **5.6** (which is also

poorly soluble in $CDCl_3$) matched the species observed in the spectra of the isolated precipitate (**Figure 5.4**). Finally, it was shown that only 1 equiv. of $HNTf_2$ (out of 2 equiv.) reacts with *di*-bromo pyrazabole **5.2**. This was done by adding 2 equiv. of DBP at the end of the "activation" reaction (18 hours, 100 °C). The ^1H NMR spectrum showed the immediate formation of 1 equiv. of [DBP-H][NTf_2].

Two possible mechanistic pathways to the formation of *tetra*-bromo pyrazabole **5.6** and *di*-NTf_2 pyrazabole **5.5** were proposed. The first possible pathway proceeds via the substitution of the B-H bonds in *di*-bromo pyrazabole **5.2** by $HNTf_2$, forming *di*-bromo *di*-NTf_2 pyrazabole **5.4** and evolving H_2 (**Scheme 5.11**). Following this, it is proposed that *di*-bromo *di*-NTf_2 pyrazabole **5.4** reacts rapidly with unreacted *di*-bromo pyrazabole **5.2** via a substituent exchange (similar to the observed exchange between *di*-NTf_2 pyrazabole and pyrazabole to form *mono*-NTf_2 pyrazabole *in situ*, discussed in **Chapter 3**).[3] This forms *di*-NTf_2 pyrazabole **5.5** and *tetra*-bromo pyrazabole **5.6**, where the insolubility of **5.5** provides a driving force to the substituent exchange. This therefore prevents the build-up of **5.4** in solution and would explain why approximately 1 equiv. of $HNTf_2$ is left unreacted, as neither **5.5** or **5.6** reacts with further $HNTf_2$.

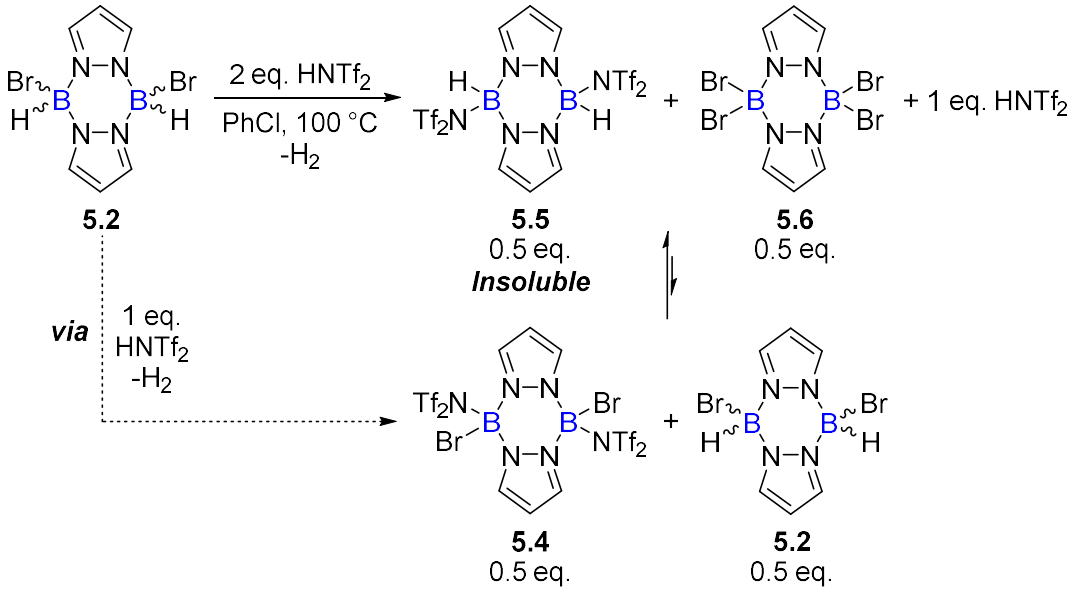

Scheme 5.11: Proposed mechanism for the formation of *di*-NTf_2 pyrazabole and *tetra*-bromo pyrazabole in the "activation" of *di*-bromo pyrazabole with $HNTf_2$.

Alternatively, a second pathway was also proposed, where *di*-bromo pyrazabole **5.2** react with $HNTf_2$ at the B-Br bonds, forming *di*-NTf_2 pyrazabole **5.5** and HBr. The formation of *tetra*-bromo pyrazabole **5.6** could then arise through the reaction of HBr with leftover **5.2**, evolving H_2 as the by-product. Again, this would leave approximately 1 equiv. of $HNTf_2$ unreacted. The second pathway is believed to be more unlikely than the first pathway, as $HNTf_2$ should react with the B-H bond over B-Br, and the evolution of H_2 should provide a greater driving force. However, the overall outcome of the two processes is the same.

Finally, attempts were made to prevent overreaction to *tetra*-bromo pyrazabole **5.6** and *di*-NTf_2 pyrazabole **5.5** by stopping the activation reaction earlier. However, when the reaction was monitored by *in situ* ^{1}H NMR spectroscopy, partial formation of **5.6** was observed after only 30 minutes at room temperature, with **5.2** still present and no additional ^{11}B resonances that could correspond to **5.4** observed (**Figure 5.8**).

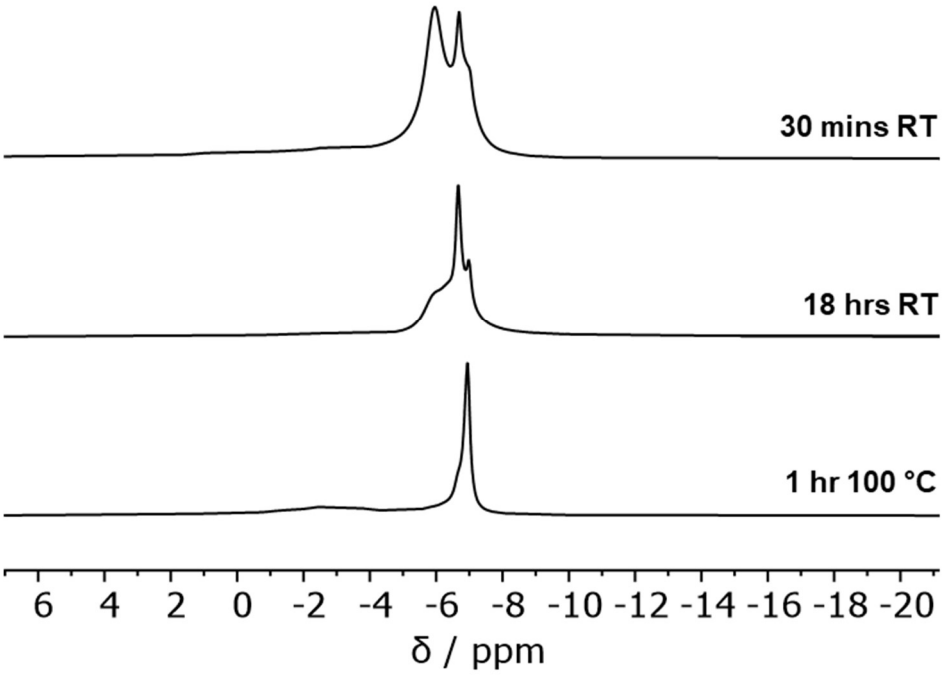

Figure 5.8: Stacked $^{11}B\{^{1}H\}$ NMR spectra showing the formation of *tetra*-bromo pyrazabole (δ_{11B} = -6.7 ppm) following addition of 2 equiv. $HNTf_2$ to *di*-bromo pyrazabole (δ_{11B} = -5.9, -6.9 ppm). *(Solvent = C_6H_5Cl, NMR temperature = 300 K).*

This suggests that the rate of substituent exchange between *di*-bromo *di*-NTf_2 pyrazabole **5.4**, and *di*-bromo pyrazabole **5.2** is faster than the rate of formation of *di*-bromo *di*-NTf_2 pyrazabole **5.4**. Note, the ^{11}B NMR spectra reveal that one of the isomers of **5.2** reacts more rapidly, but both are ultimately fully consumed.

Explaining Observed Reactivity

Knowing that the pyrazabole species formed from the reaction of *di*-bromo pyrazabole **5.2** and 2 equiv. $HNTf_2$ was a mixture of *tetra*-bromo pyrazabole **5.6** and *di*-NTf_2 pyrazabole **5.5**, with approximately 1 equiv. $HNTf_2$ leftover, further studies were necessary to rationalise the evidence of C2/C3-diborylation in the reactions with DBP and *N*-methyl indole.

In these reactions, two equiv. of DBP was added following the "activation" of *di*-bromo pyrazabole **5.2**. This will have quickly reacted with the leftover $HNTf_2$, forming 1 equiv. [DBP-H][NTf_2] and leaving 1 equiv. of DBP unreacted. *N*-methyl indole was then added to the reaction, with the *in situ* NMR spectra recorded approximately 15 minutes later. At this point, 2 equiv. of [DBP-H][NTf_2] was observed, indicating that the 1 equiv. of DBP leftover was protonated via the C-H borylation of *N*-methyl indole. However, it is not clear which pyrazabole species had enabled C-H borylation.

Control reactions were performed using either *tetra*-bromo pyrazabole **5.6** or *di*-NTf_2 pyrazabole **5.5**, to see if either of these pyrazabole species were individually responsible for the observed reactivity with *N*-methyl indole. As expected, *tetra*-bromo pyrazabole **5.6** showed no reactivity with *N*-methyl indole, even with extended heating at 100 °C. In contrast, the reaction with *di*-NTf_2 pyrazabole **5.5** resulted in the complete consumption of *N*-methyl indole, and protonation of 2 equiv. DBP after 18 hours at room temperature. A complex mixture of indole and indoline products were observed in the *in situ* ^{1}H / ^{13}C NMR spectra (**Figure 5.9a**). One of the indoline products was identified as the C3/N-borylated indoline derivative formed from the hydroboration of *N*-methyl indole, matching the species synthesised by Dr Jürgen Pahl in **Chapter 3**.[3] Regardless of the exact composition, the outcome of the reaction of *di*-NTf_2 pyrazabole **5.5** with *N*-methyl indole (**Figure 5.9a**) is distinctively different to the outcome of the

reaction following the "activation" of *di*-bromo pyrazabole **5.2** with $HNTf_2$ (**Figure 5.9b**), where no evidence of reduction/indoline formation was observed in the $^{1}H/^{13}C$ NMR spectra. This indicates that *di*-NTf_2 pyrazabole **5.5** is not the reactive pyrazabole species effecting indole C-H borylation in these reactions.

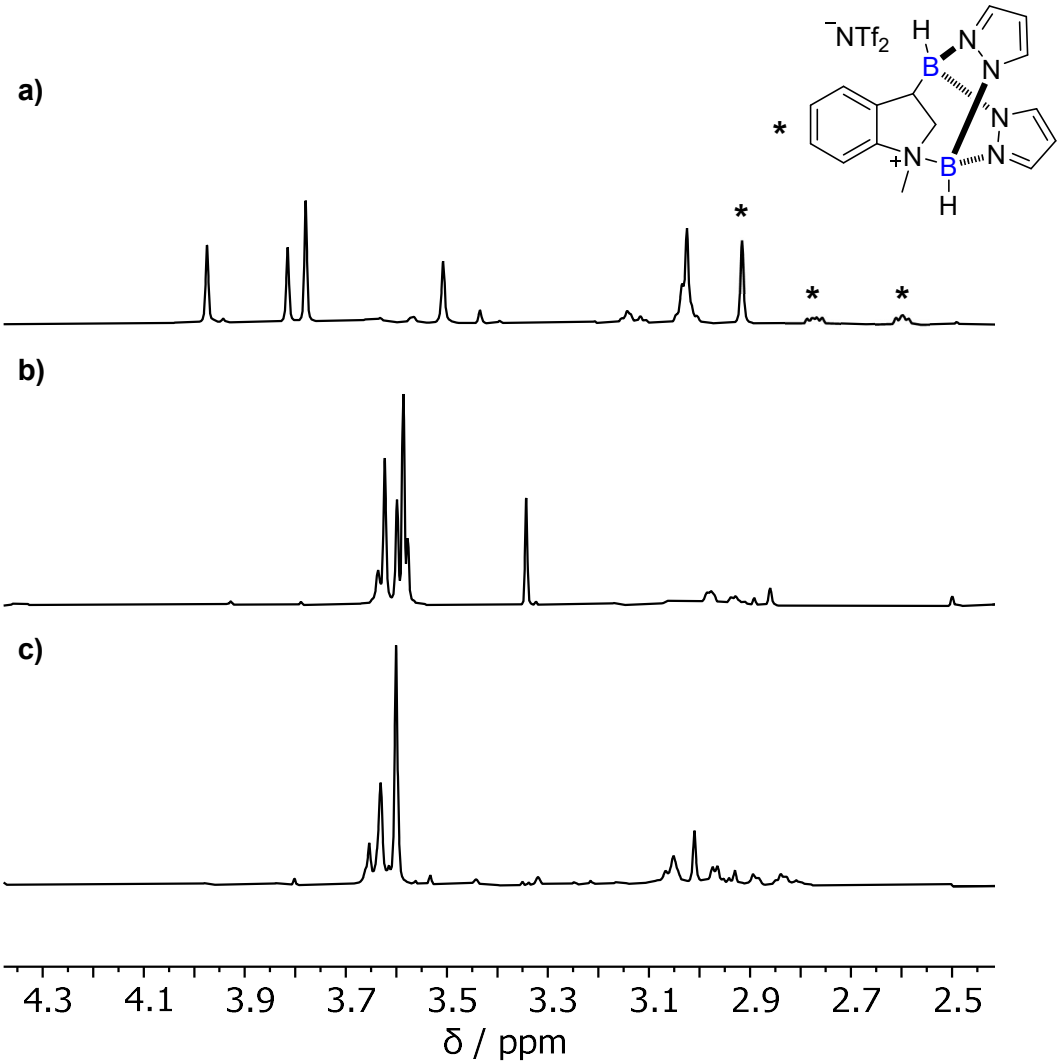

Figure 5.9: *In situ* ^{1}H NMR spectra recorded following the reaction of 1 equiv. *N*-methyl indole and 2 equiv. DBP with either: **a)** 1 equiv. *di*-NTf_2 pyrazabole **5.5**, **b)** crude products following the "activation" of *di*-bromo pyrazabole **5.2** with 2 equiv. $HNTf_2$, 18 hrs 100 °C, and **c)** 0.5 equiv. *tetra*-bromo pyrazabole **5.6**, 0.5 equiv. *di*-NTf_2 pyrazabole **5.5** and 1 equiv. $HNTf_2$. All spectra recorded after 18 hours at RT. *Note: Resonance at 3.34 ppm is due to unreacted N-methyl indole. (Solvent = C_6H_5Cl, NMR Temperature = 300 K).*

To rationalise this, it was hypothesised that reversible substituent exchange between *tetra*-bromo pyrazabole **5.6** and *di*-NTf_2 pyrazabole **5.5** may occur to some extent to form other pyrazabole species *in situ.* These could go on to react

with *N*-methyl indole, forming the indole products observed in **Figure 5.9b**. To probe this theory, 2 equiv. DBP and 1 equiv. *N*-methyl indole were added to a mixture of 0.5 equiv. *tetra*-bromo pyrazabole **5.6**, 0.5 equiv. *di*-NTf_2 pyrazabole **5.5** and 1 equiv. $HNTf_2$ (replicating the mixture formed from the "activation" of *di*-bromo pyrazabole **5.2**). After 18 hours at room temperature, the ^1H NMR spectrum (**Figure 5.9c**) had some of the same '*N*-methyl' resonances observed in **Figure 5.9b**. This indicates that products from the reaction of *tetra*-bromo pyrazabole **5.6** and *di*-NTf_2 pyrazabole **5.5** causes the reactivity with *N*-methyl indole to change, supporting the theory that substituent exchange is occurring within the reaction.

If this substituent exchange enables the partial formation of *di*-bromo *di*-NTf_2 pyrazabole **5.4** *in situ*, this could react and enable the C2/C3-diborylation of *N*-methyl indole, which would explain the observation of 2-Bpin *N*-methyl indole and 3-Bpin *N*-methyl indole species following pinacol addition (**Scheme 5.12**).

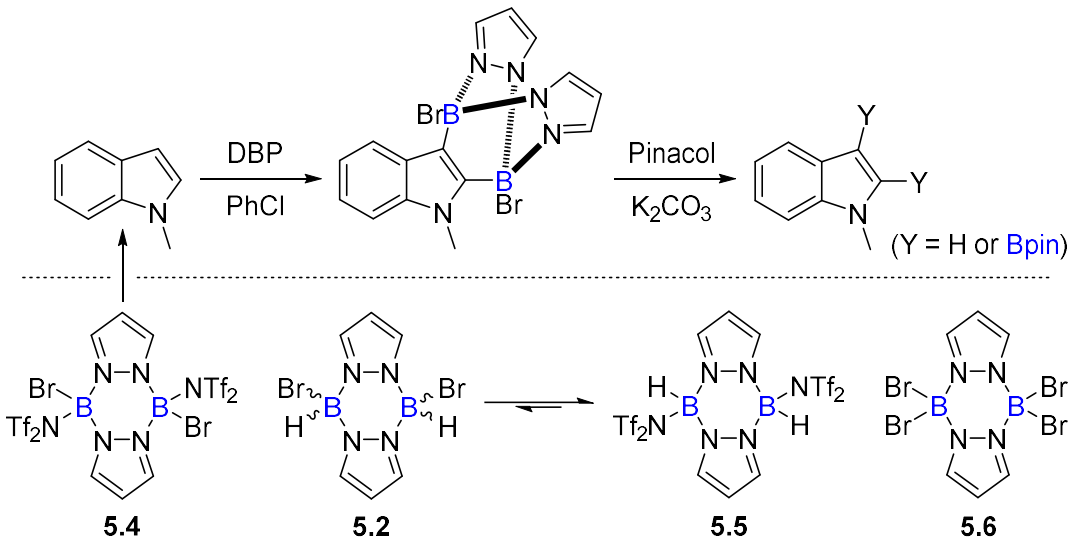

Scheme 5.12: The partial formation of *di*-bromo *di*-NTf_2 pyrazabole via the proposed *in situ* substituent exchange between *tetra*-bromo pyrazabole and *di*-NTf_2 pyrazabole, could enable some C2/C3-borylation of *N*-methyl indole.

However, the amount of both Bpin species formed was low, and *N*-methyl indole was not fully consumed, showing that the amount of the reactive pyrazabole species present in solution is not substantial. Therefore, though the "activation" of *di*-bromo pyrazabole **5.2** (or the addition of 1:1 *tetra*-bromo pyrazabole **5.6**

and *di*-NTf_2 pyrazabole **5.5**) may form minor amounts of *di*-bromo *di*-NTf_2 pyrazabole **5.4** *in situ*, this is not a suitable way to produce the electrophile for use as a stoichiometric directing group / borylating reagent, as the equilibrium (**Scheme 5.12**, bottom) does not appear to favour the formation of **5.4** (based on the above reactivity studies).

Comparing Reactivity to that of *Di*-Chloro Pyrazabole

In an attempt to form the chloro-analogue of the desired halo-substituted pyrazabole electrophile, *di*-chloro *di*-NTf_2 pyrazabole **5.7**, the activation of *di*-chloro pyrazabole **5.3** with 2 equiv. $HNTf_2$ was also attempted (**Scheme 5.13**). It was hoped that the more coordinating chloride substituents (compared to bromide) would slow the rate of substituent exchange and increase the amount of *di*-chloro *di*-NTf_2 pyrazabole **5.7** formed. However, this was not the case.

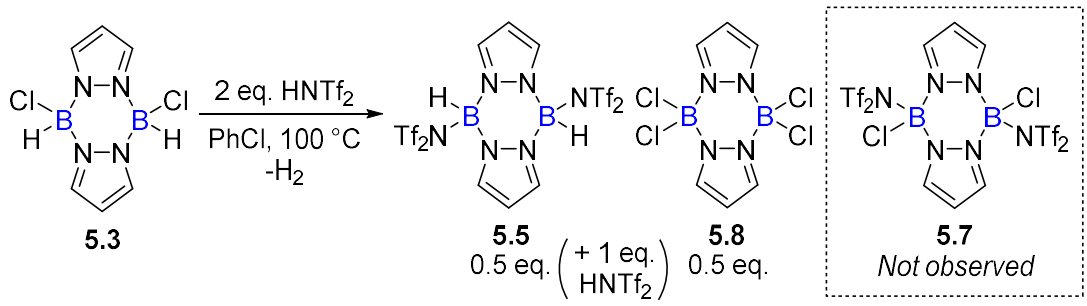

Scheme 5.13: Attempted activation of *di*-chloro pyrazabole with $HNTf_2$, instead forming *di*-NTf_2 pyrazabole and *tetra*-chloro pyrazabole, with no ^{11}B resonances that could correspond to *di*-chloro *di*-NTf_2 pyrazabole observed.

The near-complete conversion of *di*-chloro pyrazabole **5.3** was observed in the ^{11}B NMR spectrum after 18 hours at room temperature, with a singlet resonance (δ_{11B} = 2.1 ppm, C_6H_5Cl) observed as the only product (in solution), matching previously reported *tetra*-chloro pyrazabole **5.8**.[14] The formation of *di*-NTf_2 pyrazabole **5.5** was again shown by dissolving the crude mixture in d_3-MeCN, forming [*di*-MeCN pyrazabole][NTf_2]$_2$ (**5.5[MeCN]**). No other ^{11}B resonances were observed. Addition of 2 equiv. DBP to the crude mixture formed 1 equiv. [DBP-H][NTf_2], demonstrating that only 1 equiv. of $HNTf_2$ had been consumed.

The reaction of *di*-chloro pyrazabole **5.3** with $HNTf_2$ is significantly faster than the equivalent reaction of *di*-bromo pyrazabole **5.2**, which required heating to

100 °C. This is presumably because the more coordinating chloride substituents increase the hydridity of the B-H units, and may also help to stabilise the dehydrocoupled product, *di*-chloro *di*-NTf_2 pyrazabole **5.7**, to a greater extent than bromide substituents. This therefore lowers the barrier to the formation of *di*-chloro *di*-NTf_2 pyrazabole **5.7**. However, substituent exchange between **5.7** and *di*-chloro pyrazabole **5.3** still proceeds rapidly, suggesting that the driving force of the formation of insoluble *di*-NTf_2 pyrazabole **5.5** dominates, hence no **5.7** is observed in solution.

Consequently, the activation of *di*-halo pyrazaboles with $HNTf_2$ as a method to form *di*-halo *di*-NTf_2 pyrazabole electrophiles (**Route 1**) appears to be unfeasible as the propensity of the reaction to form *di*-NTf_2 pyrazabole **5.5** is too great to overcome (given the limited solvent options available). Therefore, an activation mode that avoids the use of B-H containing pyrazaboles is required. Thus, at this point focus shifted to exploring '**Route 2**', with a method to form the desired halo-substituted pyrazabole electrophiles via the activation of *tetra*-halo (Cl or Br) pyrazaboles targeted.

5.3.3 Synthesis of *Tetra*-Halo Pyrazaboles

As previously reported, *tetra*-bromo pyrazabole **5.6** was readily synthesised via the bromination of pyrazabole with excess BBr_3 (**Scheme 5.14**).[15] It was found that refluxing the reaction for two hours improved the outcome, and **5.6** was recrystallised from THF / hexane and isolated in a 48% yield. *Tetra*-bromo pyrazabole **5.6** is poorly soluble in many organic solvents, but weak NMR spectroscopy data could be obtained from a sample of **5.6** in $CDCl_3$. The ^1H NMR spectrum showed the expected two resonances at relative 2:1 integral, indicating a symmetrical pyrazabole species, whilst the ^{11}B NMR spectrum showed a singlet resonance at -6.9 ppm.

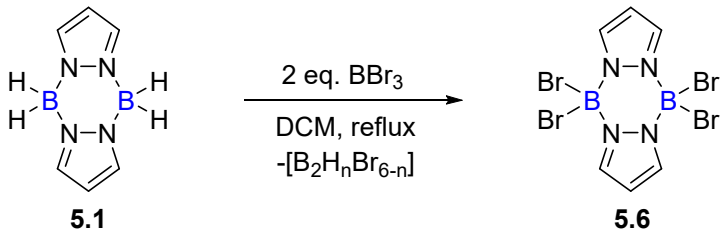

Scheme 5.14: Bromination of pyrazabole to form *tetra*-bromo pyrazabole.

The previously reported synthesis of *tetra*-chloro pyrazabole **5.8** was achieved via the chlorination of pyrazabole using excess chlorine gas.[14] Since this process was undesirable, other synthetic routes to **5.8** were explored. The reaction of pyrazabole **5.1** with excess BCl_3 formed very little *tetra*-chloro pyrazabole **5.8**, even at higher temperatures (60 °C), with *di*-chloro pyrazabole **5.3** formed as the major product with significant unreacted BCl_3 leftover. A subsequent reaction saw *di*-chloro pyrazabole **5.3** heated with HCl (in diethyl ether). The activation of B-H bonds in NHC-boranes using HCl has been previously reported,[26] but very little **5.8** was formed under these conditions in this case.

Attempts to form *tetra*-chloro pyrazabole **5.8** directly via the reaction of pyrazole and BCl_3 were unsuccessful, with no **5.8** observed. Lithiation of pyrazole using *n*-BuLi, followed by addition of BCl_3, was also unsuccessful. This was attributed to the poor solubility of the lithiated pyrazole intermediate, preventing reactivity with BCl_3. This issue was circumvented by addition of chlorotrimethylsilane

(TMSCl) to the lithiated pyrazole intermediate, which formed the more soluble pyrazole-TMS *in situ*. This species reacted with BCl_3 upon heating, forming *tetra*-chloro pyrazabole **5.8** which precipitated from the reaction and was isolated in an unoptimized 33% yield without any further purification (**Scheme 5.15**).

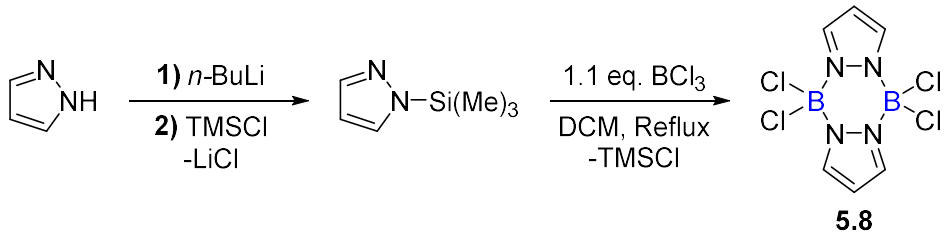

Scheme 5.15: Synthesis of *tetra*-chloro pyrazabole via the lithiation and silylation of pyrazole, followed by addition of BCl_3.

The ^1H NMR spectrum of **5.8** in $CDCl_3$ showed the two expected pyrazole resonances in 2:1 relative integral, and the ^{11}B NMR spectrum showed a singlet at 2.3 ppm, matching the reported data for the species synthesised using Cl_2.[14] Further optimisation is necessary to improve this synthetic route to make it a useful method to form large amounts of **5.8**.

5.3.4 Reactivity of *Tetra*-Halo Pyrazaboles with $TMSNTf_2$: 'Route 2'

With *tetra*-bromo pyrazabole **5.6** readily synthesised via the previously reported method,[15] this compound was successfully isolated in good yield before *tetra*-chloro pyrazabole **5.8** was, hence its activation and reactivity were studied first.

Initial Studies: Activation of *Tetra*-Bromo Pyrazabole

To form the desired *di*-electrophile, *di*-bromo *di*-NTf_2 pyrazabole **5.4**, from *tetra*-bromo pyrazabole **5.6**, substitution of two B-Br bonds is required. As expected, *tetra*-bromo pyrazabole **5.6** showed no reactivity with 2 equiv. $HNTf_2$, even upon extending heating at 100 °C. The formation of HBr as by-product, rather than H_2, reduces the driving force to the substitution. Attempts to activate **5.6** with 2 equiv. $LiNTf_2$ were also unsuccessful with no reactivity observed.

The use of Me_3Si-NTf_2 ($TMSNTf_2$) as an activator of *tetra*-bromo pyrazabole **5.6** was explored, where the formation of TMSBr as by-product was hoped to provide a sufficient driving force (**Scheme 5.16**). $TMSNTf_2$ can be readily prepared *in situ* via the protodesilylation of PhTMS with $HNTf_2$ (with benzene as a by-product), prior to the addition of *tetra*-bromo pyrazabole **5.6**.[27] Following activation, TMSBr and benzene could be removed prior to the addition of *N*-methyl indole by concentration of the reaction mixture *in vacuo*.

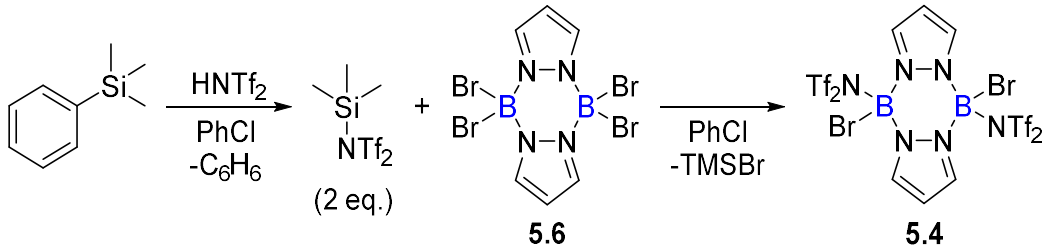

Scheme 5.16: Proposed reaction between *tetra*-bromo pyrazabole and *in situ* generated $TMSNTf_2$, to form *di*-bromo *di*-NTf_2 pyrazabole and TMSBr.

Monitoring the preparation of $TMSNTf_2$ in PhCl by *in situ* NMR spectroscopy showed that PhTMS (δ_{29Si} = -4.7 ppm) was fully consumed after 2 hours at room temperature, with the formation of $TMSNTf_2$ (δ_{29Si} = 54.5 ppm) observed. The minor formation of a second 'TMS' species was also observed (δ_{29Si} = 6.7 ppm). This is believed to be $(TMS)_2O$, or similar, based on previously reported ^{29}Si

resonances.[28,29] In addition, minor amounts of $HNTf_2$ was observed in the ^1H NMR spectrum. These side-products are presumably formed by a small amount of hydrolysis of $TMSNTf_2$, with the source of the trace water believed to be the solvent/PhTMS. However, this should not hinder reactivity if the minor loss of $TMSNTf_2$ (<5%) is accounted for in the reaction stoichiometry.

Following the *in situ* preparation of 2.2 equiv. $TMSNTf_2$, 1 equiv. *tetra*-bromo pyrazabole **5.6** was added to the reaction. After 1 hour at room temperature **5.6** had fully dissolved. *In situ* NMR spectroscopy of the now homogenous sample showed the full conversion of **5.6**, alongside the formation of TMSBr (δ_{29Si} = 26.6 ppm). However, only partial consumption of $TMSNTf_2$ was observed, suggesting the reactivity with **5.6** was not in the desired 2:1 ratio. No further reactivity was observed after stirring the reaction at room temperature for 18 hours.

The *in situ* ^1H NMR spectrum of the reaction showed the formation of two new pyrazabole species (**Figure 5.10a**). For the major product, three pyrazole resonances were observed in a 1:1:1 ratio, whilst the minor product had two pyrazole resonances in a 2:1 ratio. The $^{13}C\{^1H\}$ NMR spectrum also showed the same pattern: one pyrazabole species had three inequivalent pyrazole resonances, whilst the second had two (confirmed by ^1H-^1H COSY and ^1H-^{13}C HSQC NMR spectroscopy). This demonstrates that the major pyrazabole species is unsymmetrically substituted, so must have different substituents on the two boron atoms. The minor pyrazabole species is symmetrical with the same substituents on the two boron atoms. The ^{11}B NMR spectrum showed two singlet resonances (**Figure 5.10b**). The resonance at -7.6 ppm is close in chemical shift to the starting material, *tetra*-bromo pyrazabole **5.6** (δ_{11B} = -7.0 ppm). However, the $^1H/^{13}C$ NMR spectra confirmed that there was no **5.6** leftover in the reaction.

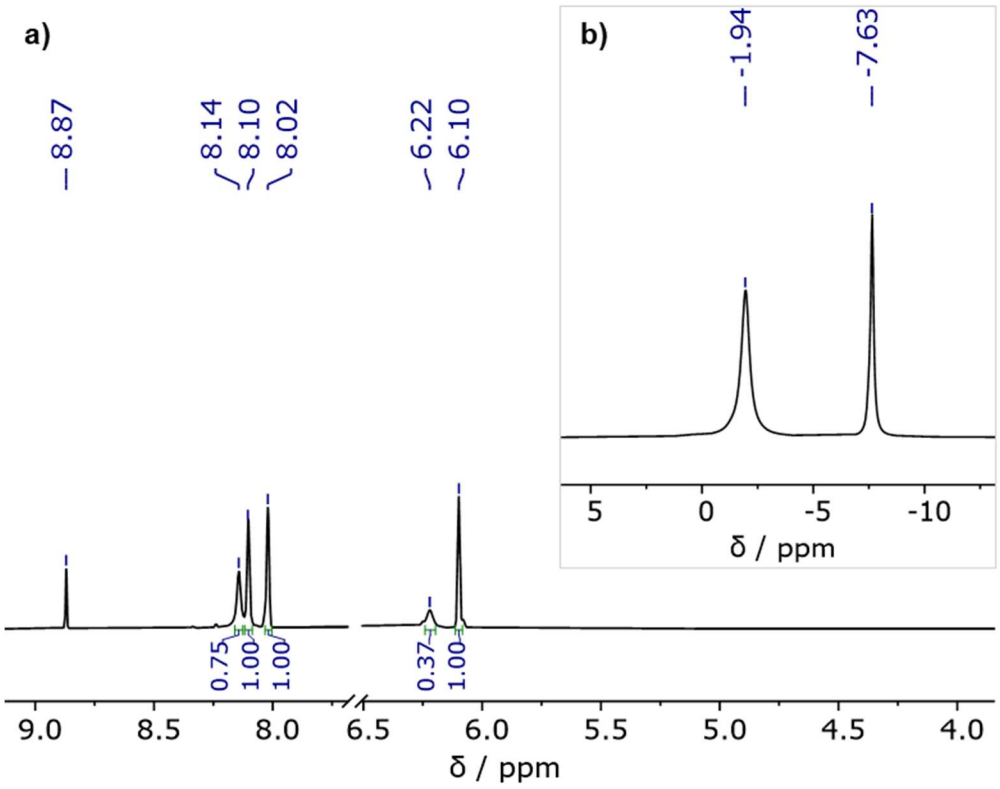

Figure 5.10: *In situ* **a)** ^{1}H NMR and **b)** ^{11}B NMR spectra of the reaction of *tetra*-bromo pyrazabole and 2.2 equiv. $TMSNTf_2$, after 18 hours at RT. *Note: The ^{1}H resonance at 8.87 ppm corresponds to $HNTf_2$, and the ^{1}H solvent resonance has been omitted for clarity. (Solvent = C_6H_5Cl, NMR temperature = 300 K).*

Considering this spectral data, the major pyrazabole species was assigned as the *mono*-electrophile, *tri*-bromo *mono*-NTf_2 pyrazabole (**5.9**, **Scheme 5.17**), formed via the activation of one boron unit in **5.6** with $TMSNTf_2$. This unsymmetrical pyrazabole species would have three inequivalent pyrazole resonances in the ^{1}H/^{13}C NMR spectra, and two resonances in the ^{11}B NMR spectrum, matching **Figure 5.10**. The ^{11}B resonance at -7.6 ppm is believed to be the $[BBr_2]$ unit, whilst the resonance at -1.9 ppm is proposed to be the $[B(Br)NTf_2]$ unit.

The minor species was assigned as the *di*-electrophile, *di*-bromo *di*-NTf_2 pyrazabole (**5.4, Scheme 5.17**), with two pyrazole resonances in the ^{1}H/^{13}C NMR spectra and one resonance in the ^{11}B NMR spectrum. The ^{11}B resonance of the two equivalent $[B(Br)NTf_2]$ units in **5.4** is believed to be overlapping with the $[B(Br)NTf_2]$ resonance of **5.9** at -1.9 ppm, as these ^{11}B nuclei are in very similar chemical environments.

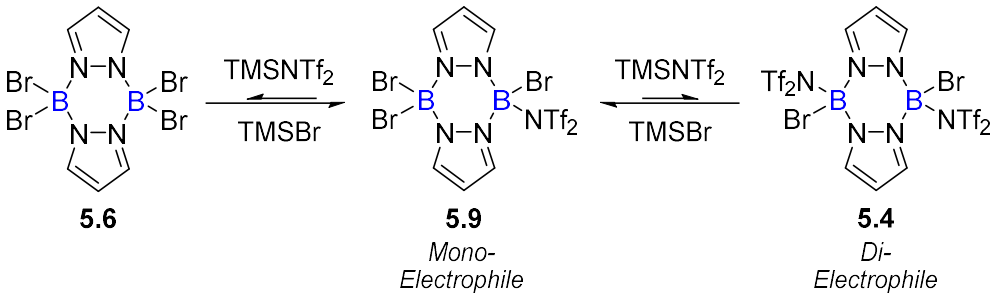

Scheme 5.17: The activation of *tetra*-bromo pyrazabole with $TMSNTf_2$.

This attempted double activation reaction did not go to completion, with a considerable amount of $TMSNTf_2$ unreacted, and only a small amount of the (assumed) *di*-electrophile, **5.4**, was formed. This implies that the reaction is in equilibrium. The reversibility of this reaction was shown by the addition and removal of the by-product, TMSBr, which shifted the equilibrium position and the relative ratios of the pyrazabole species.

Concentration of the sample *in vacuo* removed some TMSBr. The ^1H NMR spectrum of the redissolved reaction mixture showed a small increase in the amount of **5.4** present (**Figure 5.11b**). However, the reaction still had a significant amount of unreacted $TMSNTf_2$ present. Subsequent addition of TMSBr to the reaction favoured the reverse reaction, reducing the amount of *di*-electrophile **5.4** present and increasing the amount of *mono*-electrophile **5.9** (**Figure 5.11c-e**). This also resulted in small amounts of *tetra*-bromo pyrazabole **5.6** being formed (δ_{1H} = 8.03, 6.07 ppm), showing that the first activation step is also reversible. This initial work suggests that the formation of the *di*-electrophile **5.4** is possible, though it appears that the second activation step is endergonic whereas the first activation step to form the *mono*-electrophile **5.9** is exergonic. According to Le Chatelier's principle, increasing the amount of $TMSNTf_2$ and/or decreasing the amount of TMSBr present in the reaction should shift the equilibrium position to favour the formation of the *di*-electrophile **5.4**.

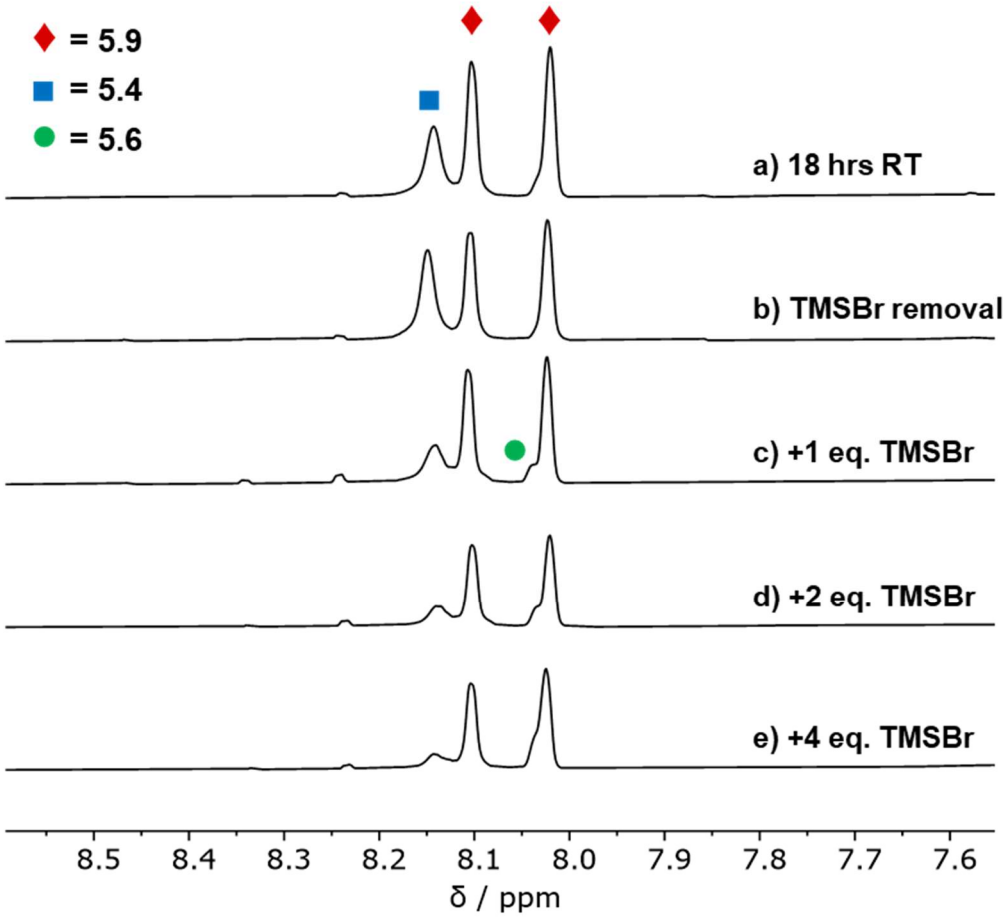

Figure 5.11: Stacked *in situ* ^{1}H NMR spectra of the reaction of *tetra*-bromo pyrazabole with 2 equiv. $TMSNTf_2$. *(Solvent = C_6H_5Cl, NMR temperature = 300 K).*

The observed formation of the unsymmetrical *mono*-electrophile **5.9** is interesting. The *mono*-electrophiles that have been studied previously (*mono*-NTf_2 pyrazabole and *mono*-iodo pyrazabole)[3,4] were both only formed *in situ* and any attempt to isolate/characterise them led to rapid disproportionation to form the two symmetrical pyrazabole counterparts. The observation that this doesn't appear to happen with **5.9** may indicate that the disproportionation of this *mono*-electrophile is disfavoured because of the high energy of one of the symmetrical counterparts (presumably **5.4**, which is expected to be highly electrophilic). Therefore, the clean synthesis and characterisation of both the *mono*- and *di*-electrophiles was attempted, to confirm their assignment and to potentially enable studies into their reactivity with *N*-methyl indole.

Synthesis and Characterisation of the *Mono*-Electrophiles

The single activation of *tetra*-bromo pyrazabole using 1.2 equiv. $TMSNTf_2$ proceeds readily at room temperature, but the reaction does not go to completion and some minor double activation is also observed, giving a mixture of three pyrazabole species (**5.9**, **5.6** and **5.4**) in the *in situ* NMR spectra. The conversion of *tetra*-bromo pyrazabole **5.6** was calculated to be 84% (based on the relative ^1H integrals of the three pyrazabole species present). The ratio of the two products, the *mono*-electrophile (**5.9**) and the *di*-electrophile (**5.4**), was 9.5:1. In an attempt to increase the conversion of **5.6**, 1.5 equiv. $TMSNTf_2$ was used. This increased the conversion of **5.6** to 90%, but the amount of *di*-electrophile formed also increased, with the ratio of the *mono*:*di*-electrophile (**5.9**:**5.4**) now 4.5:1.

To characterise the *mono*-electrophile **5.9** and confirm its assignment, the competitive overreaction to form the *di*-electrophile **5.4** needed to be prevented. The conditions that maximised the conversion of **5.6**, whilst preventing any observable double activation, were found to be 0.9 equiv. $TMSNTf_2$ and 1 equiv. **5.6** (**Scheme 5.18**). This resulted in 76% conversion of **5.6** (based on the relative ^1H integrals of the two pyrazabole species present), with the *mono*-electrophile **5.9** observed as the only new pyrazabole species. Some minor unreacted $TMSNTf_2$ was initially observed, but this (and the TMSBr by-product) were removed by concentration of the reaction *in vacuo*.

Attempts were made to purify **5.9** and remove the unreacted *tetra*-bromo pyrazabole **5.6** by precipitation or extraction, but these were unsuccessful. The *mono*-electrophile **5.9**, was therefore characterised by *in situ* NMR spectroscopy with **5.6** present. The electrophile was characterised in d_2-DCM, as it was shown to be stable in this solvent, with no halogen exchange observed, up to 50 °C.

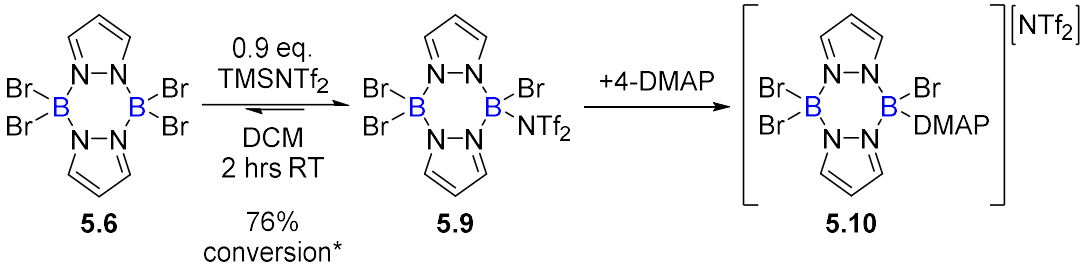

Scheme 5.18: Optimised conditions for the synthesis of *tri*-bromo *mono*-NTf_2 pyrazabole, from *tetra*-bromo pyrazabole. Subsequent addition of 4-DMAP forms the corresponding boronium ion. **(Conversion is calculated from the relative ^1H integrals of the pyrazabole species).*

Attempts to characterise the *mono*-electrophile **5.9** by mass spectrometry were unsuccessful. To enable further support for its formulation, **5.9** was converted into the corresponding boronium cation (**5.10**, **Scheme 5.18**) by addition of 0.9 equiv. of 4-DMAP. ^{11}B NMR spectroscopy showed that the resonance corresponding to the [B(Br)NTf_2] unit of **5.9** (δ_{11B} = -1.1 ppm) was shifted downfield upon addition of 4-DMAP (**Figure 5.12**), demonstrating the substitution of $[NTf_2]^-$ to form a [BBr(DMAP)] unit (δ_{11B} = -0.1 ppm). The (overlapping) resonances corresponding to the [BBr_2] units of **5.9** and of the unreacted *tetra*-bromo pyrazabole **5.6** (δ_{11B} = -6.9 ppm) were unchanged upon addition of 4-DMAP, showing that these boron units are not electrophilic.

The boronium ion **5.10** was more robust and hence was observed by ESI^+ mass spectrometry, supporting the assignment of the observed unsymmetrical pyrazabole product as the *mono*-electrophile, **5.9**. Multiple efforts to form single crystals of either **5.9** or **5.10** for X-ray diffraction studies were unsuccessful, however, with only *tetra*-bromo pyrazabole **5.6** precipitating from the samples.

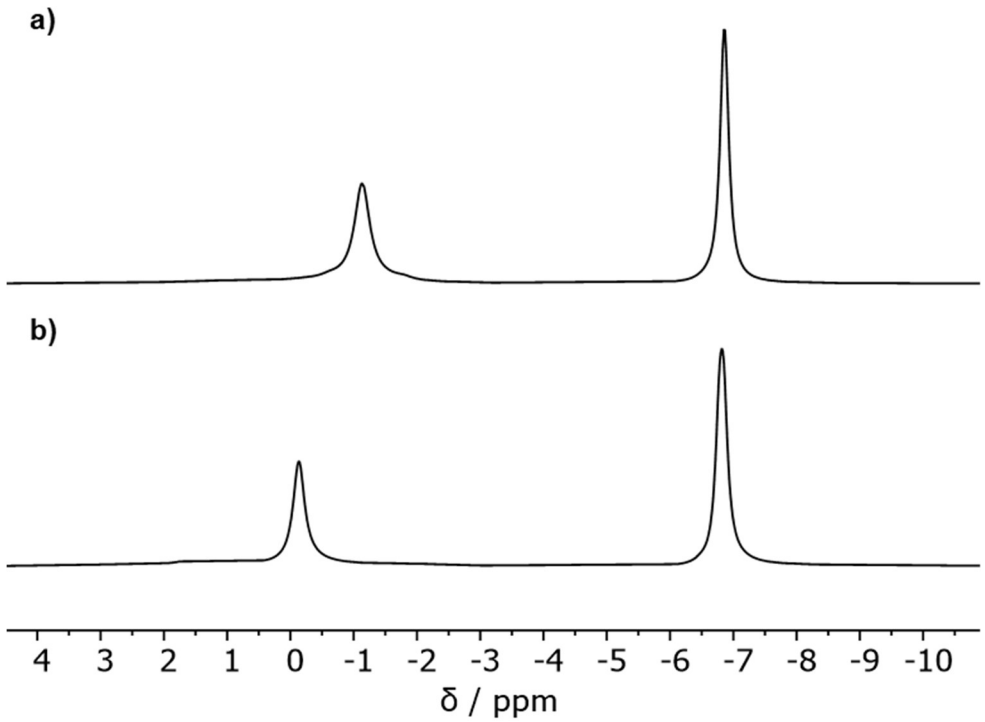

Figure 5.12: Stacked ^{11}B NMR spectra of **a)** *tri*-bromo *mono*-NTf_2 pyrazabole, formed via the activation of *tetra*-bromo pyrazabole with 0.9 equiv. $TMSNTf_2$ and **b)** the corresponding boronium ion formed after addition of 4-DMAP. *(Solvent = CD_2Cl_2, NMR temperature = 300 K).*

The single activation of *tetra*-chloro pyrazabole **5.8** was also achieved using these optimised conditions. Addition of **5.8** to 0.9 equiv. $TMSNTf_2$ resulted in 75% conversion of **5.8** (based on the relative ^1H integrals of the two pyrazabole species present), with the formation of the corresponding *mono*-electrophile, *tri*-chloro *mono*-NTf_2 pyrazabole **5.11**, observed as the only new pyrazabole species (**Scheme 5.19**). Following the removal of the unreacted $TMSNTf_2$ and TMSCl by-product *in vacuo*, the *mono*-electrophile **5.11** was characterised in d_2-DCM with a small amount of leftover **5.8** present. The ^1H NMR spectrum appeared to show only two pyrazole resonances for the new pyrazabole species in a 2:1 ratio. This implied that was not the unsymmetrical *mono*-electrophile **5.11**. However, analysis of the ^1H-^{13}C HSQC spectrum showed that there were three inequivalent pyrazole environments, as expected for **5.11**, with two of the resonances overlapping in the ^1H NMR spectrum. The ^{11}B NMR spectrum showed two resonances at 2.3 and -1.8 ppm. The downfield shift corresponds to the $[BCl_2]$ unit

of **5.11** (and the leftover **5.8**), whilst the more upfield corresponds to the [B(Cl)NTf$_2$] unit of **5.11**.

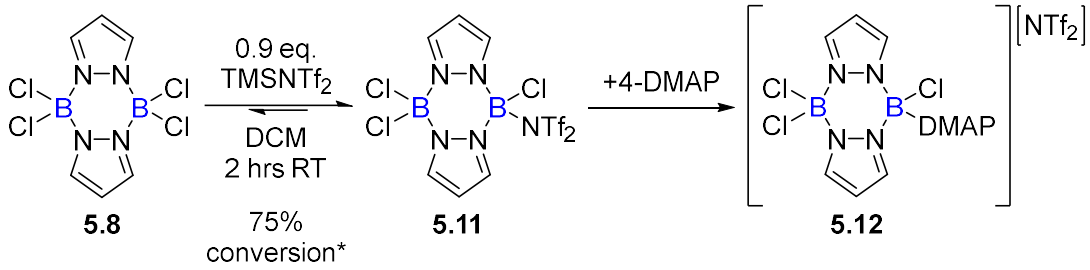

Scheme 5.19: Optimised conditions for the synthesis of *tri*-chloro *mono*-NTf$_2$ pyrazabole, from *tetra*-chloro pyrazabole. Subsequent addition of 4-DMAP forms the corresponding boronium ion. **(Conversion is calculated by the relative ^{1}H integrals of the pyrazabole species).*

As with the bromo analogue, the chloro-substituted *mono*-electrophile **5.11** could not be characterised by mass spectrometry, presumably because of the high sensitivity of these pyrazabole electrophiles. Hence the *mono*-electrophile **5.11** was converted into the boronium ion **5.12** by the addition of 0.9 equiv. 4-DMAP to the sample. The ^{11}B NMR spectrum showed the loss of the [B(Cl)NTf$_2$] resonance of **5.11** at -1.8 ppm, alongside the formation of a new resonance at 2.0 ppm, corresponding to the new [BCl(DMAP)] unit. As before, the resonances of the [BCl$_2$] units in both **5.11** and **5.8** were not affected by the addition of 4-DMAP. Characterisation of the boronium ion **5.12** by mass spectrometry supported the assignment of the unsymmetrical pyrazabole species as **5.11**, though again single crystals of **5.11** and **5.12** could not be formed, with only *tetra*-chloro pyrazabole **5.8** isolated. This precluded full characterisation of the *mono*-electrophiles and their corresponding boronium salts.

Therefore, the single activation of both *tetra*-bromo pyrazabole **5.6** and *tetra*-chloro pyrazabole **5.8** using TMSNTf$_2$ proceeds readily at room temperature, forming unsymmetrical *mono*-electrophiles which have been characterised *in situ*. However, the formation of an equilibrium prevents the complete activation of the *tetra*-halo pyrazabole to form the *mono*-electrophiles cleanly.

Synthesis and Characterisation of the *Di*-Electrophiles

The previous efforts to form the bromo-substituted *di*-electrophile, **5.4**, via the double activation of *tetra*-bromo pyrazabole, **5.6**, used 2.2 equiv. $TMSNTf_2$. However, this resulted in very little of the *di*-electrophile **5.4** formed, with the *mono*-electrophile **5.9** the major product and considerable $TMSNTf_2$ leftover.

In an attempt to favour more double activation, *tetra*-bromo pyrazabole **5.6** was reacted with 3 equiv. $TMSNTf_2$. After 1 hour at room temperature, **5.6** had fully dissolved. The *in situ* ^1H NMR spectrum showed full conversion of **5.6**, giving a mixture of the *mono*- and *di*-electrophiles (**5.9**:**5.4**) in a 3:2 ratio, respectively (**Figure 5.13a**). This indicates that approximately 0.14 mmol (47%) of the added $TMSNTf_2$ (0.3 mmol) had reacted. The sample was heated to 60 °C for 22 hours, in the hope that this would push the double-activation further, but no change in the ratio of the two pyrazabole products was observed, indicating the equilibrium position had been reached (**Figure 5.13b**).

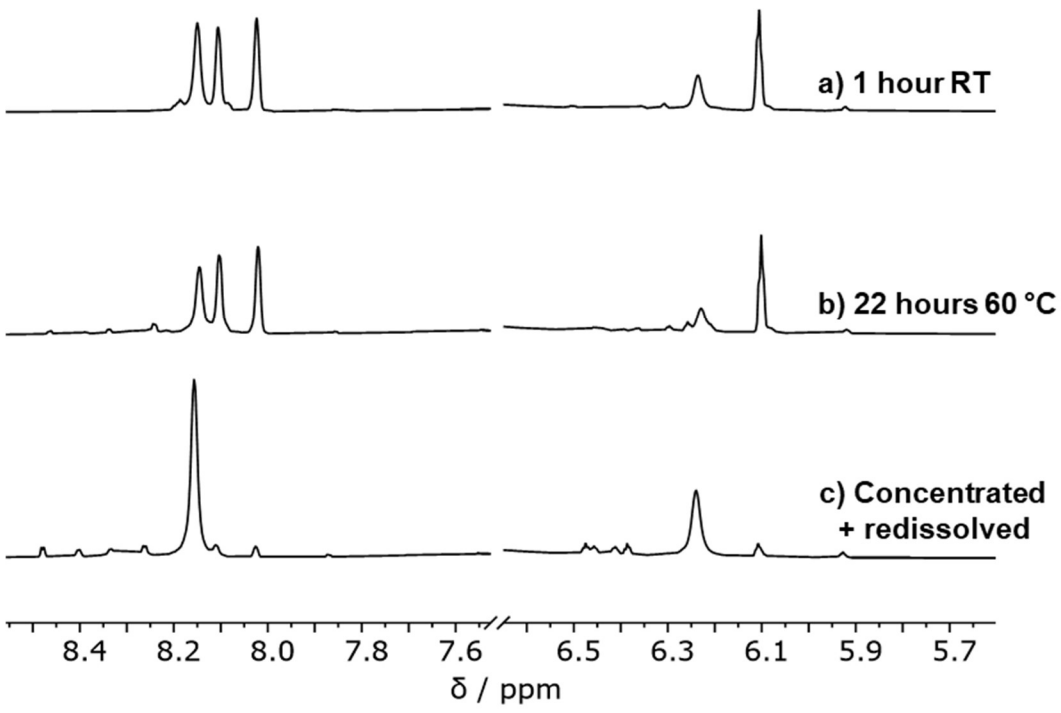

Figure 5.13: Stacked *in situ* ^1H NMR spectra of the reaction of *tetra*-bromo pyrazabole with 3 equiv. $TMSNTf_2$. *Note: The ^1H solvent resonance has been omitted for clarity. (Solvent = C_6H_5Cl, NMR temperature = 300 K).*

To try to shift the reaction towards the formation of more of the *di*-electrophile **5.4**, the reaction was concentrated *in vacuo* to remove TMSBr. It was hoped that removal of the by-product would enable more of the *mono*-electrophile **5.9** to react. It should be noted that while $TMSNTf_2$ is also volatile,[27] it is less so than TMSBr,[30] so controlled concentration is essential to enable the double activation before any significant $TMSNTf_2$ is removed. Following concentration, the ^1H NMR spectrum of the redissolved sample showed the *di*-electrophile **5.4** as the major pyrazabole species present, with almost all of the *mono*-electrophile **5.9** converted (**Figure 5.13c**). However, the $^1H/^{13}C$ NMR spectra are not clean, with several other minor species observed. This implies that other side reactions may occur under these conditions, or the highly sensitive *di*-electrophile **5.4** is degrading/reacting further.

In addition, a significant amount of $TMSNT_2$ was still present in the sample, which could not be entirely removed from the reaction (via further concentrations) without causing more degradation of the *di*-electrophile **5.4**. Removal of $TMSNTf_2$ is essential if **5.4** is to be used in reactions, e.g. with *N*-methyl indole, as the presence of this silyl electrophile would result in competitive electrophilic C-H silylation of the indole substrate.[31] Therefore, efforts were made to selectively form the *di*-electrophile **5.4** using smaller excesses of $TMSNTf_2$. However, with ≤2.8 equiv. $TMSNTf_2$ and removal of TMSBr *in vacuo*, a significant amount of *mono*-electrophile, **5.9**, was still present that did not undergo a second activation.

An alternative 'stepwise activation' approach was also explored, where *tetra*-bromo pyrazabole **5.6** was initially reacted with 1.2 equiv. $TMSNTf_2$, then concentrated *in vacuo* to remove TMSBr, followed by the addition of a further 1.2 equiv. $TMSNTf_2$ and concentration again. This led to complete consumption of **5.6**, but the *mono*-electrophile **5.9** was still the major pyrazabole species present. Addition of a further 1.2 equiv. $TMSNTf_2$ and concentration resulted in the apparent degradation of the *di*-electrophile **5.4**, suggesting that this species is even more sensitive than the *mono*-electrophile **5.9**. Therefore, thus far the *di*-electrophile **5.4** has only been selectively formed as the major product when

using 3 equiv. $TMSNTf_2$, with concentration of the reaction required to force the second activation step towards completion (**Scheme 5.20**).

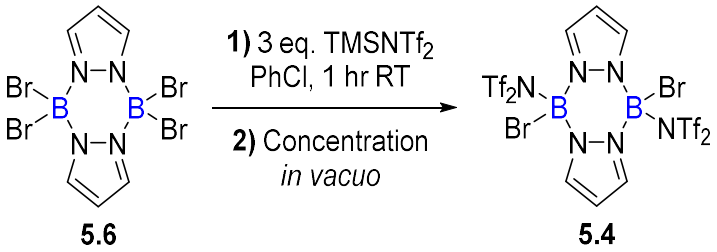

Scheme 5.20: Optimised conditions for the synthesis of *di*-bromo *di*-NTf_2 pyrazabole from *tetra*-bromo pyrazabole.

A sample of **5.4** formed via these conditions was characterised by NMR spectroscopy in d_2-DCM. The ^{11}B NMR spectrum showed a single resonance for the two equivalent [B(Br)NTf_2] resonances at -1.1 ppm (**Figure 5.14b**). The ^{1}H NMR spectrum showed two resonances for **5.4** (**Figure 5.14a**), but these are much broader than was seen for the *mono*-electrophile **5.9**. This peak broadening is even more significant in the $^{13}C\{^{1}H\}$ NMR spectrum. The two $[NTf_2]^-$ substituents shifting between the '*N*-bound' and '*O*-bound' coordination modes can be precluded as the origin of this broadening as the two CF_3 groups are equivalent, indicative of only the '*N*-bound' coordination mode.[32] A definitive explanation for this peak broadening has not been found, but it may be due to *cis*-*trans* isomerism (as observed with *di*-bromo pyrazabole **5.2**).

In addition to **5.4**, several minor impurities / side-products are also observed in the $^{1}H/^{13}C$ NMR spectra alongside $TMSNTf_2$. Therefore, before the reactivity with *N*-methyl indole can be evaluated, a purification method, or more selective activation conditions, must be found. Attempts to recrystallise the *di*-electrophile **5.4** from this reaction mixture have been unsuccessful, with degradation of the samples observed. Furthermore, **5.4** was not observed when analysing the reaction mixture by mass spectrometry.

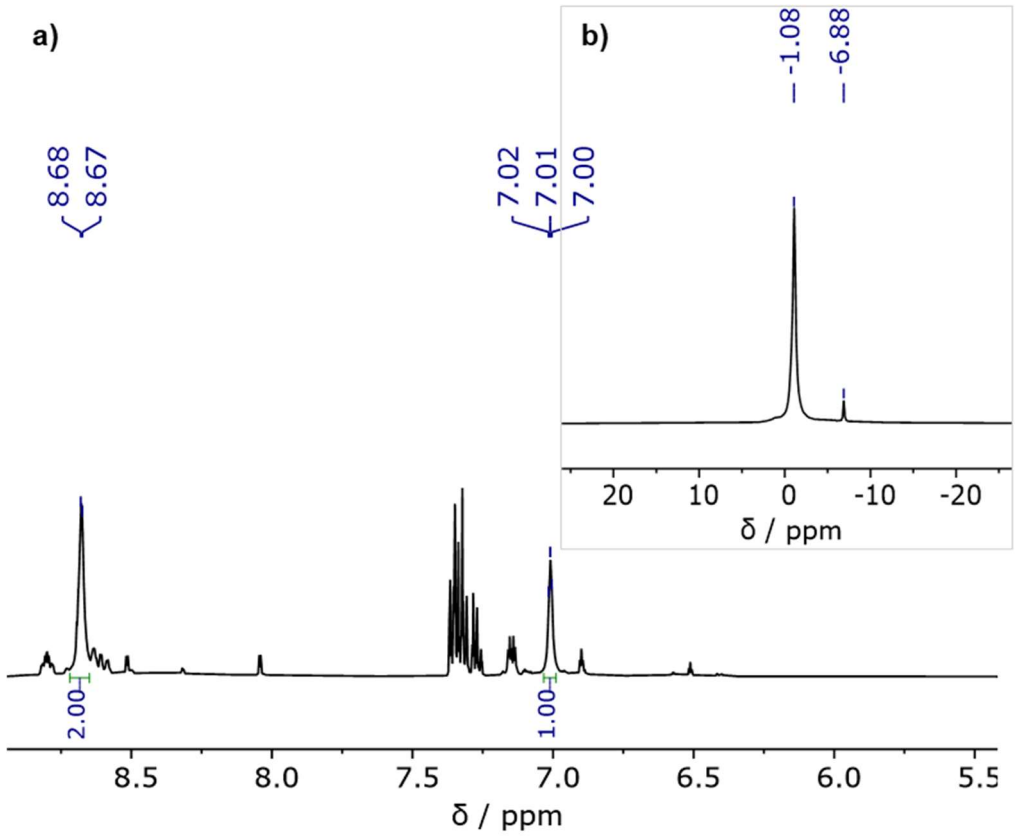

Figure 5.14: **a)** ^{1}H NMR and **b)** ^{11}B NMR spectra of (predominantly) *di*-bromo *di*-NTf_2 pyrazabole, formed via double activation of *tetra*-bromo pyrazabole with 3 equiv. $TMSNTf_2$ and concentration *in vacuo*.
Note: The ^{1}H resonance around 7.33 ppm corresponds to residual PhCl. (Solvent = CD_2Cl_2, NMR temperature = 300 K).

The double activation of *tetra*-chloro pyrazabole **5.8** was also explored in the hope of forming *di*-chloro *di*-NTf_2 pyrazabole **5.7**. Initially, 2.2 equiv. $TMSNTf_2$ was used, and **5.8** was fully dissolved after 1 hour at room temperature. Analysis of the sample by *in situ* NMR spectroscopy showed full consumption of **5.8**, with the *mono*- and *di*-electrophiles (**5.11**:**5.7**) formed in a ratio of 7:3, respectively. Concentration of the sample to remove the by-product, TMSCl, and redissolution resulted in a significant increase in the amount of *di*-electrophile **5.7** formed, with the ratio of the *mono*- and *di*-electrophile products now 1:3, respectively. In the hopes of pushing the double activation reaction to completion, an additional 1 equiv. $TMSNTf_2$ was added. This caused no change to the ratio of the two electrophile species initially, but a second concentration of the sample resulted in the clean and selective formation of the *di*-electrophile **5.7** (**Scheme 5.21**).

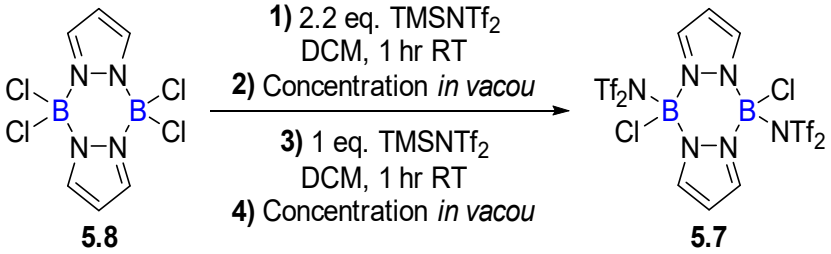

Scheme 5.21: Optimised conditions for the synthesis of *di*-chloro *di*-NTf_2 pyrazabole, from *tetra*-chloro pyrazabole.

The *di*-electrophile **5.7** was characterised by NMR spectroscopy in d_2-DCM. The ^1H NMR spectrum showed two resonances in a 2:1 ratio (**Figure 5.15a**), with these resonances significantly more resolved than observed with the bromo-equivalent (**5.4**). The spectrum is also significantly cleaner than in the formation of **5.4**, suggesting that the double activation of *tetra*-chloro pyrazabole **5.8** is more selective (compared to *tetra*-bromo pyrazabole **5.6**).

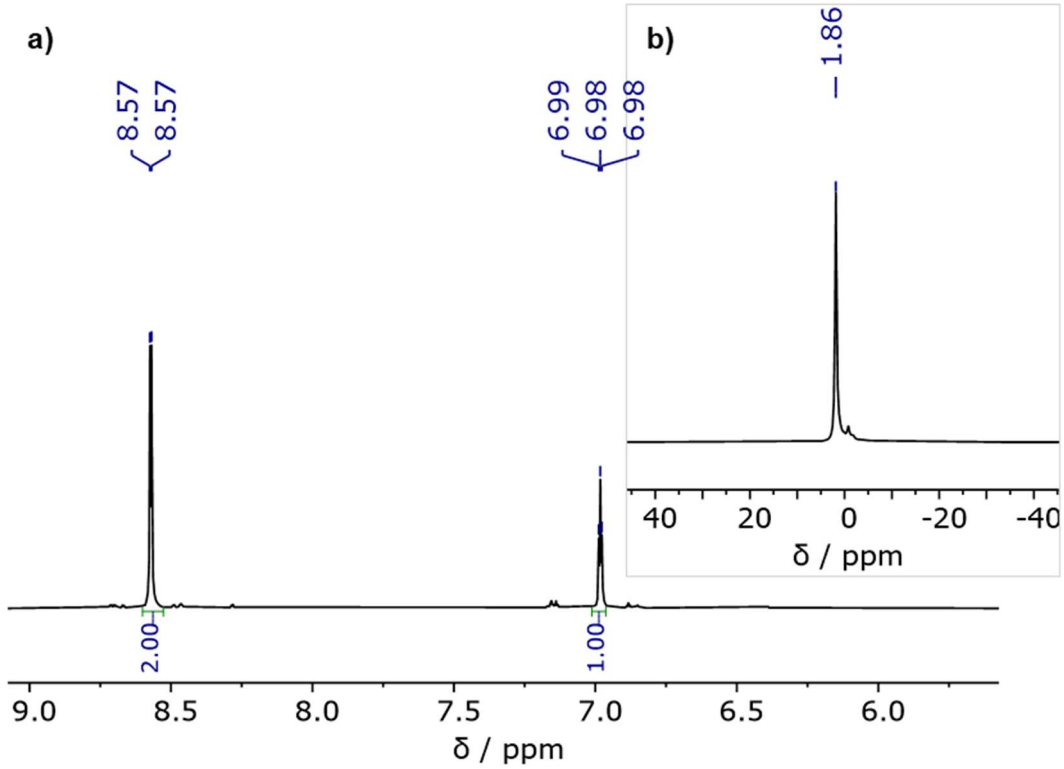

Figure 5.15: **a)** ^1H NMR and **b)** ^{11}B NMR spectra of *di*-chloro *di*-NTf_2 pyrazabole, formed via the stepwise double activation of *tetra*-chloro pyrazabole with 3.2 equiv. $TMSNTf_2$ (total) and two concentrations *in vacuo*.
(Solvent = CD_2Cl_2, NMR temperature = 300 K).

The ^{11}B NMR spectrum of **5.7** showed a single resonance for the two equivalent [B(Cl)NTf$_2$] resonances at 1.9 ppm (**Figure 5.15b**). A significant amount of TMSNTf$_2$ was still present in the sample, however, which means this sample could not be used in reactions with *N*-methyl indole without further purification. The *di*-electrophile **5.7** was also not observed by mass spectrometry and attempts to recrystallise from these samples were unsuccessful.

The double activation of both *tetra*-bromo pyrazabole **5.6** and *tetra*-chloro pyrazabole **5.8** with TMSNTf$_2$ is feasible, but this has not been achieved to give the desired *di*-electrophiles (**5.4** and **5.7**, respectively) as the only species present in solution. Therefore, at present this approach is not a suitable method to form *di*-electrophiles that can be used in subsequent reactions with *N*-methyl indole. More work is needed to optimise the activation methods (or explore alternative activators), with the clean formation of *di*-chloro *di*-NTf$_2$ pyrazabole **5.7** looking more feasible than the bromo-equivalent (**5.4**).

Reactivity of the *Mono*-Electrophiles with *N*-Methyl Indole

As the single activation of *tetra*-halo pyrazaboles to form the *mono*-electrophiles **5.9** and **5.11** proceeds more readily (than the double-activation) and large excesses of TMSNTf$_2$ are not necessary, we explored whether these *mono*-electrophiles could be utilised in the C3/C4- (or C2/C3)-diborylation of *N*-methyl indole. Two possible ways to achieve double C-H borylation using a *mono*-electrophilic pyrazabole species were proposed (**Scheme 5.22**).

First, C3-H borylation of *N*-methyl indole (requiring 1 equiv. DBP) could proceed, forming intermediate **5.13**, where the second boron unit of the pyrazabole directing group is a [BX$_2$] unit. If the B-X bond is sufficiently labile, a second, intramolecular C-H borylation (at C4 or C2) could proceed. This would likely be more feasible using the bromo-substituted *mono*-electrophile, **5.9**, as this halide is less coordinating (than chloride).

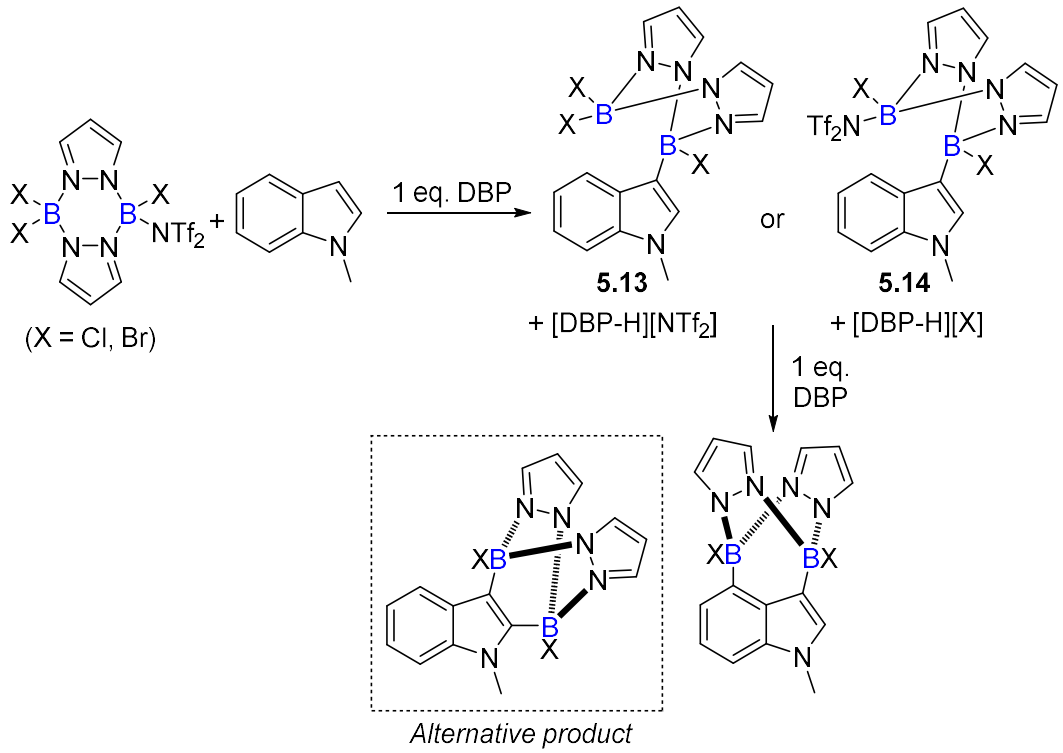

Scheme 5.22: Proposed routes to achieve double C-H borylation of *N*-methyl indole (either C3/C4, or C2/C3) using halo-substituted *mono*-electrophiles.

Alternatively, following C3-H borylation, anion exchange between [DBP-H][NTf_2] and an 'X' substituent of the [BX_2] unit of **5.13** could occur. This would produce [DBP-H][X] and intermediate **5.14**, where an electrophilic [B(X)NTf_2] unit is generated. This intermediate could then undergo a second C-H borylation at C4 or C2. Here, the formation of less soluble [DBP-H][X] could provide a driving force to the anion exchange. There is some precedence for this approach (albeit with a different base, Et_3N) as discussed in **Chapter 4**.[4] A possible, but undesirable, side reaction with this system is double, undirected, C-H borylation using 2 equiv. of the *mono*-electrophile. This would give C3, C5-diborylated indoles, with one pyrazabole unit at C3 and another at C5.[25]

Initial test reactions used *tetra*-bromo pyrazabole **5.6**, which was activated using 1.2 equiv. $TMSNTf_2$. Following activation, minor amounts of leftover $TMSNTf_2$, and the by-product, TMSBr, were both removed *in vacuo*. This resulted in 86% conversion of **5.6**, forming the *mono*-electrophile **5.9** (with a small amount of the *di*-electrophile **5.4** also formed). To this sample was added excess (3 equiv.) DBP, and 1 equiv. *N*-methyl indole. After 18 hours at room temperature, a significant

amount of precipitate had crashed out, believed to be protonated base. Concentration of the sample, and addition of d_2-DCM fully dissolved the precipitate, and the now homogeneous sample was analysed by *in situ* NMR spectroscopy (**Figure 5.16**).

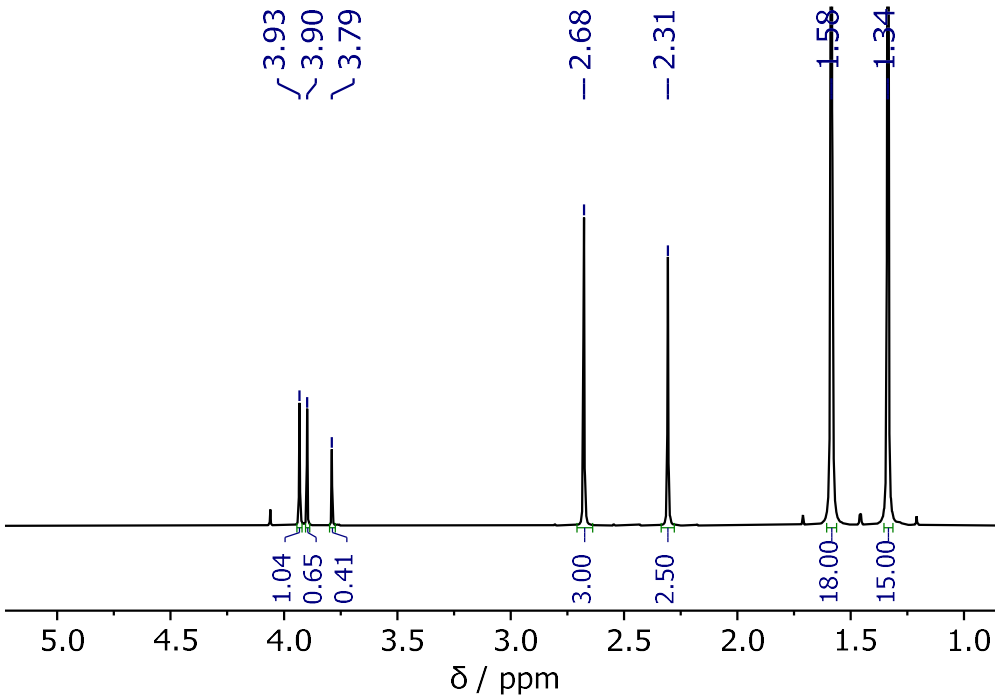

Figure 5.16: ^{1}H NMR spectrum of the reaction of *tri*-bromo *mono*-NTf_2 pyrazabole with 3 equiv. DBP and 1 equiv. *N*-methyl indole, after 18 hours at RT. *Note: The resonances at 1.34 and 2.31 ppm correspond to DBP, whilst the resonances at 1.58 and 2.68 ppm correspond to [DBP-H][NTf_2].* *(Solvent = CD_2Cl_2, NMR temperature = 300 K).*

The ^{1}H NMR spectrum showed approximately 80% conversion of *N*-methyl indole (*N*-Me δ_{1H} = 3.79 ppm), which was expected considering that the activation of **5.6** did not go to completion. Two new '*N*-methyl' resonances were also observed at 3.90 and 3.93 ppm, which are assigned as two different borylated indole species. A mixture of protonated and unprotonated DBP was also observed. Based on the relative integrals of these resonances, it was calculated that 0.14 mmol of DBP (47%) was protonated following the addition of *N*-methyl indole. The formation of >1 equiv. protonated base, and the observation of two indole species suggests there may be a mixture of *mono*- and *di*-borylated *N*-methyl indole present. Note the aromatic region of the ^{1}H NMR spectrum was complicated by residual C_6H_5Cl. The ^{11}B NMR spectrum indicated that the

[B(Br)NTf_2] unit of the *mono*-electrophile **5.9** had fully reacted, with the resonance shifting from -1.1 ppm to -1.4 ppm and becoming much broader. This new broad resonance may correspond to several inequivalent, but overlapping, carbon-bonded [B(Br)R] units. The [BBr_2] resonance of **5.9** at -6.9 ppm was still observed, which suggests that the *mono*-electrophile had only reacted at one 'end' to form the intermediate **5.13**. From this data, it could not be concluded whether any diborylation had occurred, or if the *mono*-electrophile had only reacted in one C-H borylation reaction.

To characterise the indole products, the borylated species were converted into the 'Bpin' derivates using the previously established conditions,[3] albeit with the reaction heated to 50 °C for just 4 hours (as C3-Bpin indole derivatives are sensitive to protodeboronation). The reaction was then analysed directly any without further work-up. The ^{11}B NMR spectrum showed a significant 'ArBpin' resonance at 30.2 ppm, with this chemical shift consistent with 3-Bpin *N*-methyl indole (**Figure 5.17**).[24] The other ^{11}B resonance at -6.8 ppm was attributed to leftover *tetra*-bromo pyrazabole **5.6**. Furthermore, the ^{1}H NMR spectrum showed two indole species, the first being unreacted *N*-methyl indole and the second matching the reported resonances of 3-Bpin *N*-methyl indole.[24] Therefore, it appears that only C3-H borylation has occurred, with no evidence of diborylation (or C-H borylation at other positions), obtained from this reaction.

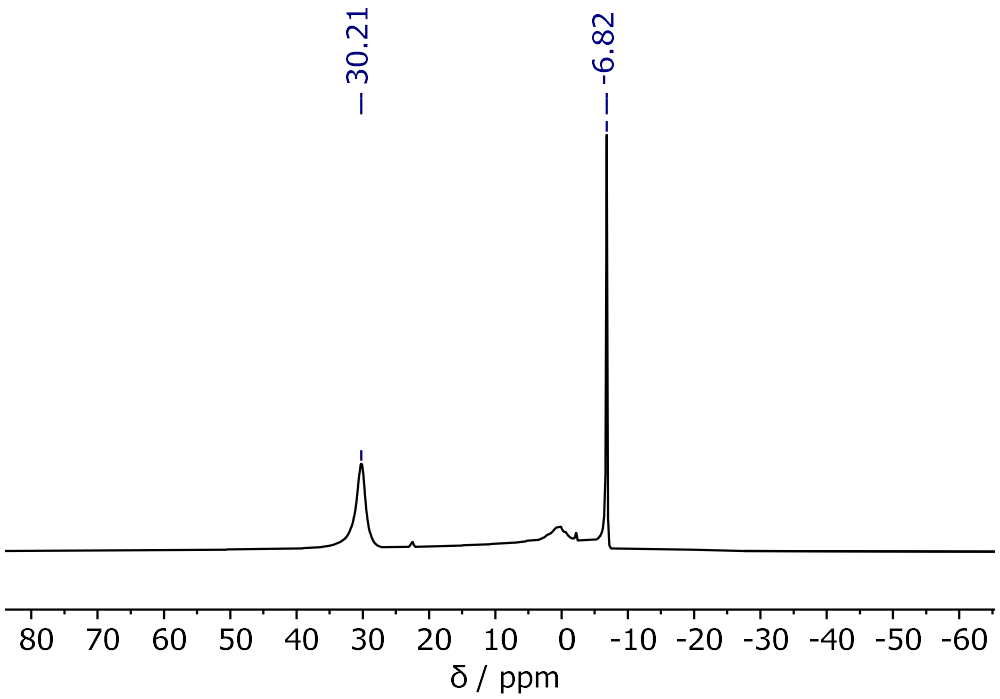

Figure 5.17: ^{11}B NMR spectrum following 'pinacol protection' of the reaction between *tri*-bromo *mono*-NTf_2 pyrazabole, DBP and *N*-methyl indole. *(Solvent = CD_2Cl_2, NMR temperature = 300 K).*

To ensure there was no protodeboronation of any other C-B bonds (which could indicate diborylation), the reaction of the *mono*-electrophile **5.9** and *N*-methyl indole was repeated under identical conditions, but the pinacol protection was performed using deuterated water instead. Therefore, if protodeboronation was occurring during this step, there would be deuterium incorporation at that carbon position. This could then be detected by ^{2}H NMR spectroscopy. However, the resulting ^{2}H NMR spectrum only showed a small amount of 3-deutero *N*-methyl indole, hence there is no evidence of any other carbon positions undergoing C-H borylation. This is presumably because the [BBr_2] unit of the C3-borylated intermediate (**5.13**) is insufficiently reactive to perform an intramolecular C-H borylation (requiring S_N2 at boron).

The reactivity of the chloro-substituted *mono*-electrophile **5.11** with *N*-methyl indole was also studied under the same conditions. This resulted in near-identical NMR spectra to the bromo-equivalent, with only 3-Bpin *N*-methyl indole formed after pinacol protection. No evidence of any C-B protodeboronation was observed either. Therefore, whilst the two synthesised *mono*-electrophiles **5.9** and **5.11** are

suitable boron electrophiles for the C3-H borylation of *N*-methyl indole, the [BX_2] units do not react to enable a second, intramolecular C-H borylation.

Therefore, a 'stepwise' activation approach using the *mono*-electrophile **5.9** was attempted in the hope of enabling double C-H borylation of *N*-methyl indole (**Scheme 5.23**). The *mono*-electrophile **5.9** was generated *in situ*, which was followed by the addition of 1.2 equiv. DBP and 1 equiv. *N*-methyl indole. This resulted in C3-H borylation of *N*-methyl indole to form the intermediate **5.13**. To this was added a further 1.2 equiv. $TMSNTf_2$ (and another 1 equiv. DBP), where it was hoped this would activate the [BBr_2] unit of **5.13** to form intermediate **5.14** with a reactive [$B(Br)NTf_2$] unit, which could undergo a second C-H borylation. However, when this reaction was pinacol protected (in the presence of D_2O) and analysed by NMR spectroscopy, very little 3-Bpin *N*-methyl indole was formed, and no resonances corresponding to other C-B (or C-D) bonds were observed indicating a second C-H borylation had not proceeded.

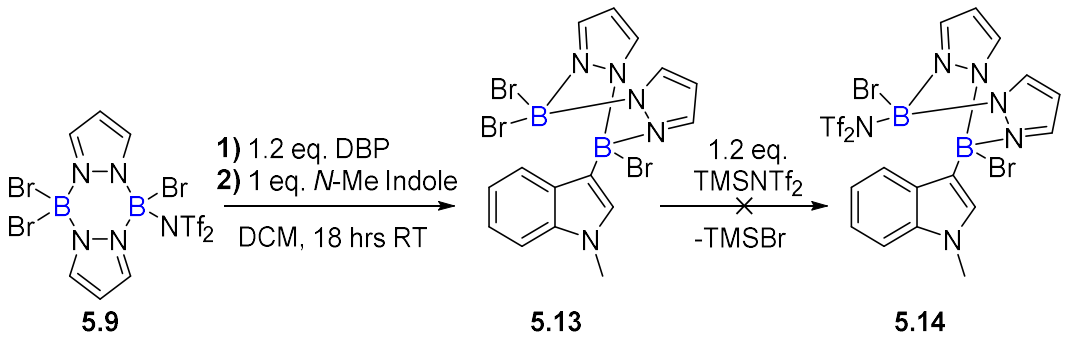

Scheme 5.23: Attempted 'stepwise' activation of *tri*-bromo *mono*-NTf_2 pyrazabole in the reaction with DBP and *N*-methyl indole.

Therefore, the addition of $TMSNTf_2$ to the C3-H borylated intermediate **5.13** is not a suitable way to 're-activate' the *mono*-electrophile to enable a second C-H borylation. This may be due to side reactions between the substrate and the silyl electrophile.

5.4 Conclusions

In this work, two possible routes to synthesise halo/NTf_2-substituted pyrazabole electrophiles, for the purpose of targeting the C3/C4 (or C2/C3)-diborylation of indoles, were evaluated.

In '**Route 1**', *di*-halo pyrazaboles were reacted with $HNTf_2$. This did not yield the desired halo-substituted pyrazabole *di*-electrophiles, however, and instead the respective *tetra*-halo pyrazabole and *di*-NTf_2 pyrazabole were isolated due to the extremely low solubility of these compounds driving the substituent exchange equilibrium. Despite this, studies on the reactivity with *N*-methyl indole provided some evidence of indole C2/C3-diborylation indicating that this route may facilitate the formation of a small amount of the desired *di*-electrophile *in situ*. Therefore, though this is not a viable route to produce large amounts of the halo-substituted pyrazabole electrophiles of interest, it does imply that these electrophiles will be suitable traceless directing groups for the C2/C3-, or C3/C4-diborylation of indole if they can be produced selectively. For example, with more soluble pyrazabole derivatives (e.g. using alkylated pyrazoles), this approach could be feasible.

With '**Route 2**', the single and double activation of *tetra*-halo pyrazaboles has been demonstrated using $TMSNTf_2$. The single activation of *tetra*-halo pyrazaboles occurs at room temperature, forming *mono*-electrophiles as the major products that have been characterised and shown be adequate boron electrophiles for the C3-H borylation of *N*-methyl indole. The target of indole diborylation has not been achieved using these *mono*-electrophiles due to the inability to form a second electrophilic boron unit *in situ* using further $TMSNTf_2$, Other activators, such as AlX_3, may be more effective at increasing the reactivity of the second boron unit to enable the second C-H borylation, hence future work should explore this.

The formation of *di*-electrophiles via '**Route 2**' is disfavoured as the second halide abstraction is energetically uphill, and has only been achieved using an excess of the activator, $TMSNTf_2$. This has prevented the application of these *di*-

electrophiles in reactions with *N*-methyl indole. Encouragingly, the double activation of *tetra*-chloro pyrazabole gave significant amounts of the corresponding *di*-electrophile with only 2.2 equiv. $TMSNTf_2$. This implies that the formation of chloro-substituted *di*-electrophiles may be more accessible (than the bromo-equivalents), hence the optimisation of this process is a promising area for further studies.

5.5 Experimental

*For general experimental considerations, see **Chapter 2**.*

The NMR spectra for these reactions can be found in the appendix of this thesis.

5.5.1 Synthesis of Halogen-Substituted Pyrazaboles

Di-Bromo Pyrazabole – 5.2

This modified procedure is based on a previous report by Nöth and co-workers.[15]

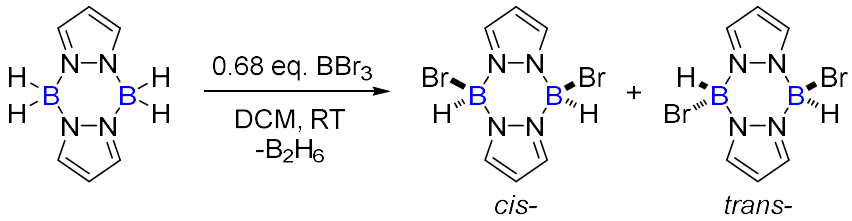

A solution of BBr_3 (0.66 mL, 6.8 mmol, 0.68 equiv.) in CH_2Cl_2 (17 mL) was prepared and then added dropwise over the course of 15 minutes to a solution of pyrazabole **5.1** (1.6 g, 10 mmol) in CH_2Cl_2 (12 mL) at 0 °C. Following complete addition, the reaction was stirred at room temperature for 18 hours. Diborane gas generated during the reaction was quenched by bubbling the nitrogen outflow through degassed methanol. A white solid precipitated during the course of the reaction. The precipitate was filtered, washed with hexane (2 x 10 mL) and dried *in vacuo* to afford the title product as a white solid in 88% yield (2.280 g, 8.82 mmol). Analytical data are in accordance with literature values.[15] The title product undergoes isomerisation upon dissolution in solvent, giving a 1:1 mixture of the *cis*- and *trans*- isomers after <2 hours at room temperature in halocarbon solvents (*see **Figure 5.2** and appendix*). The characterisation data below is for a 1:1 mixture of isomers, where the sample was dissolved in $CDCl_3$ and left at room temperature for 2 hours before recording NMR spectra.

^{1}H NMR (500 MHz, $CDCl_3$) δ 8.08 (d, $^3J_{HH}$ = 2.5 Hz, 4H, N=C*H*-CH), 7.99 (d, $^3J_{HH}$ = 2.5 Hz, 4H, N=C*H*-CH), 6.64 (t, $^3J_{HH}$ = 2.5 Hz, 2H, N=CH-C*H*), 6.59 (t, $^3J_{HH}$ = 2.5 Hz, 2H, N=CH-C*H*), 5.50-4.43 (br m, 4H, B*H*Br);

^{1}H{^{11}B} NMR (500 MHz, $CDCl_3$) δ 8.08 (d, $^3J_{HH}$ = 2.5 Hz, 4H, N=C*H*-CH), 7.99 (d, $^3J_{HH}$ = 2.5 Hz, 4H, N=C*H*-CH), 6.64 (t, $^3J_{HH}$ = 2.5 Hz, 2H, N=CH-C*H*), 6.59 (t, $^3J_{HH}$ = 2.5 Hz, 2H, N=CH-C*H*), 5.05 (s, 2H, B*H*Br), 4.90 (s, 2H, B*H*Br);

^{11}B NMR (160 MHz, $CDCl_3$) δ -5.7 (d, $^1J_{BH}$ = 143 Hz, *B*HBr), -6.7 (d, $^1J_{BH}$ = 121 Hz, *B*HBr);

^{11}B {^{1}H} NMR (160 MHz, $CDCl_3$) δ -5.7 (s, *B*HBr), -6.7 (s, *B*HBr);

^{13}C{^{1}H} NMR (126 MHz, $CDCl_3$) δ 138.70, 138.59, 108.78, 108.04 ppm.

The title compound was not observed via mass spectrometry (both ESI and EI).

Elemental Analysis: Calculated for $C_6H_8B_2Br_2N_4$: C 22.69%, H 2.54%, N 17.64%; Observed: C 22.50%, H 2.40%, N 16.71%

Di-Chloro Pyrazabole – 5.3

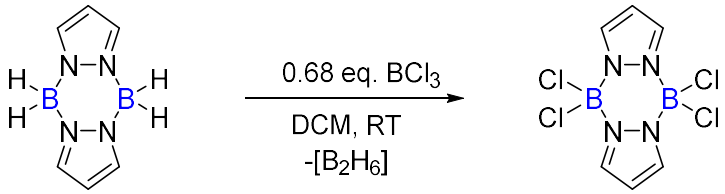

A solution of BCl_3 (0.4 M in CH_2Cl_2, 17 mL, 6.8 mmol, 0.68 equiv.) was added dropwise over the course of 15 minutes to a solution of pyrazabole **5.1** (1.6 g, 10 mmol) in CH_2Cl_2 (12 mL) at 0 °C. Following complete addition, the reaction was stirred at room temperature for 18 hours. Diborane gas generated during the reaction was quenched by bubbling the nitrogen outflow through degassed methanol. A white solid precipitated upon cooling the reaction flask in an ice bath. This was filtered, washed with hexane (2 x 10 mL) and dried *in vacuo* to afford the title product as a white solid in a 56% yield (1.292 g, 5.56 mmol) as a single stereoisomer, confirmed as the *cis*-isomer by single-crystal X-ray diffraction. Crystals suitable for X-ray diffraction were produced by DCM / hexane vapour diffusion at room temperature. The product appears as one stereoisomer in solution, with no isomerisation observed at room temperature or heating to 100 °C for 18 hours.

^{1}H NMR (500 MHz, $CDCl_3$) δ 7.96 (d, $^{3}J_{HH}$ = 2.5 Hz, 4H, N=C*H*-CH), 6.57 (t, $^{3}J_{HH}$ = 2.5 Hz, 2H, N=CH-C*H*), 4.62 (1:1:1:1 q, $^{1}J_{BH}$ = 130 Hz, 2H, B*H*Cl);

^{1}H{^{11}B} NMR (500 MHz, $CDCl_3$) δ 7.96 (d, $^{3}J_{HH}$ = 2.5 Hz, 4H, N=C*H*-CH), 6.57 (t, $^{3}J_{HH}$ = 2.5 Hz, 2H, N=CH-C*H*), 4.62 (s, 2H, B*H*Cl);

^{11}B NMR (160 MHz, $CDCl_3$) δ -2.8 (d, $^{1}J_{BH}$ = 130 Hz, *B*HCl);

^{11}B {^{1}H} NMR (160 MHz, $CDCl_3$) δ -2.8 (s, *B*HCl);

^{13}C{^{1}H} NMR (126 MHz, $CDCl_3$) δ 137.77, 107.87 ppm.

HRMS (ESI^{+}) m/z calcd for $C_6H_8B_2Cl_2N_4Na^{+}$: 251.02043 $[M+Na]^{+}$, found 251.0209.

Tetra-Bromo Pyrazabole – 5.6

This modified procedure is based on a previous report by Nöth and co-workers.[15]

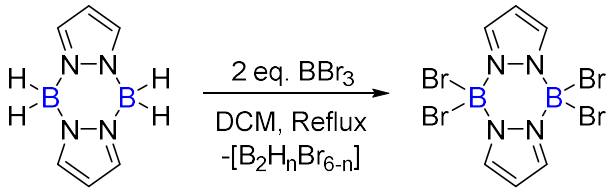

A solution of BBr_3 (1.2 mL, 12.6 mmol, 2 equiv.) in CH_2Cl_2 (20 mL) was prepared and then added dropwise over the course of 15 minutes to a solution of pyrazabole **5.1** (1.0 g, 6.3 mmol) in CH_2Cl_2 (20 mL) at 0 °C. Following complete addition, the reaction was refluxed for 2 hours. Gaseous boranes generated during the reaction was quenched by bubbling the nitrogen outflow through degassed methanol. The volatiles were then removed *in vacuo*, and the obtained white solid was washed with hexane (2 x 10 mL) and dried *in vacuo.* The product was recrystallised from THF (40 ml) / hexane (10 ml) at -20 °C, washed with hexane (2 x 5 mL) and dried *in vacuo* to afford the title product as a white crystalline solid in 48% yield (1.429 g, 3.01 mmol). Analytical data are in accordance with literature values.[14,15]

^{1}H NMR (500 MHz, $CDCl_3$) δ 8.53 (br, 4H, N=C*H*-CH), 6.83 (t, $^3J_{HH}$ = 3 Hz, 2H, N=CH-C*H*);

^{11}B NMR (160 MHz, $CDCl_3$) δ -6.8 (s);

^{13}C{^{1}H} NMR (126 MHz, $CDCl_3$) δ 141.27, 110.38 ppm.

The title compound was not observed via mass spectrometry (both ESI and EI).

Elemental Analysis: Calculated for $C_6H_6B_2Br_4N_4$: C 15.16%, H 1.27%, N 11.79%; Observed: C 15.38%, H 1.25%, N 11.52 %

Tetra-Chloro Pyrazabole – 5.8

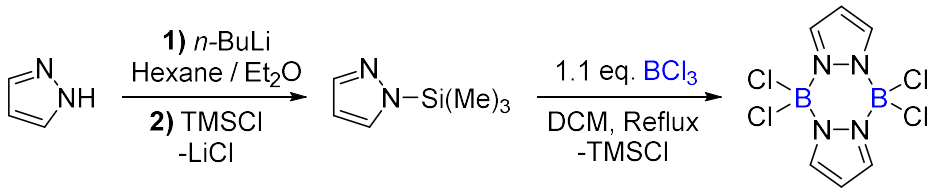

A solution of *n*-BuLi (1.6 M in hexanes, 3.44 mL, 5.5 mmol, 1.1 equiv.) was added dropwise over the course of 30 minutes to a solution of pyrazole (0.340 g, 5 mmol) in diethyl ether (15 mL) at -78 °C. Following complete addition, the reaction was stirred at -78 °C for 1 hour, then warmed to room temperature for 1 hour. The reaction was cooled to -78 °C and chlorotrimethylsilane (0.7 mL, 5.5 mmol, 1.1 equiv.) was added dropwise over the course of 5 minutes. The reaction was stirred at -78 °C for 1 hour, then warmed to room temperature and stirred for 18 hours. The by-product, LiCl, precipitated during the course of the reaction and was removed by filtration. The filtrate was cooled to 0 °C, and BCl_3 (1 M in CH_2Cl_2, 5.5 mL, 5.5 mmol, 1 equiv.) was added dropwise over the course of 30 minutes. The reaction was stirred at 0 °C for 1 hour, then refluxed for 18 hours. A white solid precipitated upon cooling the flask in an ice bath. The precipitate was filtered and dried *in vacuo* to afford the title product as a white solid in 33% yield (0.229 g, 0.77 mmol). Analytical data are in accordance with literature values.[14]

^{1}H NMR (500 MHz, $CDCl_3$) δ 8.35 (d, $^{3}J_{HH}$ = 3 Hz, 4H, N=C*H*-CH), 6.75 (t, $^{3}J_{HH}$ = 3 Hz, 2H, N=CH-C*H*);

^{11}B NMR (160 MHz, $CDCl_3$) δ 2.3 (s);

^{13}C{^{1}H} NMR (126 MHz, $CDCl_3$) δ 139.18, 109.56 ppm.

HRMS (ESI^{-}) m/z calcd for $C_6H_5B_2Cl_4N_4^-$: 294.94599 $[M-H]^-$, found 294.9449.

5.5.2 Control Reactions: Pyrazaboles and *N*-Methyl Indole

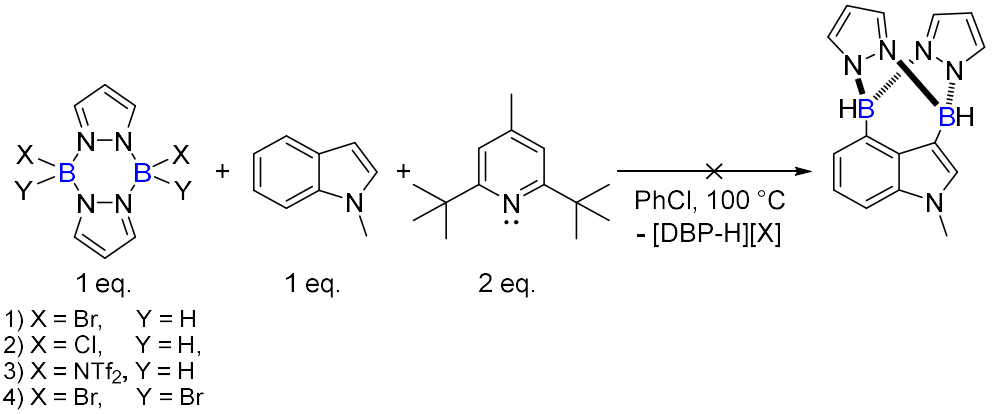

To a J. Young's NMR tube was added the corresponding substituted pyrazabole species (0.1 mmol), and chlorobenzene (0.5 mL). To this was added 2,6-di-*tert*-butyl-4-methylpyridine (0.041 g, 0.2 mmol, 2 equiv.), followed by *N*-methyl indole (0.012 mL, 0.1 mmol, 1 equiv.). This was mixed by inversion (approx. 1 rotation / s) at room temperature and analysed by NMR spectroscopy at regular time points. Samples were also heated to 100 °C in a heating block without inversion / external heating.

5.5.3 Reactivity of *Di*-Bromo Pyrazabole with $HNTf_2$ (Route 1)

General Procedure 5.1: "Activation" of *Di*-Bromo Pyrazabole (5.2)

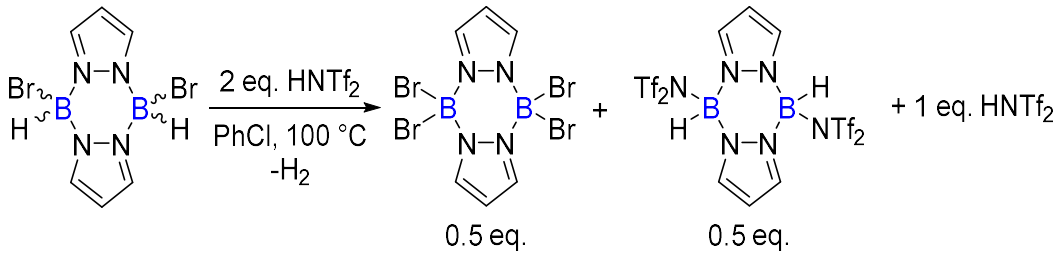

Di-bromo pyrazabole **5.2** (0.160 g, 0.5 mmol, 1 equiv.) and $HNTf_2$ (0.281 g, 1 mmol, 2 equiv.) were added to an ampule and suspended in chlorobenzene (3 mL). The reaction was refluxed at 100 °C for 18 hours, with gas evolution observed and precipitation of a white solid. At the end of the reaction, the ampule was cooled to -20 °C to further facilitate precipitation. The precipitate was then filtered, washed with pentane (2 x 10 mL) and dried *in vacuo*.

A sample of the precipitate was partially dissolved in $CDCl_3$ and analysed by NMR spectroscopy. The spectra showed a single pyrazabole species in solution, matching literature values for *tetra*-bromo pyrazabole **5.6**.[14,15] The precipitate was also dissolved in d_3-MeCN, stirred for 2 hours, and analysed by NMR spectroscopy. The spectra showed two pyrazabole species in solution, the first being *tetra*-bromo pyrazabole **5.6**, and the second [*di*-MeCN pyrazabole][NTf_2]$_2$ (**5.5[MeCN]**).[3]

Reactivity with *N*-Methyl Indole

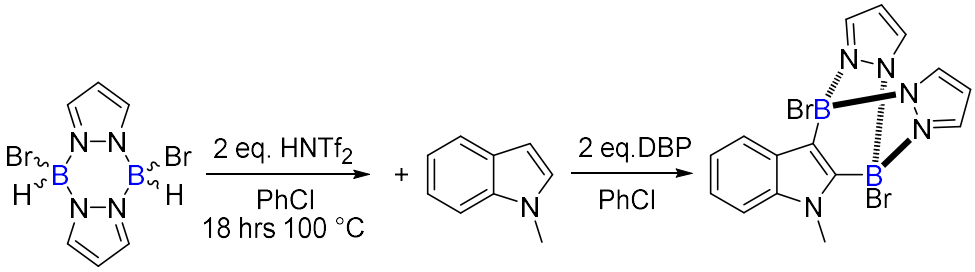

In a J. Young's NMR tube, *di*-bromo pyrazabole **5.2** (0.032 g, 0.1 mmol) was "activated" following **General Procedure 5.1** in chlorobenzene (0.5 mL). The crude reaction mixture was used directly without any further purification. To this mixture was added DBP (0.041 g, 0.2 mmol, 2 equiv.), followed by *N*-methyl indole (0.013 mL, 0.1 mmol, 1 equiv.). The reaction was stirred at room temperature for 18 hours by inversion (approx. 1 rotation / s) and analysed by NMR spectroscopy at regular time points.

General Procedure 5.2: Conversion of Borylated Intermediates to 'ArBpin'

The crude reaction mixture was transferred to an ampule, to which pinacol (0.059 g, 0.5 mmol, 5 equiv.), K_2CO_3 (0.069 g, 0.5 mmol, 5 equiv.), DCM (1 mL) and water (or D_2O, 1 mL) were added sequentially. The ampule was sealed and heated to 50 °C for 4 or 18 hours, with rapid stirring to facilitate some mixing of the biphasic mixture. Upon returning to room temperature, a sample was taken of the organic layer and analysed by NMR spectroscopy.

Alternative Conditions: *Tetra*-Bromo Pyrazabole 5.6, *Di*-NTf$_2$ Pyrazabole 5.5 and *N*-Methyl Indole

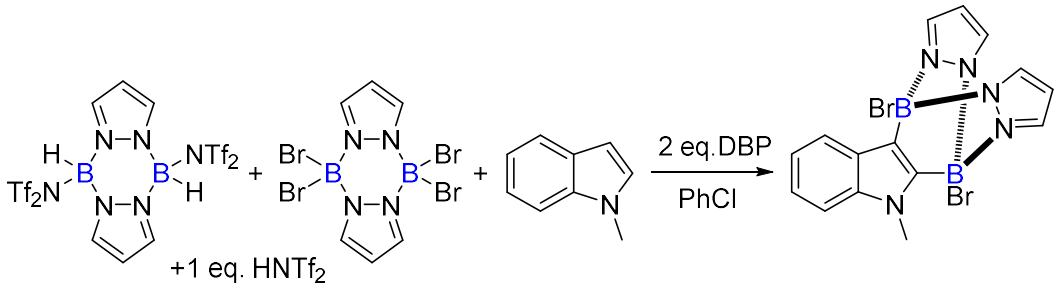

To a J. Young's NMR tube was added *tetra*-bromo pyrazabole **5.6** (0.024 g, 0.05 mmol, 0.5 equiv.), *di*-NTf$_2$ pyrazabole **5.5** (0.036 g, 0.05 mmol, 0.5 equiv.), and HNTf$_2$ (0.028 g, 0.1 mmol, 1 equiv.), which were suspended in chlorobenzene (0.5 mL). To this mixture was added DBP (0.041 g, 0.2 mmol, 2 equiv.), followed by *N*-methyl indole (0.013 mL, 0.1 mmol, 1 equiv.). The sample was mixed by inversion (approx. 1 rotation / s) at room temperature and analysed by NMR spectroscopy at regular time points.

5.5.4 Reactivity of *Di*-Chloro Pyrazabole with HNTf$_2$ (Route 1)

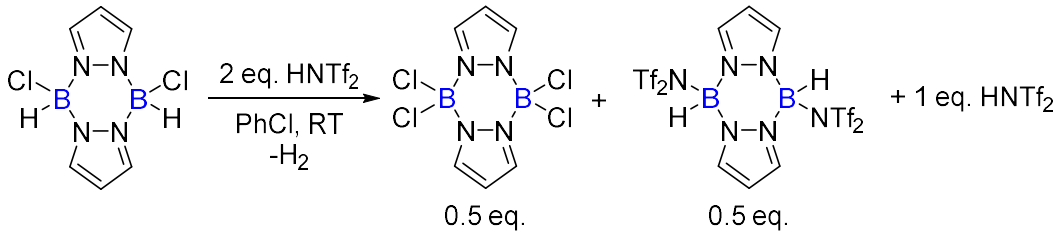

Di-chloro pyrazabole **5.3** (0.023 g, 0.1 mmol, 1 equiv.) and HNTf$_2$ (0.057 g, 0.2 mmol, 2 equiv.) were added to J. Young's NMR tube and suspended in chlorobenzene (0.5 mL). Gas evolution was observed almost immediately. Once the majority of gas evolution had ceased, the NMR tube was sealed. The sample was mixed by inversion (approx. 1 rotation / s) at room temperature for 18 hours, during which time a white solid precipitated. Analysis of the crude reaction mixture showed the near complete conversion of *di*-chloro pyrazabole **5.3** alongside the formation of single pyrazabole species in solution, matching literature values for *tetra*-chloro pyrazabole **5.8**.[14] Concentration of the crude reaction mixture *in vacuo*, and redissolving in d$_3$-MeCN enabled the observation

of a second pyrazabole species matching the literature values for [*di*-MeCN pyrazabole][NTf_2]$_2$ (**5.5[MeCN]**).[3]

5.5.5 Reactivity of *Tetra*-Bromo Pyrazabole with $TMSNTf_2$ (Route 2)

General Procedure 5.3: Preparation of $TMSNTf_2$ *in situ*

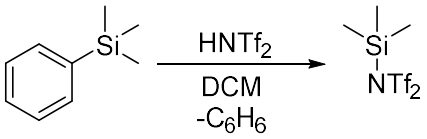

To a J. Young's NMR tube was added $HNTf_2$ (1 equiv.), PhTMS (1 equiv.) and DCM. The reaction was mixed by inversion (approx. 1 rotation / s) at room temperature for 2 hours. ^{29}Si NMR spectroscopy showed the conversion of PhTMS and the formation of $TMSNTf_2$, with analytical data in accordance with literature values.[27]

***Tri*-Bromo *Mono*-NTf_2 Pyrazabole – 5.9**

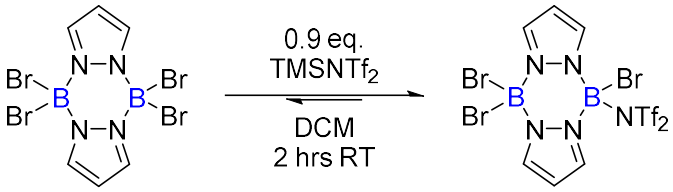

In a J. Young's NMR tube, $TMSNTf_2$ (0.09 mmol, 0.9 equiv.) was prepared *in situ* following **General Procedure 5.3** in DCM (0.5 mL). To this was added *tetra*-bromo pyrazabole **5.6** (0.048 g, 0.1 mmol, 1 equiv.). The reaction was mixed by inversion (approx. 1 rotation / s) at room temperature for 2 hours, until **5.6** had fully dissolved. All volatiles were removed *in vacuo*, and the reaction mixture was redissolved in d_2-DCM (0.5 mL). Analysis by NMR spectroscopy showed 76% conversion of **5.6** to *tri*-bromo *mono*-NTf_2 pyrazabole **5.9**. The title product was characterised directly from this mixture.

^{1}H NMR (500 MHz, CD_2Cl_2) δ 8.64 (br, 2H, N=C*H*-CH), 8.61 (d, $^3J_{HH}$ = 2 Hz, 2H, N=C*H*-CH), 6.90 (t, $^3J_{HH}$ = 2 Hz, 2H, N=CH-C*H*);

^{11}B NMR (160 MHz, CD_2Cl_2) δ -1.1 (s, *B*(Br)NTf_2), -6.9 (s, *B*Br_2);

^{13}C{^{1}H} NMR (126 MHz, CD_2Cl_2) δ 143.16, 142.91, 119.06 (q, $^1J_{CF}$ = 321 Hz, S*C*F_3), 110.92;

^{19}F NMR (471 MHz, CD_2Cl_2) δ -76.56 (s, SC*F*$_3$) ppm.

*The title compound was not observed via mass spectrometry (both ESI and EI), and elemental analysis could not be obtained as **5.9** could not be isolated cleanly.*

Subsequent Conversion of 5.9 to the 4-DMAP-Boronium Ion (5.10)

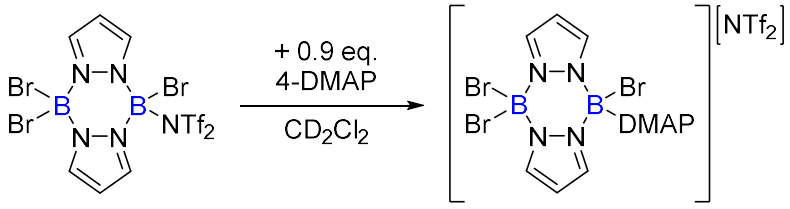

To the sample of **5.9** in CD_2Cl_2 was added 4-DMAP (0.010 g, 0.09 mmol, 0.9 equiv.). The reaction was mixed by inversion (approx. 1 rotation / s) at room temperature for 15 minutes, until 4-DMAP had fully dissolved. Analysis by NMR spectroscopy showed complete conversion of **5.9** to the title boronium ion, **5.10**, with any leftover **5.6** unreacted.

^{1}H NMR (500 MHz, CD_2Cl_2) δ 8.68 (br, 2H, N=C*H*-CH), 8.62 (br, 2H, N=C*H*-CH), 7.59 (m, 2H, 4-DMAP), 6.99 (t, $^{3}J_{HH}$ = 2.5 Hz, 2H, N=CH-C*H*) 6.77 (m, 2H, 4-DMAP), 3.20 (s, 6H, 4-DMAP);

^{11}B NMR (160 MHz, CD_2Cl_2) δ -0.1 (s, *B*Br(4-DMAP)), -6.8 (s, *B*Br$_2$);

^{13}C{^{1}H} NMR (126 MHz, CD_2Cl_2) δ 157.25, 143.26, 143.03, 140.43, 120.16 (q, $^{1}J_{CF}$ = 321 Hz, S*C*F$_3$), 111.30, 107.55, 40.53;

^{19}F NMR (471 MHz, CD_2Cl_2) δ -79.36 (s, SC*F*$_3$) ppm.

HRMS (ESI$^+$) *m/z* calcd for $C_{13}H_{16}B_2Br_3N_6^+$: 514.91726 [M]$^+$, found 514.92079.

Reactivity of *Mono*-Electrophile 5.9 with *N*-Methyl Indole

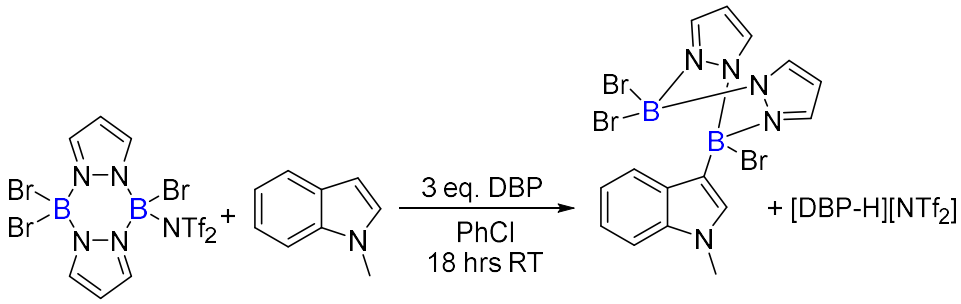

In a J. Young's NMR tube, $TMSNTf_2$ (0.12 mmol, 1.2 equiv.) was prepared *in situ* following **General Procedure 5.3** in PhCl (0.5 mL). To this was added *tetra*-bromo pyrazabole **5.6** (0.048 g, 0.1 mmol, 1 equiv.). The reaction was mixed by inversion (approx. 1 rotation / s) at room temperature for 18 hours. All volatiles were then removed *in vacuo*, and the reaction mixture was redissolved in PhCl (0.5 mL). To the tube was then added DBP (0.062 g, 0.3 mmol, 3 equiv.), and the reaction was mixed by inversion at room temperature for 1 hour. To this was added *N*-methyl indole (0.013 mL, 0.1 mmol, 1 equiv.), and the reaction was mixed by inversion at room temperature for 18 hours, during which time an orange solid precipitated. All volatiles were then removed *in vacuo*, and the resulting solid was redissolved in d_2-DCM (2 mL) and mixed by inversion until fully homogeneous. The sample was then analysed by NMR spectroscopy.

Conversion of the borylated intermediates to 'ArBpin' was achieved following **General Procedure 5.2**. The major Bpin product had analytical data that are in accordance with literature values for 3-Bpin *N*-methyl indole.[24]

***Di*-Bromo *Di*-NTf_2 Pyrazabole – 5.4**

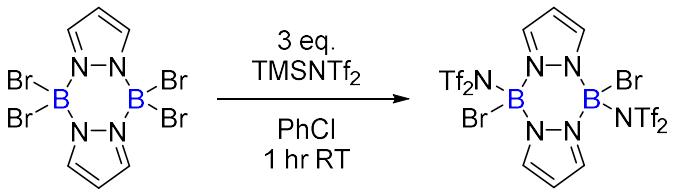

In a J. Young's NMR tube, $TMSNTf_2$ (0.3 mmol, 3 equiv.) was prepared *in situ* following **General Procedure 5.3** in PhCl (0.5 mL). To this was added *tetra*-bromo pyrazabole **5.6** (0.048 g, 0.1 mmol, 1 equiv.). The reaction was mixed by

inversion (approx. 1 rotation / s) at room temperature for 1 hour, until **5.6** had fully dissolved. The volatile TMSBr by-product was removed *in vacuo,* giving an oily residue. The reaction mixture was redissolved in d_2-DCM (0.5 mL). Analysis by NMR spectroscopy showed the conversion of **5.6** to *di*-bromo *di*-NTf_2 pyrazabole **5.4**, but with a significant amount of $TMSNTf_2$ leftover. The title product was characterised directly from this mixture.

^{1}H NMR (500 MHz, CD_2Cl_2) δ 8.68 (br, 4H, N=C*H*-CH), 7.01 (br, 2H, N=CH-C*H*);
^{11}B NMR (160 MHz, CD_2Cl_2) δ -1.1 (s, *B*(Br)NTf_2);
^{13}C{^{1}H} NMR (126 MHz, CD_2Cl_2) δ 144.51, 119.32 (q, $^1J_{CF}$ = 321 Hz, S*C*F_3), 111.72;
^{19}F NMR (471 MHz, CD_2Cl_2) δ -77.44 (s, SC*F*$_3$) ppm.
The title compound was not observed via mass spectrometry (both ESI and EI).

5.5.6 Reactivity of *Tetra*-Chloro Pyrazabole with $TMSNTf_2$ (Route 2)

Tri-Chloro _Mono_-NTf_2 Pyrazabole – 5.11

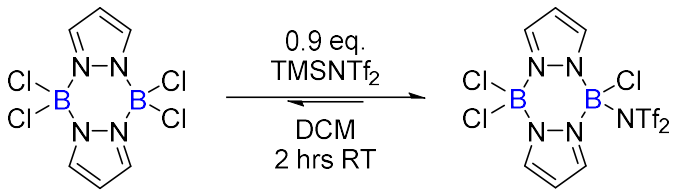

In a J. Young's NMR tube, $TMSNTf_2$ (0.09 mmol, 0.9 equiv.) was prepared *in situ* following **General Procedure 5.3** in DCM (0.5 mL). To this was added *tetra*-chloro pyrazabole **5.8** (0.030 g, 0.1 mmol, 1 equiv.). The reaction was mixed by inversion (approx. 1 rotation / s) at room temperature for 2 hours, until **5.8** had fully dissolved. All volatiles were removed *in vacuo*, and the reaction mixture was redissolved in d_2-DCM (0.5 mL). Analysis by NMR spectroscopy showed 75% conversion of **5.8** to *tri*-chloro *mono*-NTf_2 pyrazabole **5.11**. The title product was characterised directly from this mixture.

^{1}H NMR (500 MHz, CD_2Cl_2) δ 8.47 (br, 2H, N=C*H*-CH), 8.47 (br, 2H, N=C*H*-CH), 6.85 (t, $^3J_{HH}$ = 2.5 Hz, 2H, N=CH-C*H*);
^{11}B NMR (160 MHz, CD_2Cl_2) δ 2.2 (s, *B*(Cl)NTf_2), -1.8 (s, *B*Cl_2);
^{13}C{^{1}H} NMR (126 MHz, CD_2Cl_2) δ 141.37, 141.05, 119.03 (q, $^1J_{CF}$ = 321 Hz, S*C*F_3), 110.30;

^{19}F NMR (471 MHz, CD_2Cl_2) δ -77.40 (s, SC*F*$_3$) ppm.

*The title compound was not observed via mass spectrometry (both ESI and EI) and elemental analysis could not be obtained as **5.11** could not be isolated cleanly.*

Subsequent Conversion of 5.11 to the 4-DMAP-Boronium Ion (5.12)

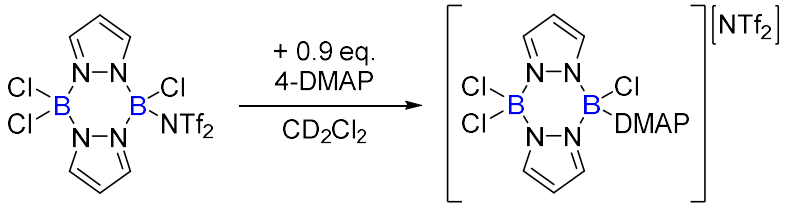

To the sample of **5.11** in CD_2Cl_2 was added 4-DMAP (0.010 g, 0.09 mmol, 0.9 equiv.). The reaction was mixed by inversion (approx. 1 rotation / s) at room temperature for 15 minutes, until 4-DMAP had fully dissolved. Analysis by NMR spectroscopy showed complete conversion of **5.11** to the title boronium ion, **5.12**, with any leftover **5.8** unreacted.

^{1}H NMR (500 MHz, CD_2Cl_2) δ 8.50 (br, 2H, N=C*H*-CH), 8.50 (br, 2H, N=C*H*-CH), 7.55 (m, 2H, 4-DMAP), 6.95 (t, $^{3}J_{HH}$ = 3 Hz, 2H, N=CH-C*H*) 6.75 (m, 2H, 4-DMAP), 3.20 (s, 6H, 4-DMAP);

^{11}B NMR (160 MHz, CD_2Cl_2) δ 2.2 (s, *B*Cl(4-DMAP)), 2.0 (s, *B*Cl$_2$);

^{13}C{^{1}H} NMR (126 MHz, CD_2Cl_2) δ 156.89, 141.11, 140.93, 140.93, 119.99 (q, $^{1}J_{CF}$ = 321 Hz, S*C*F$_3$), 110.43, 107.85, 40.06;

^{19}F NMR (471 MHz, CD_2Cl_2) δ -79.42 (s, SC*F*$_3$) ppm.

HRMS (ESI$^+$) *m/z* calcd for $C_{13}H_{16}B_2Cl_3N_6^+$: 383.06893 [M]$^+$, found 383.07021.

Reactivity of *Mono*-Electrophile 5.11 with *N*-Methyl Indole

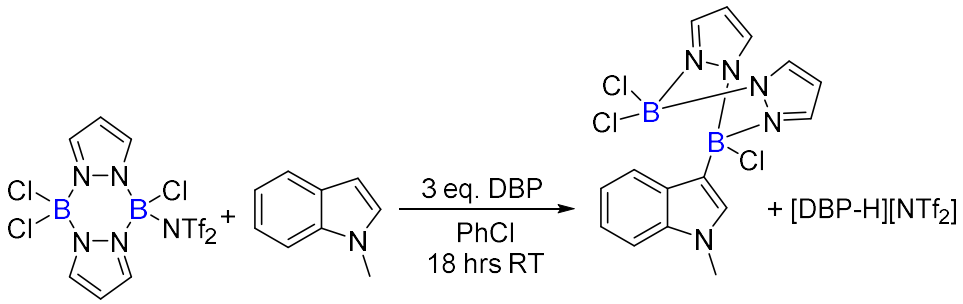

In a J. Young's NMR tube, $TMSNTf_2$ (0.12 mmol, 1.2 equiv.) was prepared *in situ* following **General Procedure 5.3** in PhCl (0.5 mL). To this was added *tetra*-

chloro pyrazabole **5.8** (0.030 g, 0.1 mmol, 1 equiv.). The reaction was mixed by inversion (approx. 1 rotation / s) at room temperature for 18 hours. All volatiles were then removed *in vacuo*, and the reaction mixture was redissolved in PhCl (0.5 mL). To the tube was then added DBP (0.062 g, 0.3 mmol, 3 equiv.), and the reaction was mixed by inversion at room temperature for 1 hour. To this was added *N*-methyl indole (0.013 mL, 0.1 mmol, 1 equiv.), and the reaction was mixed by inversion at room temperature for 18 hours, during which time a brown solid precipitated. All volatiles were then removed *in vacuo*, and the resulting solid was redissolved in d_2-DCM (2 mL) and mixed by inversion until fully homogeneous. The sample was then analysed by NMR spectroscopy.

Conversion of the borylated intermediates to 'ArBpin' was achieved following **General Procedure 5.2**. The major Bpin product had analytical data that are in accordance with literature values for 3-Bpin *N*-methyl indole.[24]

***Di*-Chloro *Di*-NTf$_2$ Pyrazabole – 5.7**

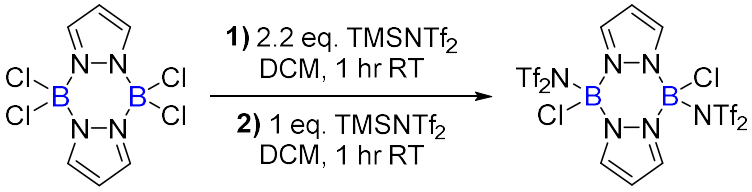

In a J. Young's NMR tube, TMSNTf$_2$ (0.22 mmol, 2.2 equiv.) was prepared *in situ* following **General Procedure 5.3** in DCM (0.5 mL). To this was added *tetra*-chloro pyrazabole **5.8** (0.048 g, 0.1 mmol, 1 equiv.). The reaction was mixed by inversion (approx. 1 rotation / s) at room temperature for 1 hour, until **5.8** had fully dissolved. The volatile TMSCl by-product was removed *in vacuo,* giving an oily residue. To the residue was added TMSNTf$_2$ (0.1 mmol, 1 equiv., prepared following **General Procedure 5.3**) in DCM (0.5 mL). The reaction was mixed by inversion (approx. 1 rotation / s) at room temperature for 1 hour, and the volatiles were again removed *in vacuo*. The residue was then redissolved in d_2-DCM (0.5 mL). Analysis by NMR spectroscopy showed the complete conversion of **5.8** to *di*-chloro *di*-NTf$_2$ pyrazabole **5.7**, but with a significant amount of TMSNTf$_2$ leftover. The title product was characterised directly from this mixture.

^{1}H NMR (500 MHz, CD_2Cl_2) δ 8.57 (d, $^{3}J_{HH}$ = 3 Hz, 4H, N=C*H*-CH), 6.98 (d, $^{3}J_{HH}$ = 3 Hz, 2H, N=CH-C*H*);

^{11}B NMR (160 MHz, CD_2Cl_2) δ 1.9 (s, *B*(Cl)NTf_2);

^{13}C{^{1}H} NMR (126 MHz, CD_2Cl_2) δ 143.03, 119.23 (q, $^{1}J_{CF}$ = 321 Hz, S*C*F_3), 111.43;

^{19}F NMR (471 MHz, CD_2Cl_2) δ -77.37 (s, SC*F*$_3$) ppm.

The title compound was not observed via mass spectrometry (both ESI and EI).

5.5.7 X-Ray Crystallography

_Di_-Chloro Pyrazabole – 5.3

Experimental: Single colourless plate-shaped crystals of **5.3** were recrystallised from a mixture of hexane and dichloromethane by vapour diffusion. A suitable crystal with dimensions 0.36 × 0.23 × 0.03 mm^3 was selected and mounted on a MITIGEN holder in Paratone oil on a Bruker APEX-II CCD diffractometer. The crystal was kept at a steady T = 100.00 K during data collection. The structure was solved with the ShelXT 2018/2[33] solution program using dual methods and by using Olex2 1.5-beta[34] as the graphical interface. The model was refined with olex2.refine 1.5-beta[35] using full matrix least squares minimisation on F^2.

Crystal Data:

Formula	$C_6H_8B_2Cl_2N_4$
$D_{calc.}$ / g cm^{-3}	1.552
μ /mm^{-1}	0.622
Formula Weight	228.711
Colour	Colourless
Shape	Plate-Shaped
Size/ mm^3	0.36 × 0.23 × 0.03
T/ K	100.00
Crystal System	Triclinic
Space Group	*P*-1
a /Å	7.1489(3)
b /Å	7.1845(3)
c /Å	10.7250(4)
α /°	100.601(1)
β /°	94.102(2)
γ /°	113.637(1)
V / Å^3	489.52(4)
Z	2
Z'	1
Wavelength / Å	0.71073
Radiation type	Mo K_α
Θ_{min} /°	3.15
Θ_{max} /°	36.33
Measured Refl's.	48005
Indep't Refl's	4720
Refl's I≥2 σ(I)	4067
R_{int}	0.0360
Parameters	199
Restraints	0
Largest Peak	0.2385
Deepest Hole	-0.2556
GooF	1.0703
wR_2 (all data)	0.0323
wR_2	0.0297
R_1 (all data)	0.0255
R_1	0.0182

5.6 References

1 J. Kalepu, P. Gandeepan, L. Ackermann and L. T. Pilarski, *Chem. Sci.*, 2018, **9**, 4203–4216.

2 J. Wen and Z. Shi, *Acc. Chem. Res.*, 2021, **54**, 1723–1736.

3 J. Pahl, E. Noone, M. Uzelac, K. Yuan and M. J. Ingleson, *Angew. Chem. Int. Ed.*, 2022, **61**, e202206230.

4 C. R. P. Millet, E. Noone, A. V. Schellbach, J. Pahl, J. Łosiewicz, G. S. Nichol and M. J. Ingleson, *Chem. Sci.*, 2023, **14**, 12041–12048.

5 V. A. Kallepalli, F. Shi, S. Paul, E. N. Onyeozili, R. E. Maleczka Jr. and M. R. Smith III, *J. Org. Chem.*, 2009, **74**, 9199–9201.

6 S. M. Preshlock, D. L. Plattner, P. E. Maligres, S. W. Krska, R. E. Maleczka Jr. and M. R. Smith III, *Angew. Chem. Int. Ed.*, 2013, **52**, 12915–12919.

7 J. S. Wright, P. J. H. Scott and P. G. Steel, *Angew. Chem. Int. Ed.*, 2021, **60**, 2796–2821.

8 H. C. Brown and B. C. S. Rao, *J. Am. Chem. Soc.*, 1956, **78**, 5694–5695.

9 H. C. Brown and M. V. Rangaishenvi, *J. Heterocycl. Chem.*, 1990, **27**, 13–24.

10 S. Kirschner, K. Yuan and M. J. Ingleson, *New J. Chem.*, 2021, **45**, 14855–14868.

11 C. Wang and M. Uchiyama, *Eur. J. Org. Chem.*, 2012, **2012**, 6548–6554.

12 S. Trofimenko, *J. Am. Chem. Soc.*, 1967, **89**, 4948–4952.

13 N. A. Lange and J. A. Dean, *Lange's handbook of chemistry*, McGraw-Hill, New York, 15th ed., 1998.

14 K. Niedenzu and H. Nöth, *Chem. Ber.*, 1983, **116**, 1132–1153.

15 E. Hanecker, T. G. Hodgkins, K. Niedenzu and H. Noeth, *Inorg. Chem.*, 1985, **24**, 459–462.

16 W. J. Layton, K. Niedenzu, P. M. Niedenzu and S. Trofimenko, *Inorg. Chem.*, 1985, **24**, 1454–1457.

17 C. M. Clarke, M. K. Das, E. Hanecker, J. F. Mariategui, K. Niedenzu, P. M. Niedenzu, H. Noeth and K. R. Warner, *Inorg. Chem.*, 1987, **26**, 2310–2317.

18 C. I. Nieto, D. Sanz, R. M. Claramunt, I. Alkorta and J. Elguero, *Coord. Chem. Rev.*, 2022, **473**, 214812.

19 S. Nerkar and D. P. Curran, *Org. Lett.*, 2015, **17**, 3394–3397.

20 E. R. Clark, A. Del Grosso and M. J. Ingleson, *Chem. Eur. J.*, 2013, **19**, 2462–2466.

21 J. M. Farrell, J. A. Hatnean and D. W. Stephan, *J. Am. Chem. Soc.*, 2012, **134**, 15728–15731.

22 K. Yuan, D. Volland, S. Kirschner, M. Uzelac, G. S. Nichol, A. Nowak-Król and M. J. Ingleson, *Chem. Sci.*, 2022, **13**, 1136–1145.

23 A. Escande, D. L. Crossley, J. Cid, I. A. Cade, I. Vitorica-Yrezabal and M. J. Ingleson, *Dalton Trans.*, 2016, **45**, 17160–17167.

24 L. Britton, J. H. Docherty, G. S. Nichol, A. P. Dominey and S. P. Thomas, *Chin. J. Chem.*, 2022, **40**, 2875–2881.

25 S. Zhang, Y. Han, J. He and Y. Zhang, *J. Org. Chem.*, 2018, **83**, 1377–1386.

26 A. Solovyev, Q. Chu, S. J. Geib, L. Fensterbank, M. Malacria, E. Lacôte and D. P. Curran, *J. Am. Chem. Soc.*, 2010, **132**, 15072–15080.

27 B. Mathieu and L. Ghosez, *Tetrahedron*, 2002, **58**, 8219–8226.

28 Q. Zhuo, J. Yang, Z. Mo, X. Zhou, T. Shima, Y. Luo and Z. Hou, *J. Am. Chem. Soc.*, 2022, **144**, 6972–6980.

29 A. Glüer, J. I. Schweizer, U. S. Karaca, C. Würtele, M. Diefenbach, M. C. Holthausen and S. Schneider, *Inorg. Chem.*, 2018, **57**, 13822–13828.

30 A. Shvartsbart and A. Smith, *J. Am. Chem. Soc.*, 2014, **136**, 870–873.

31 Q.-A. Chen, H. F. T. Klare and M. Oestreich, *J. Am. Chem. Soc.*, 2016, **138**, 7868–7871.

32 A. Prokofjevs, J. Jermaks, A. Borovika, J. W. Kampf and E. Vedejs, *Organometallics*, 2013, **32**, 6701–6711.

33 G. M. Sheldrick, *Acta Cryst. A*, 2015, **71**, 3–8.

34 O. V. Dolomanov, L. J. Bourhis, R. J. Gildea, J. a. K. Howard and H. Puschmann, *J. Appl. Cryst.*, 2009, **42**, 339–341.

35 L. J. Bourhis, O. V. Dolomanov, R. J. Gildea, J. a. K. Howard and H. Puschmann, *Acta Cryst. A*, 2015, **71**, 59–75.

Chapter 6

Thesis Summary and Outlook

Chapter 6: Thesis Summary and Outlook

This thesis sought to extend the scope of directed electrophilic C-H borylation of (hetero)arenes by addressing two under-developed areas: (i) the use of O-H as a directing group, and (ii) the use of transient directing groups.

In **Chapter 2**, the potential utility of the O-H of benzyl alcohols as a directing group was investigated, with the aim of producing medicinally relevant benzoxaboroles via an oxygen-directed electrophilic C-H borylation process. However, this work was unsuccessful and conditions to facilitate intramolecular arene C-H borylation could not be identified. Though the O-H directing group was able to covalently bond to the boron electrophiles, this either resulted in benzyl cleavage (with haloborane electrophiles) or the generation of insufficiently electrophilic NHC-borenium ions for arene C-H borylation (with NHC-BH_2NTf_2 electrophiles). The synthesis of benzoxaboroles via directed electrophilic C-H borylation was later achieved by Rej and Chatani via the *in situ* conversion of the carbonyl moiety of benzaldehyde for a transient imine directing group, therefore avoiding the issues observed in this chapter.

The work by Rej and Chatani demonstrates that the development of transient directing groups for electrophilic C-H borylation is likely to be a important area of future research within this field. **Chapters 3**, **4** and **5** focussed on the application of a ditopic boron electrophile, pyrazabole, as a transient directing group in the electrophilic C-H borylation of indoles and indolines. **Chapter 3** provides an initial proof of concept that activated pyrazabole electrophiles can act as traceless directing groups for the C7-H borylation of indoles/indolines, owing to their suitable B···B distance for double N/C7-H borylation and their ability to be converted into useful organoborane units (C-Bpin) within a one-pot process. This was initially achieved using $HNTf_2$ as the activator (**Chapter 3**), but subsequent work has also demonstrated the use of I_2 as a cheaper and easier to handle alternative (**Chapter 4**). However, the higher coordination strength of I^- (relative to $[NTf_2]^-$) decreases the yields of C7-H borylation.

Other activators (e.g. HOTf, $B(C_6F_5)_3$, and $[Ph_3C]^+$ salts) may also be suitable for this process, but the current requirement for stoichiometric amounts of the activator reduces the efficiency of this process. Establishing conditions that enable the reaction to be catalytic in activator is therefore a key area for future study. This will likely require a dehydrocoupling step between the Brønsted acidic by-product from C-H borylation and the starting pyrazabole species, therefore enabling regeneration of the active pyrazabole electrophile.

Further variation of the pyrazabole unit may enable pyrazabole-based transient directing groups to be applied to other substrates, or enable the regioselectivity of electrophilic C-H borylation to be altered. To this end, **Chapter 5** explored synthetic routes to ditopic pyrazabole electrophiles that lack B-H bonds. It was hoped that by replacing the B-H bonds with B-X bonds, this would prevent indole reduction and enable C3/C4-diborylation. However, studies with NTf_2-based activators have thus far not been successful in generating significant amounts of the desired *di*-NTf_2 *di*-halo pyrazabole electrophiles. Other activators, such as AlX_3, may be more suitable and enable the desired reactivity. Further modification of the pyrazabole backbone and boron substituents may also enable the scope of pyrazabole-based transient directing groups to be expanded to other (hetero)arene substrates, hence there is significantly more work that can be done in this field. The generation of other diboron electrophiles with different B···B separations is also an important avenue for further investigation.

Directed Electrophilic C-H Borylation using Lewis-Base Stabilised Boranes

Thesis Appendix

Emily Noone

School of Chemistry

University of Edinburgh

2024

Note: Any NMR spectra for data that has already been published is included in the supplementary information of that publication, and not included below.

Table of Contents

Chapter 2: Attempted Synthesis of Benzoxaboroles via O-Directed Electrophilic Borylation

2.5.2 – Reactivity with Haloboranes

Attempted C-H Borylation of 3-Fluorobenzyl alcohol with BCl_3

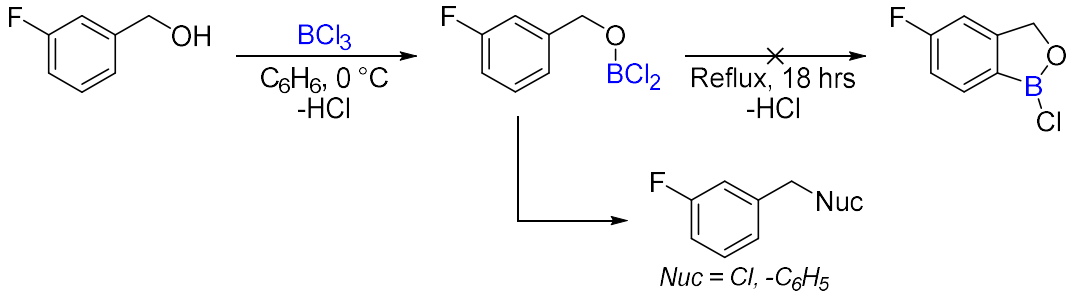

- ***In situ* NMR, 18 hrs Reflux:**

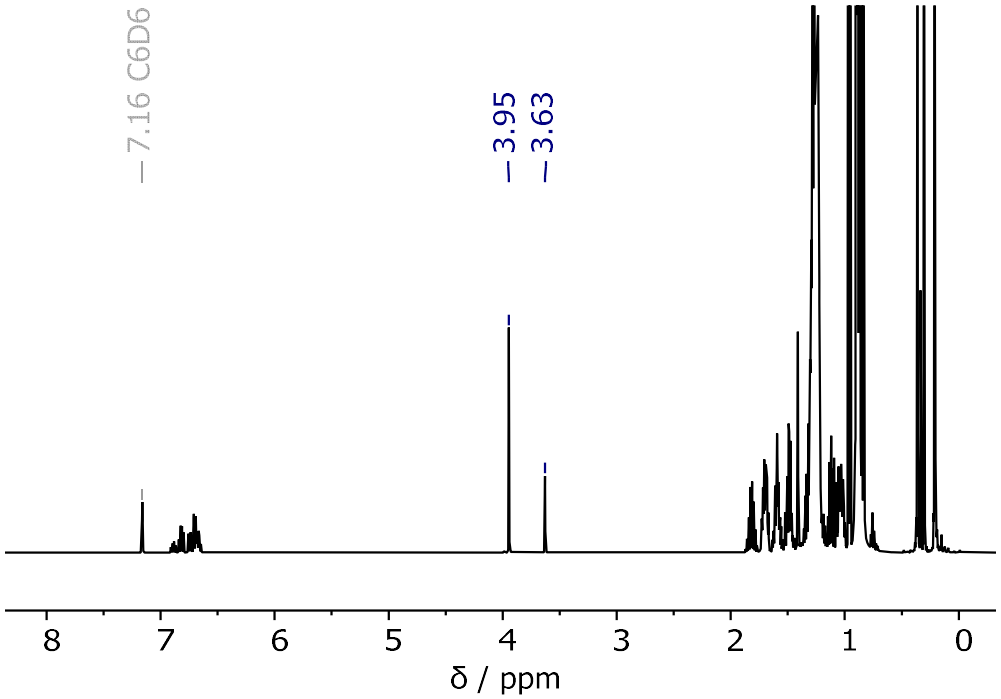

Figure 2.1: ^1H NMR (500 MHz, C_6D_6) spectrum of the reaction of 3-fluorobenzyl alcohol and 3 equiv. BCl_3, after 18 hrs at reflux.

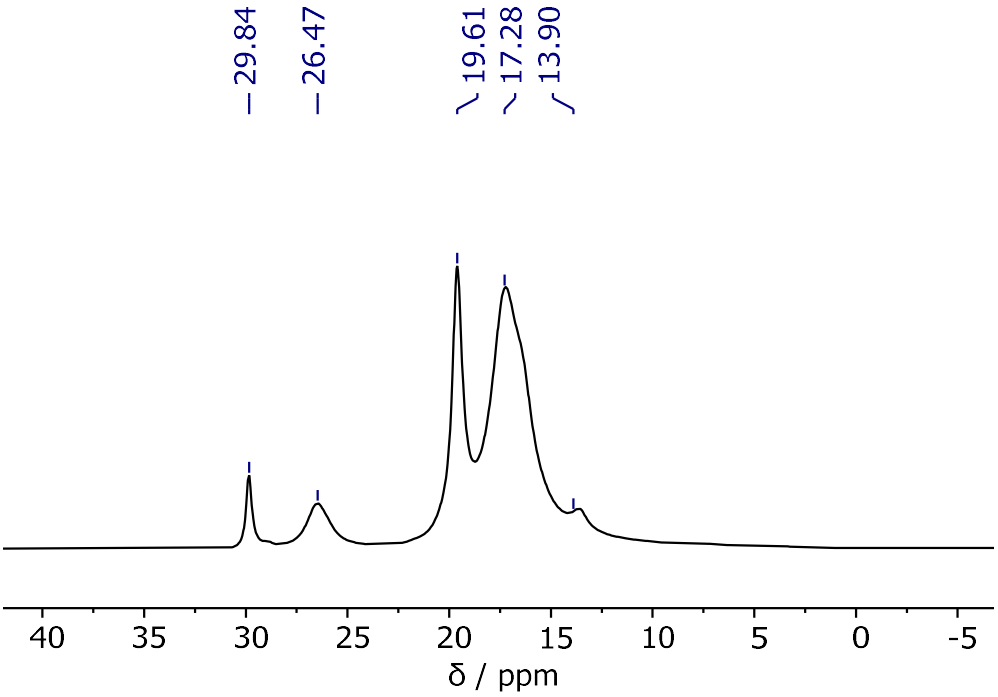

Figure 2.2: ^{11}B NMR (161 MHz, C_6D_6) spectrum of the reaction of 3-fluorobenzyl alcohol and 3 equiv. BCl_3, after 18 hrs at reflux.

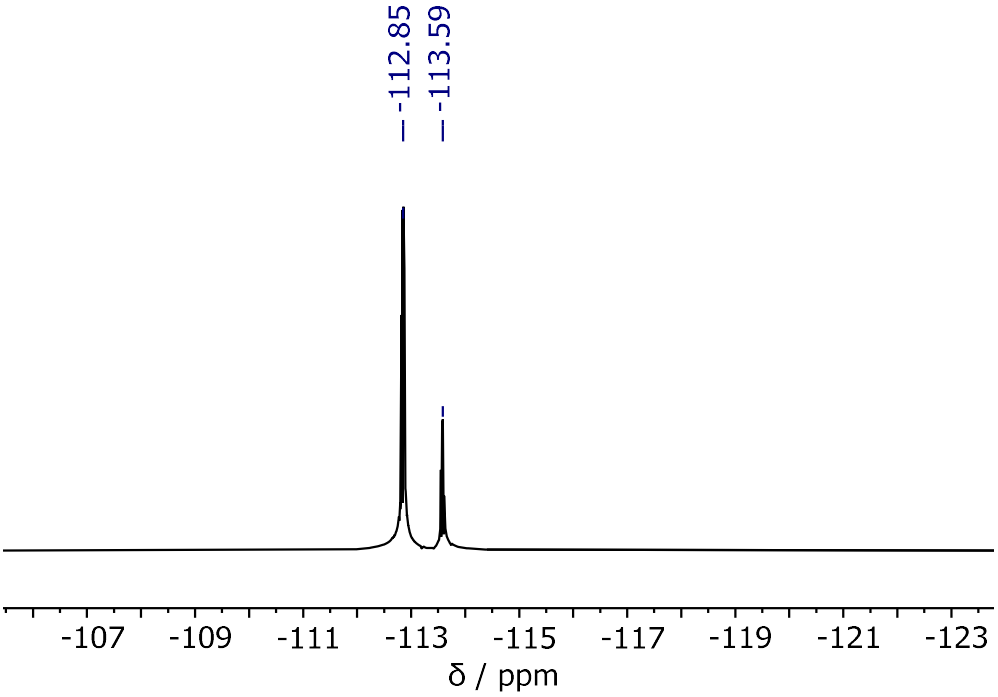

Figure 2.3: $^{13}C\{^1H\}$ NMR (126 MHz, C_6D_6) spectrum of the reaction of 3-fluorobenzyl alcohol and 3 equiv. BCl_3, after 18 hrs at reflux.

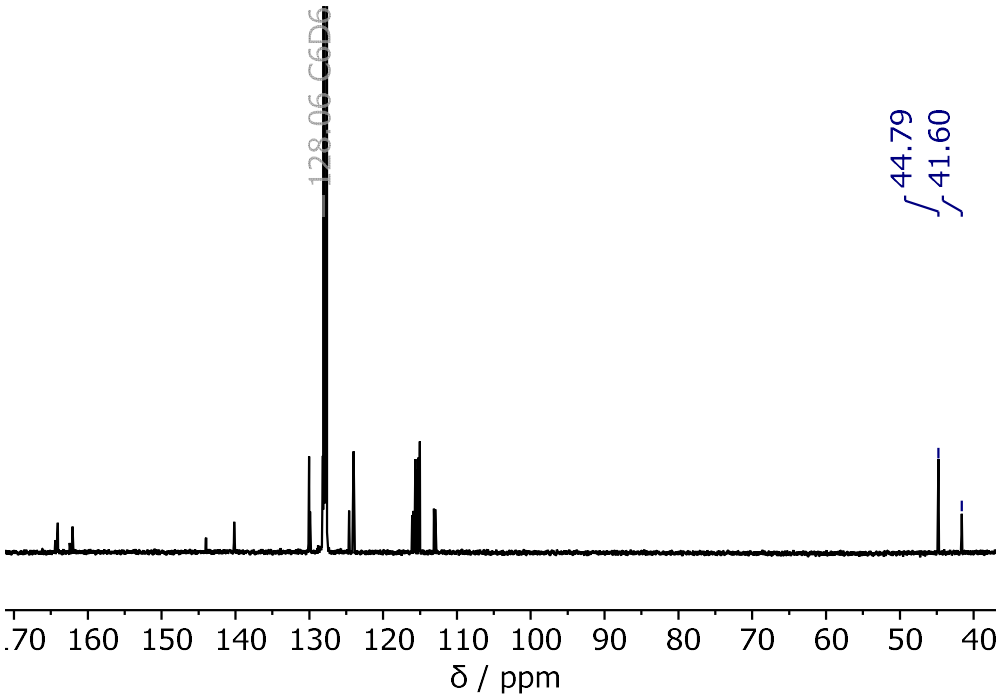

Figure 2.4: ^{19}F NMR (471 MHz, C_6D_6) spectrum of the reaction of 3-fluorobenzyl alcohol and 3 equiv. BCl_3, after 18 hrs at reflux.

- **Following chromatography: Isolated benzyl products**

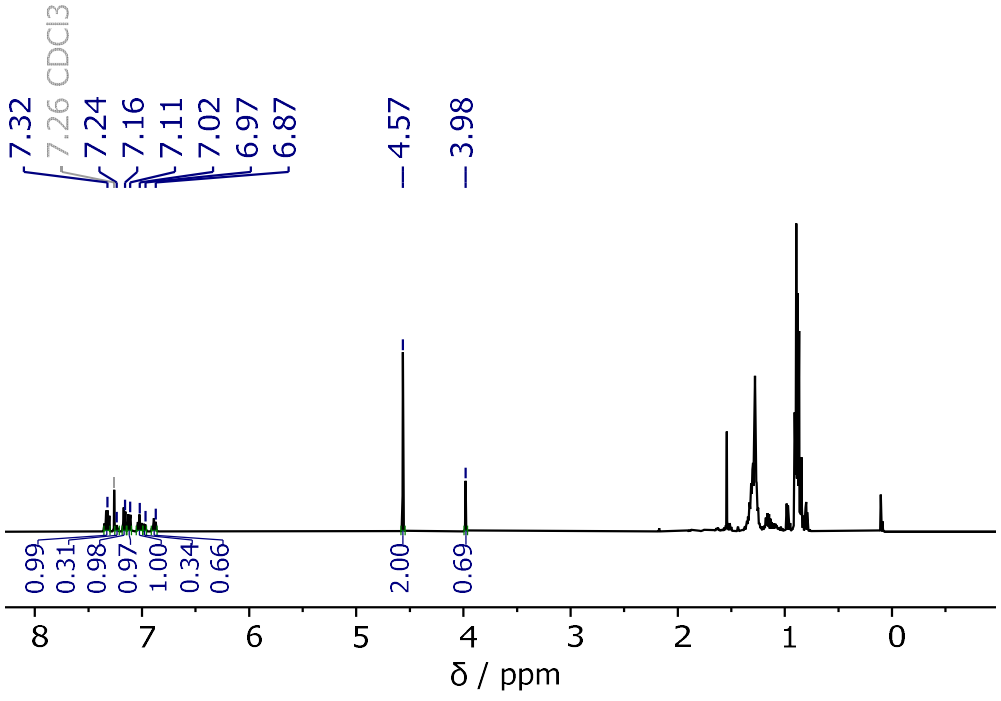

Figure 2.5: ^{1}H NMR (500 MHz, $CDCl_3$) spectrum of two benzyl products isolated from the reaction of 3-fluorobenzyl alcohol and BCl_3. *Note – some pet. ether remains.*

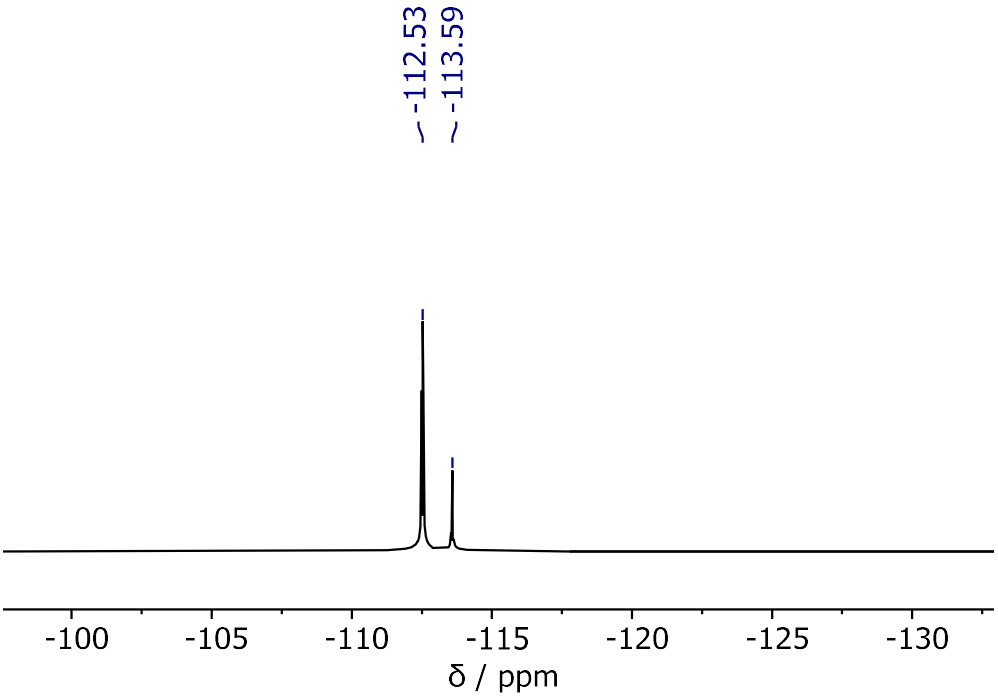

Figure 2.6: ^{19}F NMR (471 MHz, $CDCl_3$) spectrum of two benzyl products isolated from the reaction of 3-fluorobenzyl alcohol and BCl_3.

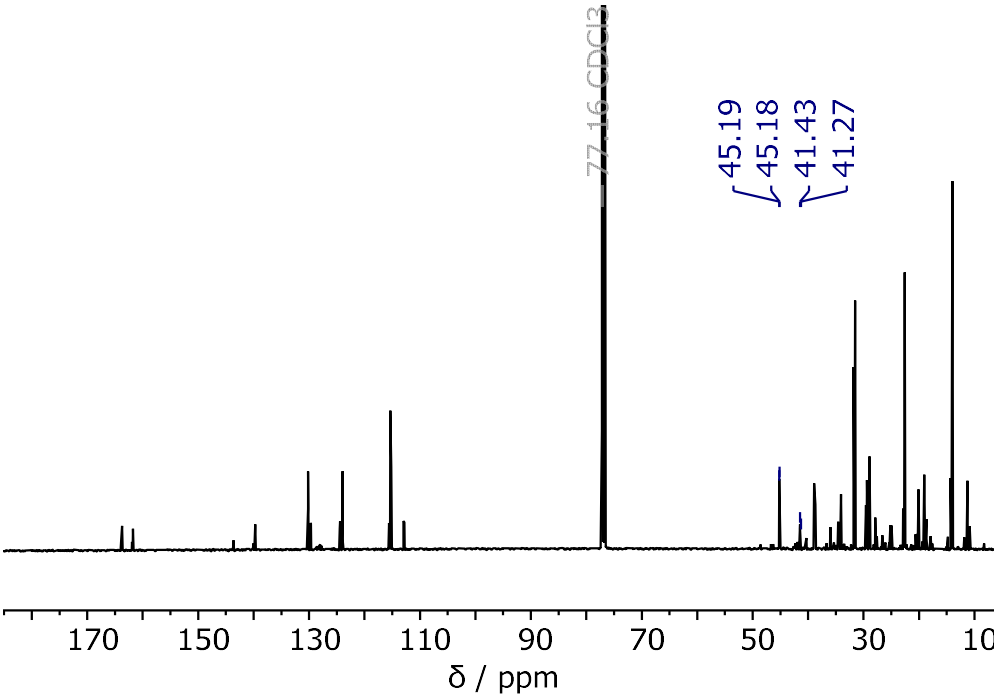

Figure 2.7: $^{13}C\{^1H\}$ NMR (126 MHz, $CDCl_3$) spectrum of two benzyl products isolated from the reaction of 3-fluorobenzyl alcohol and BCl_3. *Note – some pet. ether remains.*

Attempted Hydroboration/C-H Borylation of Benzaldehyde with $HBCl_2$

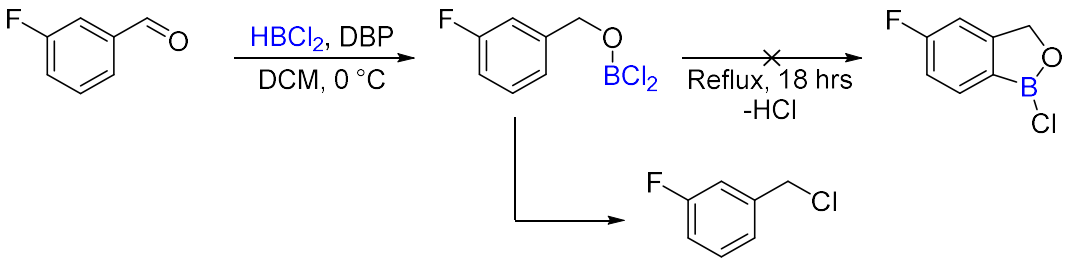

- ***In situ* NMR, 24 hrs 60 °C:**

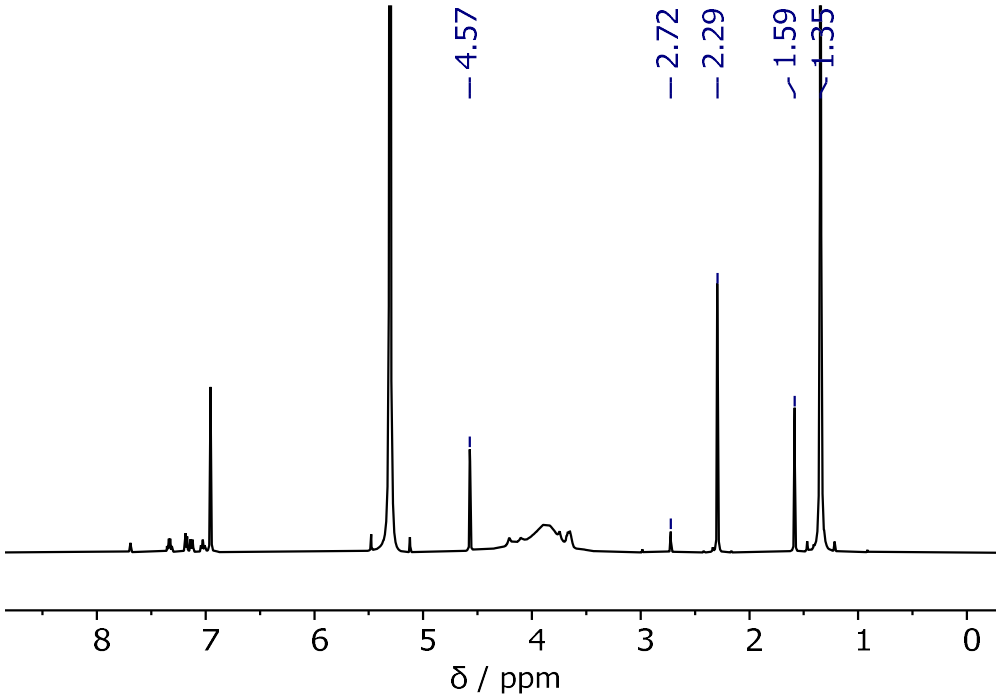

Figure 2.8: ^1H NMR (500 MHz, CH_2Cl_2) spectrum of the reaction of 3-fluorobenzaldehyde and 2 equiv. $HBCl_2$ and 2 equiv. DBP after 24 hrs at 60 °C.

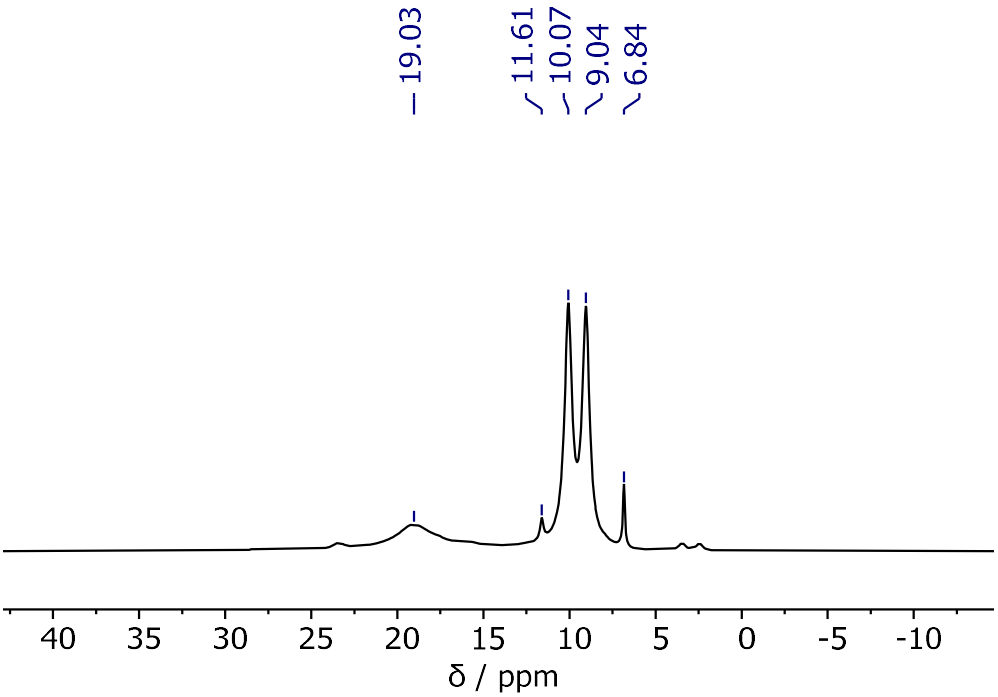

Figure 2.9: ^{11}B NMR (161 MHz, CH_2Cl_2) spectrum of the reaction of 3-fluorobenzaldehyde and 2 equiv. $HBCl_2$ and 2 equiv. DBP after 24 hrs at 60 °C.

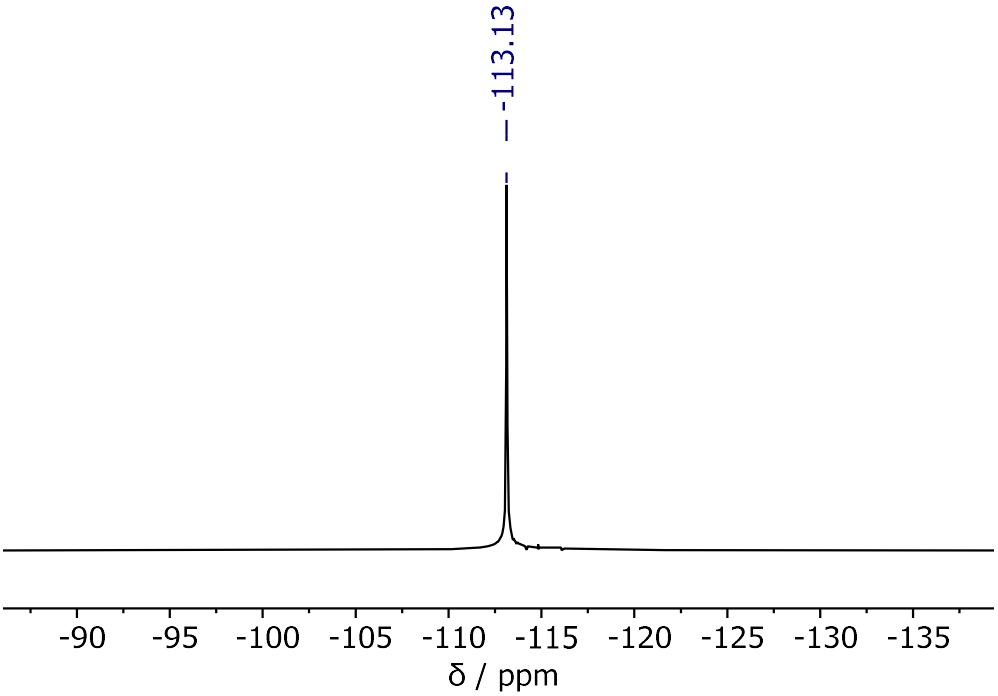

Figure 2.10: $^{13}C\{^1H\}$ NMR (126 MHz, CH_2Cl_2) spectrum of the reaction of 3-fluorobenzaldehyde and 2 equiv. $HBCl_2$ and 2 equiv. DBP after 24 hrs at 60 °C.

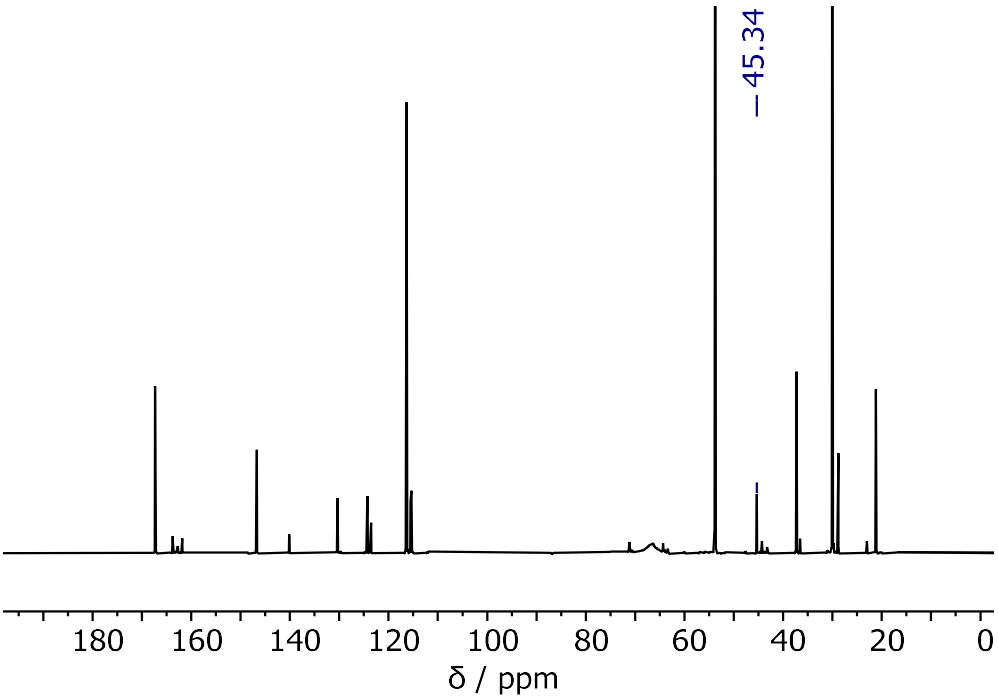

Figure 2.11: ^{19}F NMR (471 MHz, CH_2Cl_2) spectrum of the reaction of 3-fluorobenzaldehyde and 2 equiv. $HBCl_2$ and 2 equiv. DBP after 24 hrs at 60 °C.

2.5.3 – Synthesis of NHC-Boranes

$IMeBH_3$ (2.6)

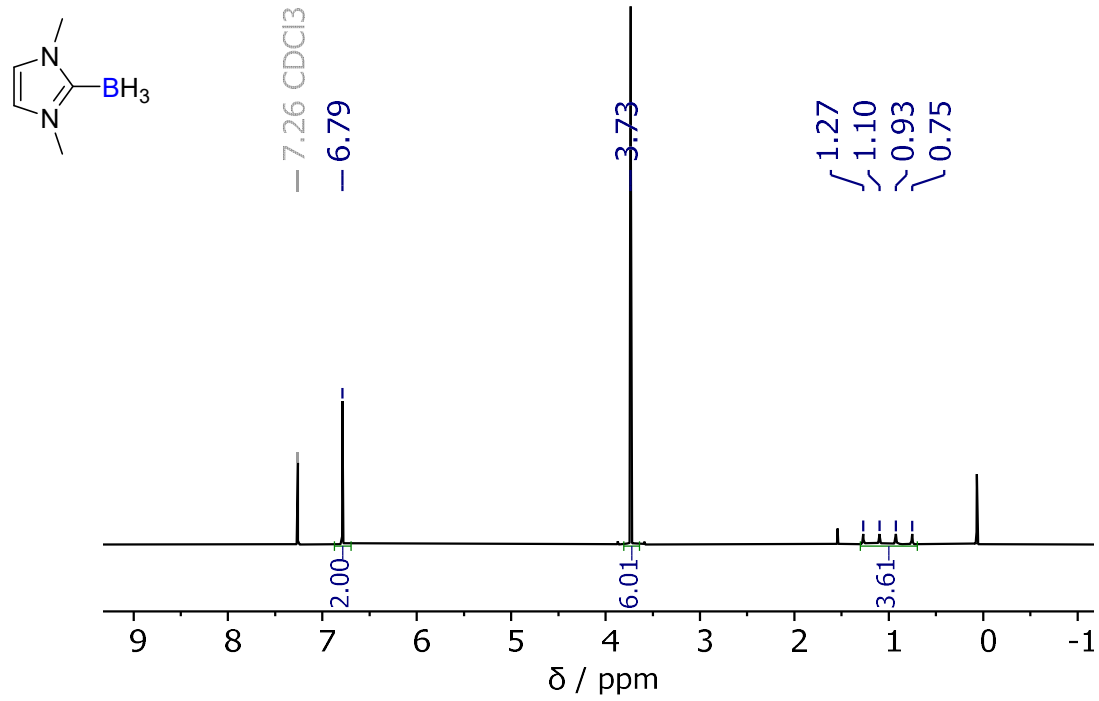

Figure 2.12: ^{1}H NMR (500 MHz, $CDCl_3$) spectrum of $IMeBH_3$.

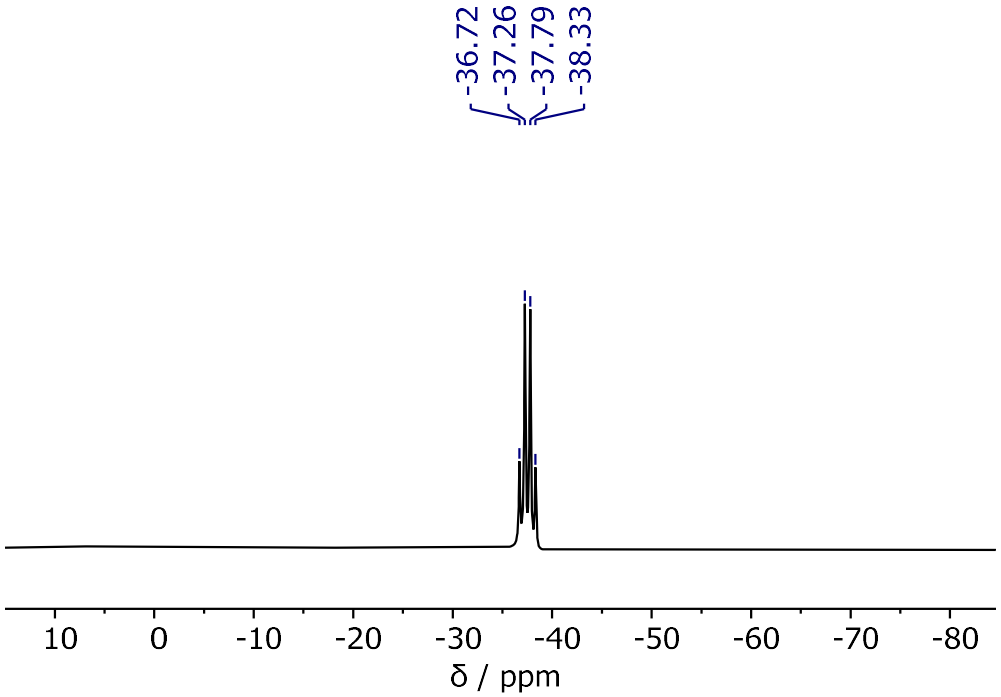

Figure 2.13: ^{11}B NMR (161 MHz, $CDCl_3$) spectrum of $IMeBH_3$.

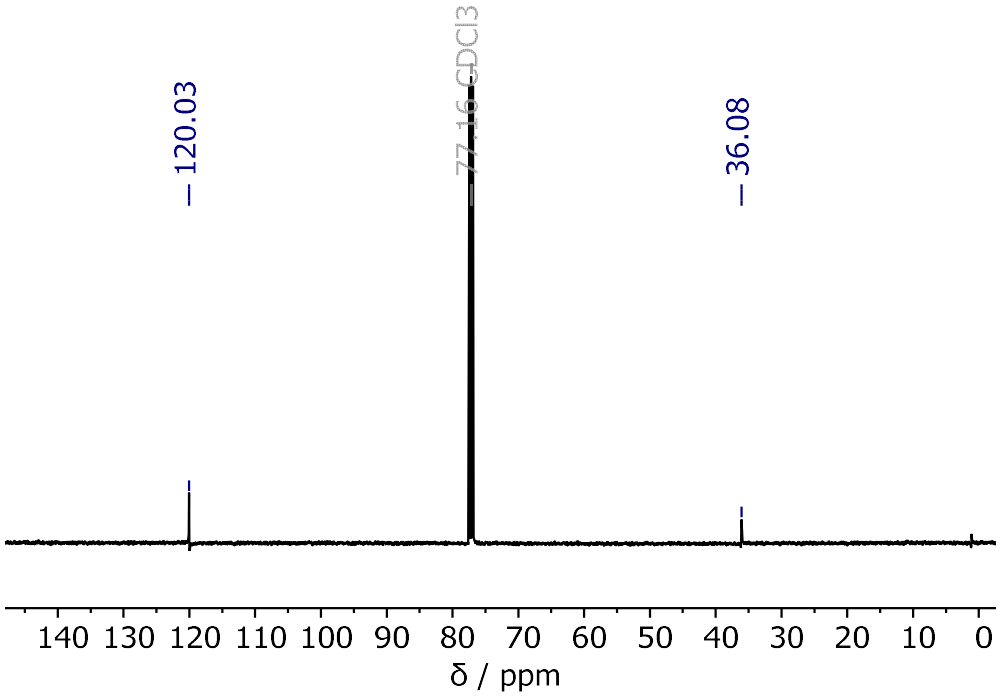

Figure 2.14: $^{13}C\{^{1}H\}$ NMR (126 MHz, $CDCl_3$) spectrum of $IMeBH_3$.

I^iPrBH_3 (2.11)

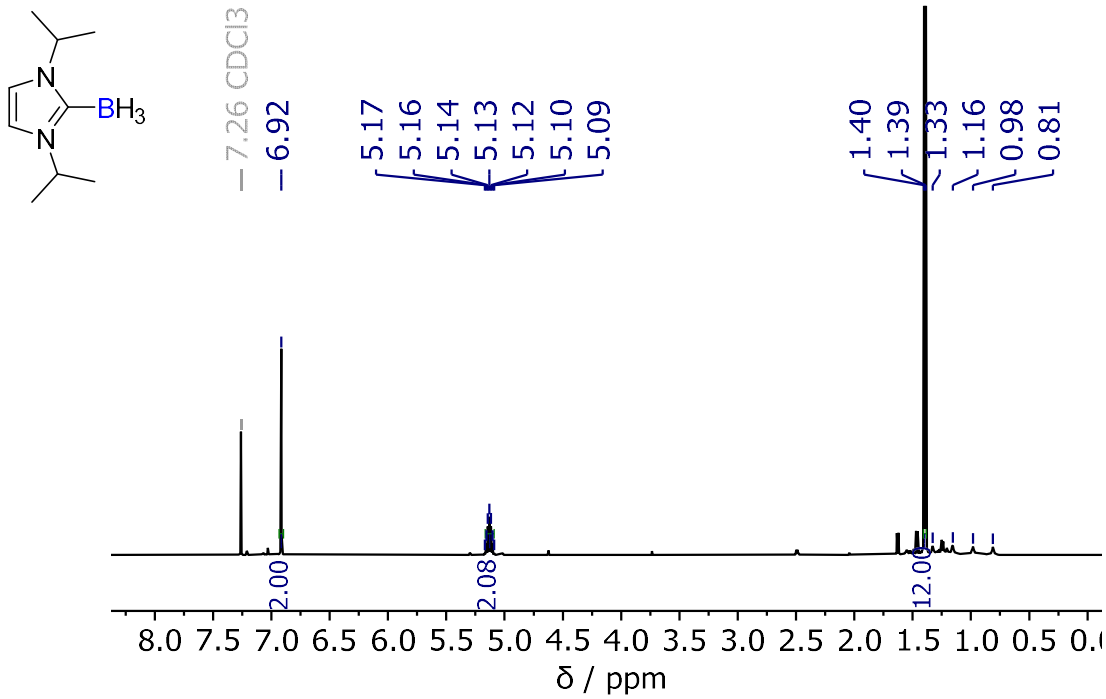

Figure 2.15: ^{1}H NMR (500 MHz, $CDCl_3$) spectrum of I^iPrBH_3.

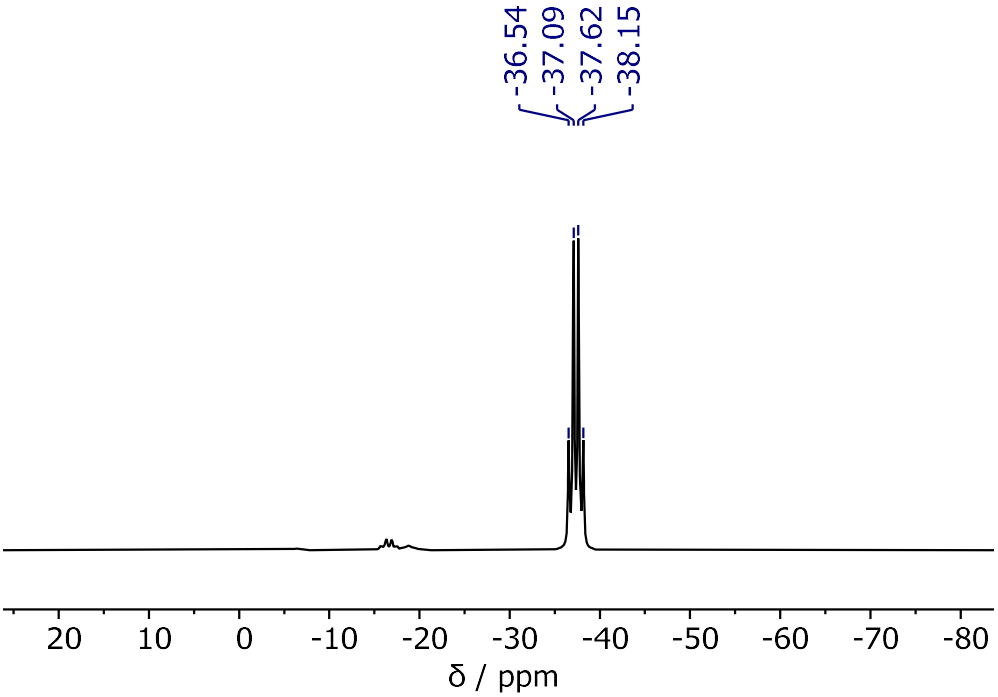

Figure 2.16: ^{11}B NMR (161 MHz, $CDCl_3$) spectrum of I^iPrBH_3.

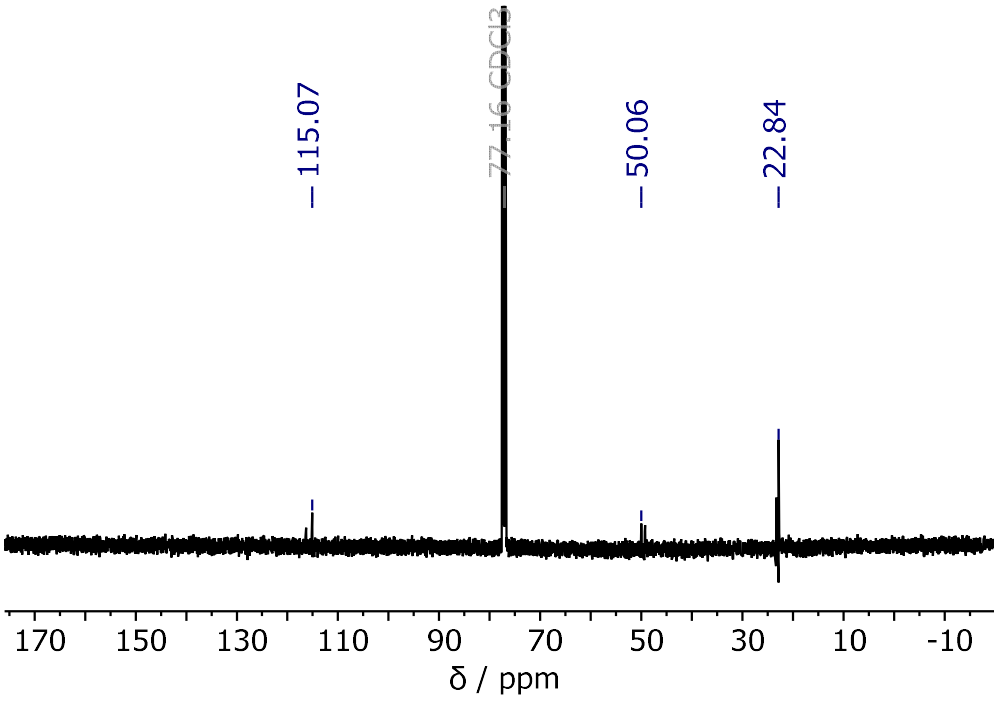

Figure 2.17: $^{13}C\{^1H\}$ NMR (126 MHz, $CDCl_3$) spectrum of I^iPrBH_3.

$IMesBH_3$ (2.15)

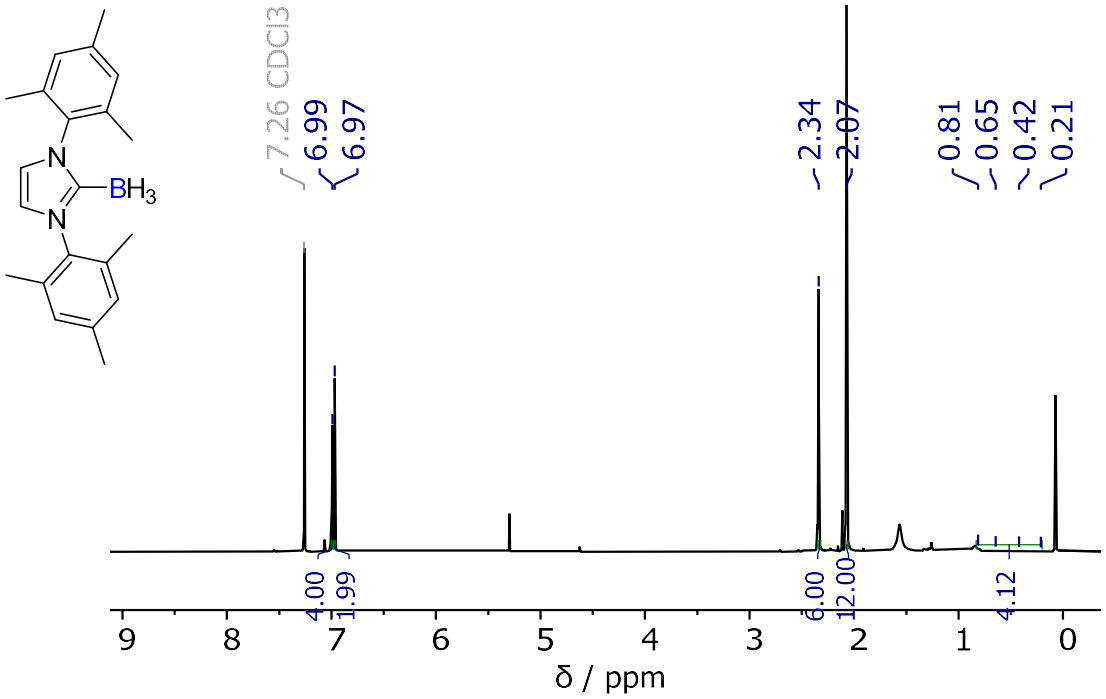

Figure 2.18: ^{1}H NMR (400 MHz, $CDCl_3$) spectrum of $IMesBH_3$.

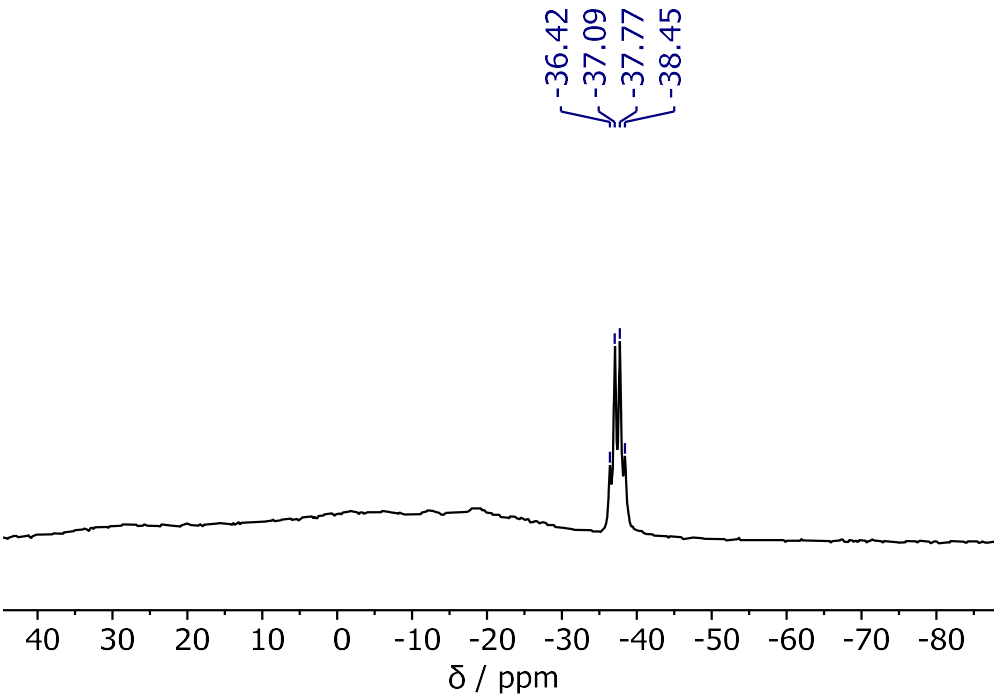

Figure 2.19: ^{11}B NMR (128 MHz, $CDCl_3$) spectrum of $IMesBH_3$.

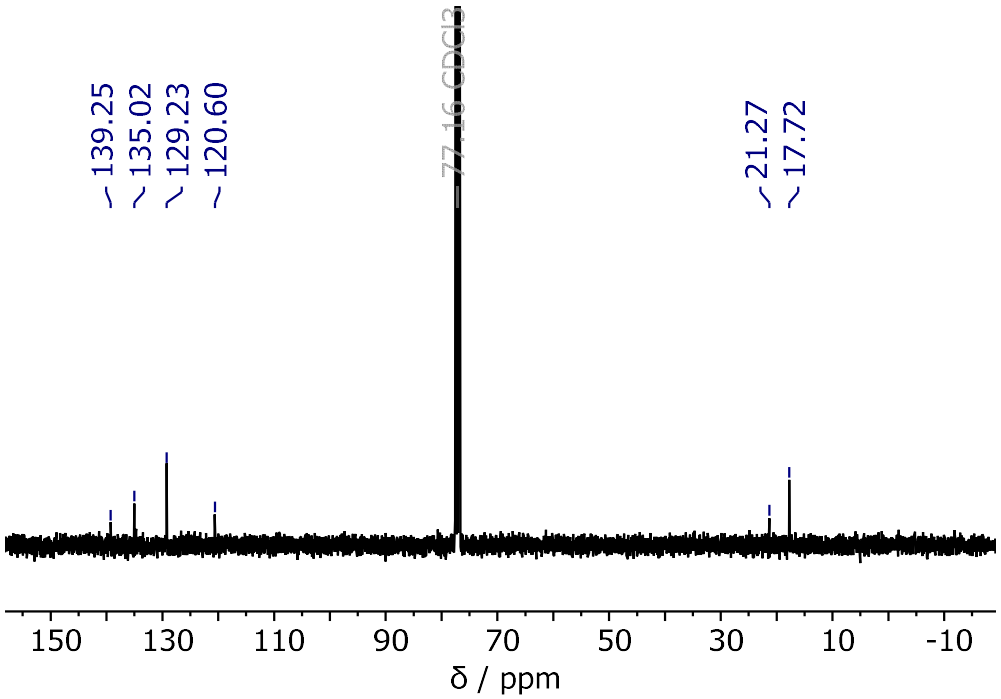

Figure 2.20: $^{13}C\{^{1}H\}$ NMR (101 MHz, $CDCl_3$) spectrum of $IMesBH_3$.

2.5.4 – Characterising Addition Products: 3-Fluorobenzyl Alcohol and NHC-Boranes

Activation of $IMeBH_3$ to $IMeBH_2NTf_2$ (2.7)

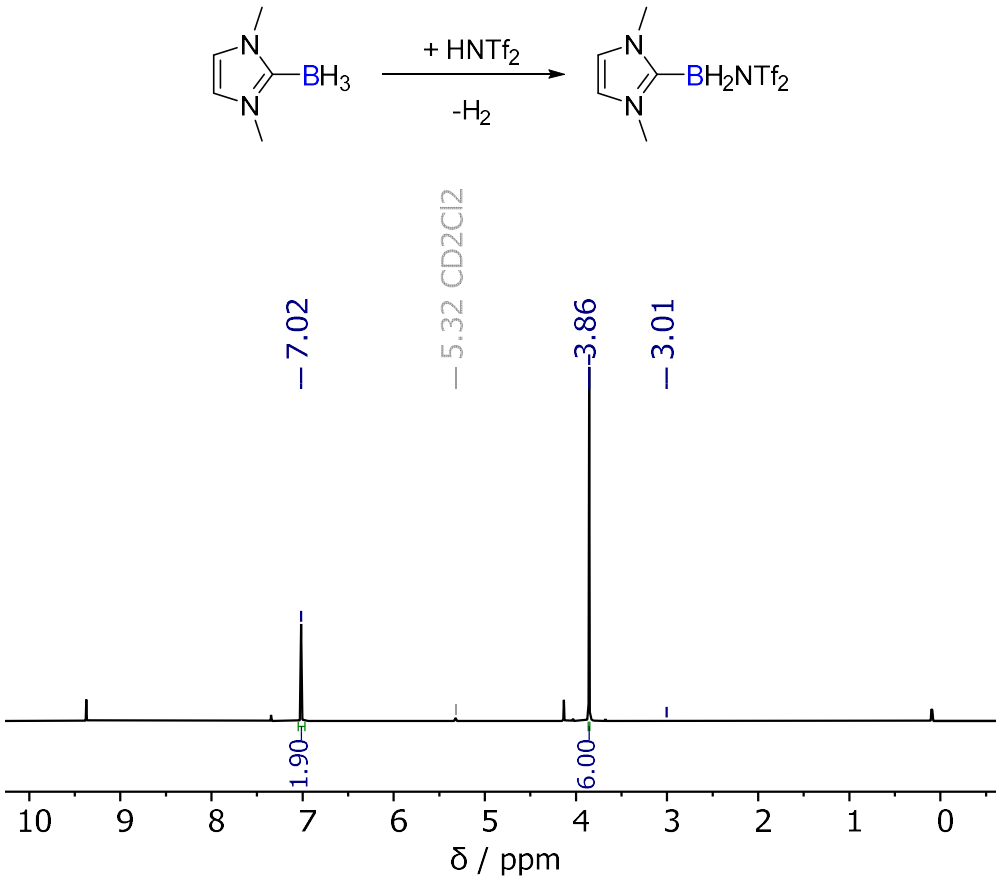

Figure 2.21: ^1H NMR (400 MHz, CD_2Cl_2) spectrum of $IMeBH_2NTf_2$.

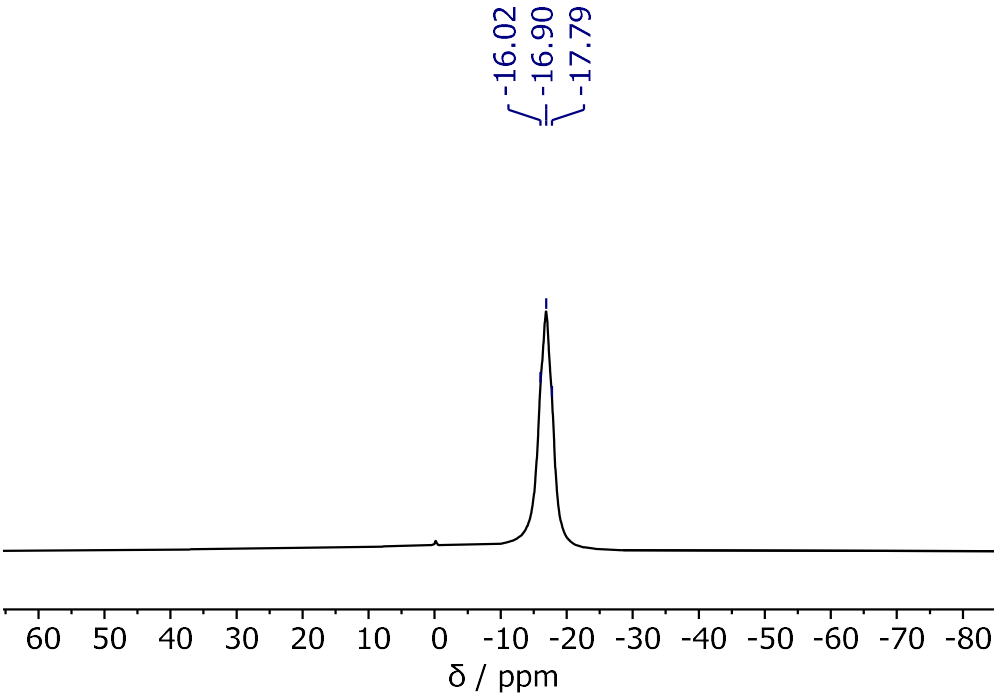

Figure 2.22: ^{11}B NMR (128 MHz, CD_2Cl_2) spectrum of $IMeBH_2NTf_2$.

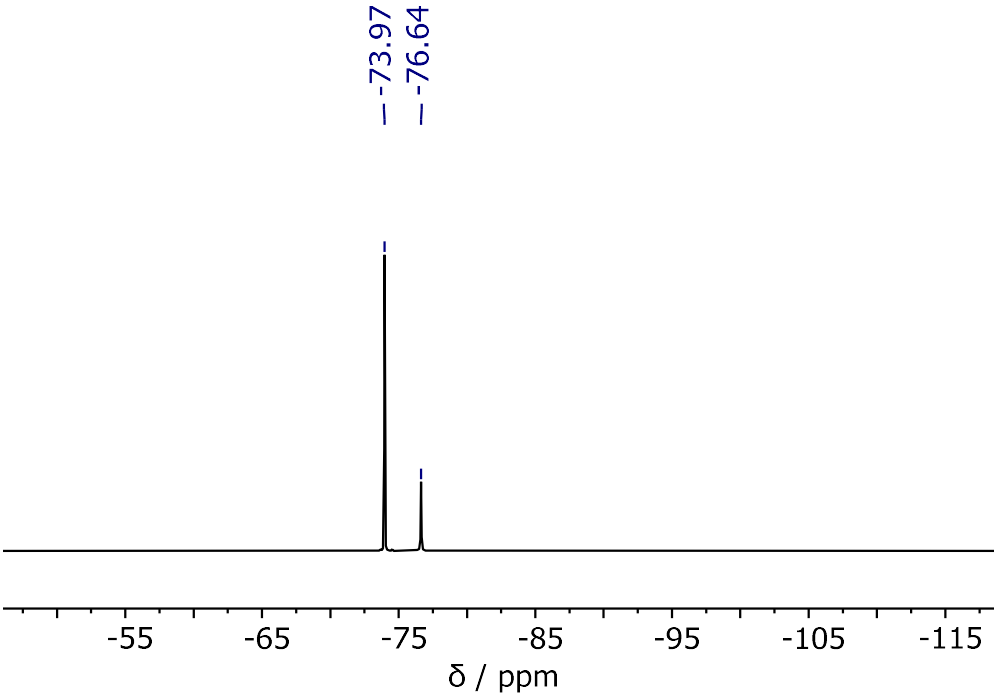

Figure 2.23: ^{19}F NMR (376 MHz, CD_2Cl_2) spectrum of $IMeBH_2NTf_2$.

Addition of 3-Fluorobenzyl Alcohol to $IMeBH_2NTf_2$: 1:1 reaction

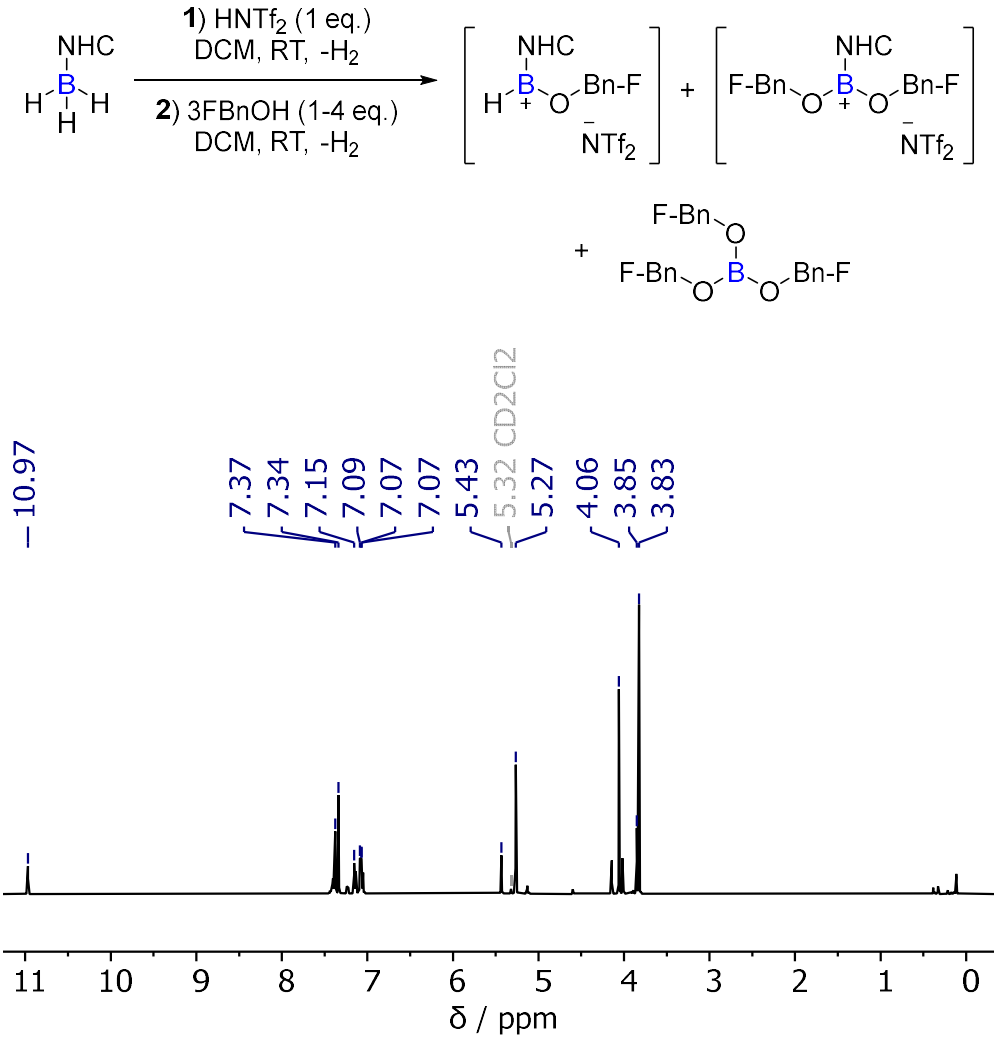

Figure 2.24: ^1H NMR (500 MHz, CD_2Cl_2) spectrum of the 1:1 reaction of $IMeBH_2NTf_2$ with 3-fluorobenzyl alcohol, 15 mins RT.

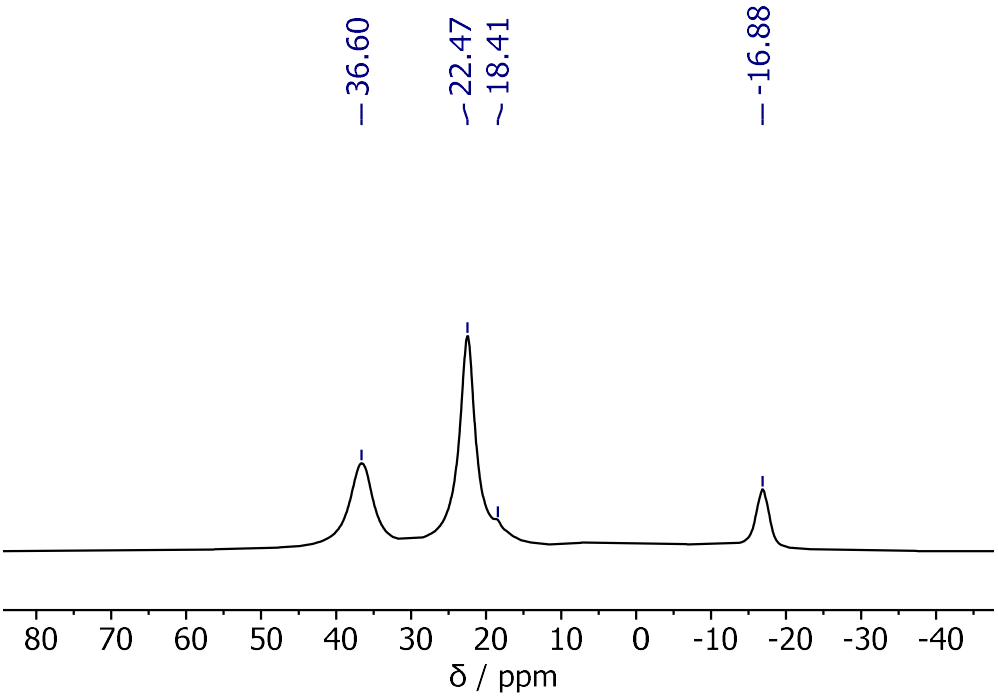

Figure 2.25: ^{11}B NMR (161 MHz, CD_2Cl_2) spectrum of the 1:1 reaction of $IMeBH_2NTf_2$ with 3-fluorobenzyl alcohol, 15 mins RT.

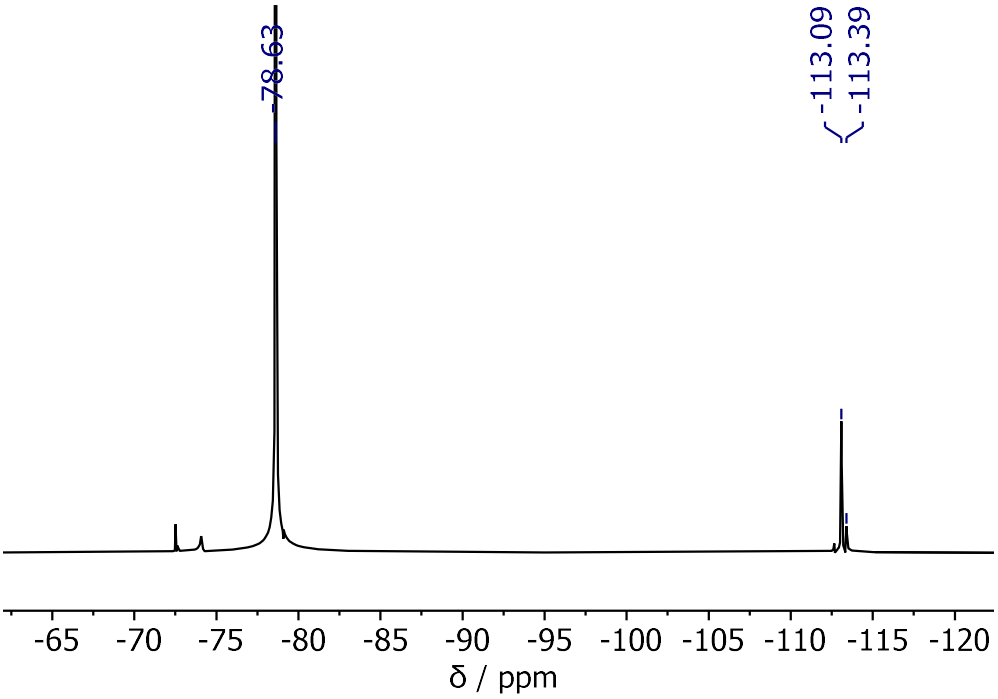

Figure 2.26: ^{19}F NMR (471 MHz, CD_2Cl_2) spectrum of the 1:1 reaction of $IMeBH_2NTf_2$ with 3-fluorobenzyl alcohol, 15 mins RT.

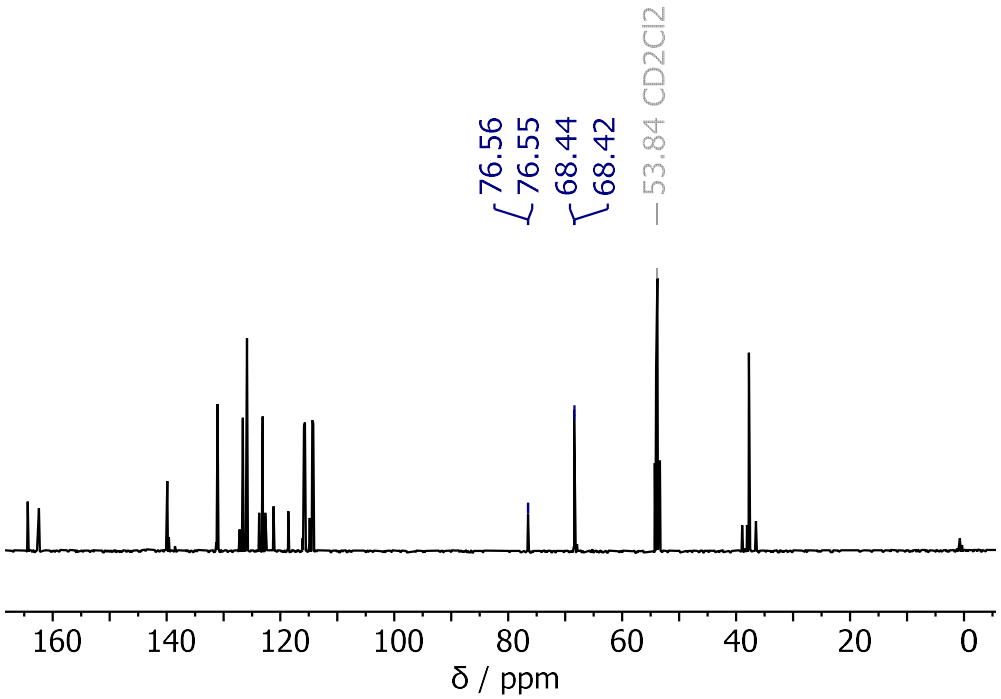

Figure 2.27: $^{13}C\{^{1}H\}$ NMR (126 MHz, CD_2Cl_2) spectrum of the 1:1 reaction of $IMeBH_2NTf_2$ with 3-fluorobenzyl alcohol, 15 mins RT.

Addition of 3-Fluorobenzyl Alcohol to $IMeBH_2NTf_2$: 1:2 reaction (2.8)

- **Characterisation of 2.8 *in situ*:**

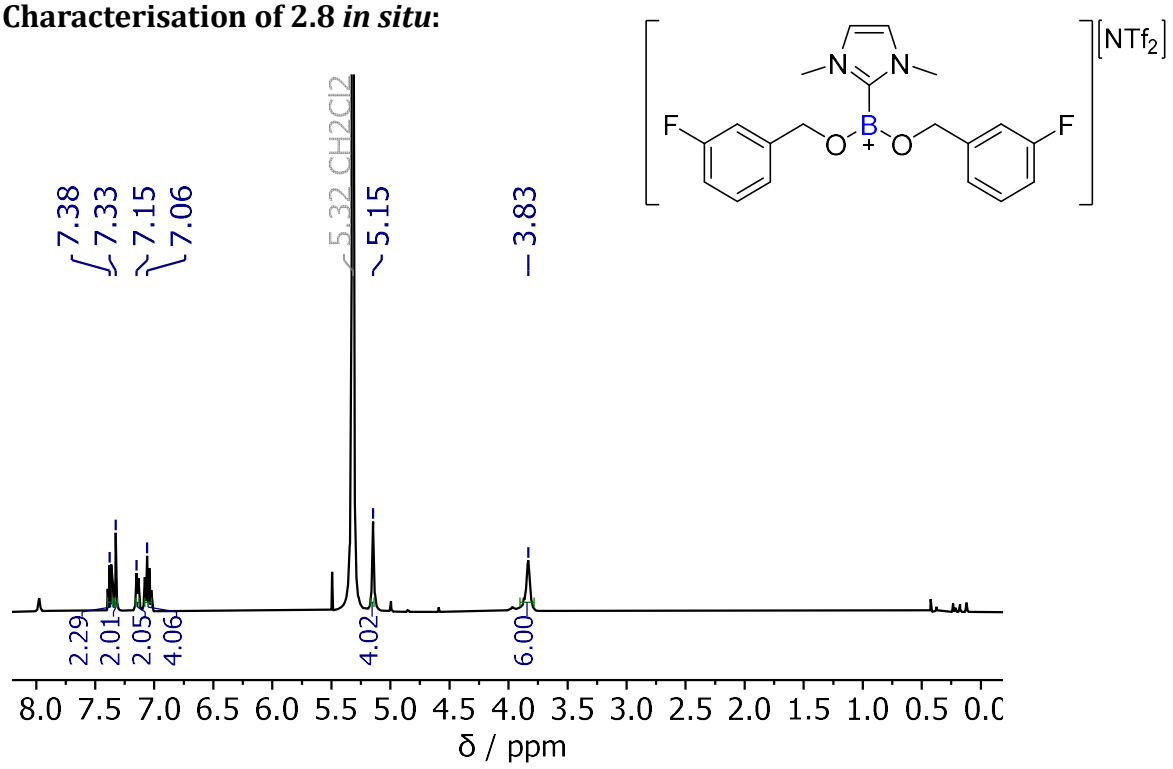

Figure 2.28: ^{1}H NMR (500 MHz, CH_2Cl_2) spectrum of the 1:2 reaction of $IMeBH_2NTf_2$ with 3-fluorobenzyl alcohol, 15 mins RT: *In situ* characterisation of **2.8**.

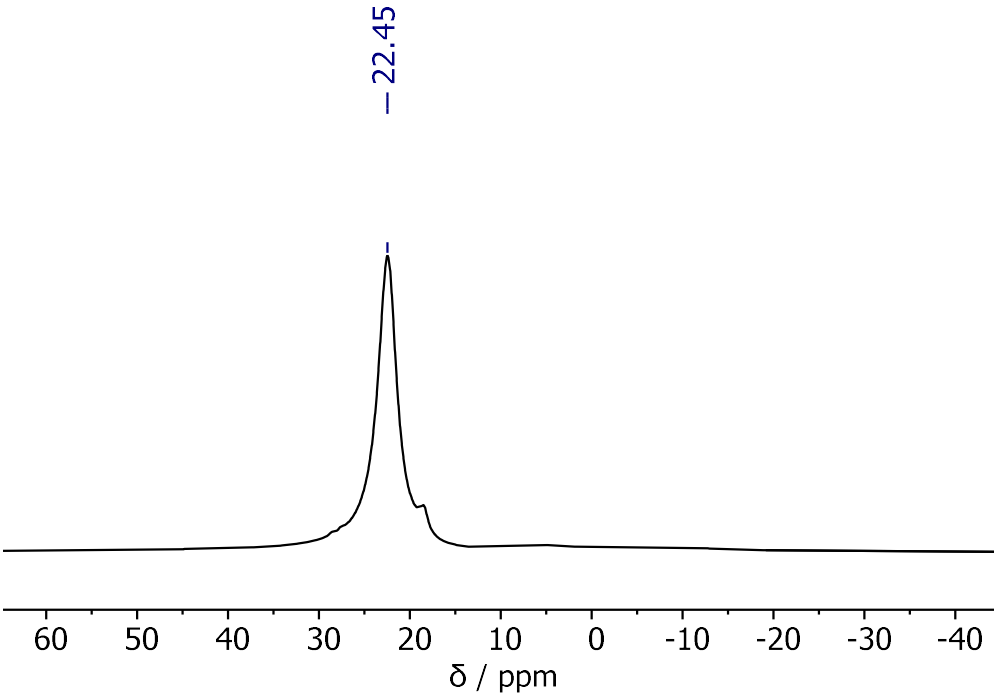

Figure 2.29: ^{11}B NMR (161 MHz, CH_2Cl_2) spectrum of the 1:2 reaction of $IMeBH_2NTf_2$ with 3-fluorobenzyl alcohol, 15 mins RT: *In situ* characterisation of **2.8**.

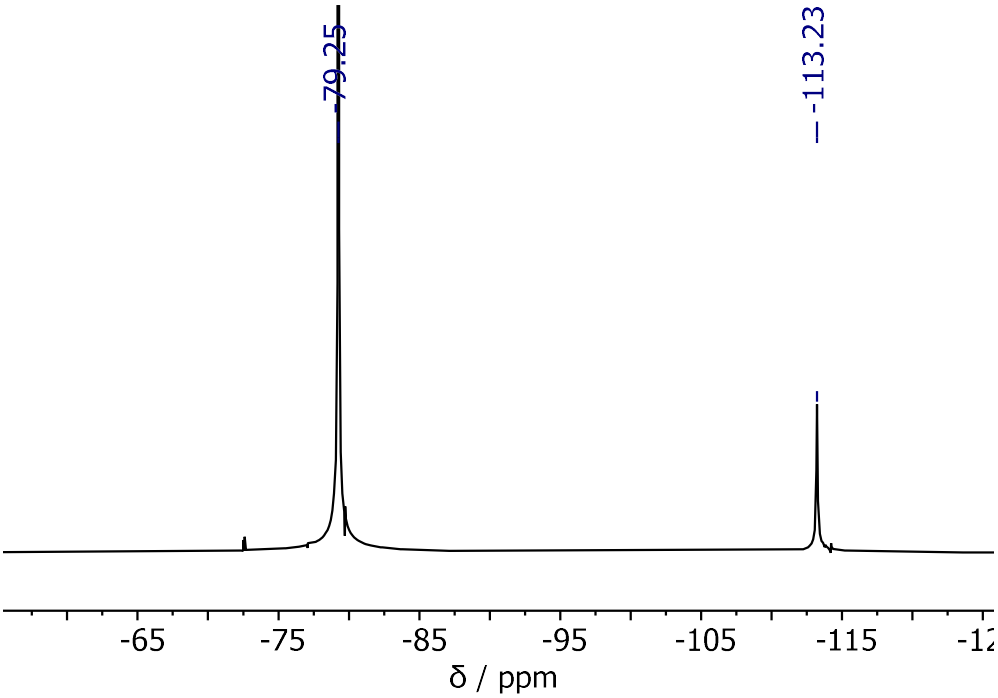

Figure 2.30: ^{19}F NMR (471 MHz, CH_2Cl_2) spectrum of the 1:2 reaction of $IMeBH_2NTf_2$ with 3-fluorobenzyl alcohol, 15 mins RT: *In situ* characterisation of **2.8**.

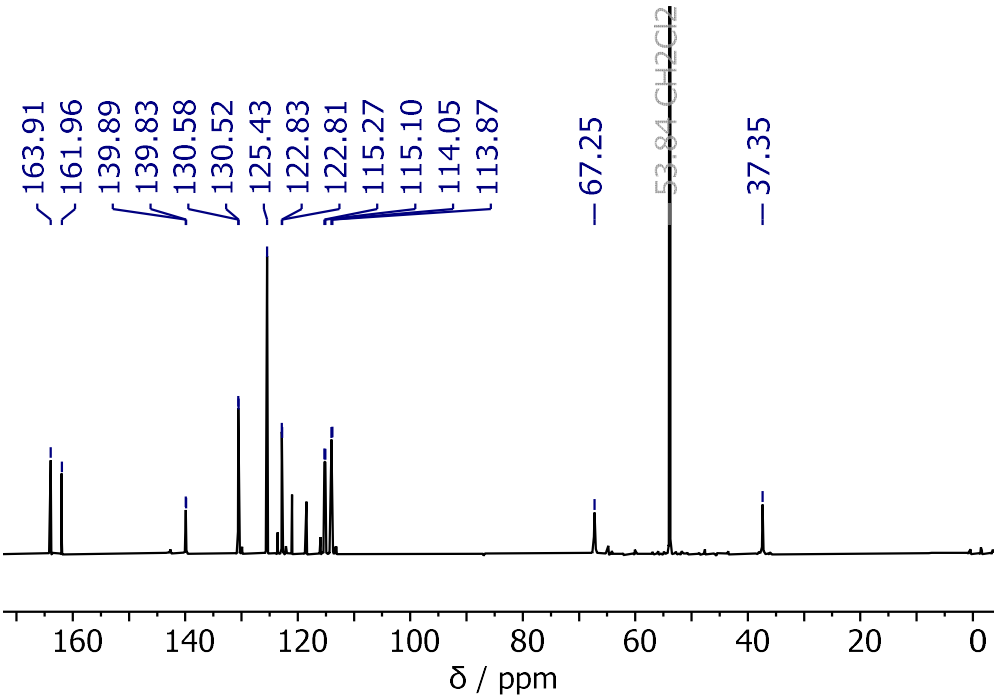

Figure 2.31: $^{13}C\{^{1}H\}$ NMR (126 MHz, CH_2Cl_2) spectrum of the 1:2 reaction of $IMeBH_2NTf_2$ with 3-fluorobenzyl alcohol, 15 mins RT: *In situ* characterisation of **2.8**.

Tri-(3-fluorobenzyl) borate ester (2.10)

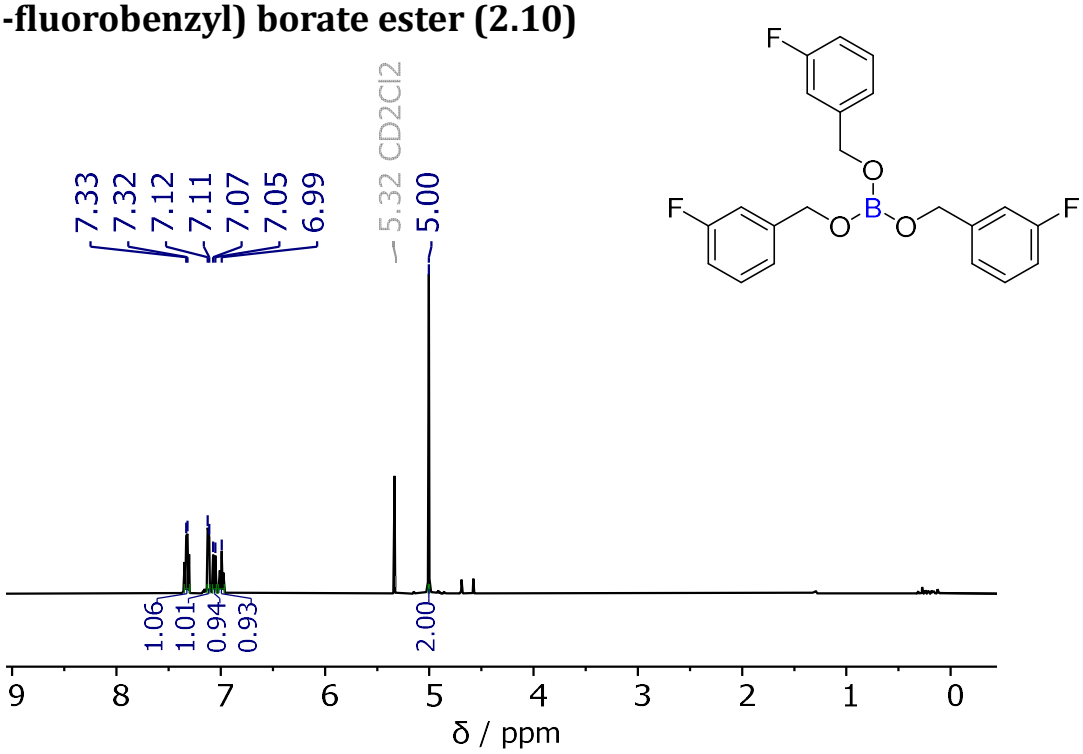

Figure 2.32: ^{1}H NMR (500 MHz, CD_2Cl_2) spectrum of tri-(3-fluorobenzyl) borate ester.

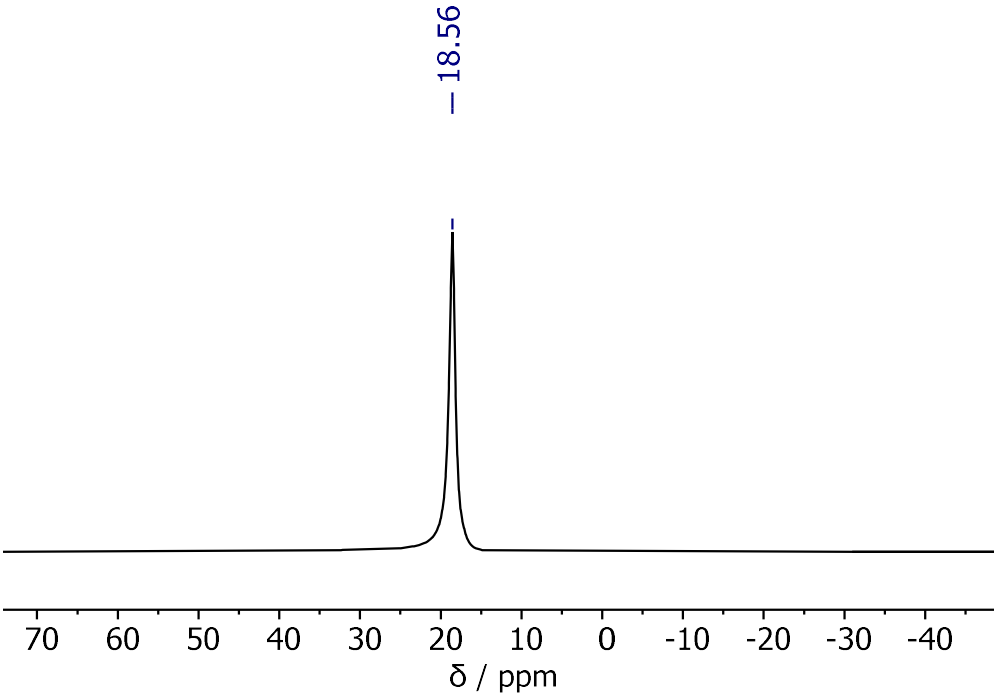

Figure 2.33: ^{11}B NMR (161 MHz, CD_2Cl_2) spectrum of tri-(3-fluorobenzyl) borate ester.

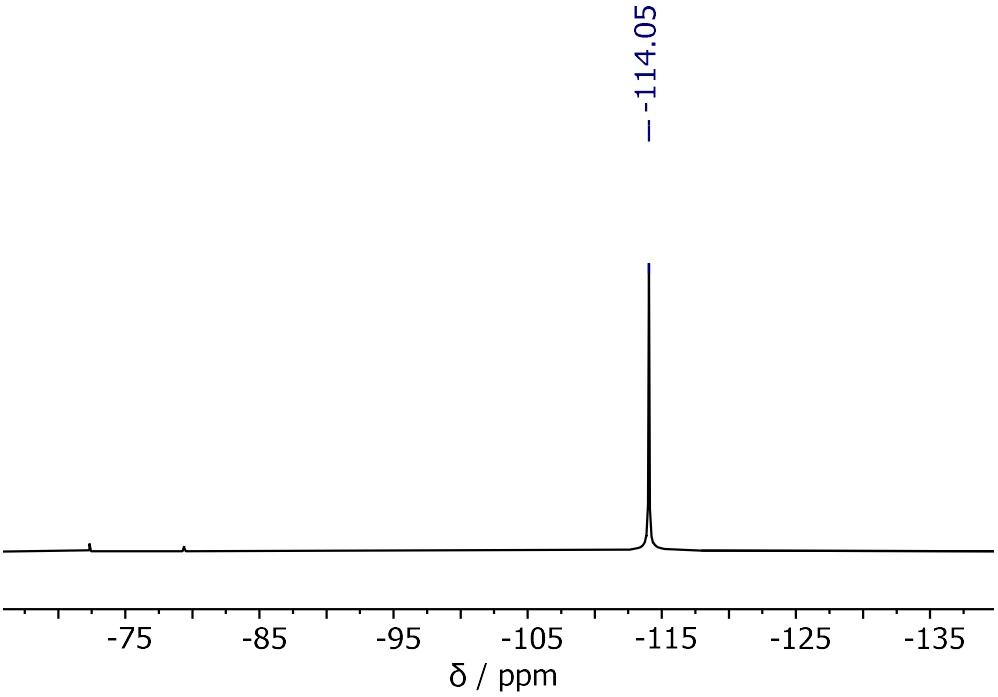

Figure 2.34: ^{19}F NMR (471 MHz, CD_2Cl_2) spectrum of tri-(3-fluorobenzyl) borate ester.

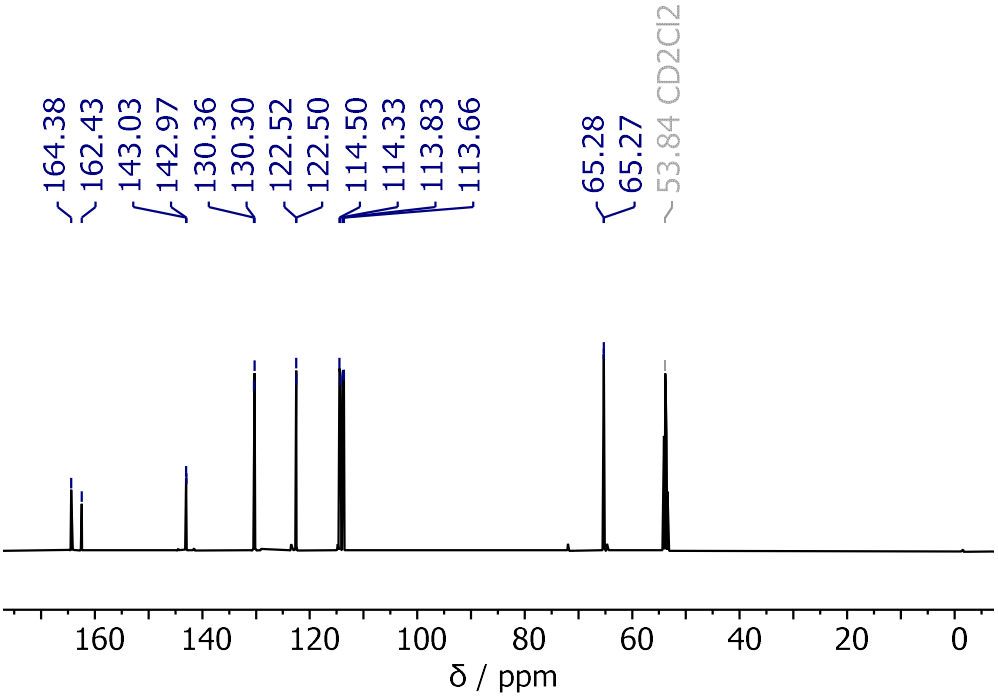

Figure 2.35: $^{13}C\{^{1}H\}$ NMR (126 MHz, CD_2Cl_2) spectrum of tri-(3-fluorobenzyl) borate ester.

Activation of I^iPrBH_3 to $I^iPrBH_2NTf_2$ (2.12)

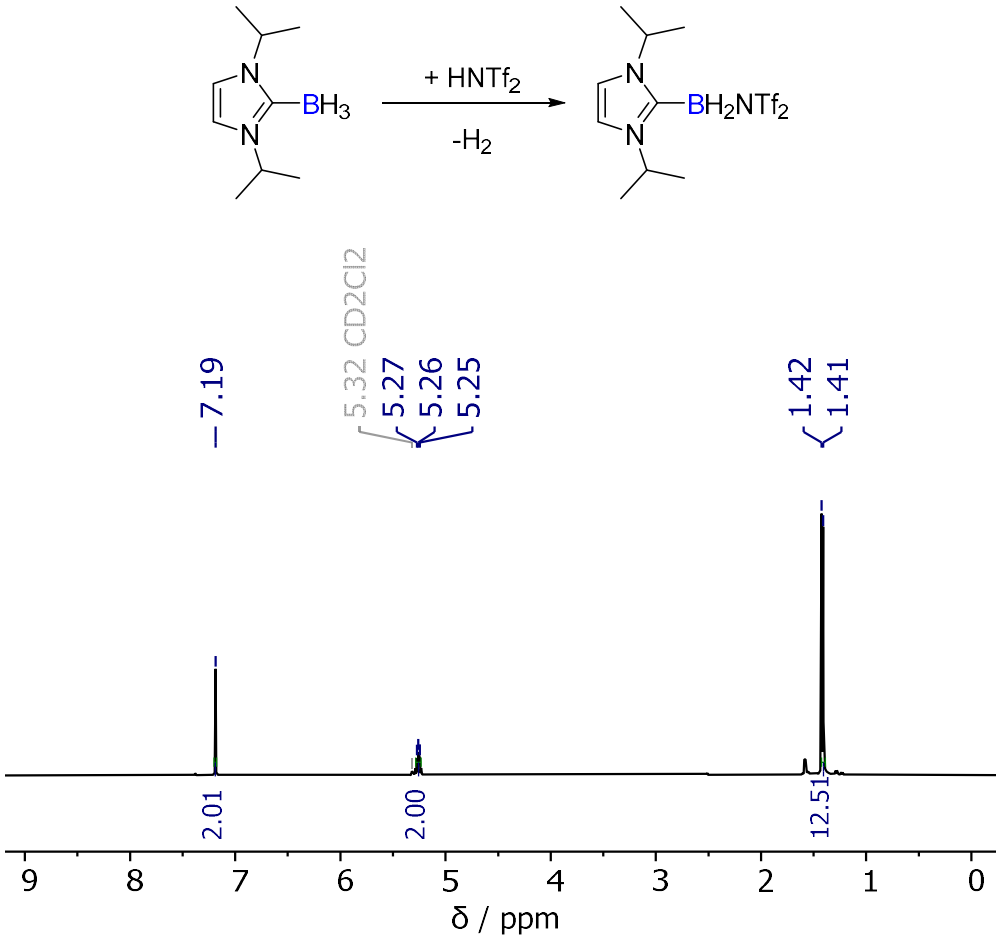

Figure 2.36: ^1H NMR (500 MHz, CD_2Cl_2) spectrum of $I^iPrBH_2NTf_2$.

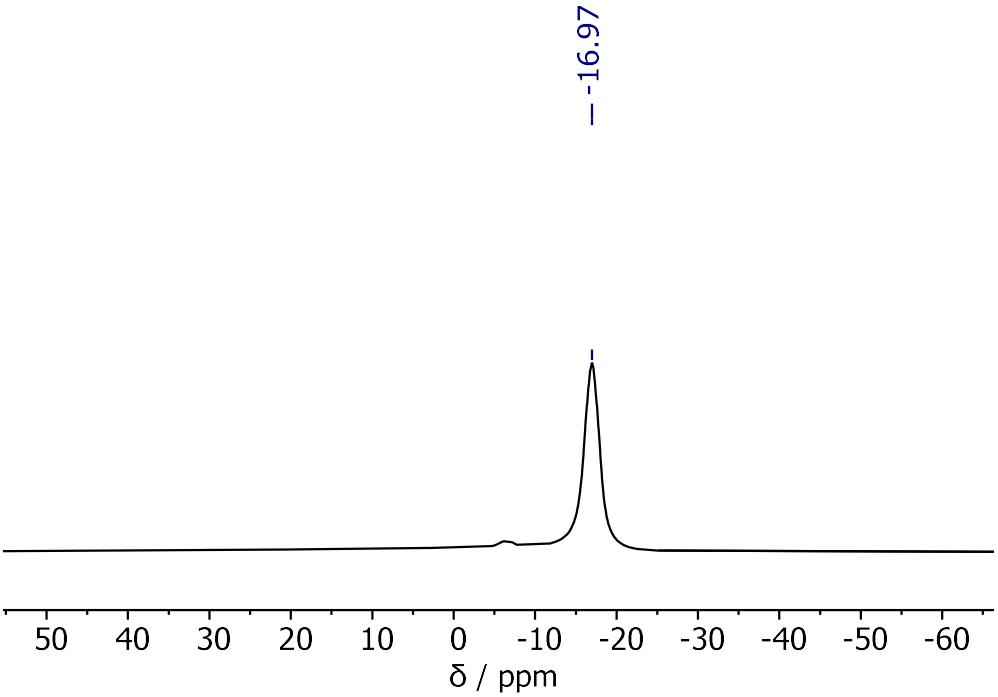

Figure 2.37: ^{11}B NMR (161 MHz, CD_2Cl_2) spectrum of I^{i}PrBH$_2$NTf$_2$.

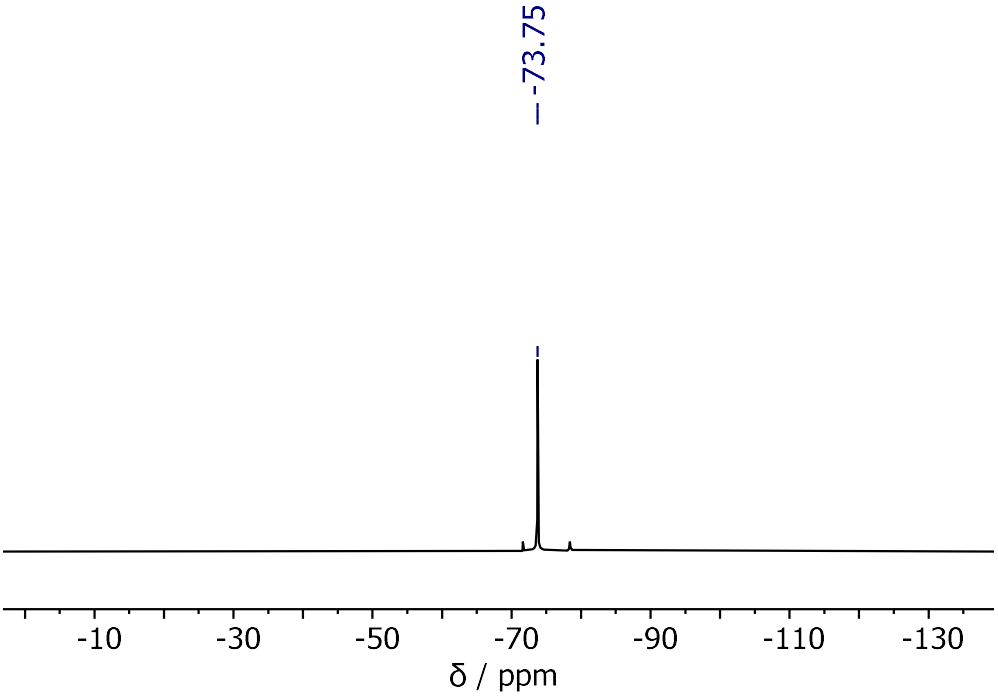

Figure 2.38: ^{19}F NMR (471 MHz, CD_2Cl_2) spectrum of I^{i}PrBH$_2$NTf$_2$.

Addition of 3-Fluorobenzyl Alcohol to $I^iPrBH_2NTf_2$: 1:1 reaction

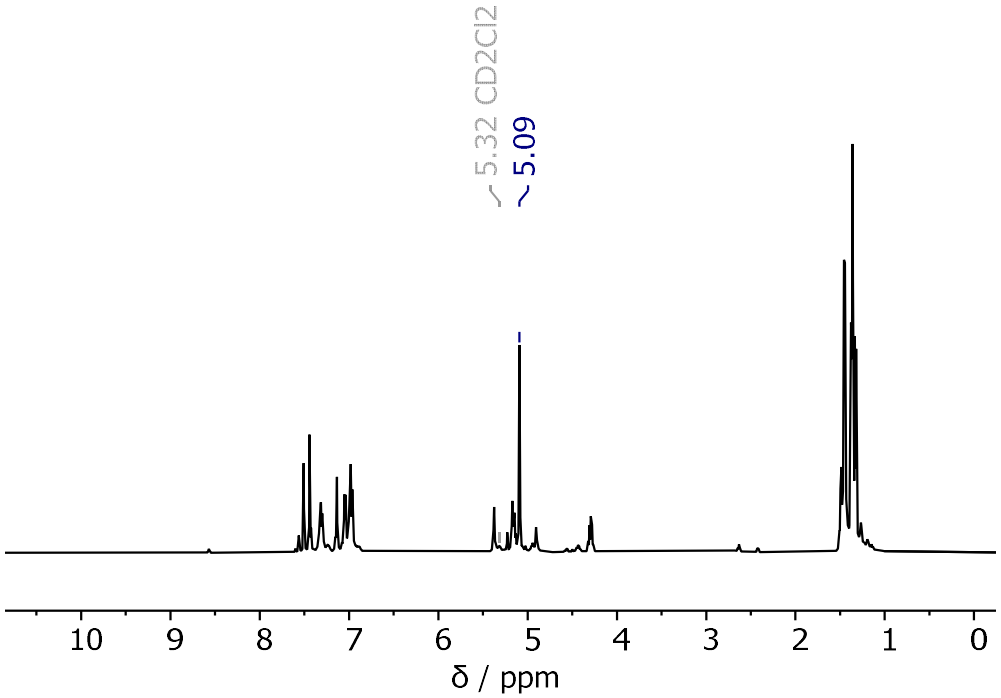

Figure 2.39: ^1H NMR (500 MHz, CD_2Cl_2) spectrum of the 1:1 reaction of $I^iPrBH_2NTf_2$ with 3-fluorobenzyl alcohol, 15 mins RT.

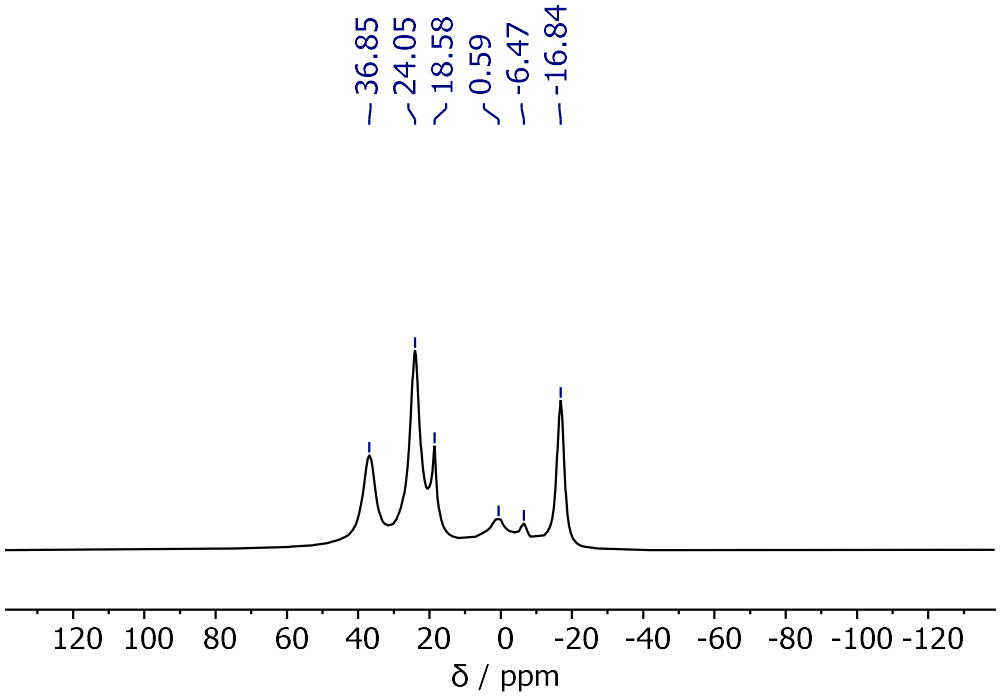

Figure 2.40: ^{11}B NMR (161 MHz, CD_2Cl_2) spectrum of the 1:1 reaction of $I^iPrBH_2NTf_2$ with 3-fluorobenzyl alcohol, 15 mins RT.

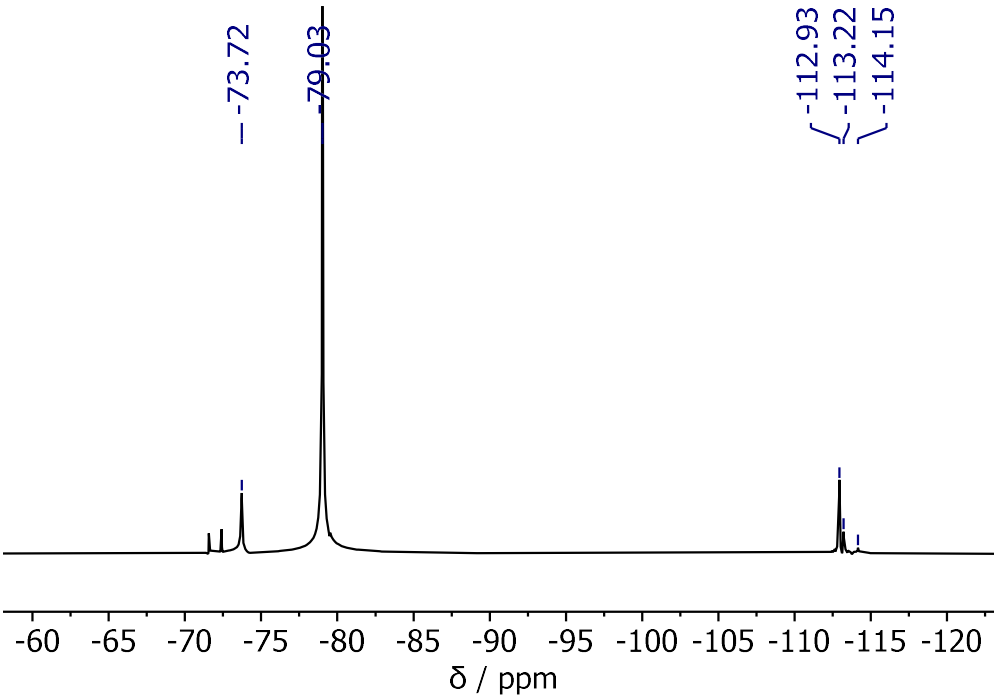

Figure 2.41: ^{19}F NMR (471 MHz, CD_2Cl_2) spectrum of the 1:1 reaction of I^{i}PrBH$_2$NTf$_2$ with 3-fluorobenzyl alcohol, 15 mins RT.

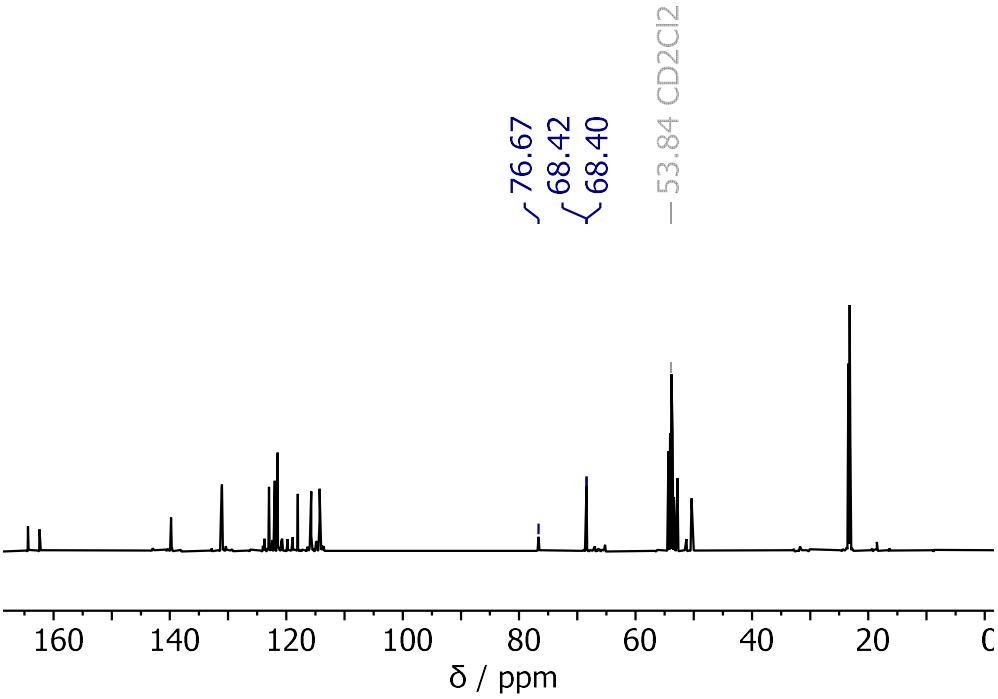

Figure 2.42: $^{13}C\{^1H\}$ NMR (126 MHz, CD_2Cl_2) spectrum of the 1:1 reaction of I^{i}PrBH$_2$NTf$_2$ with 3-fluorobenzyl alcohol, 15 mins RT.

Activation of $IMesBH_3$ to $IMesBH_2NTf_2$ (2.16)

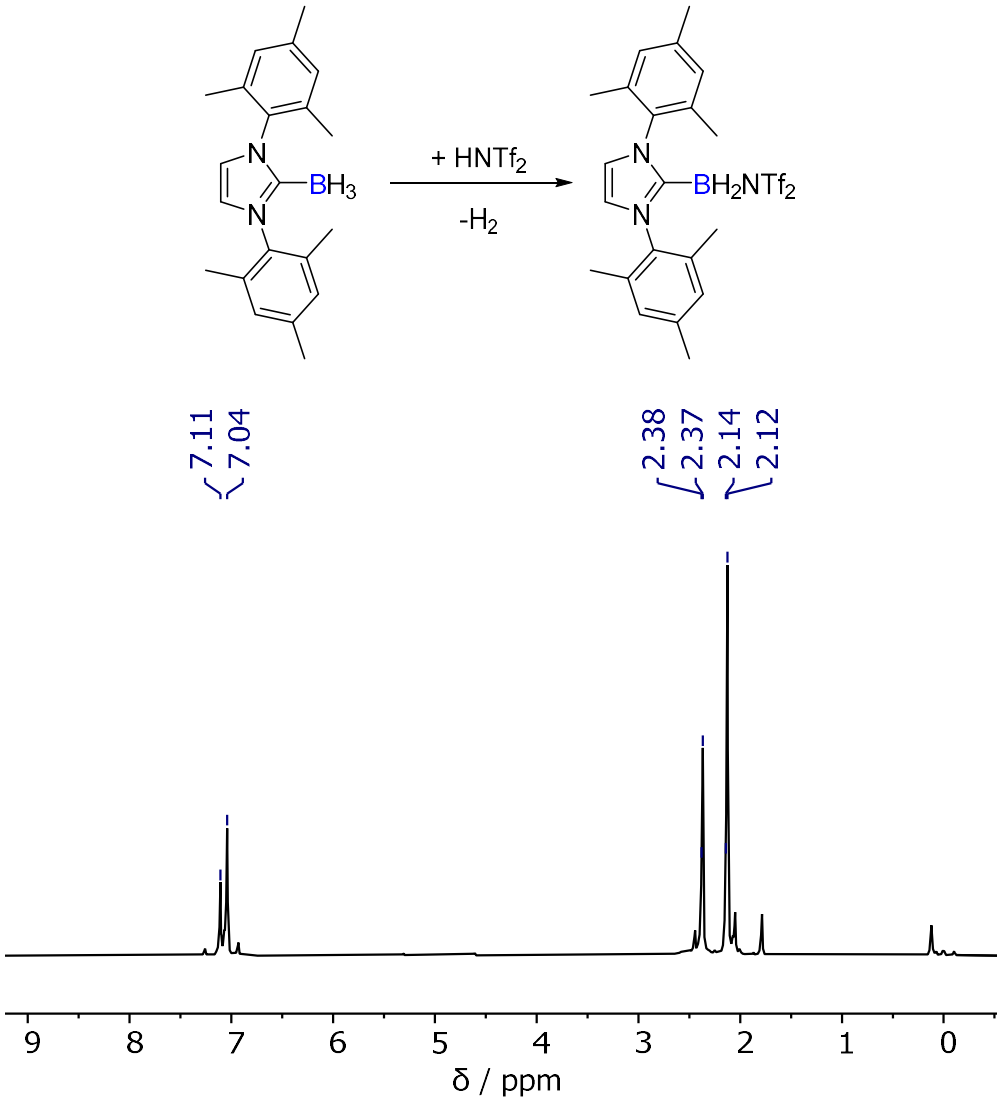

Figure 2.43: ^1H NMR (500 MHz, CD_2Cl_2) spectrum of $IMesBH_2NTf_2$.

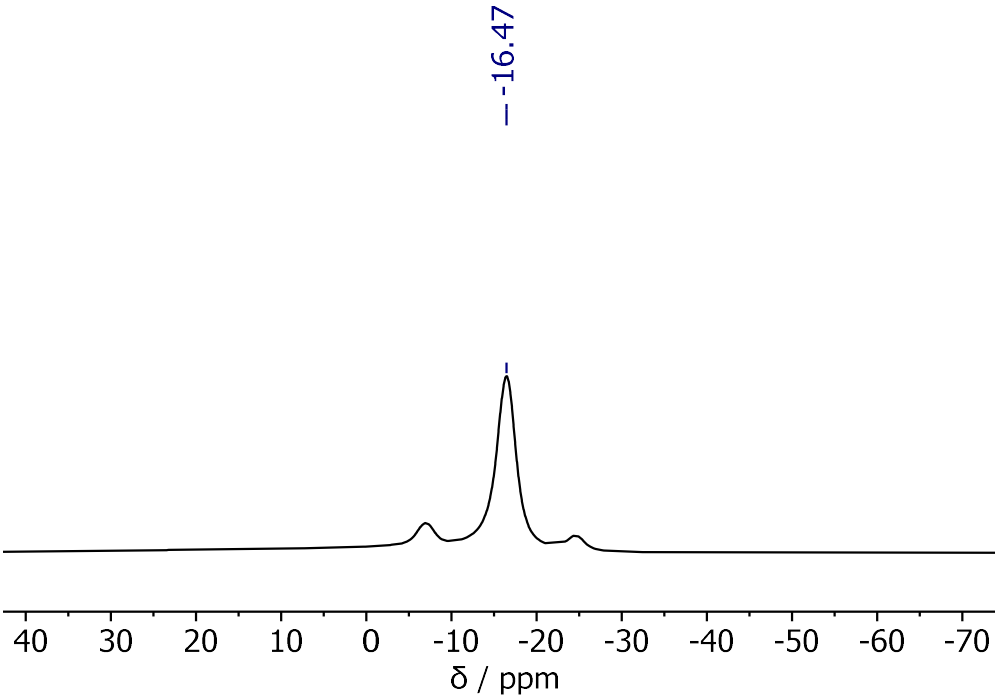

Figure 2.44: ^{11}B NMR (161 MHz, CD_2Cl_2) spectrum of $IMesBH_2NTf_2$.

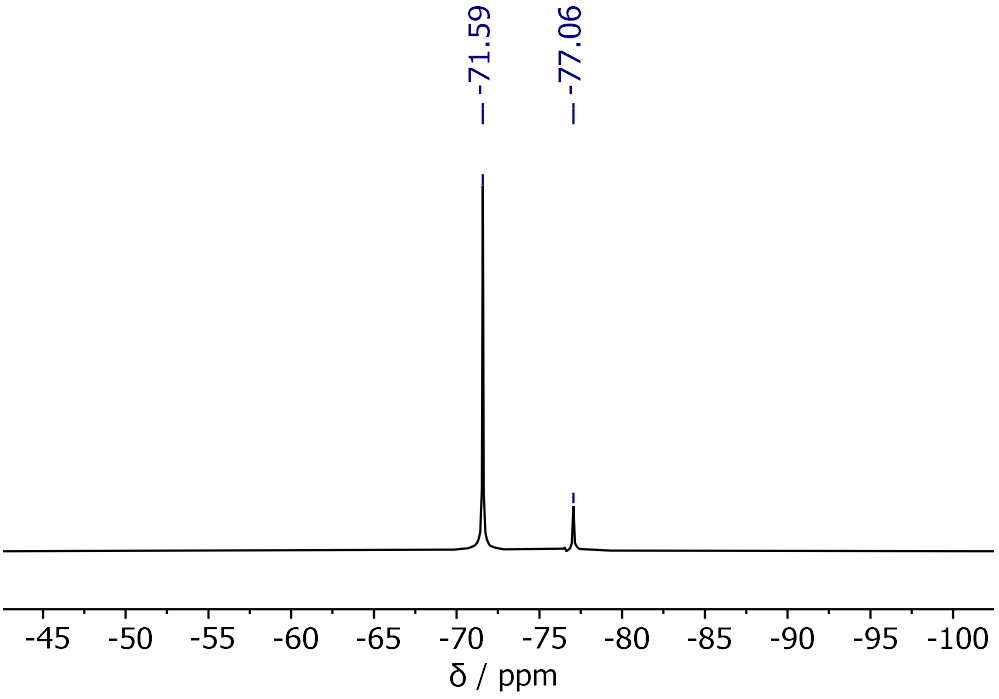

Figure 2.45: ^{19}F NMR (471 MHz, CD_2Cl_2) spectrum of $IMesBH_2NTf_2$.

Addition of 3-Fluorobenzyl Alcohol to $IMesBH_2NTf_2$: 1:1 reaction (RT)

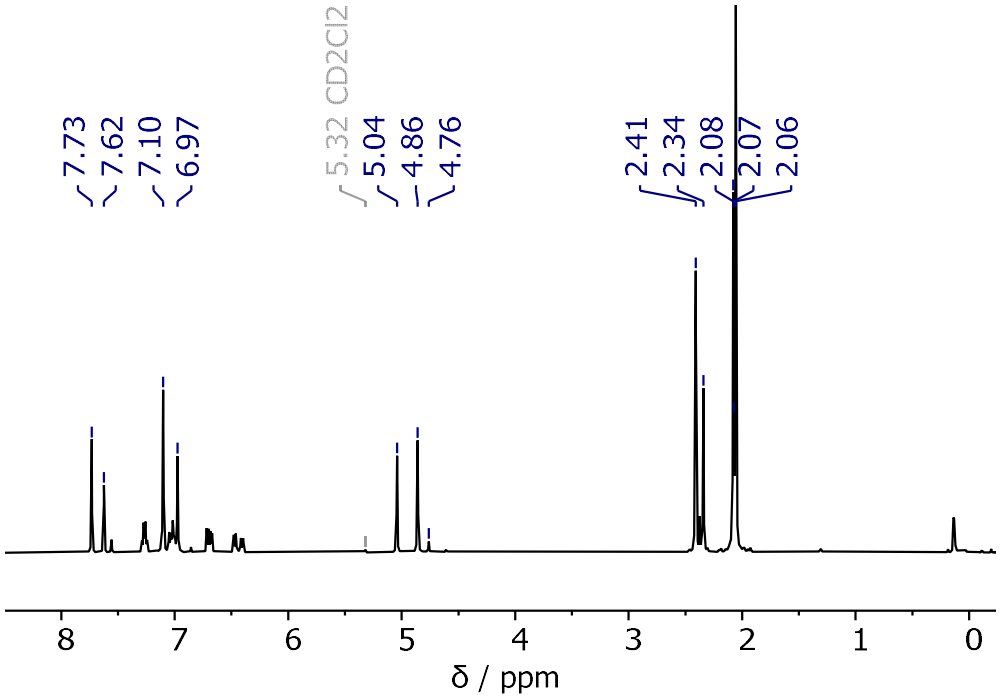

Figure 2.46: ^{1}H NMR (500 MHz, CD_2Cl_2) spectrum of the 1:1 reaction of $IMesBH_2NTf_2$ with 3-fluorobenzyl alcohol, 15 mins RT.

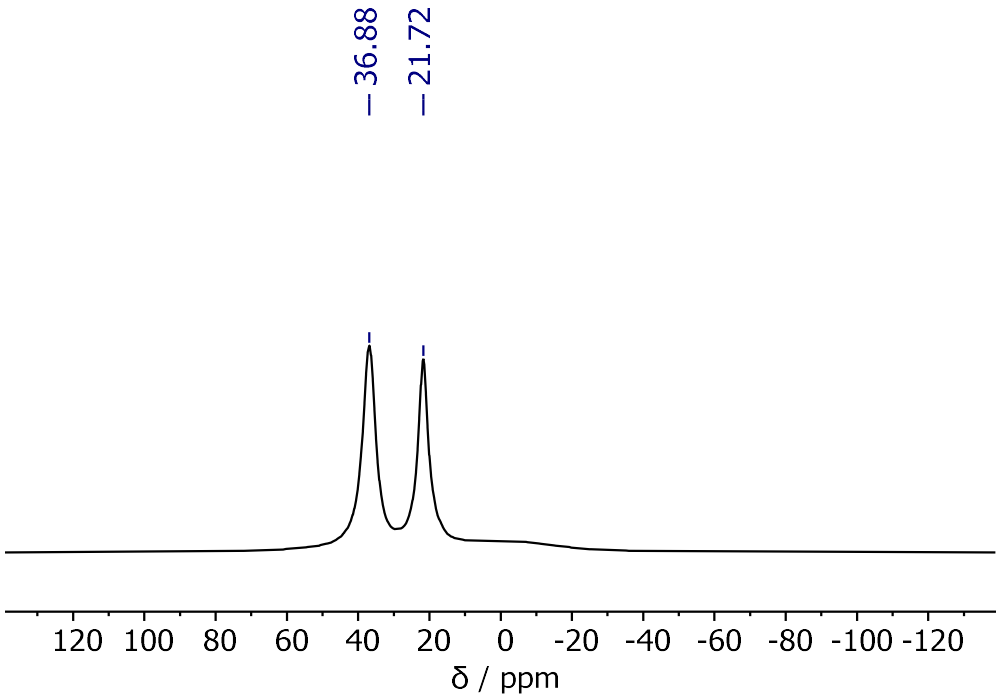

Figure 2.47: ^{11}B NMR (161 MHz, CD_2Cl_2) spectrum of the 1:1 reaction of $IMesBH_2NTf_2$ with 3-fluorobenzyl alcohol, 15 mins RT.

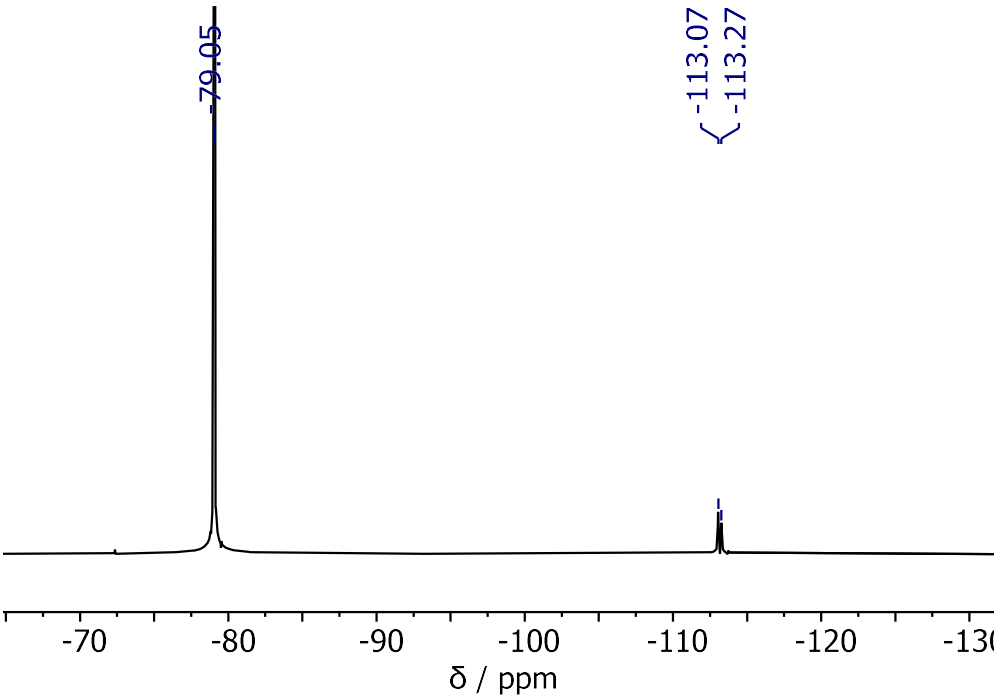

Figure 2.48: ^{19}F NMR (471 MHz, CD_2Cl_2) spectrum of the 1:1 reaction of $IMesBH_2NTf_2$ with 3-fluorobenzyl alcohol, 15 mins RT.

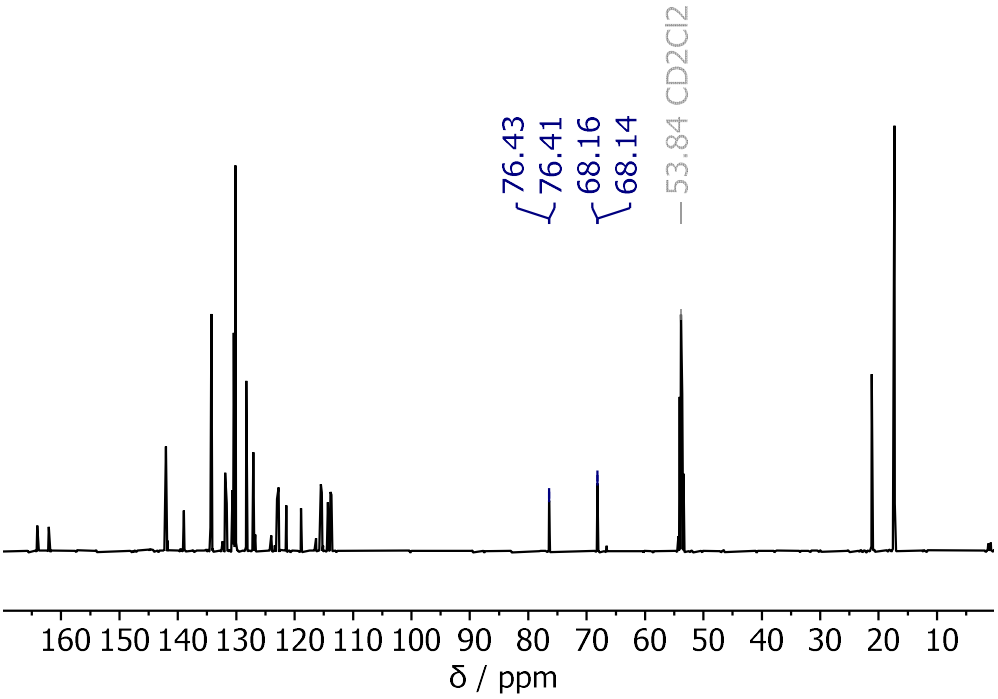

Figure 2.49: $^{13}C\{^1H\}$ NMR (126 MHz, CD_2Cl_2) spectrum of the 1:1 reaction of $IMesBH_2NTf_2$ with 3-fluorobenzyl alcohol, 15 mins RT.

Addition of 3-Fluorobenzyl Alcohol to $IMesBH_2NTf_2$: 1:1 rxn at 0 °C

- **Characterisation of 2.17 *in situ*:**

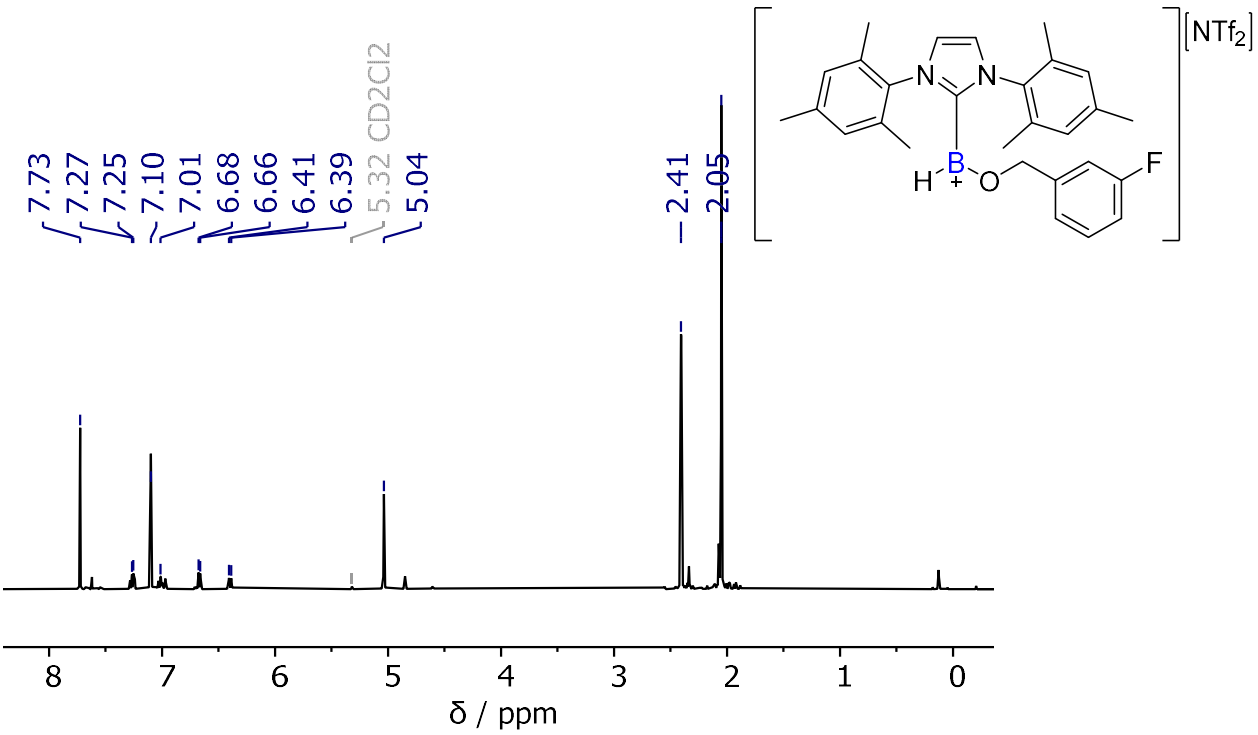

Figure 2.50: ^{1}H NMR (500 MHz, CD_2Cl_2) spectrum of the 0 °C 1:1 reaction of $IMesBH_2NTf_2$ with 3-fluorobenzyl alcohol, 15 mins RT: *In situ* characterisation of **2.17**.

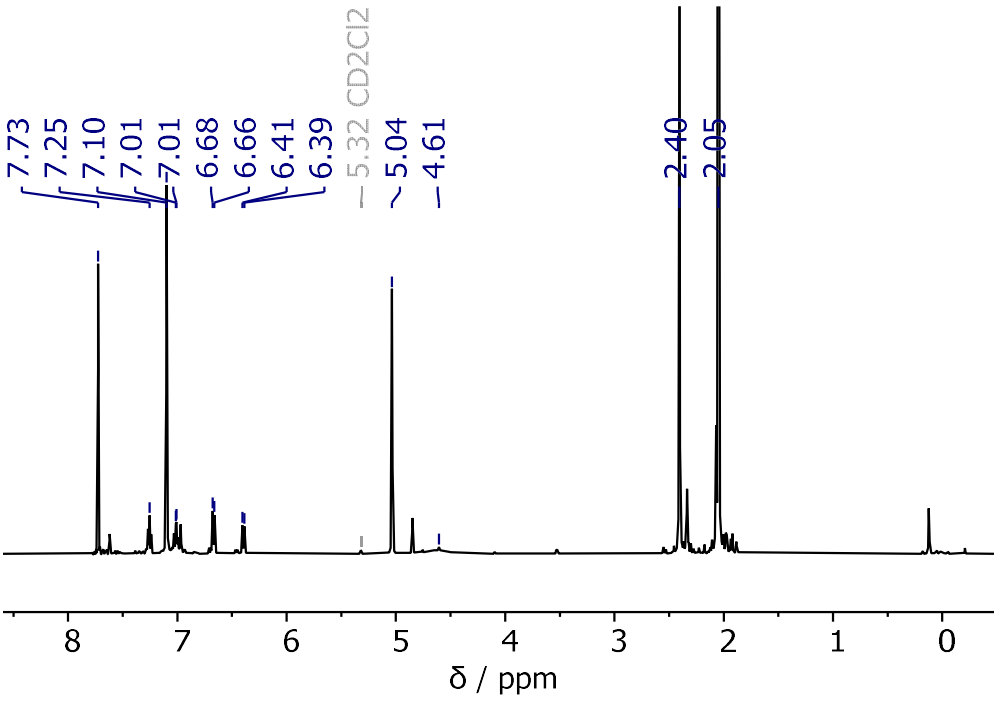

Figure 2.51: $^{1}H\{^{11}B\}$ NMR (500 MHz, CD_2Cl_2) spectrum of the 0 °C 1:1 reaction of $IMesBH_2NTf_2$ with 3-fluorobenzyl alcohol, 15 mins RT: *In situ* characterisation of **2.17**.

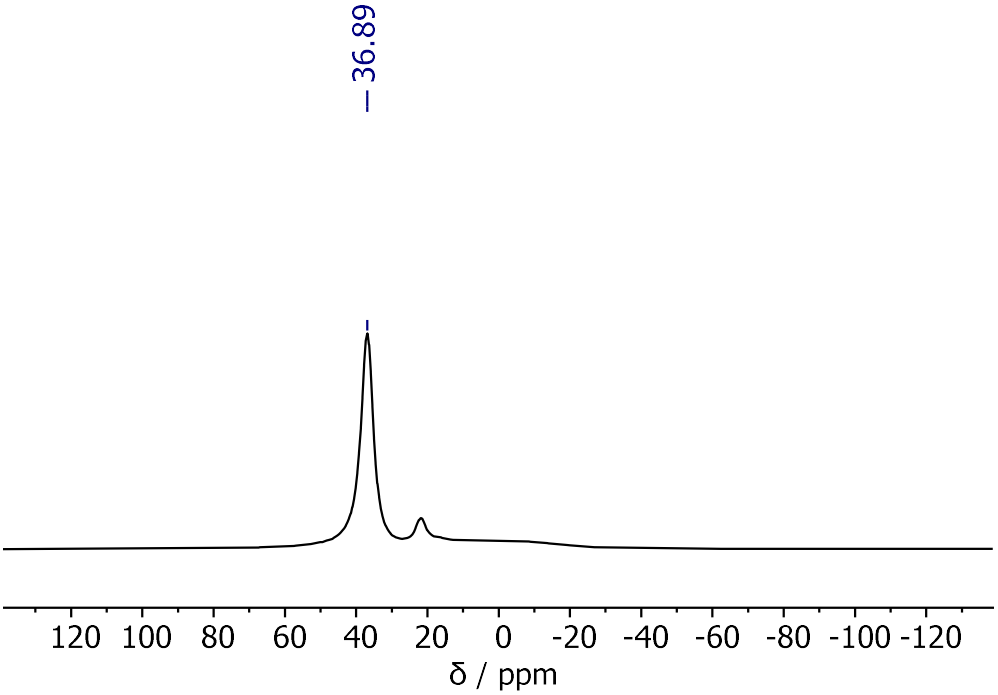

Figure 2.52: ^{11}B NMR (161 MHz, CD_2Cl_2) spectrum of the 0 °C 1:1 reaction of $IMesBH_2NTf_2$ with 3-fluorobenzyl alcohol, 15 mins RT: *In situ* characterisation of **2.17**.

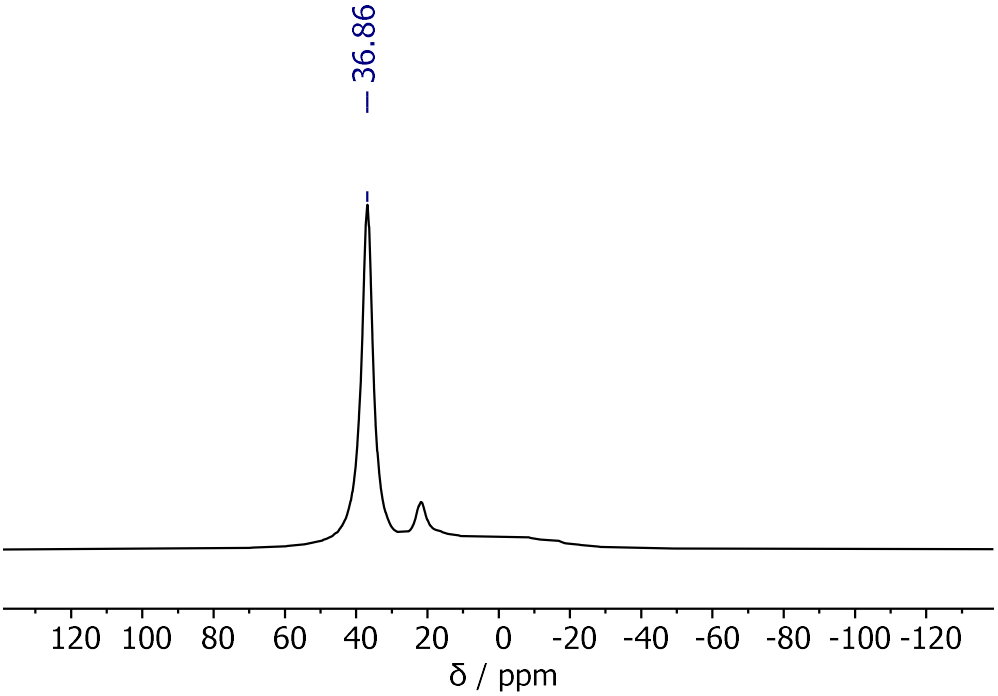

Figure 2.53: $^{11}B\{^1H\}$ NMR (161 MHz, CD_2Cl_2) spectrum of the 0 °C 1:1 reaction of $IMesBH_2NTf_2$ with 3-fluorobenzyl alcohol, 15 mins RT: *In situ* characterisation of **2.17**.

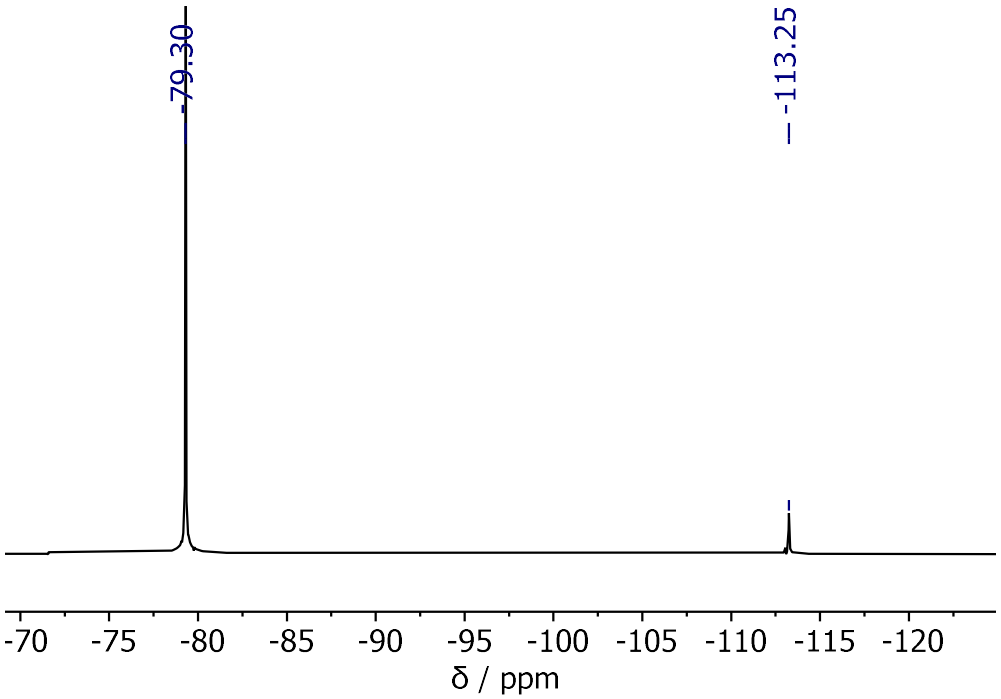

Figure 2.54: ^{19}F NMR (471 MHz, CD_2Cl_2) spectrum of the 0 °C 1:1 reaction of $IMesBH_2NTf_2$ with 3-fluorobenzyl alcohol, 15 mins RT: *In situ* characterisation of **2.17**.

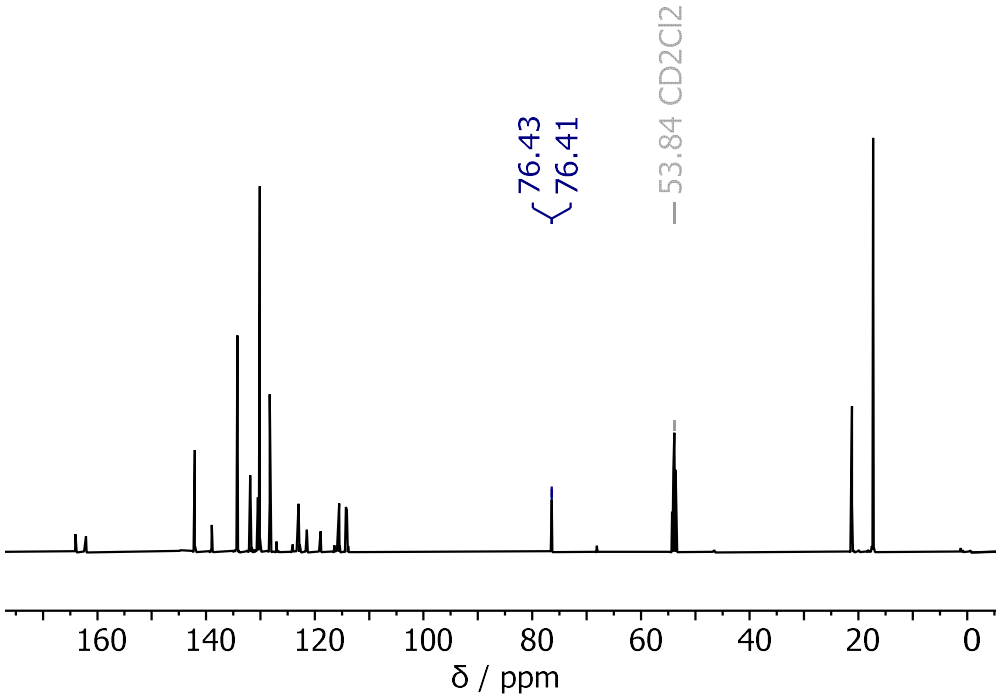

Figure 2.55: $^{13}C\{^1H\}$ NMR (126 MHz, CD_2Cl_2) spectrum of the 0 °C 1:1 reaction of $IMesBH_2NTf_2$ with 3-fluorobenzyl alcohol, 15 mins RT: *In situ* characterisation of **2.17**.

Addition of 3-Fluorobenzyl Alcohol to $IMesBH_2NTf_2$: 1:2 rxn at 0 °C

- **Characterisation of 2.18 *in situ*:**

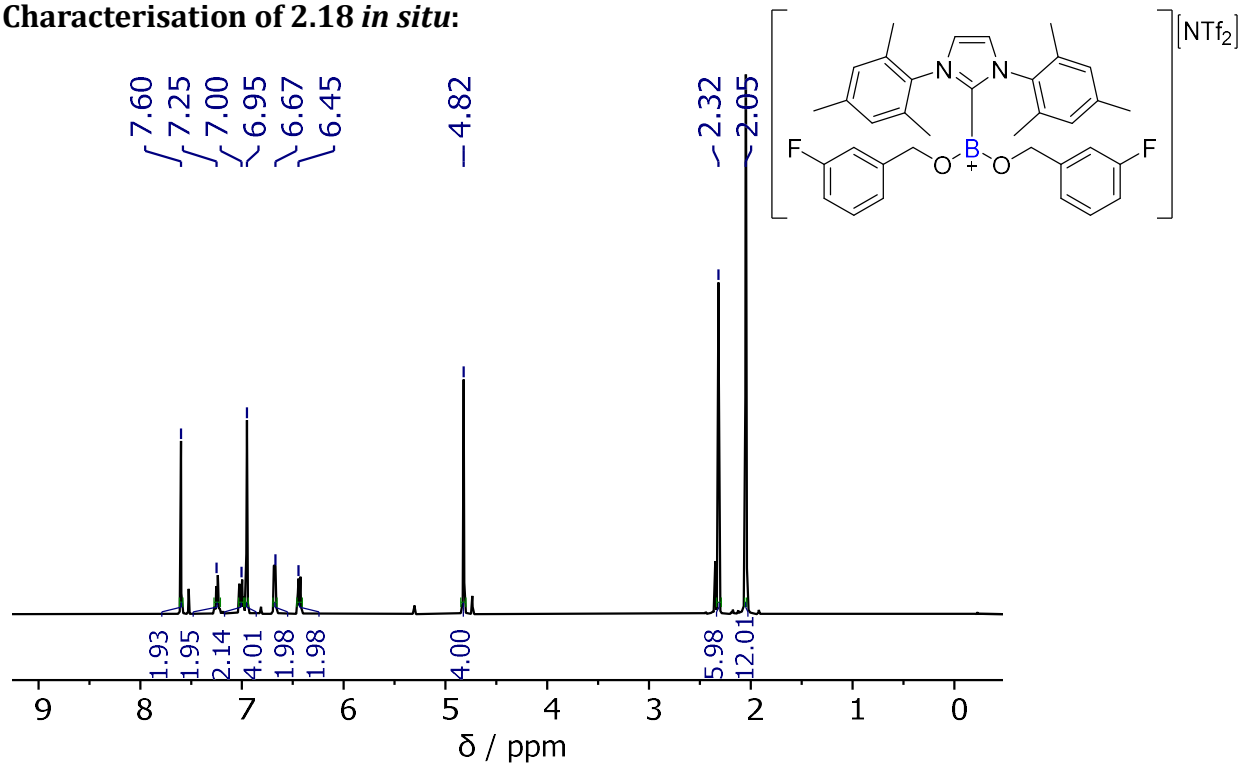

Figure 2.56: ^{1}H NMR (500 MHz, CD_2Cl_2) spectrum of the 0 °C 1:2 reaction of $IMesBH_2NTf_2$ with 3-fluorobenzyl alcohol, 15 mins RT: *In situ* characterisation of **2.18**.

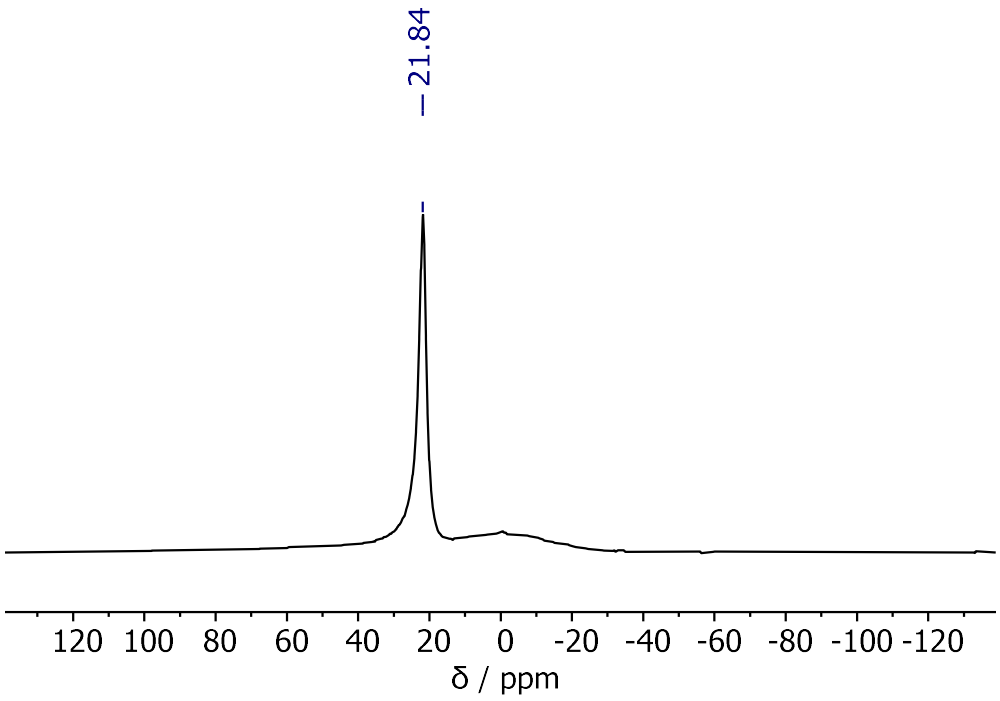

Figure 2.57: ^{11}B NMR (161 MHz, CD_2Cl_2) spectrum of the 0 °C 1:2 reaction of $IMesBH_2NTf_2$ with 3-fluorobenzyl alcohol, 15 mins RT: *In situ* characterisation of **2.18**.

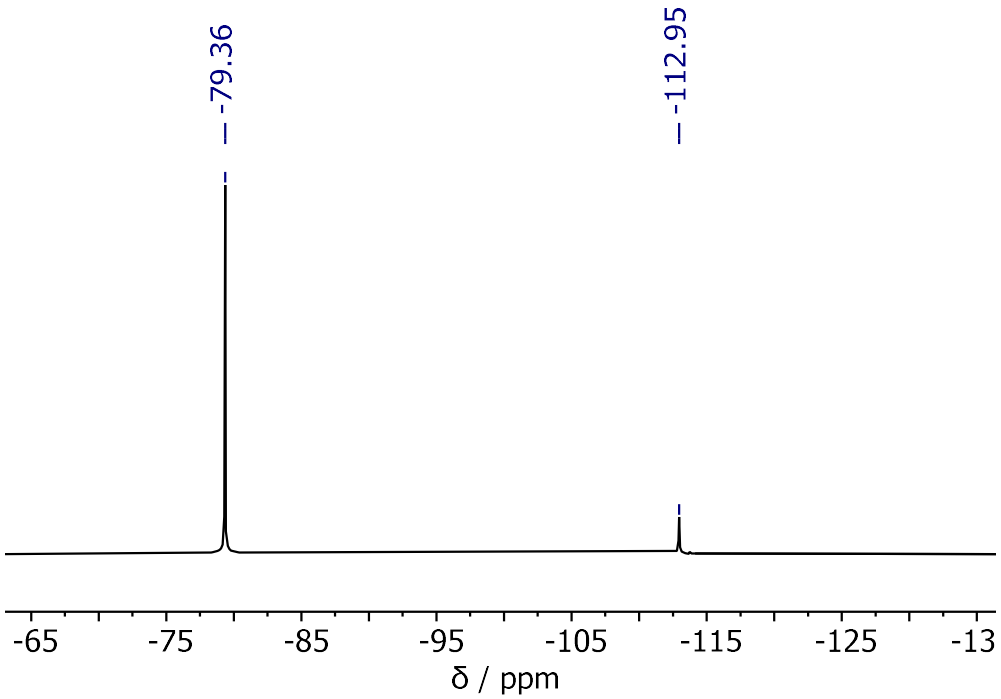

Figure 2.58: ^{19}F NMR (471 MHz, CD_2Cl_2) spectrum of the 0 °C 1:2 reaction of $IMesBH_2NTf_2$ with 3-fluorobenzyl alcohol, 15 mins RT: *In situ* characterisation of **2.18**.

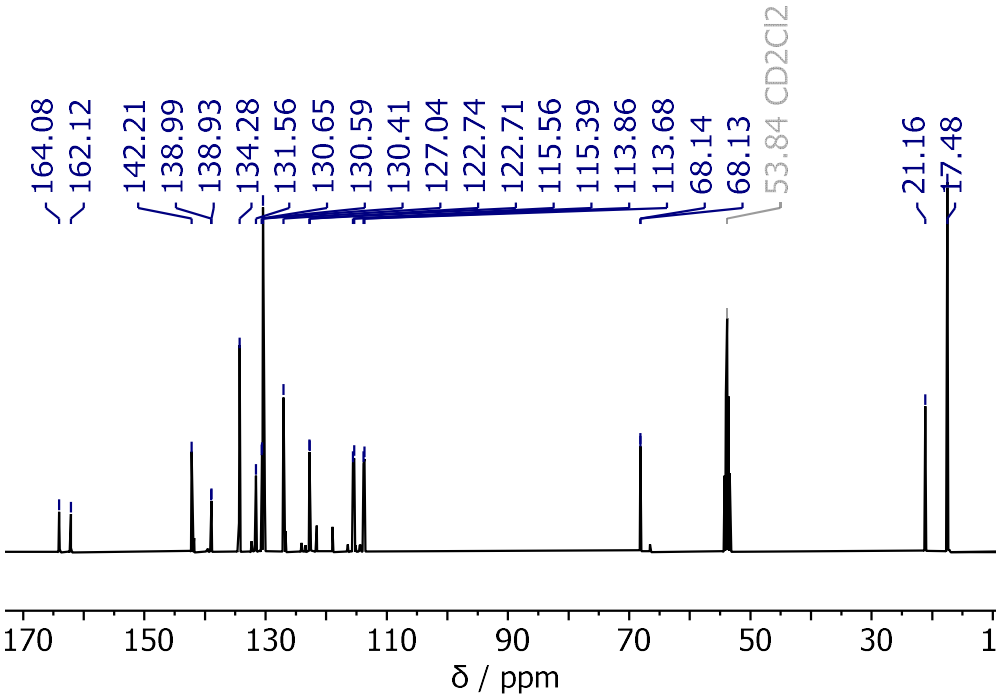

Figure 2.59: $^{13}C\{^1H\}$ NMR (126 MHz, CD_2Cl_2) spectrum of the 0 °C 1:2 reaction of $IMesBH_2NTf_2$ with 3-fluorobenzyl alcohol, 15 mins RT: *In situ* characterisation of **2.18**.

2.5.5 - Attempts to Induce Intramolecular Arene C-H Borylation

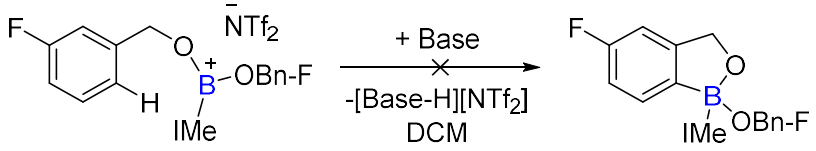

Reaction of 2.8 with 1 equiv. DBP at RT

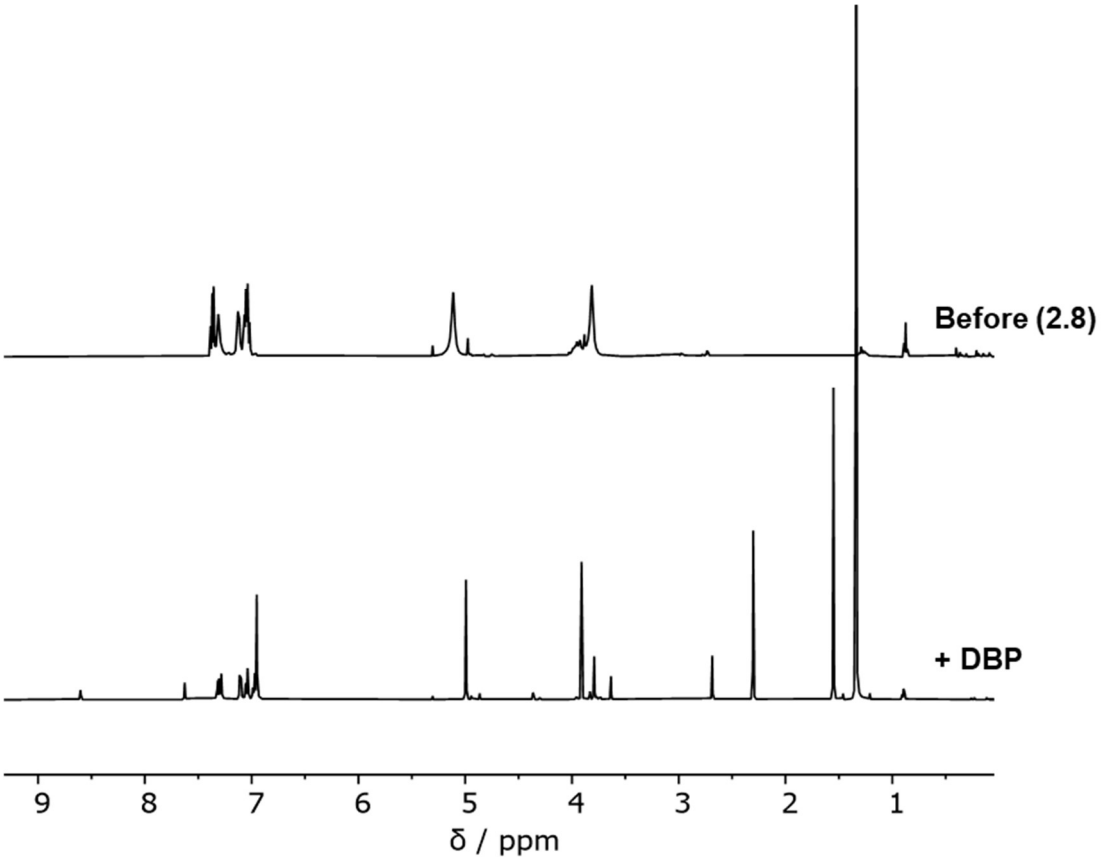

Figure 2.60: Stacked ^{1}H NMR (500 MHz, CD_2Cl_2) spectrum of the reaction of **2.8** with 1 equiv. DBP at RT.

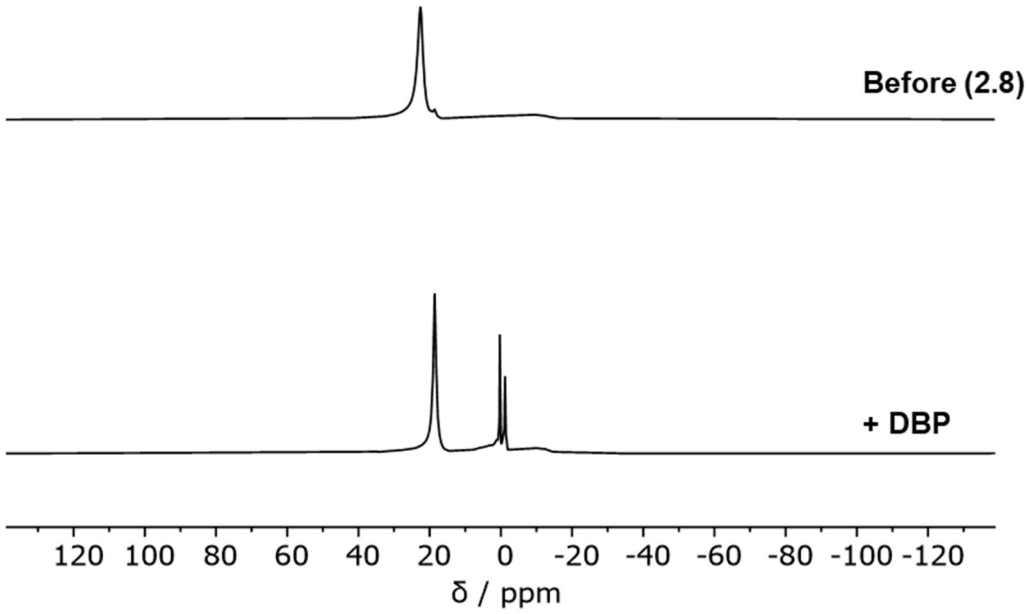

Figure 2.61: Stacked ^{11}B NMR (161 MHz, CD_2Cl_2) spectrum of the reaction of **2.8** with 1 equiv. DBP at RT.

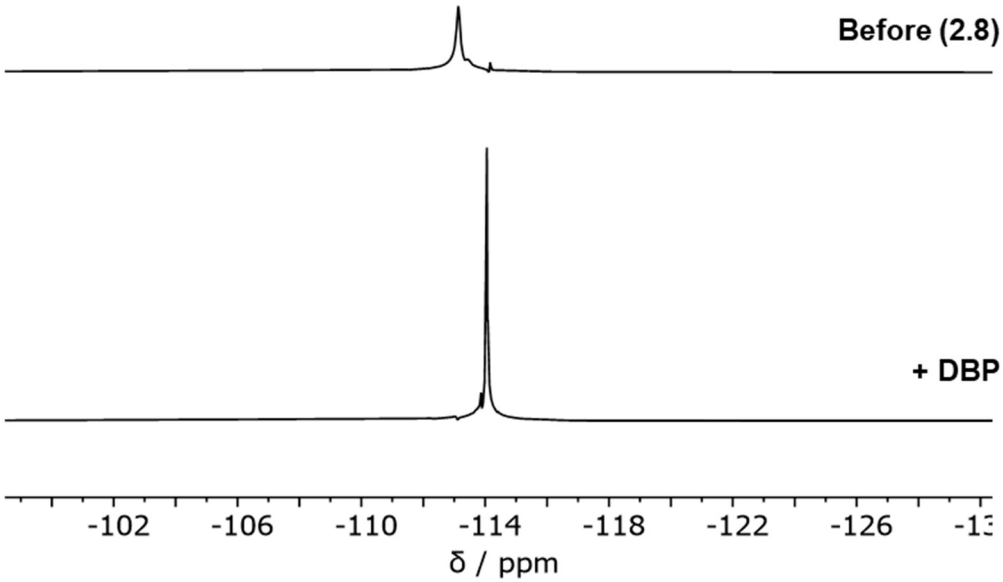

Figure 2.62: Stacked ^{19}F NMR (471 MHz, CD_2Cl_2) spectrum of the reaction of **2.8** with 1 equiv. DBP at RT.

Reaction of 2.8 with 1 equiv. DIPEA at RT

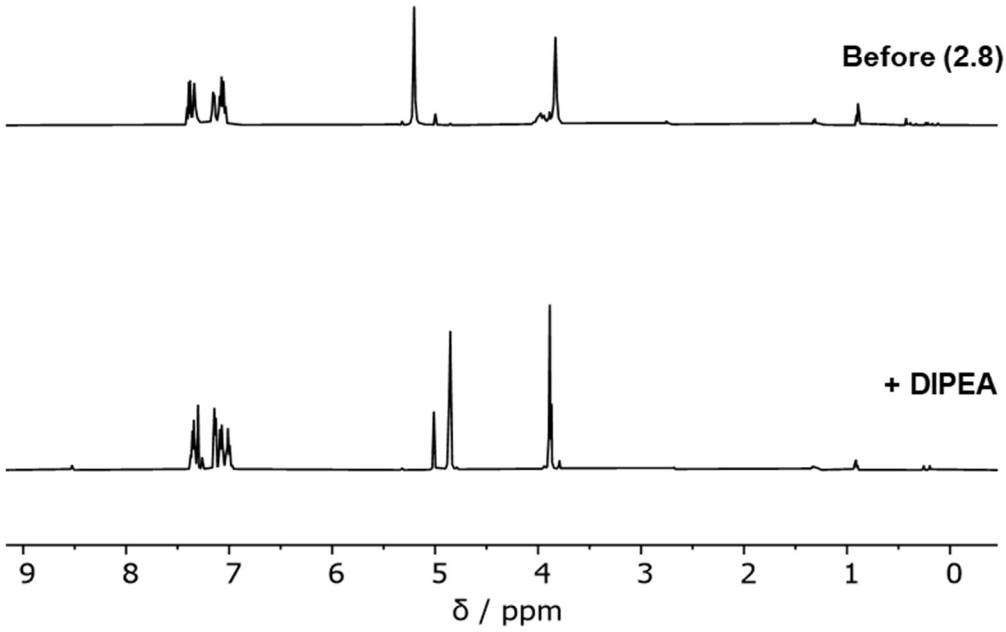

Figure 2.63: Stacked ^{1}H NMR (500 MHz, CD_2Cl_2) spectrum of the reaction of **2.8** with 1 equiv. DIPEA at RT.

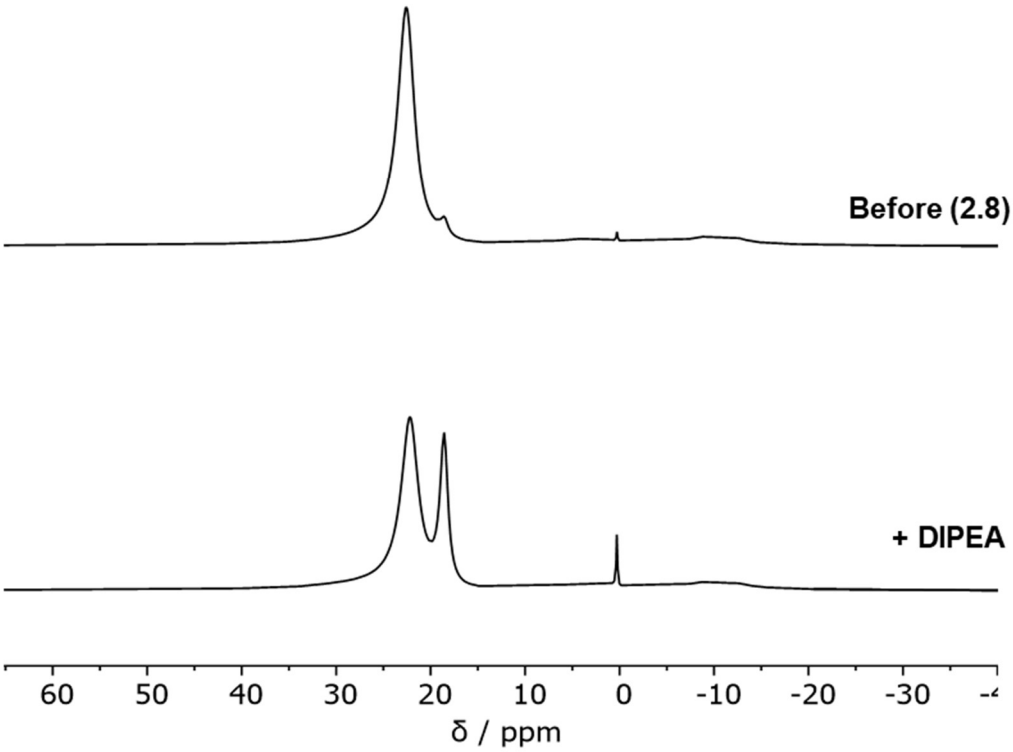

Figure 2.64: Stacked ^{11}B NMR (161 MHz, CD_2Cl_2) spectrum of the reaction of **2.8** with 1 equiv. DIPEA at RT.

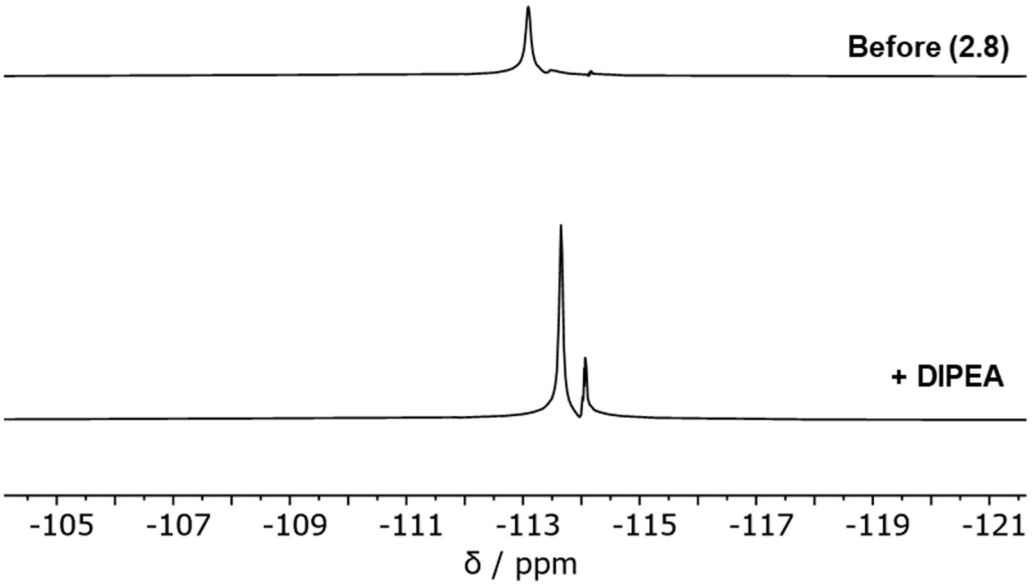

Figure 2.65: Stacked ^{19}F NMR (471 MHz, CD_2Cl_2) spectrum of the reaction of **2.8** with 1 equiv. DIPEA at RT.

Reaction of $IMeBH_2NTf_2$ with Benzyl Alcohol and 1 equiv. DBP at RT

- **Addition of 2 equiv. BnOH to $IMeBH_2NTf_2$: *in situ* NMR**

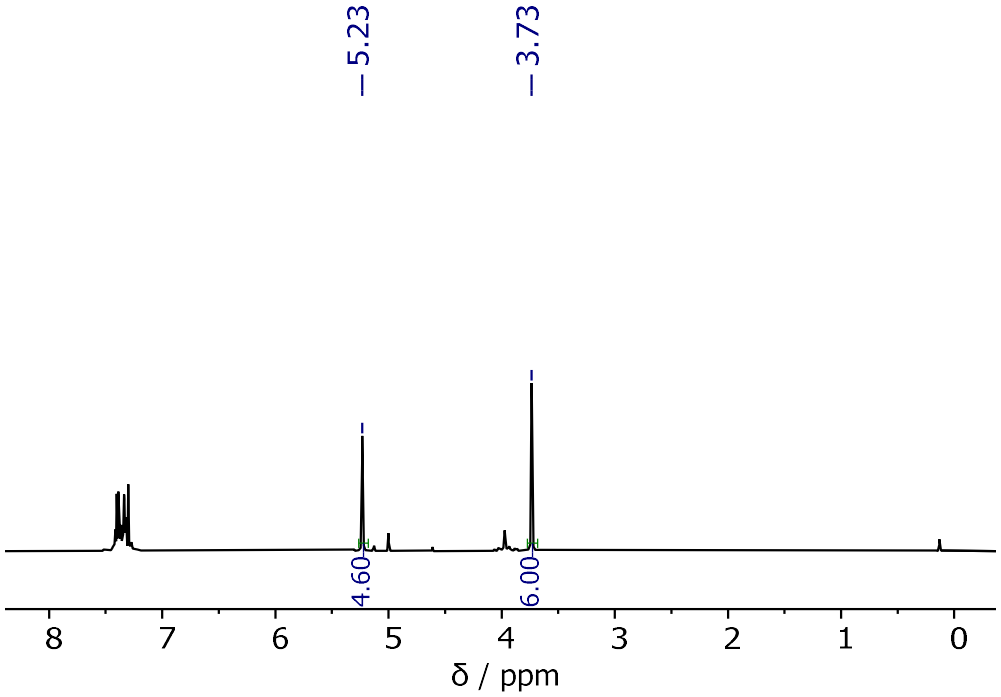

Figure 2.66: ^{1}H NMR (500 MHz, CD_2Cl_2) spectrum of the 1:2 reaction of $IMeBH_2NTf_2$ with benzyl alcohol, 15 mins RT

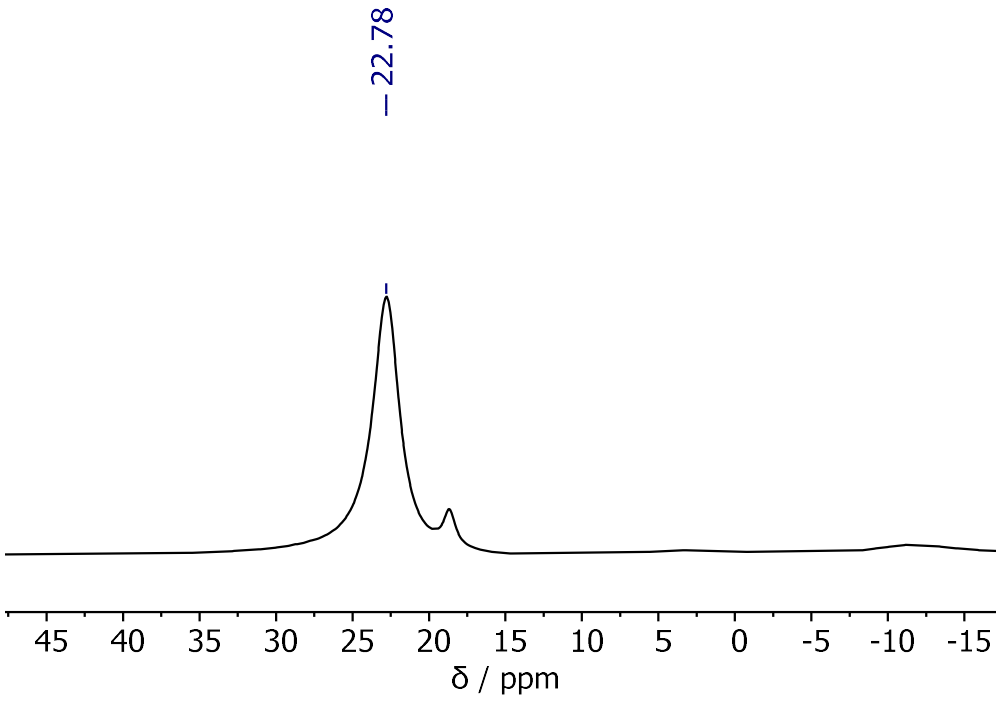

Figure 2.67: ^{11}B NMR (161 MHz, CD_2Cl_2) spectrum of the 1:2 reaction of $IMeBH_2NTf_2$ with benzyl alcohol, 15 mins RT

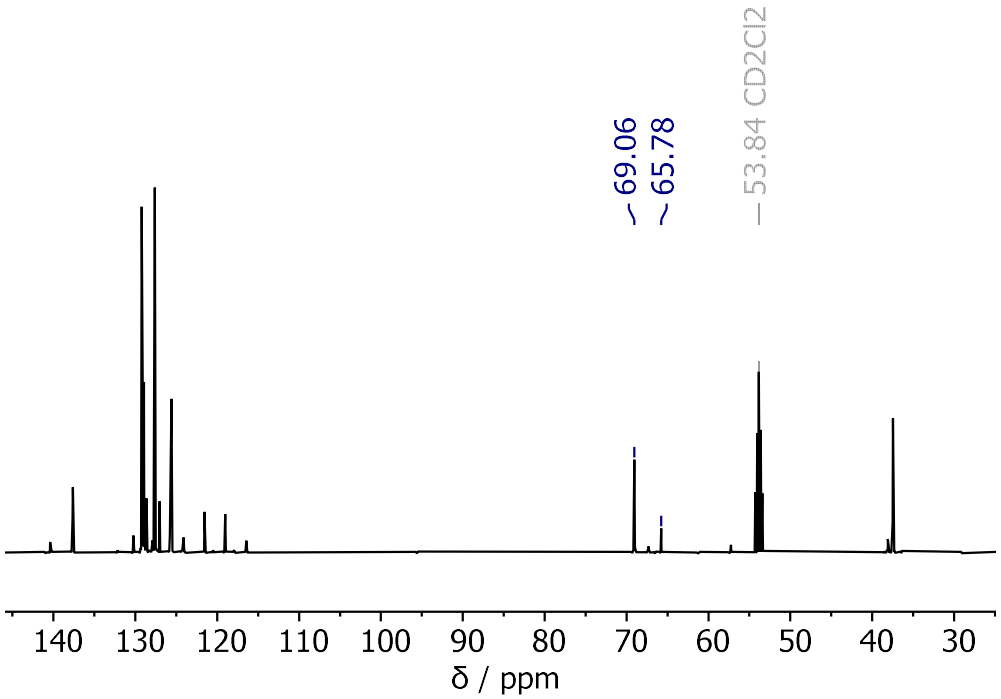

Figure 2.68: $^{13}C\{^{1}H\}$ NMR (126 MHz, CD_2Cl_2) spectrum of the 1:2 reaction of $IMeBH_2NTf_2$ with benzyl alcohol, 15 mins RT

- **Addition of 1 equiv. DBP:**

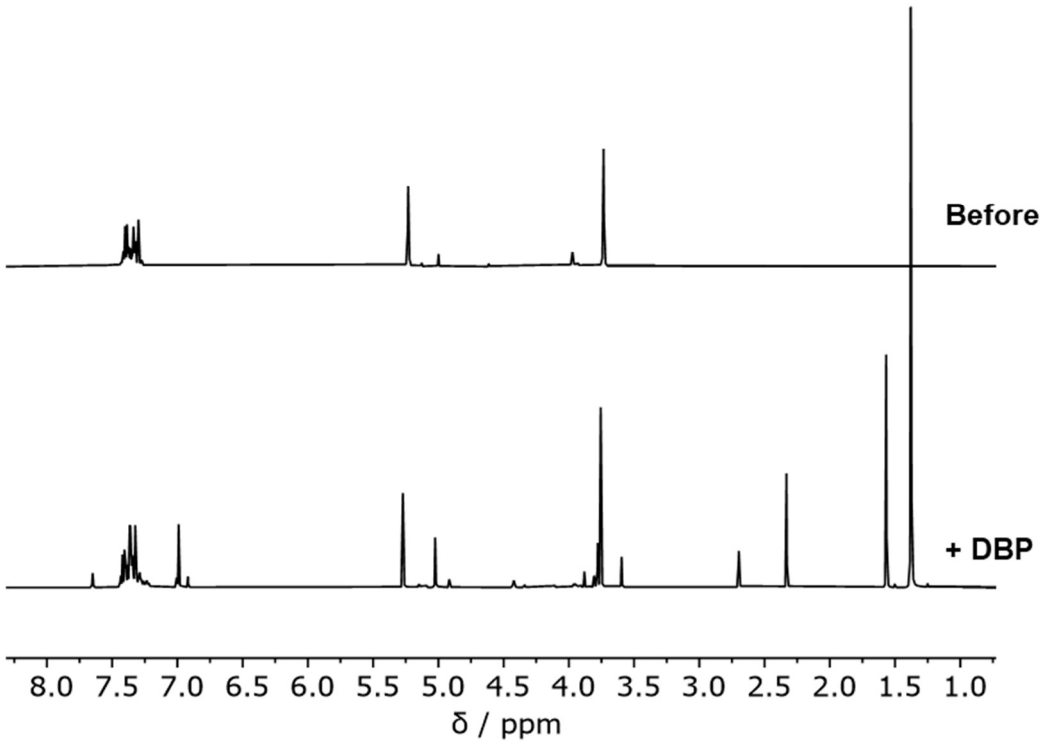

Figure 2.69: Stacked ^{1}H NMR (500 MHz, CD_2Cl_2) spectrum of the reaction of $IMeBH_2NTf_2$, 2 equiv. BnOH with 1 equiv. DBP at RT.

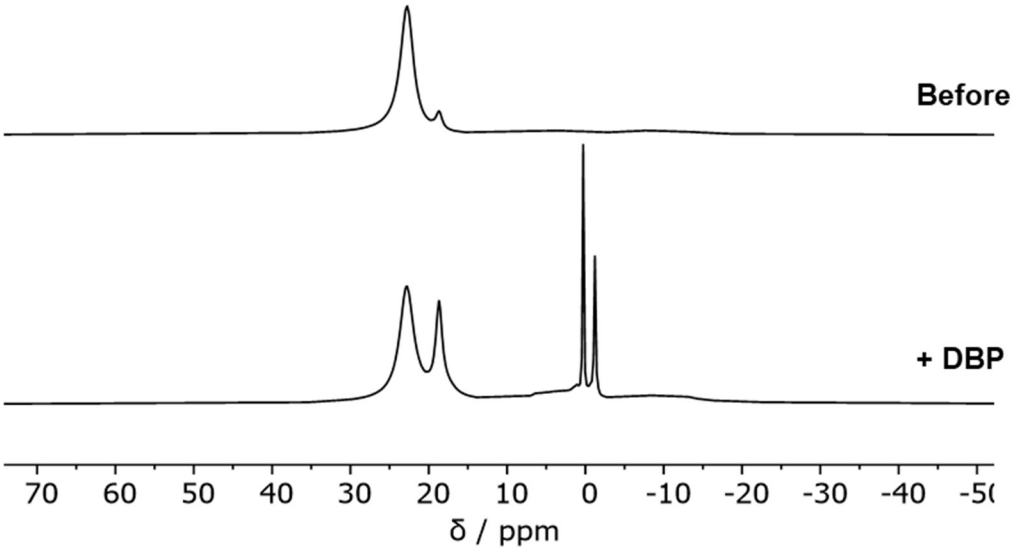

Figure 2.70: Stacked ^{11}B NMR (161 MHz, CD_2Cl_2) spectrum of the reaction of $IMeBH_2NTf_2$, 2 equiv. BnOH with 1 equiv. DBP at RT.

Chapter 3: ‘Borylation Directed Borylation’ of Indoles using Pyrazabole Electrophiles

3.6.2 – Directed C7-H Borylation of N-H Indoles

Scaled-up Synthesis of 7-Bpin Indoline (3.7)

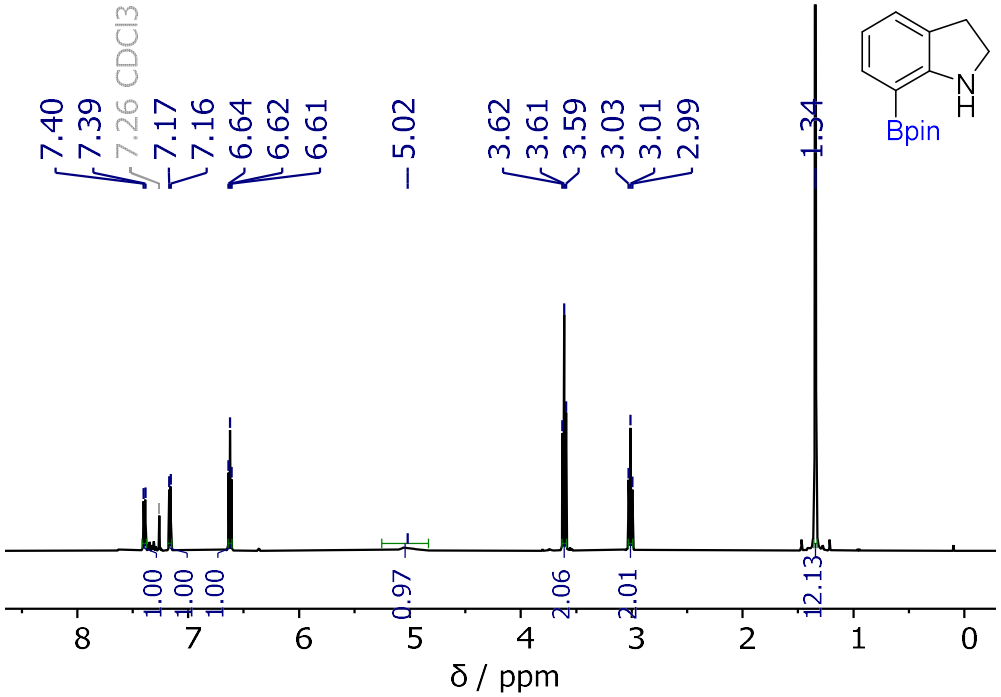

Figure 3.1: ^{1}H NMR (500 MHz, $CDCl_3$) spectrum of 7-Bpin indoline from the scaled-up reaction of indole.

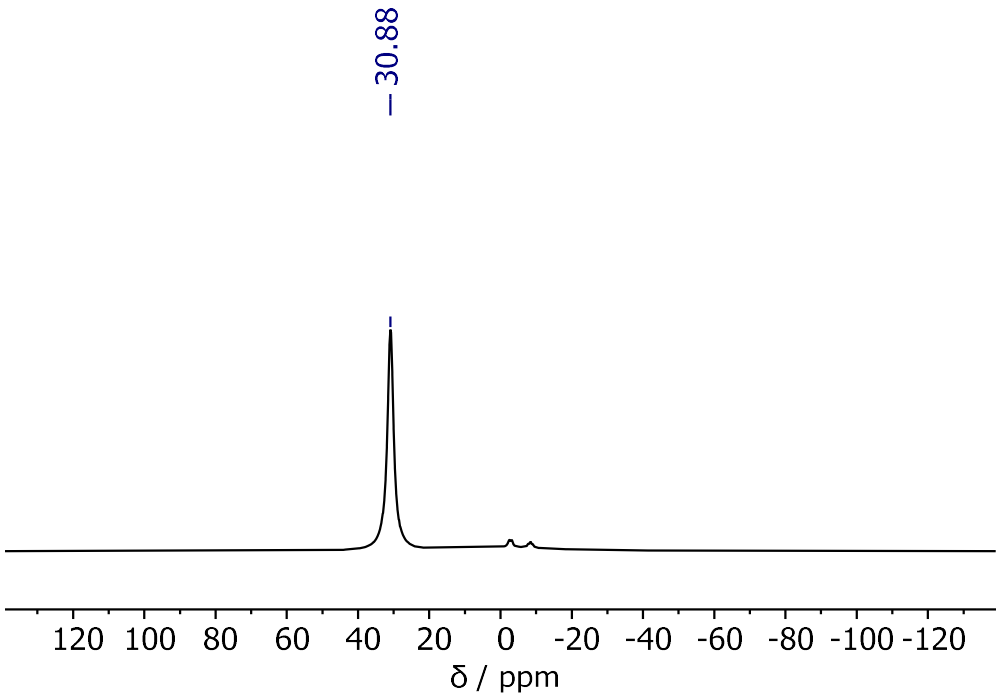

Figure 3.2: ^{11}B NMR (161 MHz, $CDCl_3$) spectrum of 7-Bpin indoline from the scaled-up reaction of indole.

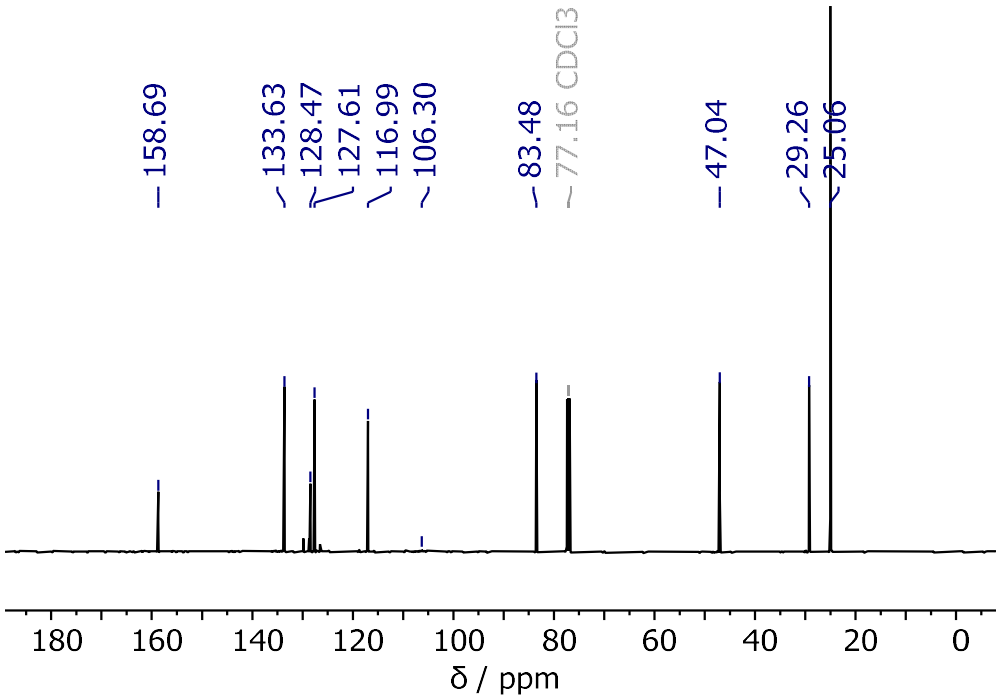

Figure 3.3: $^{13}C\{^{1}H\}$ NMR (126 MHz, $CDCl_3$) spectrum of 7-Bpin indoline from the scaled-up reaction of indole.

Suzuki-Miyaura Cross-Coupling: 7-Phenyl *N*-H Indoline

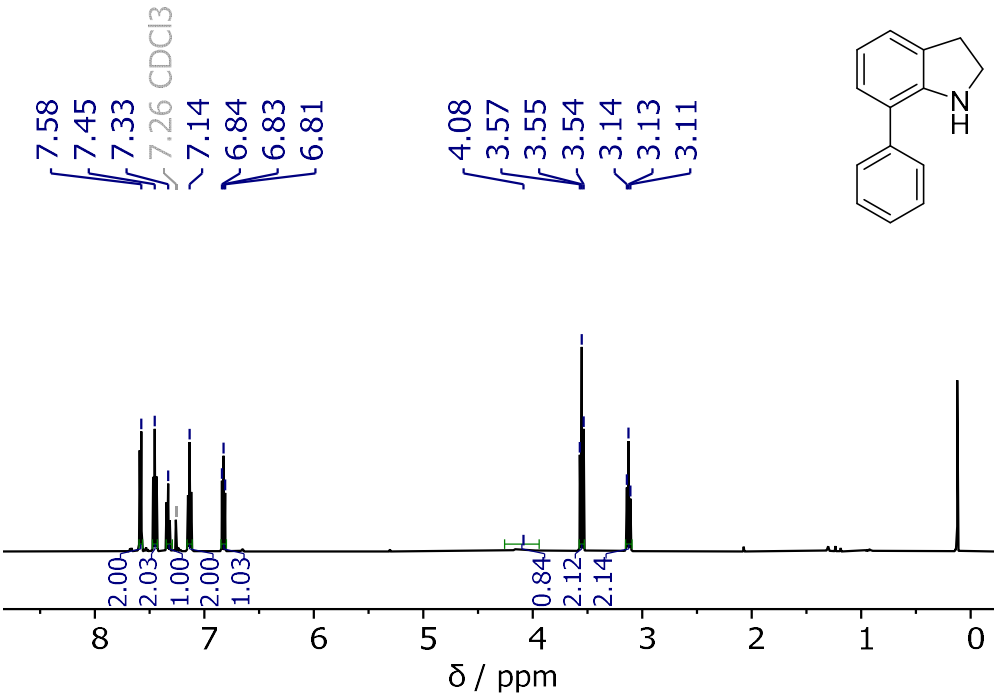

Figure 3.4: ^{1}H NMR (500 MHz, $CDCl_3$) spectrum of 7-phenyl indoline via the Suzuki-Miyaura cross coupling of 7-Bpin indoline and bromobenzene.

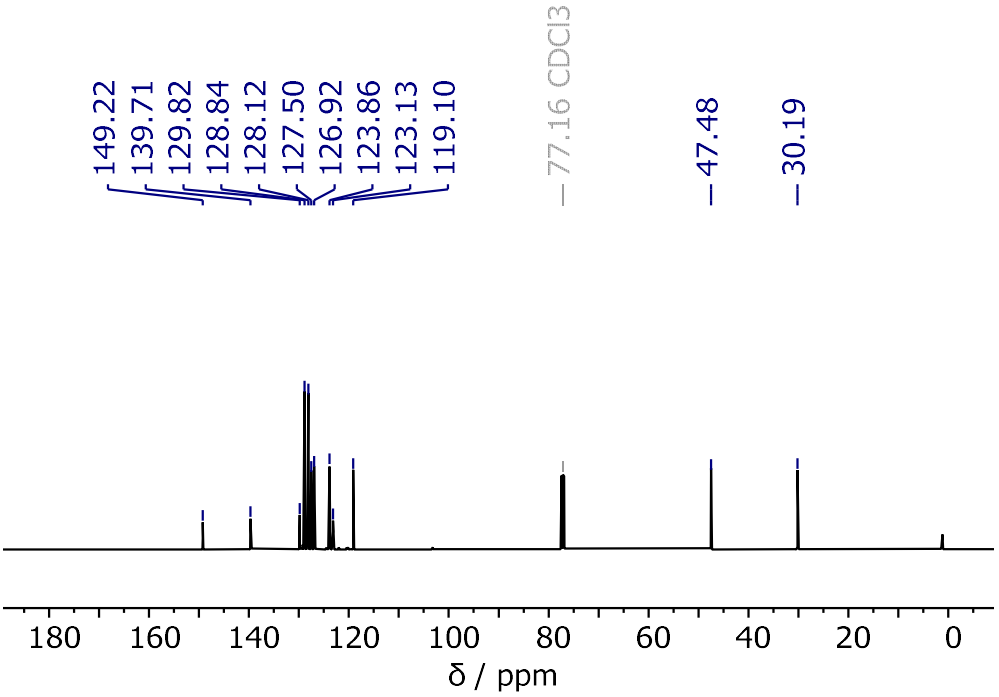

Figure 3.5: $^{13}C\{^{1}H\}$ NMR (126 MHz, $CDCl_3$) spectrum of 7-phenyl indoline via the Suzuki-Miyaura cross coupling of 7-Bpin indoline and bromobenzene.

3.6.3 – Directed *Ortho* C-H Borylation of Indoline and Aniline Derivatives

Indoline (3.7) from *N*-H Indoline

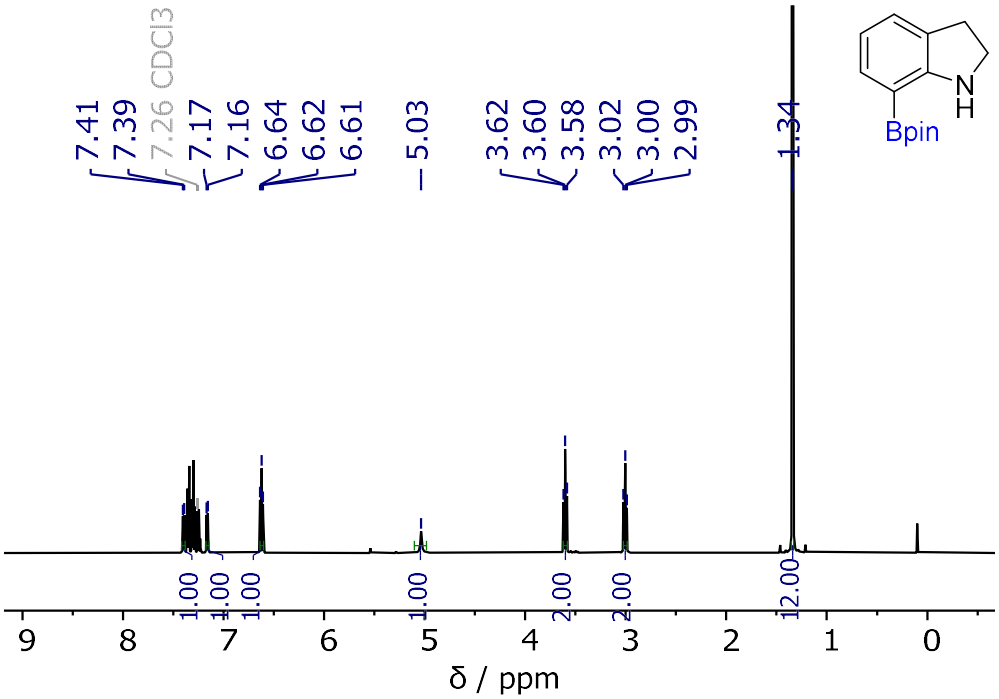

Figure 3.6: ^{1}H NMR (500 MHz, $CDCl_3$) spectrum of 7-Bpin indoline from *N*-H Indoline. *Note: Some residual PhCl is observed at 7.3 ppm.*

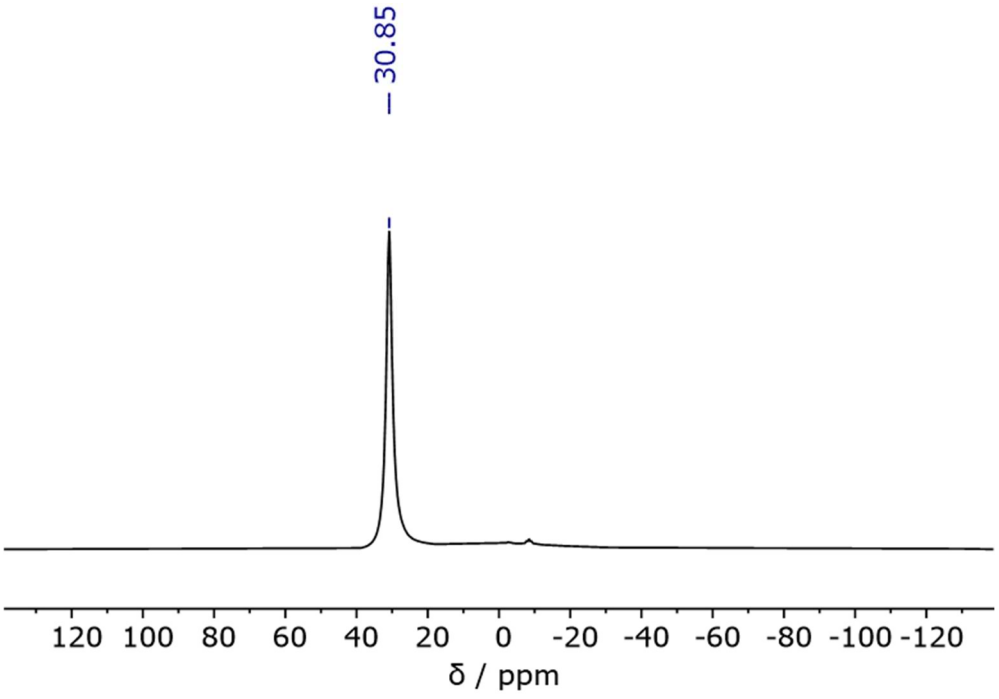

Figure 3.7: ^{11}B NMR (161 MHz, $CDCl_3$) spectrum of 7-Bpin indoline from *N*-H Indoline

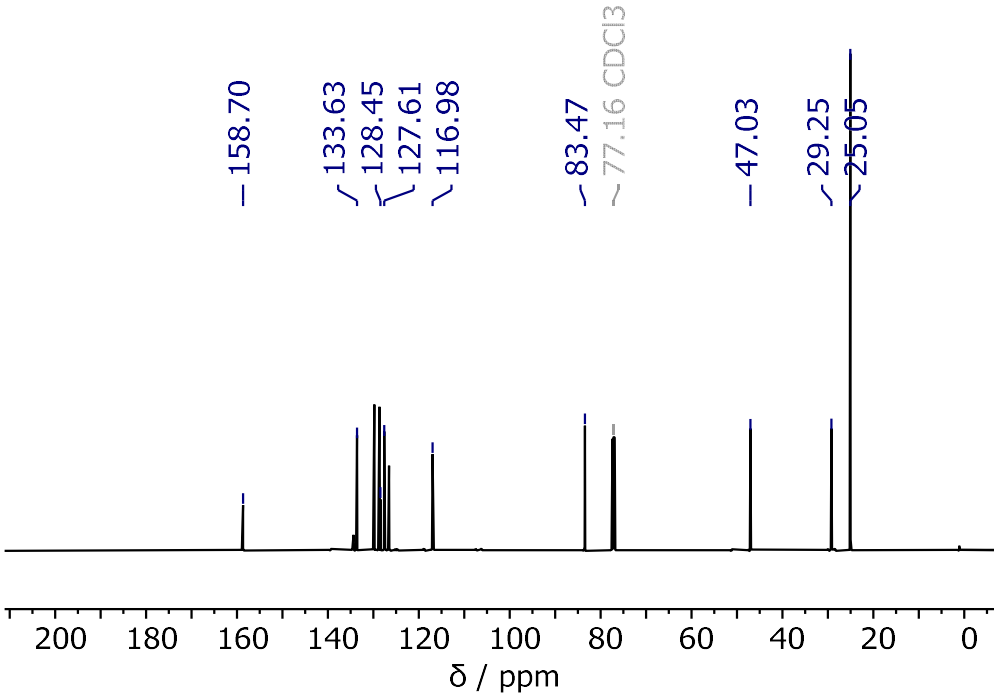

Figure 3.8: $^{13}C\{^{1}H\}$ NMR (126 MHz, $CDCl_3$) spectrum of 7-Bpin indoline from N-H Indoline. *Note: Some residual PhCl is observed at 130 ppm.*

N/C7-Diborylated Indoline Intermediate (3.6) from *N*-H Indoline

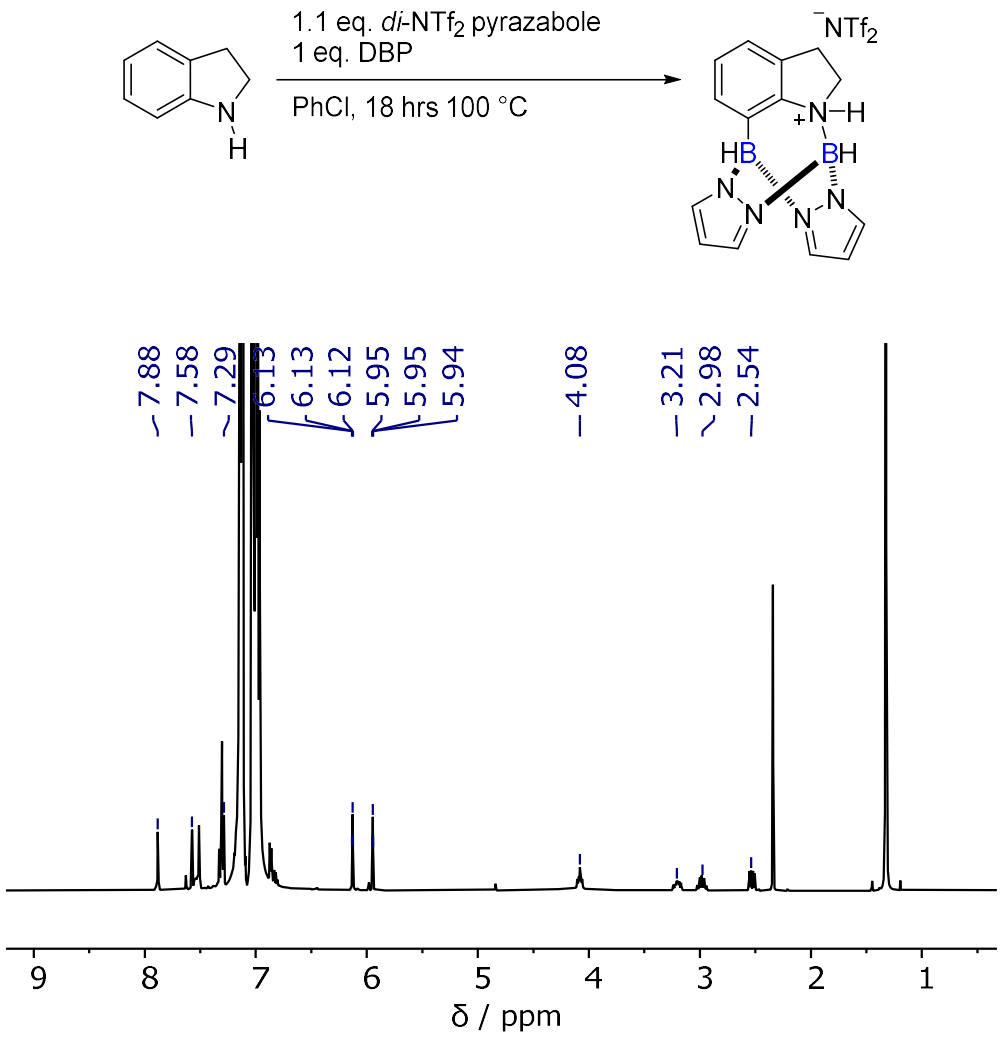

Figure 3.9: ^{1}H NMR (500 MHz, C_6H_5Cl) spectrum of N/C7-borylated indoline intermediate **3.6** following the reaction of *N*-H indoline, *di*-NTf_2 pyrazabole and DBP, 18 hrs 100 °C. The resonances at 10.77, 7.32, 2.35 and 1.34 ppm correspond to [DBP-H][NTf_2].

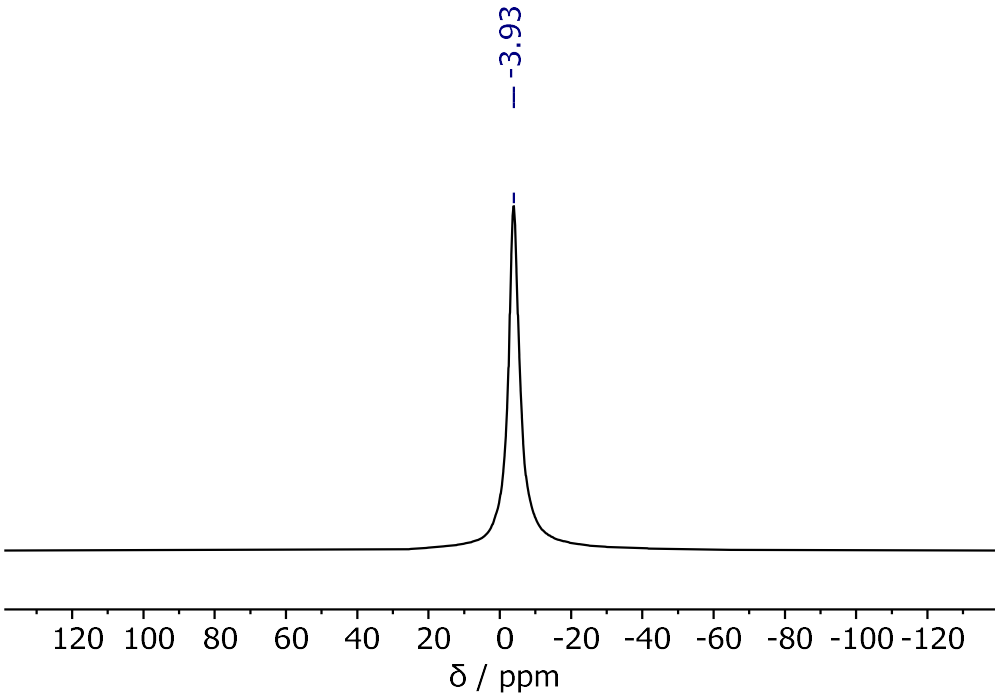

Figure 3.10: ^{11}B NMR (161 MHz, C_6H_5Cl) spectrum of N/C7-borylated indoline intermediate **3.6** following the reaction of *N*-H indoline, *di*-NTf_2 pyrazabole and DBP, 18 hrs 100 °C. The resonances at 10.77, 7.32, 2.35 and 1.34 ppm correspond to [DBP-H][NTf_2].

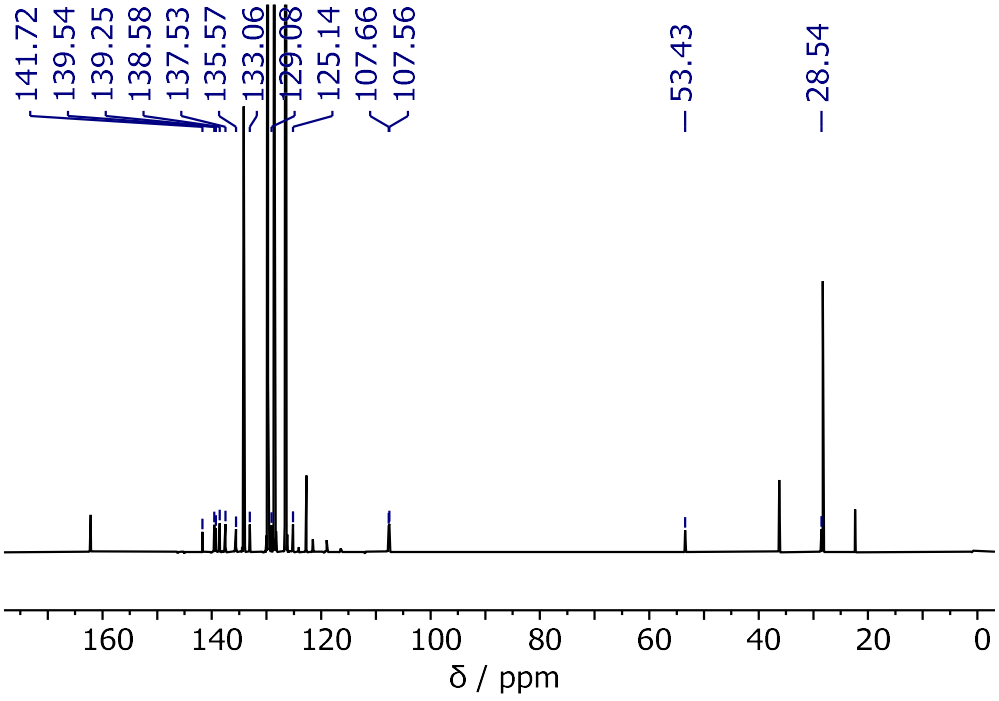

Figure 3.11: $^{13}C\{^1H\}$ NMR (126 MHz, C_6H_5Cl) spectrum of N/C7-borylated indoline intermediate **3.6** following the reaction of *N*-H indoline, *di*-NTf_2 pyrazabole and DBP, 18 hrs 100 °C.

8-Bpin Tetrahydroquinoline (3.30)

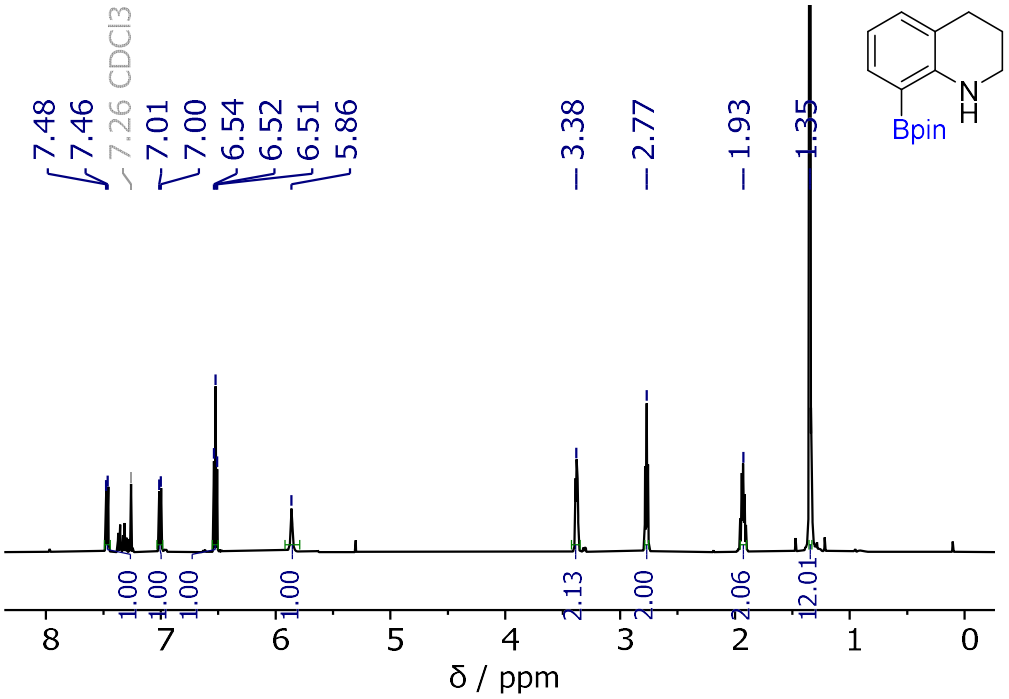

Figure 3.12: ^{1}H NMR (500 MHz, $CDCl_3$) spectrum of 8-Bpin tetrahydroquinoline.

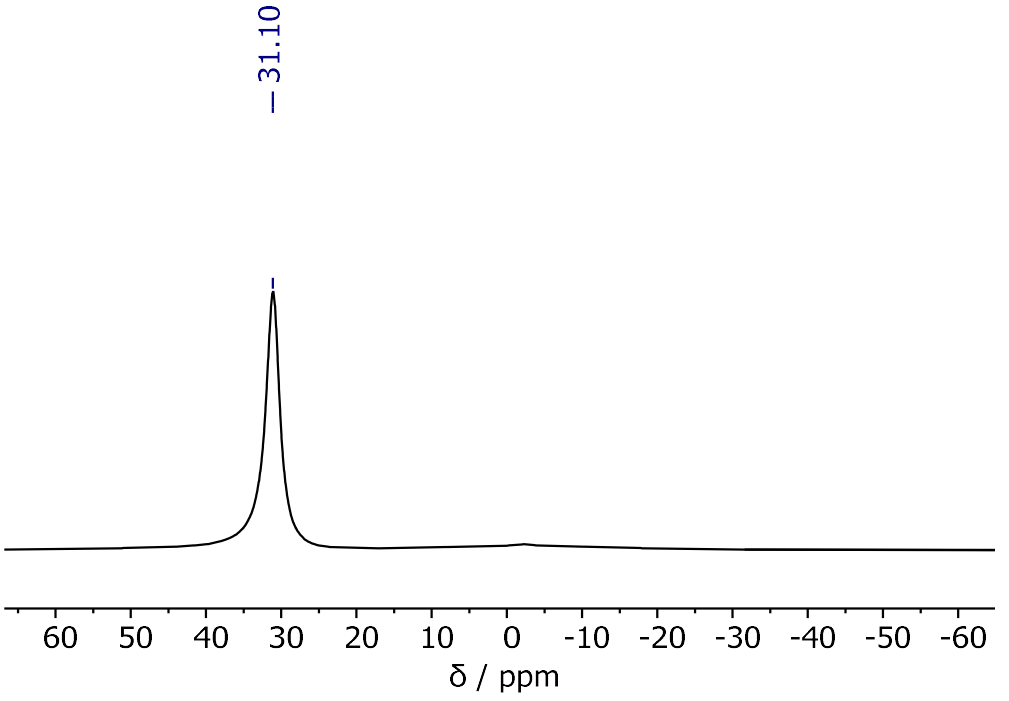

Figure 3.13: ^{11}B NMR (161 MHz, $CDCl_3$) spectrum of 8-Bpin tetrahydroquinoline.

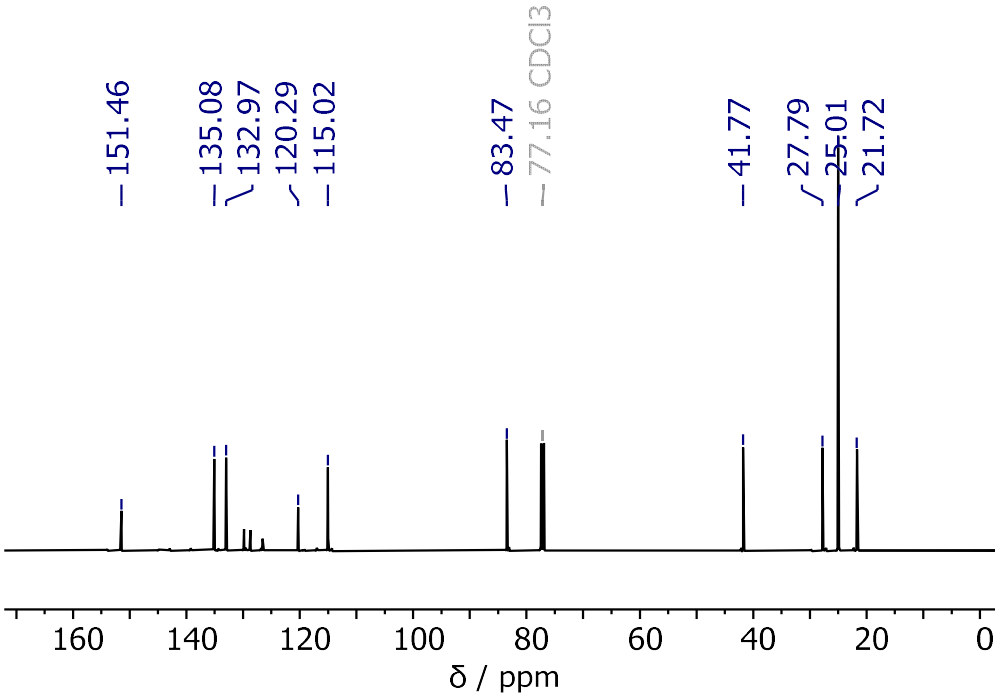

Figure 3.14: $^{13}C\{^{1}H\}$ NMR (126 MHz, $CDCl_3$) spectrum of 8-Bpin tetrahydroquinoline

3.6.5 – Reaction Profiling using *in situ* NMR Spectroscopy

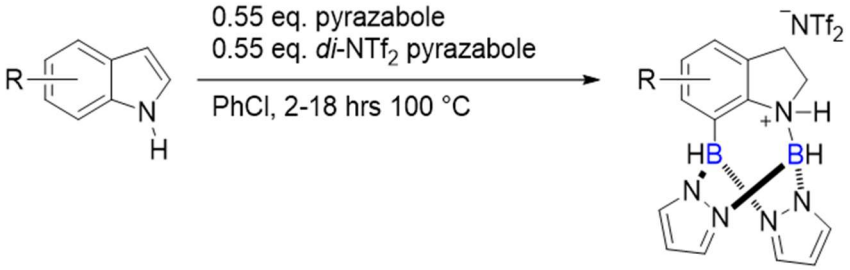

Indole to 3.6: Reaction Profile

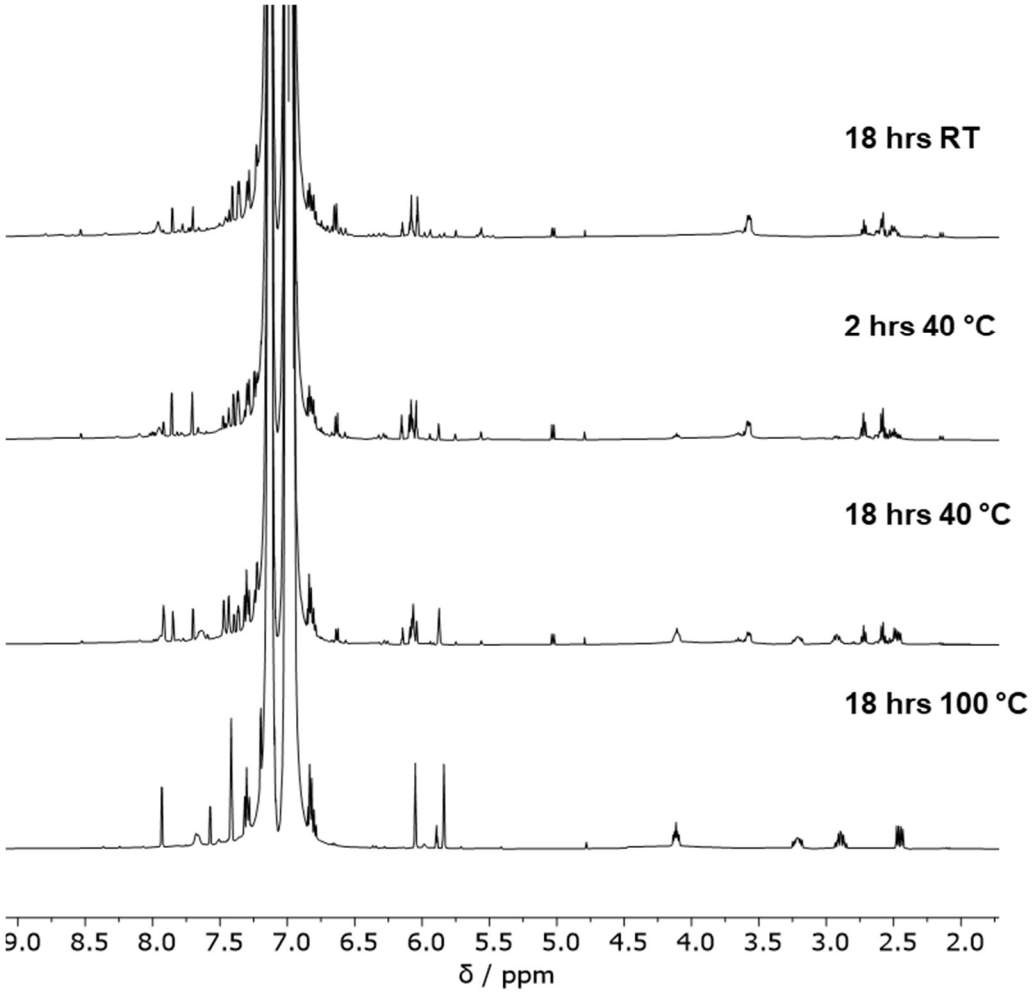

Figure 3.15: Stacked ^{1}H NMR (500 MHz, C_6H_5Cl) spectra of the formation of the N/C7-borylated indoline intermediate **3.6** in the reaction of *N*-H indole and *mono*-NTf_2 pyrazabole.

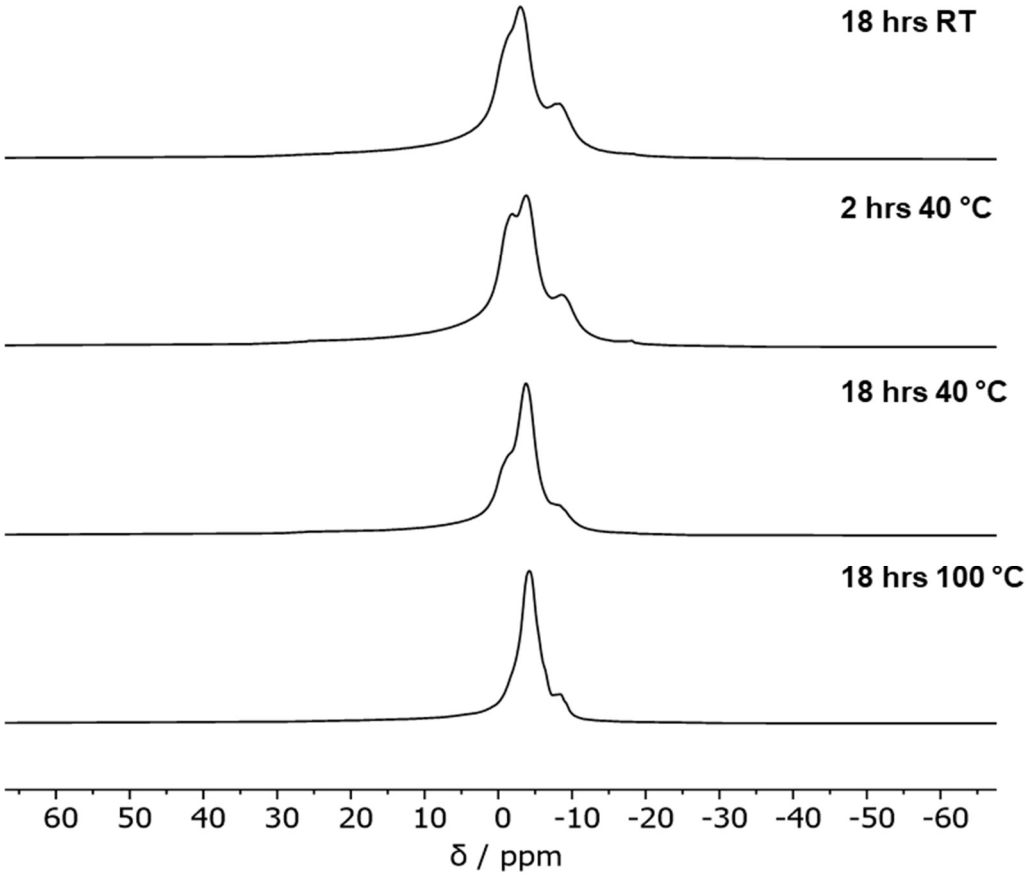

Figure 3.16: Stacked ^{11}B NMR (161 MHz, C_6H_5Cl) spectra of the formation of the N/C7-borylated indoline intermediate **3.6** in the reaction of *N*-H indole and *mono*-NTf_2 pyrazabole.

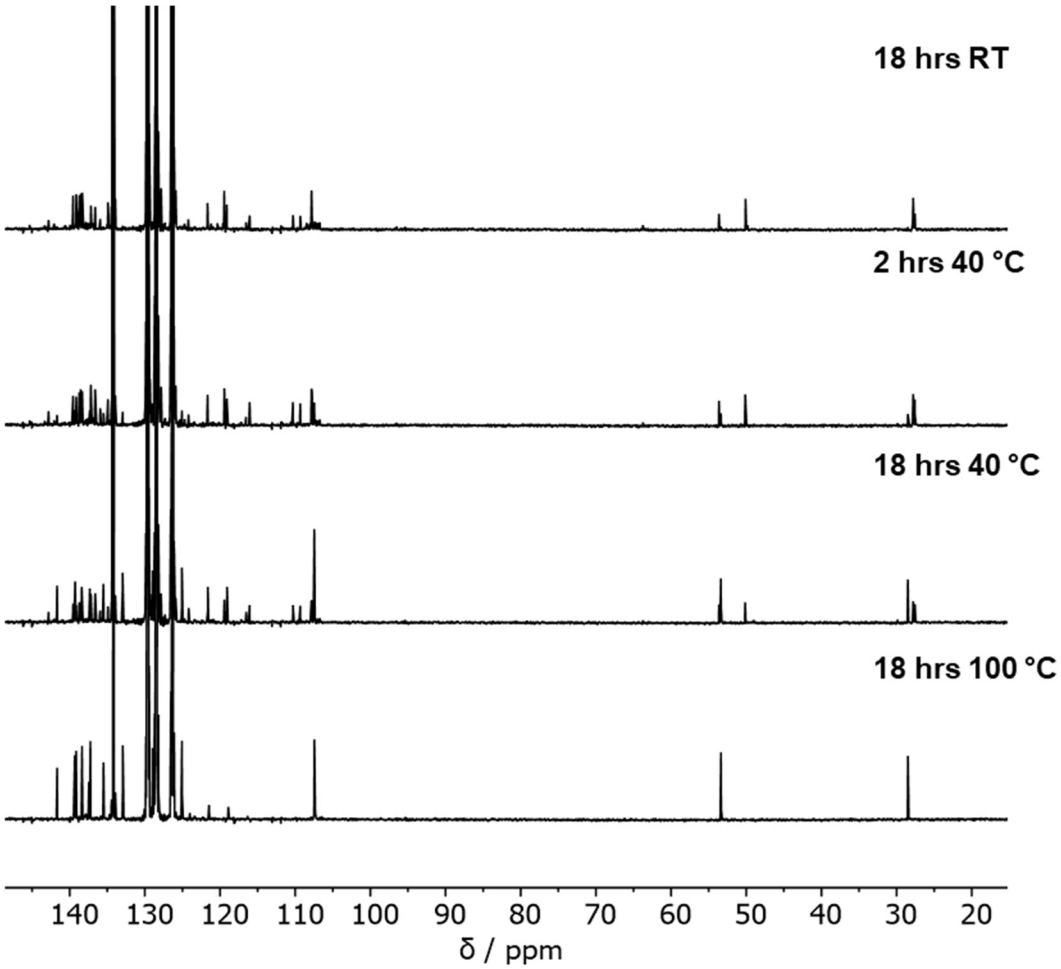

Figure 3.17: Stacked $^{13}C\{^{1}H\}$ NMR (126 MHz, C_6H_5Cl) spectra of the formation of the N/C7-borylated indoline intermediate **3.6** in the reaction of *N*-H indole and *mono*-NTf_2 pyrazabole.

5-Cl Indole to 3.15: Reaction Profile

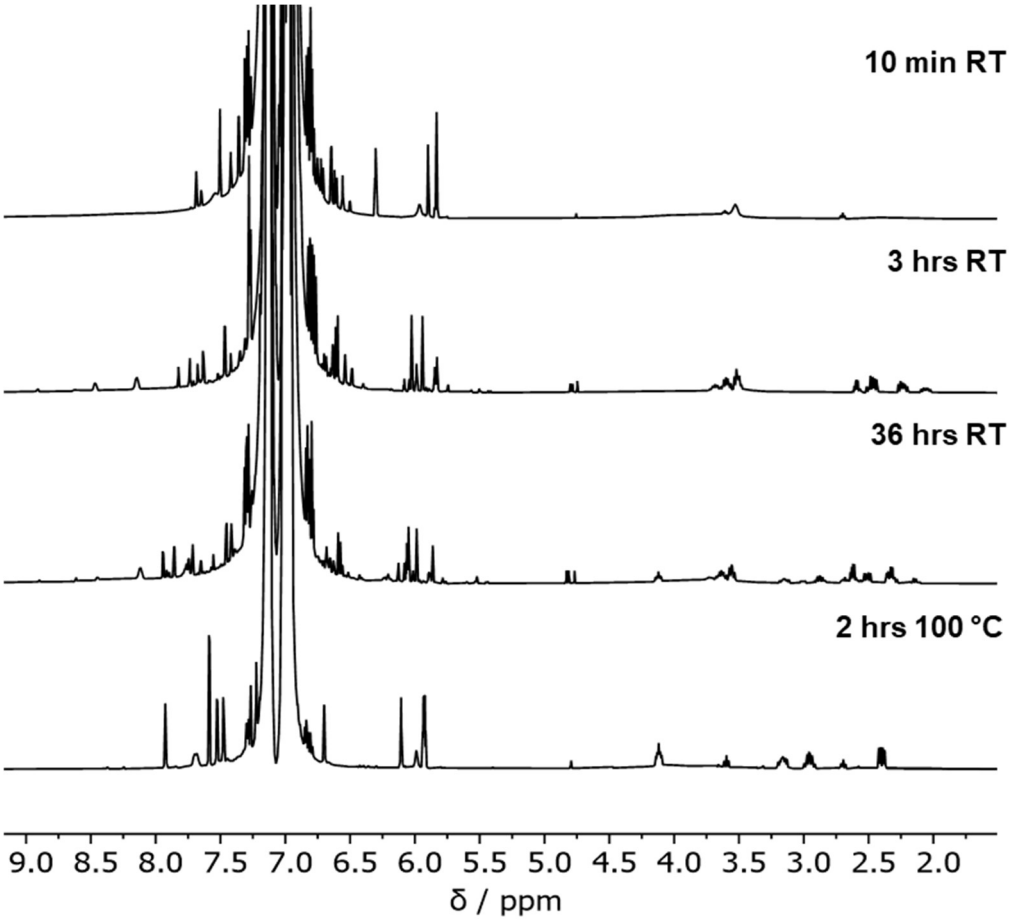

Figure 3.18: Stacked ^{1}H NMR (500 MHz, C_6H_5Cl) spectra of the formation of the N/C7-borylated indoline intermediate **3.15** in the reaction of 5-Cl indole and *mono*-NTf_2 pyrazabole.

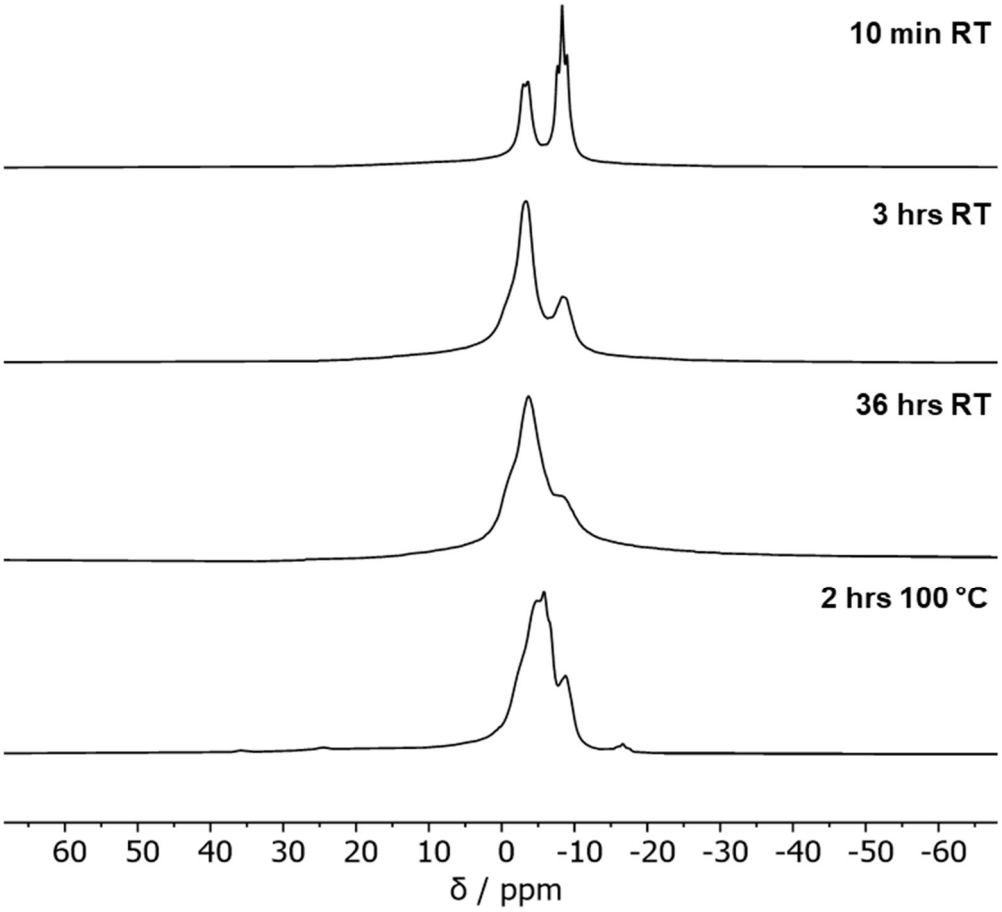

Figure 3.19: Stacked ^{11}B NMR (161 MHz, C_6H_5Cl) spectra of the formation of the N/C7-borylated indoline intermediate **3.15** in the reaction of 5-Cl indole and *mono*-NTf_2 pyrazabole.

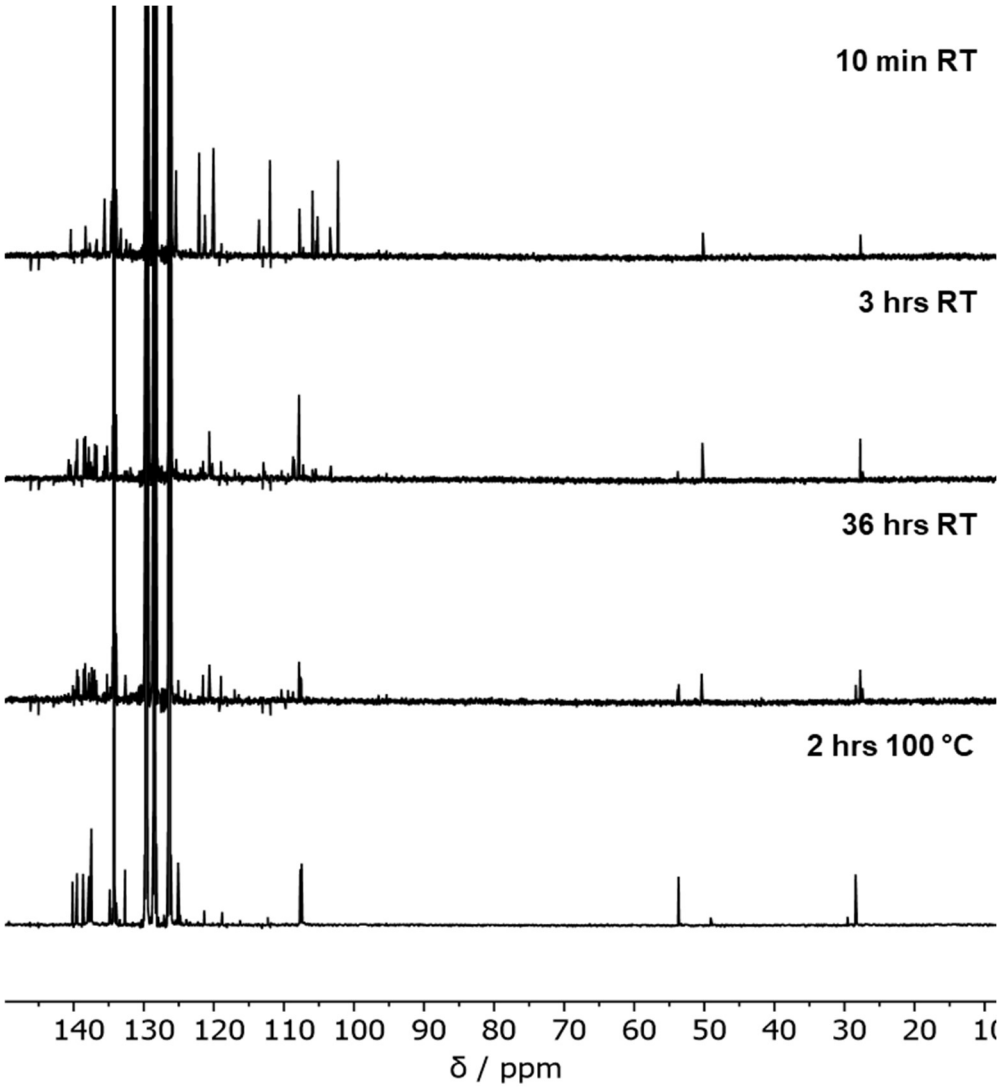

Figure 3.20: Stacked $^{13}C\{^{1}H\}$ NMR (126 MHz, C_6H_5Cl) spectra of the formation of the N/C7-borylated indoline intermediate **3.15** in the reaction of 5-Cl indole and *mono*-NTf_2 pyrazabole.

Attempted Catalytic Reaction of 5-Cl Indole

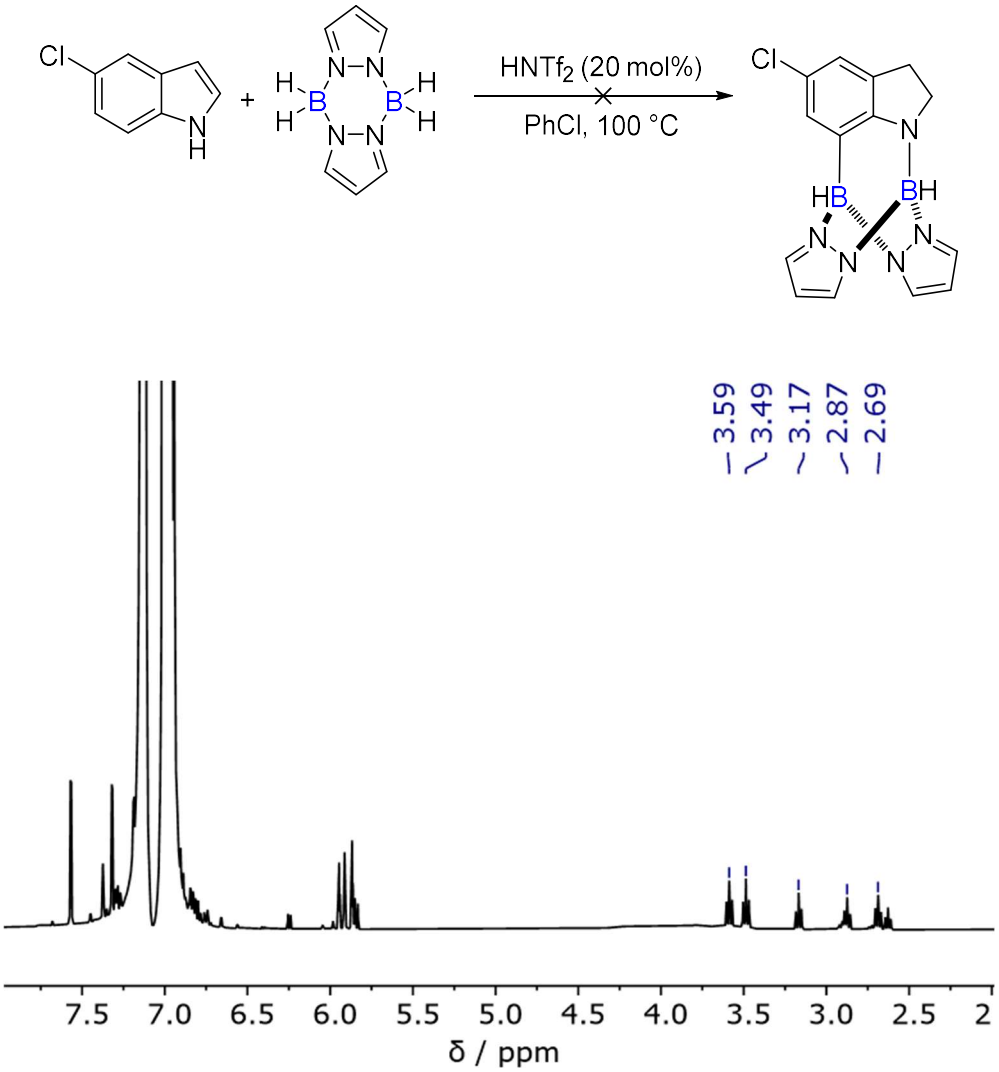

Figure 3.21: ^{1}H NMR (500 MHz, C_6H_5Cl) spectrum of the reaction of 5-Cl indole with pyrazabole and 20 mol% $HNTf_2$, after 24 hours at 100 °C.

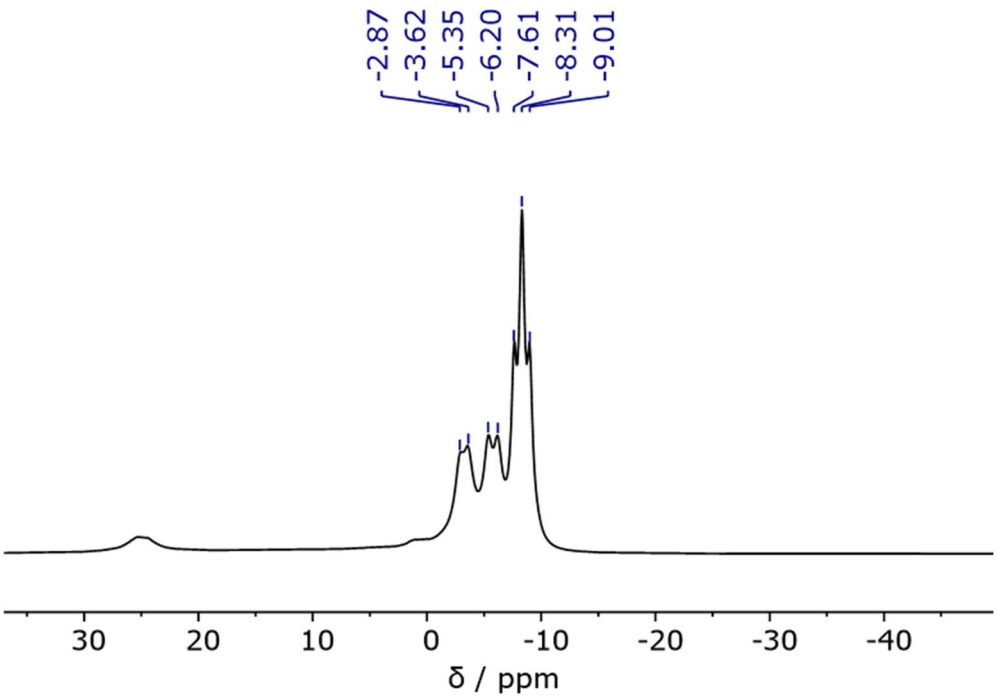

Figure 3.22: ^{11}B NMR (161 MHz, C_6H_5Cl) spectrum of the reaction of 5-Cl indole with pyrazabole and 20 mol% $HNTf_2$, after 24 hours at 100 °C.

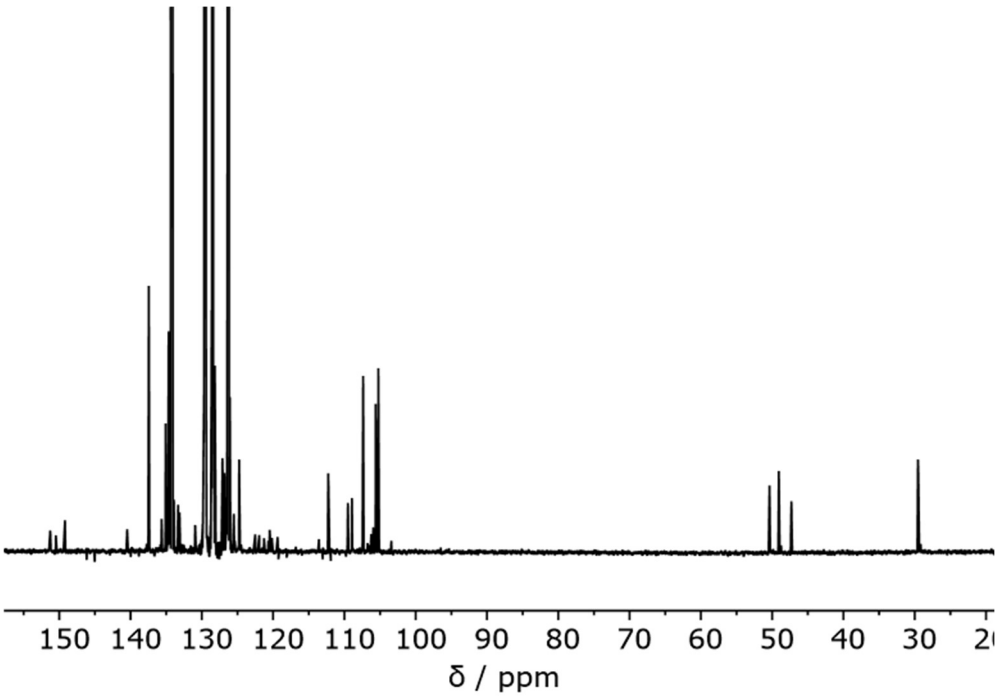

Figure 3.23: $^{13}C\{^1H\}$ NMR (126 MHz, C_6H_5Cl) spectrum of the reaction of 5-Cl indole with pyrazabole and 20 mol% $HNTf_2$, after 24 hours at 100 °C.

3.6.6 – Deuterium-Labelling Experiments

N-D Indole

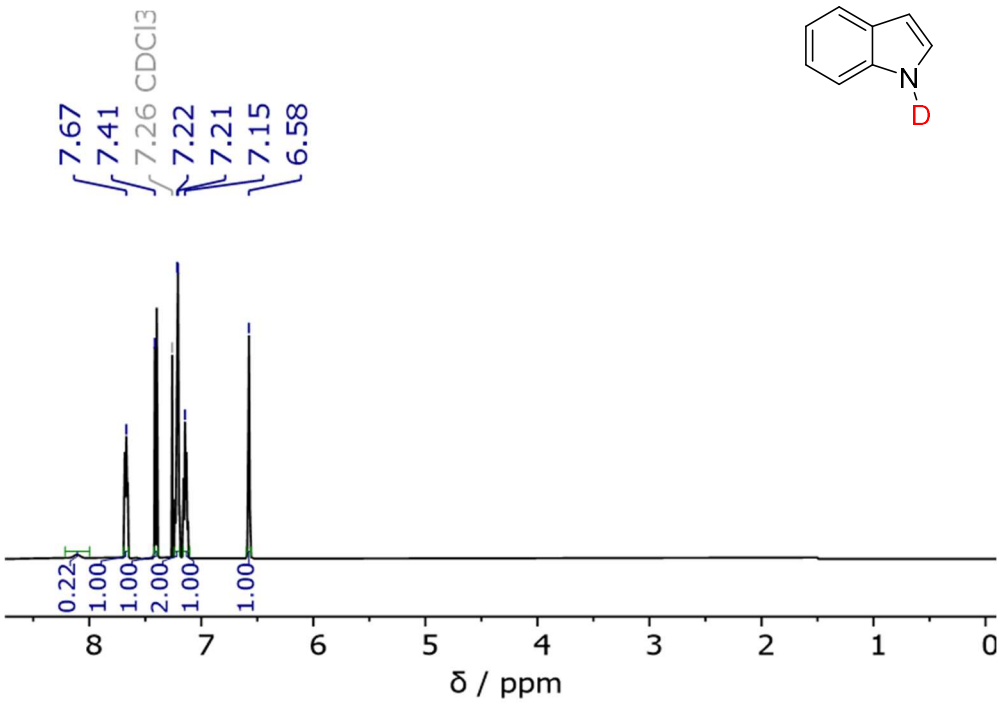

Figure 3.24: ^{1}H NMR (500 MHz, $CDCl_3$) spectrum of *N*-D Indole.

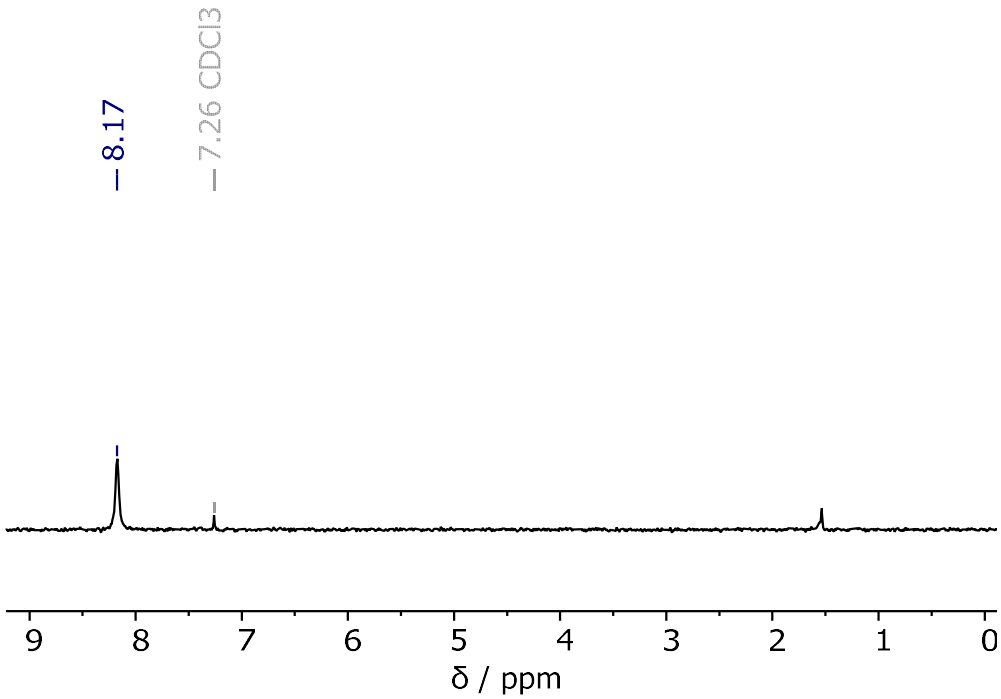

Figure 3.25: ^{2}H NMR (77 MHz, $CHCl_3$) spectrum of *N*-D Indole.

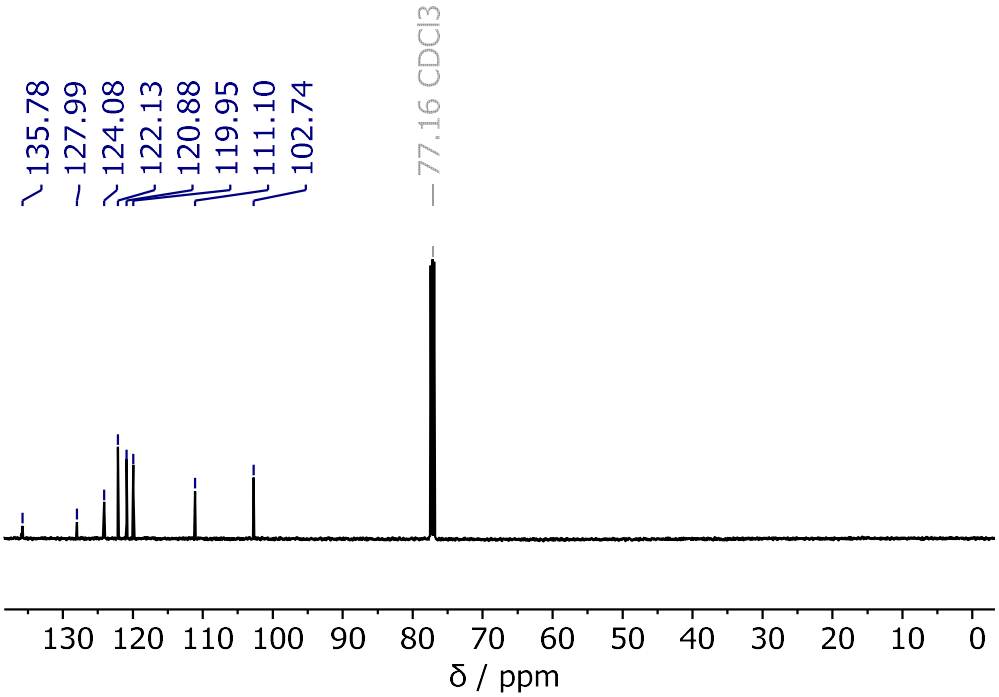

Figure 3.26: $^{13}C\{^{1}H\}$ NMR (126 MHz, $CDCl_3$) spectrum of *N*-D Indole.

N-D Indole to Intermediate 3.6-D: Reaction Profile

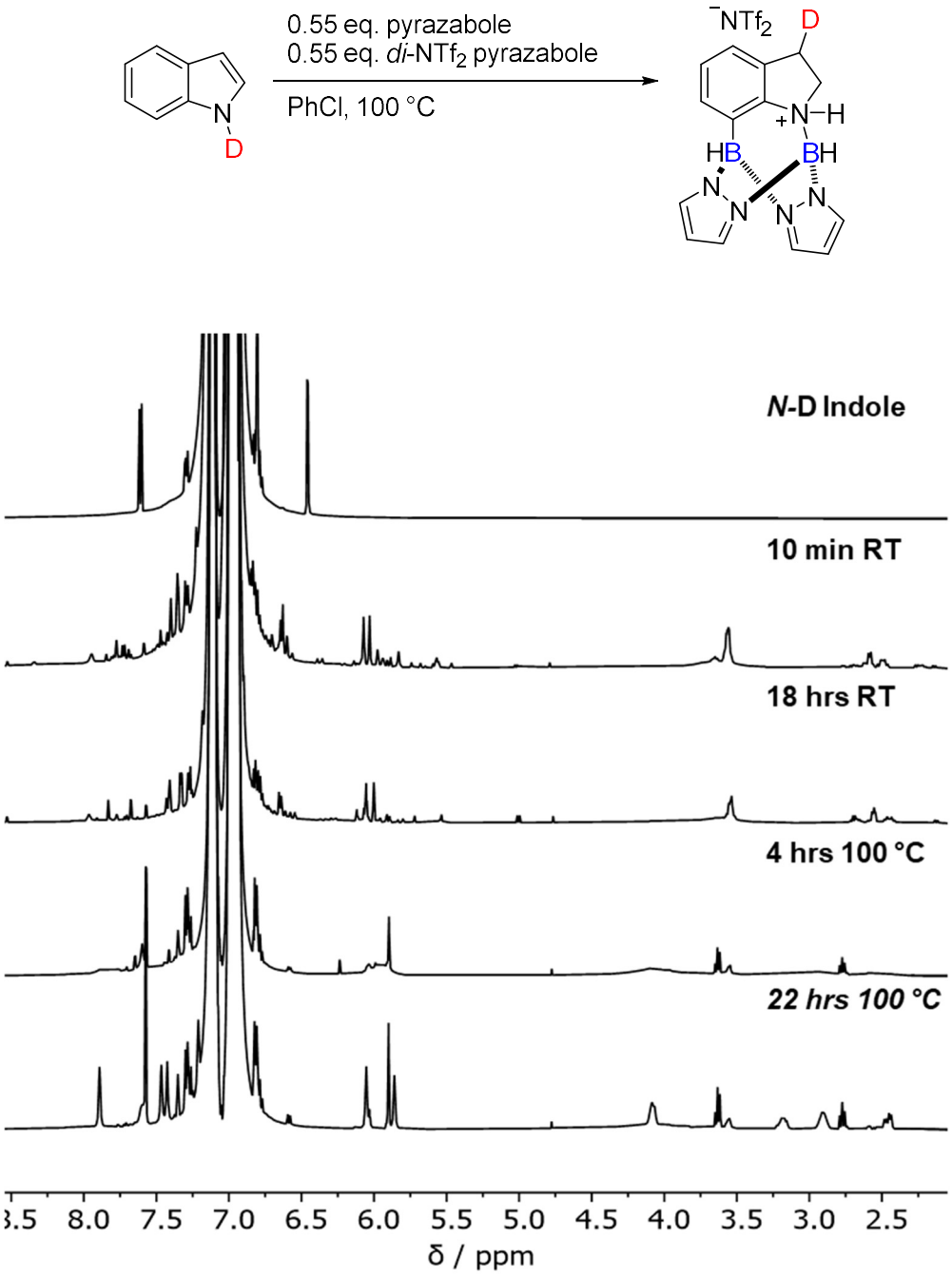

Figure 3.27: Stacked ^{1}H NMR (500 MHz, C_6H_5Cl) spectra of the formation of the N/C7-borylated indoline intermediate **3.6-D** in the reaction of *N*-D indole and *mono*-NTf_2 pyrazabole.

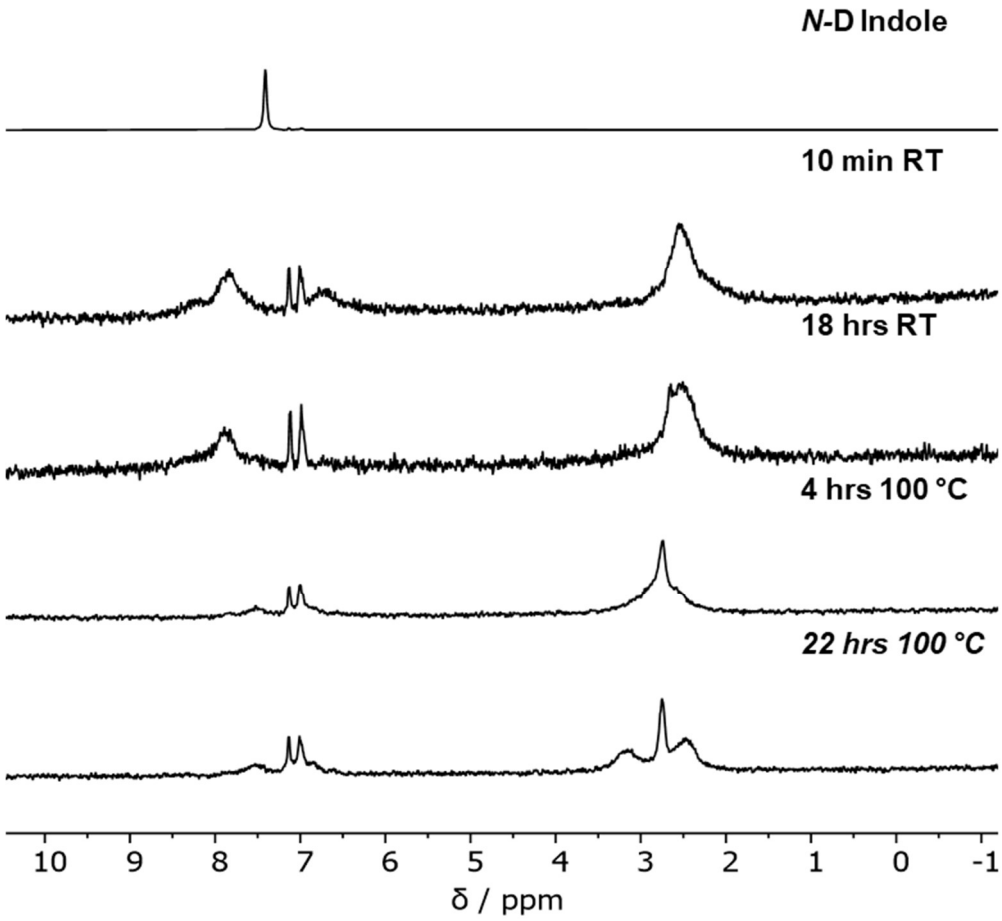

Figure 3.28: Stacked ^{2}H NMR (77 MHz, C_6H_5Cl) spectra of the formation of the N/C7-borylated indoline intermediate **3.6-D** in the reaction of *N*-D indole and *mono*-NTf_2 pyrazabole.

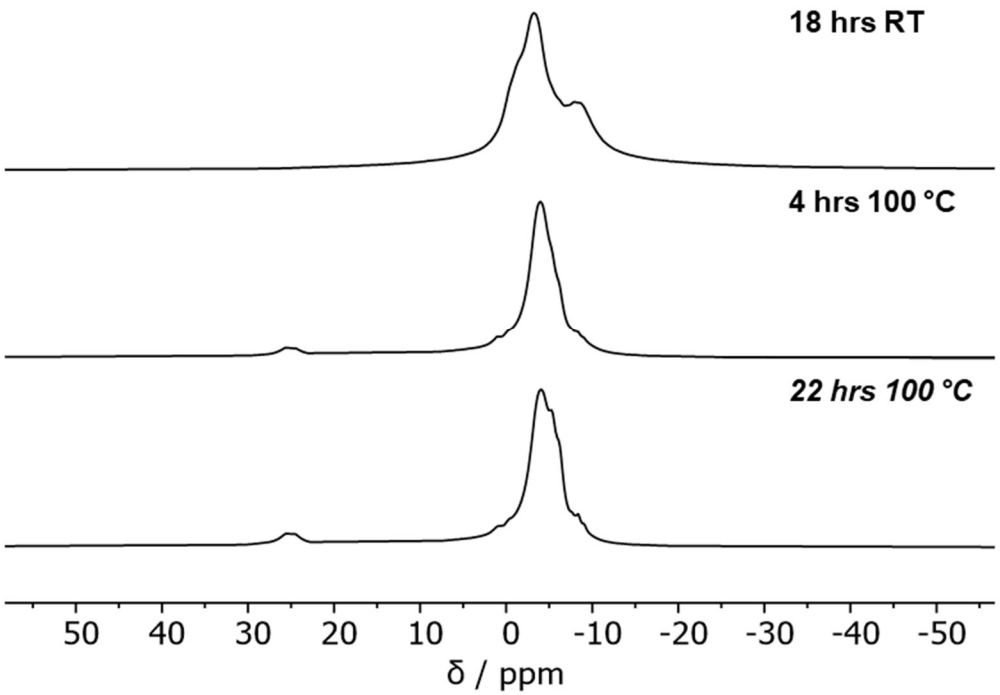

Figure 3.29: Stacked ^{11}B NMR (161 MHz, C_6H_5Cl) spectra of the formation of the N/C7-borylated indoline intermediate **3.6-D** in the reaction of *N*-D indole and *mono*-NTf_2 pyrazabole.

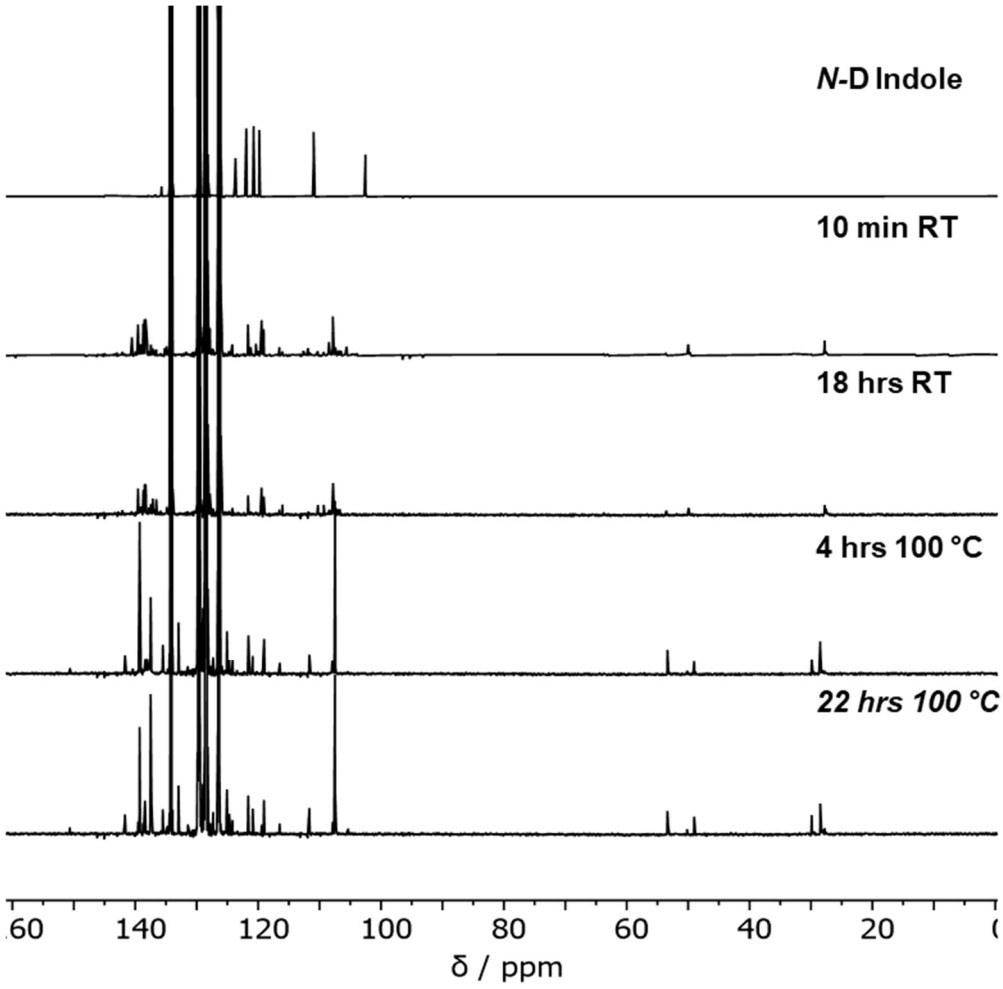

Figure 3.30: Stacked $^{13}C\{^{1}H\}$ NMR (126 MHz, C_6H_5Cl) spectra of the formation of the N/C7-borylated indoline intermediate **3.6-D** in the reaction of *N*-D indole and *mono*-NTf_2 pyrazabole.

3-Deutero 7-Bpin Indoline (3.7-D)

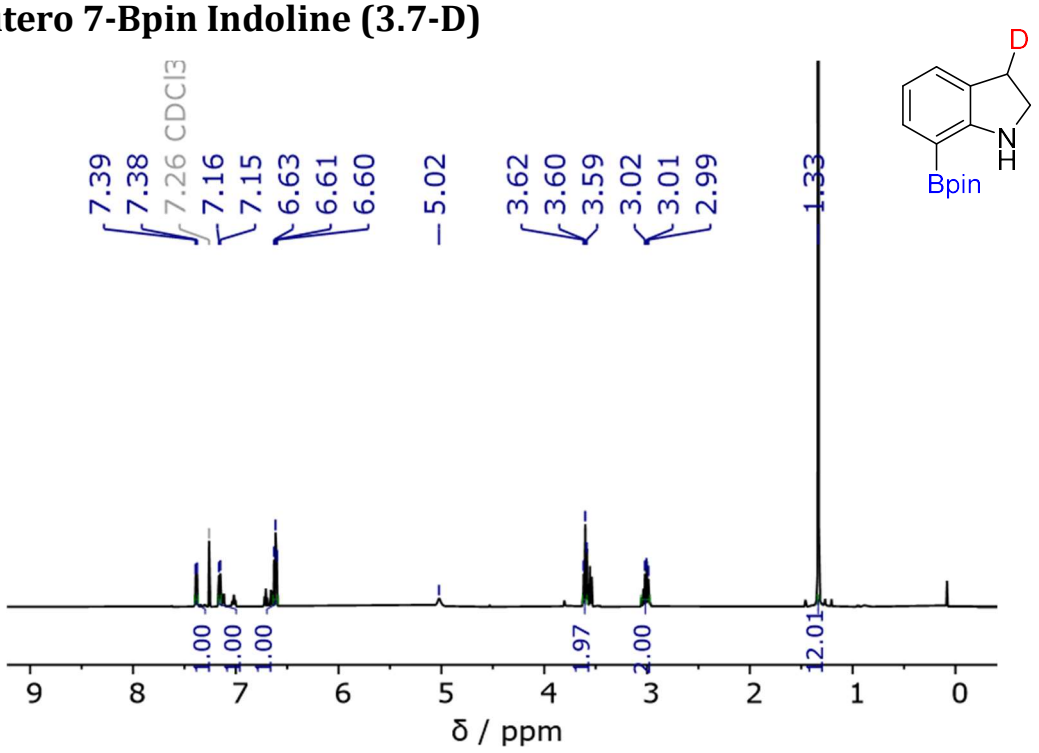

Figure 3.31: ^{1}H NMR (500 MHz, $CDCl_3$) spectrum of 3-D 7-Bpin indoline. Note: some minor 3-H 7-Bpin indoline is present, resulting in minor overlapping resonances.

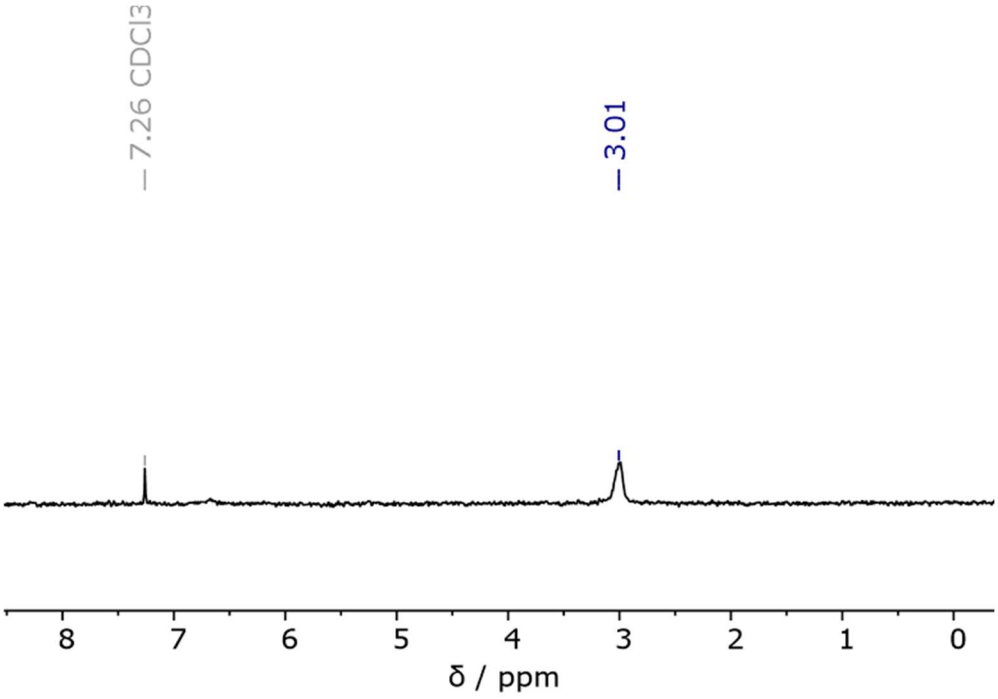

Figure 3.32: ^{2}H NMR (77 MHz, $CHCl_3$) spectrum of 3-D 7-Bpin indoline.

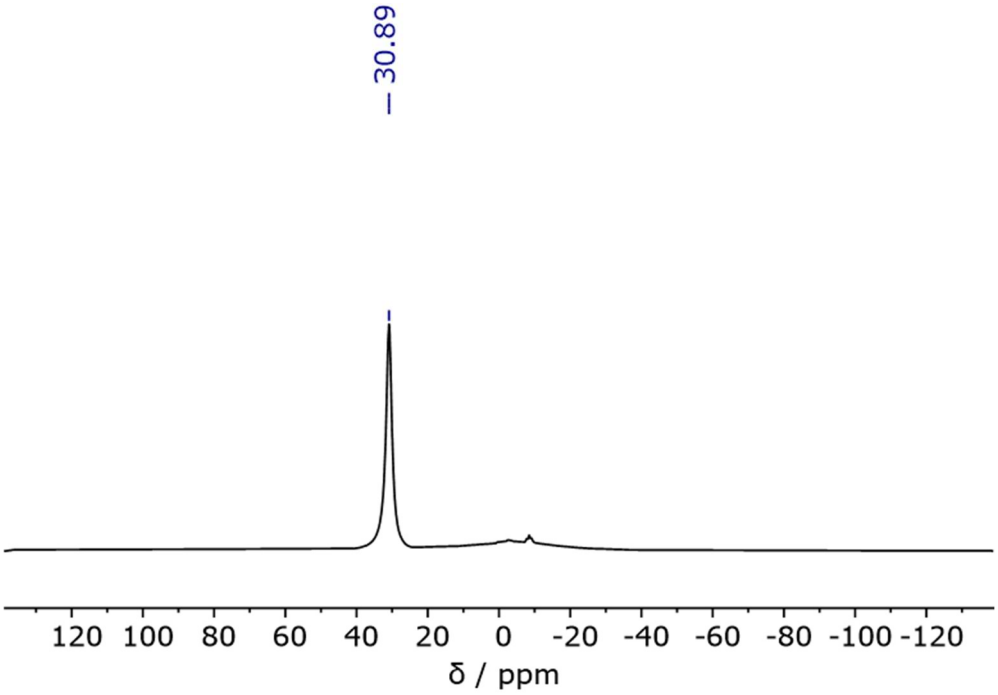

Figure 3.33: ^{11}B NMR (161 MHz, $CDCl_3$) spectrum of 3-D 7-Bpin indoline.

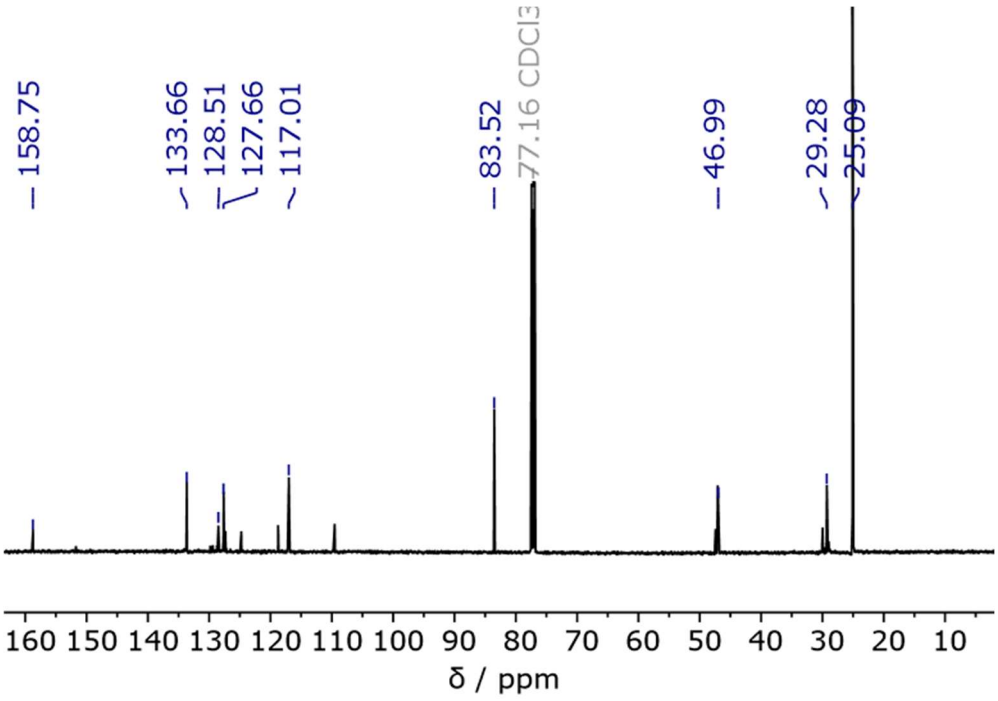

Figure 3.34: $^{13}C\{^1H\}$ NMR (126 MHz, $CDCl_3$) spectrum of 3-D 7-Bpin indoline. Note: some minor 3-H 7-Bpin indoline is present, resulting in minor overlapping resonances.

3.6.7 – Hydrodehalogenation Studies

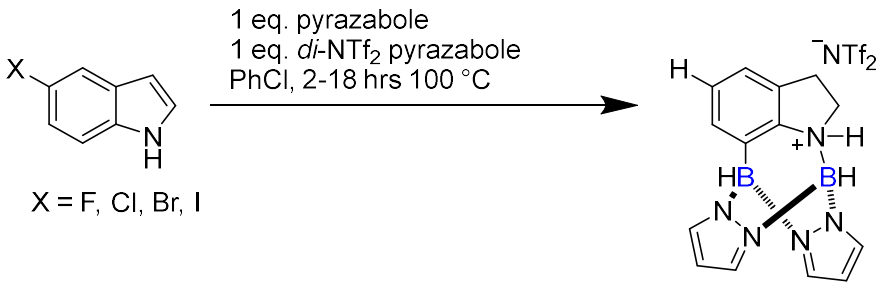

5-F Indole: Reaction Profile

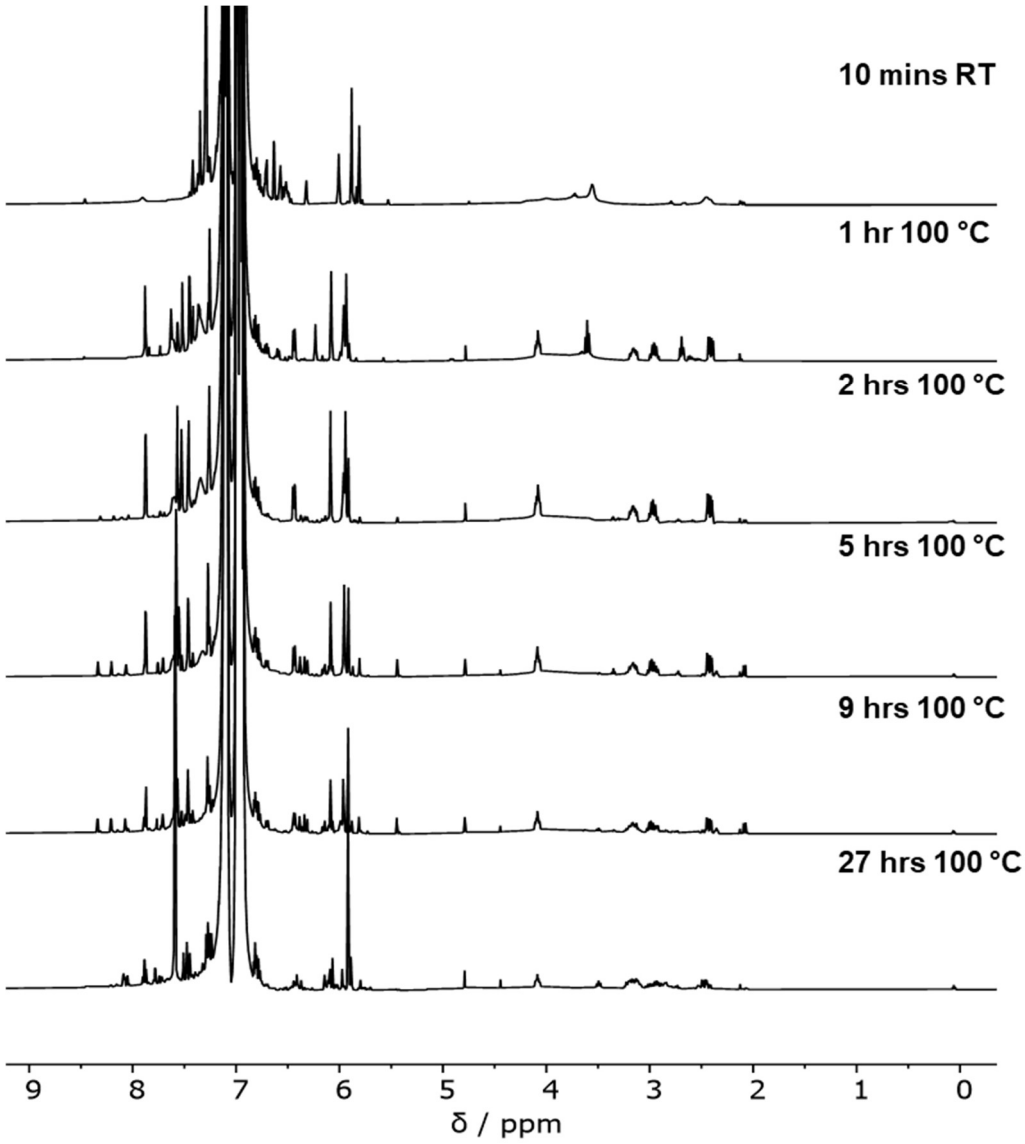

Figure 3.35: Stacked ^{1}H NMR (500 MHz, C_6H_5Cl) spectra of the N/C7-borylation and subsequent slow hydrodehalogenation (assumably, but may be decomposition) in the reaction of 5-F Indole and *mono*-NTf_2 pyrazabole.

5-Cl Indole: Reaction Profile

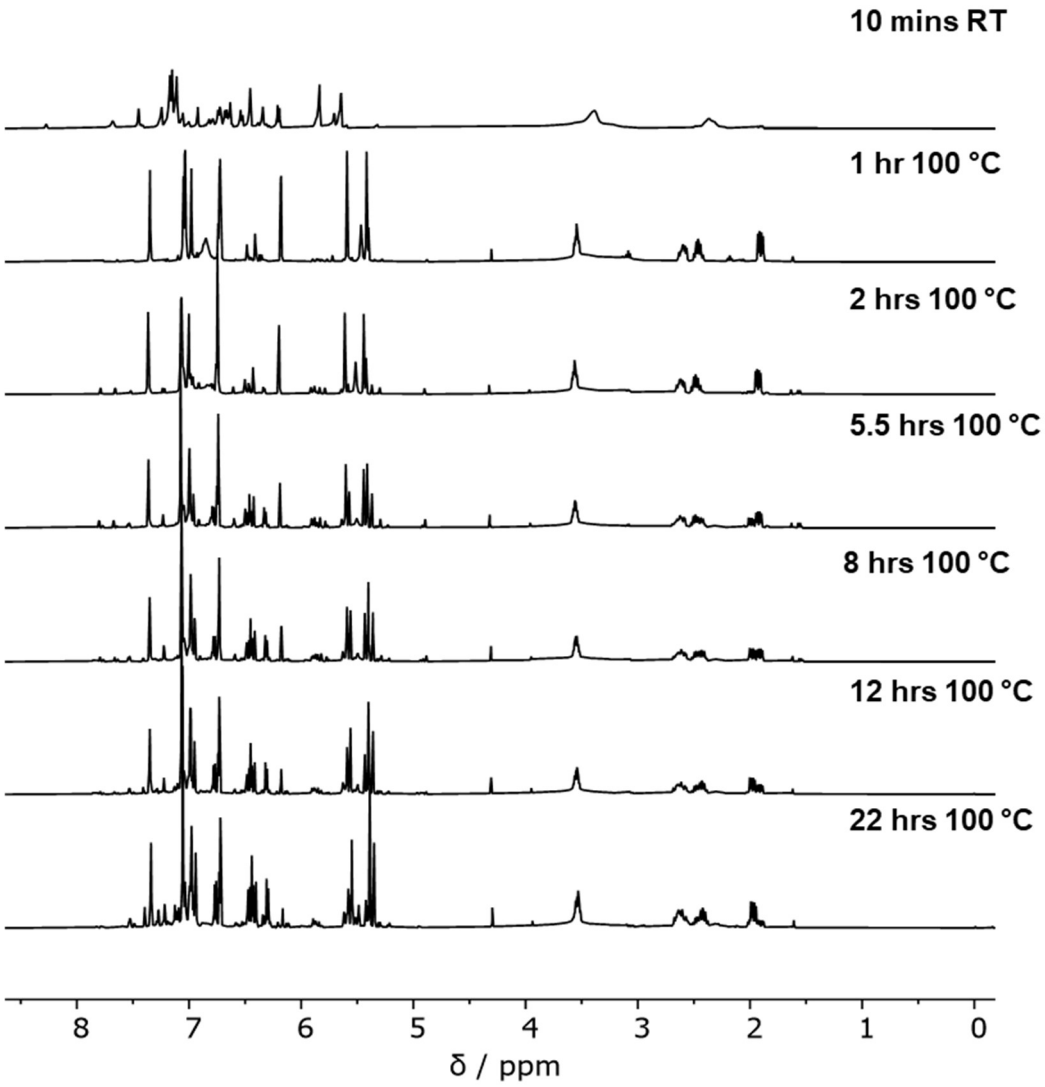

Figure 3.36: Stacked ^{1}H NMR (500 MHz, C_6H_5Cl) spectra of the N/C7-borylation and hydrodehalogenation in the reaction of 5-Cl Indole and *mono*-NTf_2 pyrazabole.

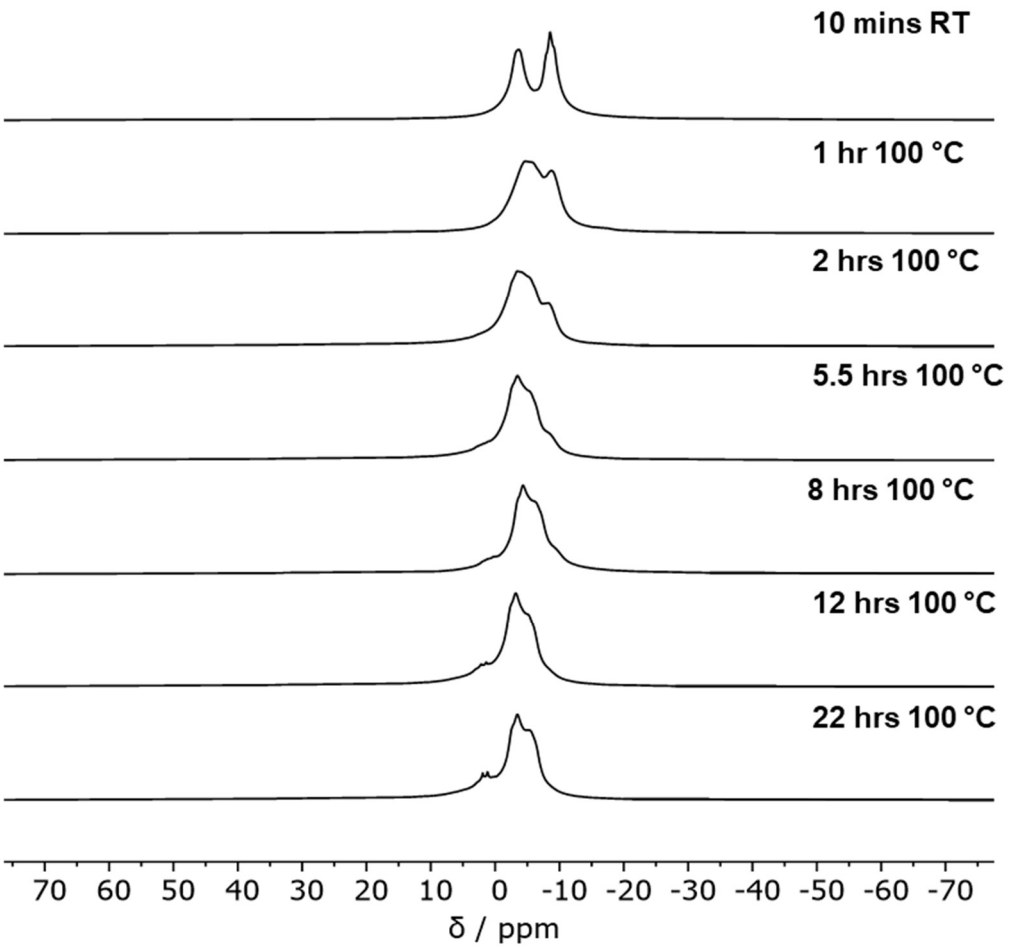

Figure 3.37: Stacked ^{11}B NMR (161 MHz, C_6H_5Cl) spectra of the N/C7-borylation and hydrodehalogenation in the reaction of 5-Cl Indole and *mono*-NTf_2 pyrazabole.

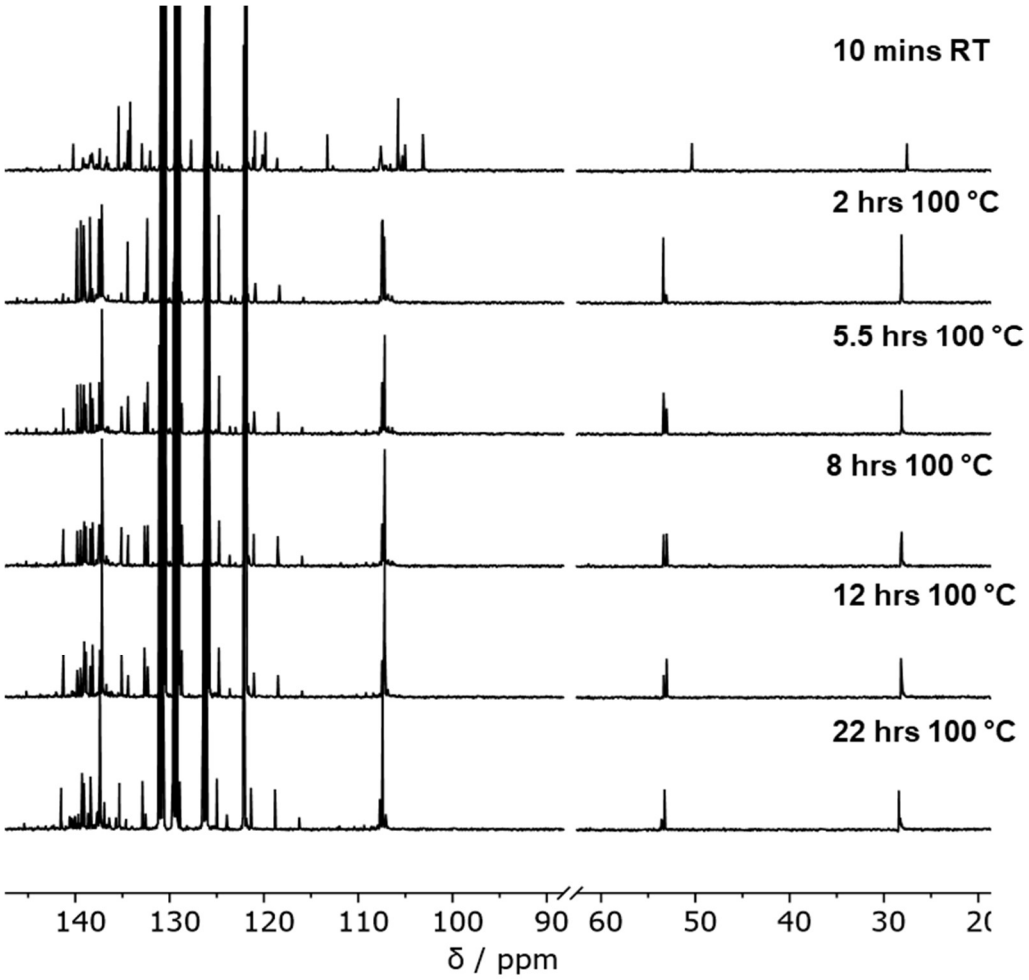

Figure 3.38: Stacked $^{13}C\{^{1}H\}$ NMR (126 MHz, C_6H_5Cl) spectra of the N/C7-borylation and hydrodehalogenation in the reaction of 5-Cl Indole and *mono*-NTf_2 pyrazabole.

5-Br Indole: Reaction Profile

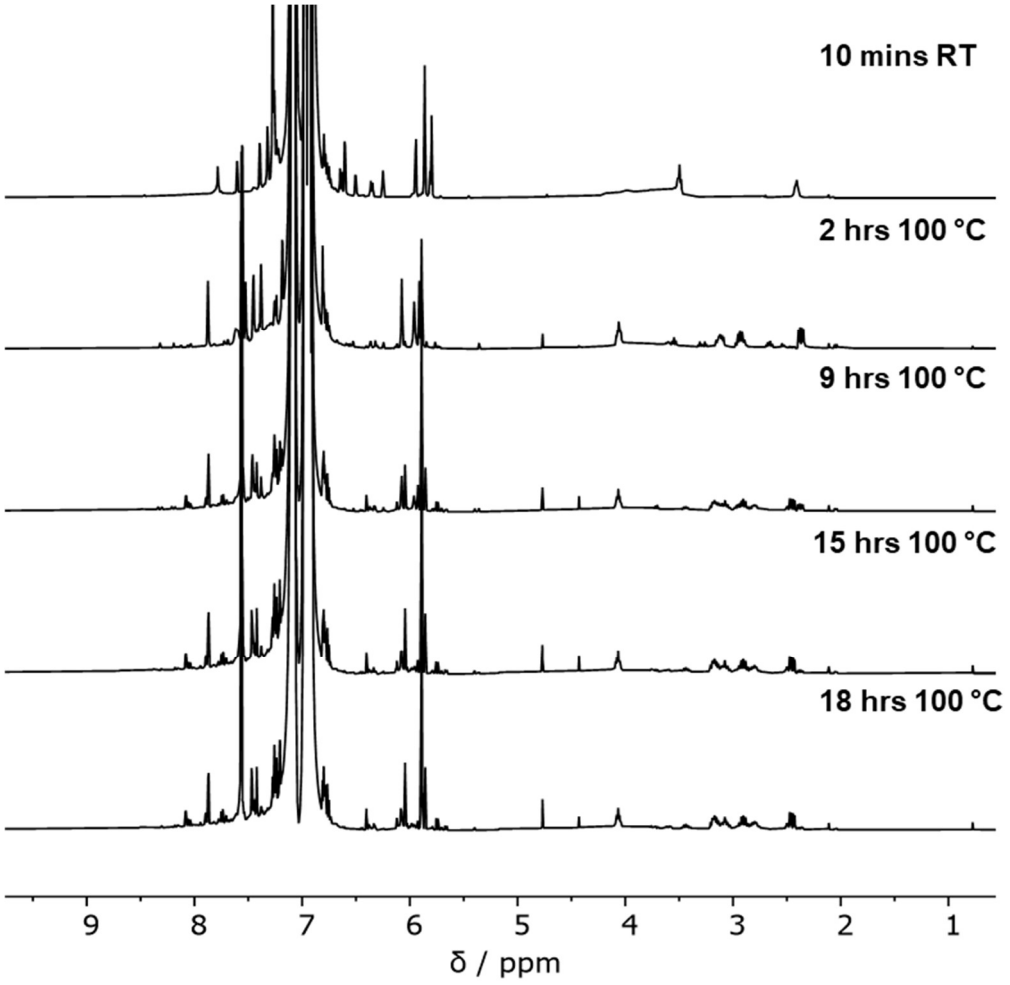

Figure 3.39: Stacked ^{1}H NMR (500 MHz, C_6H_5Cl) spectra of the N/C7-borylation and hydrodehalogenation in the reaction of 5-Br Indole and *mono*-NTf_2 pyrazabole.

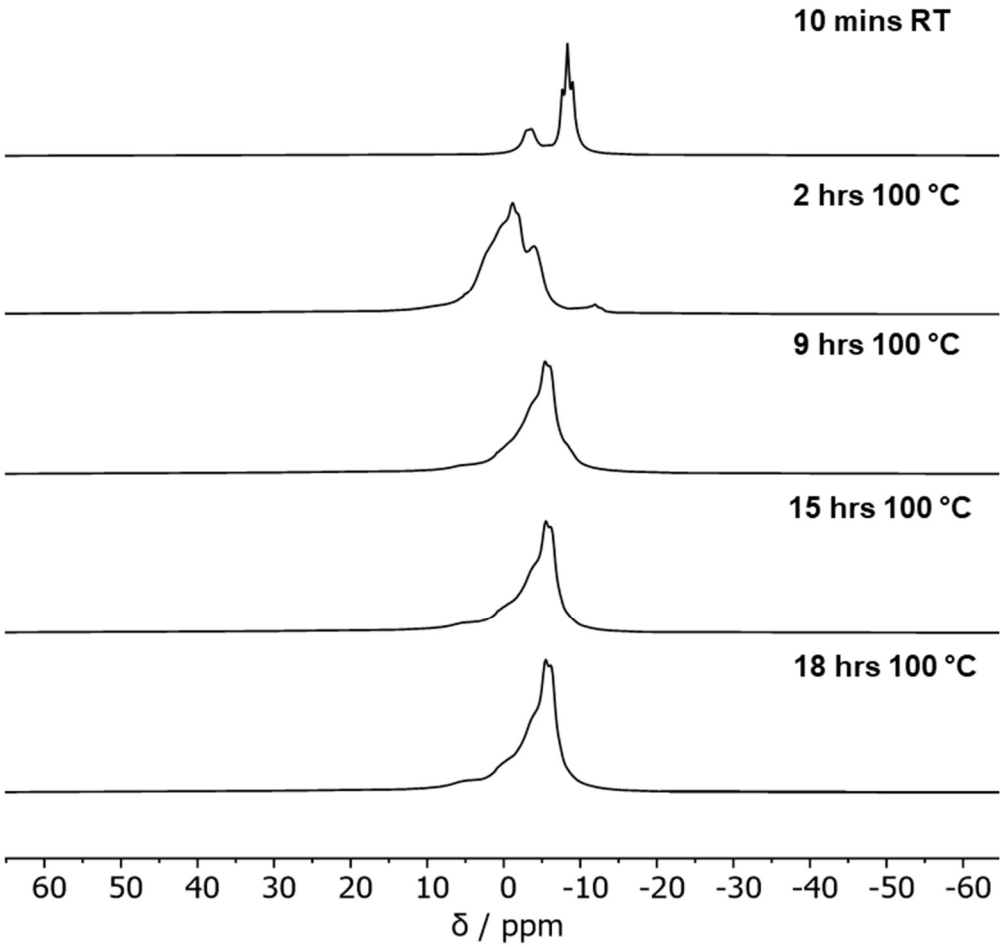

Figure 3.40: Stacked ^{11}B NMR (161 MHz, C_6H_5Cl) spectra of the N/C7-borylation and hydrodehalogenation in the reaction of 5-Br Indole and *mono*-NTf_2 pyrazabole.

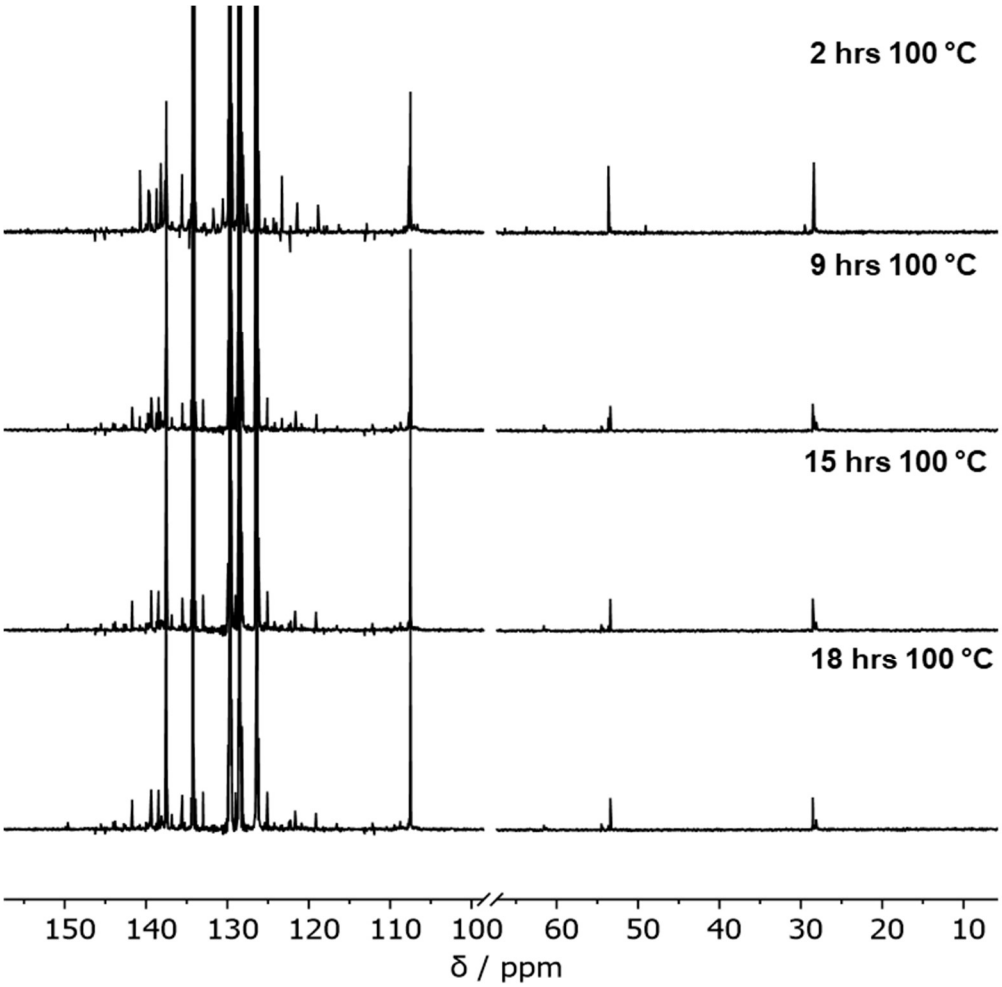

Figure 3.41: Stacked $^{13}C\{^{1}H\}$ NMR (126 MHz, C_6H_5Cl) spectra of the N/C7-borylation and hydrodehalogenation in the reaction of 5-Br Indole and *mono*-NTf_2 pyrazabole.

5-I Indole: Reaction Profile

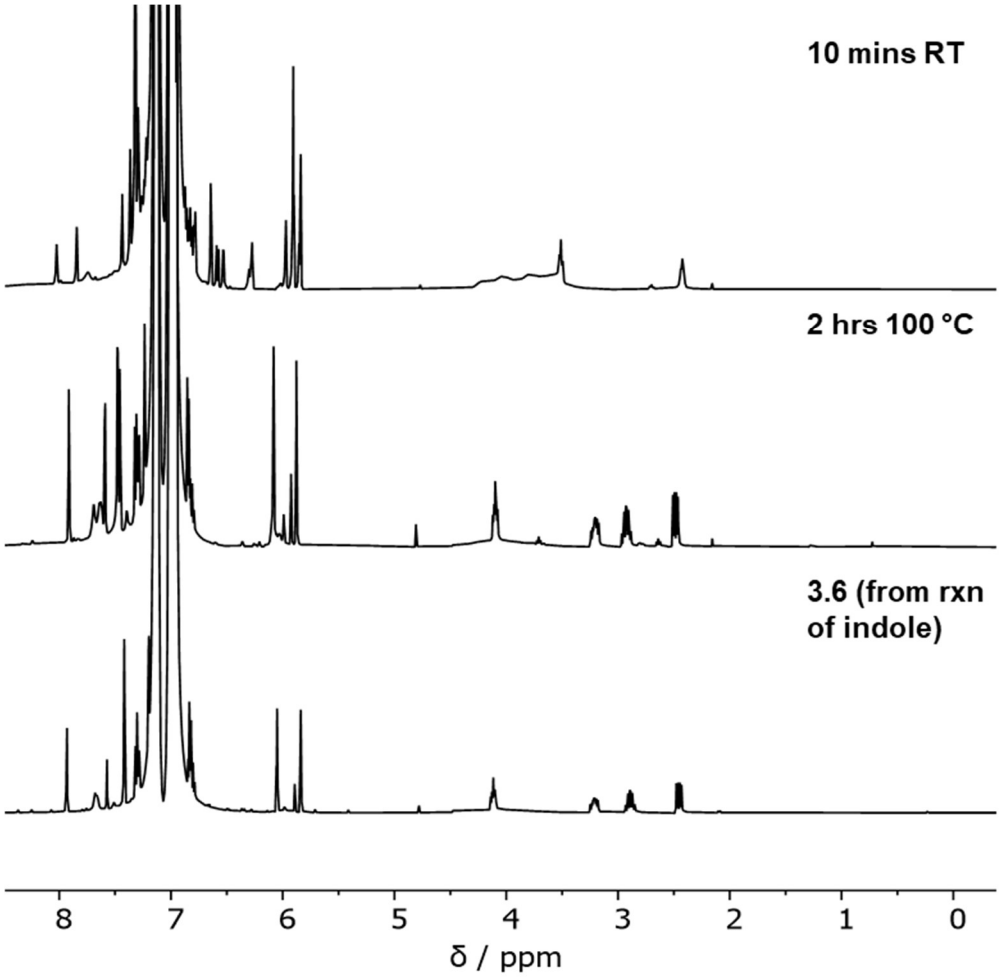

Figure 3.42: Stacked ^{1}H NMR (500 MHz, C_6H_5Cl) spectra of the N/C7-borylation and hydrodehalogenation in the reaction of 5-I Indole and *mono*-NTf_2 pyrazabole, with only the hydrodehalogenated product **3.6** observed after 2 hours 100 °C.

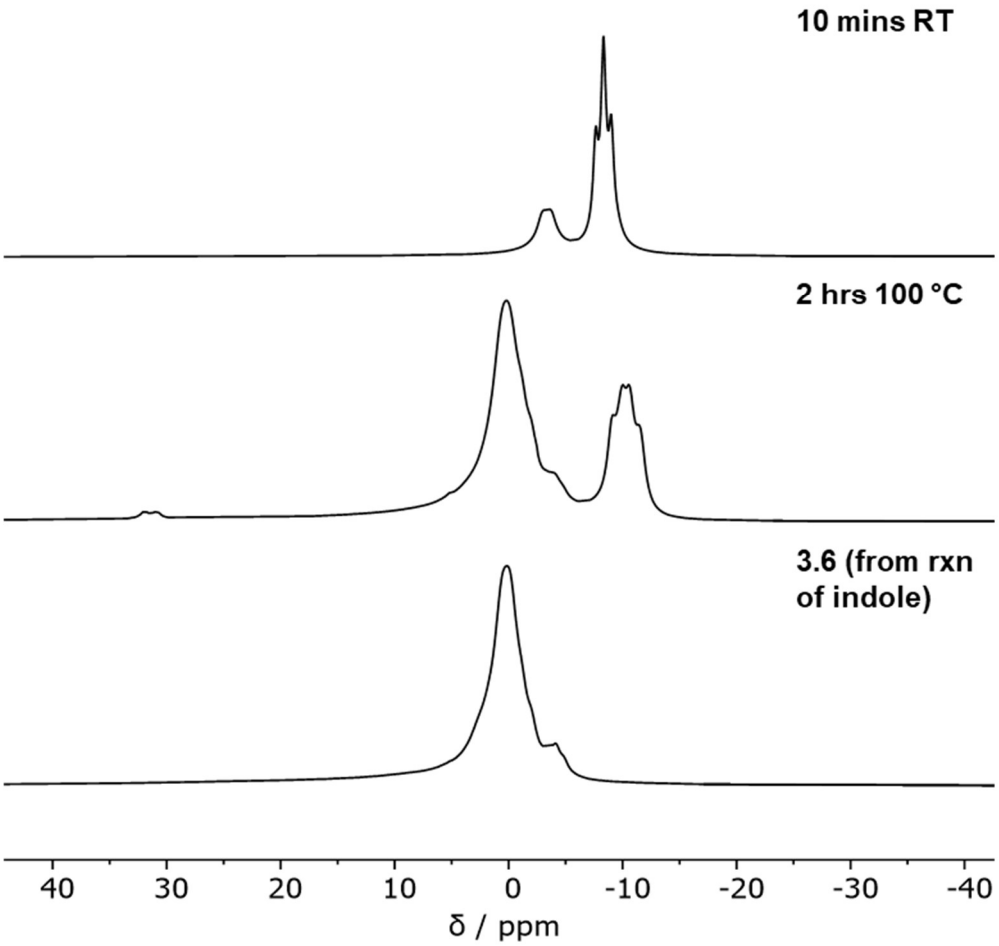

Figure 3.43: Stacked ^{11}B NMR (161 MHz, C_6H_5Cl) spectra of the N/C7-borylation and hydrodehalogenation in the reaction of 5-I Indole and *mono*-NTf_2 pyrazabole, with only the hydrodehalogenated product **3.6** observed after 2 hours 100 °C.

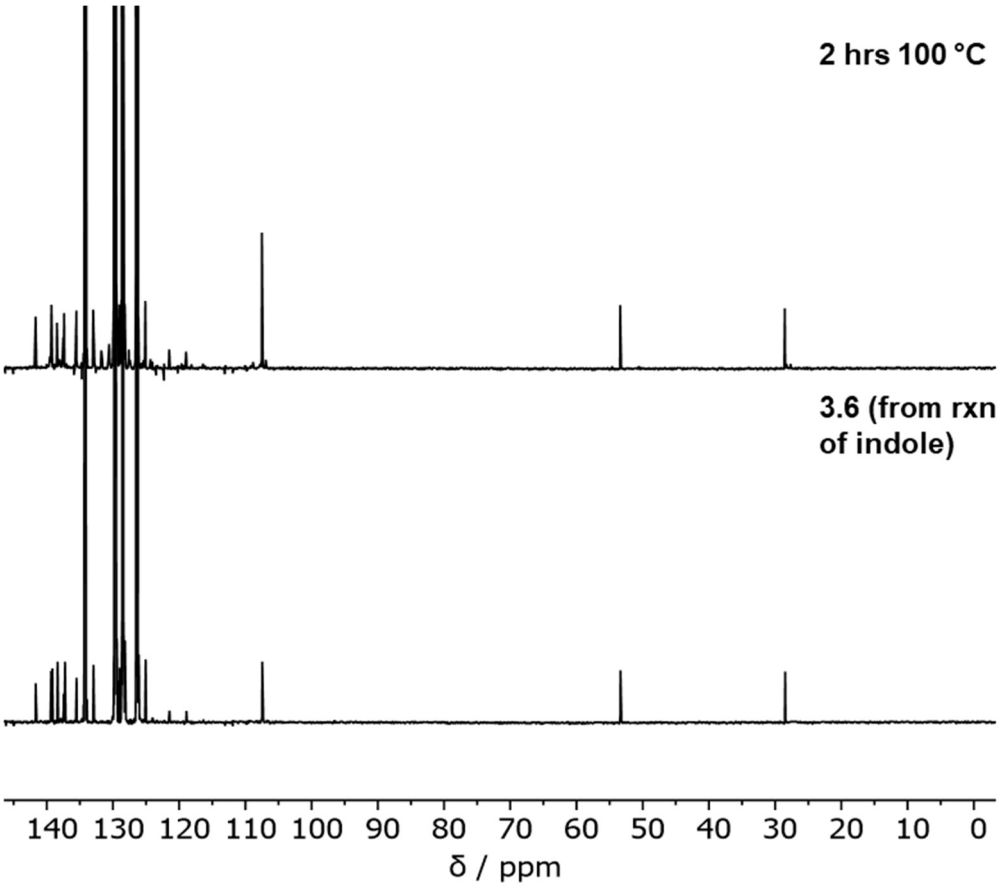

Figure 3.44: Stacked $^{13}C\{^{1}H\}$ NMR (126 MHz, C_6H_5Cl) spectra of the N/C7-borylation and hydrodehalogenation in the reaction of 5-I Indole and *mono*-NTf_2 pyrazabole, with only the hydrodehalogenated product **3.6** observed after 2 hours 100 °C.

6-Cl Indole: Reaction Profile

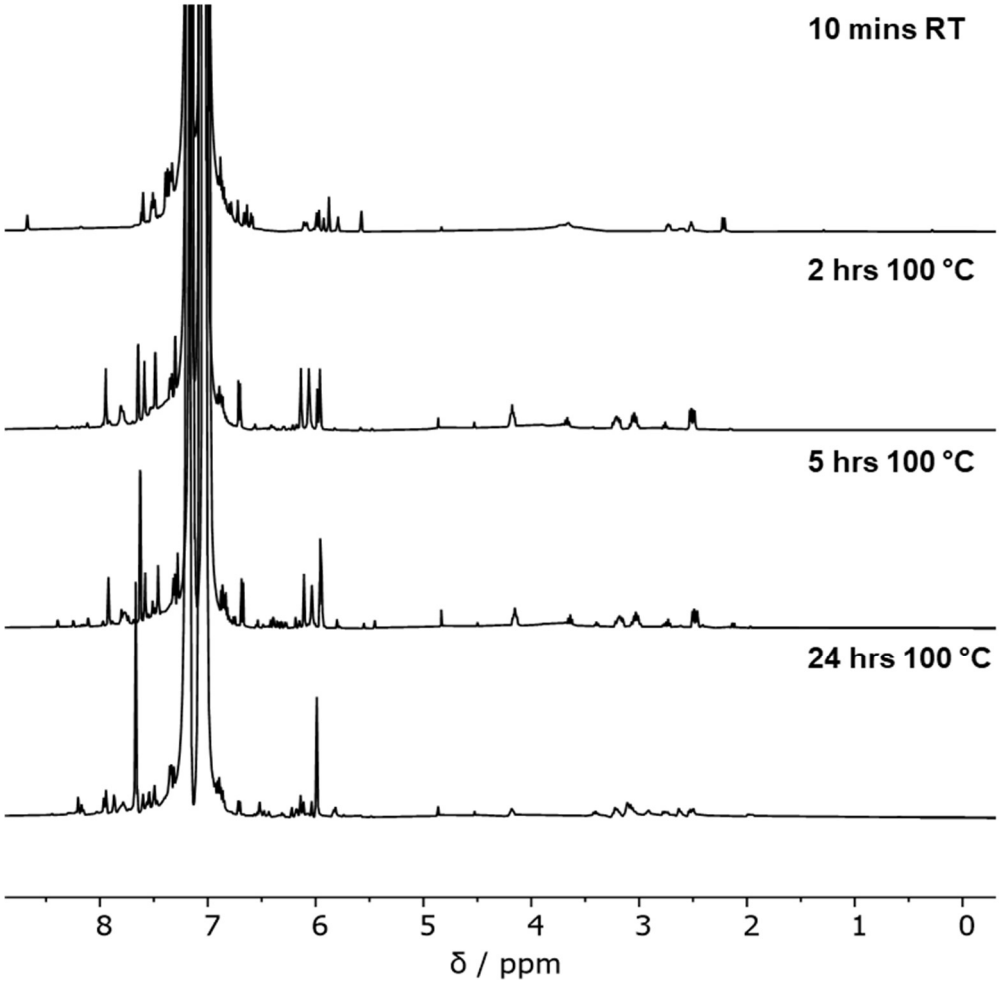

Figure 3.45: Stacked ^{1}H NMR (500 MHz, C_6H_5Cl) spectra of the N/C7-borylation and subsequent slow hydrodehalogenation (assumably, but may be decomposition) in the reaction of 6-Cl Indole and *mono*-NTf_2 pyrazabole.

Hydrodehalogenation of 3.15 using *mono*-NTf_2 pyrazabole (3.3)

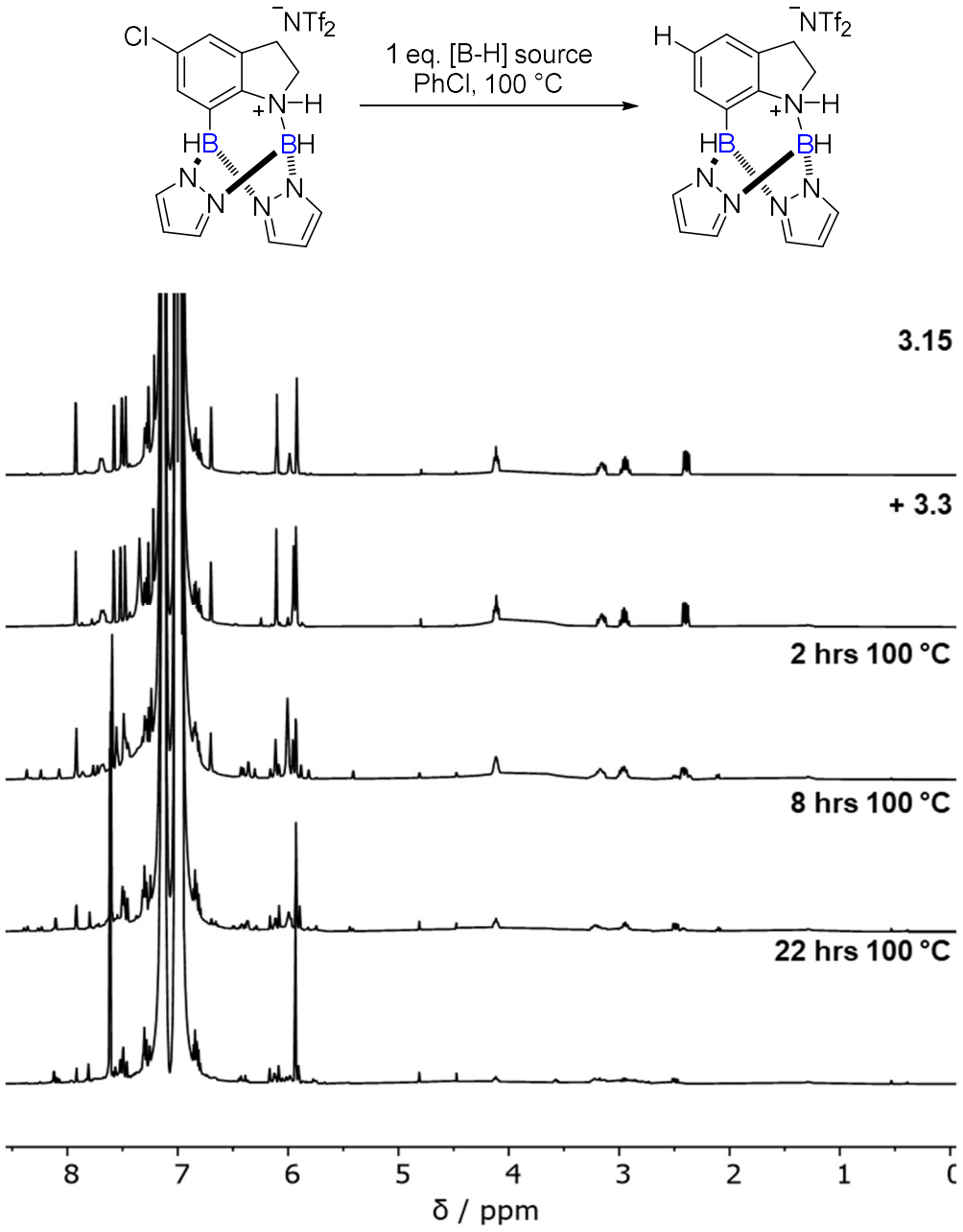

Figure 3.46: Stacked ^{1}H NMR (500 MHz, C_6H_5Cl) spectra of the hydrodehalogenation of N/C7-borylated indoline intermediate **3.15** using *mono*-NTf_2 pyrazabole.

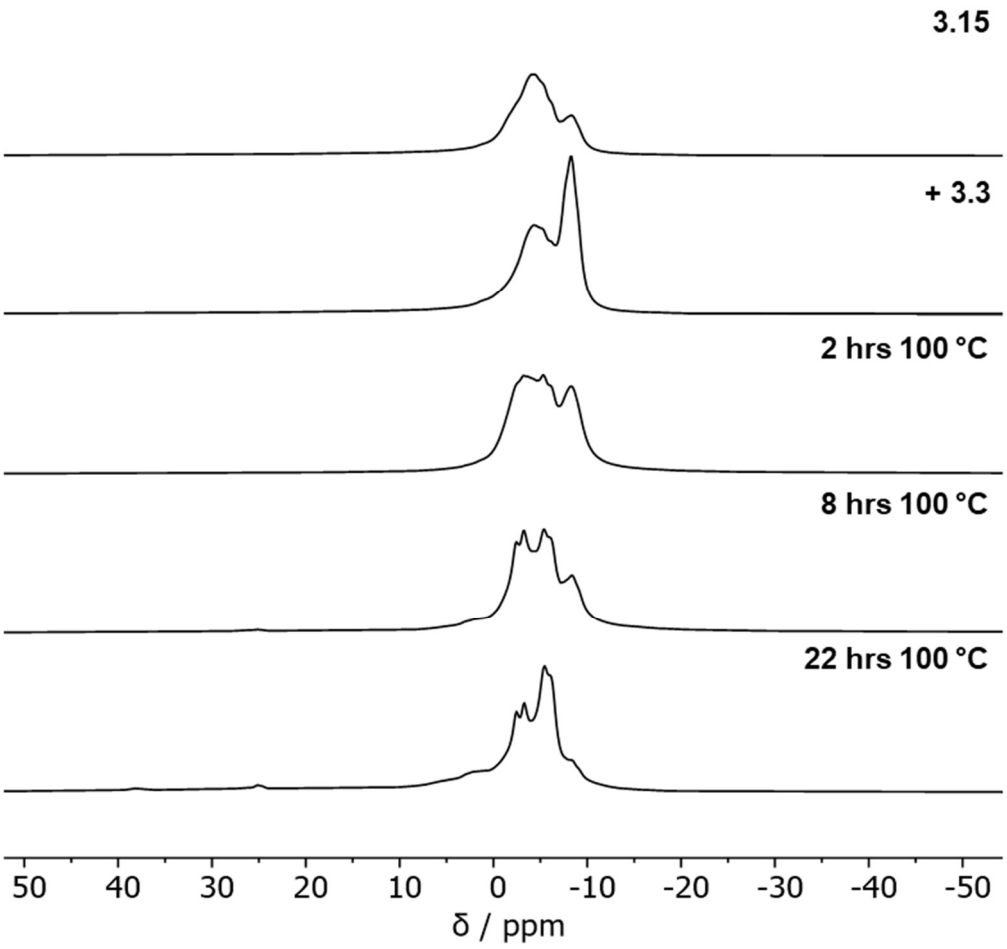

Figure 3.47: Stacked ^{11}B NMR (161 MHz, C_6H_5Cl) spectra of the hydrodehalogenation of N/C7-borylated indoline intermediate **3.15** using *mono*-NTf_2 pyrazabole.

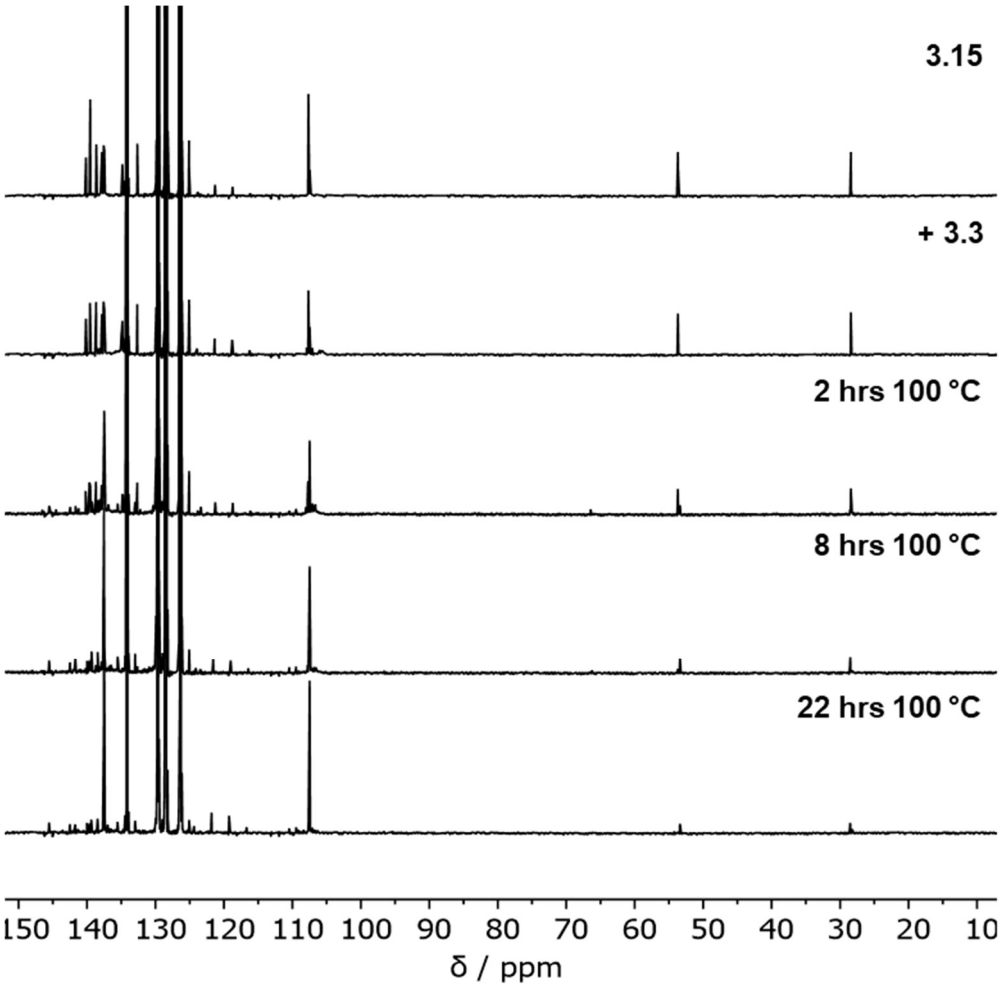

Figure 3.48: Stacked ^{1}H NMR (126 MHz, C_6H_5Cl) spectra of the hydrodehalogenation of N/C7-borylated indoline intermediate **3.15** using *mono*-NTf_2 pyrazabole.

Hydrodehalogenation of 3.15 using *di*-NTf_2 pyrazabole 3.2

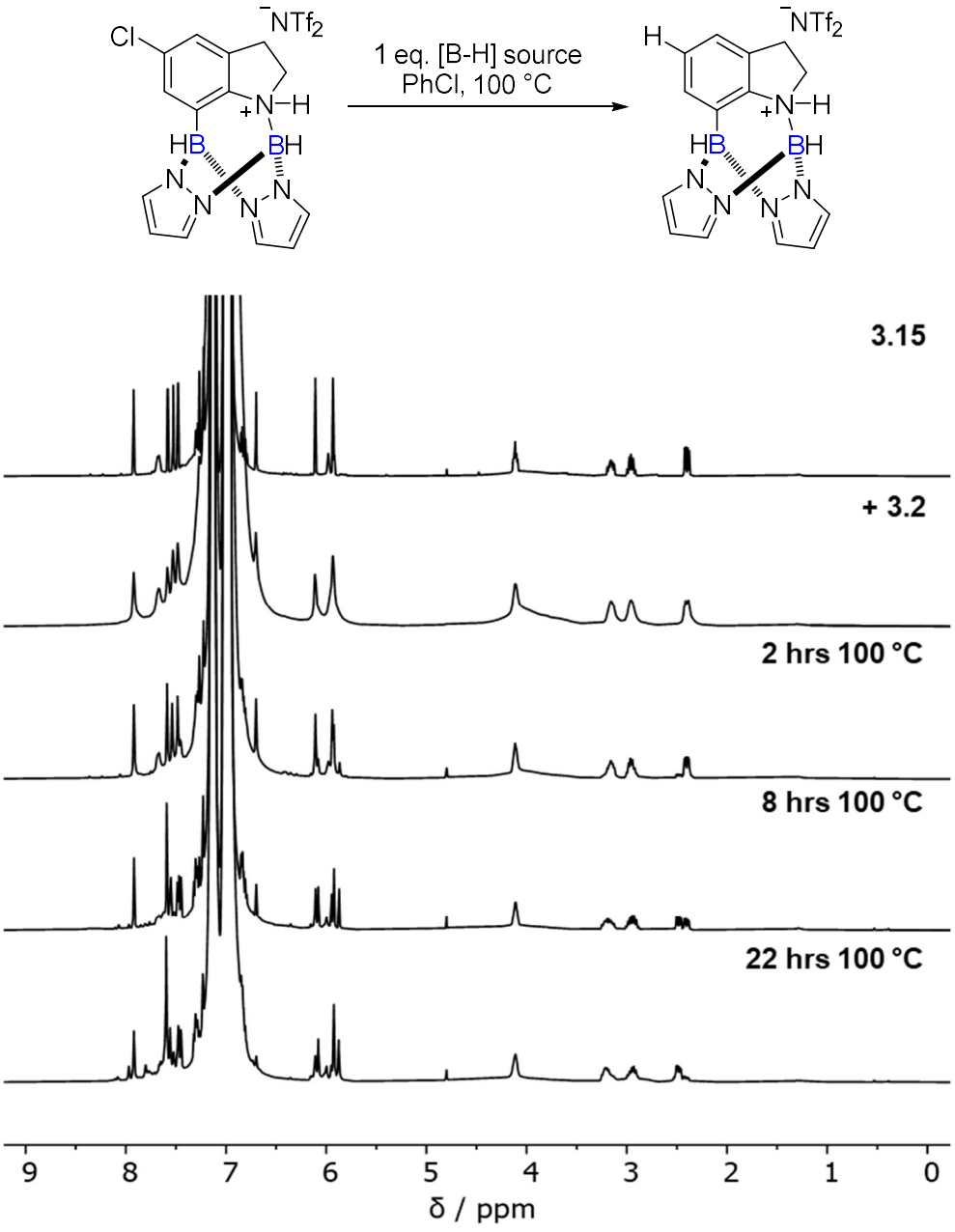

Figure 3.49: Stacked ^{1}H NMR (500 MHz, C_6H_5Cl) spectra of the hydrodehalogenation of N/C7-borylated indoline intermediate **3.15** using *di*-NTf_2 pyrazabole.

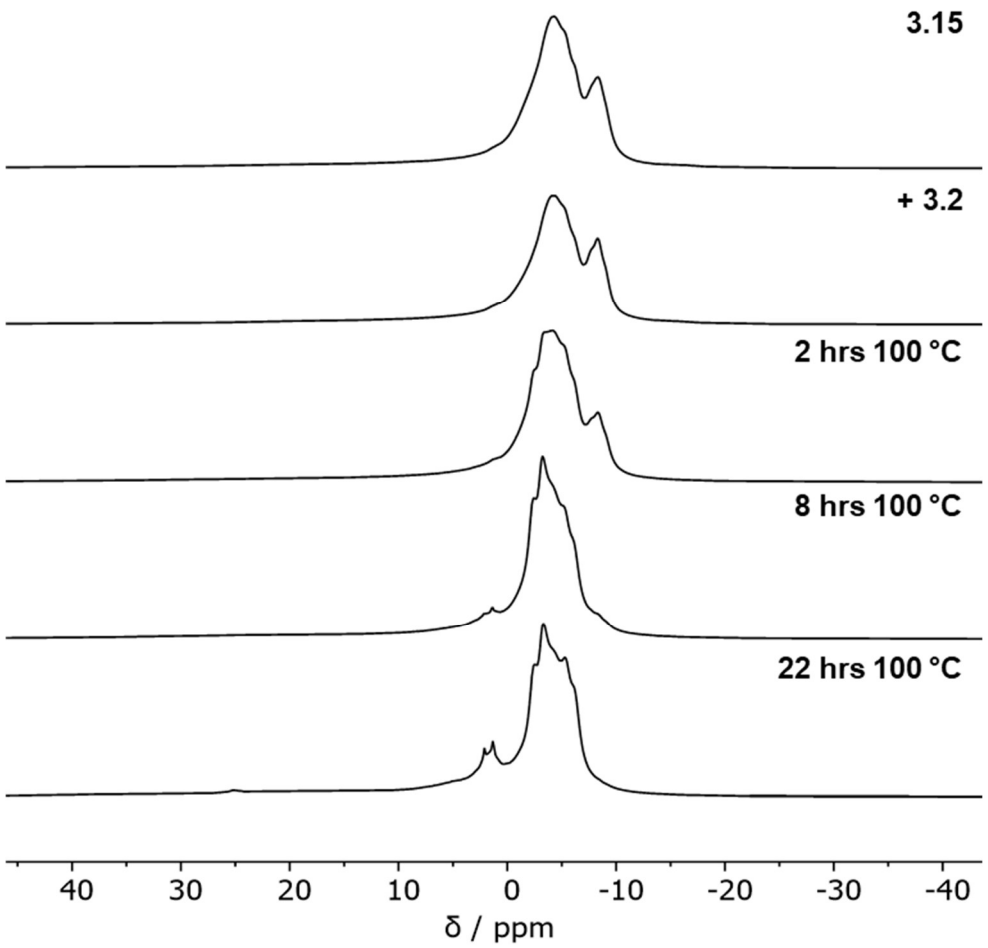

Figure 3.50: Stacked ^{11}B NMR (161 MHz, C_6H_5Cl) spectra of the hydrodehalogenation of N/C7-borylated indoline intermediate **3.15** using *di*-NTf_2 pyrazabole.

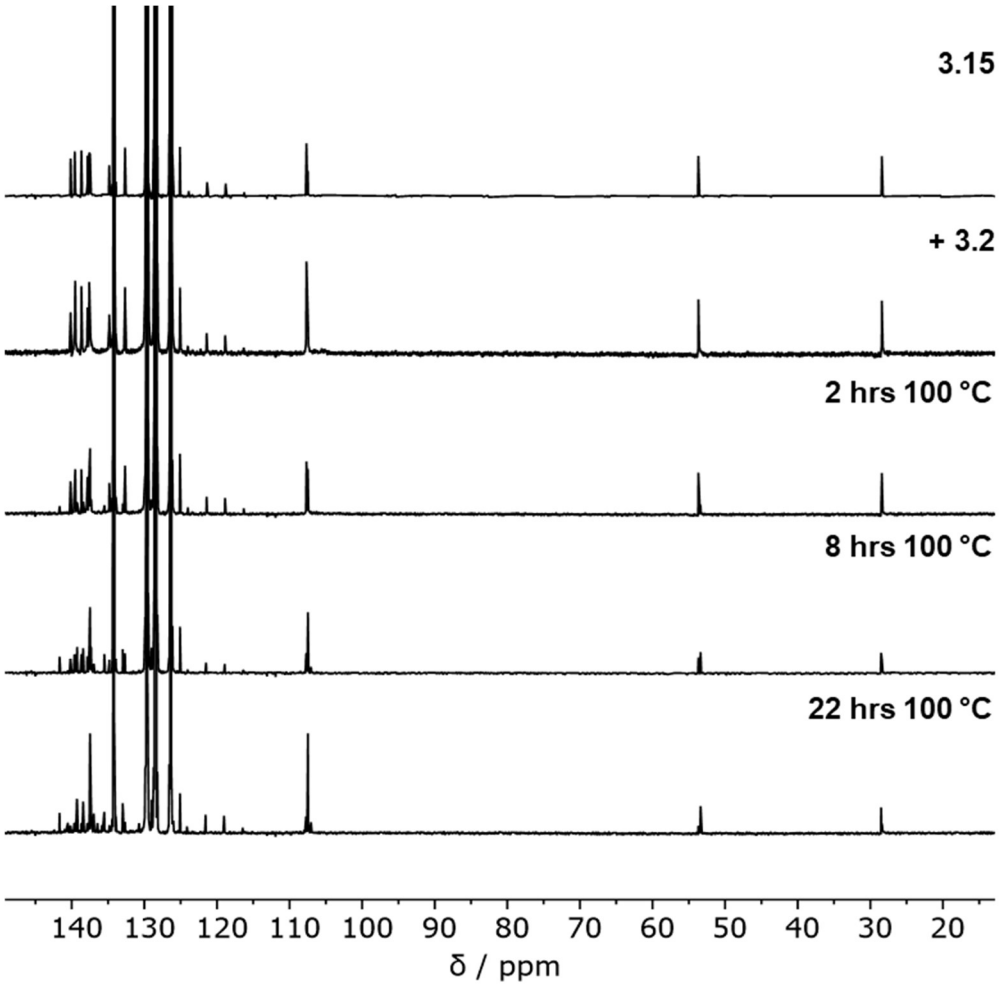

Figure 3.51: Stacked ^{1}H NMR (126 MHz, C_6H_5Cl) spectra of the hydrodehalogenation of N/C7-borylated indoline intermediate **3.15** using *di*-NTf_2 pyrazabole.

Chapter 4: Reactivity of Iodine-Activated Pyrazaboles

4.5.1 – Synthesis of Iodine-Activated Pyrazaboles

Di-Iodo Pyrazabole (4.2)

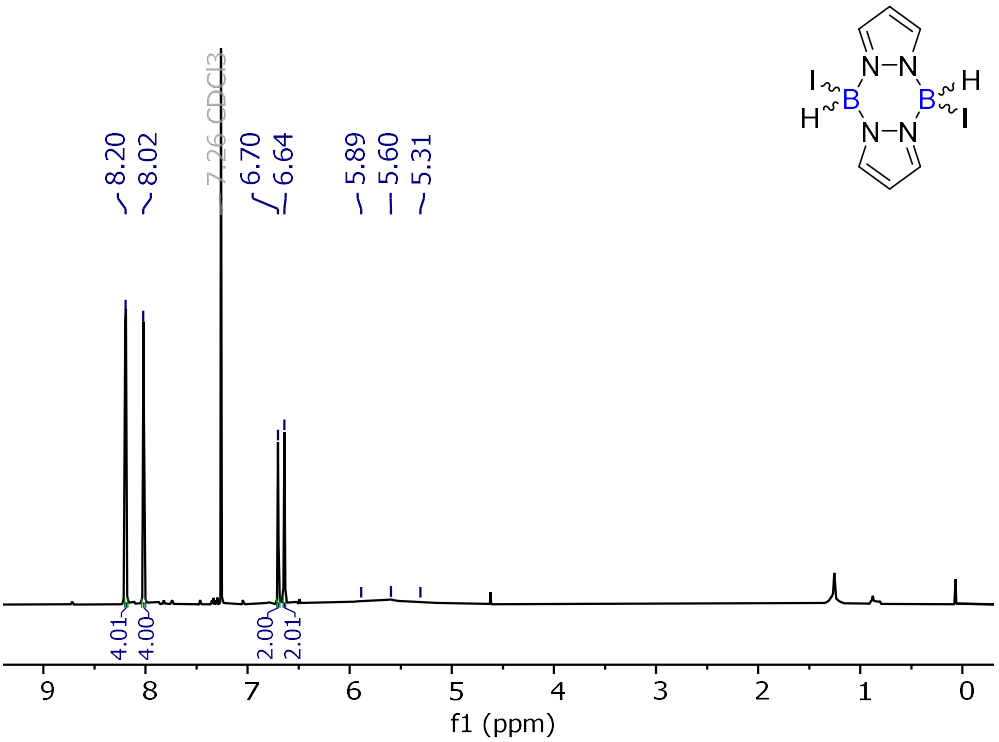

Figure 4.1: ^{1}H NMR (500 MHz, $CDCl_3$) spectrum of *di*-iodo pyrazabole.

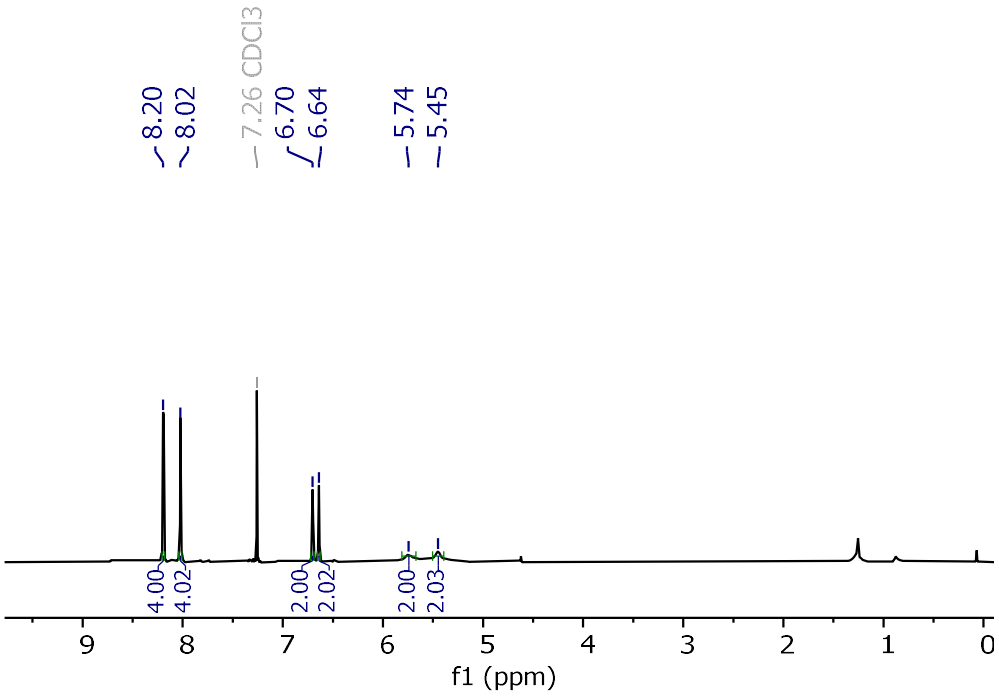

Figure 4.2: $^{1}H\{^{11}B\}$ NMR (500 MHz, $CDCl_3$) spectrum of *di*-iodo pyrazabole.

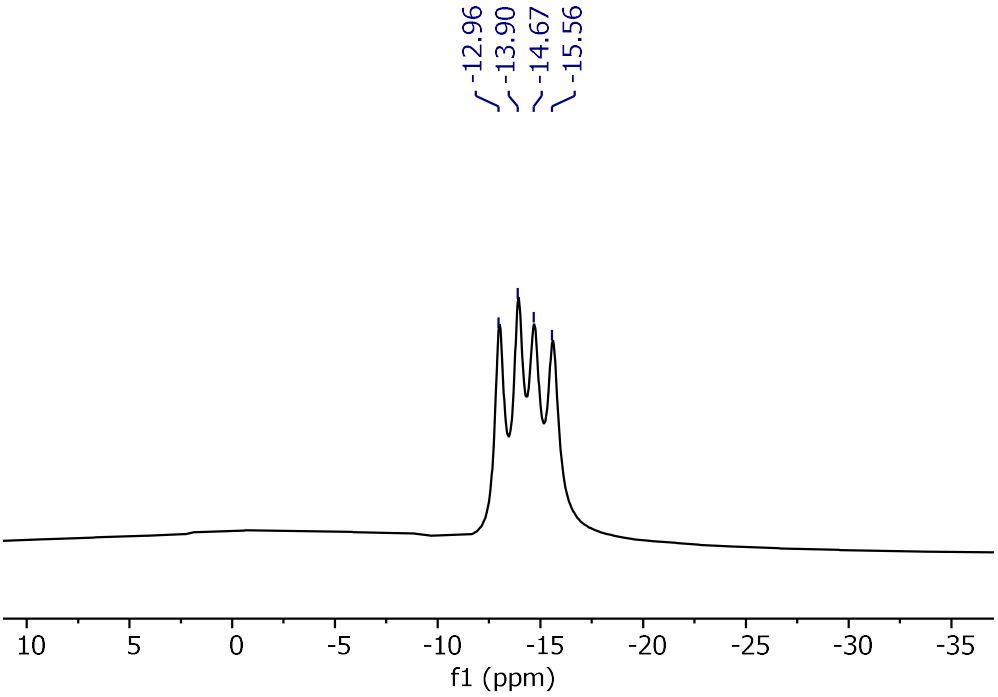

Figure 4.3: ^{11}B NMR (161 MHz, $CDCl_3$) spectrum of *di*-iodo pyrazabole.

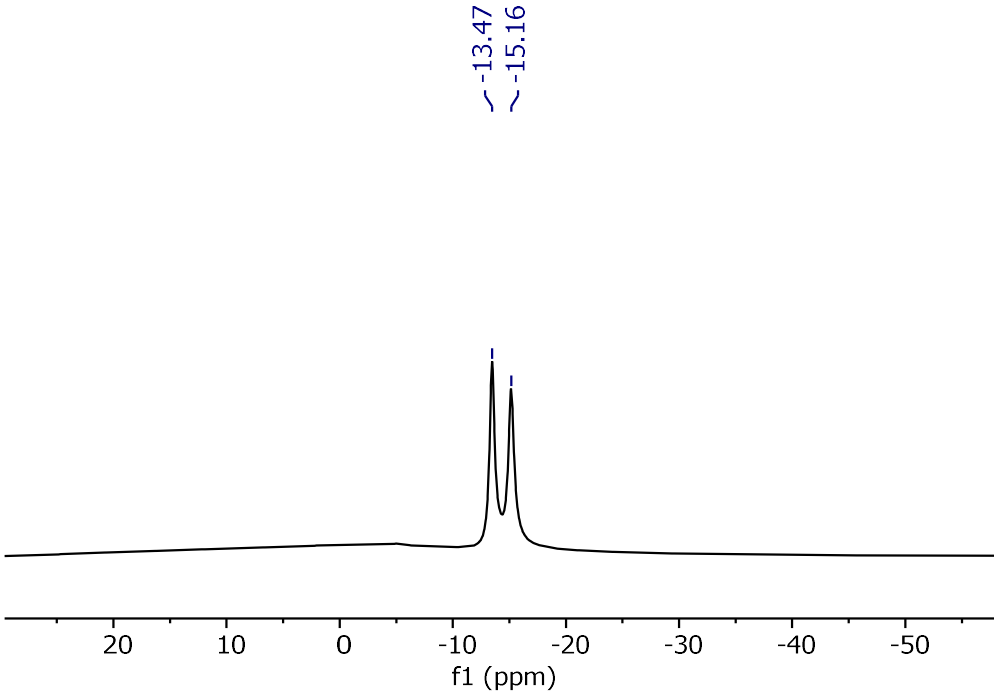

Figure 4.4: $^{11}B\{^1H\}$ NMR (161 MHz, $CDCl_3$) spectrum of *di*-iodo pyrazabole.

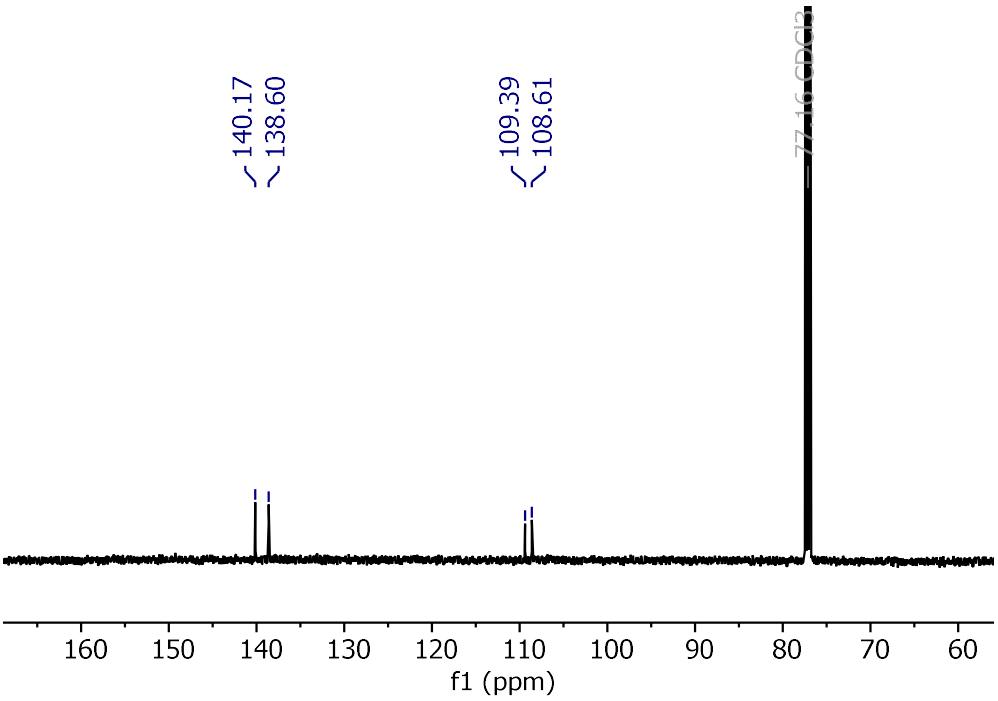

Figure 4.5: $^{13}C\{^{1}H\}$ NMR (126 MHz, $CDCl_3$) spectrum of *di*-iodo pyrazabole.

Formation of *Mono*-Iodo Pyrazabole (4.3) *in situ*

- **Via Conditions A: Pyrazabole + 0.5 equiv. I_2**

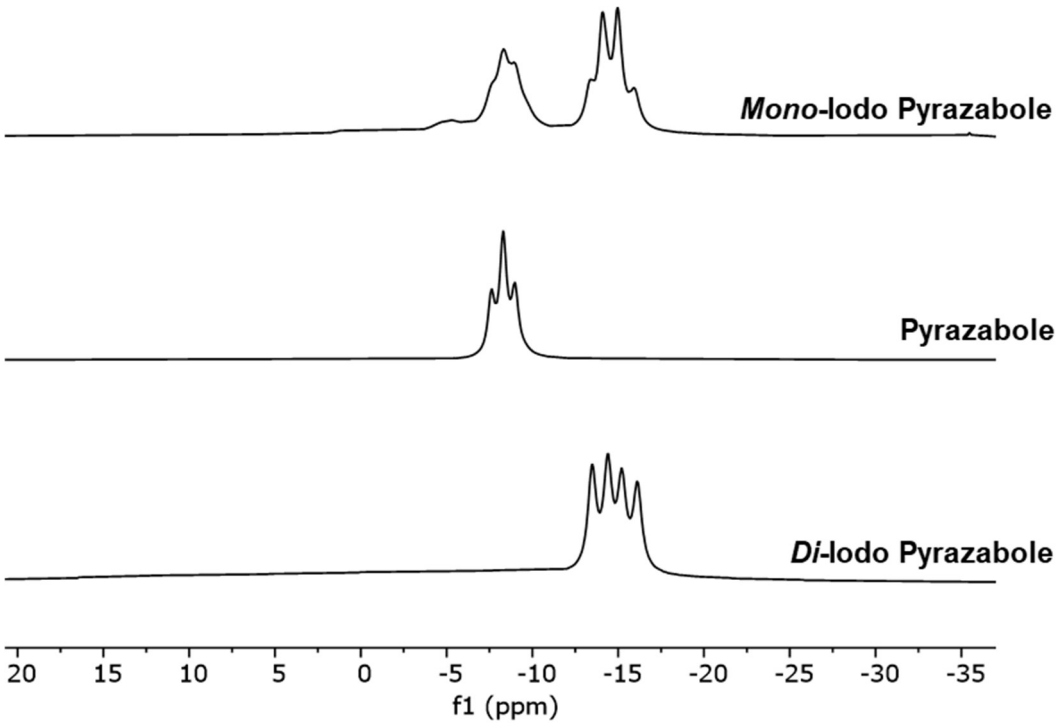

Figure 4.6: Stacked *in situ* ^{11}B NMR (161 MHz, C_6H_5Cl) spectra of:
Top = The reaction of pyrazabole and 0.5 equiv. I_2 (**Conditions A**). Partial formation of *mono*-iodo pyrazabole **4.3** is observed, alongside some pyrazabole **4.1** and *di*-iodo pyrazabole **4.2**. **Middle** = Pyrazabole **4.1**, for comparison. **Bottom** = *Di*-iodo pyrazabole **4.2**, for comparison.

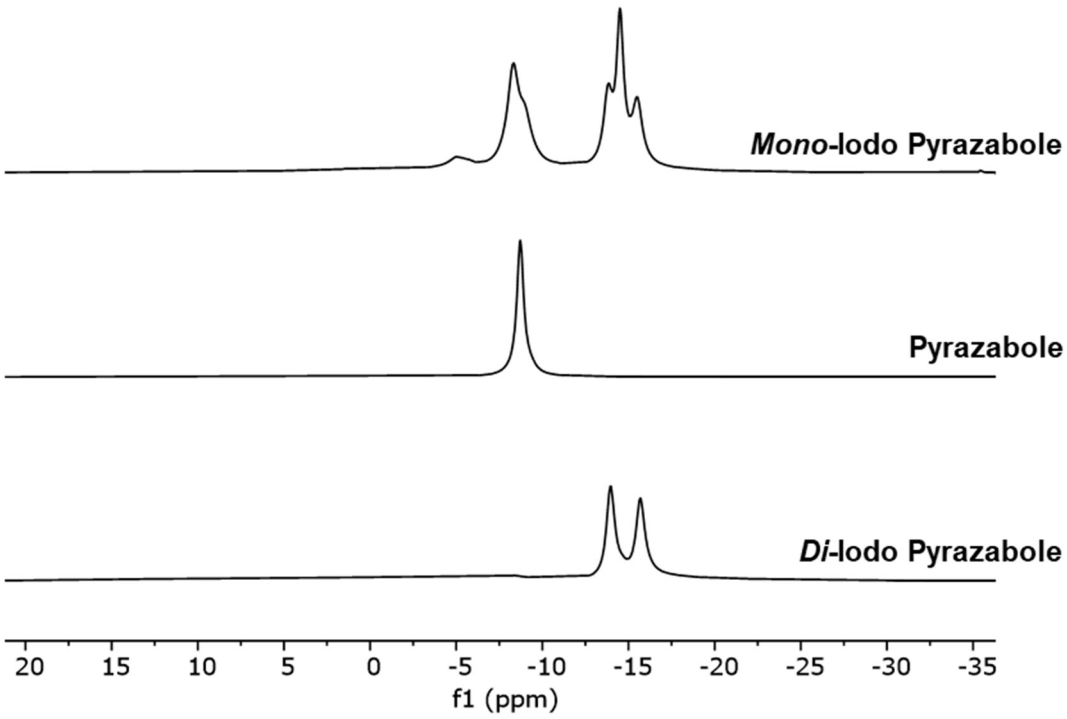

Figure 4.7: Stacked *in situ* $^{11}B\{^{1}H\}$ NMR (161 MHz, C_6H_5Cl) spectra of:
Top = The reaction of pyrazabole and 0.5 equiv. I_2 (**Conditions A**). Partial formation of *mono*-iodo pyrazabole **4.3** is observed, alongside some pyrazabole **4.1** and *di*-iodo pyrazabole **4.2**. **Middle** = Pyrazabole **4.1**, for comparison. **Bottom** = *Di*-iodo pyrazabole **4.2**, for comparison.

- **Via Conditions B: Pyrazabole + *Di*-Iodo Pyrazabole**

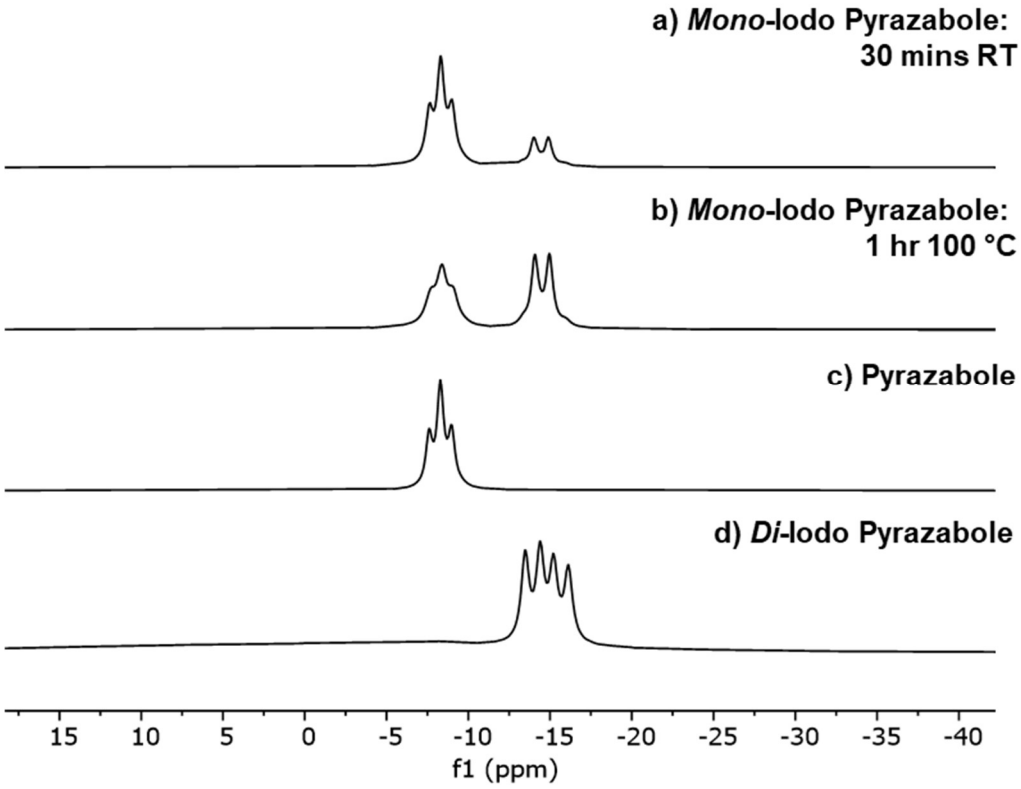

Figure 4.8 : Stacked *in situ* ^{11}B NMR (161 MHz, C_6H_5Cl) spectra of:
a) The reaction of equimolar pyrazabole **4.1** and *di*-iodo pyrazabole **4.2** (**Conditions B**) after 30 minutes at room temperature, and **b)** after 1 hour at 100 °C.
c) Pyrazabole **4.1**, for comparison. **d)** *Di*-iodo pyrazabole **4.2**, for comparison.

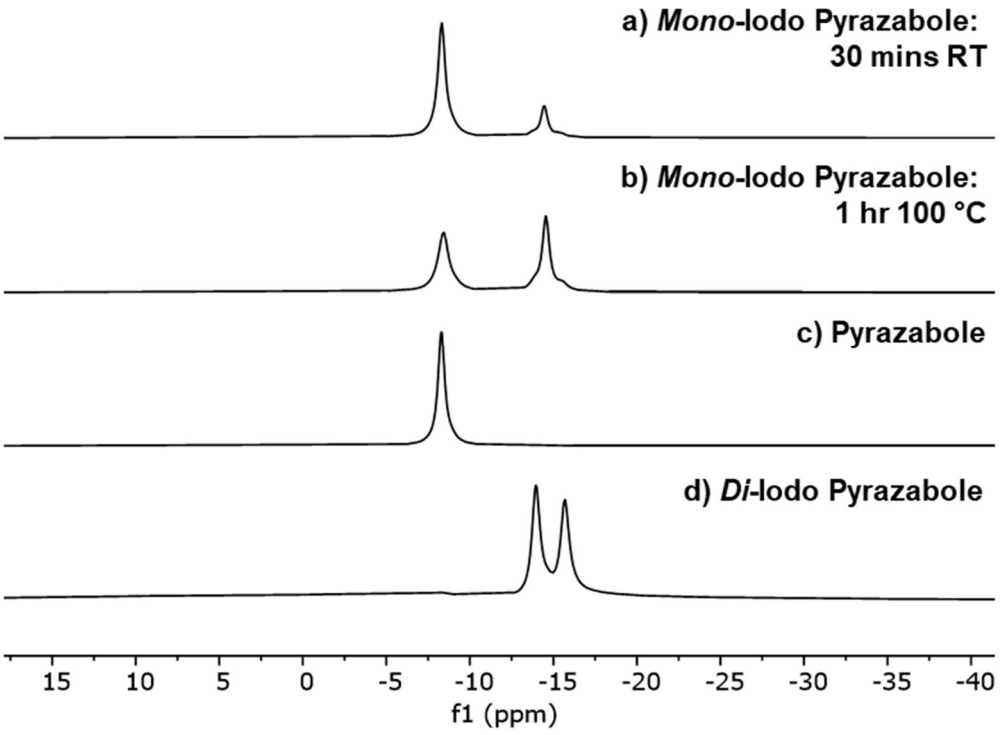

Figure 4.9: Stacked *in situ* $^{11}B\{^{1}H\}$ NMR (161 MHz, C_6H_5Cl) spectra of:
a) The reaction of equimolar pyrazabole **4.1** and *di*-iodo pyrazabole **4.2** (**Conditions B**) after 30 minutes at room temperature, and **b)** after 1 hour at 100 °C.
c) Pyrazabole **4.1**, for comparison. **d)** *Di*-iodo pyrazabole **4.2**, for comparison.

4.5.2 - Directed C7-H Borylation of *N*-H Indoles

Reactivity of Indole with *Mono*-Iodo Pyrazabole (4.3)

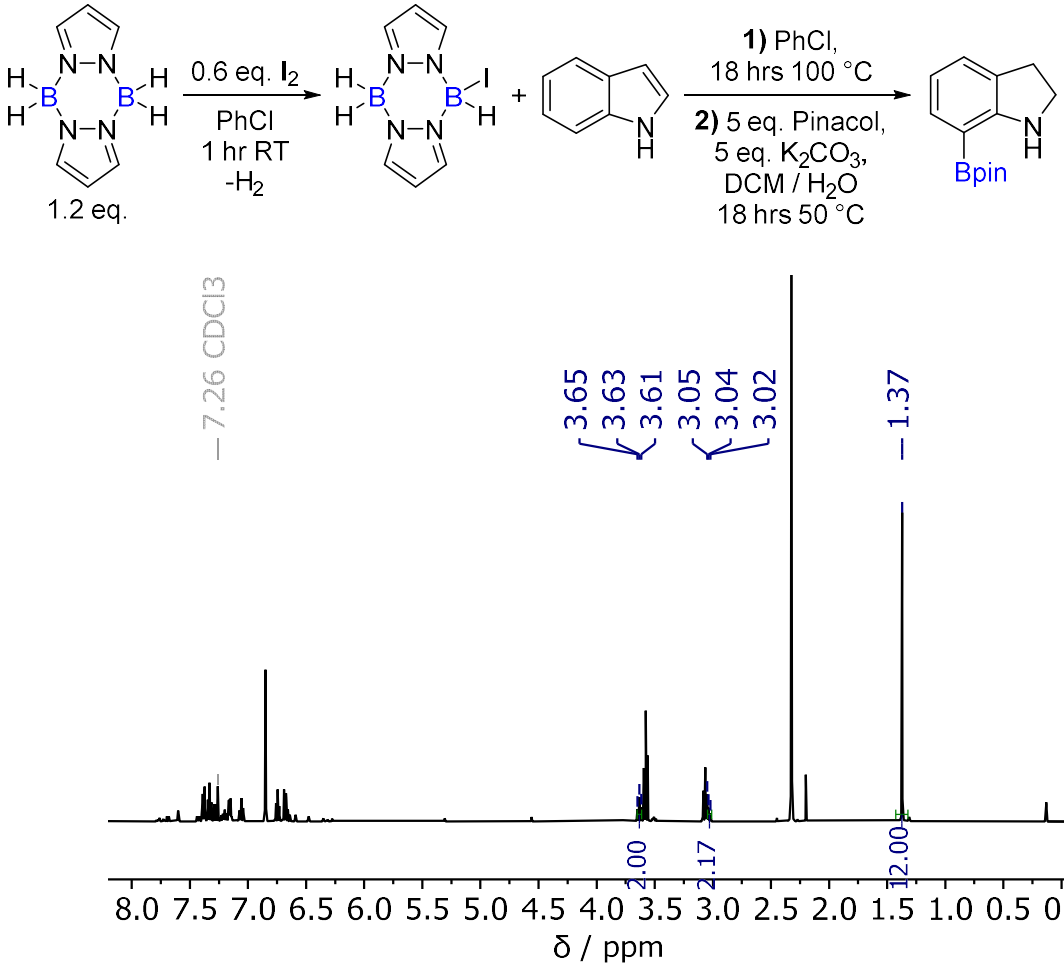

Figure 4.10: ^{1}H NMR (500 MHz, $CDCl_3$) spectrum of 7-Bpin indoline formed via the reaction of indole and *mono*-iodo pyrazabole. The major species present is *N*-H Indoline. *Note: The resonance at 2.32 ppm is mesitylene, used as an internal standard.*

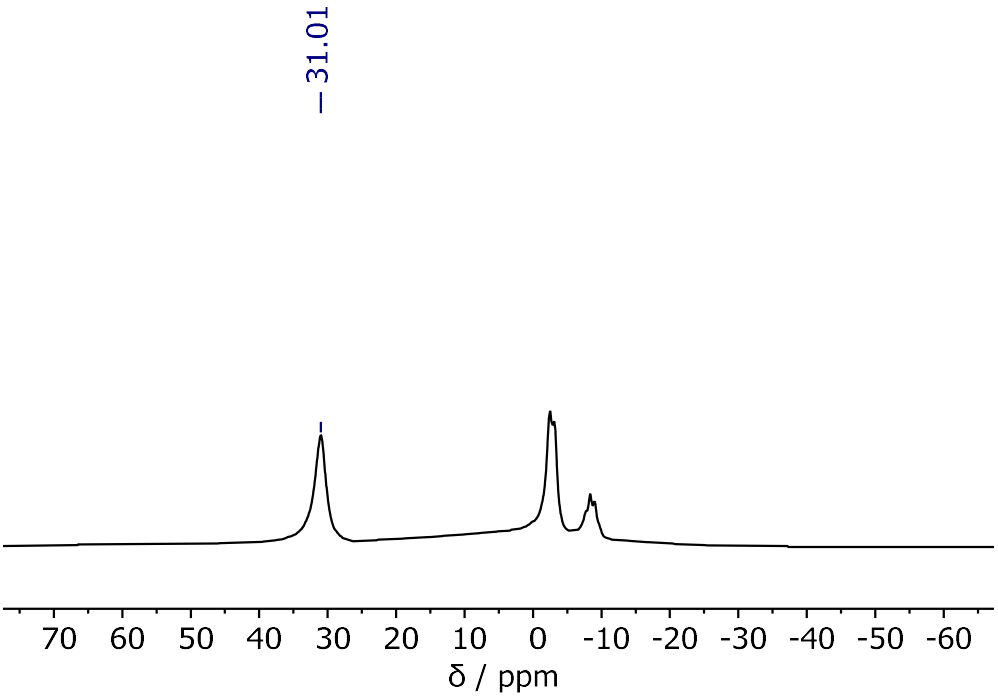

Figure 4.11: ^{11}B NMR (161 MHz, $CDCl_3$) spectrum of 7-Bpin indoline formed via the reaction of indole and *mono*-iodo pyrazabole.

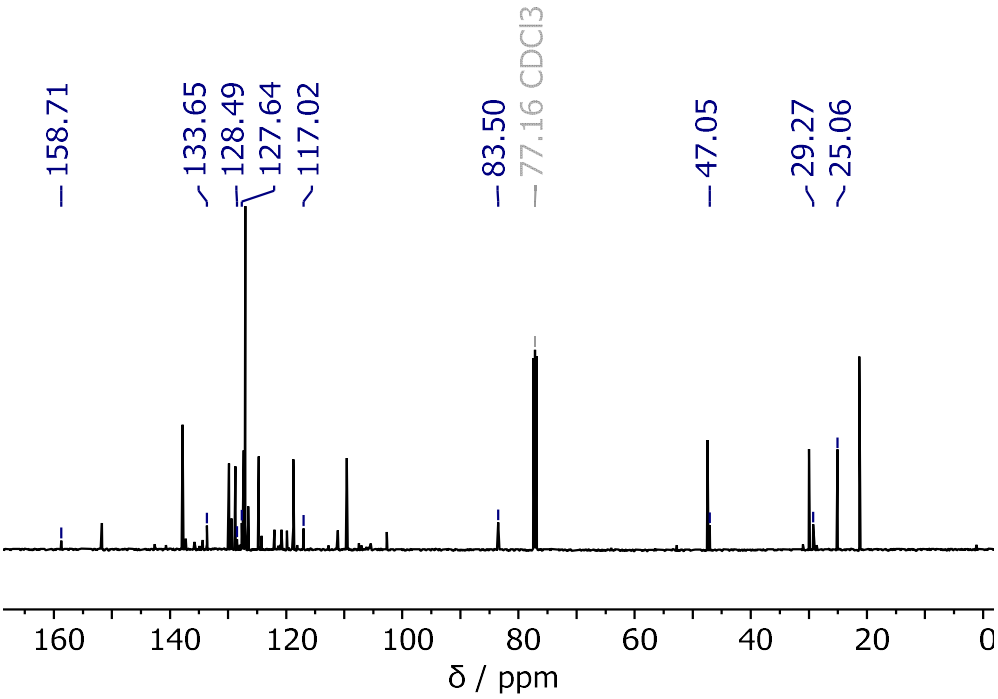

Figure 4.12: $^{13}C\{^1H\}$ NMR (126 MHz, $CDCl_3$) spectrum of 7-Bpin indoline formed via the reaction of indole and *mono*-iodo pyrazabole. The major species present is *N*-H Indoline. *Note: The resonances at 21.3, 127.7 and 137.3 ppm are mesitylene, used as an internal standard.*

Reactivity of Indole with *Di*-Iodo Pyrazabole (4.2)

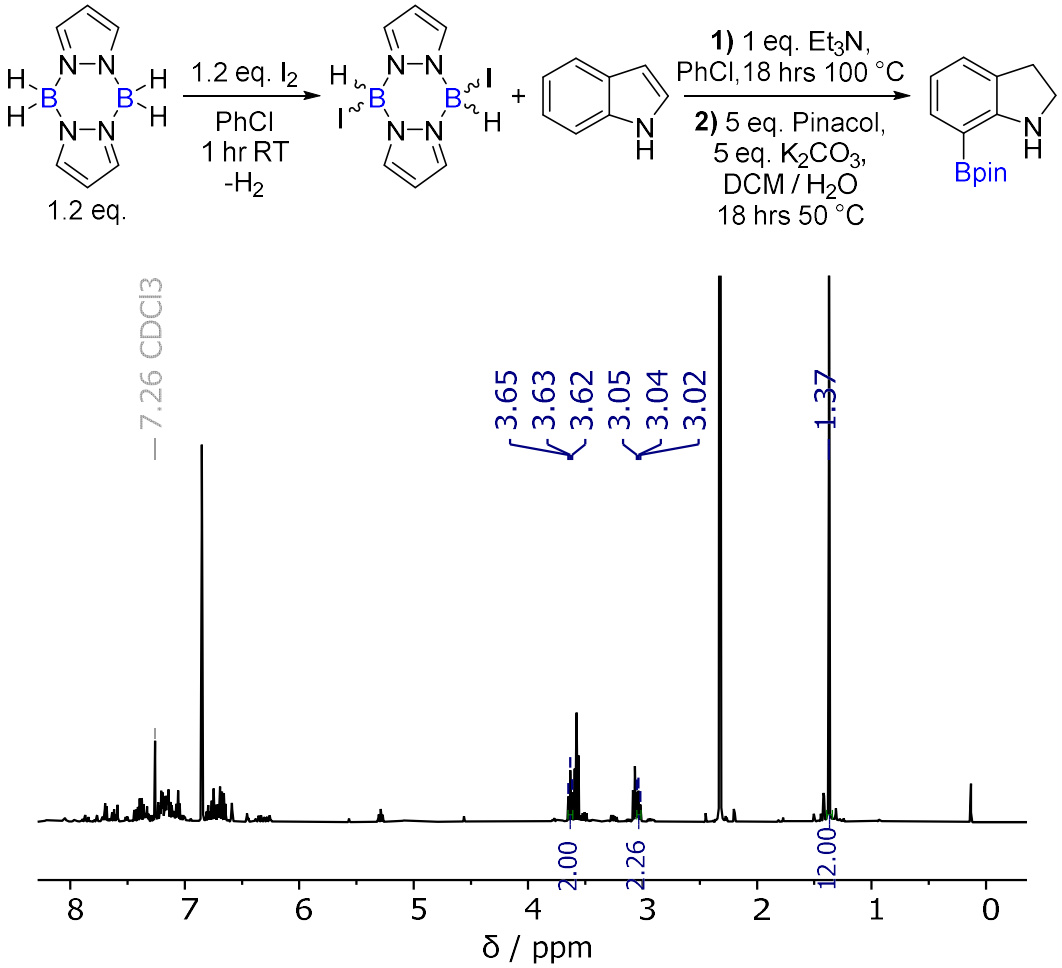

Figure 4.13: ^{1}H NMR (500 MHz, $CDCl_3$) spectrum of 7-Bpin indoline formed via the reaction of indole and *di*-iodo pyrazabole (and Et_3N). The major species present is *N*-H Indoline. *Note: The resonances at 2.32 and 6.86 ppm are due to mesitylene, used as an internal standard.*

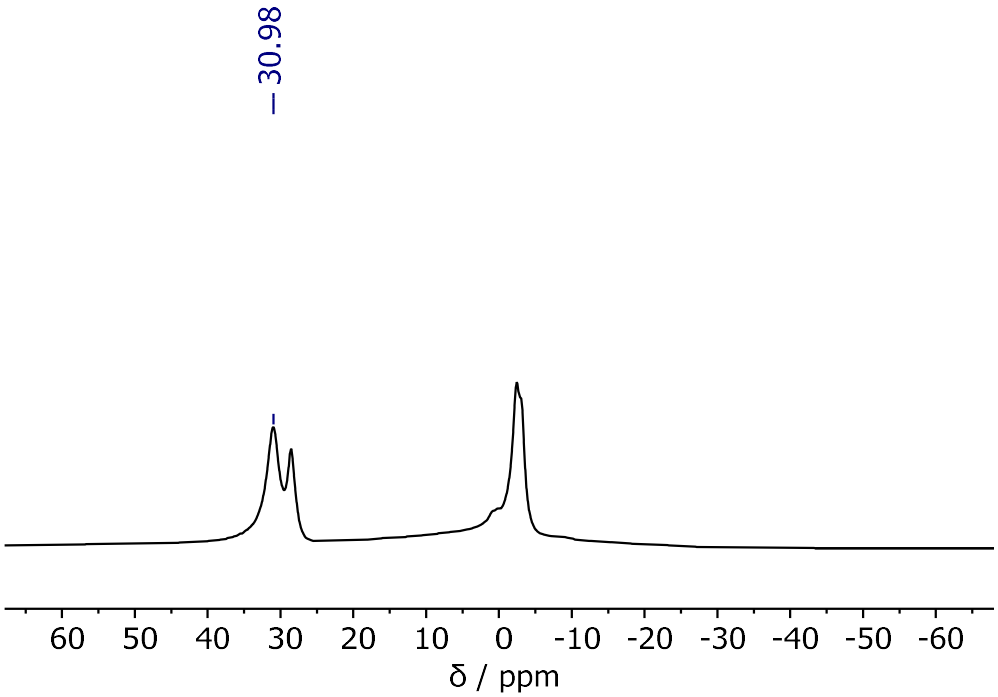

Figure 4.14: ^{11}B NMR (161 MHz, $CDCl_3$) spectrum of 7-Bpin indoline formed via the reaction of indole and *di*-iodo pyrazabole (and Et_3N).

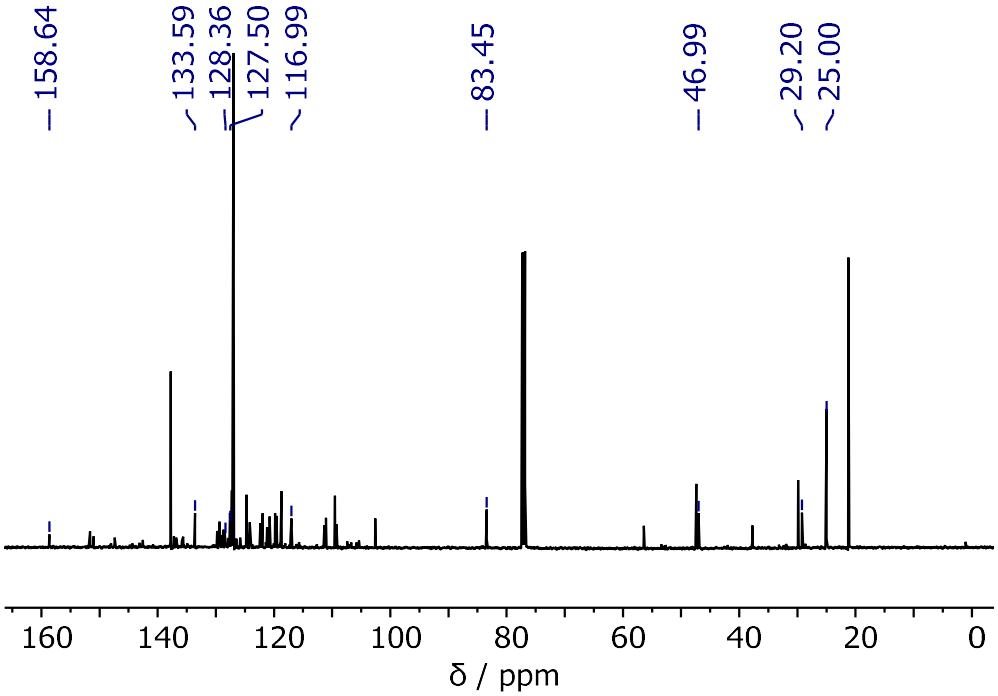

Figure 4.15: $^{13}C\{^1H\}$ NMR (126 MHz, $CDCl_3$) spectrum of 7-Bpin indoline formed via the reaction of indole and *di*-iodo pyrazabole (and Et_3N). The major species present is *N*-H Indoline. *Note: The resonances at 21.3, 127.7 and 137.3 ppm are due to mesitylene, used as an internal standard.*

4.5.3 – Directed *Ortho* C-H Borylation of Indoline and Tetrahydroquinoline

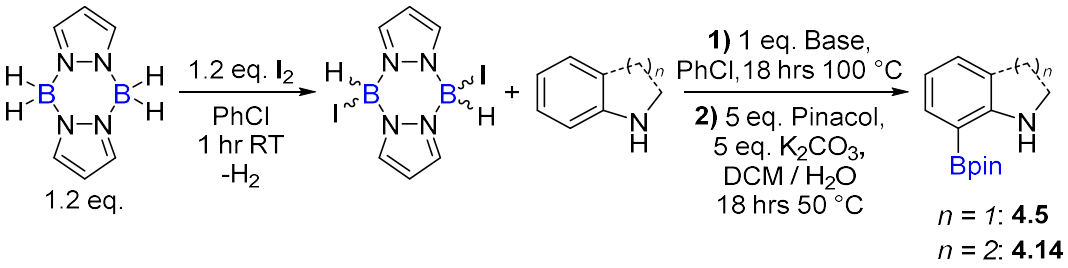

Entry 1: Indoline, *Di*-Iodo Pyrazabole and DBP

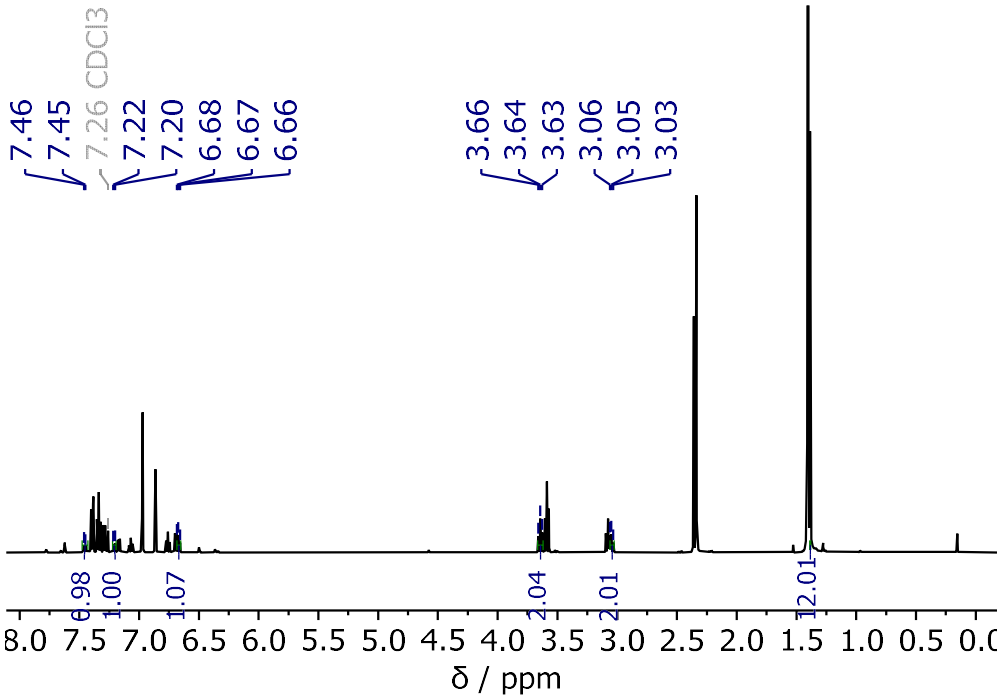

Figure 4.16: ^{1}H NMR (500 MHz, $CDCl_3$) spectrum of 7-Bpin indoline formed via the reaction of indoline, *di*-iodo pyrazabole and DBP. The major species present is *N*-H Indoline. *Note: The resonances at 2.32 and 6.86 ppm are due mesitylene, used as an internal standard. The resonances at 1.40, 2.36 and 6.97 ppm are due to DBP.*

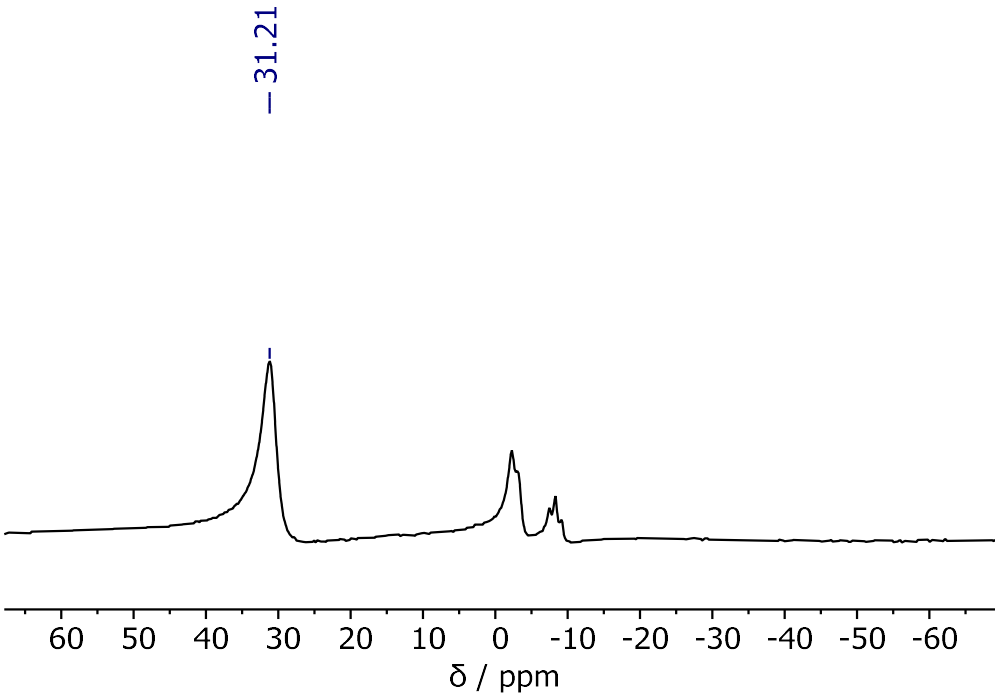

Figure 4.17: ^{11}B NMR (161 MHz, $CDCl_3$) spectrum of 7-Bpin indoline formed via the reaction of indoline, *di*-iodo pyrazabole and DBP.

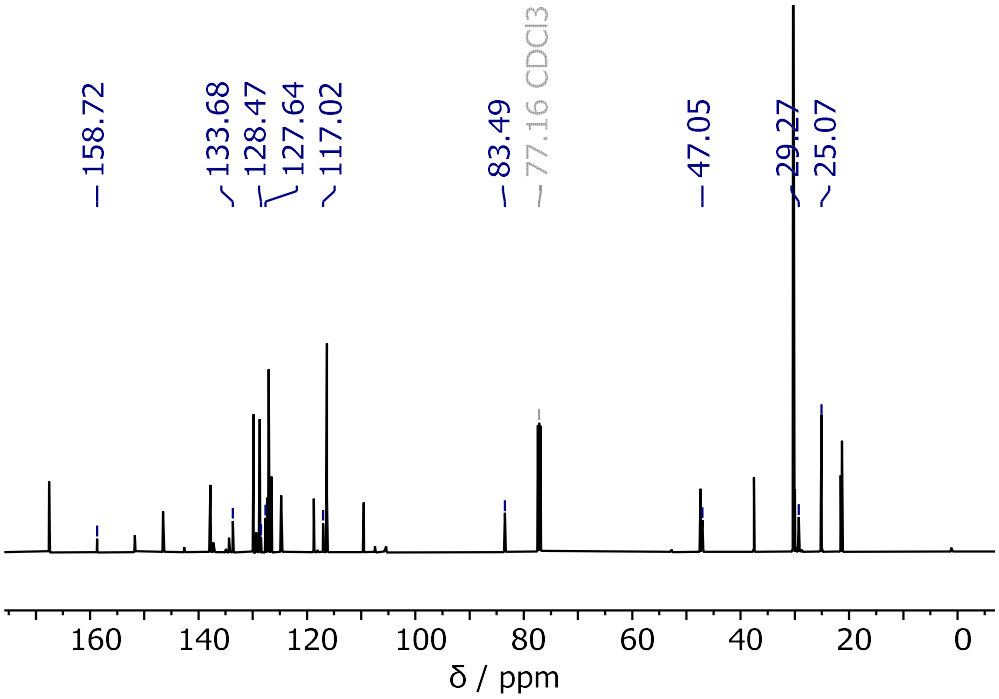

Figure 4.18: $^{13}C\{^1H\}$ NMR (126 MHz, $CDCl_3$) spectrum of 7-Bpin indoline formed via the reaction of indoline, *di*-iodo pyrazabole and DBP. The major species present is *N*-H Indoline. *Note: The resonances at 21.3, 127.7 and 137.3 ppm are due to mesitylene, used as an internal standard. The resonances at 21.3, 29.8, 37.1, 117.5, 147.4 and 166.7 ppm are due to DBP.*

Entry 2: Indoline, *Di*-Iodo Pyrazabole and DIPEA

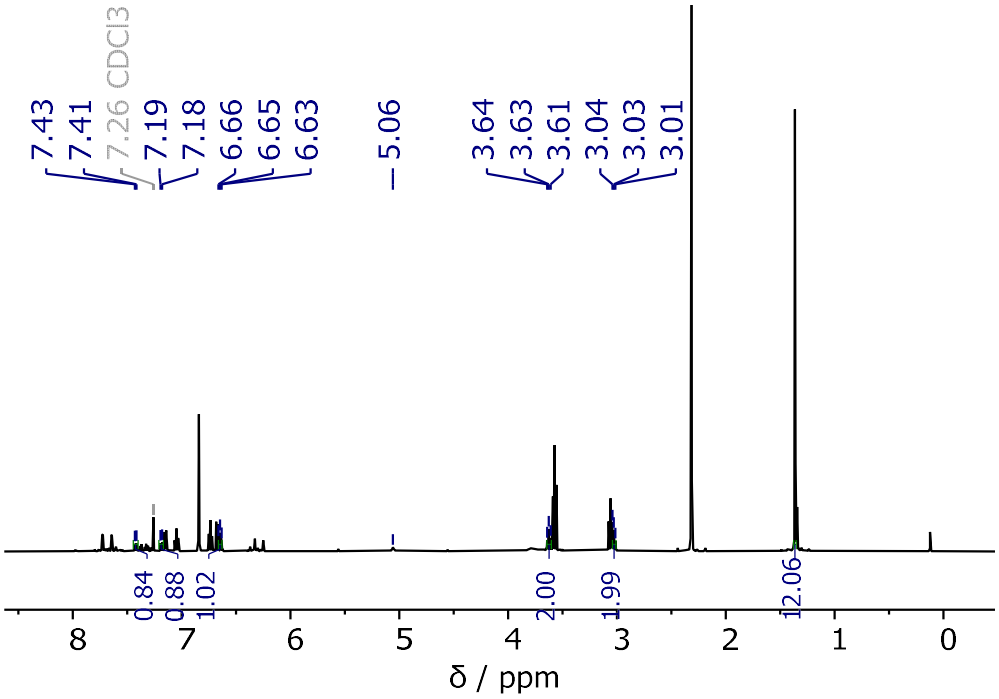

Figure 4.19: ^{1}H NMR (500 MHz, $CDCl_3$) spectrum of 7-Bpin indoline formed via the reaction of indoline, *di*-iodo pyrazabole and DIPEA. The major species present is *N*-H Indoline. *Note: The resonances at 2.32 and 6.86 ppm are due mesitylene, used as an internal standard.*

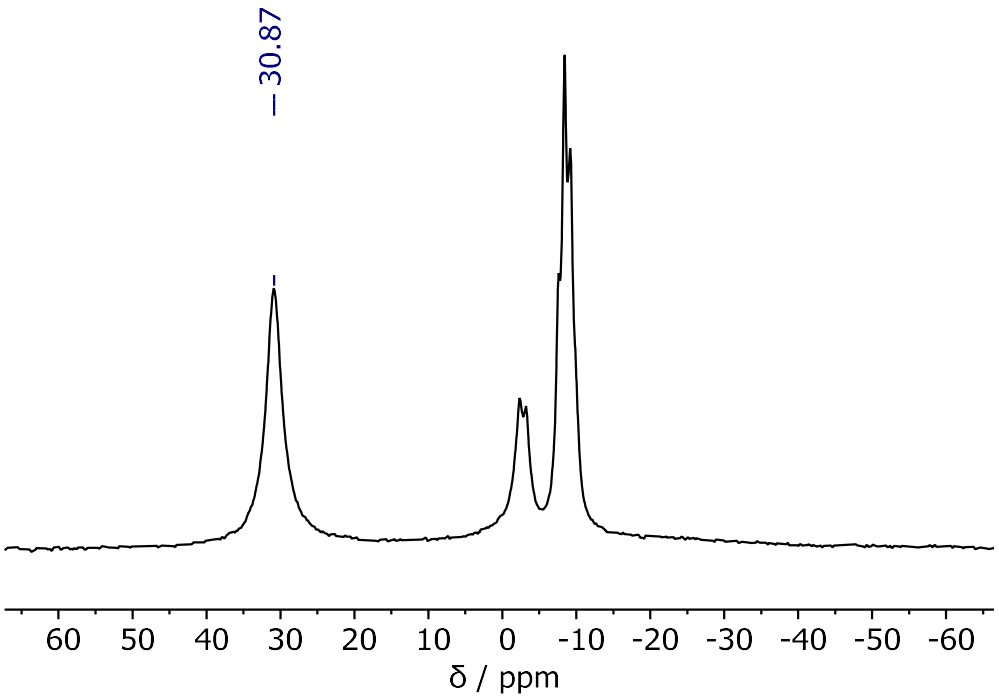

Figure 4.20: ^{11}B NMR (161 MHz, $CDCl_3$) spectrum of 7-Bpin indoline formed via the reaction of indoline, *di*-iodo pyrazabole and DIPEA

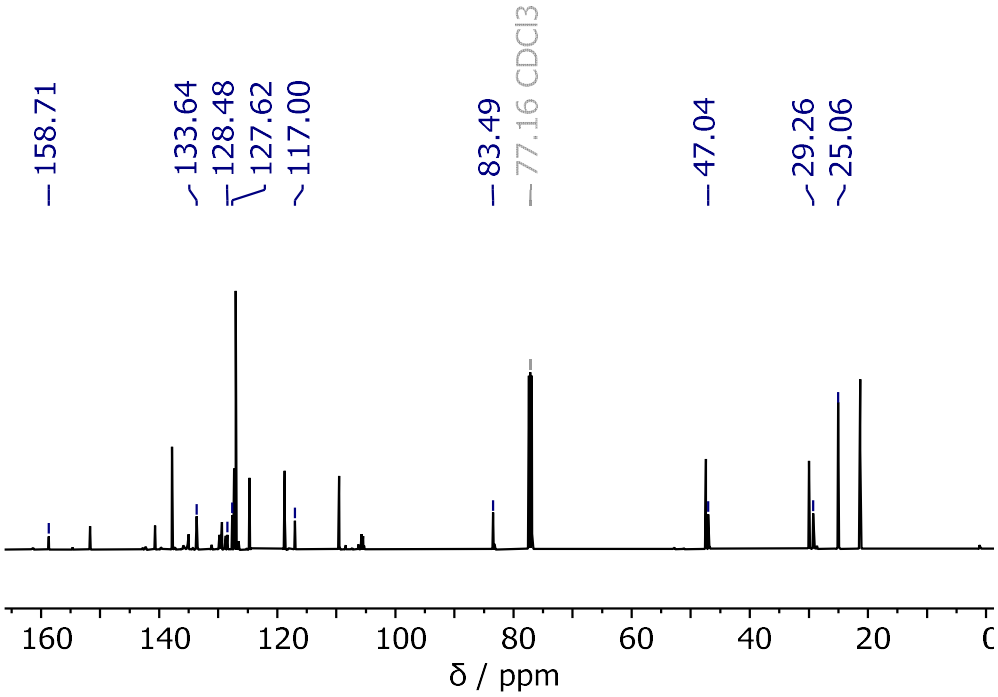

Figure 4.21: $^{13}C\{^{1}H\}$ NMR (126 MHz, $CDCl_3$) spectrum of 7-Bpin indoline formed via the reaction of indoline, *di*-iodo pyrazabole and DIPEA. The major species present is *N*-H Indoline. *Note: The resonances at 21.3, 127.7 and 137.3 ppm are due to mesitylene, used as an internal standard.*

Entry 3: Indoline, *Di*-Iodo Pyrazabole and Et_3N

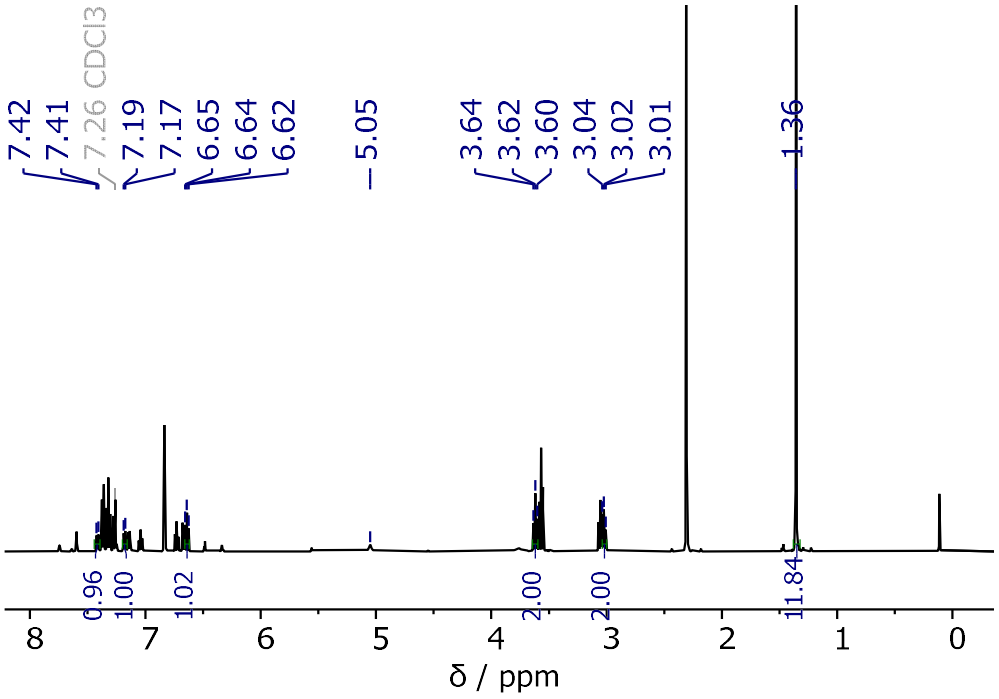

Figure 4.22: ^{1}H NMR (500 MHz, $CDCl_3$) spectrum of 7-Bpin indoline formed via the reaction of indoline, *di*-iodo pyrazabole and Et_3N. The major species present is *N*-H Indoline. *Note: The resonances at 2.32 and 6.86 ppm are due mesitylene, used as an internal standard.*

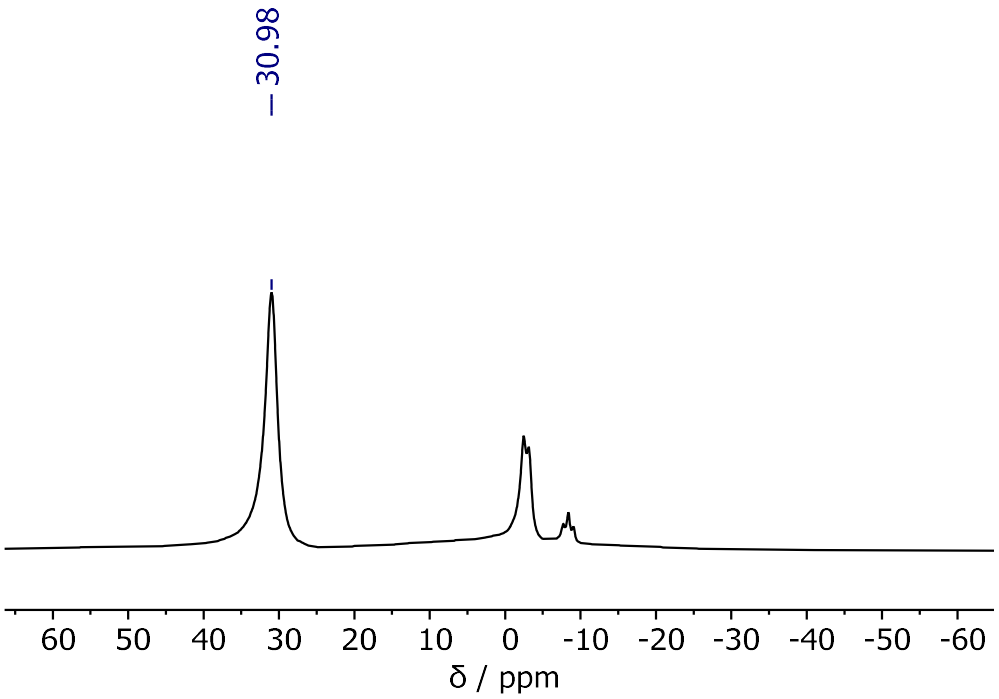

Figure 4.23: ^{11}B NMR (161 MHz, $CDCl_3$) spectrum of 7-Bpin indoline formed via the reaction of indoline, *di*-iodo pyrazabole and Et_3N.

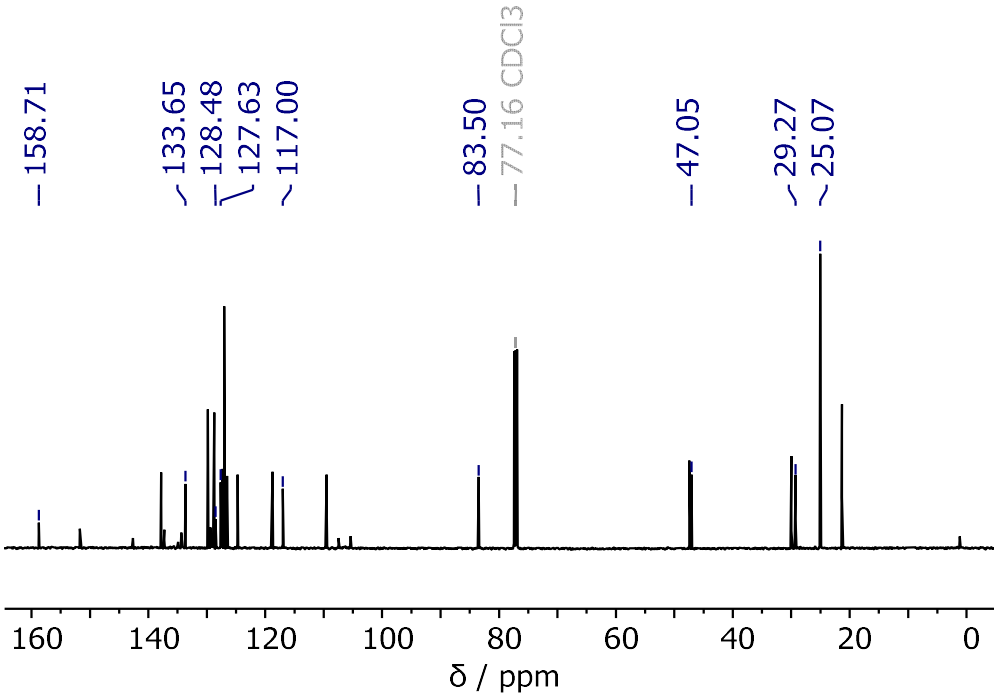

Figure 4.24: $^{13}C\{^{1}H\}$ NMR (126 MHz, $CDCl_3$) spectrum of 7-Bpin indoline formed via the reaction of indoline, *di*-iodo pyrazabole and Et_3N. The major species present is *N*-H Indoline. *Note: The resonances at 21.3, 127.7 and 137.3 ppm are due to mesitylene, used as an internal standard.*

Entry 4: Indoline, *Di*-Iodo Pyrazabole and Et_3N (Order of Addition Switched)

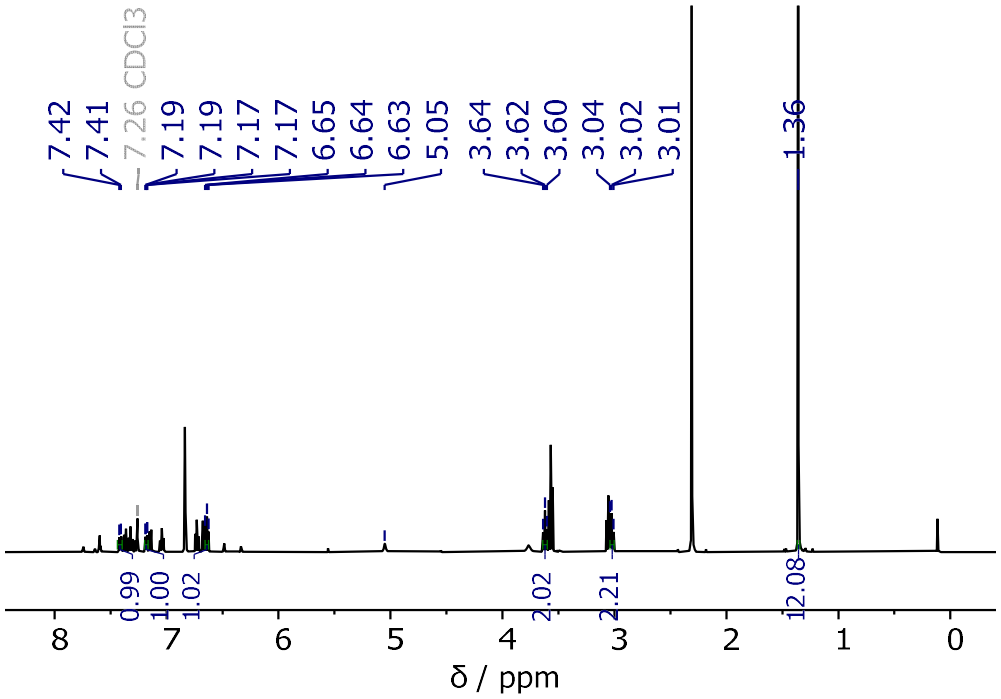

Figure 4.25: ^{1}H NMR (500 MHz, $CDCl_3$) spectrum of 7-Bpin indoline formed via the reaction of indoline, *di*-iodo pyrazabole and Et_3N. The major species present is *N*-H Indoline. *Note: The resonances at 2.32 and 6.86 ppm are due mesitylene, used as an internal standard.*

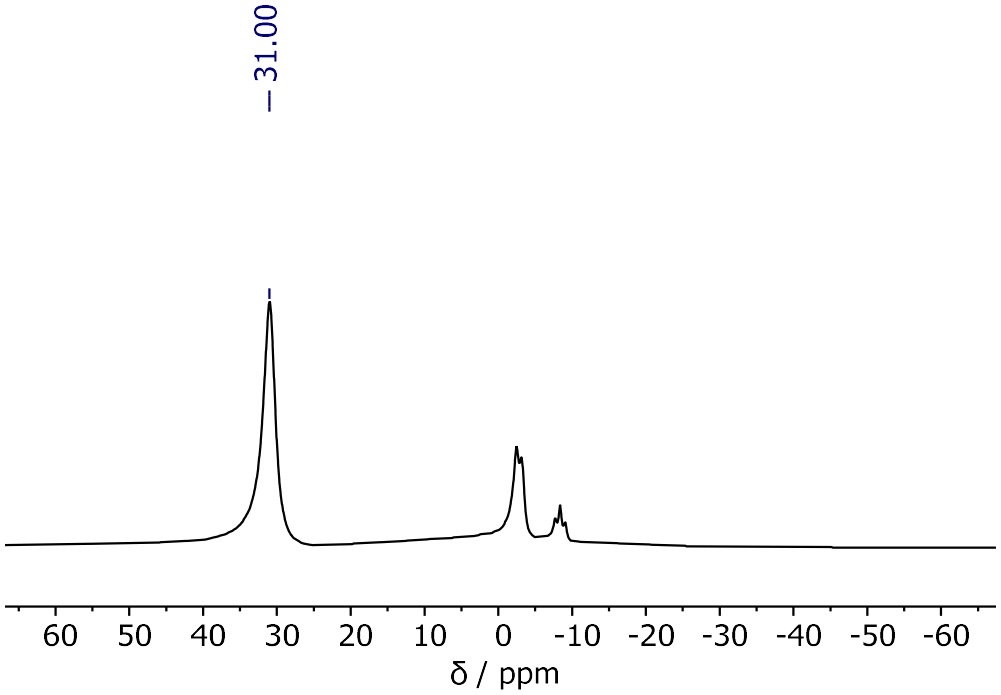

Figure 4.26: ^{11}B NMR (161 MHz, $CDCl_3$) spectrum of 7-Bpin indoline formed via the reaction of indoline, *di*-iodo pyrazabole and Et_3N.

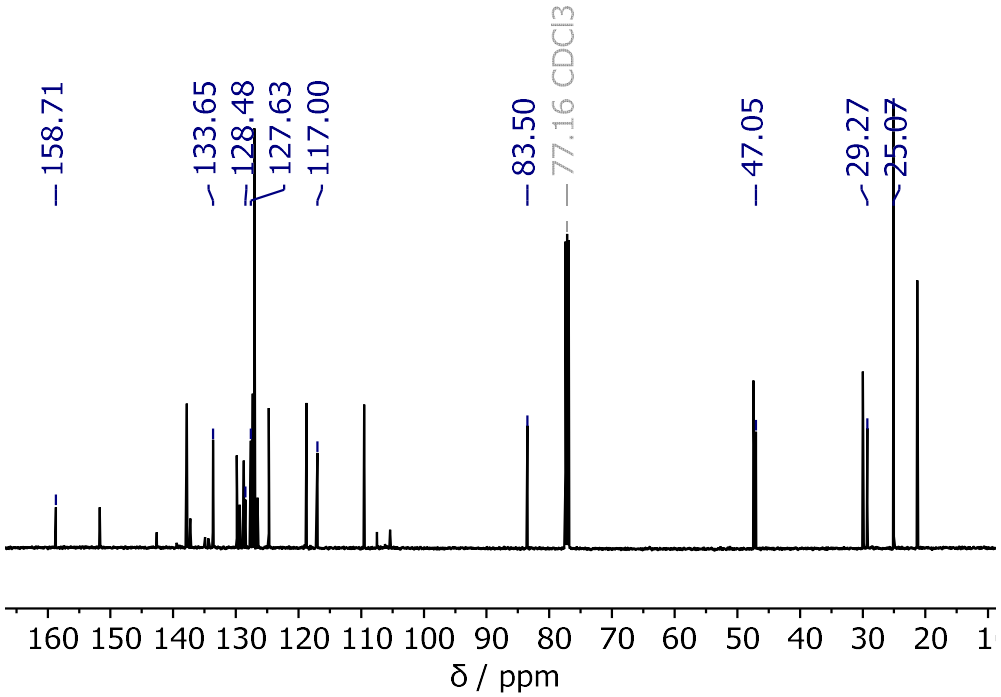

Figure 4.27: $^{13}C\{^{1}H\}$ NMR (126 MHz, $CDCl_3$) spectrum of 7-Bpin indoline formed via the reaction of indoline, *di*-iodo pyrazabole and Et_3N. The major species present is *N*-H Indoline. *Note: The resonances at 21.3, 127.7 and 137.3 ppm are due to mesitylene, used as an internal standard.*

Entry 5: Indoline, *Di*-Iodo Pyrazabole and Et_3N (Simultaneously)

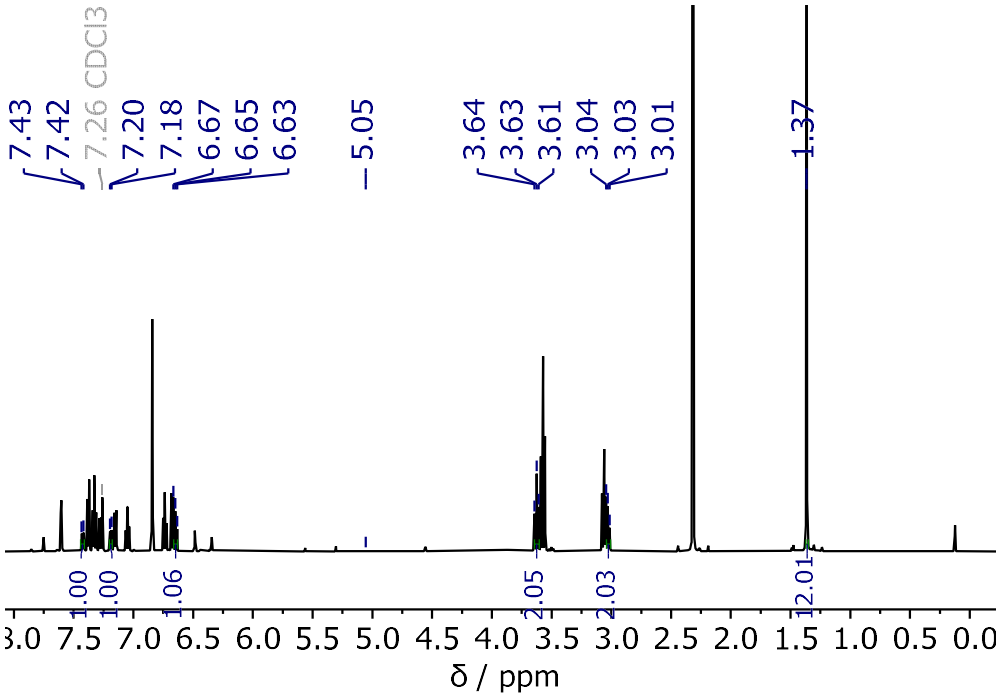

Figure 4.28: ^{1}H NMR (500 MHz, $CDCl_3$) spectrum of 7-Bpin indoline formed via the reaction of indoline, *di*-iodo pyrazabole and Et_3N. The major species present is *N*-H Indoline. *Note: The resonances at 2.32 and 6.86 ppm are due mesitylene, used as an internal standard.*

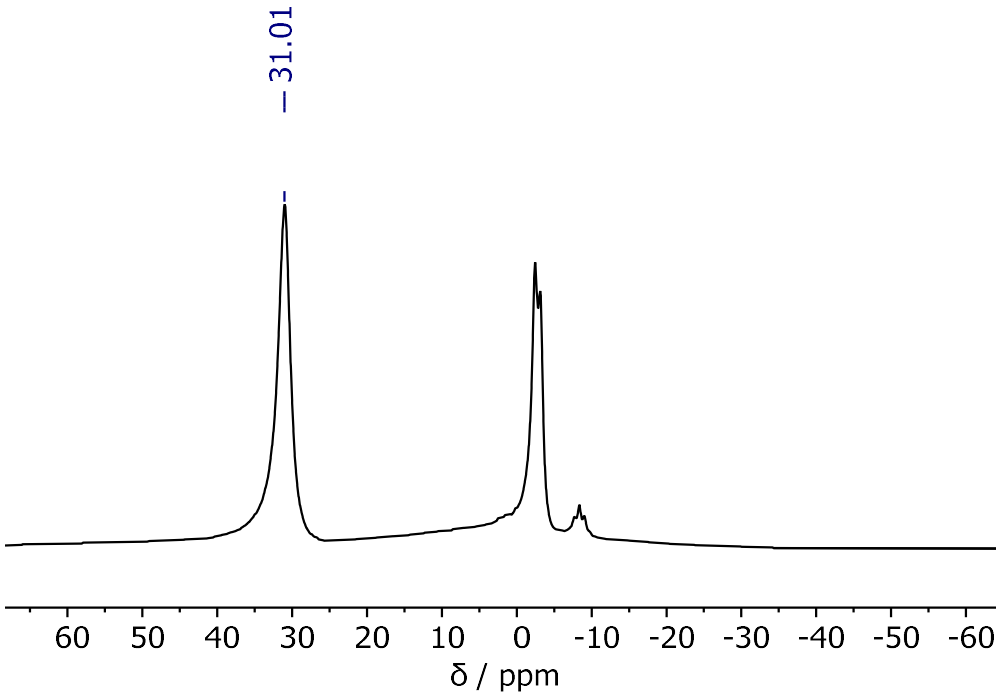

Figure 4.29: ^{11}B NMR (161 MHz, $CDCl_3$) spectrum of 7-Bpin indoline formed via the reaction of indoline, *di*-iodo pyrazabole and Et_3N.

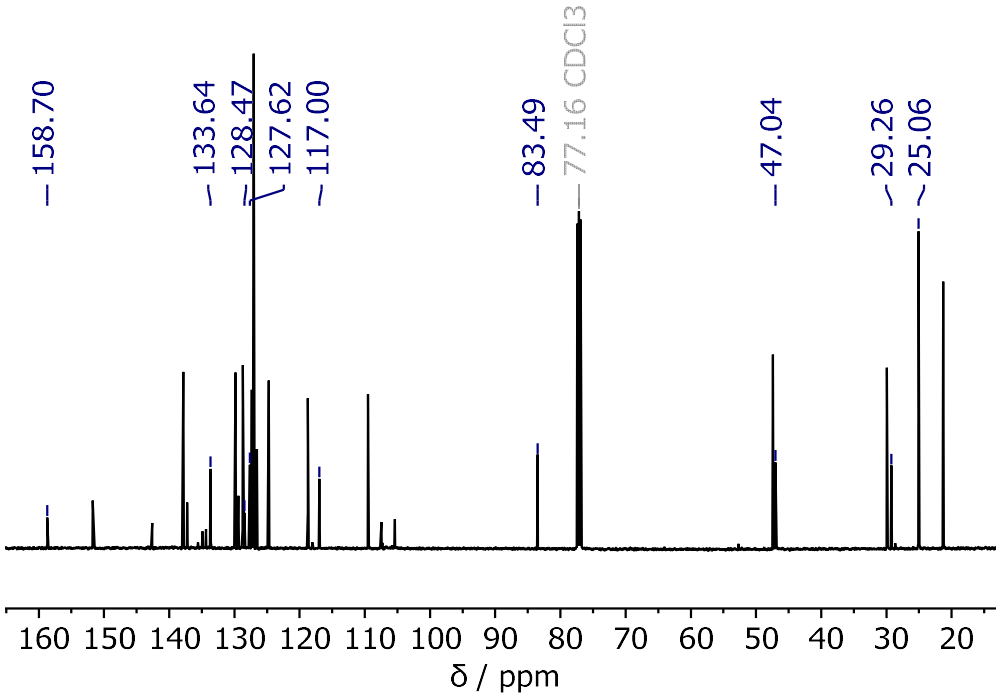

Figure 4.30: $^{13}C\{^{1}H\}$ NMR (126 MHz, $CDCl_3$) spectrum of 7-Bpin indoline formed via the reaction of indoline, *di*-iodo pyrazabole and Et_3N. The major species present is *N*-H Indoline. *Note: The resonances at 21.3, 127.7 and 137.3 ppm are due to mesitylene, used as an internal standard.*

Entry 6: Tetrahydroquinoline, *Di*-Iodo Pyrazabole and DBP

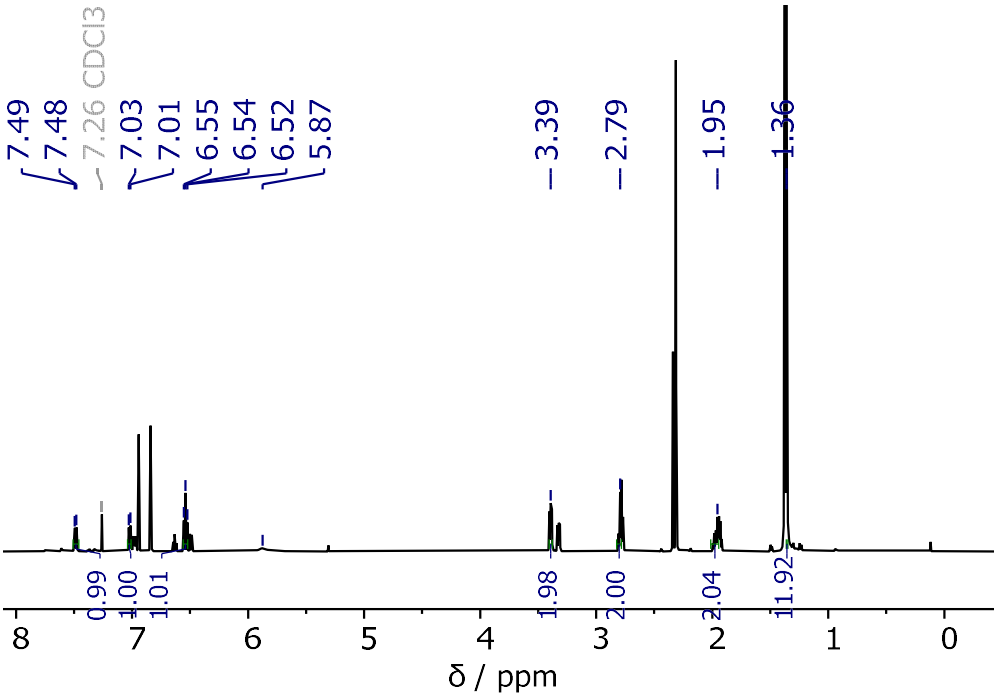

Figure 4.31: ^{1}H NMR (500 MHz, $CDCl_3$) spectrum of 8-Bpin tetrahydroquinoline formed via the reaction of tetrahydroquinoline, *di*-iodo pyrazabole and DBP. The major species is tetrahydroquinoline. *Note: Resonances at 2.32, 6.86 ppm are due mesitylene, an internal standard. The resonances at 1.40, 2.36 and 6.97 ppm are due to DBP.*

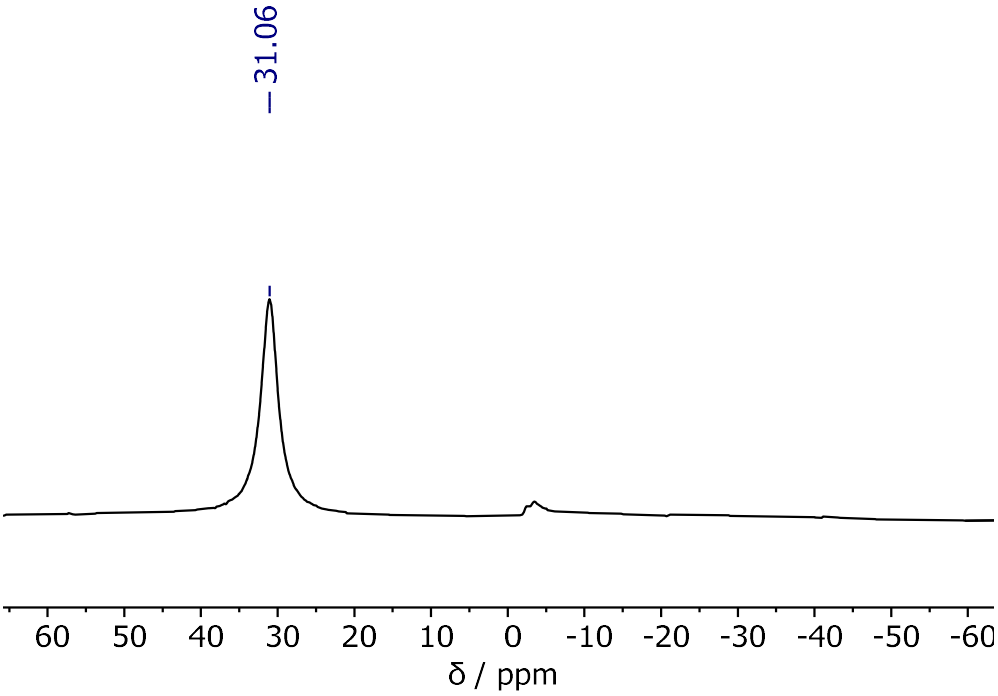

Figure 4.32: ^{11}B NMR (161 MHz, $CDCl_3$) spectrum of 8-Bpin tetrahydroquinoline formed via the reaction of tetrahydroquinoline, *di*-iodo pyrazabole and DBP.

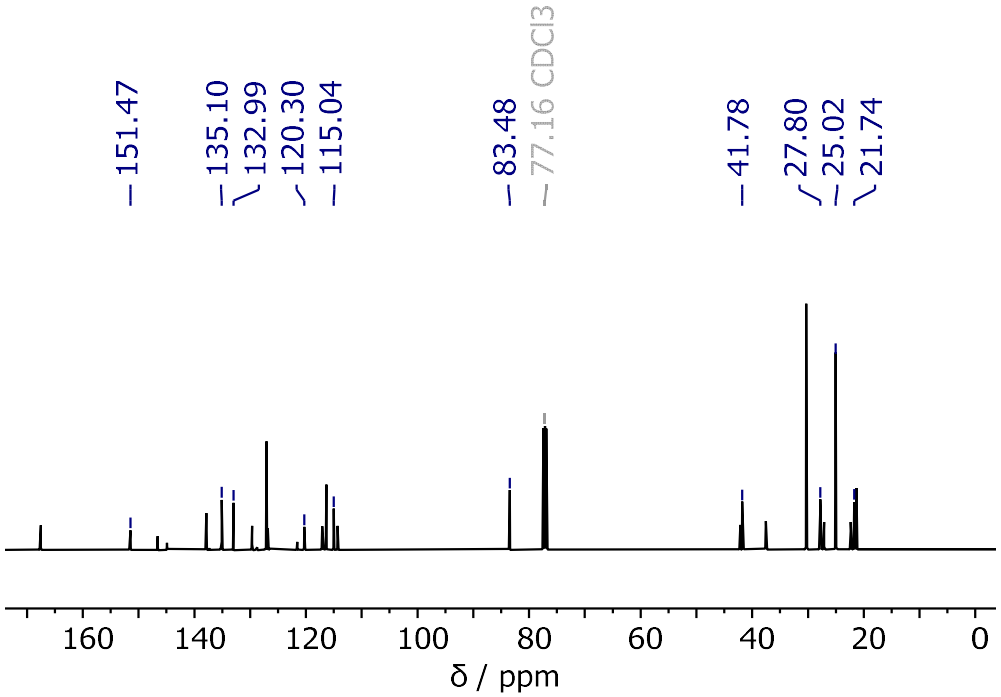

Figure 4.33: $^{13}C\{^{1}H\}$ NMR (126 MHz, $CDCl_3$) spectrum of 8-Bpin tetrahydroquinoline formed via the reaction of tetrahydroquinoline, *di*-iodo pyrazabole and DBP. The major species present is tetrahydroquinoline. *Note: Resonances at 21.3, 127.7 and 137.3 ppm are due to mesitylene, an internal standard. The resonances at 21.3, 29.8, 37.1, 117.5, 147.4 and 166.7 ppm are due to DBP.*

Entry 7: Tetrahydroquinoline, *Di*-Iodo Pyrazabole and DIPEA

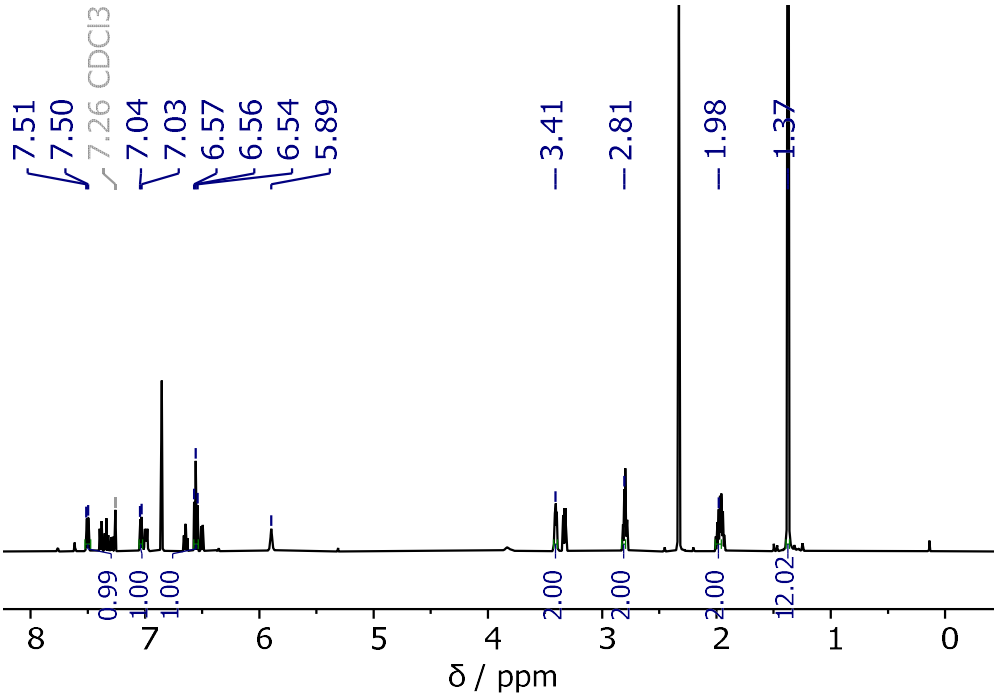

Figure 4.34: ^{1}H NMR (500 MHz, $CDCl_3$) spectrum of 8-Bpin tetrahydroquinoline formed via the reaction of tetrahydroquinoline, *di*-iodo pyrazabole and DIPEA. The major species is tetrahydroquinoline. *Note: Resonances at 2.32, 6.86 ppm are due mesitylene, an internal standard.*

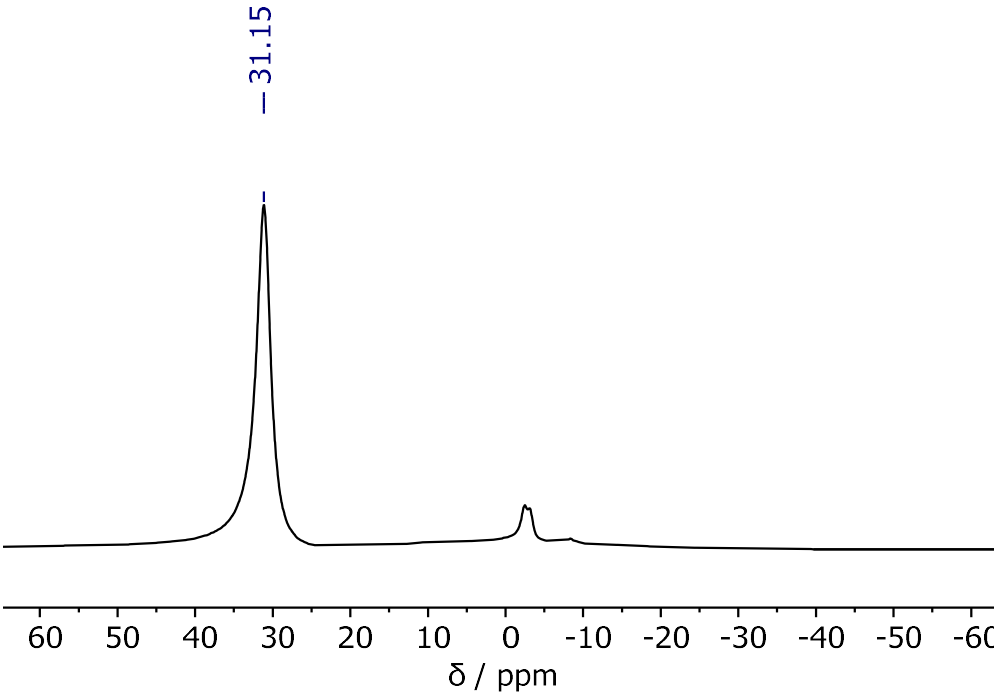

Figure 4.35: ^{11}B NMR (161 MHz, $CDCl_3$) spectrum of 8-Bpin tetrahydroquinoline formed via the reaction of tetrahydroquinoline, *di*-iodo pyrazabole and DIPEA.

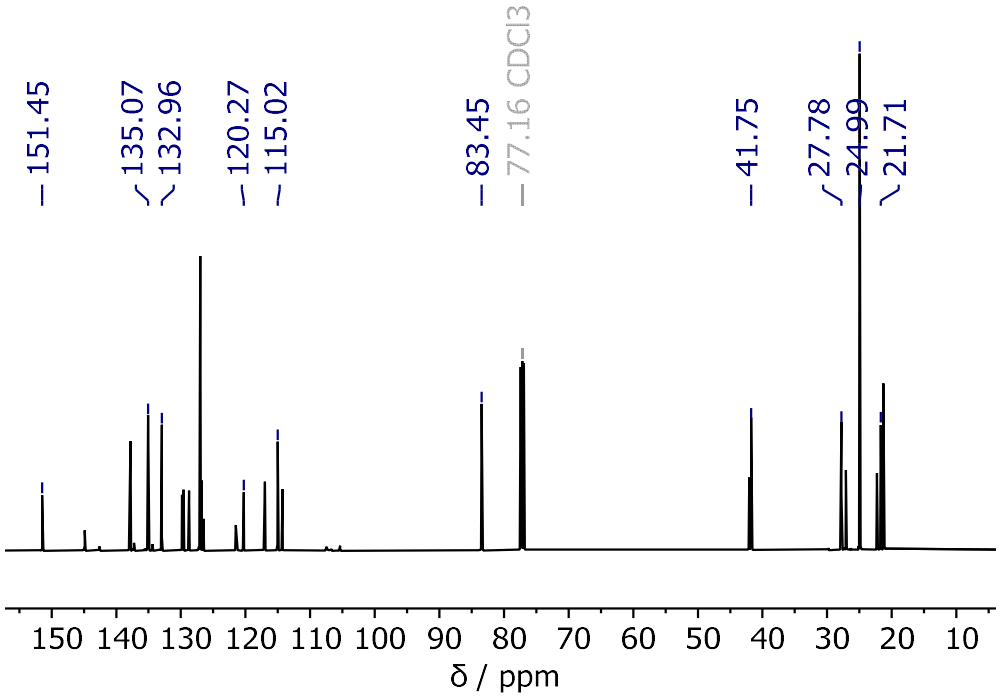

Figure 4.36: $^{13}C\{^{1}H\}$ NMR (126 MHz, $CDCl_3$) spectrum of 8-Bpin tetrahydroquinoline formed via the reaction of tetrahydroquinoline, *di*-iodo pyrazabole and DIPEA. The major species present is tetrahydroquinoline. *Note: Resonances at 21.3, 127.7 and 137.3 ppm are due to mesitylene, an internal standard.*

Entry 8: Tetrahydroquinoline, *Di*-Iodo Pyrazabole and Et_3N

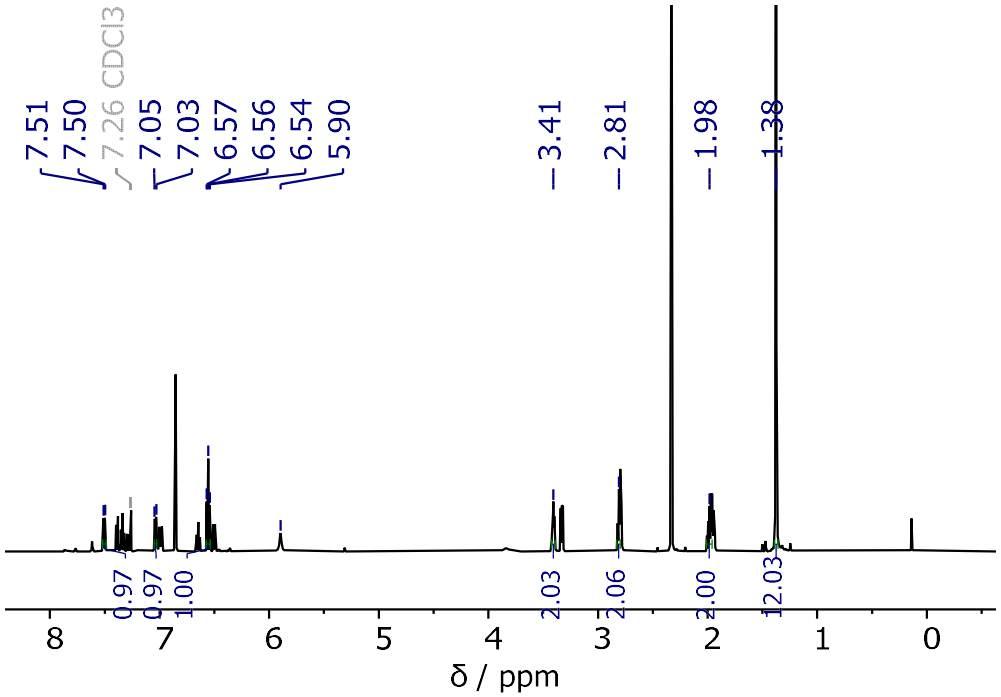

Figure 4.37: ^1H NMR (500 MHz, $CDCl_3$) spectrum of 8-Bpin tetrahydroquinoline formed via the reaction of tetrahydroquinoline, *di*-iodo pyrazabole and Et_3N. The major species is tetrahydroquinoline. *Note: Resonances at 2.32, 6.86 ppm are due mesitylene, an internal standard.*

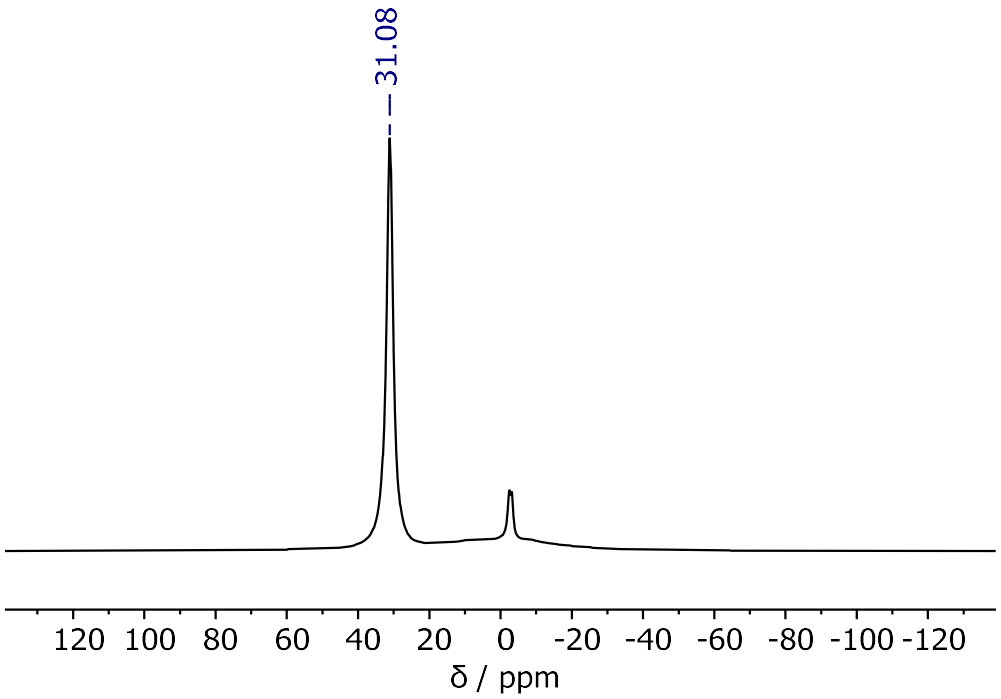

Figure 4.38: ^{11}B NMR (161 MHz, $CDCl_3$) spectrum of 8-Bpin tetrahydroquinoline formed via the reaction of tetrahydroquinoline, *di*-iodo pyrazabole and Et_3N.

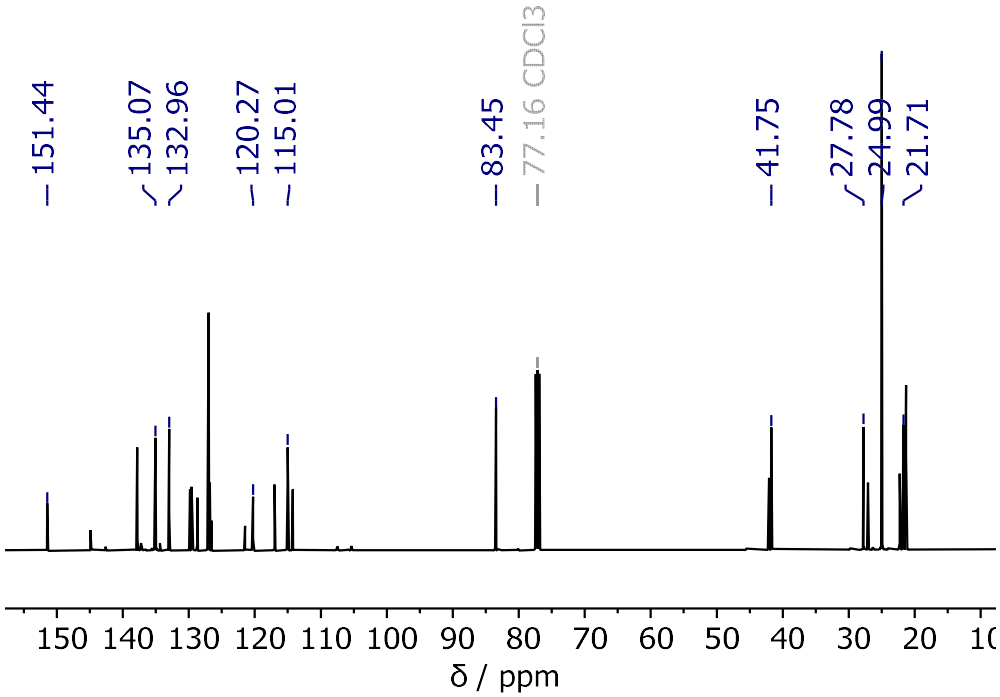

Figure 4.39: $^{13}C\{^{1}H\}$ NMR (126 MHz, $CDCl_3$) spectrum of 8-Bpin tetrahydroquinoline formed via the reaction of tetrahydroquinoline, *di*-iodo pyrazabole and Et_3N. The major species present is tetrahydroquinoline. *Note: Resonances at 21.3, 127.7 and 137.3 ppm are due to mesitylene, an internal standard.*

Entry 9: Tetrahydroquinoline, *Di*-Iodo Pyrazabole and Et_3N (Order of Addition Switched)

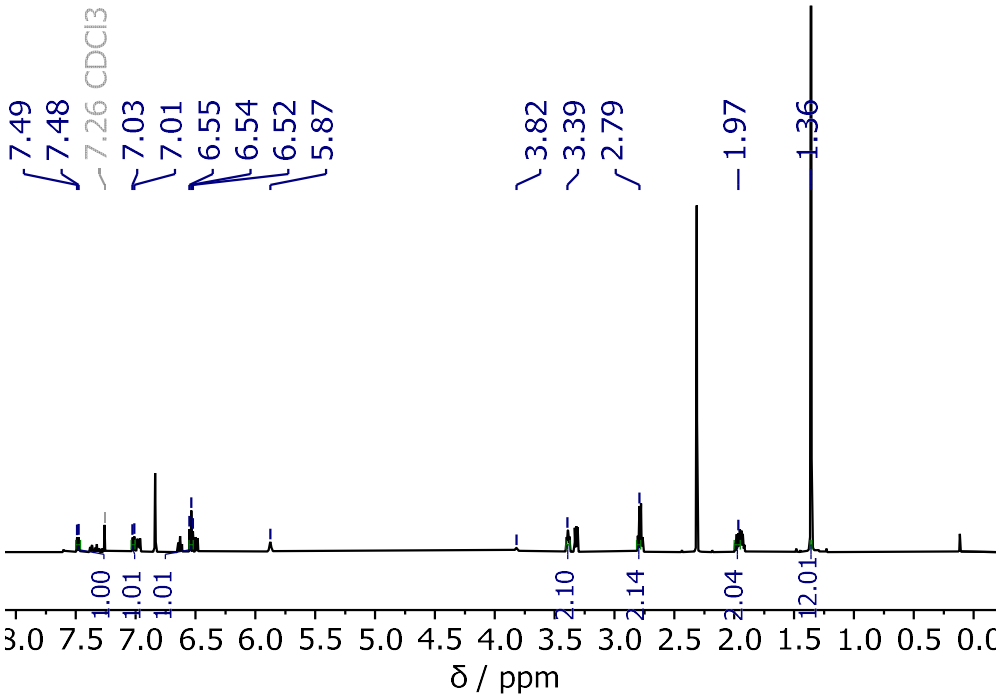

Figure 4.40: ^{1}H NMR (500 MHz, $CDCl_3$) spectrum of 8-Bpin tetrahydroquinoline formed via the reaction of tetrahydroquinoline, *di*-iodo pyrazabole and Et_3N. The major species is tetrahydroquinoline. *Note: Resonances at 2.32, 6.86 ppm are due mesitylene, an internal standard.*

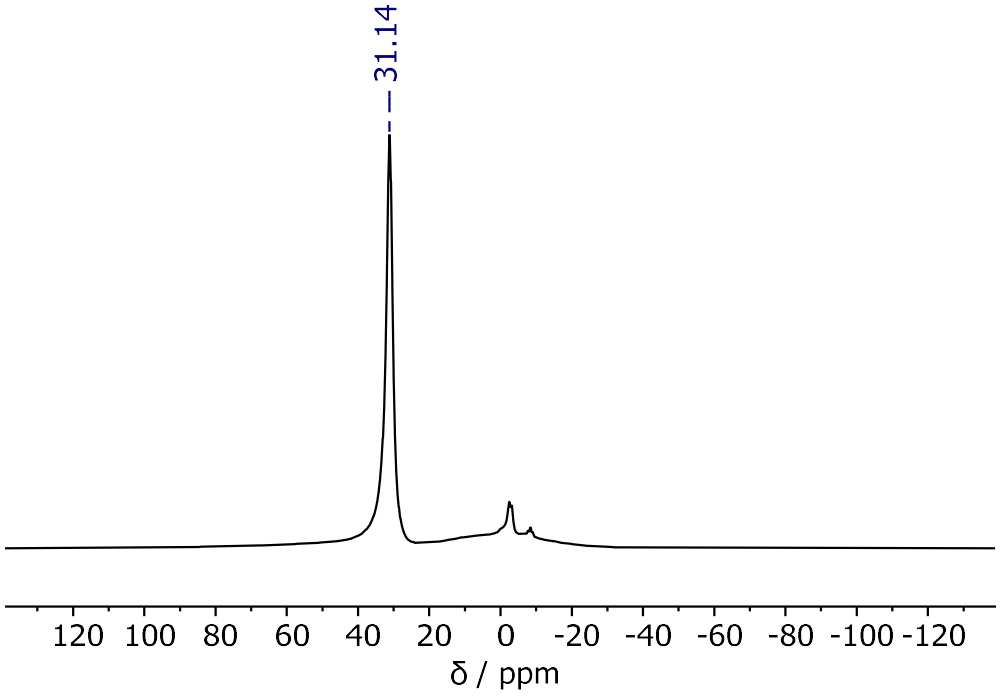

Figure 4.41: ^{11}B NMR (161 MHz, $CDCl_3$) spectrum of 8-Bpin tetrahydroquinoline formed via the reaction of tetrahydroquinoline, *di*-iodo pyrazabole and Et_3N.

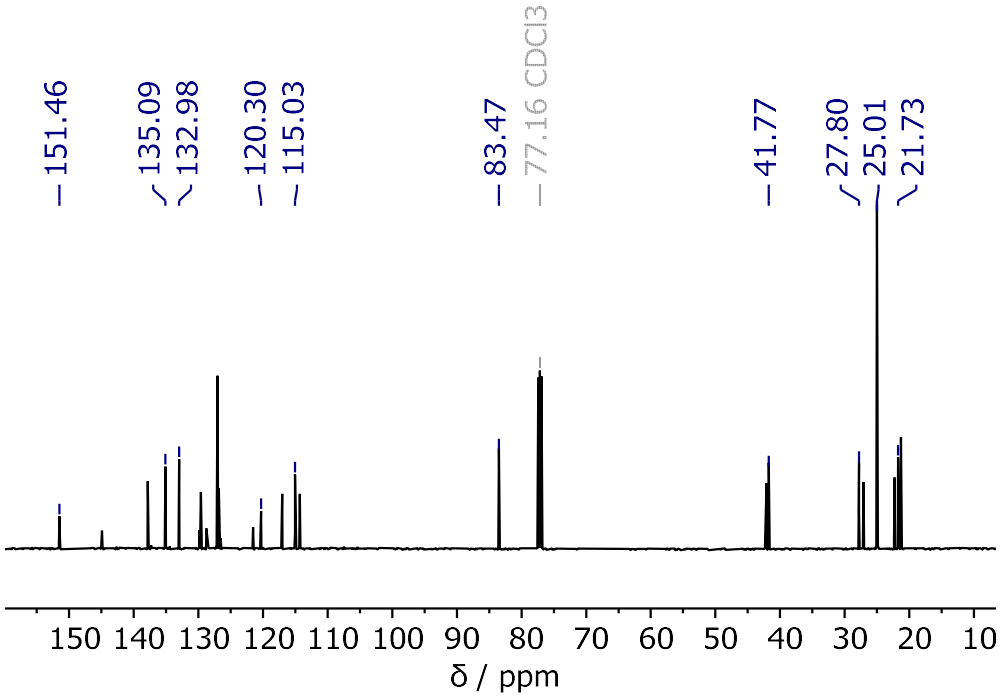

Figure 4.42: $^{13}C\{^{1}H\}$ NMR (126 MHz, $CDCl_3$) spectrum of 8-Bpin tetrahydroquinoline formed via the reaction of tetrahydroquinoline, *di*-iodo pyrazabole and Et_3N. The major species present is tetrahydroquinoline. *Note: Resonances at 21.3, 127.7 and 137.3 ppm are due to mesitylene, an internal standard.*

Entry 10: Tetrahydroquinoline, *Di*-Iodo Pyrazabole and Et_3N (Simultaneous Addition)

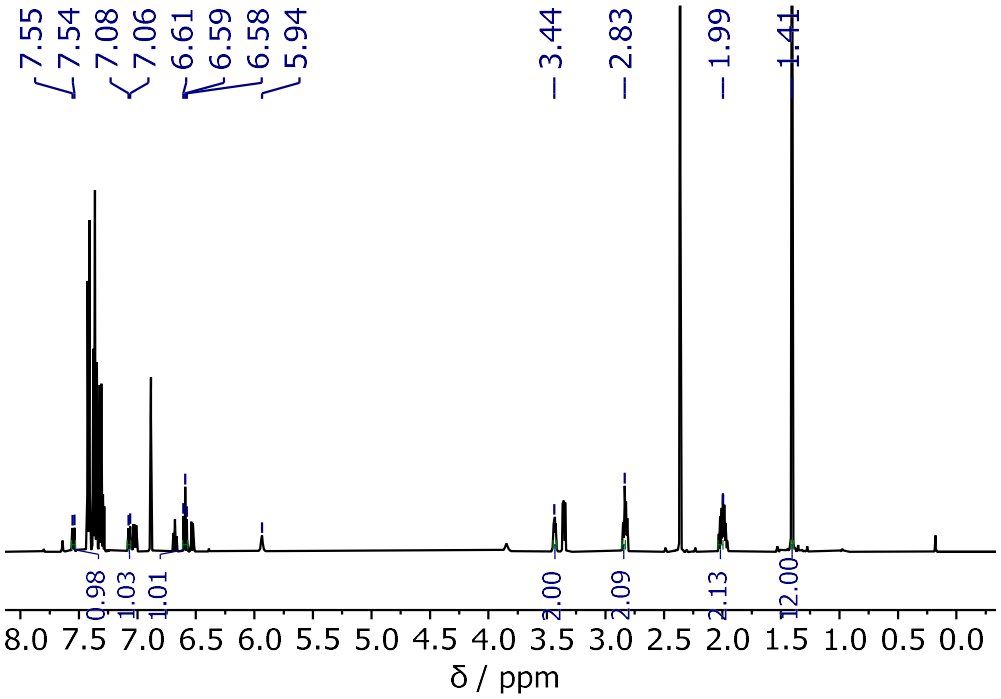

Figure 4.43: ^{1}H NMR (500 MHz, $CDCl_3$) spectrum of 8-Bpin tetrahydroquinoline formed via the reaction of tetrahydroquinoline, *di*-iodo pyrazabole and Et_3N. The major species is tetrahydroquinoline. *Note: Resonances at 2.32, 6.86 ppm are due mesitylene, an internal standard.*

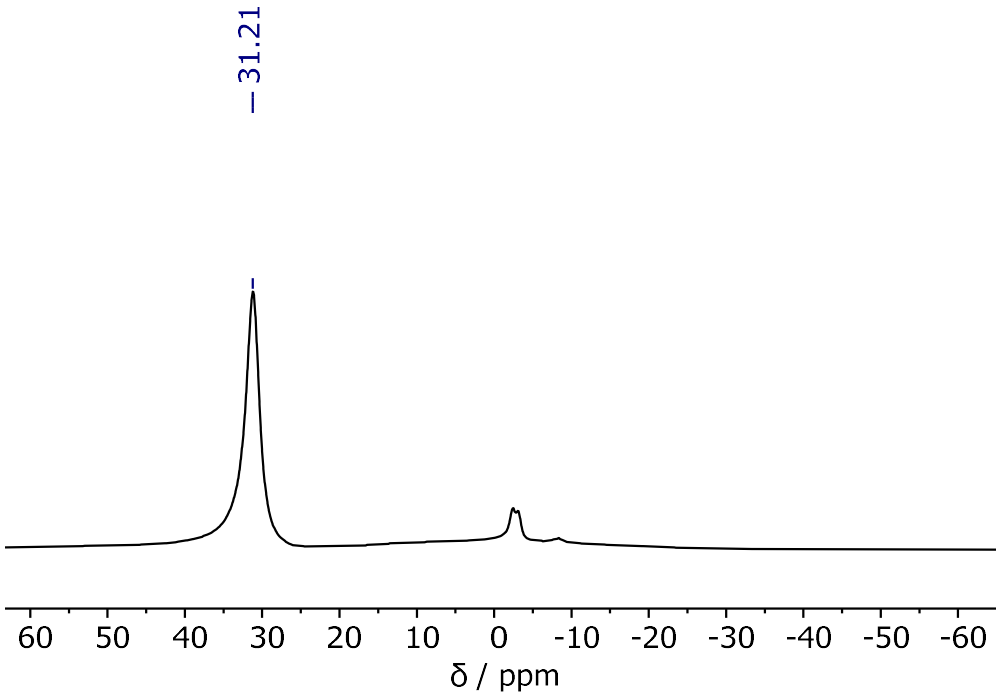

Figure 4.44: ^{11}B NMR (161 MHz, $CDCl_3$) spectrum of 8-Bpin tetrahydroquinoline formed via the reaction of tetrahydroquinoline, *di*-iodo pyrazabole and Et_3N.

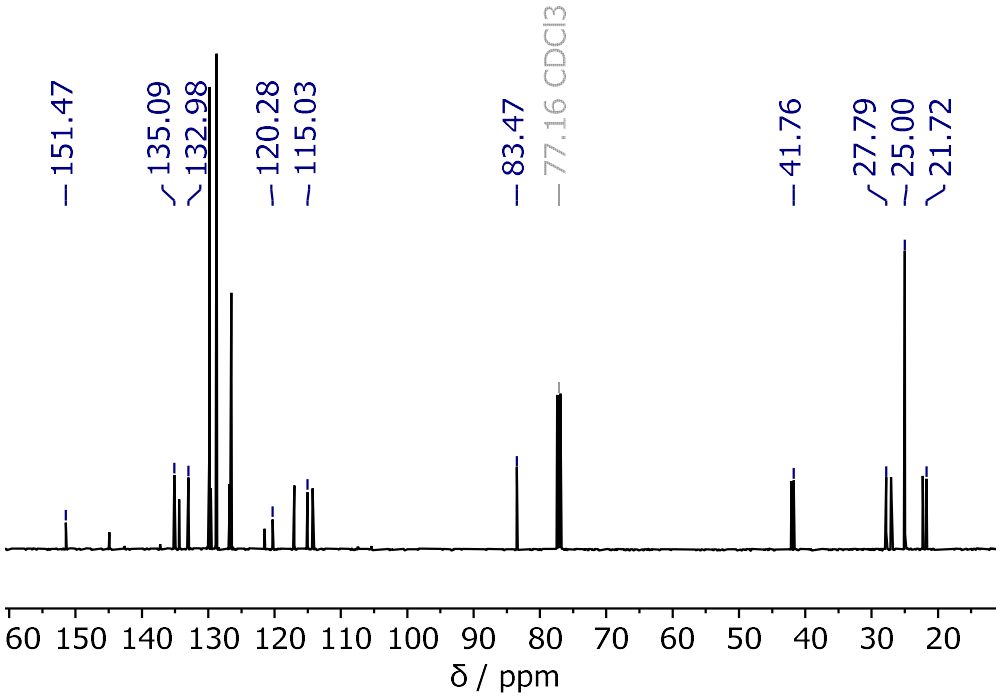

Figure 4.45: $^{13}C\{^{1}H\}$ NMR (126 MHz, $CDCl_3$) spectrum of 8-Bpin tetrahydroquinoline formed via the reaction of tetrahydroquinoline, *di*-iodo pyrazabole and Et_3N. The major species present is tetrahydroquinoline.

4.5.4 – Reaction Profiling by *in situ* NMR Spectroscopy

Reaction of Indole + *Mono* Iodo Pyrazabole

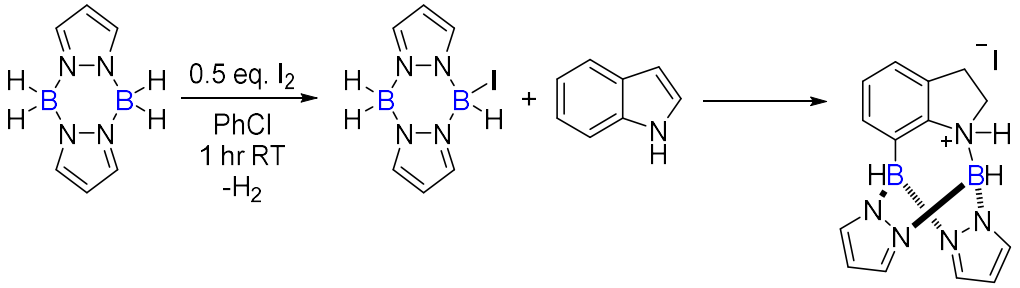

- **Reaction Profile**

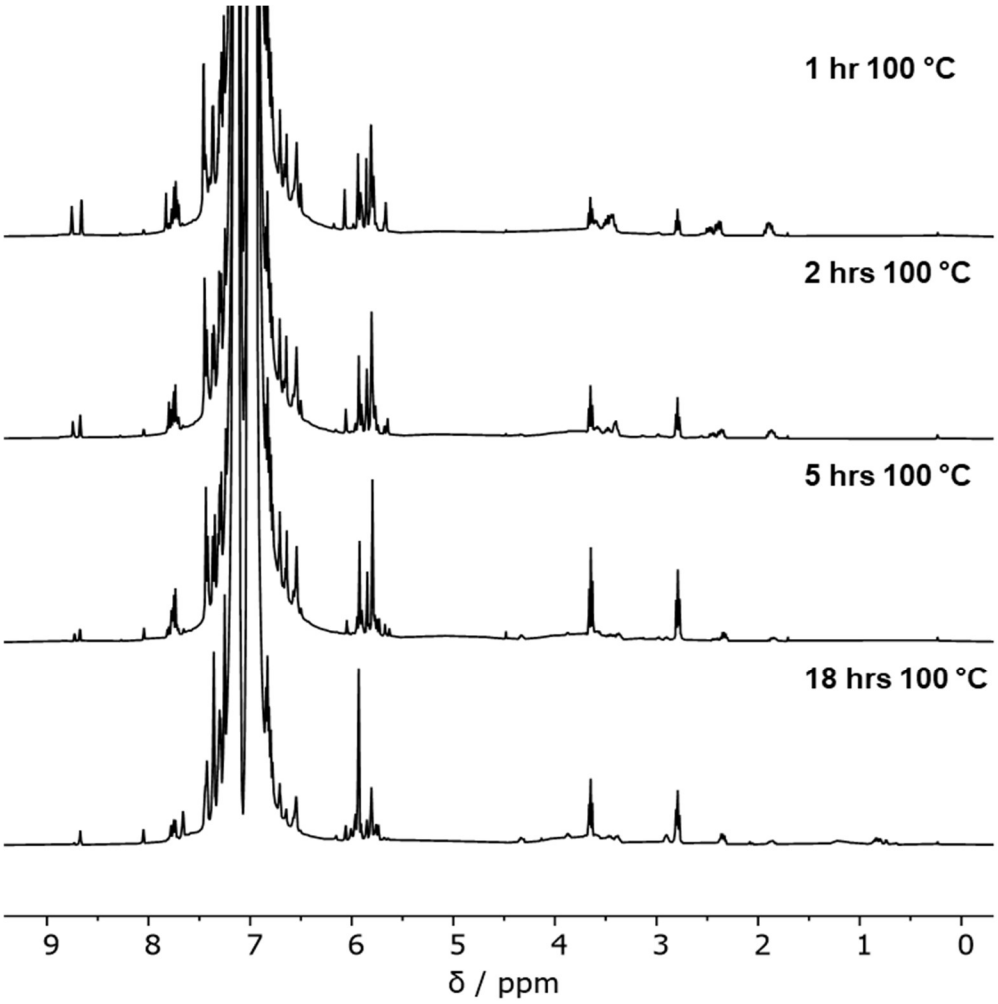

Figure 4.46: Stacked ^{1}H NMR (500 MHz, C_6H_5Cl) spectra of the reaction of *N*-H indole and *mono*-iodo pyrazabole.

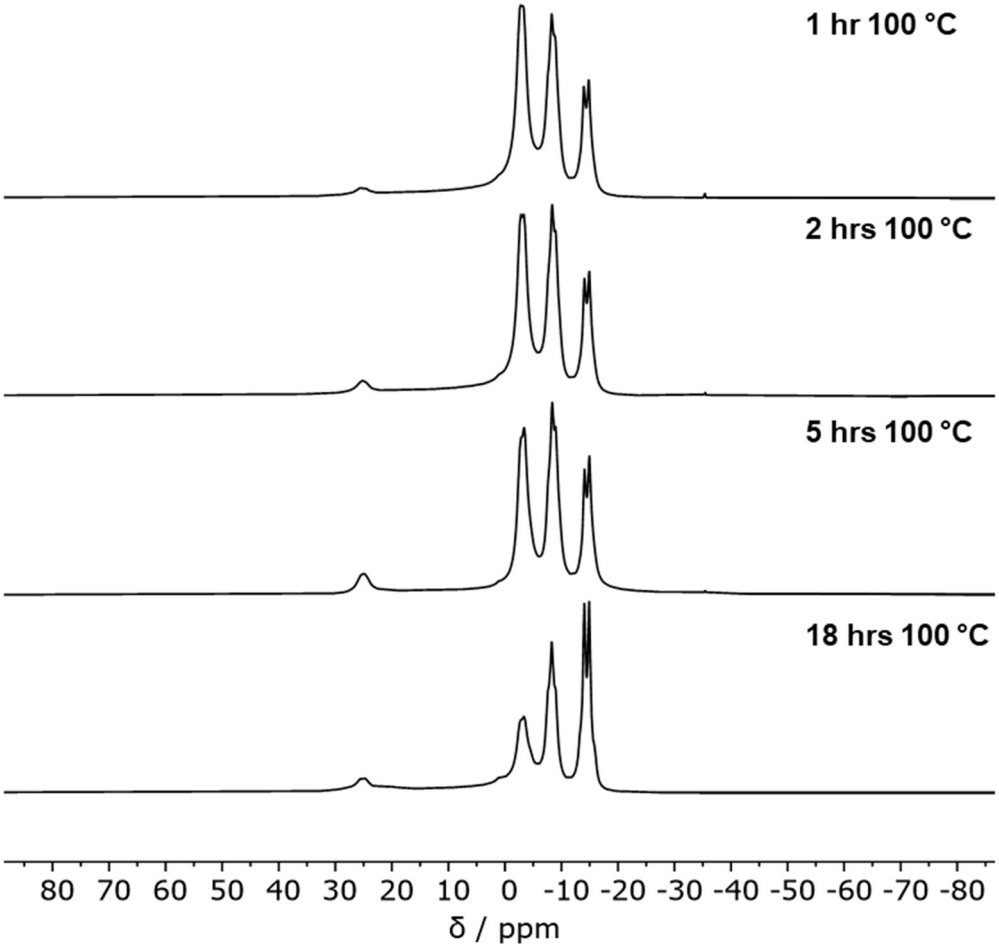

Figure 4.47: Stacked ^{11}B NMR (161 MHz, C_6H_5Cl) spectra of the reaction of *N*-H indole and *mono*-iodo pyrazabole.

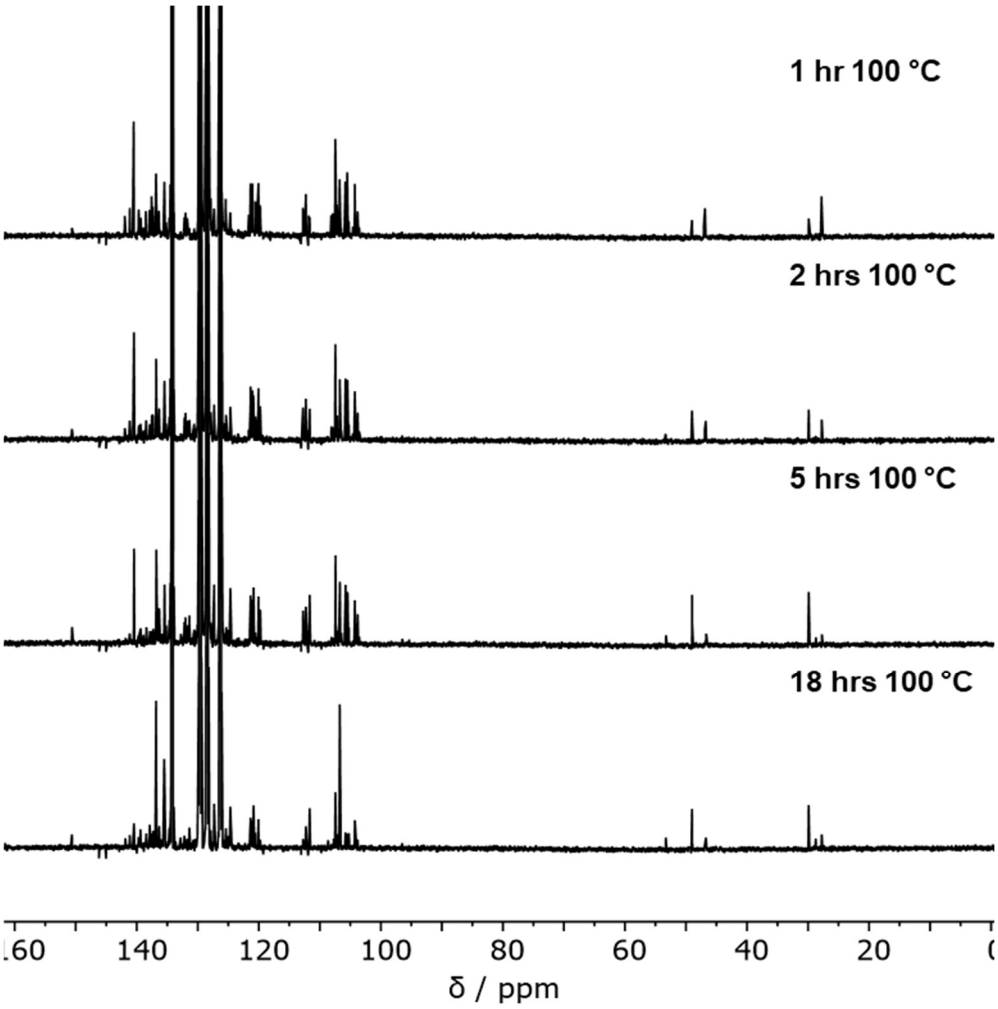

Figure 4.48: Stacked $^{13}C\{^{1}H\}$ NMR (126 MHz, C_6H_5Cl) spectra of the reaction of *N*-H indole and *mono*-iodo pyrazabole.

- **After 18 hours at 100 °C**

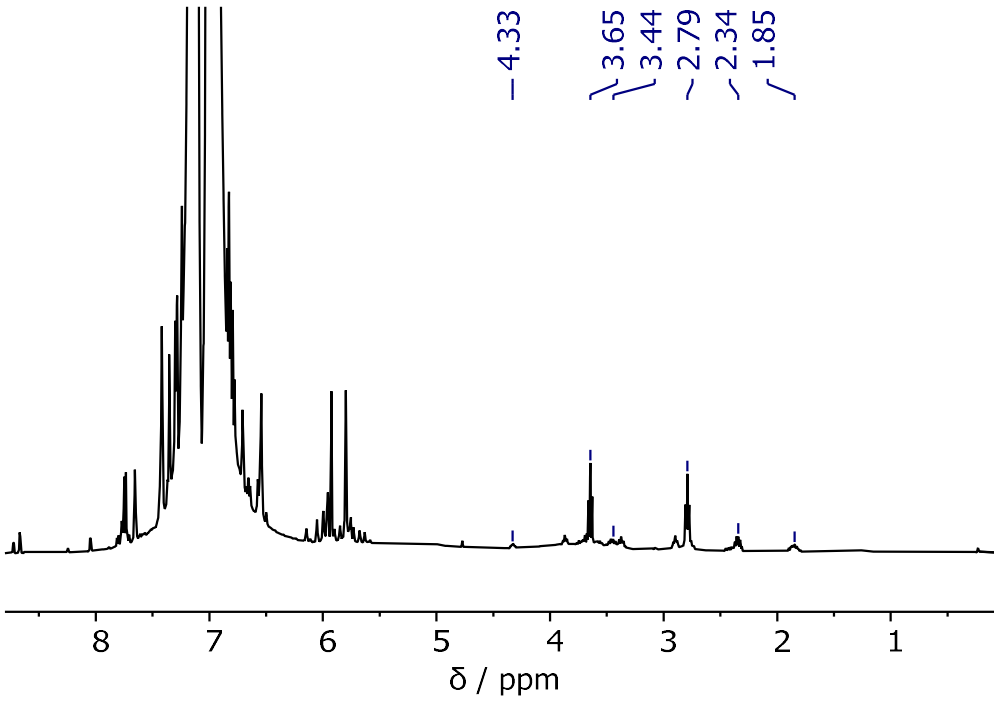

Figure 4.49: Stacked ^{1}H NMR (500 MHz, C_6H_5Cl) spectra of the reaction of *N*-H indole and *mono*-iodo pyrazabole after 18 hours at 100 °C, forming a mixture of **4.4** and **4.7**.

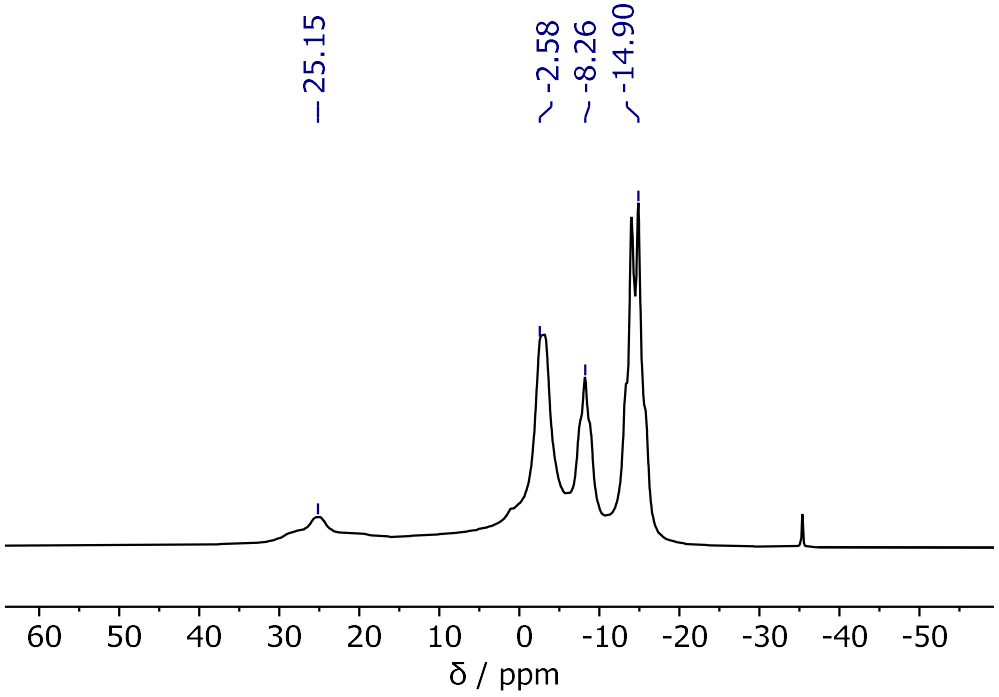

Figure 4.50: Stacked ^{11}B NMR (161 MHz, C_6H_5Cl) spectra of the reaction of *N*-H indole and *mono*-iodo pyrazabole after 18 hours at 100 °C, forming a mixture of **4.4** and **4.7**.

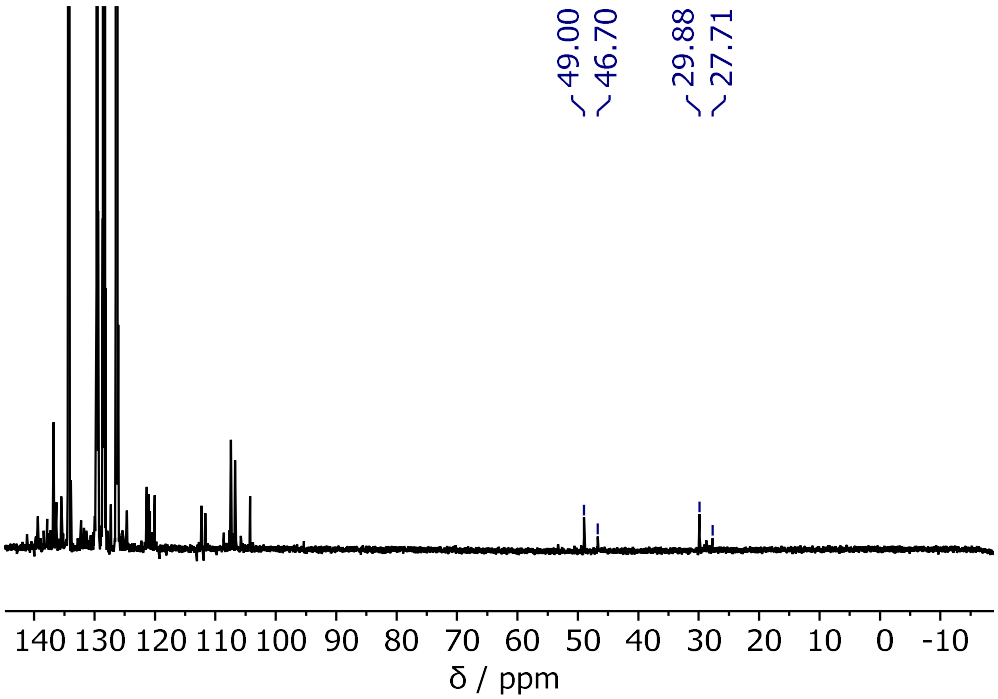

Figure 4.51: Stacked $^{13}C\{^{1}H\}$ NMR (126 MHz, C_6H_5Cl) spectra of the reaction of *N*-H indole and *mono*-iodo pyrazabole after 18 hours at 100 °C, forming a mixture of **4.4** and **4.7**.

Reaction of Indoline, *Di* Iodo Pyrazabole and Et_3N

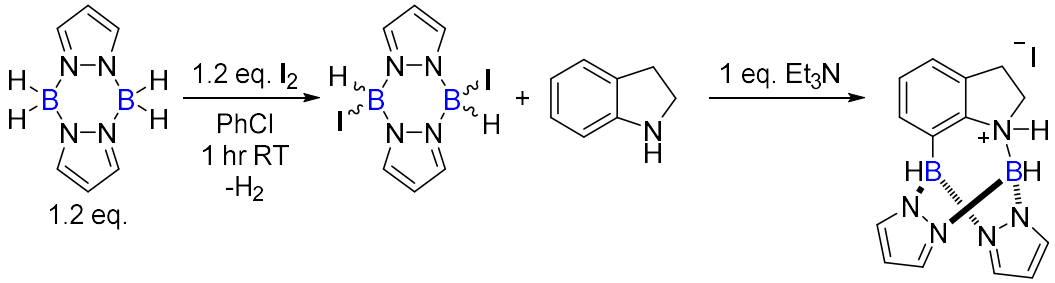

- **Reaction Profile**

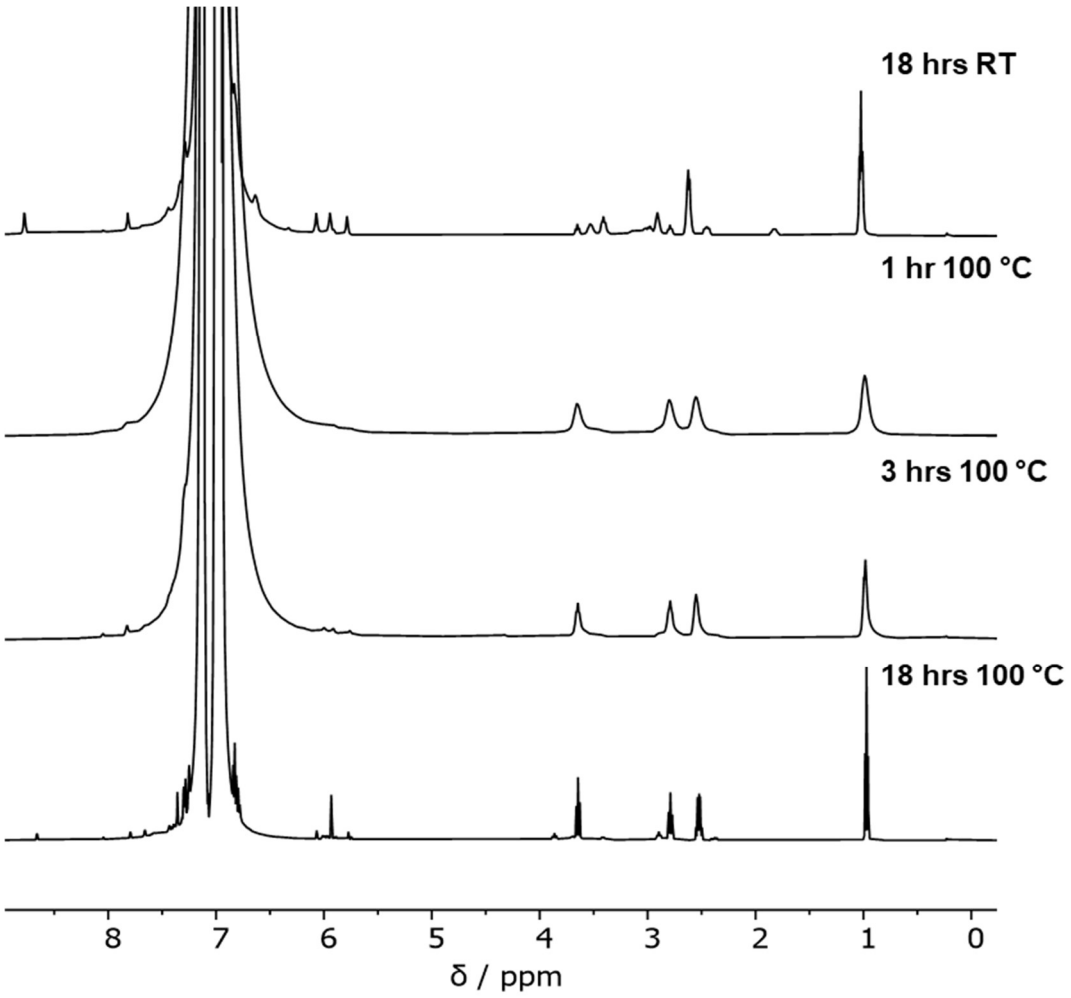

Figure 4.52: Stacked ^1H NMR (500 MHz, C_6H_5Cl) spectra of the reaction of indoline, *di*-iodo pyrazabole and Et_3N.

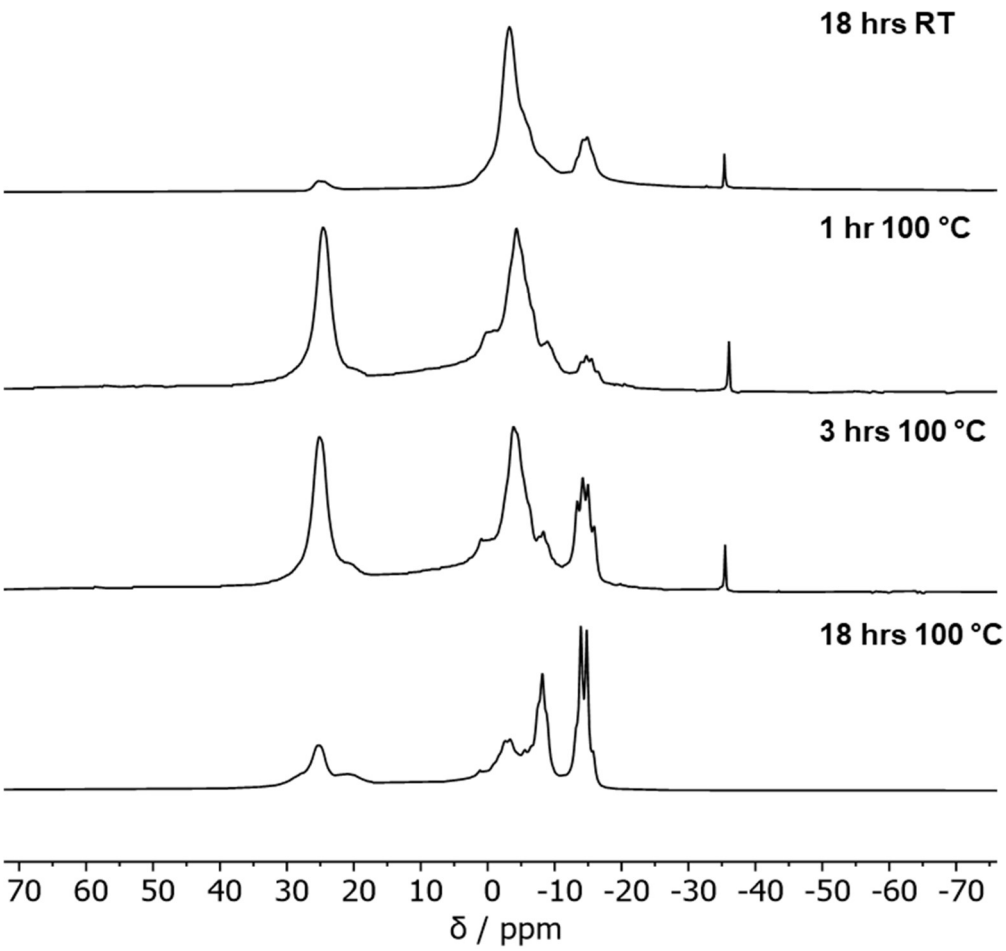

Figure 4.53: Stacked ^{11}B NMR (161 MHz, C_6H_5Cl) spectra of the reaction of indoline, *di*-iodo pyrazabole and Et_3N.

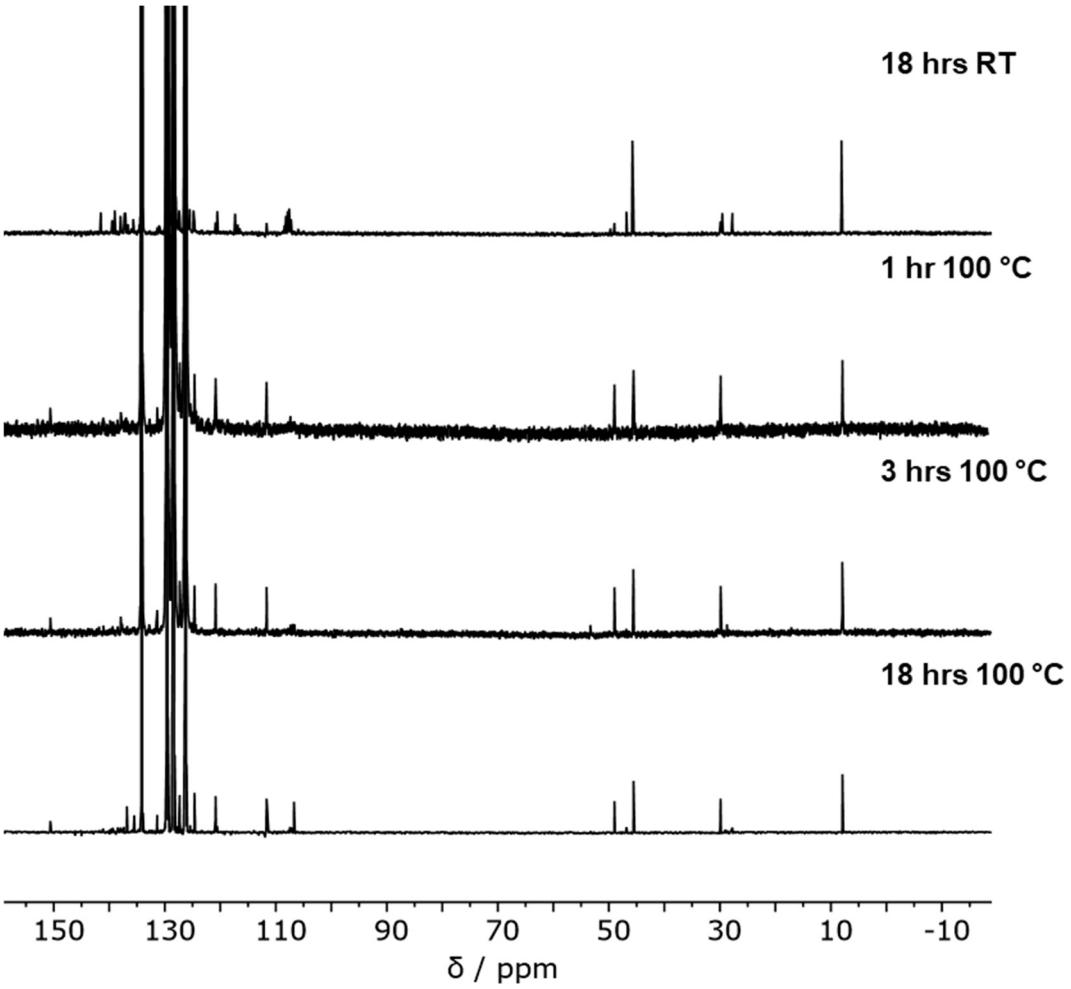

Figure 4.54: Stacked $^{13}C\{^{1}H\}$ NMR (126 MHz, C_6H_5Cl) spectra of the reaction of indoline, *di*-iodo pyrazabole and Et_3N.

- **After 18 hours at 100 °C**

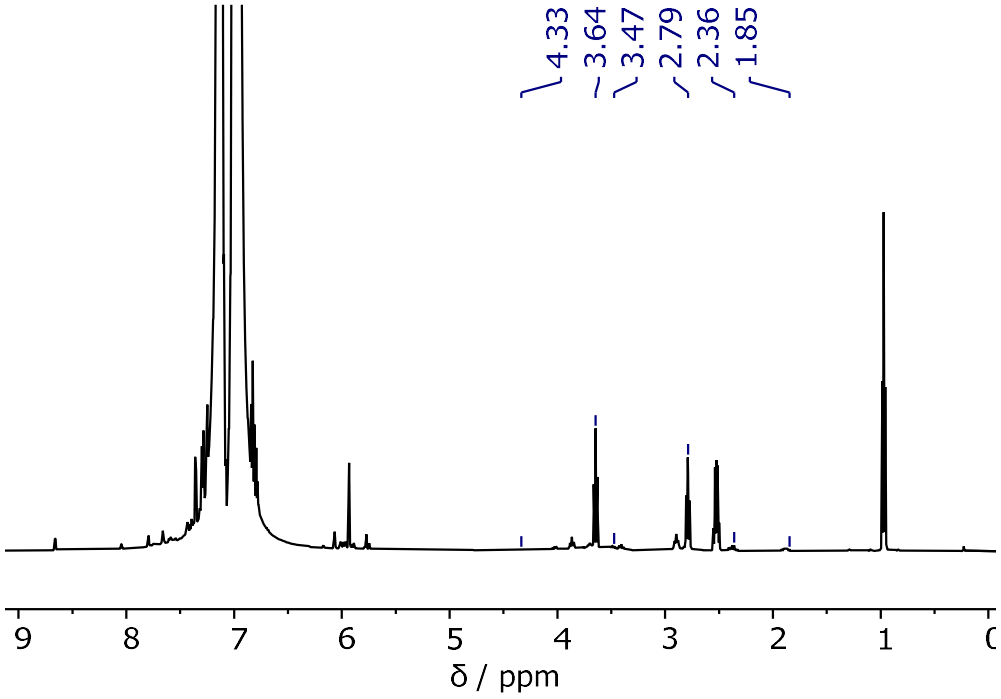

Figure 4.55: Stacked ^{1}H NMR (500 MHz, C_6H_5Cl) spectra of the reaction of indoline, *di*-iodo pyrazabole and Et_3N after 18 hours at 100 °C, forming a mixture of **4.4** and **4.7**.

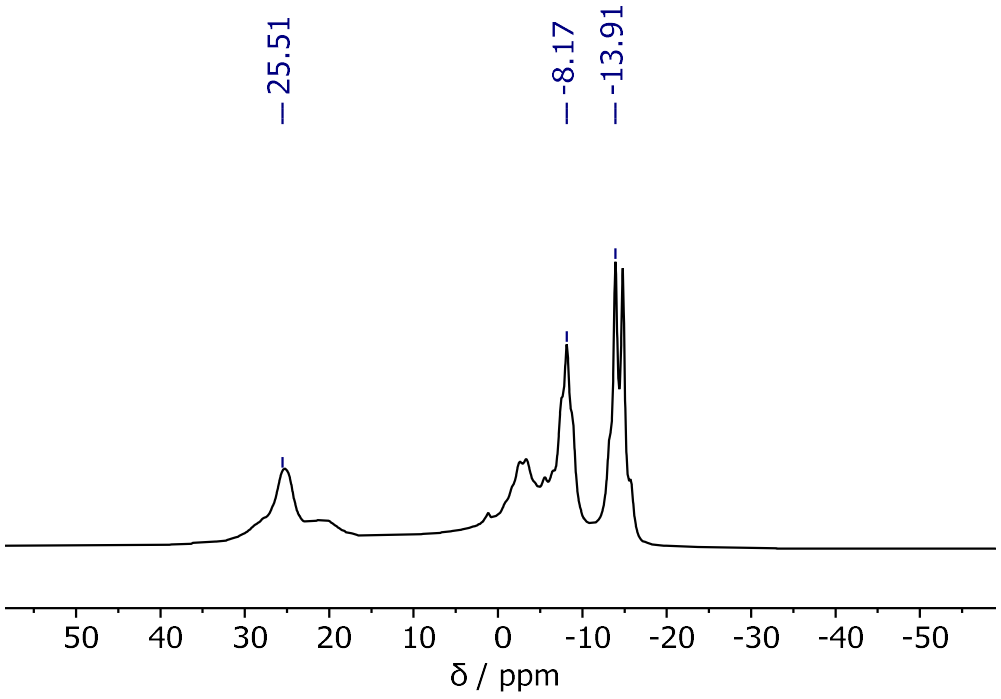

Figure 4.56: Stacked ^{11}B NMR (161 MHz, C_6H_5Cl) spectra of the reaction of indoline, *di*-iodo pyrazabole and Et_3N after 18 hours at 100 °C, forming a mixture of **4.4** and **4.7**.

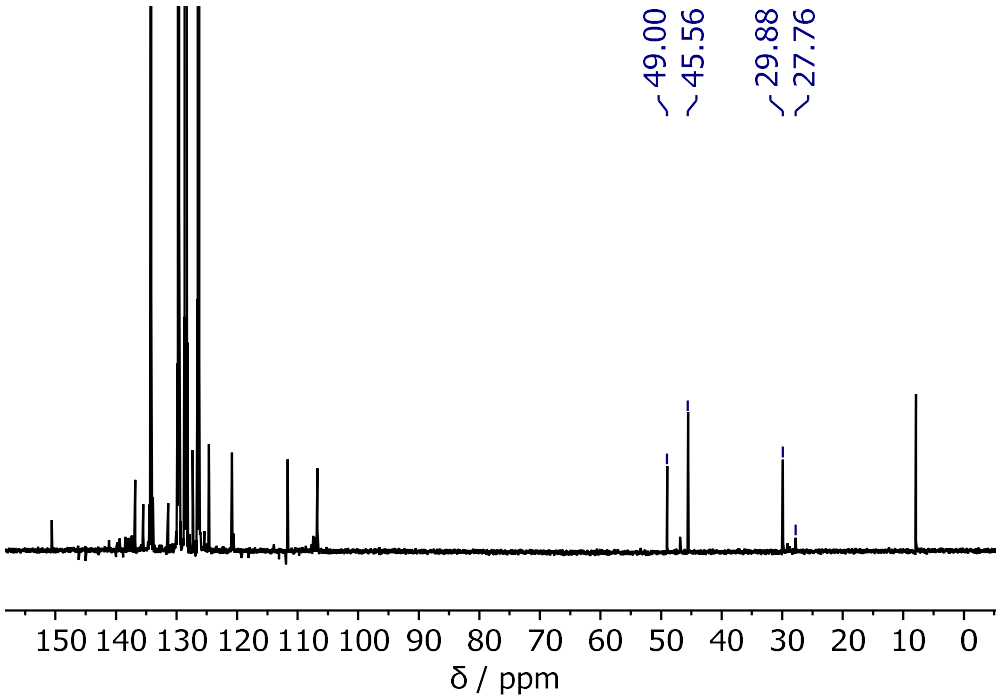

Figure 4.57: Stacked $^{13}C\{^{1}H\}$ NMR (126 MHz, C_6H_5Cl) spectra of the reaction of indoline, *di*-iodo pyrazabole and Et_3N after 18 hours at 100 °C, forming a mixture of **4.4** and **4.7**.

4.5.5 – Characterisation of Decomposition Products

[HB-(Pyrazole)$_3$-BH][I] (4.8)

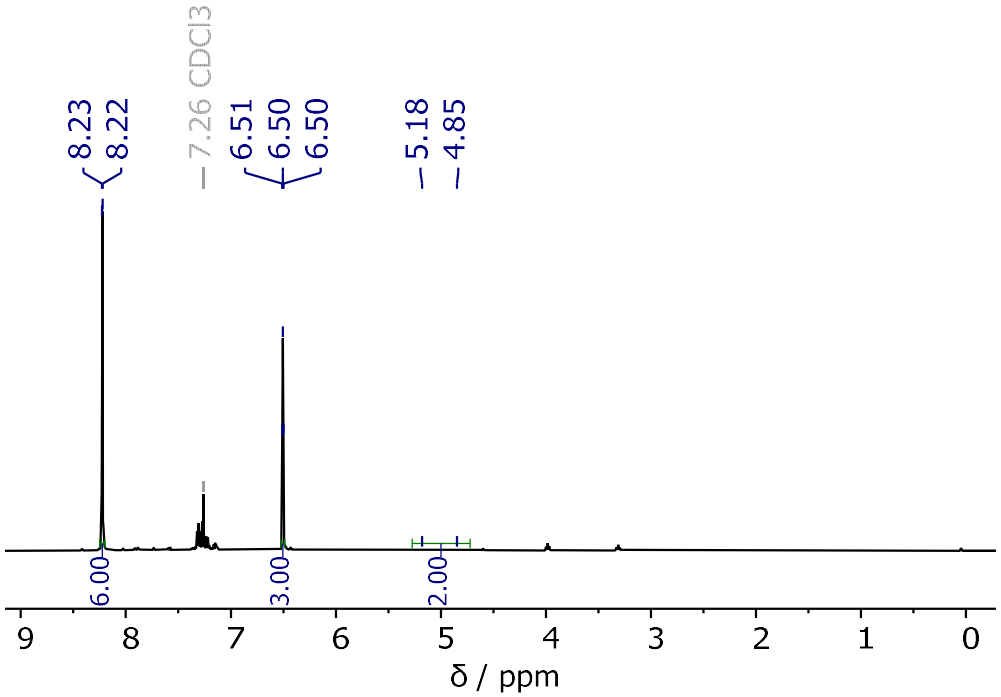

Figure 4.58: ^{1}H NMR (500 MHz, $CDCl_3$) spectrum of [HB-(Pyrazole)$_3$-BH][NTf_2], formed in the reaction of indole and *mono*-iodo pyrazabole. *Note: Some residual PhCl is observed at 7.3 ppm.*

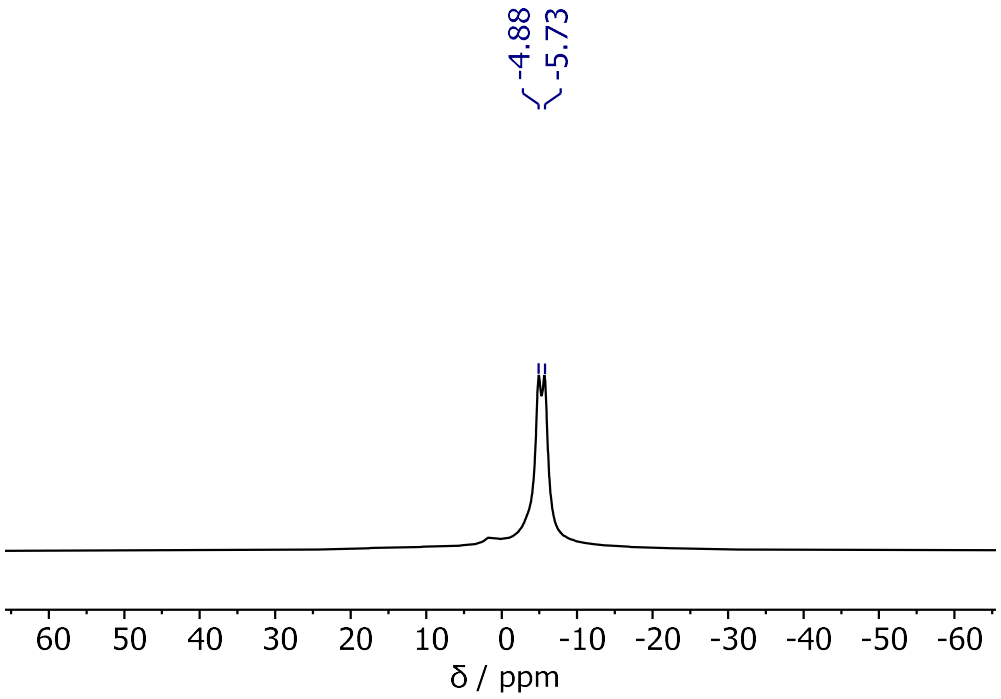

Figure 4.59: ^{11}B NMR (161 MHz, $CDCl_3$) spectrum of [HB-(Pyrazole)$_3$-BH][NTf_2], formed in the reaction of indole and *mono*-iodo pyrazabole.

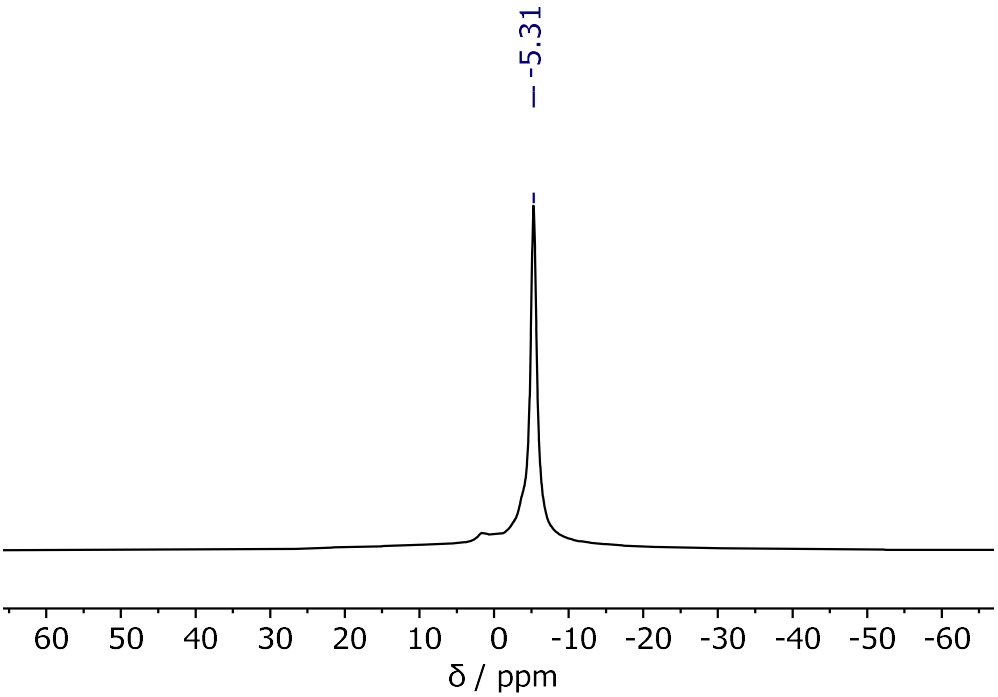

Figure 4.60: $^{11}B\{^{1}H\}$ NMR (161 MHz, $CDCl_3$) spectrum of [HB-(Pyrazole)$_3$-BH][NTf_2], formed in the reaction of indole and *mono*-iodo pyrazabole.

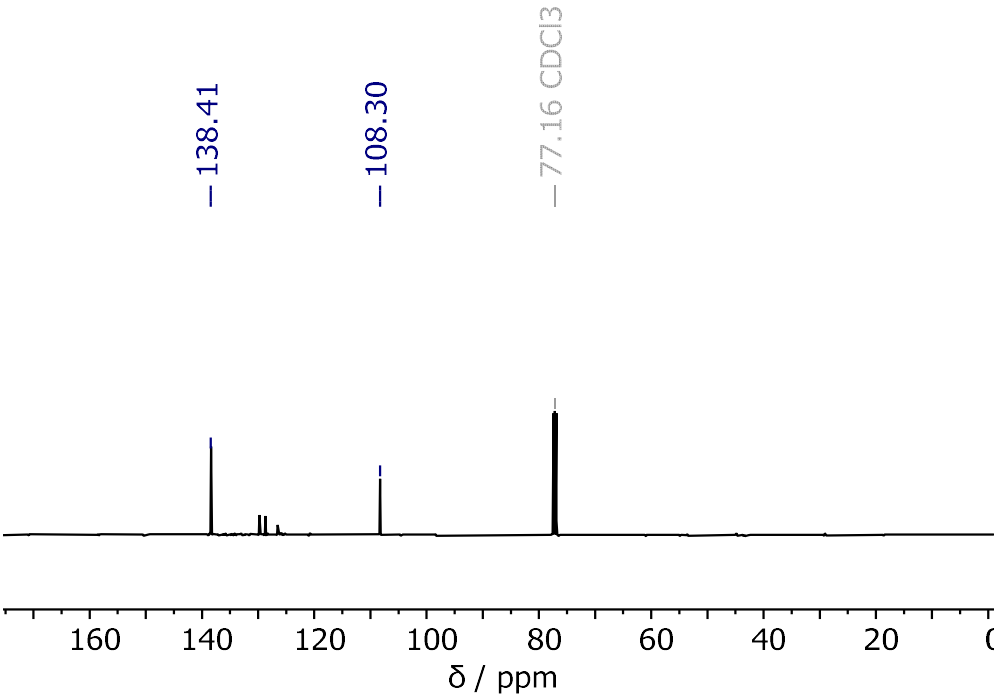

Figure 4.61: $^{13}C\{^{1}H\}$ NMR (126 MHz, $CDCl_3$) spectrum of [HB-(Pyrazole)$_3$-BH][NTf_2], formed in the reaction of indole and *mono*-iodo pyrazabole. *Note: Some residual PhCl is observed at 130 ppm.*

Chapter 5: Targeting C3/C4-Diborylation of Indoles

5.5.1 – Synthesis of Halogen-Substituted Pyrazaboles

Di-Bromo Pyrazabole – 5.2

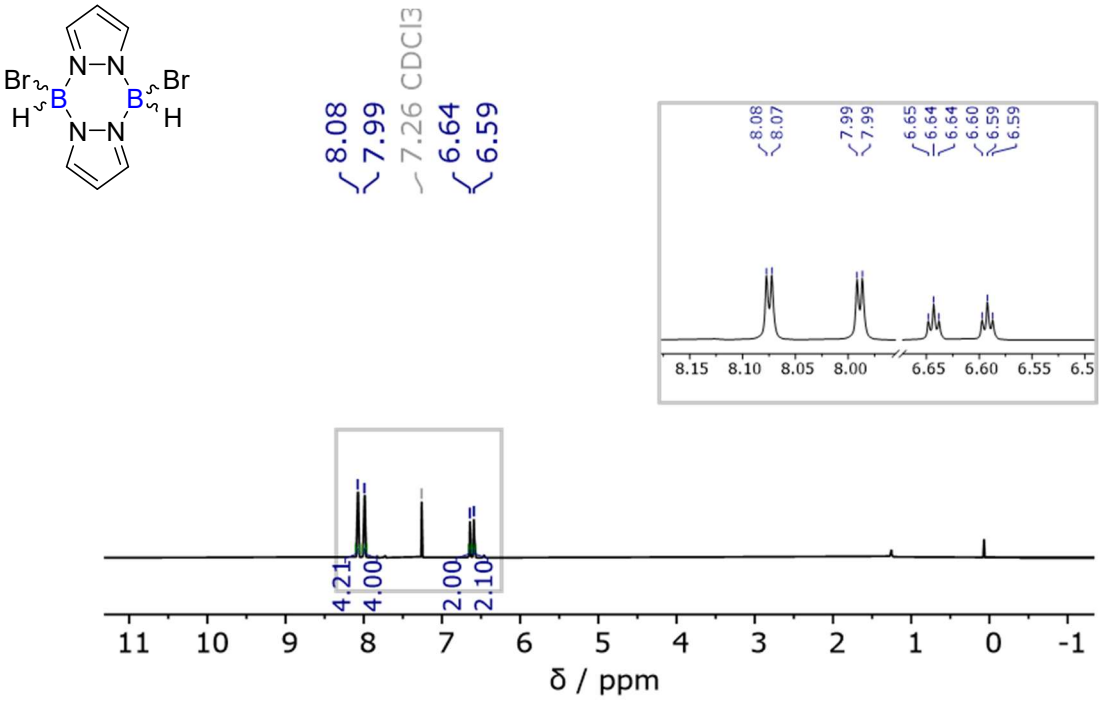

Figure 5.1: ^{1}H NMR (500 MHz, $CDCl_3$) spectrum of *di*-bromo pyrazabole.

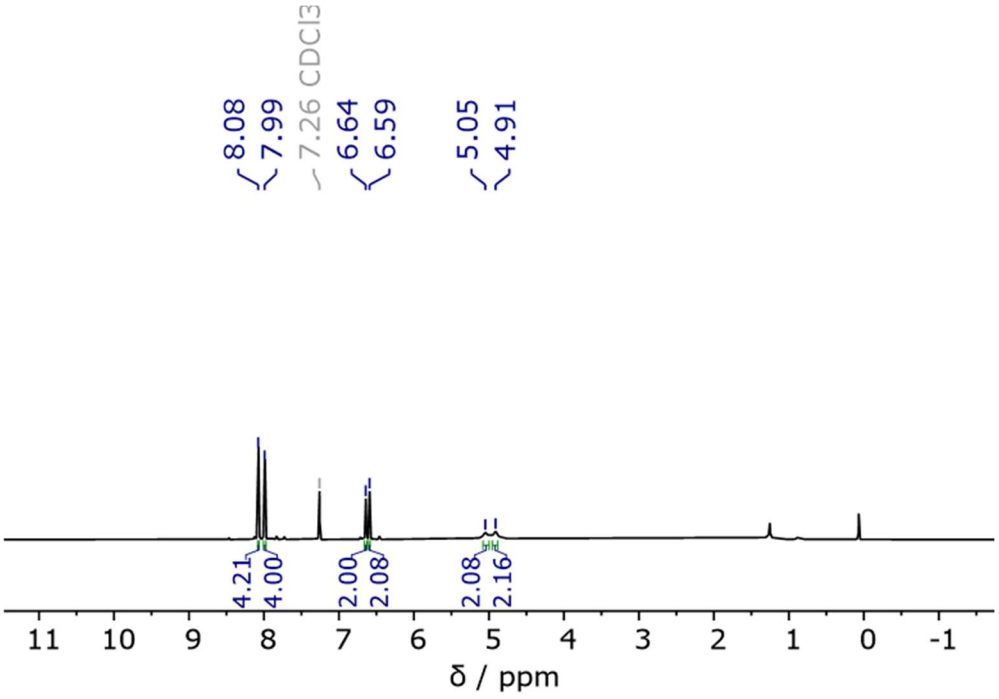

Figure 5.2: $^{1}H\{^{11}B\}$ NMR (500 MHz, $CDCl_3$) spectrum of *di*-bromo pyrazabole.

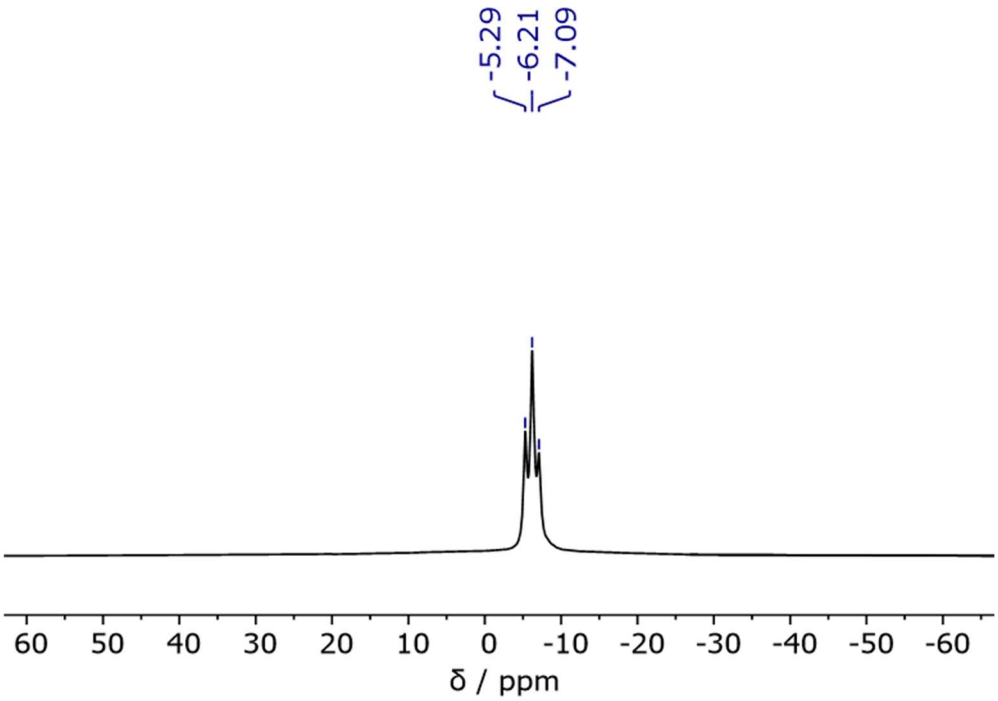

Figure 5.3: ^{11}B NMR (161 MHz, $CDCl_3$) spectrum of *di*-bromo pyrazabole.

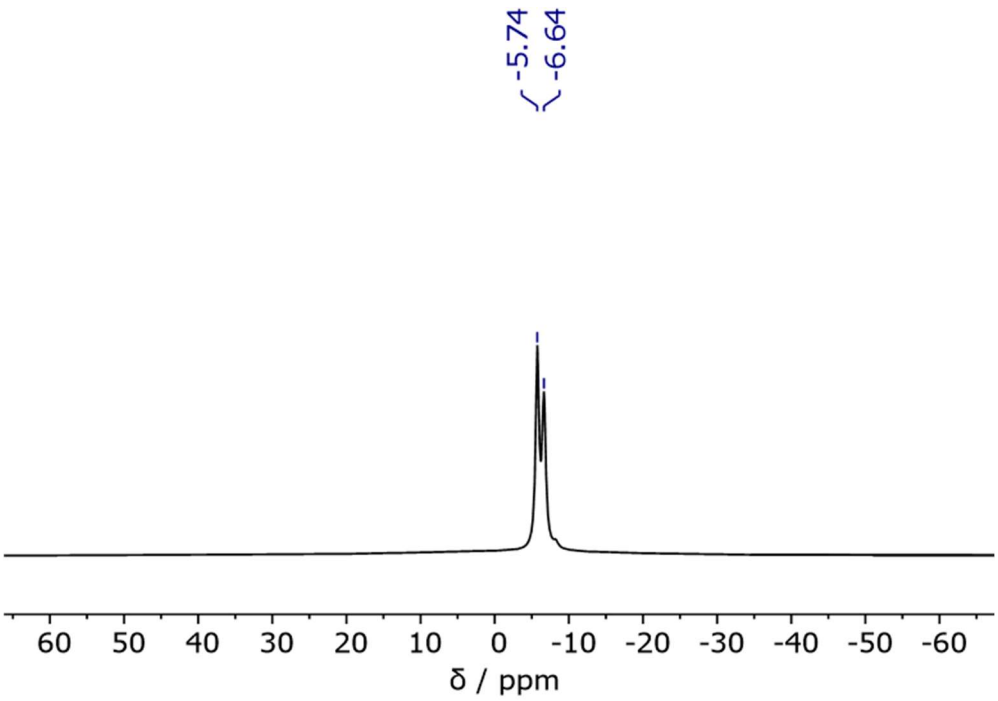

Figure 5.4: $^{11}B\{^1H\}$ NMR (161 MHz, $CDCl_3$) spectrum of *di*-bromo pyrazabole.

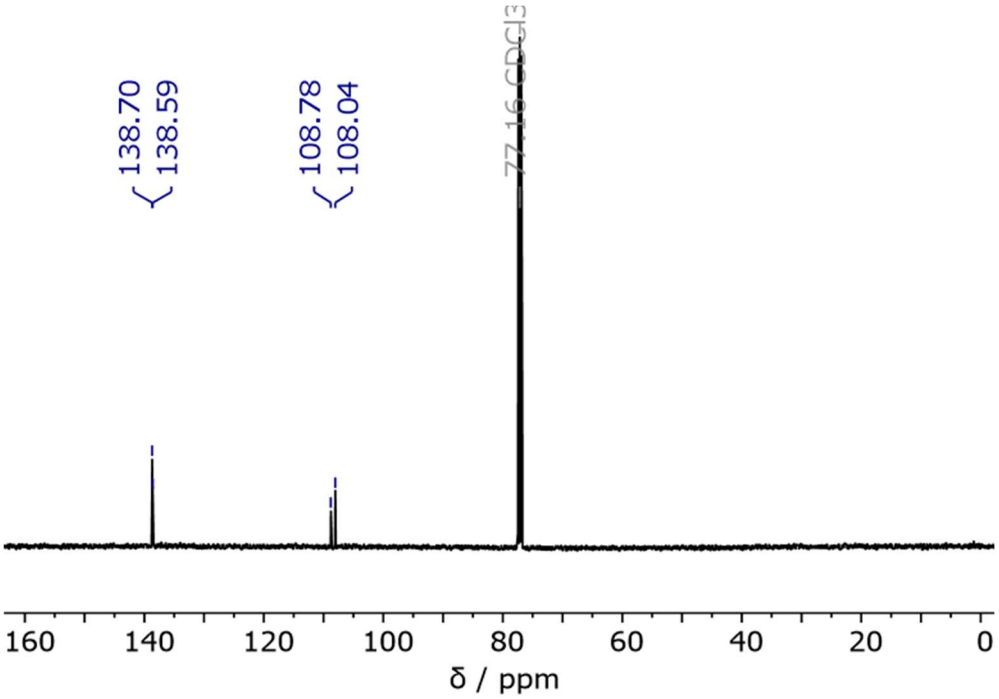

Figure 5.5: $^{13}C\{^{1}H\}$ NMR (126 MHz, $CDCl_3$) spectrum of *di*-bromo pyrazabole.

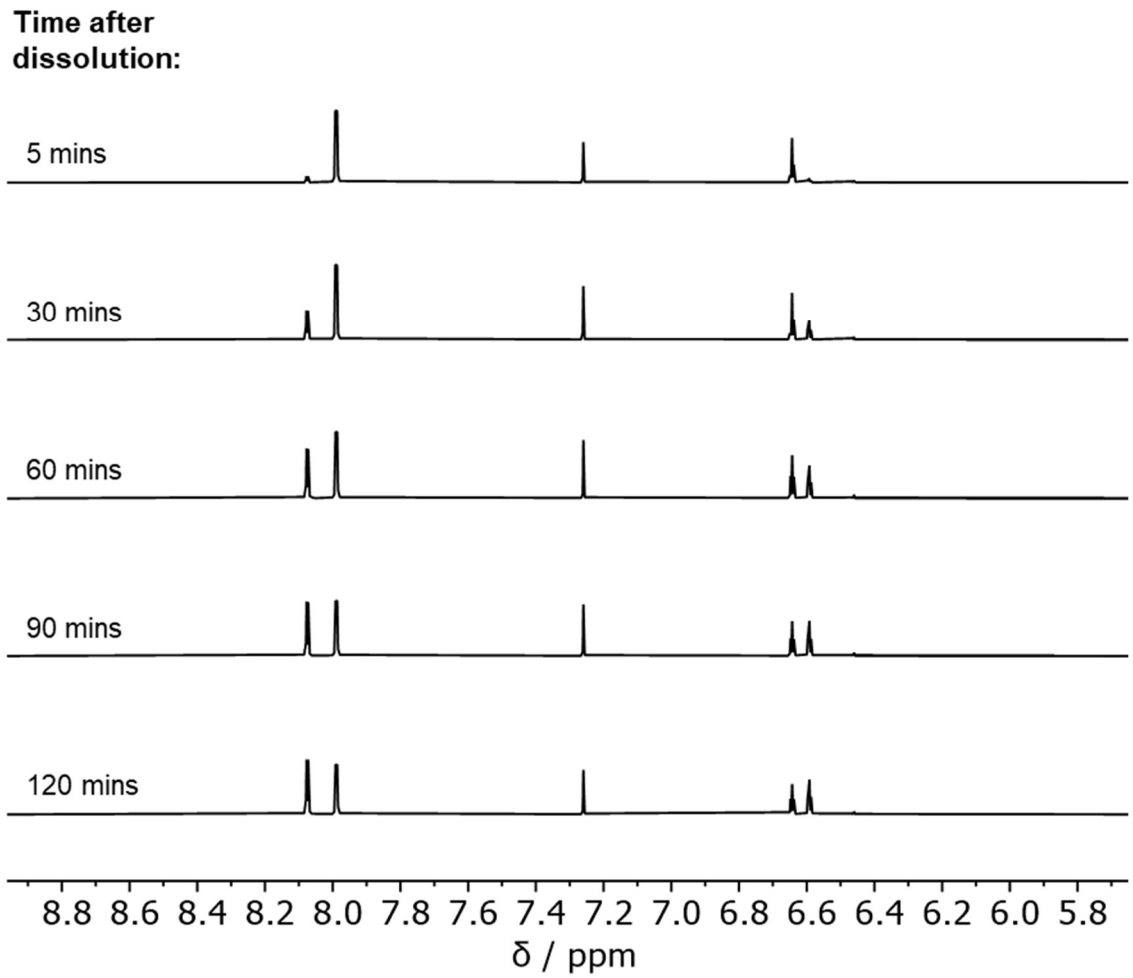

Figure 5.6: Stacked ^{1}H NMR (500 MHz, $CDCl_3$) spectra for the isomerisation of *di*-bromo pyrazabole following dissolution in $CDCl_3$ at room temperature.

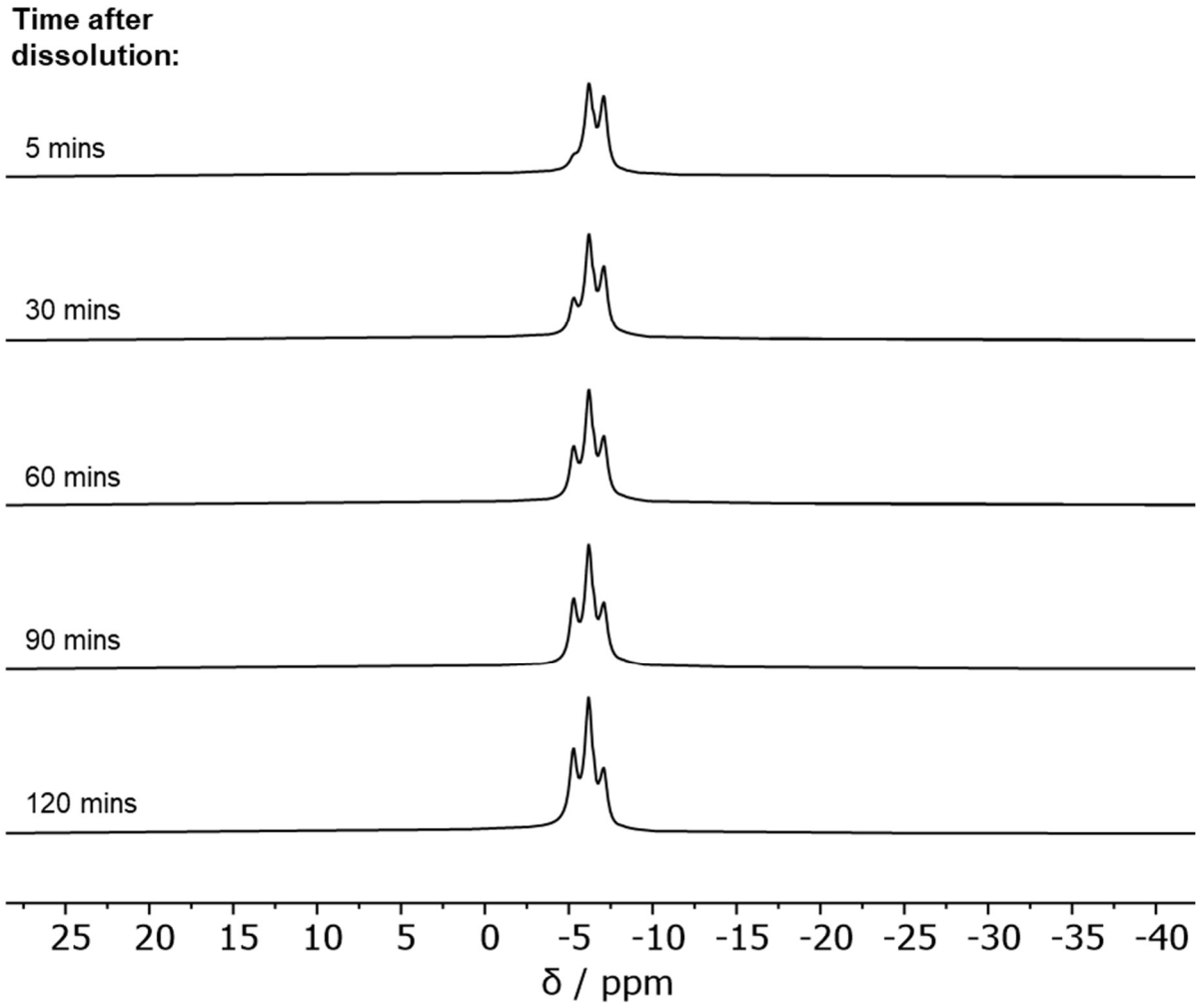

Figure 5.7: Stacked ^{11}B NMR (161 MHz, $CDCl_3$) spectra for the isomerisation of *di*-bromo pyrazabole following dissolution in $CDCl_3$ at room temperature.

Di-Chloro Pyrazabole – 5.3

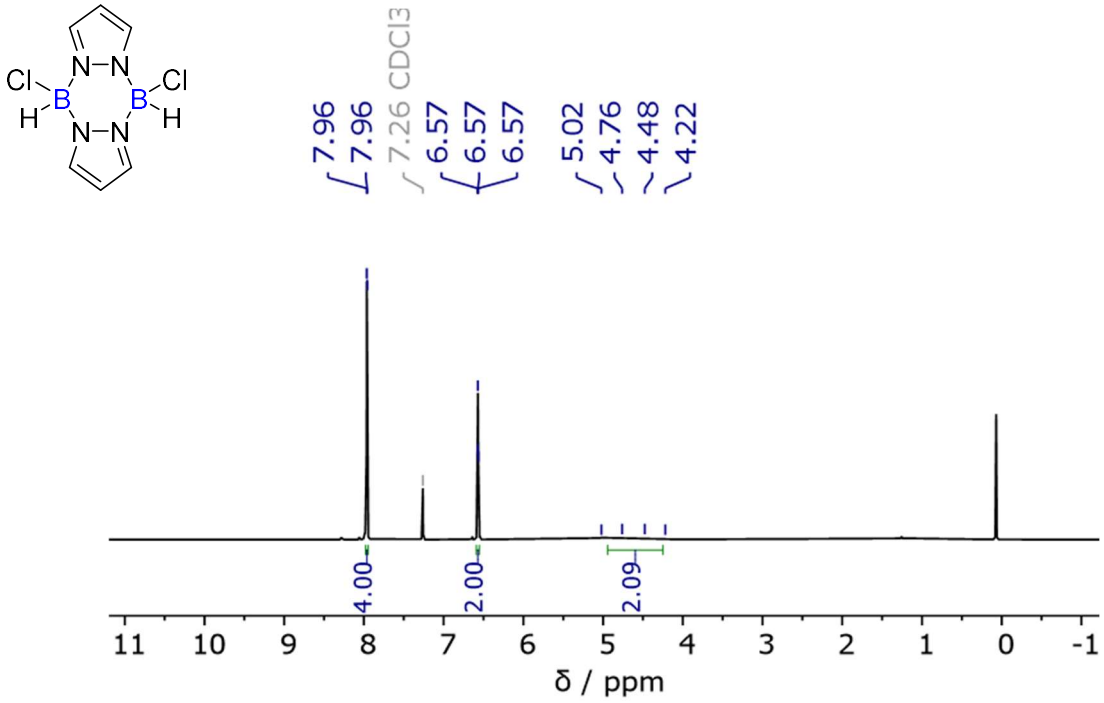

Figure 5.8: ^{1}H NMR (500 MHz, $CDCl_3$) spectrum of *di*-chloro pyrazabole.

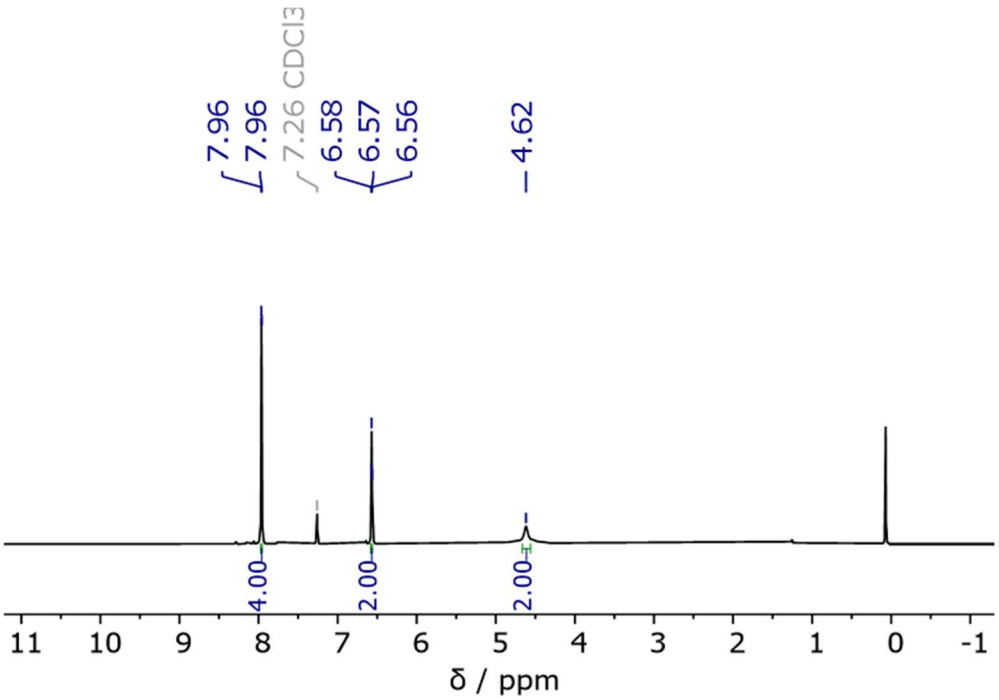

Figure 5.9: $^{1}H\{^{11}B\}$ NMR (500 MHz, $CDCl_3$) spectrum of *di*-chloro pyrazabole.

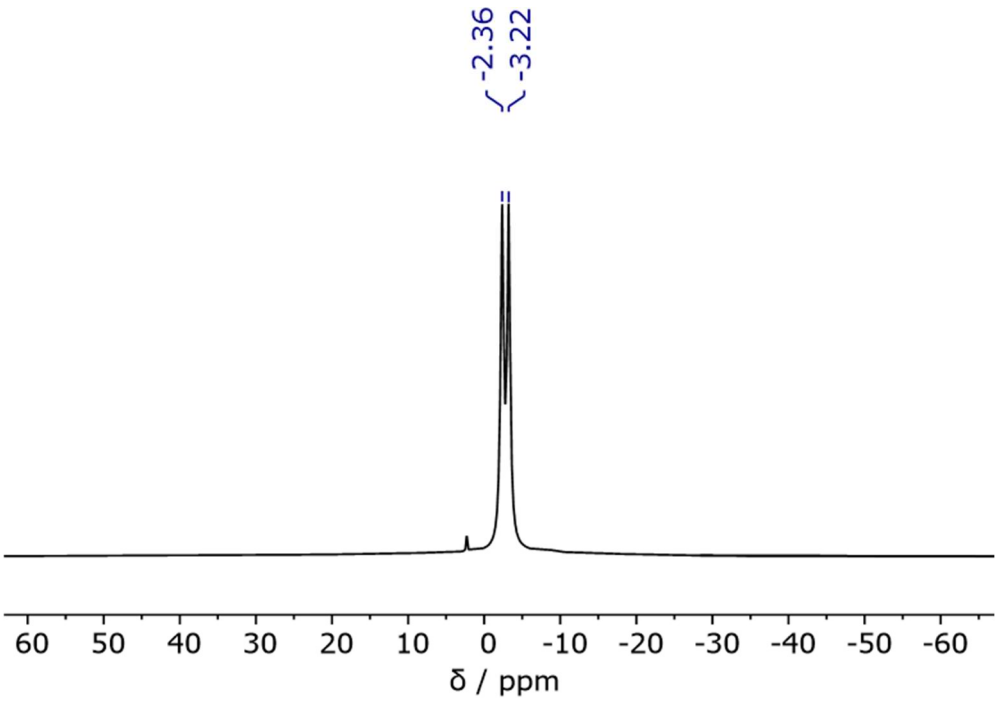

Figure 5.10: ^{11}B NMR (161 MHz, $CDCl_3$) spectrum of *di*-chloro pyrazabole.

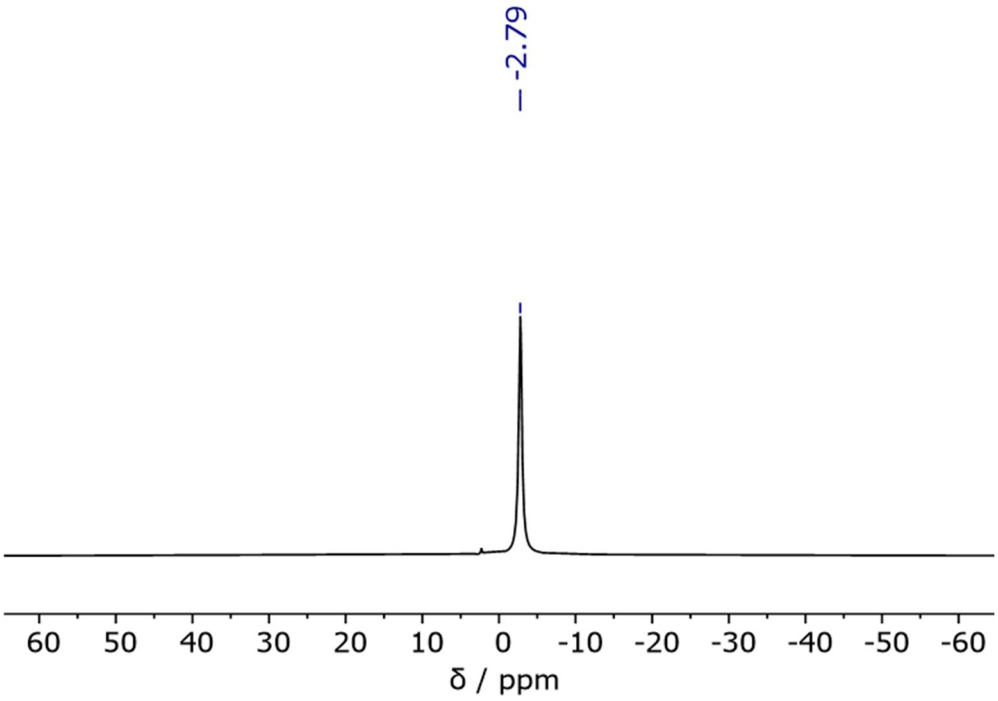

Figure 5.11: $^{11}B\{^1H\}$ NMR (161 MHz, $CDCl_3$) spectrum of *di*-chloro pyrazabole.

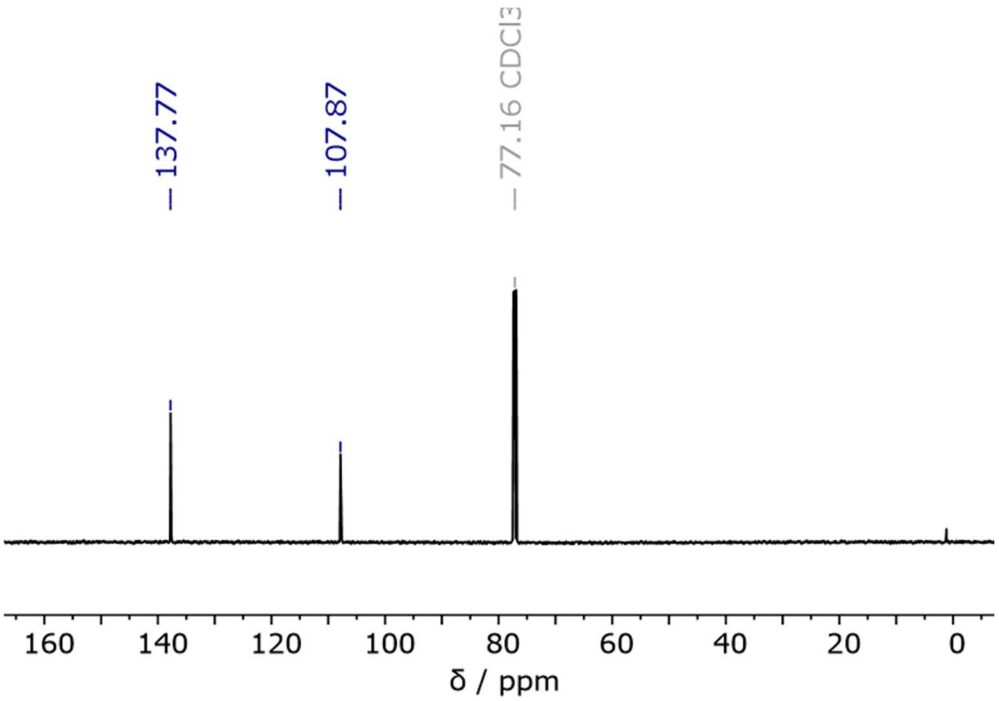

Figure 5.12: $^{13}C\{^{1}H\}$ NMR (126 MHz, $CDCl_3$) spectrum of *di*-chloro pyrazabole.

Tetra-Bromo Pyrazabole – 5.6

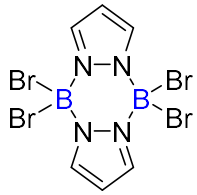

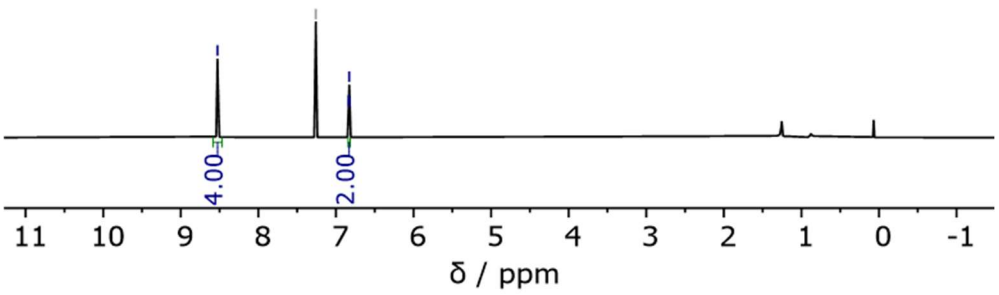

Figure 5.13: ^{1}H NMR (500 MHz, $CDCl_3$) spectrum of *tetra*-bromo pyrazabole.

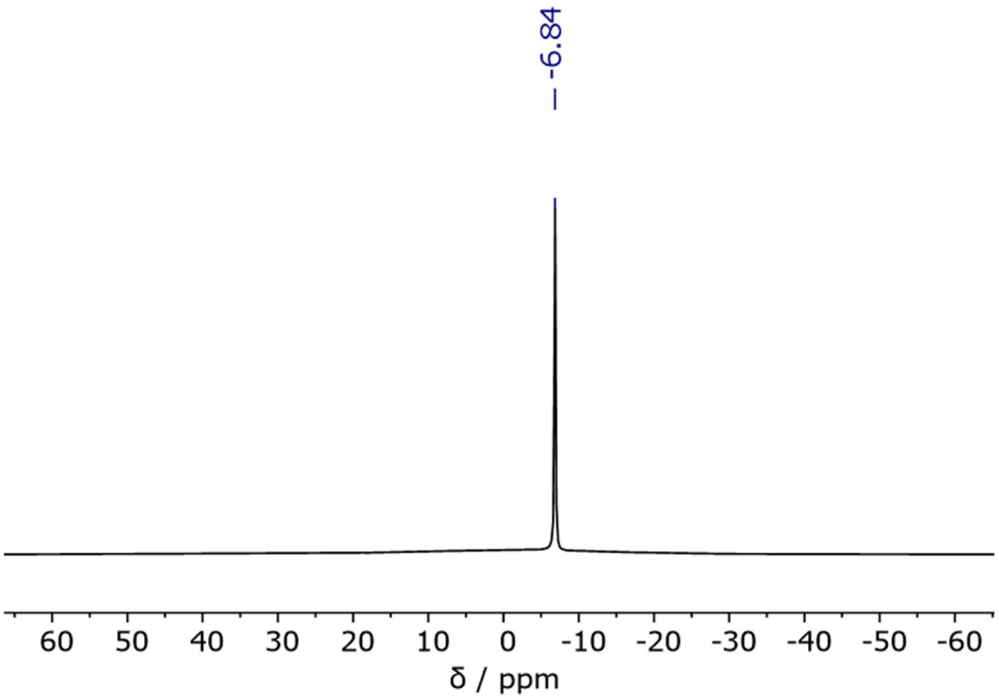

Figure 5.14: ^{11}B NMR (161 MHz, $CDCl_3$) spectrum of *tetra*-bromo pyrazabole.

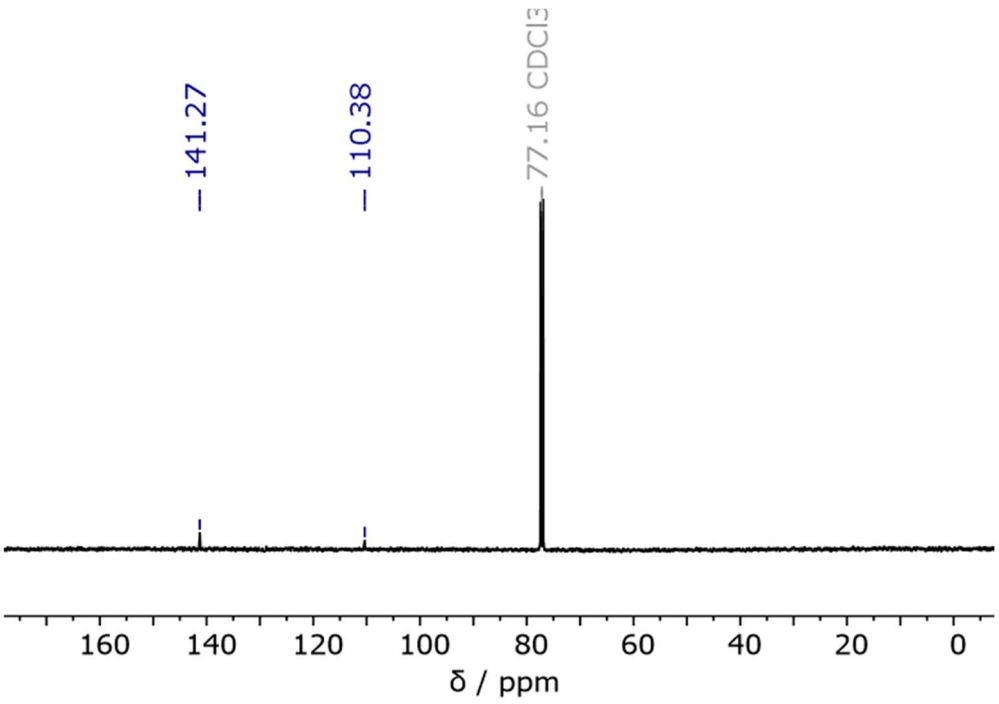

Figure 5.15: $^{13}C\{^1H\}$ NMR (126 MHz, $CDCl_3$) spectrum of *tetra*-bromo pyrazabole.

Tetra-Chloro Pyrazabole – 5.8

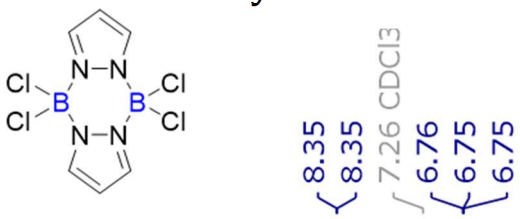

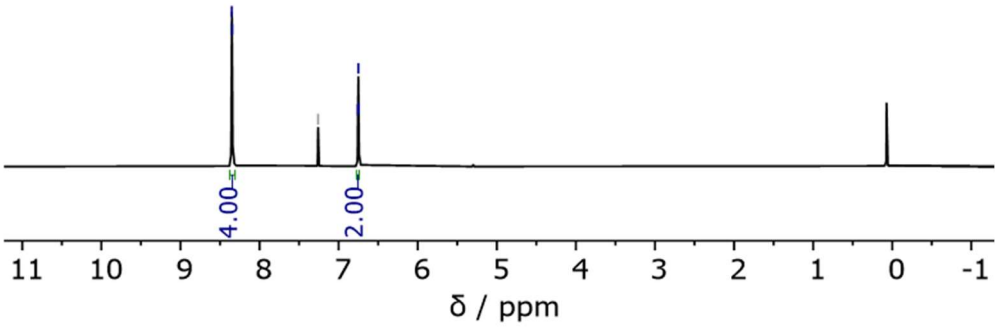

Figure 5.16: ^{1}H NMR (500 MHz, $CDCl_3$) spectrum of *tetra*-chloro pyrazabole.

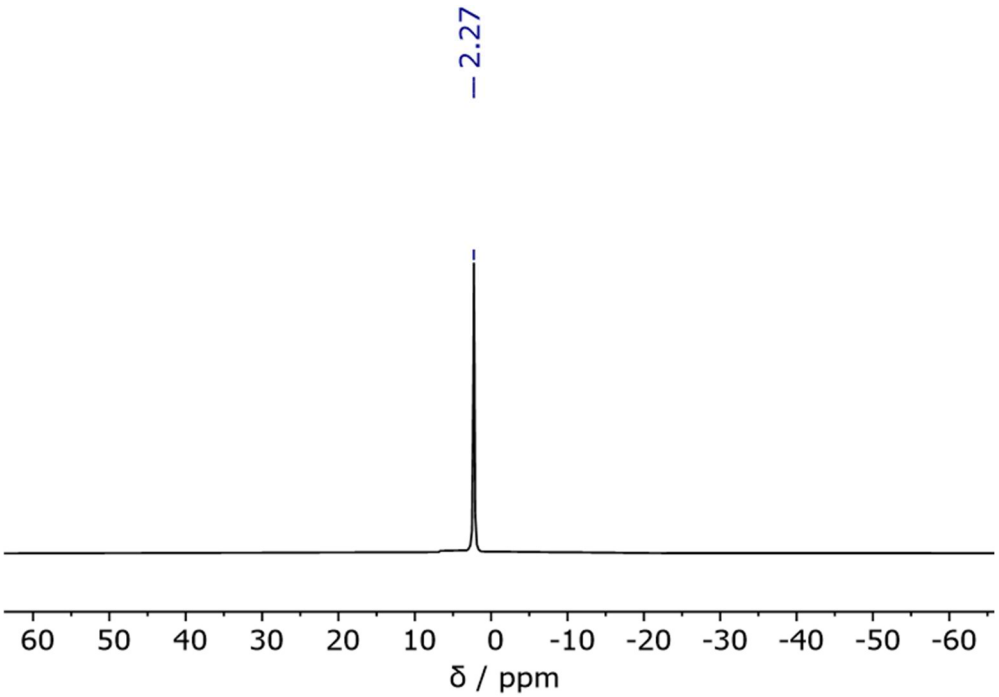

Figure 5.17: ^{11}B NMR (161 MHz, $CDCl_3$) spectrum of *tetra*-chloro pyrazabole.

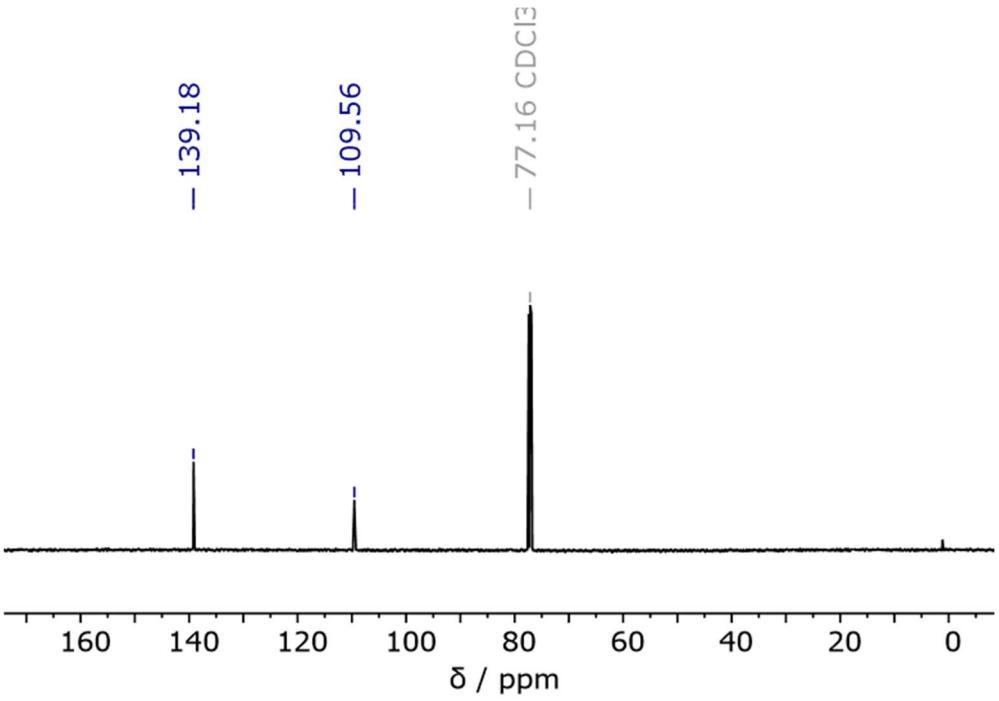

Figure 5.18: $^{13}C\{^{1}H\}$ NMR (126 MHz, $CDCl_3$) spectrum of *tetra*-chloro pyrazabole.

5.5.2 – Control Reactions with *N*-Methyl Indole

Di-NTf_2 Pyrazabole (5.5) + DBP + *N*-Methyl Indole

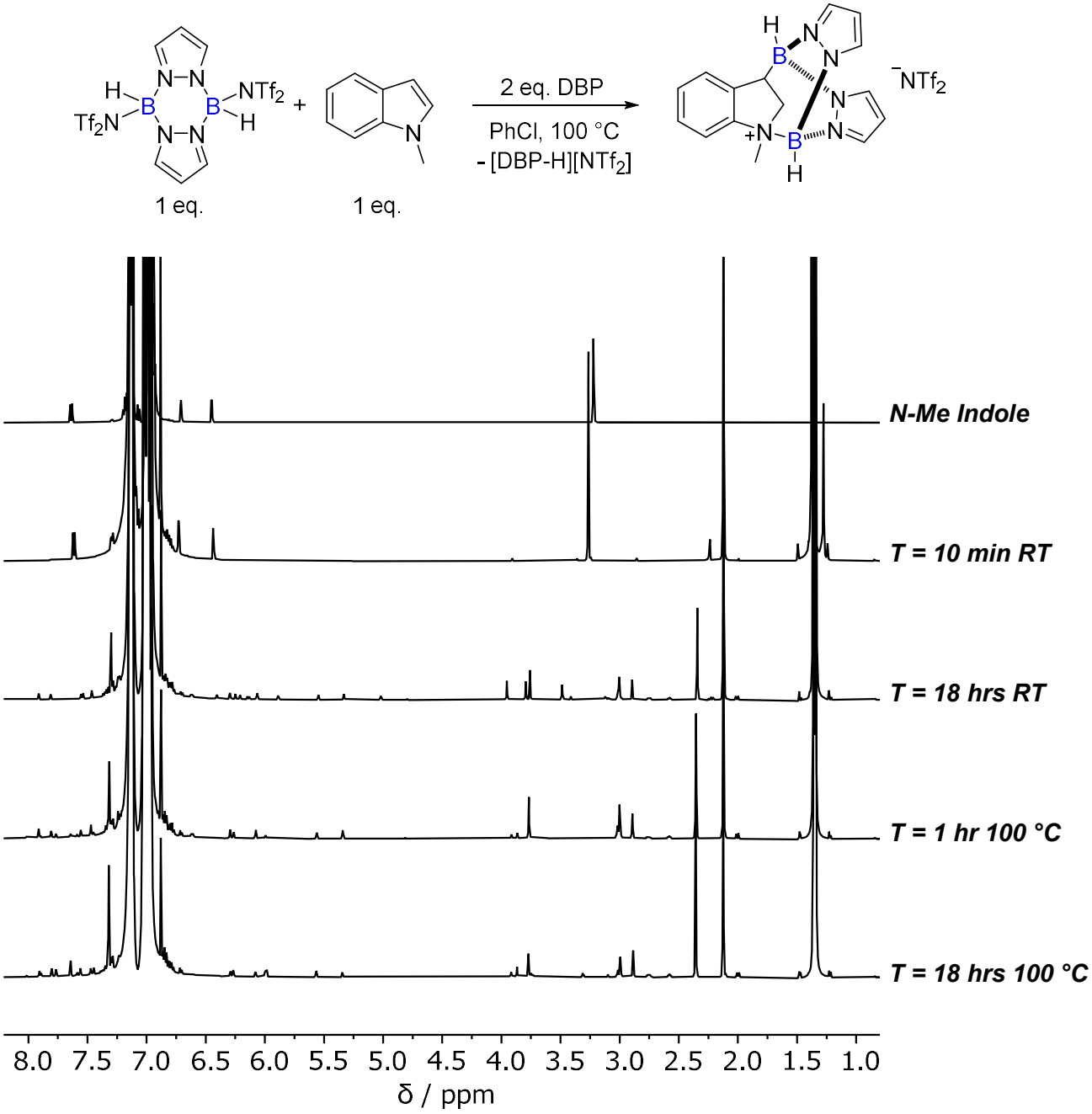

Figure 5.19: Stacked ^{1}H NMR (500 MHz, C_6H_5Cl) spectra for the reaction of *di*-NTf_2 pyrazabole, *N*-methyl indole and DBP, showing consumption of *N*-methyl indole and the formation of a complex mixture of indole and indoline species. *Note: di-NTf_2 pyrazabole is almost completely insoluble at RT, so is not observed.*

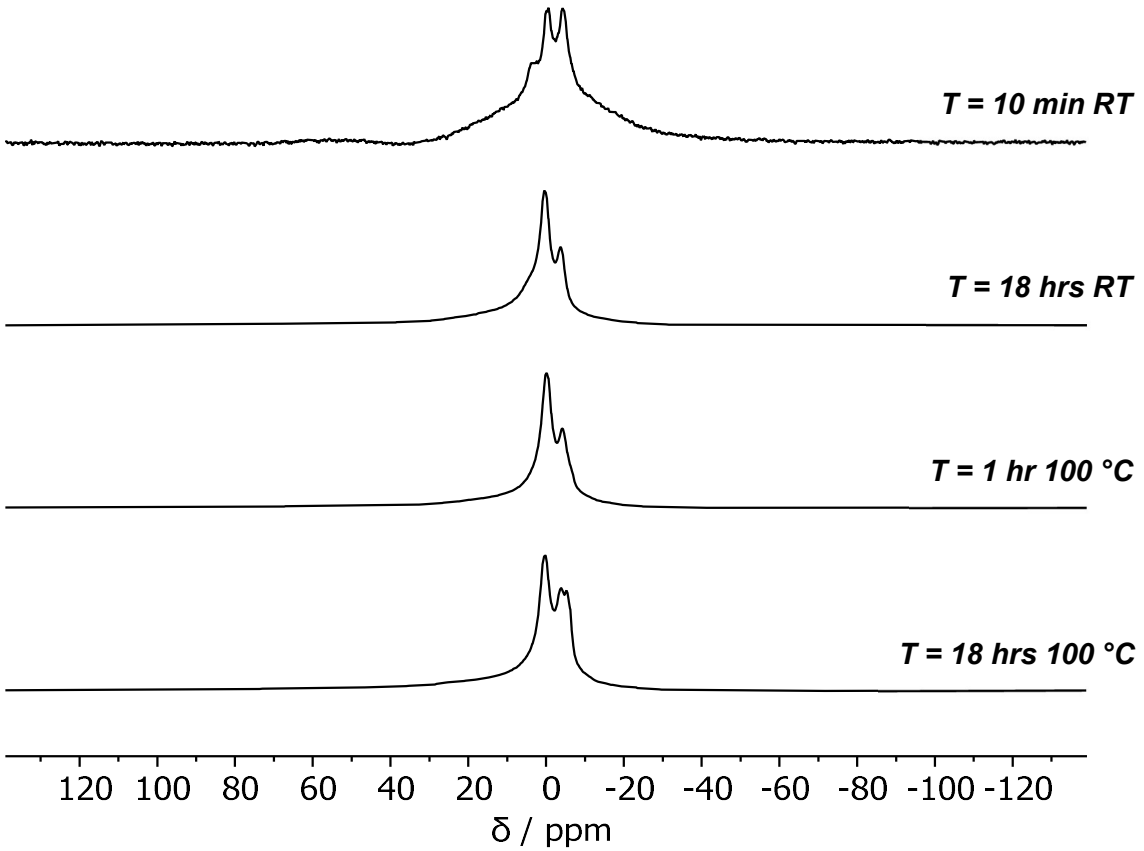

Figure 5.20: Stacked ^{11}B NMR (161 MHz, C_6H_5Cl) spectra for the reaction of *di*-NTf_2 pyrazabole, *N*-methyl indole and DBP, showing consumption of *N*-methyl indole and the formation of a complex mixture of indole and indoline species. *Note: di-NTf_2 pyrazabole is almost completely insoluble at RT, so is not observed.*

5.5.3 – Reactivity of *Di*-Bromo Pyrazabole with $HNTf_2$

'Activation' of *Di*-Bromo Pyrazabole (5.2)

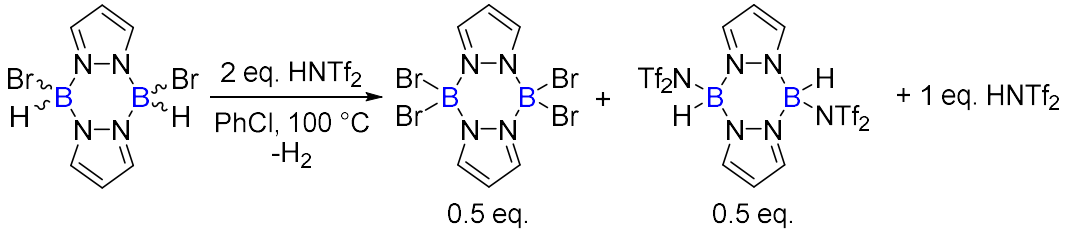

- **NMR spectra of crude reaction after 18 hours at 100 °C:**

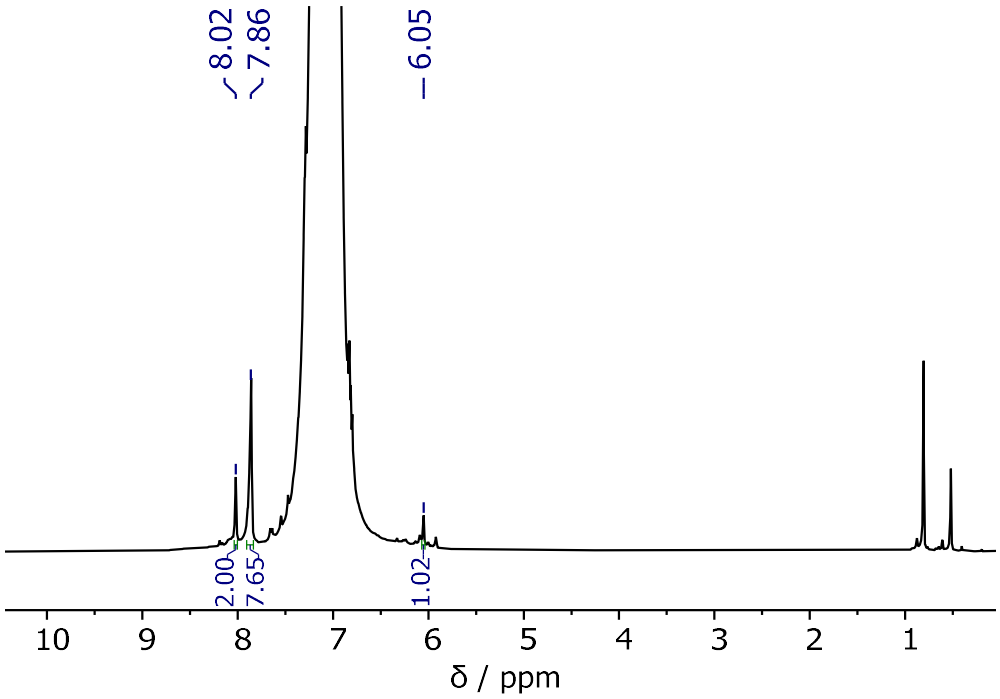

Figure 5.21: ^1H NMR (500 MHz, C_6H_5Cl) spectrum of the reaction of *di*-bromo pyrazabole and $HNTf_2$ after 18 hours at 100 °C. The resonances at 8.02 and 6.05 ppm correspond to *tetra*-bromo pyrazabole, whilst the resonance at 7.86 ppm is due to leftover $HNTf_2$. The solubility of *tetra*-bromo pyrazabole is very poor, meaning the resonances are very weak and the resonances from trace silicone grease (ca. 0.5 ppm) are exaggerated.

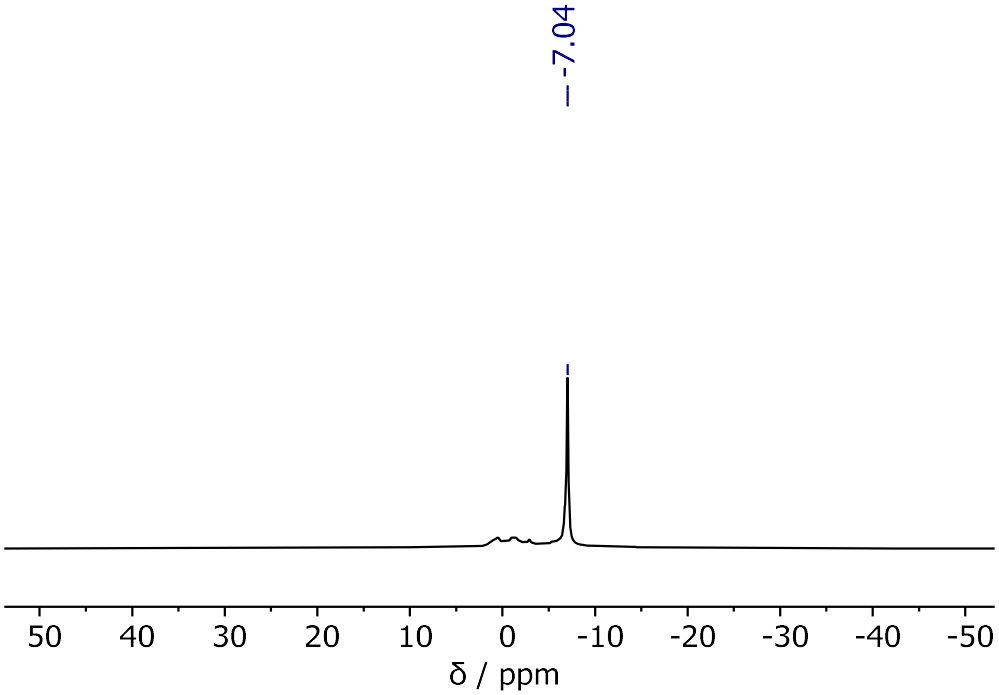

Figure 5.22: ^{11}B NMR (161 MHz, C_6H_5Cl) spectrum of the reaction of *di*-bromo pyrazabole and $HNTf_2$ after 18 hours at 100 °C. The resonance at -7.04 ppm corresponds to *tetra*-bromo pyrazabole.

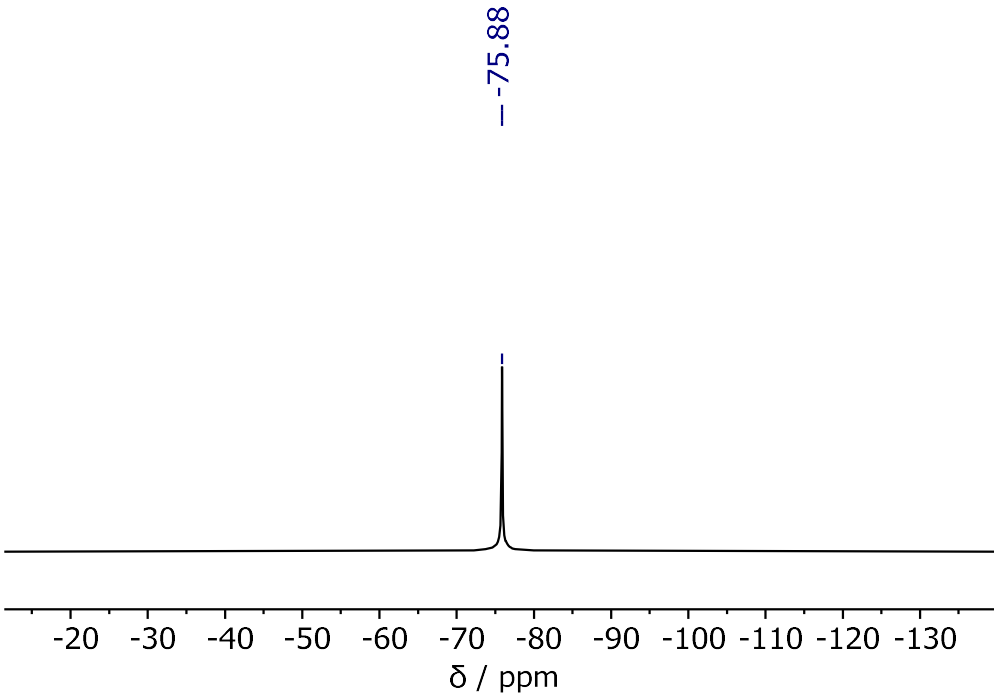

Figure 5.23: ^{19}F NMR (471 MHz, C_6H_5Cl) spectrum of the reaction of *di*-bromo pyrazabole and $HNTf_2$ after 18 hours at 100 °C. The resonance at -75.88 ppm corresponds to leftover $HNTf_2$.

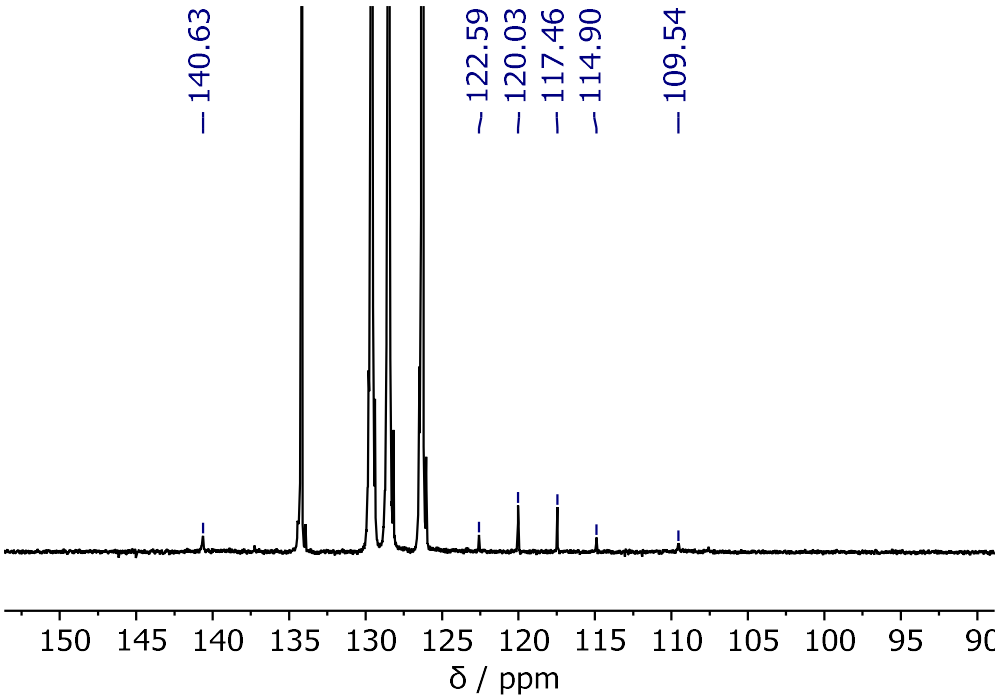

Figure 5.24: $^{13}C\{^{1}H\}$ NMR (126 MHz, C_6H_5Cl) spectrum of the reaction of *di*-bromo pyrazabole and $HNTf_2$ after 18 hours at 100 °C. The resonances at 140.63 and 109.54 ppm correspond to *tetra*-bromo pyrazabole, whilst the quartet resonance at -118.75 ppm corresponds to leftover $HNTf_2$.

- **NMR spectra of isolated precipitate in $CDCl_3$:**

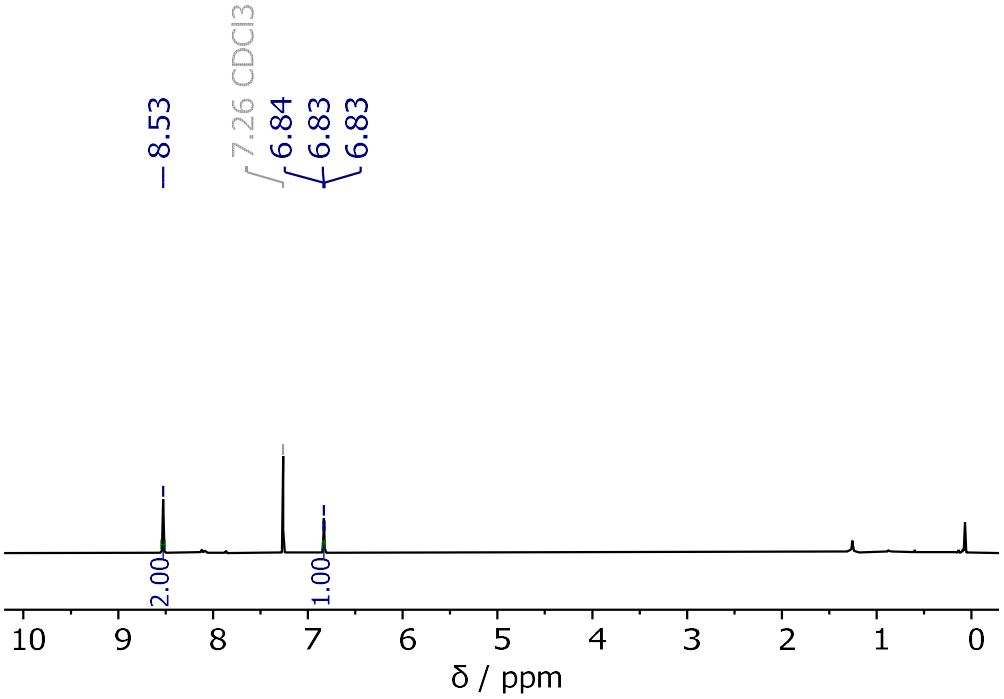

Figure 5.25: ^{1}H NMR (500 MHz, $CDCl_3$) spectrum of the precipitate isolated from the reaction of *di*-bromo pyrazabole and $HNTf_2$ after 18 hours at 100 °C. The resonances at 8.53 and 6.83 ppm correspond to *tetra*-bromo pyrazabole.

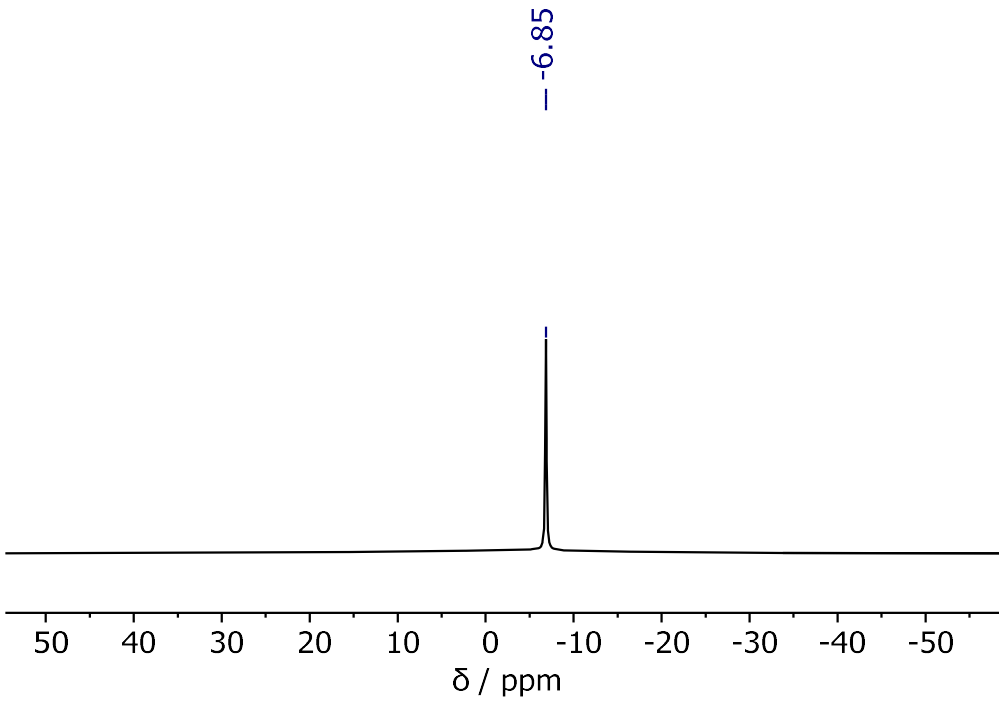

Figure 5.26: ^{11}B NMR (161 MHz, $CDCl_3$) spectrum of the precipitate isolated from the reaction of *di*-bromo pyrazabole and $HNTf_2$ after 18 hours at 100 °C. The resonance at -6.85 ppm corresponds to *tetra*-bromo pyrazabole.

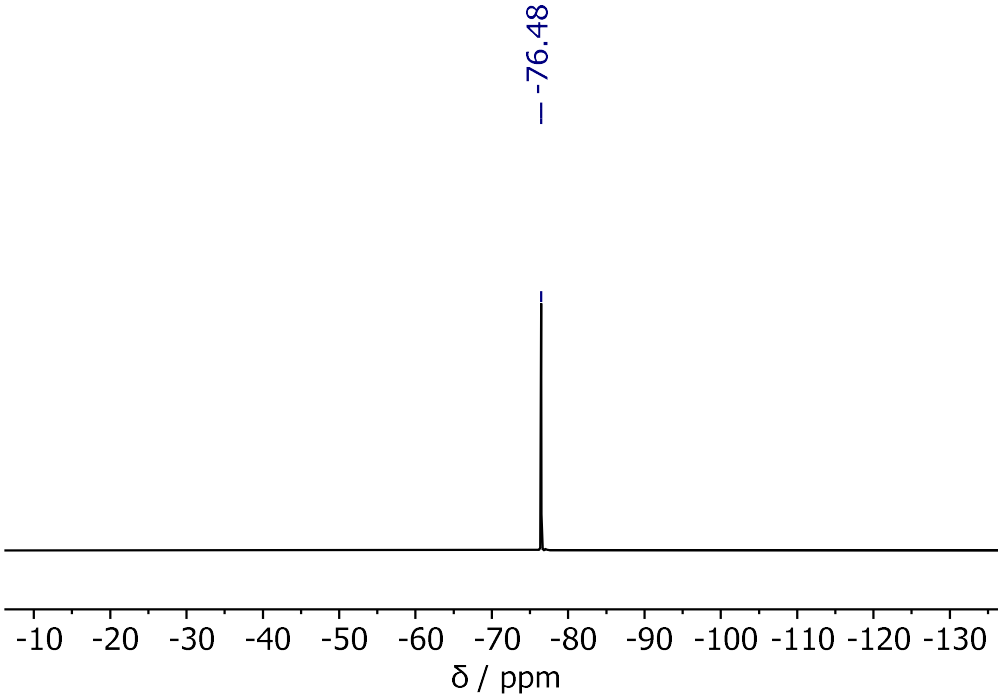

Figure 5.27: ^{19}F NMR (471 MHz, $CDCl_3$) spectrum of the precipitate isolated from the reaction of *di*-bromo pyrazabole and $HNTf_2$ after 18 hours at 100 °C. The resonance at -76.48 ppm corresponds to trace leftover $HNTf_2$.

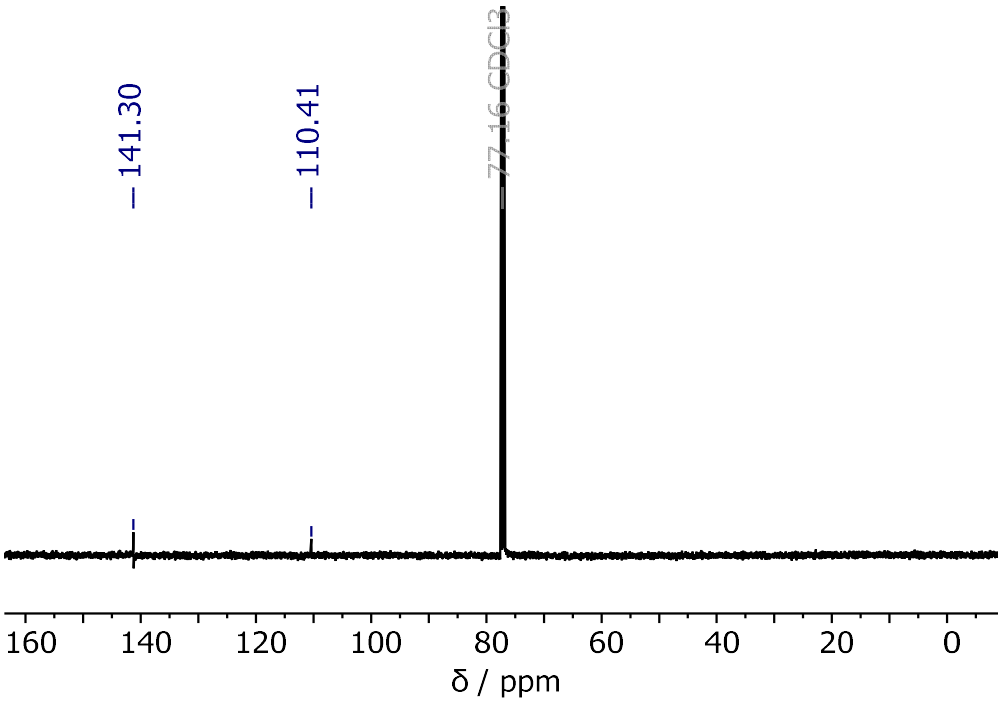

Figure 5.28: $^{13}C\{^1H\}$ NMR (126 MHz, $CDCl_3$) spectrum of the precipitate isolated from the reaction of *di*-bromo pyrazabole and $HNTf_2$ after 18 hours at 100 °C. The resonances at 141.30 and 110.41 ppm corresponds to *tetra*-bromo pyrazabole.

- **NMR spectra of isolated precipitate in d_3-MeCN:**

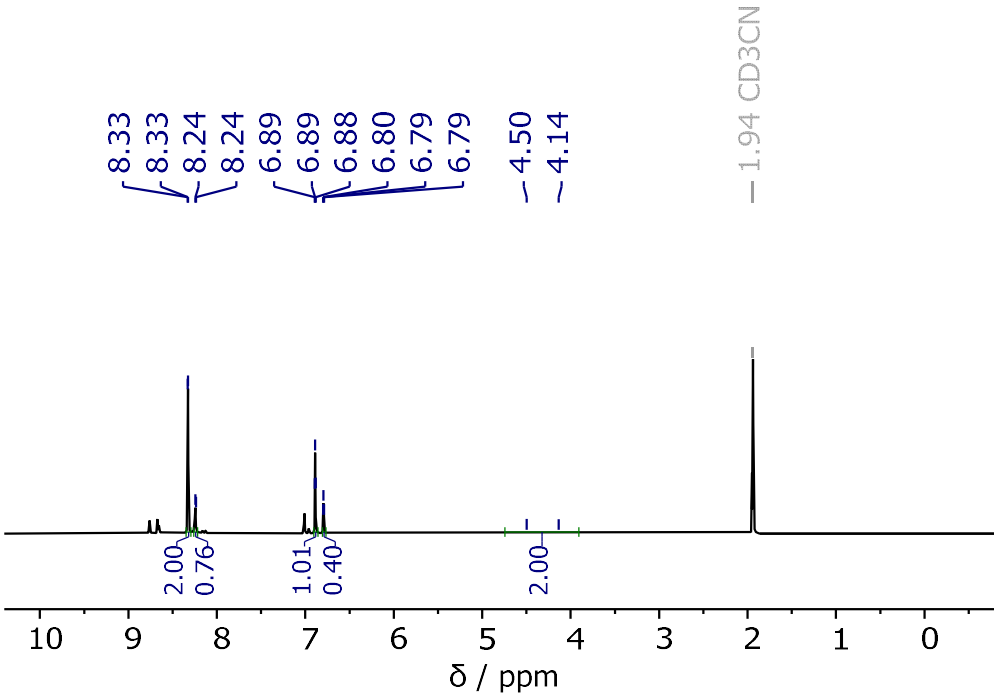

Figure 5.29: ^{1}H NMR (500 MHz, CD_3CN) spectrum of the precipitate isolated from the reaction of *di*-bromo pyrazabole and $HNTf_2$ after 18 hours at 100 °C. The resonances at 8.24 and 6.80 ppm correspond to *tetra*-bromo pyrazabole, whilst the resonances at 8.33, 6.89 and 4.33 ppm correspond to [*di*-MeCN pyrazabole][NTf_2]$_2$.

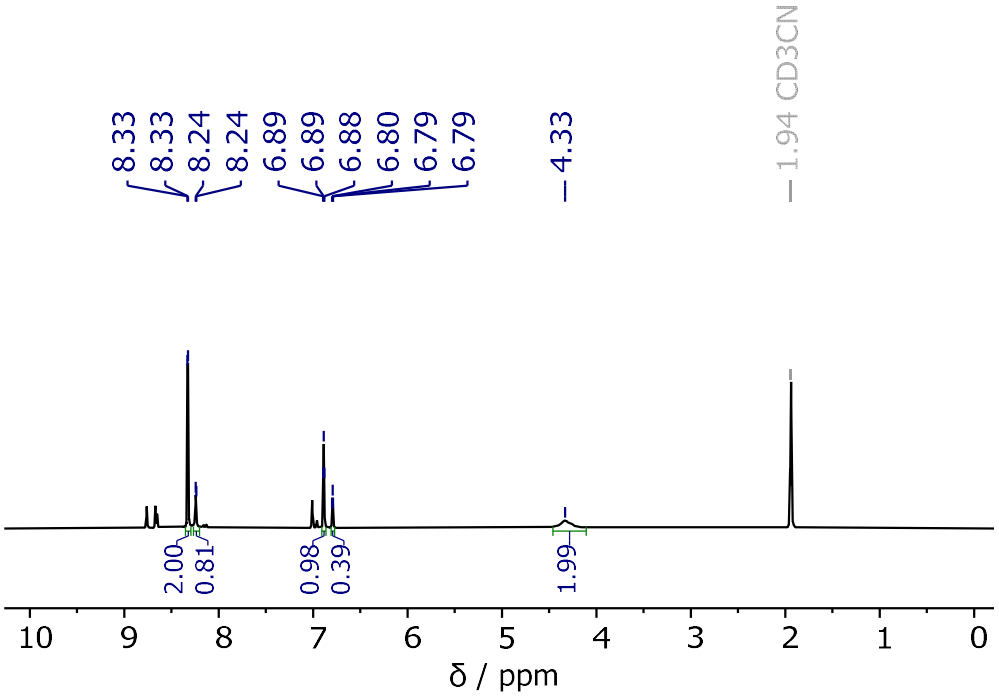

Figure 5.30: $^{1}H\{^{11}B\}$ NMR (500 MHz, CD_3CN) spectrum of the precipitate isolated from the reaction of *di*-bromo pyrazabole and $HNTf_2$ after 18 hours at 100 °C.

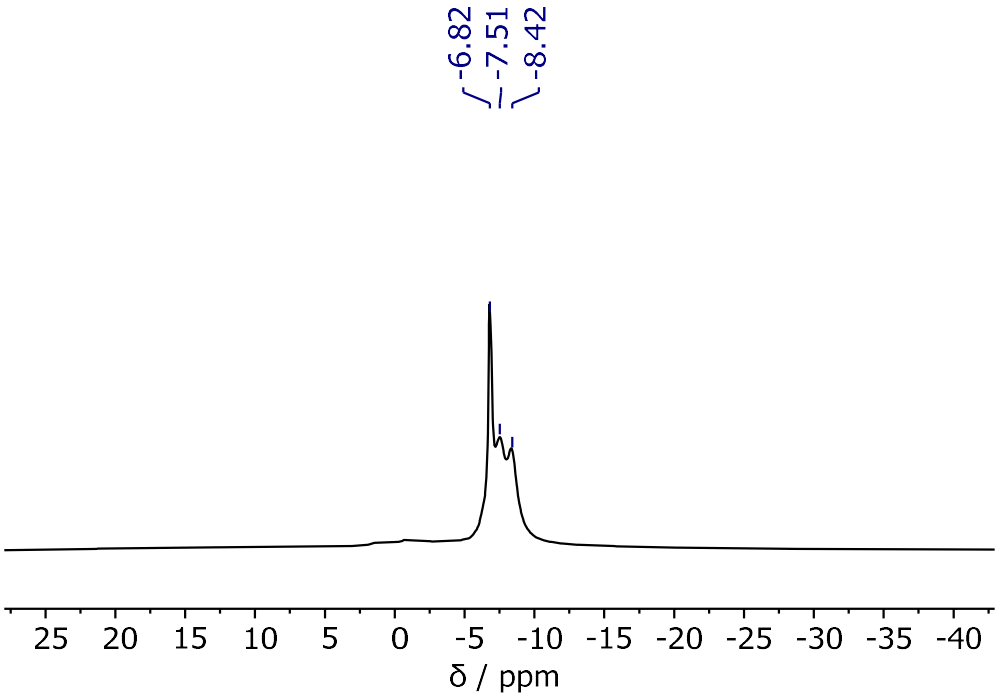

Figure 5.31: ^{11}B NMR (161 MHz, CD_3CN) spectrum of the precipitate isolated from the reaction of *di*-bromo pyrazabole and $HNTf_2$ after 18 hours at 100 °C. The resonance at -6.82 ppm corresponds to *tetra*-bromo pyrazabole, whilst the resonance at -7.97 ppm corresponds to [*di*-MeCN pyrazabole][NTf_2]$_2$.

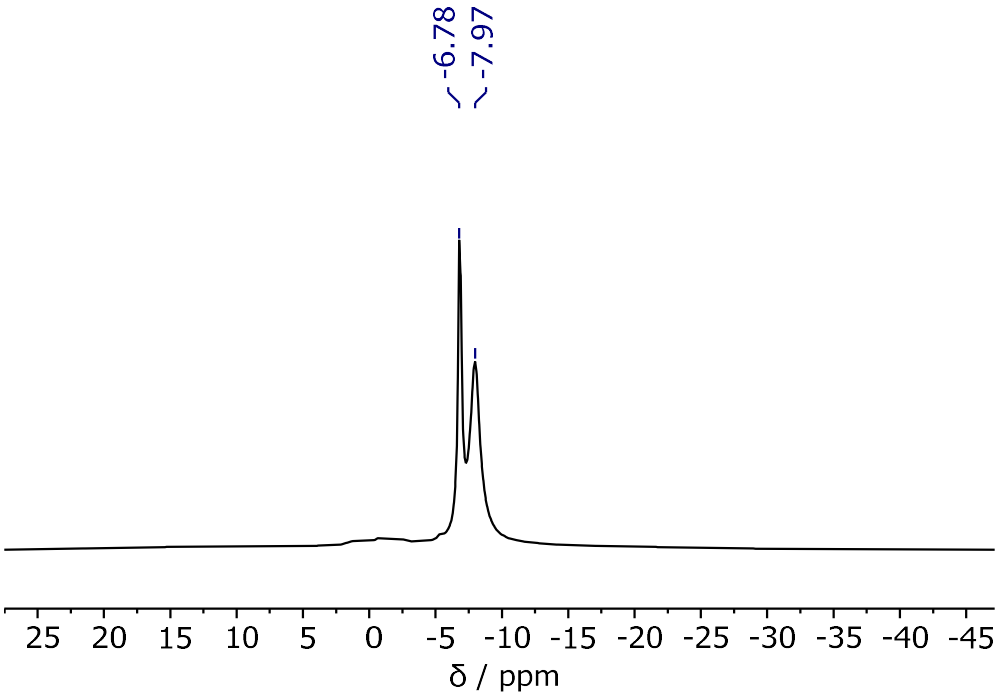

Figure 5.32: $^{11}B\{^1H\}$ NMR (161 MHz, CD_3CN) spectrum of the precipitate isolated from the reaction of *di*-bromo pyrazabole and $HNTf_2$ after 18 hours at 100 °C.

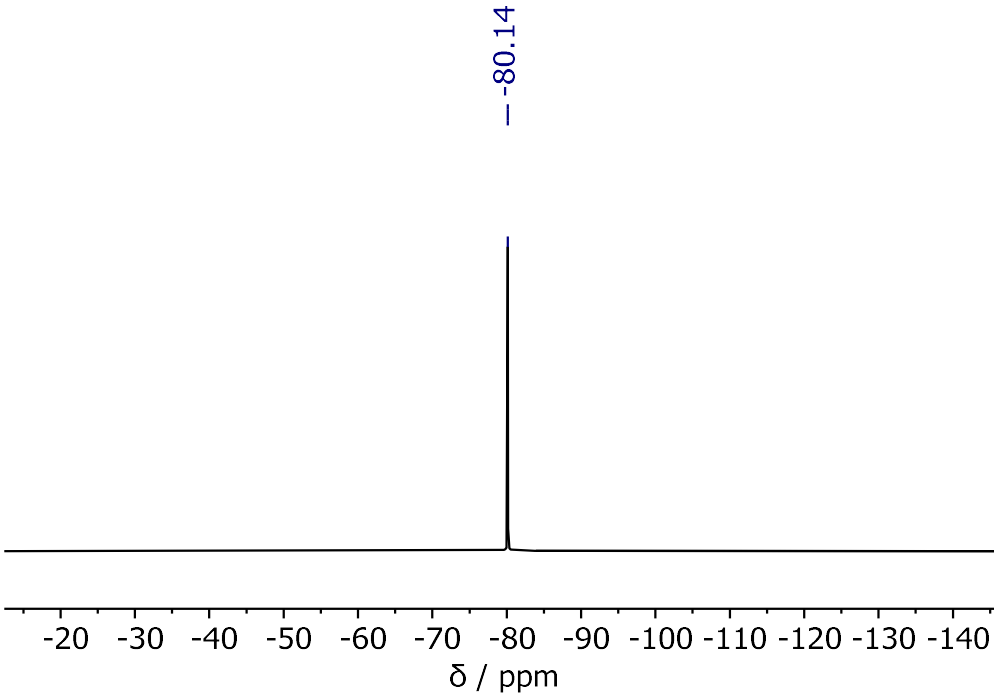

Figure 5.33: ^{19}F NMR (471 MHz, CD_3CN) spectrum of the precipitate isolated from the reaction of *di*-bromo pyrazabole and $HNTf_2$ after 18 hours at 100 °C. The resonance at -80.14 ppm corresponds to the $[NTf_2]^-$ anions.

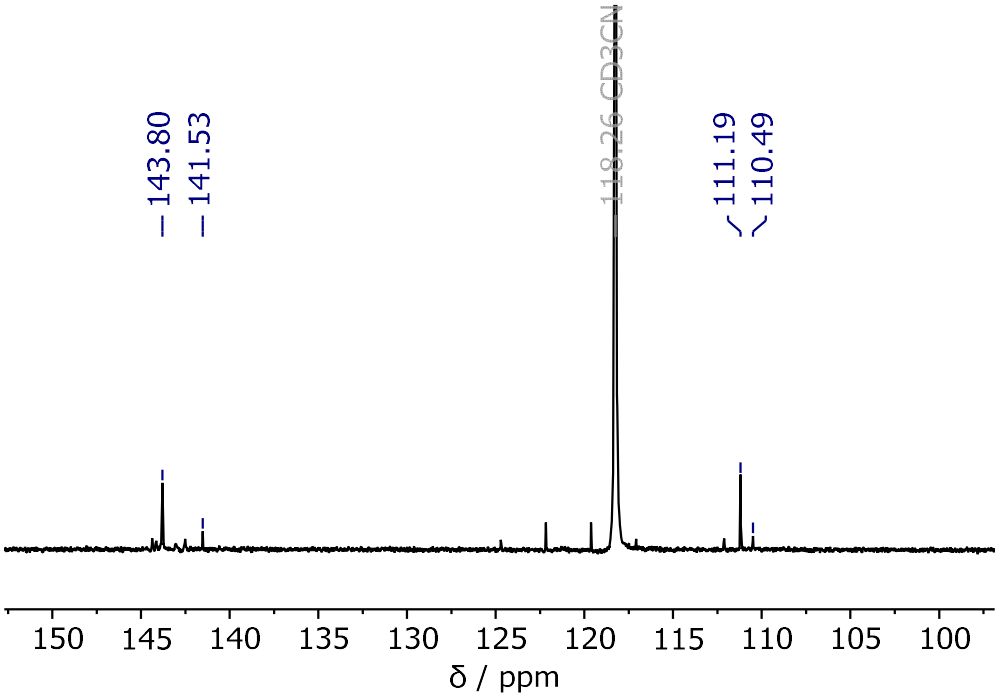

Figure 5.34: $^{13}C\{^1H\}$ NMR (126 MHz, CD_3CN) spectrum of the precipitate isolated from the reaction of *di*-bromo pyrazabole and $HNTf_2$ after 18 hours at 100 °C. The resonances at 141.53 and 110.49 ppm correspond to *tetra*-bromo pyrazabole, whilst the resonances at 143.80 and 11.19 ppm correspond to [*di*-MeCN pyrazabole][NTf_2]$_2$.

'Activated' *Di*-Bromo Pyrazabole (5.2) + *N*-Methyl Indole + DBP

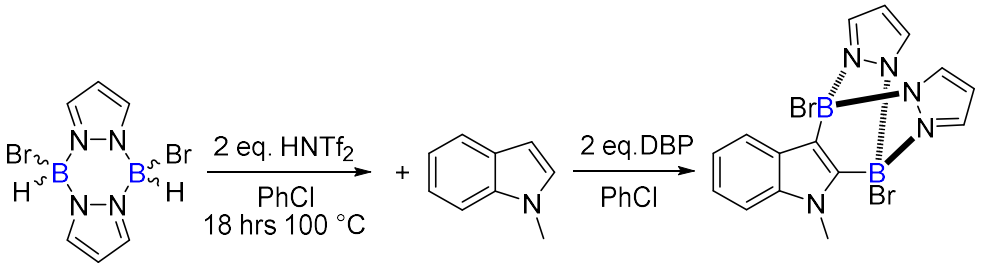

- **NMR spectra after 18 hours RT:**

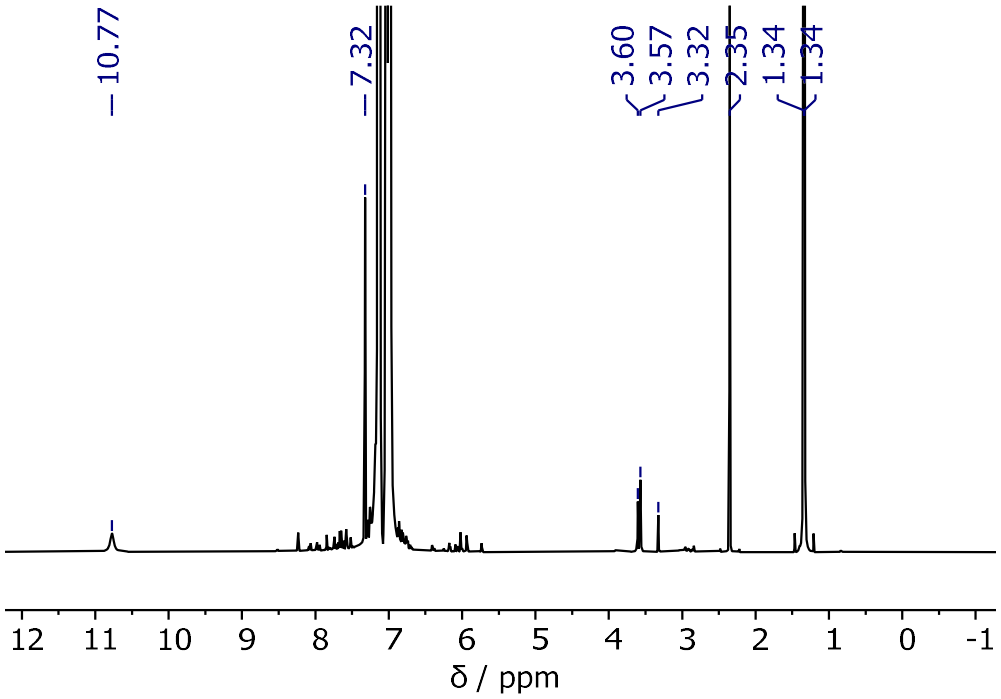

Figure 5.35: ^{1}H NMR (500 MHz, C_6H_5Cl) spectrum of the crude reaction of the 'activated' *di*-bromo pyrazabole mixture, DBP and *N*-methyl indole, after 18 hours at RT. The resonances at 10.77, 7.32, 2.35 and 1.34 ppm correspond to [DBP-H][NTf_2].

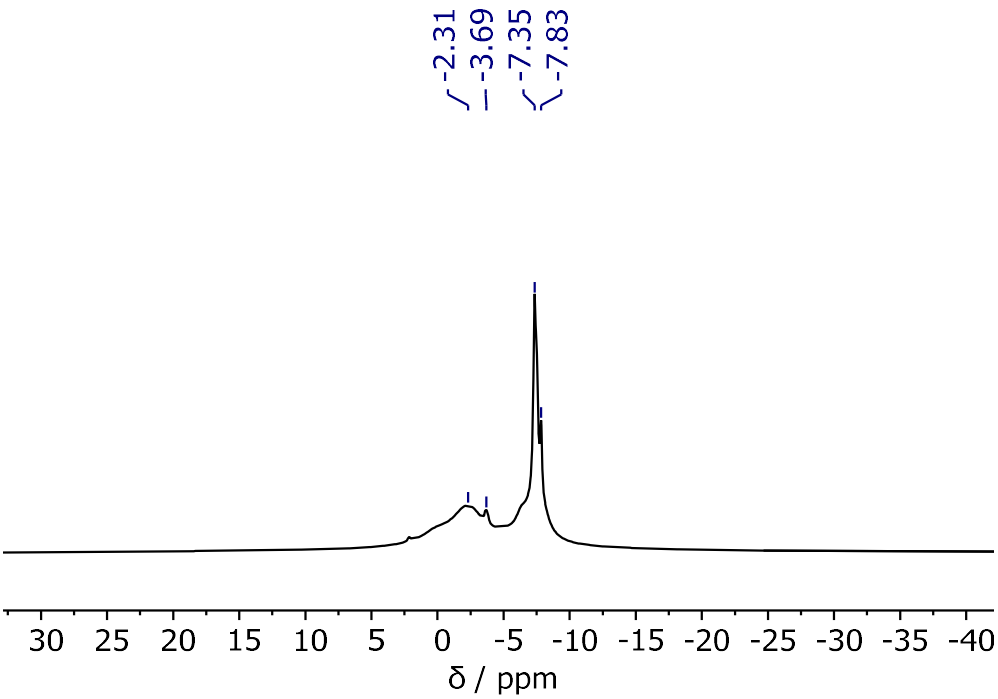

Figure 5.36: ^{11}B NMR (161 MHz, C_6H_5Cl) spectrum of the crude reaction of the 'activated' *di*-bromo pyrazabole mixture, DBP and *N*-methyl indole, after 18 hours at RT.

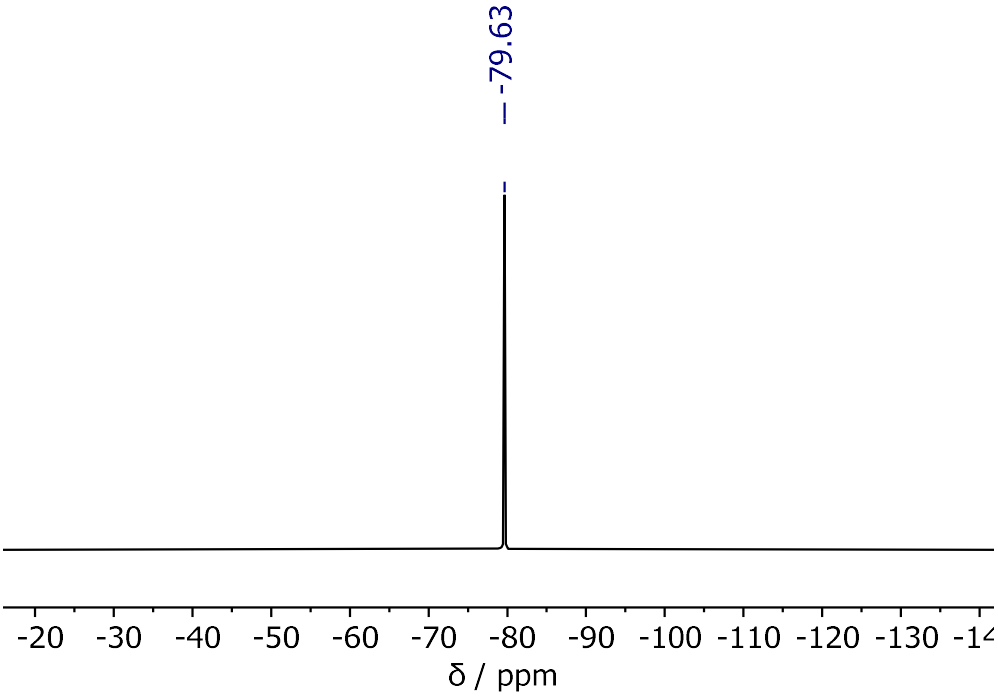

Figure 5.37: ^{19}F NMR (476 MHz, C_6H_5Cl) spectrum of the crude reaction of the 'activated' *di*-bromo pyrazabole mixture, DBP and *N*-methyl indole, after 18 hours at RT.

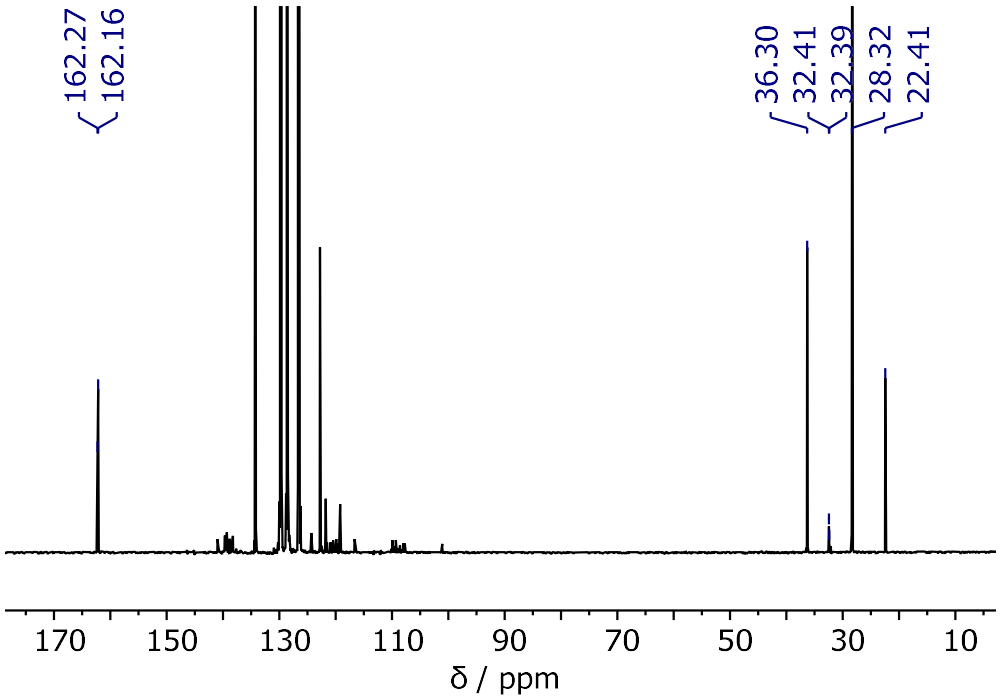

Figure 5.38: $^{13}C\{^{1}H\}$ NMR (126 MHz, C_6H_5Cl) spectrum of the crude reaction of the 'activated' *di*-bromo pyrazabole mixture, DBP and *N*-methyl indole, after 18 hours at RT.

- **NMR spectra of reaction after addition of pinacol / K_2CO_3:**

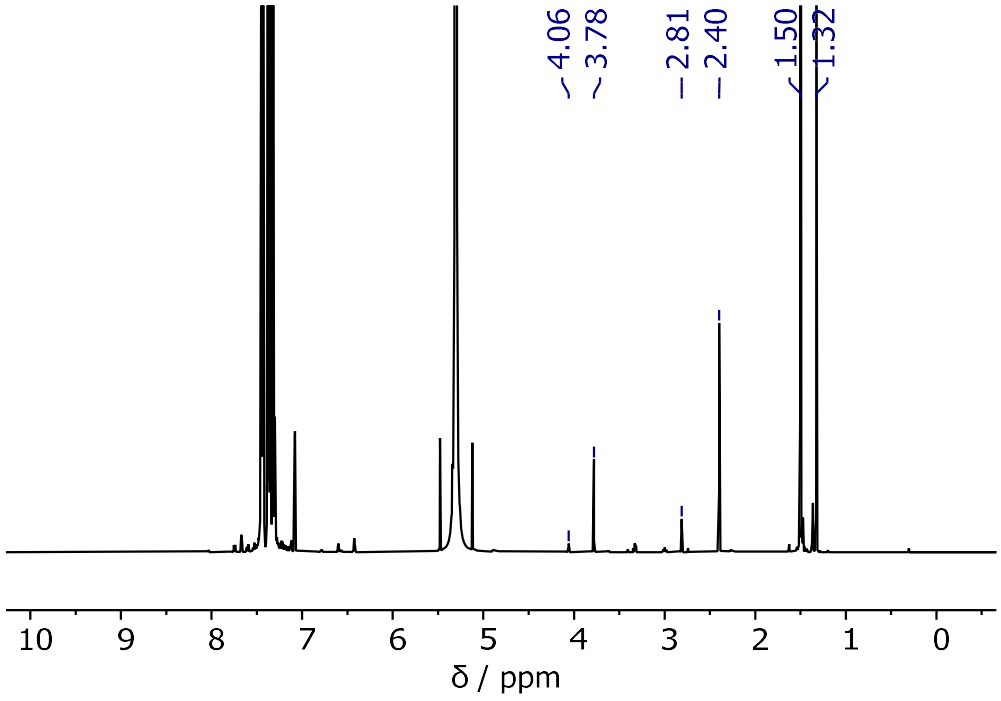

Figure 5.39: ^{1}H NMR (500 MHz, CH_2Cl_2) spectrum of the reaction of the 'activated' *di*-bromo pyrazabole mixture, DBP and *N*-methyl indole, after addition of pinacol / K_2CO_3, 18 hrs 50 °C.

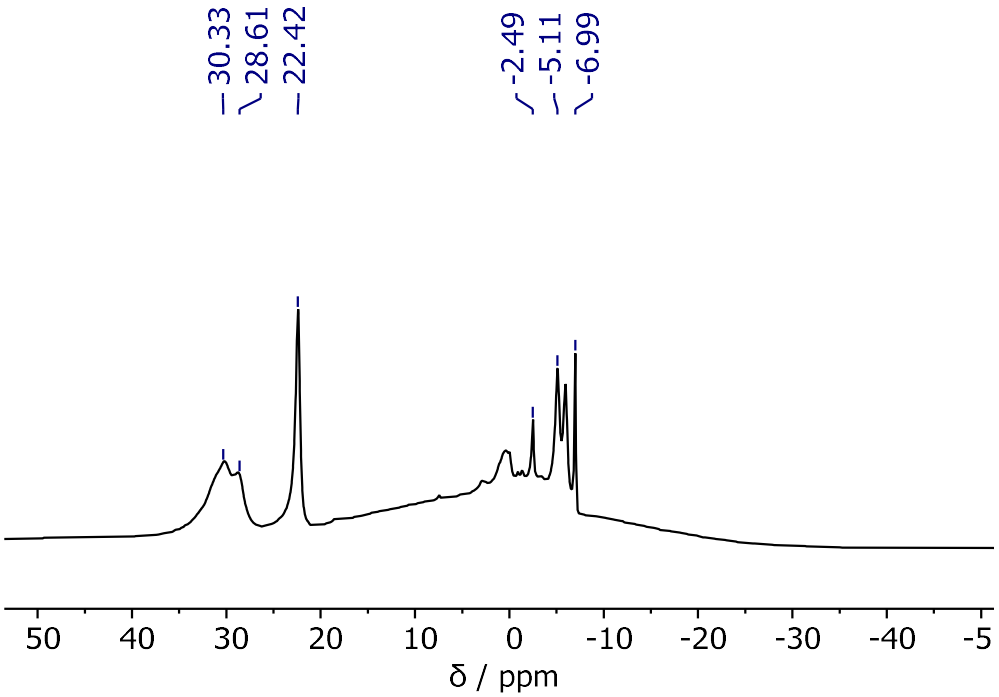

Figure 5.40: ^{11}B NMR (500 MHz, CH_2Cl_2) spectrum of the reaction of the 'activated' *di*-bromo pyrazabole mixture, DBP and *N*-methyl indole, after addition of pinacol / K_2CO_3, 18 hrs 50 °C.

Control Reaction: *Tetra*-Bromo Pyrazabole (5.6) / *Di*-NTf_2 Pyrazabole (5.5) with *N*-Methyl Indole + DBP

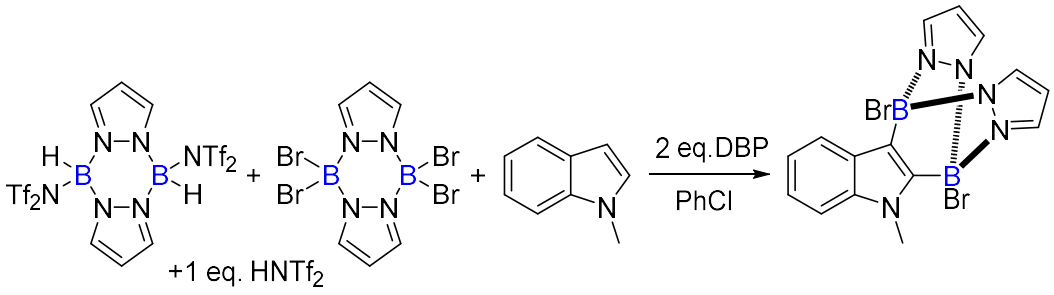

- **NMR spectra after 18 hours RT:**

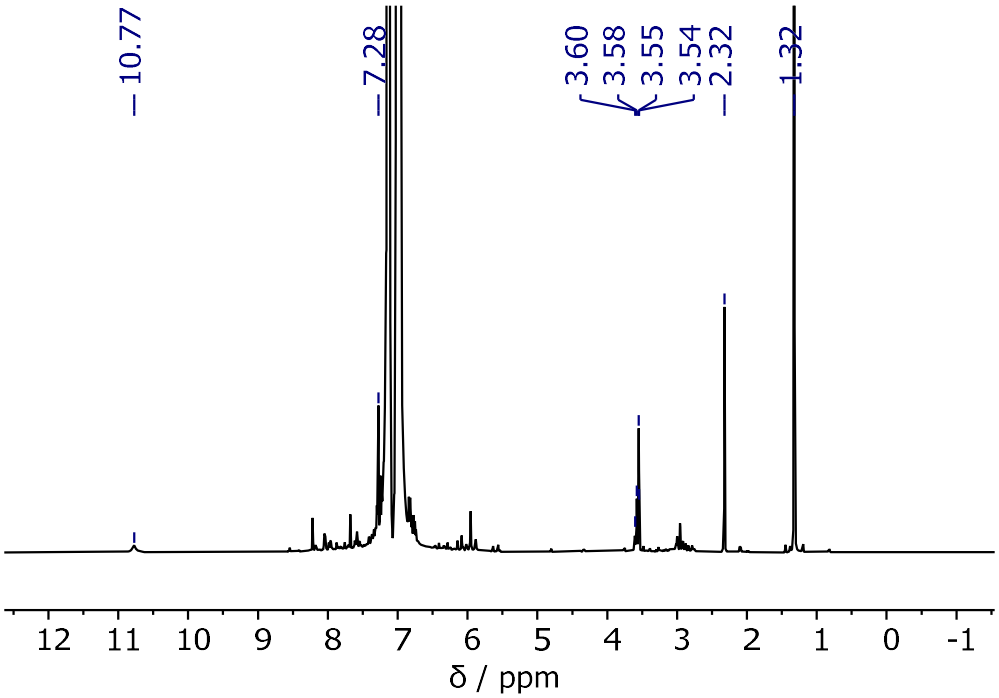

Figure 5.41: ^1H NMR (500 MHz, C_6H_5Cl) spectrum of the crude reaction of *tetra*-bromo pyrazabole, *di*-NTf_2 pyrazabole, $HNTf_2$, DBP and *N*-methyl indole, after 18 hours at RT. The resonances at 10.77, 7.28, 2.32 and 1.32 ppm correspond to [DBP-H][NTf_2].

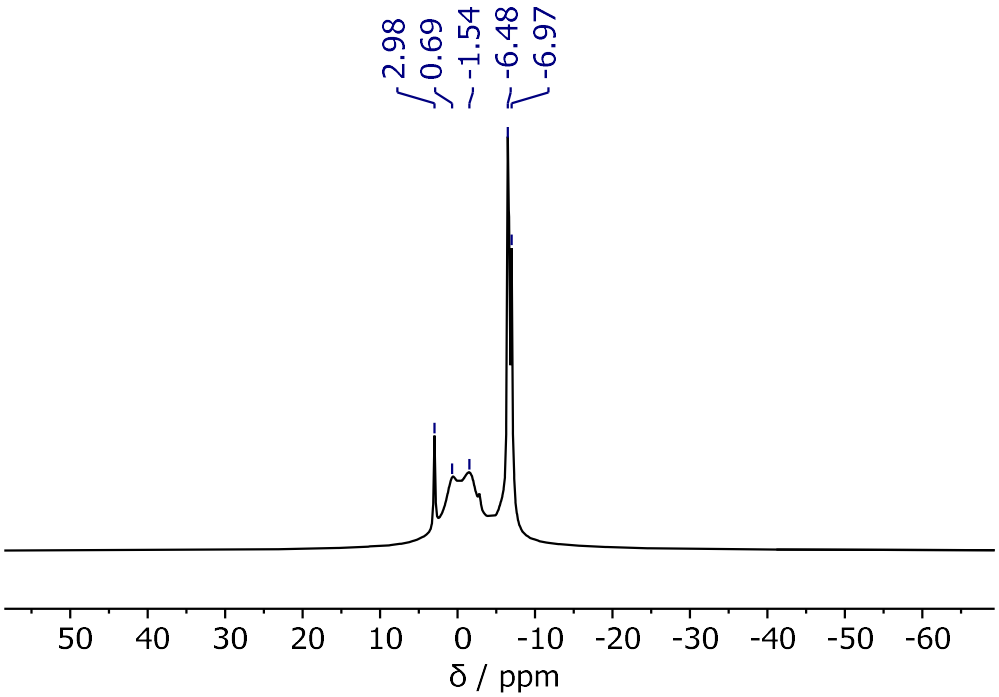

Figure 5.42: ^{11}B NMR (161 MHz, C_6H_5Cl) spectrum of the crude reaction of *tetra*-bromo pyrazabole, *di*-NTf_2 pyrazabole, $HNTf_2$, DBP and *N*-methyl indole, after 18 hours at RT.

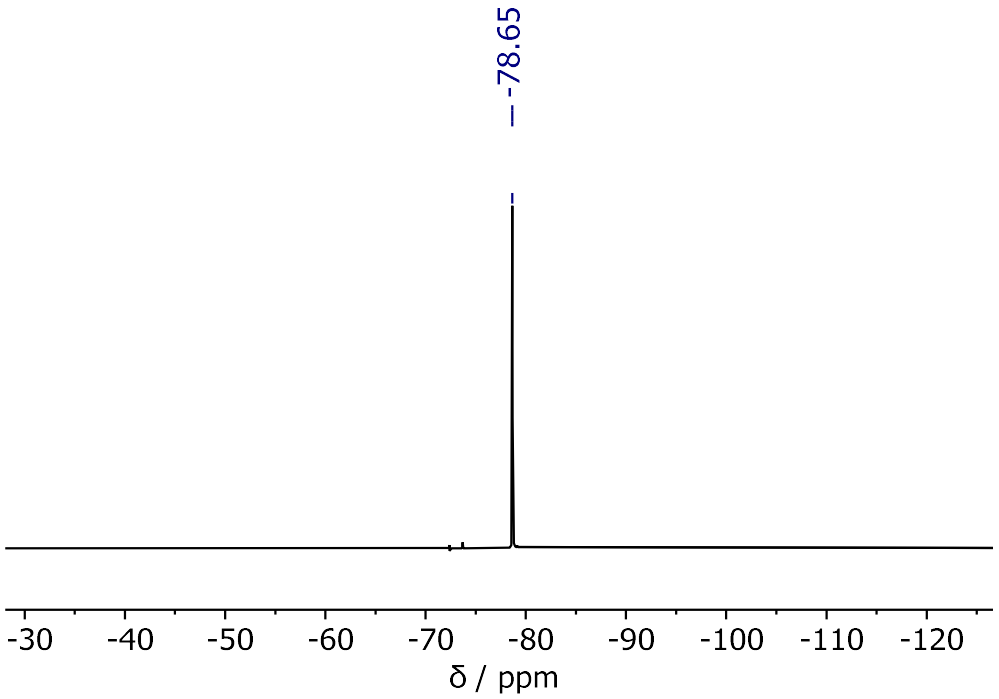

Figure 5.43: ^{19}F NMR (471 MHz, C_6H_5Cl) spectrum of the crude reaction of *tetra*-bromo pyrazabole, *di*-NTf_2 pyrazabole, $HNTf_2$, DBP and *N*-methyl indole, after 18 hours at RT.

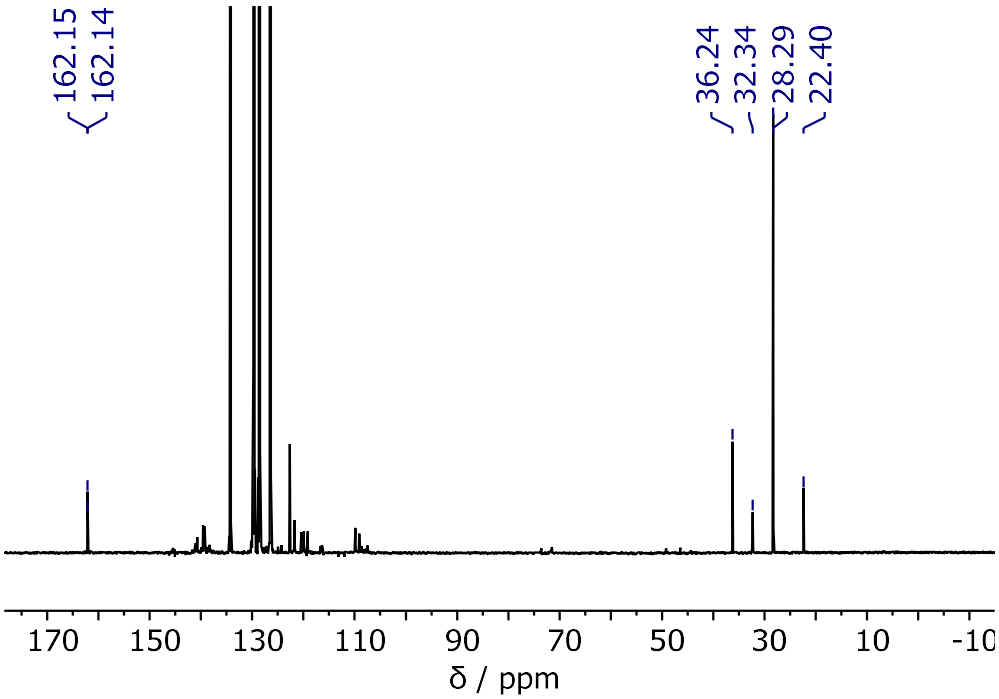

Figure 5.44: $^{13}C\{^{1}H\}$ NMR (126 MHz, C_6H_5Cl) spectrum of the crude reaction of *tetra*-bromo pyrazabole, *di*-NTf_2 pyrazabole, $HNTf_2$, DBP and *N*-methyl indole, after 18 hours at RT.

5.5.4 – Reactivity of *Di*-Chloro Pyrazabole with $HNTf_2$

'Activation' of *Di*-Chloro Pyrazabole (5.3)

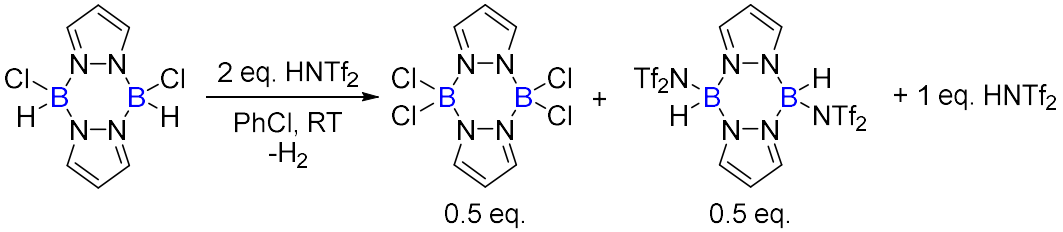

- **NMR spectra of crude reaction after 18 hours at RT:**

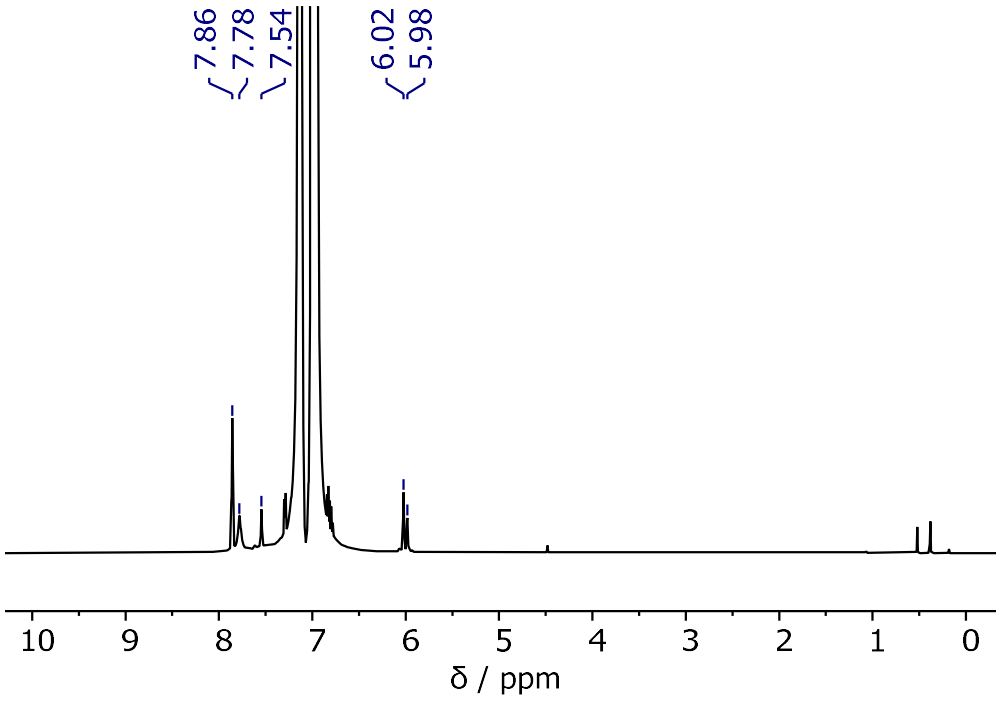

Figure 5.45: ^1H NMR (500 MHz, C_6H_5Cl) spectrum of the reaction of *di*-chloro pyrazabole and $HNTf_2$ after 18 hours at RT. The resonances at 7.86 and 6.02 ppm correspond to *tetra*-chloro pyrazabole, the resonance at 7.78 ppm is due to leftover $HNTf_2$, and the resonances at 7.54 and 5.98 ppm correspond to leftover *di*-chloro pyrazabole.

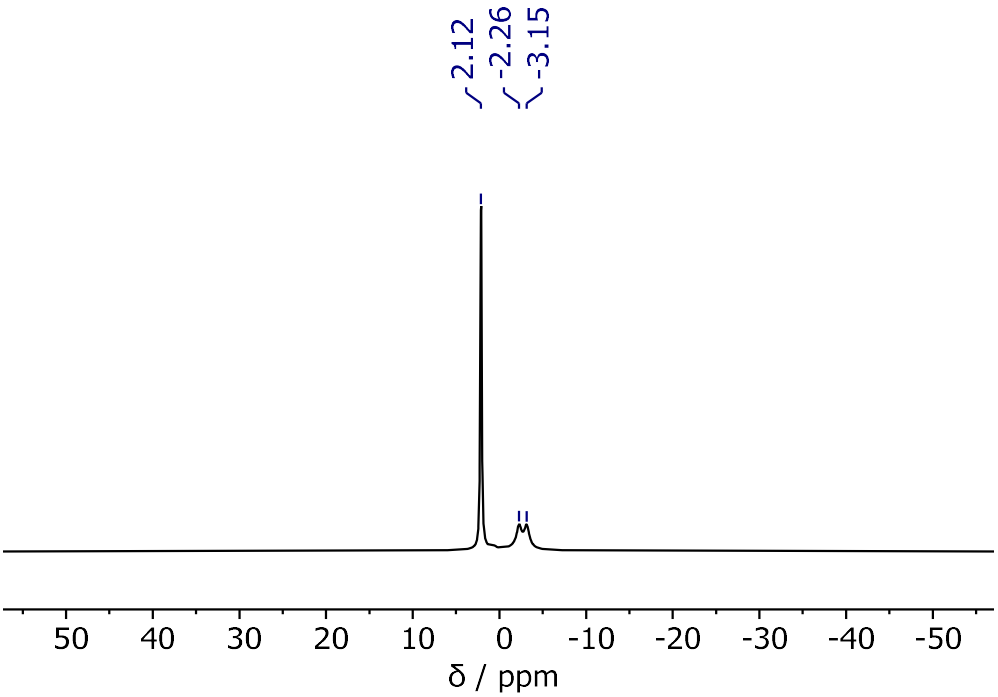

Figure 5.46: ^{11}B NMR (161 MHz, C_6H_5Cl) spectrum of the reaction of *di*-chloro pyrazabole and $HNTf_2$ after 18 hours at RT. The resonance at 2.12 ppm corresponds to *tetra*-chloro pyrazabole, whilst the resonance at -2.71 ppm corresponds to leftover *di*-chloro pyrazabole.

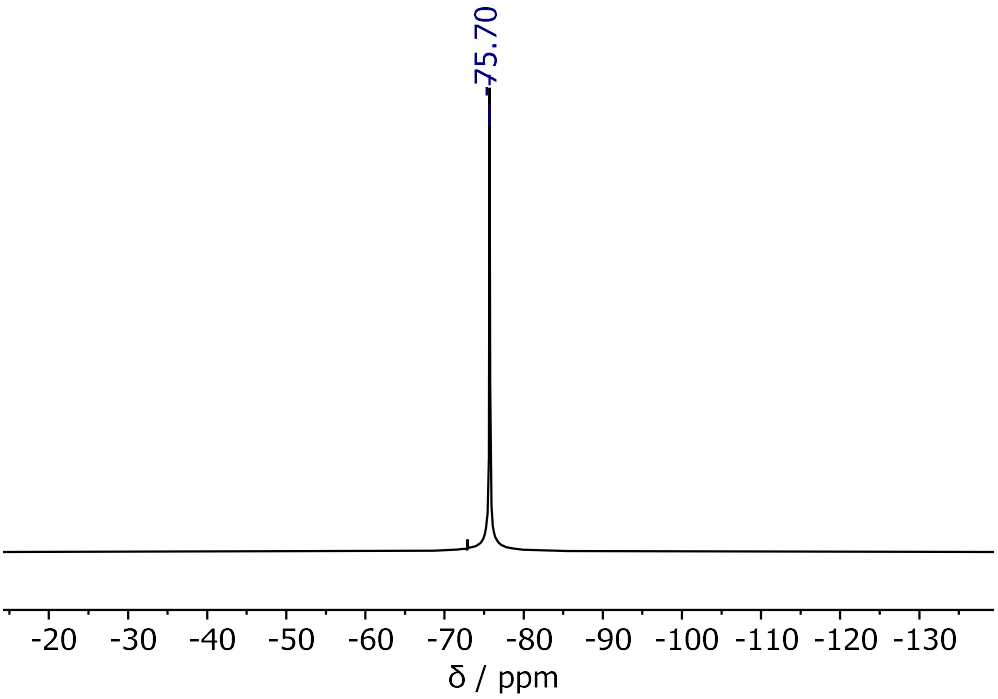

Figure 5.47: ^{19}F NMR (471 MHz, C_6H_5Cl) spectrum of the reaction of *di*-chloro pyrazabole and $HNTf_2$ after 18 hours at RT. The resonance at -75.70 ppm corresponds to leftover $HNTf_2$.

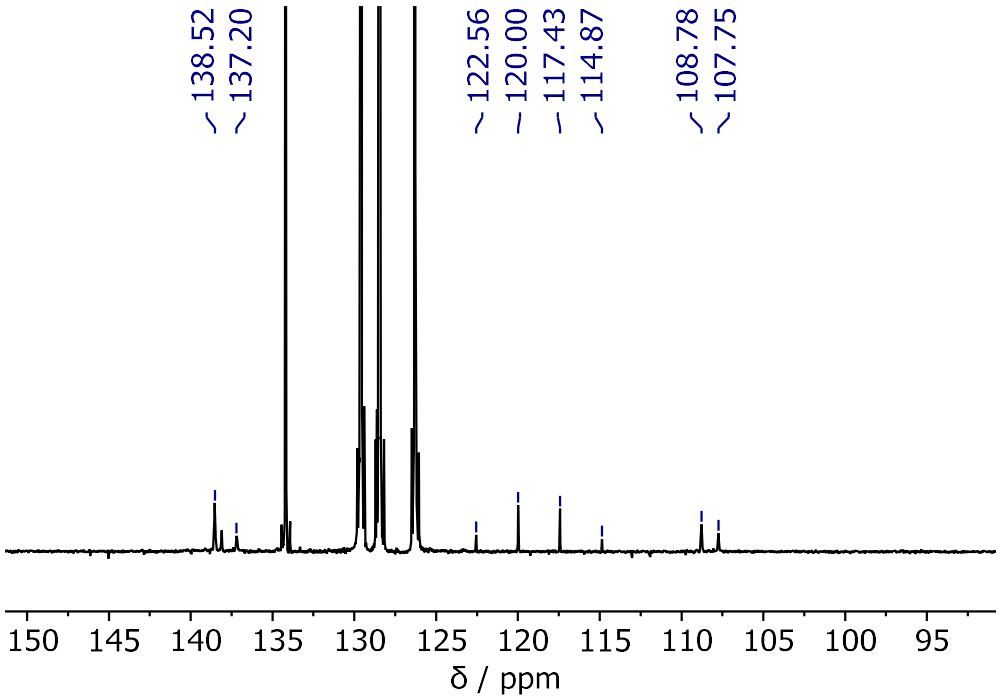

Figure 5.48: $^{13}C\{^{1}H\}$ NMR (126 MHz, C_6H_5Cl) spectrum of the reaction of *di*-chloro pyrazabole and $HNTf_2$ after 18 hours at RT. The resonances at 138.51 and 108.78 ppm correspond to *tetra*-chloro pyrazabole, the quartet resonance at -118.71 ppm corresponds to leftover $HNTf_2$, and the resonances at 137.20 and 107.75 ppm correspond to leftover *di*-chloro pyrazabole.

- **NMR spectra of crude reaction in d_3-MeCN (after addition of 2 eq. DBP):**

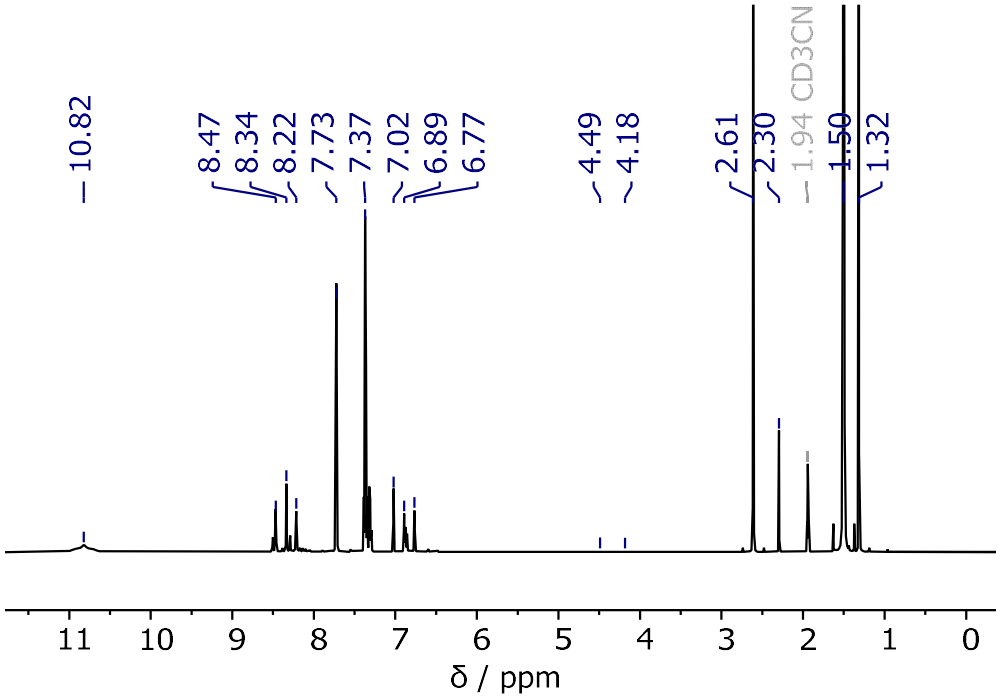

Figure 5.49: ^{1}H NMR (500 MHz, CD_3CN) spectrum of the reaction of *di*-chloro pyrazabole and $HNTf_2$ after 18 hours at RT. The resonances at 8.34, 6.89 and 4.33 ppm correspond to [*di*-MeCN pyrazabole][NTf_2]$_2$. A mixture of protonated (10.82, 7.73, 2.30 and 1.32 ppm) and unprotonated (7.37, 2.61, 1.50 ppm) DBP is also observed.

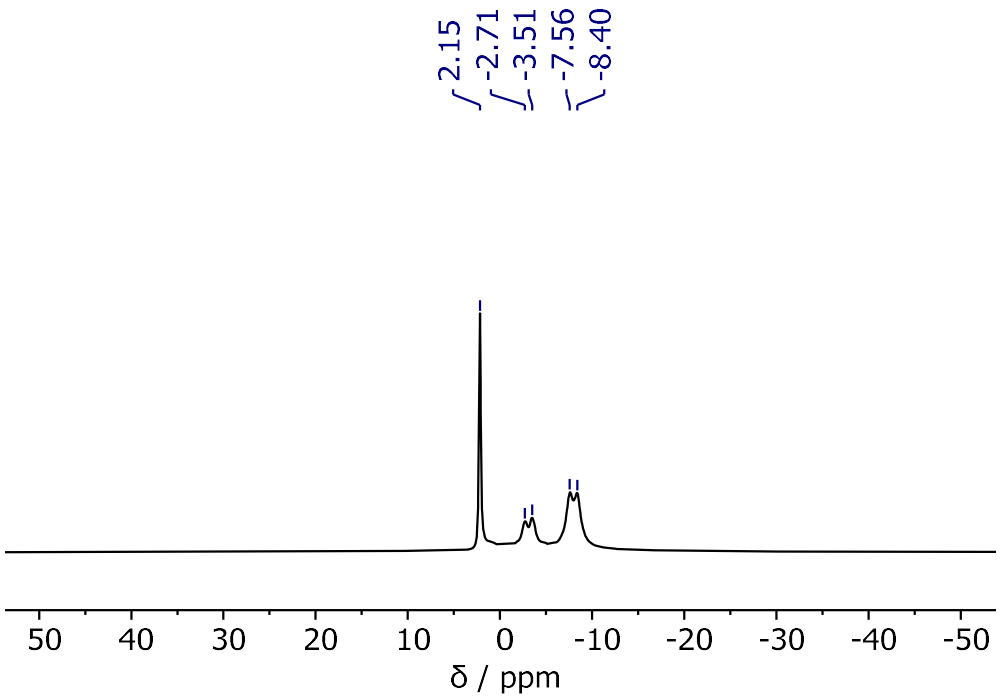

Figure 5.50: ^{11}B NMR (161 MHz, CD_3CN) spectrum of the reaction of *di*-chloro pyrazabole and $HNTf_2$ after 18 hours at RT. The resonance at 2.15 ppm corresponds to *tetra*-chloro pyrazabole, the resonance at -7.97 ppm corresponds to [*di*-MeCN pyrazabole][NTf_2]$_2$, and the resonance at -3.17 ppm corresponds to *di*-chloro pyrazabole.

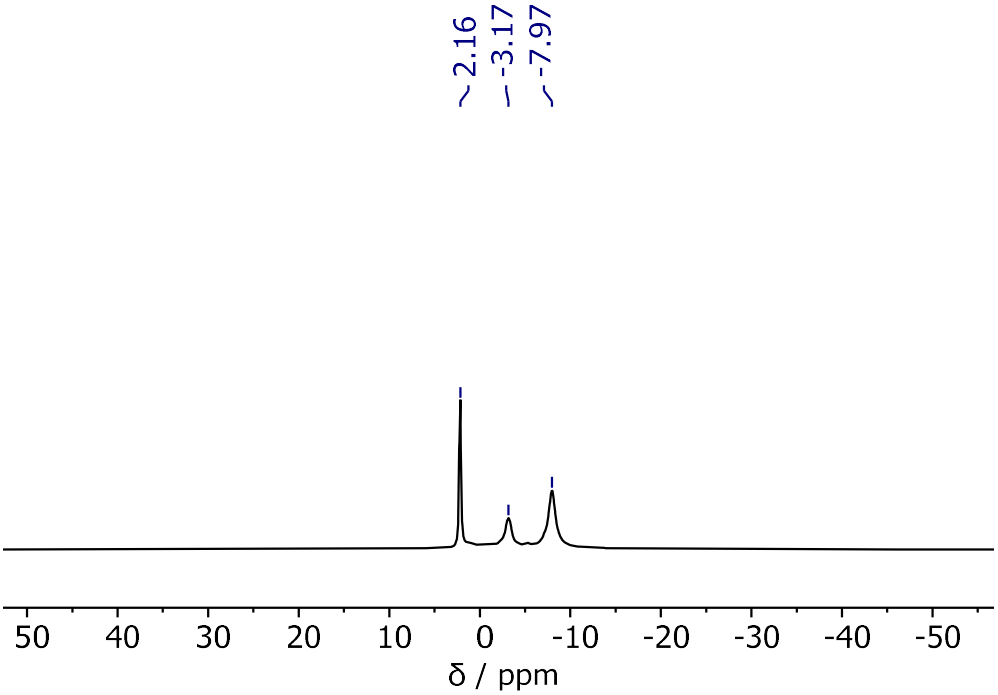

Figure 5.51: $^{11}B\{^{1}H\}$ NMR (161 MHz, CD_3CN) spectrum of the reaction of *di*-chloro pyrazabole and $HNTf_2$ after 18 hours at RT. The resonance at 2.16 ppm corresponds to *tetra*-chloro pyrazabole, the resonance at -7.97 ppm corresponds to [*di*-MeCN pyrazabole][NTf_2]$_2$, and the resonance at -3.17 ppm corresponds to *di*-chloro pyrazabole.

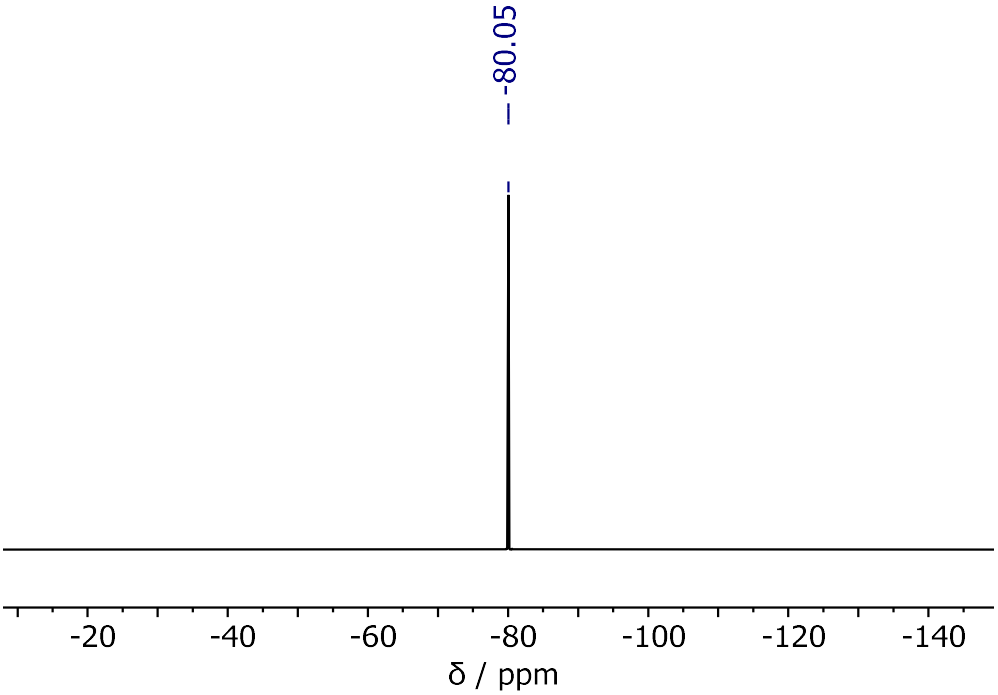

Figure 5.52: ^{19}F NMR (471 MHz, CD_3CN) spectrum of the reaction of *di*-chloro pyrazabole and $HNTf_2$ after 18 hours at RT. The resonance at -80.05 ppm corresponds to the $[NTf_2]^-$ anions.

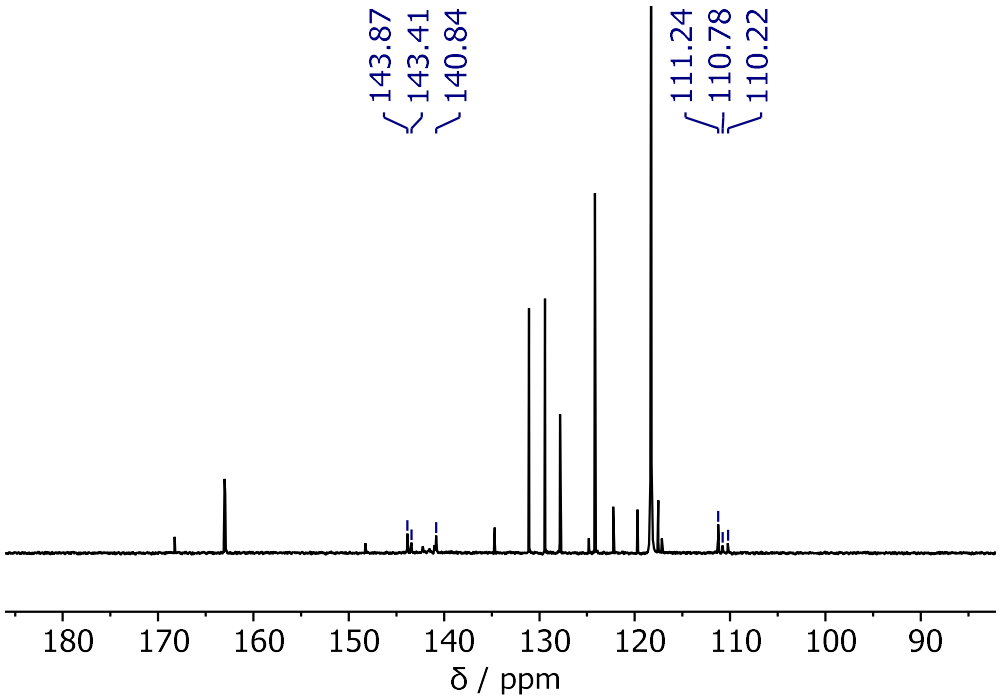

Figure 5.53: $^{13}C\{^{1}H\}$ NMR (126 MHz, CD_3CN) spectrum of the reaction of *di*-chloro pyrazabole and $HNTf_2$ after 18 hours at RT.

5.5.5 – Reactivity of *Tetra*-Bromo Pyrazabole with $TMSNTf_2$

Preparation of $TMSNTf_2$ *in situ*

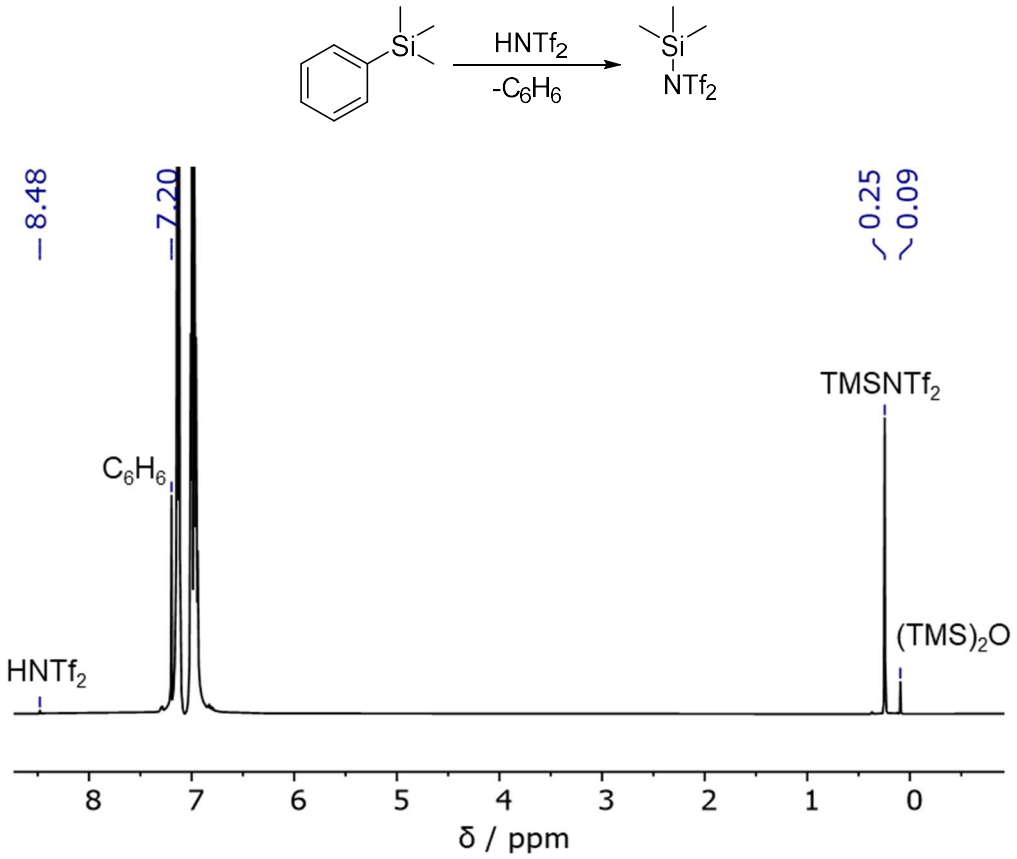

Figure 5.54: ^1H NMR (500 MHz, C_6H_5Cl) spectrum of $TMSNTf_2$, formed from PhTMS and $HNTf_2$ following 18 hours at RT.

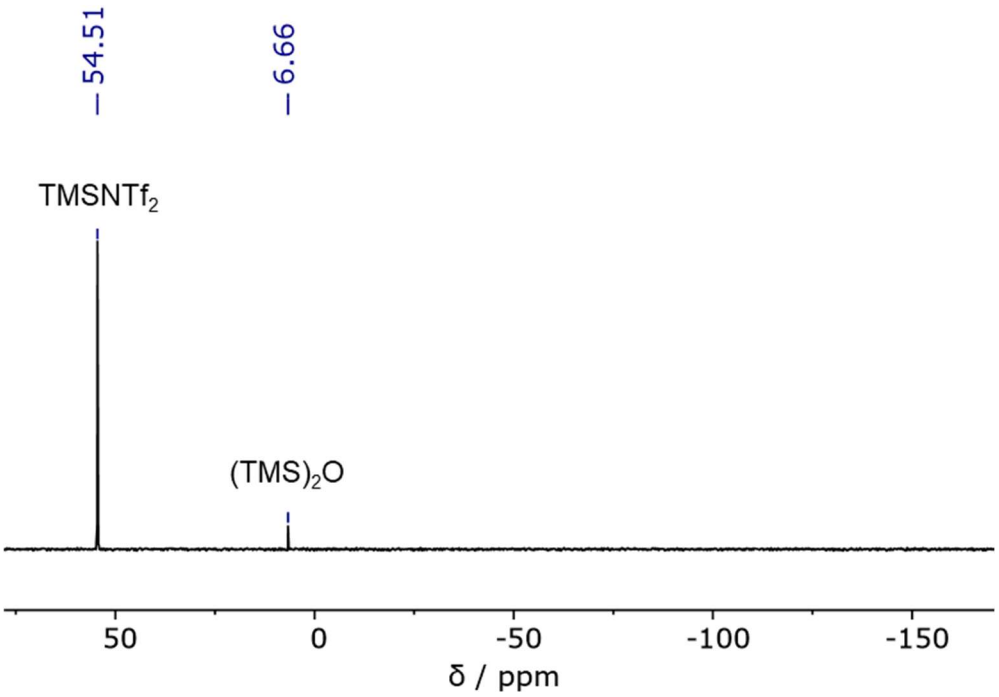

Figure 5.55: ^{29}Si NMR (99 MHz, C_6H_5Cl) spectrum of $TMSNTf_2$, formed from PhTMS and $HNTf_2$ following 18 hours at RT.

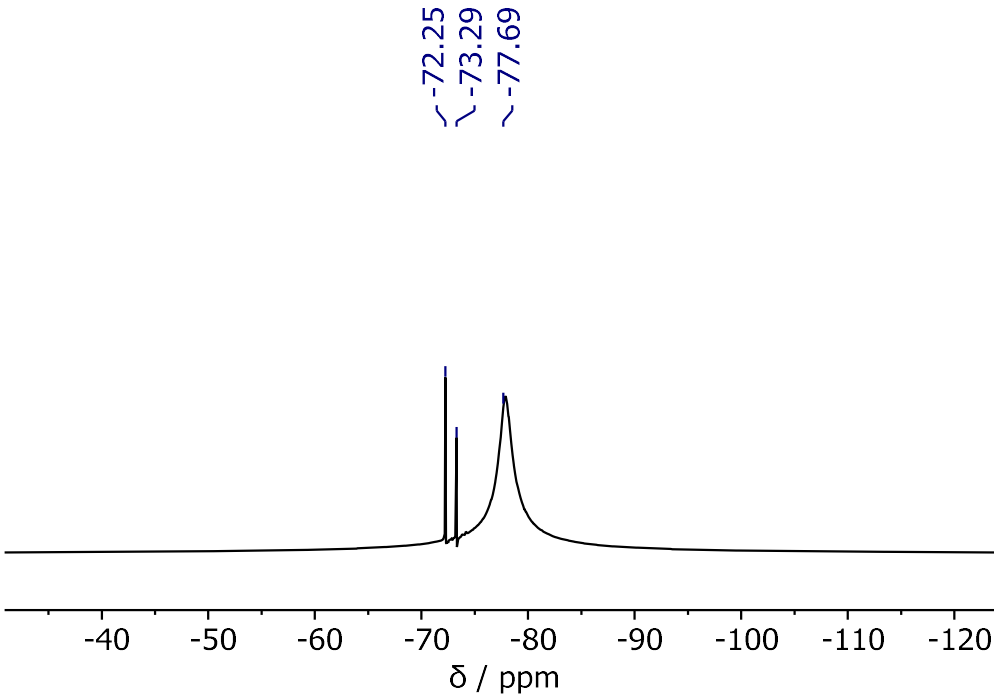

Figure 5.56: ^{19}F NMR (471 MHz, C_6H_5Cl) spectrum of $TMSNTf_2$, formed from PhTMS and $HNTf_2$ following 18 hours at RT.

Activation of *Tetra*-Bromo Pyrazabole with $TMSNTf_2$

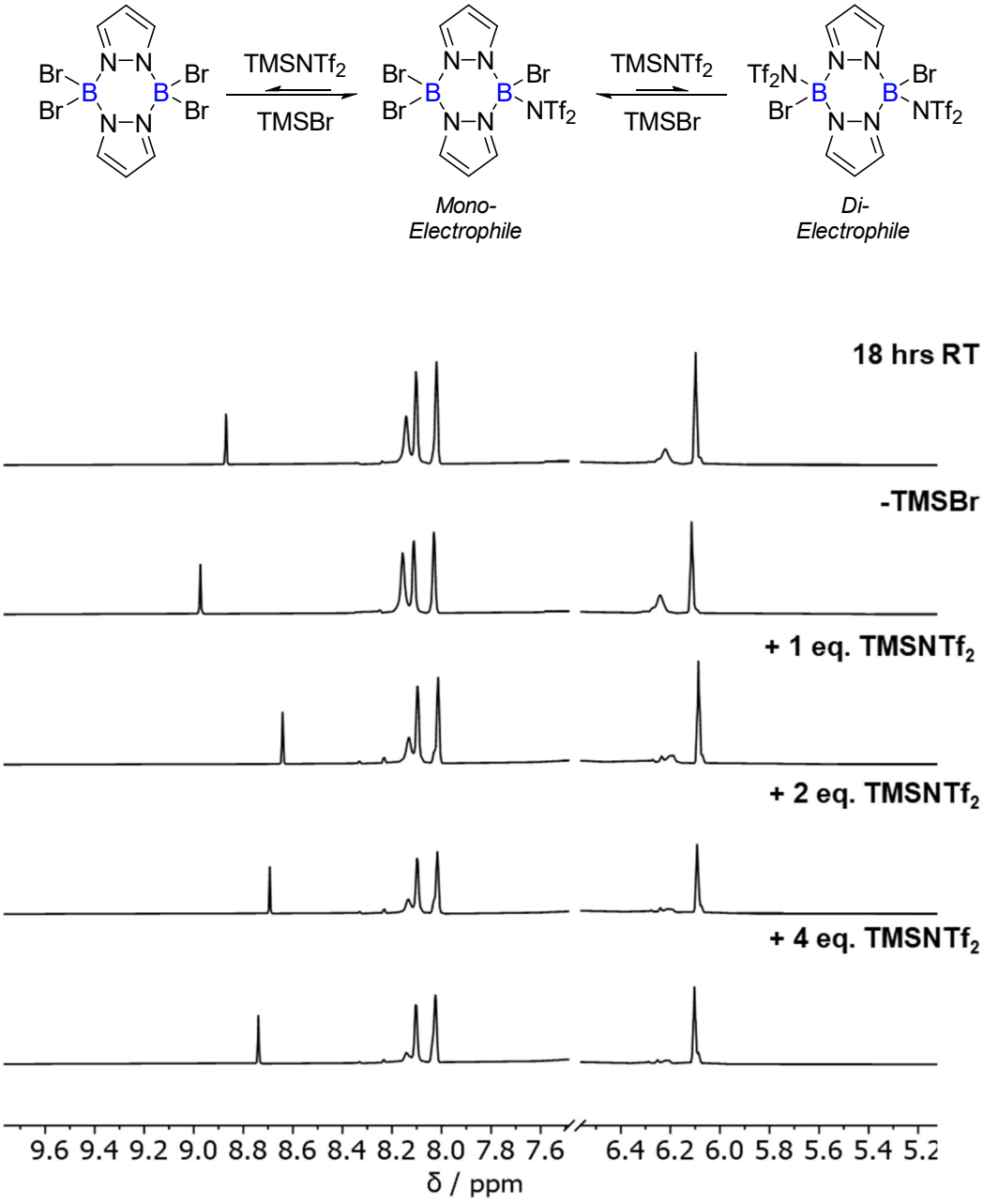

Figure 5.57: Stacked ^{1}H NMR (500 MHz, C_6H_5Cl) spectra for the reaction of *tetra*-bromo pyrazabole + 2.2 eq. $TMSNTf_2$, with subsequent removal/addition of TMSBr to demonstrate the reversibility of the reaction. *Note: the ^{1}H solvent resonance has been omitted for clarity.*

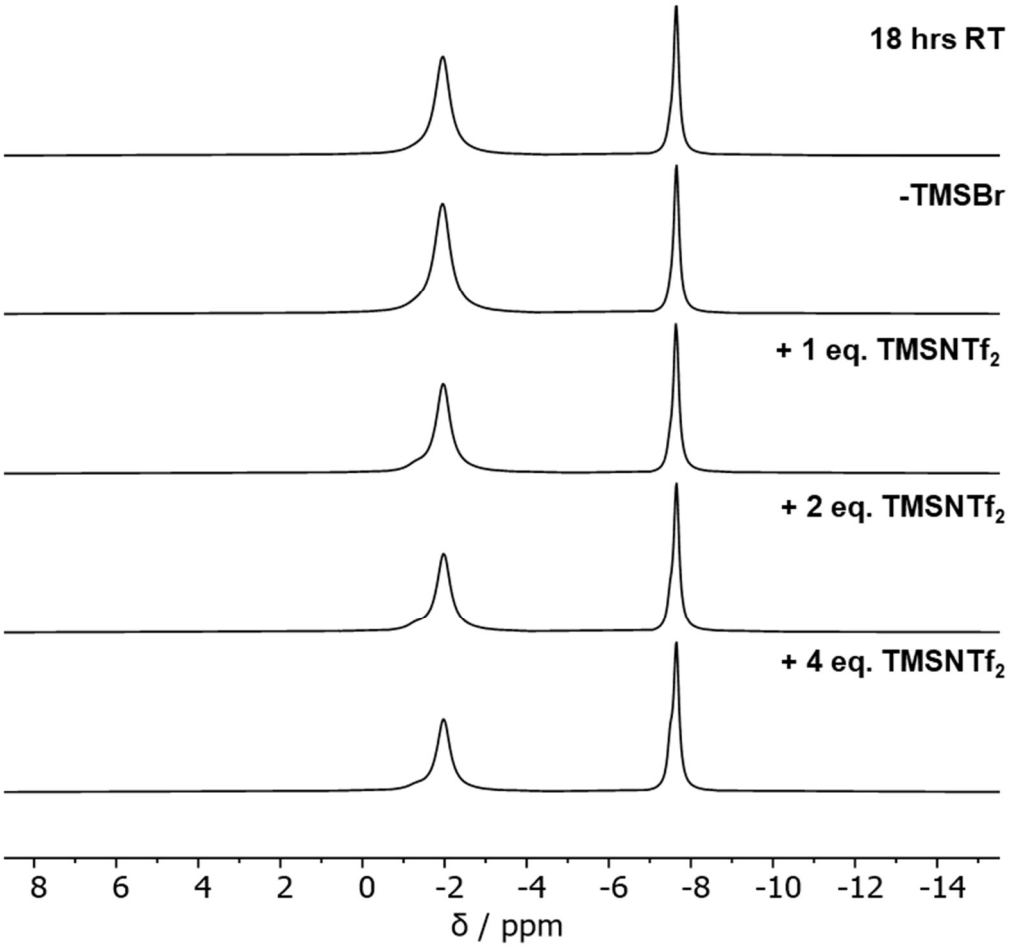

Figure 5.58: Stacked ^{11}B NMR (161 MHz, C_6H_5Cl) spectra for the reaction of *tetra*-bromo pyrazabole + 2.2 eq. $TMSNTf_2$, with subsequent removal/addition of TMSBr to demonstrate the reversibility of the reaction.

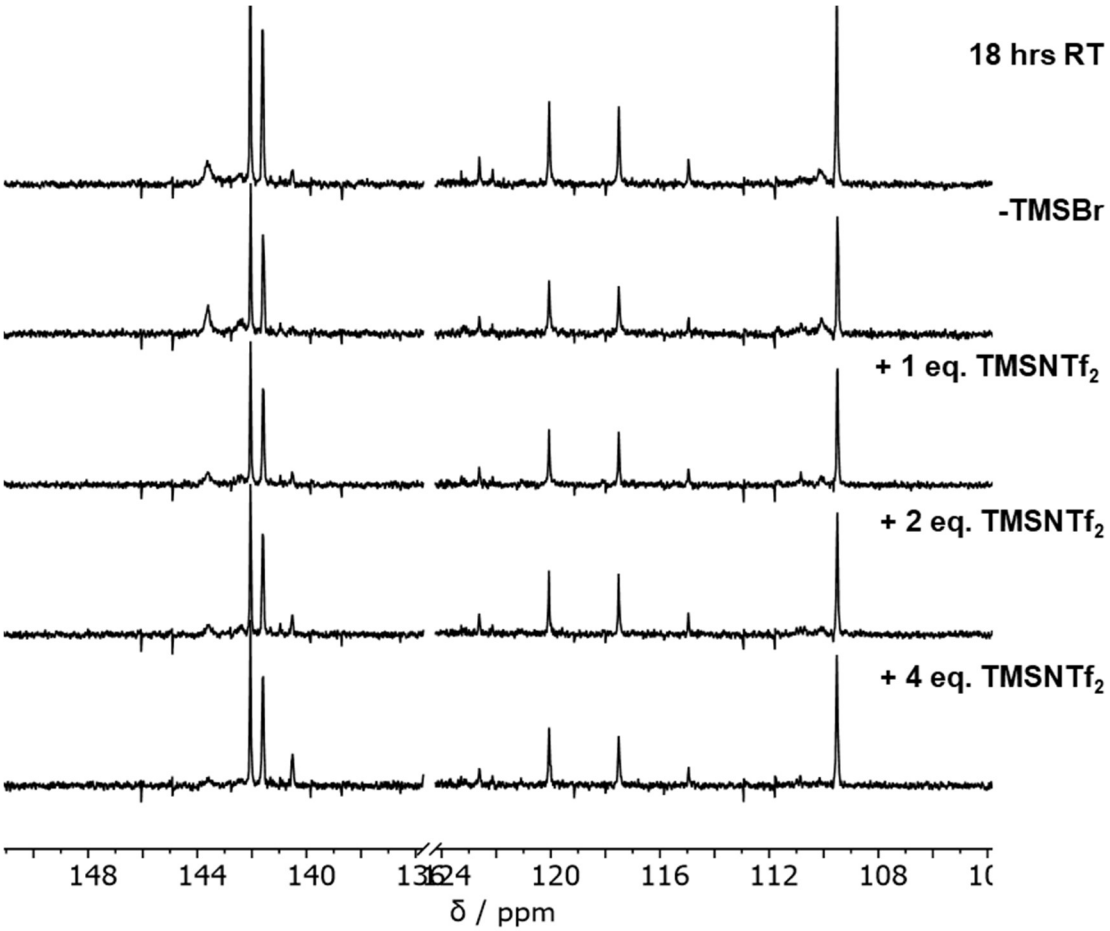

Figure 5.59: Stacked $^{13}C\{^{1}H\}$ NMR (126 MHz, C_6H_5Cl) spectra for the reaction of *tetra*-bromo pyrazabole + 2.2 eq. $TMSNTf_2$, with subsequent removal/addition of TMSBr to demonstrate the reversibility of the reaction. *Note: the ^{13}C solvent resonance has been omitted for clarity.*

Synthesis of *Tri*-Bromo *Mono*-NTf_2 Pyrazabole – 5.9

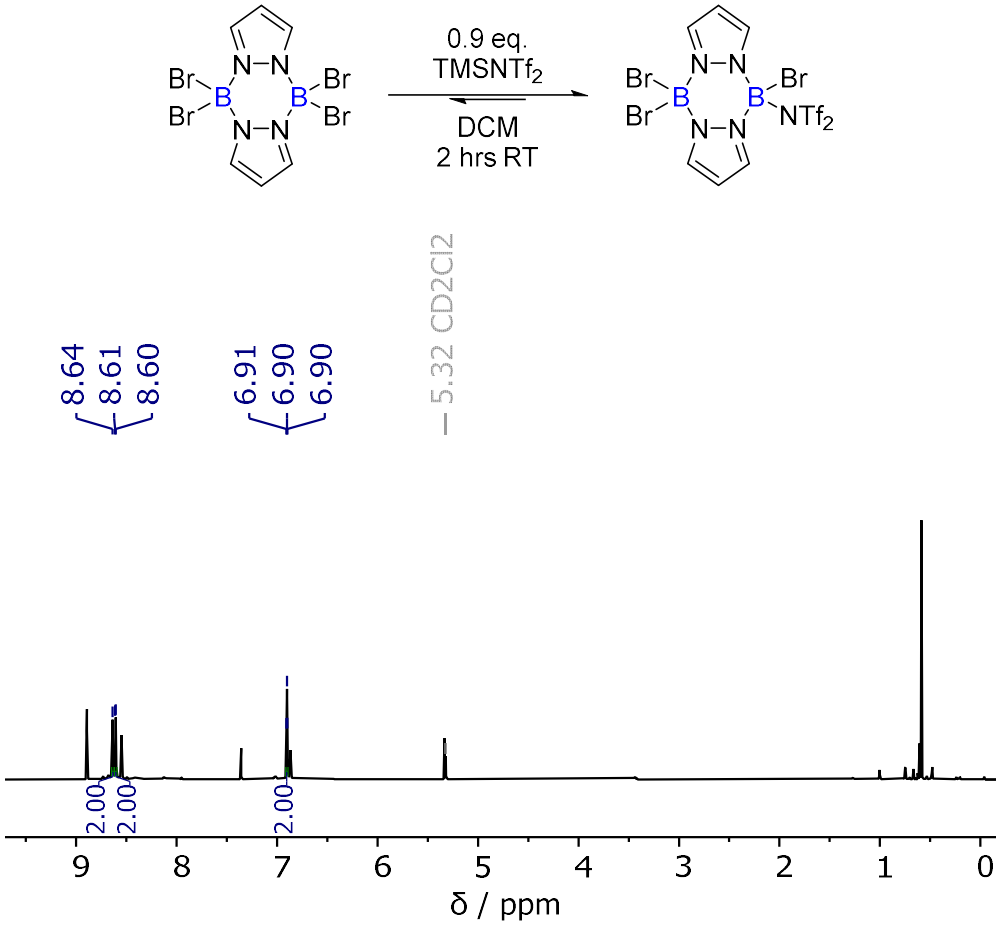

Figure 5.60: ^1H NMR (500 MHz, CD_2Cl_2) spectrum of *in situ* generated *tri*-bromo *mono*-NTf_2 pyrazabole. *Note: a small amount of residual tetra-bromo pyrazabole is also observed, along with minor $HNTf_2$ and TMSBr that was not removed in vacou*.

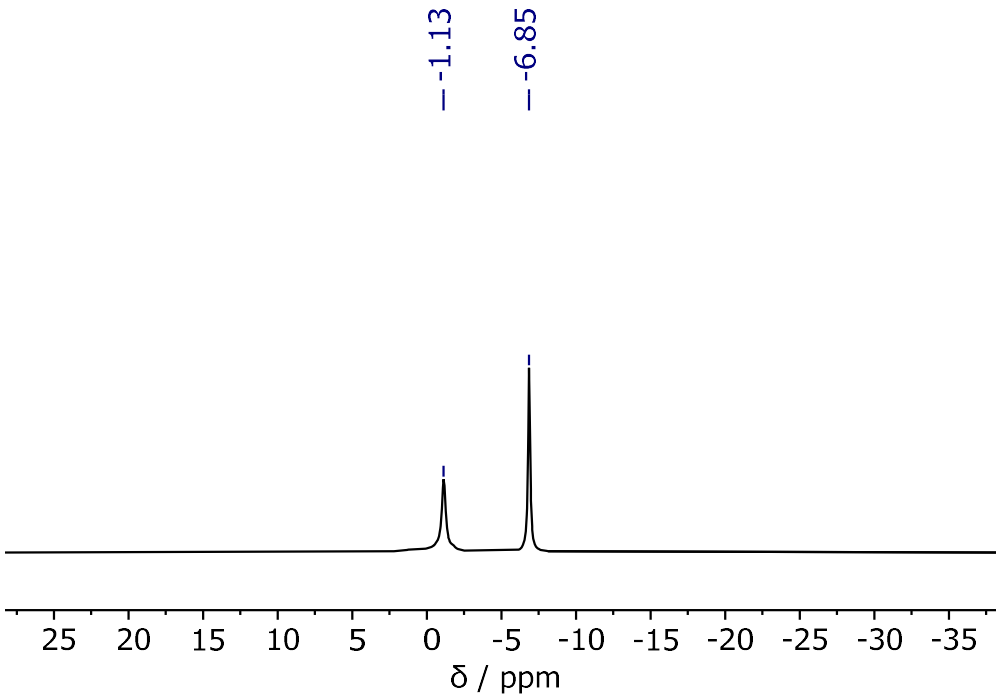

Figure 5.61: ^{11}B NMR (161 MHz, CD_2Cl_2) spectrum of *in situ* generated *tri*-bromo *mono*-NTf_2 pyrazabole. *Note: a small amount of residual tetra-bromo pyrazabole is also observed.*

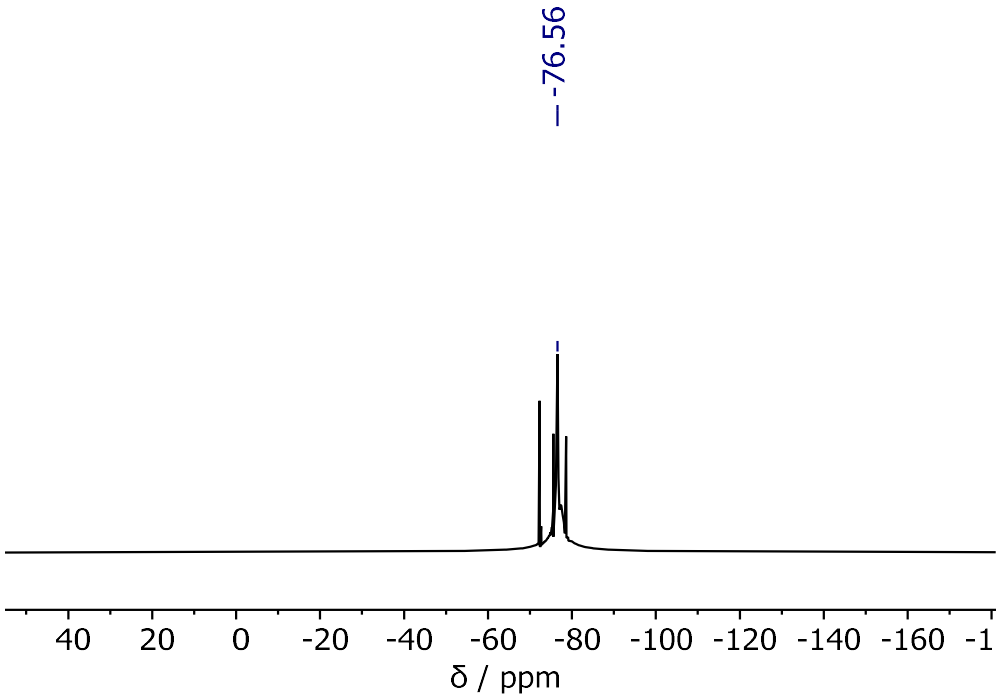

Figure 5.62: ^{19}F NMR (471 MHz, CD_2Cl_2) spectrum of *in situ* generated *tri*-bromo *mono*-NTf_2 pyrazabole.

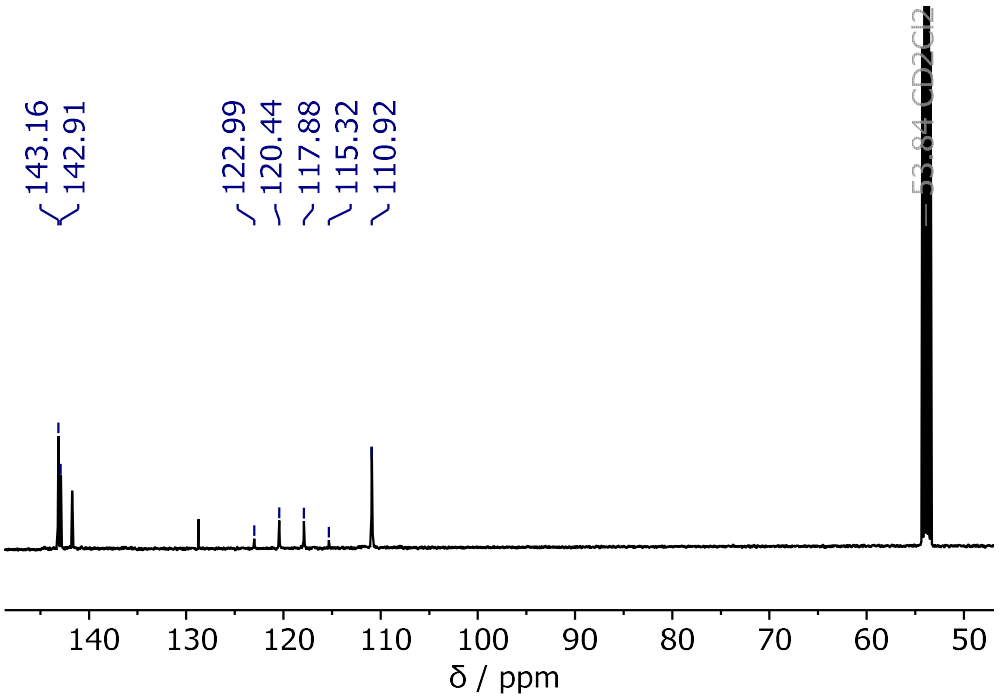

Figure 5.63: $^{13}C\{^{1}H\}$ NMR (126 MHz, CD_2Cl_2) spectrum of *in situ* generated *tri*-bromo *mono*-NTf_2 pyrazabole. *Note: a small amount of residual tetra-bromo pyrazabole is also observed, along with minor TMSBr that was not removed in vacou*.

Conversion of 5.9 to the 4-DMAP-Boronium Ion (5.10)

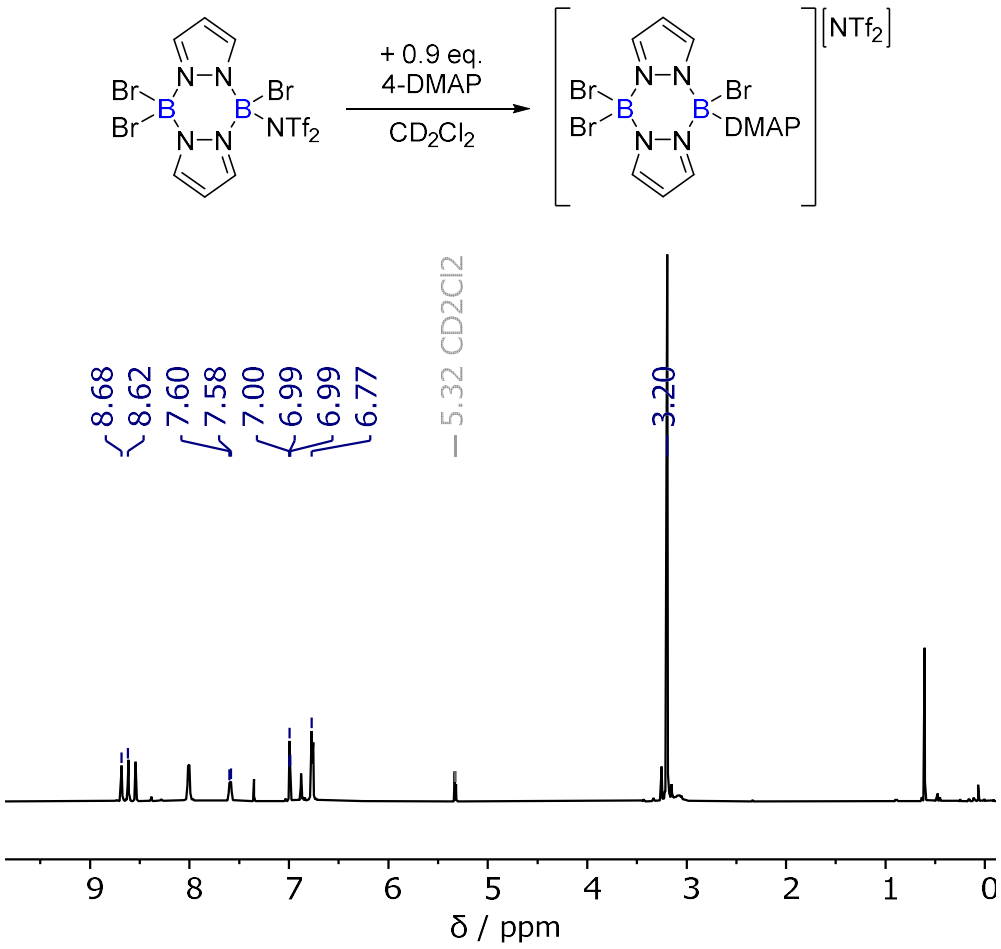

Figure 5.64: ^{1}H NMR (500 MHz, CD_2Cl_2) spectrum of the addition of 4-DMAP to *tri*-bromo *mono*-NTf_2 pyrazabole, forming the respective boronium ion. *Note: a small amount of residual tetra-bromo pyrazabole is also observed, along with minor [4DMAP-H][NTf₂].*

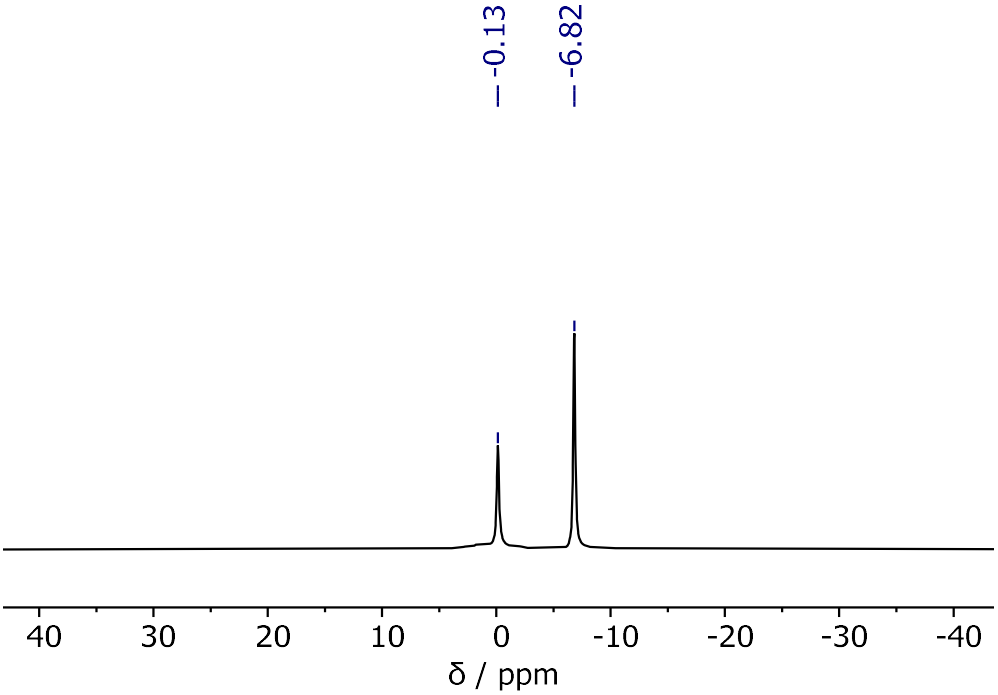

Figure 5.65: ^{11}B NMR (161 MHz, CD_2Cl_2) spectrum of the addition of 4-DMAP to *tri*-bromo *mono*-NTf_2 pyrazabole, forming the respective boronium ion. *Note: a small amount of residual tetra-bromo pyrazabole is also observed.*

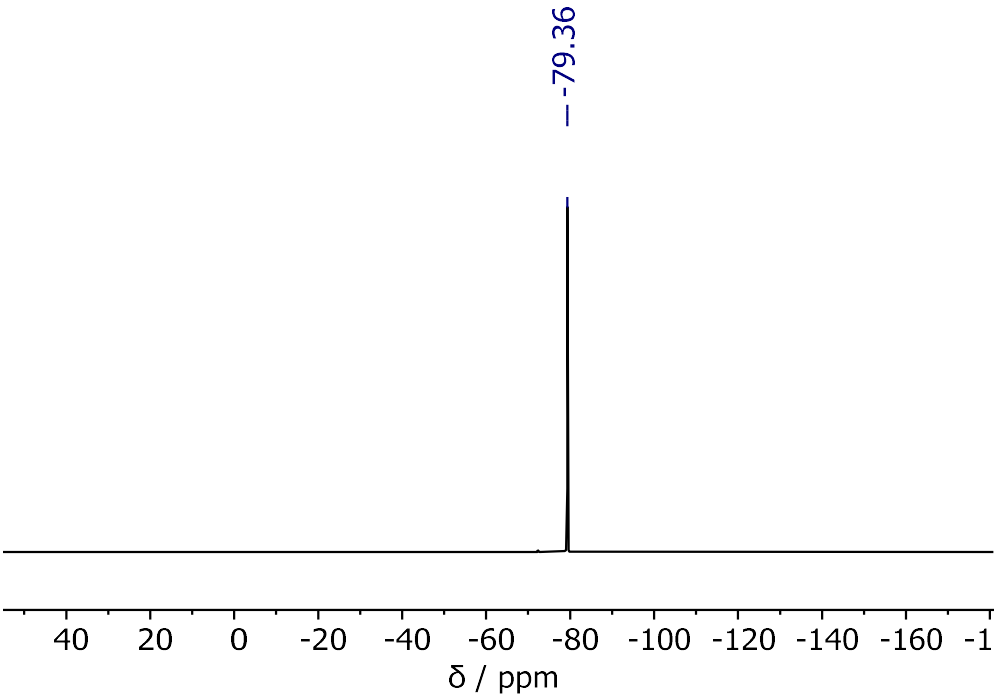

Figure 5.66: ^{19}F NMR (471 MHz, CD_2Cl_2) of the addition of 4-DMAP to *tri*-bromo *mono*-NTf_2 pyrazabole, forming the respective boronium ion.

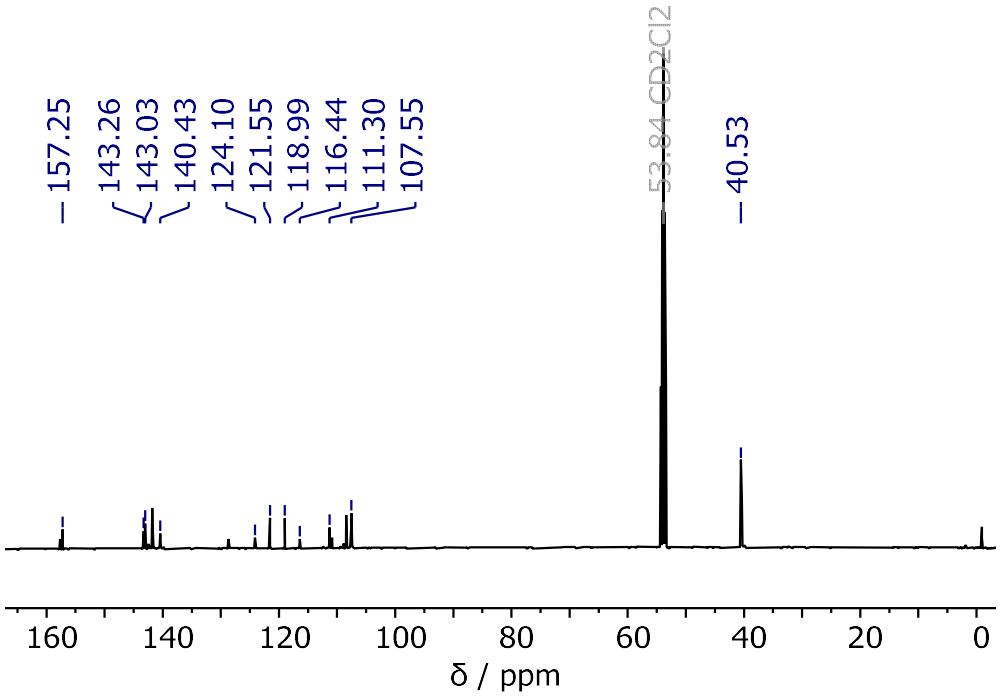

Figure 5.67: $^{13}C\{^{1}H\}$ NMR (126 MHz, CD_2Cl_2) spectrum of the addition of 4-DMAP to *tri*-bromo *mono*-NTf_2 pyrazabole, forming the respective boronium ion. *Note: a small amount of residual tetra-bromo pyrazabole is also observed, along with minor [4DMAP-H][NTf_2].*

Reactivity of *Mono*-Electrophile 5.9 with *N*-Methyl Indole

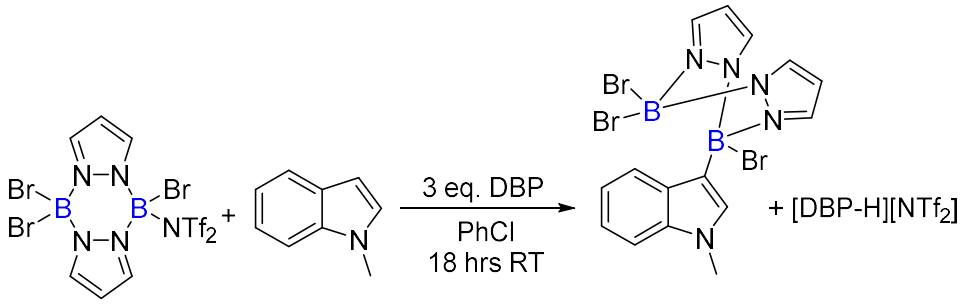

- **NMR spectra after 18 hours RT:**

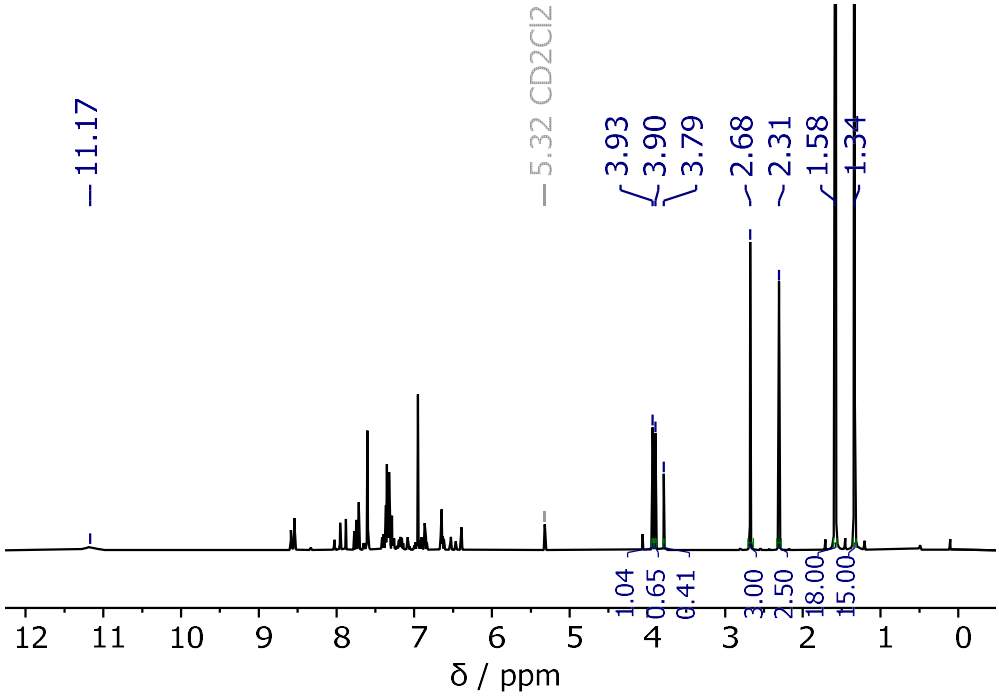

Figure 5.68: ^{1}H NMR (500 MHz, CD_2Cl_2) spectrum of the reaction of *tri*-bromo *mono*-NTf_2 pyrazabole with 3 equiv. DBP and 1 equiv. *N*-methyl indole, after 18 hours at RT.

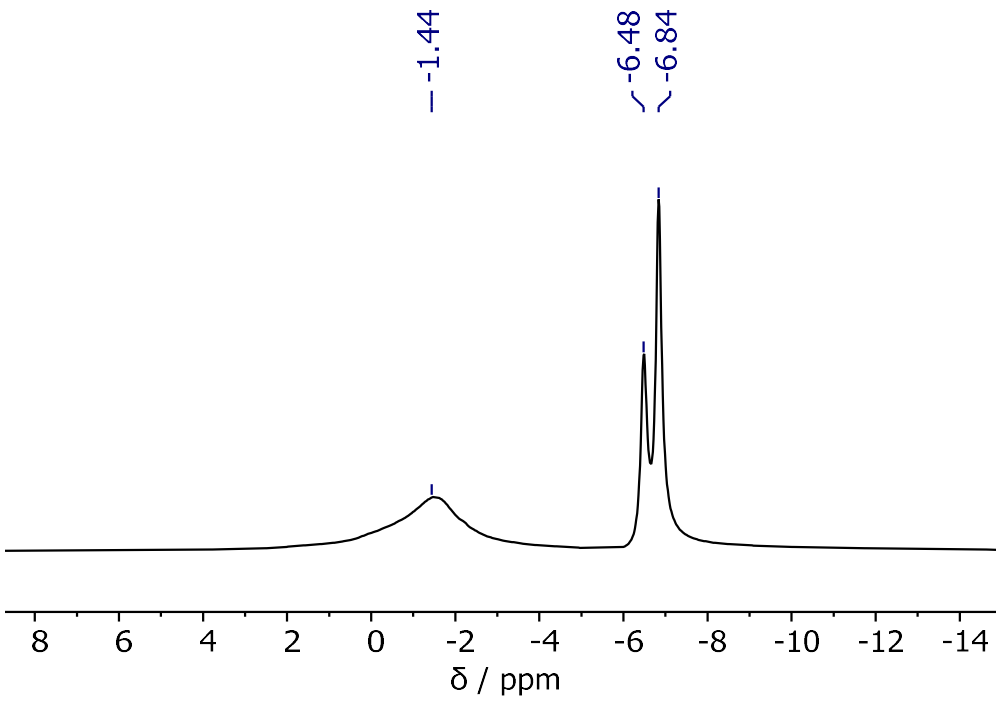

Figure 5.69: ^{11}B NMR (161 MHz, CD_2Cl_2) spectrum of the reaction of *tri*-bromo *mono*-NTf_2 pyrazabole with 3 equiv. DBP and 1 equiv. *N*-methyl indole, after 18 hours at RT.

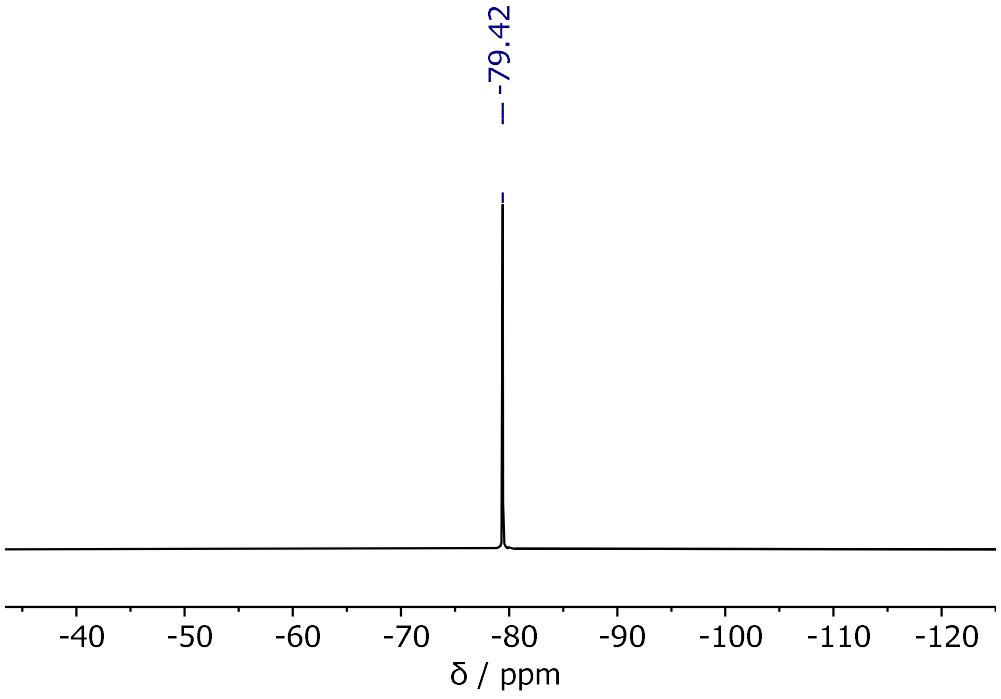

Figure 5.70: ^{19}F NMR (471 MHz, CD_2Cl_2) spectrum of the reaction of *tri*-bromo *mono*-NTf_2 pyrazabole with 3 equiv. DBP and 1 equiv. *N*-methyl indole, after 18 hours at RT.

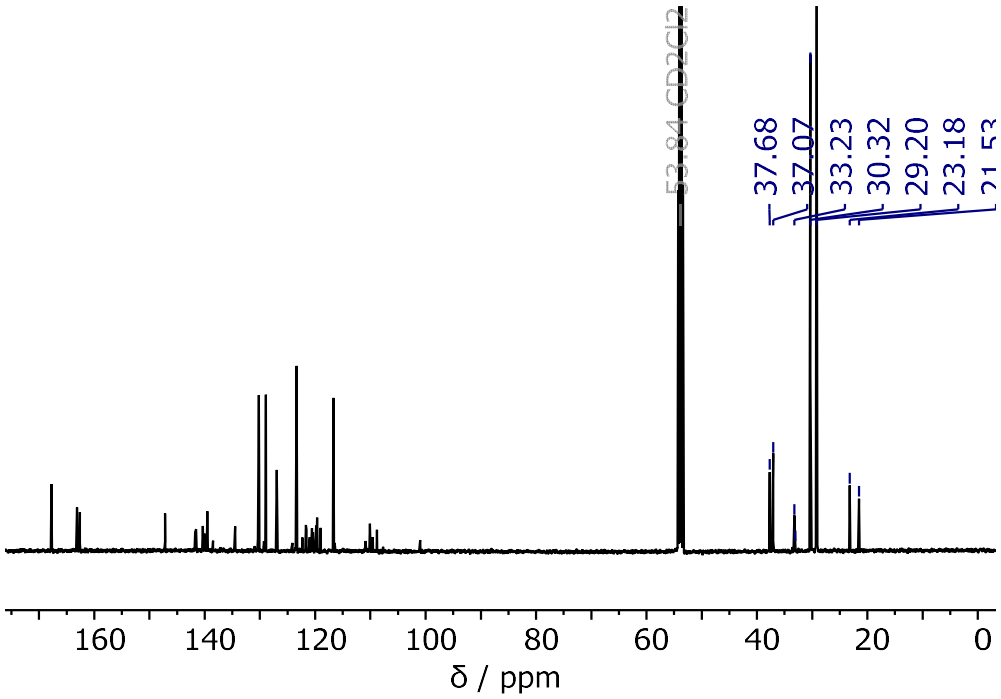

Figure 5.71: $^{13}C\{^{1}H\}$ NMR (126 MHz, CD_2Cl_2) spectrum of the reaction of *tri*-bromo *mono*-NTf_2 pyrazabole with 3 equiv. DBP and 1 equiv. *N*-methyl indole, after 18 hours at RT.

- **NMR spectra after pinacol protection in D_2O/CD_2Cl_2:**

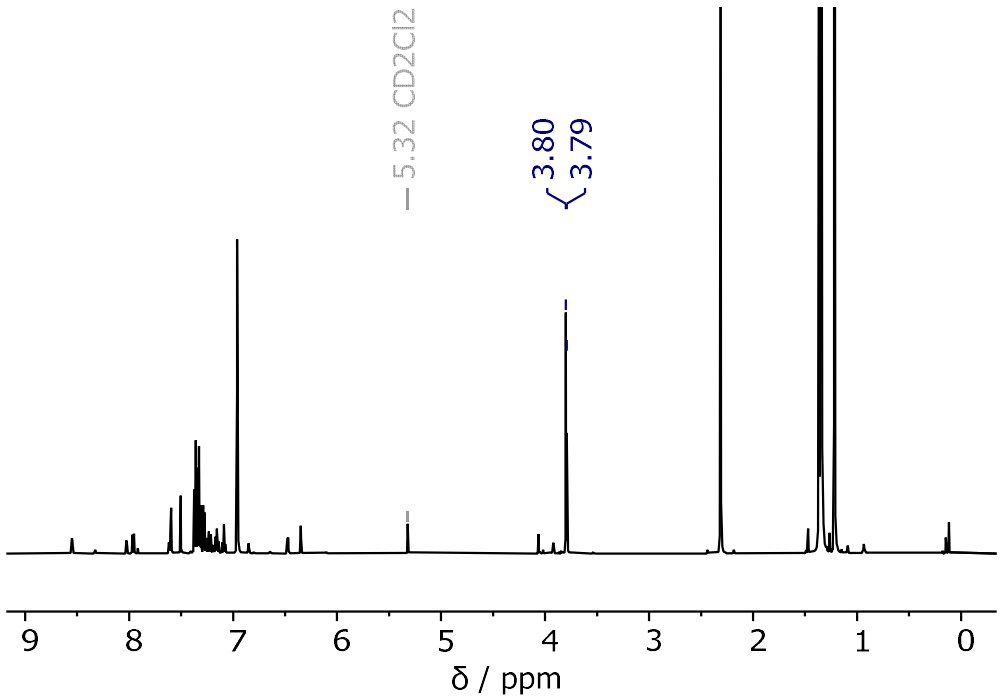

Figure 5.72: ^{1}H NMR (500 MHz, CD_2Cl_2) spectrum of the reaction of *tri*-bromo *mono*-NTf_2 pyrazabole with 3 equiv. DBP and 1 equiv. *N*-methyl indole, after pinacol protection.

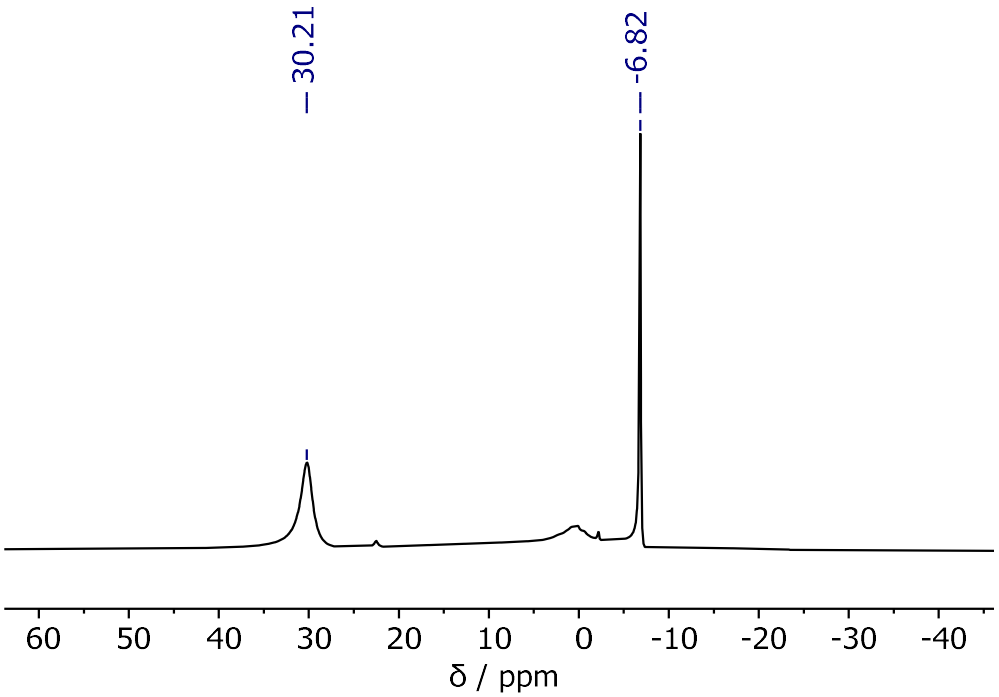

Figure 5.73: ^{11}B NMR (161 MHz, CD_2Cl_2) spectrum of the reaction of *tri*-bromo *mono*-NTf_2 pyrazabole with 3 equiv. DBP and 1 equiv. *N*-methyl indole, after pinacol protection.

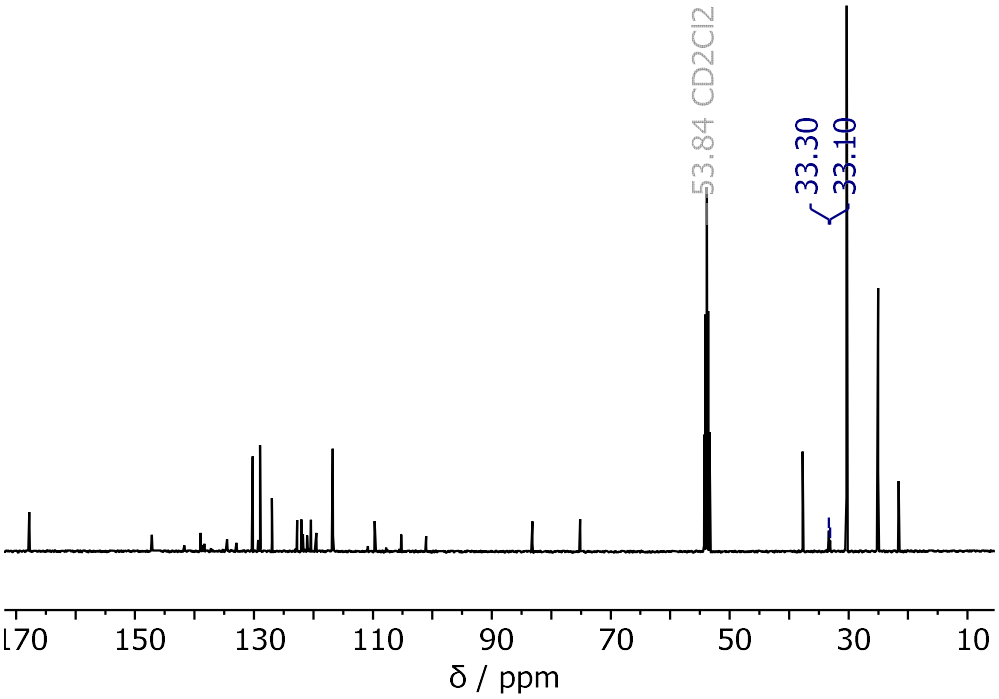

Figure 5.74: $^{13}C\{^1H\}$ NMR (126 MHz, CD_2Cl_2) spectrum of the reaction of *tri*-bromo *mono*-NTf_2 pyrazabole with 3 equiv. DBP and 1 equiv. *N*-methyl indole, after pinacol protection.

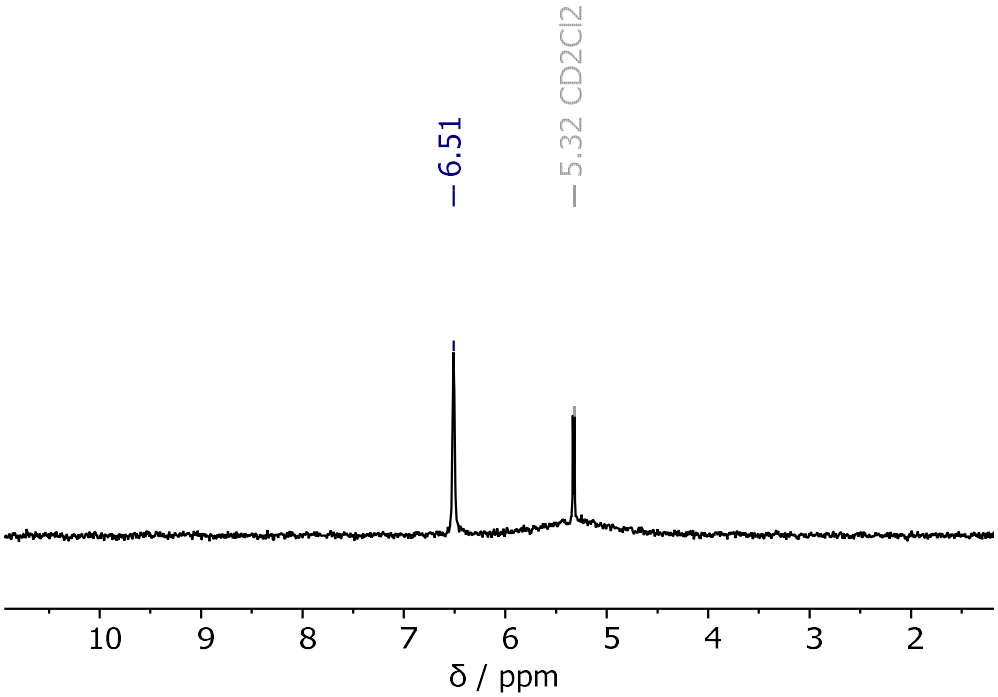

Figure 5.75: ^{2}H NMR (77 MHz, CH_2Cl_2) spectrum of the reaction of *tri*-bromo *mono*-NTf_2 pyrazabole with 3 equiv. DBP and 1 equiv. *N*-methyl indole, after pinacol protection.

Stepwise Reactivity of *Mono*-Electrophile 5.9 with *N*-Methyl Indole

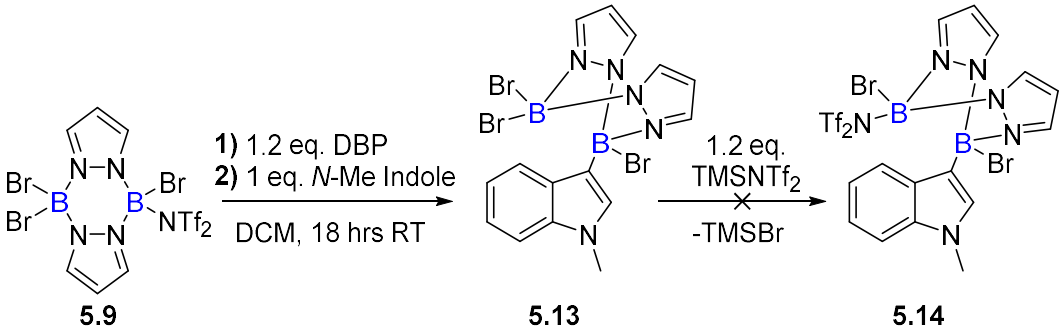

- **NMR spectra after addition of further $TMSNTf_2$, 18 hours RT:**

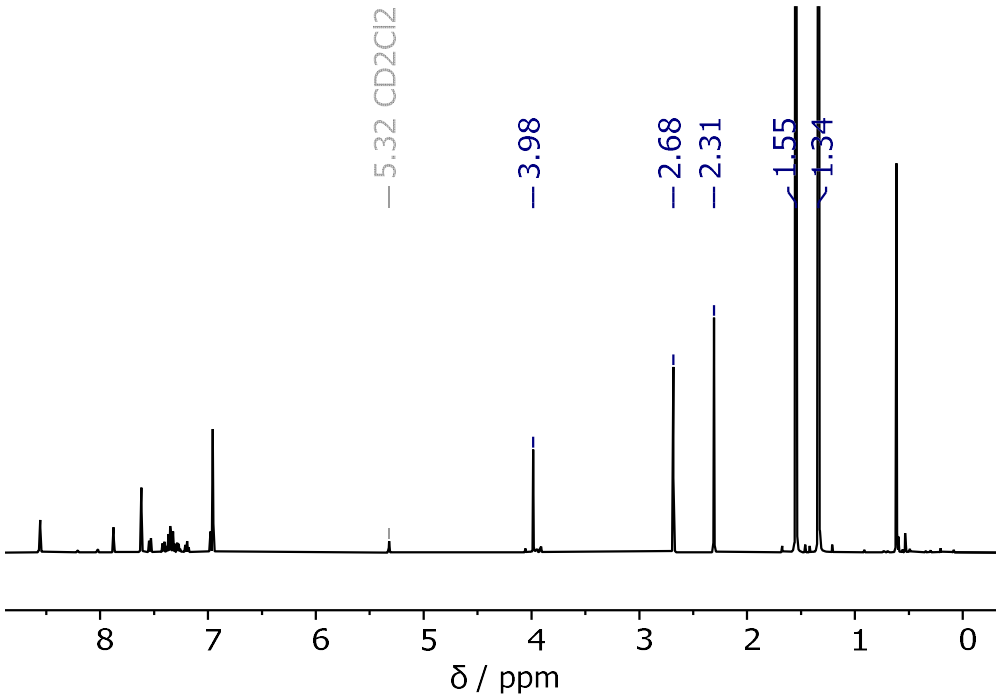

Figure 5.76: ^1H NMR (500 MHz, CD_2Cl_2) spectrum of the stepwise reaction of *tri*-bromo *mono*-NTf_2 pyrazabole with DBP and *N*-methyl indole, followed by further $TMSNTf_2$ and 18 hours at RT.

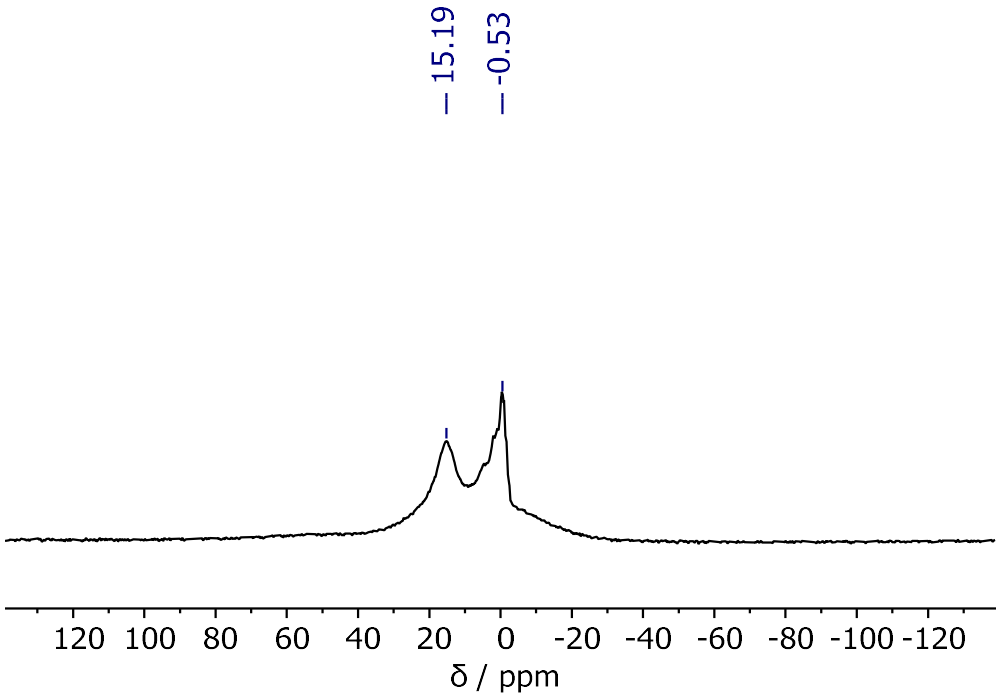

Figure 5.77: ^{11}B NMR (161 MHz, CD_2Cl_2) spectrum of the stepwise reaction of *tri*-bromo *mono*-NTf_2 pyrazabole with DBP and *N*-methyl indole, followed by further $TMSNTf_2$ and 18 hours at RT.

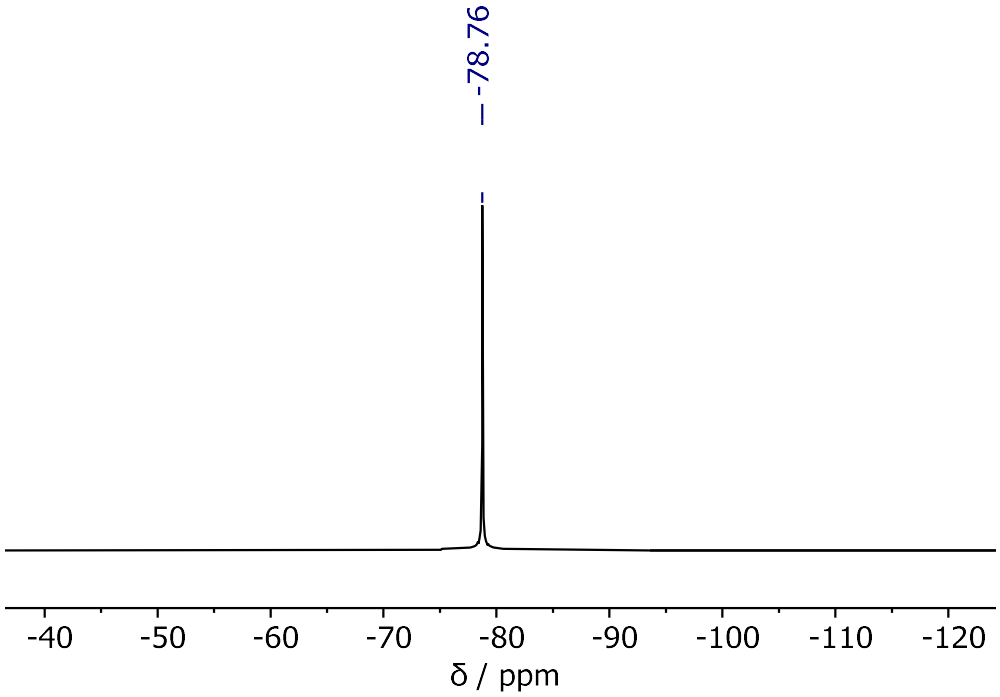

Figure 5.78: ^{19}F NMR (471 MHz, CD_2Cl_2) spectrum of the stepwise reaction of *tri*-bromo *mono*-NTf_2 pyrazabole with DBP and *N*-methyl indole, followed by further $TMSNTf_2$ and 18 hours at RT.

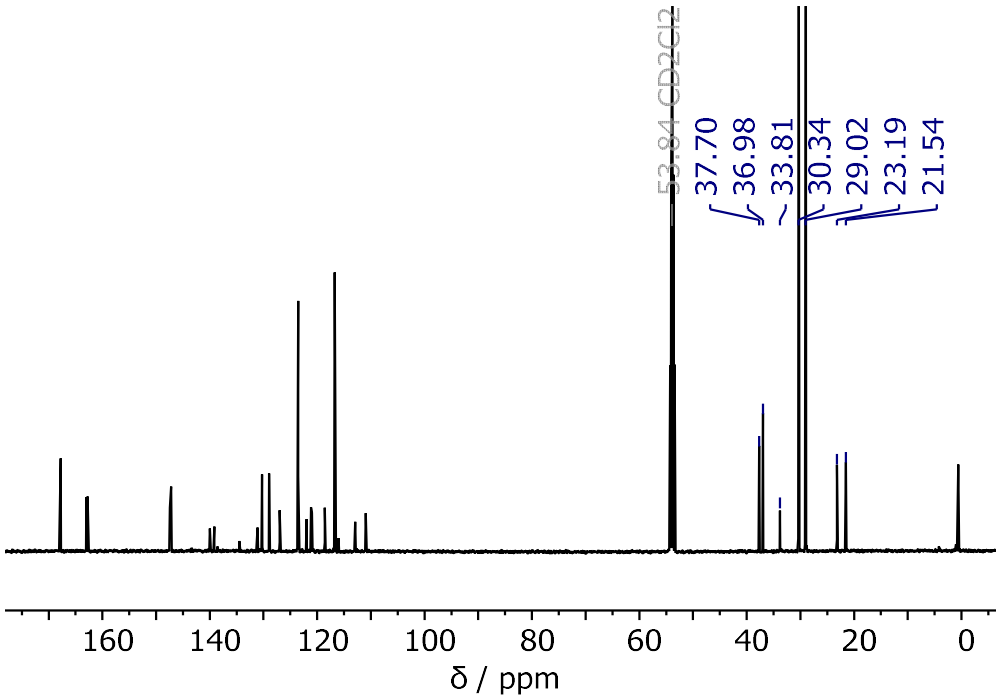

Figure 5.79: $^{13}C\{^{1}H\}$ NMR (126 MHz, CD_2Cl_2) spectrum of the stepwise reaction of *tri*-bromo *mono*-NTf_2 pyrazabole with DBP and *N*-methyl indole, followed by further $TMSNTf_2$ and 18 hours at RT.

- **NMR spectra after pinacol protection in D_2O/CD_2Cl_2:**

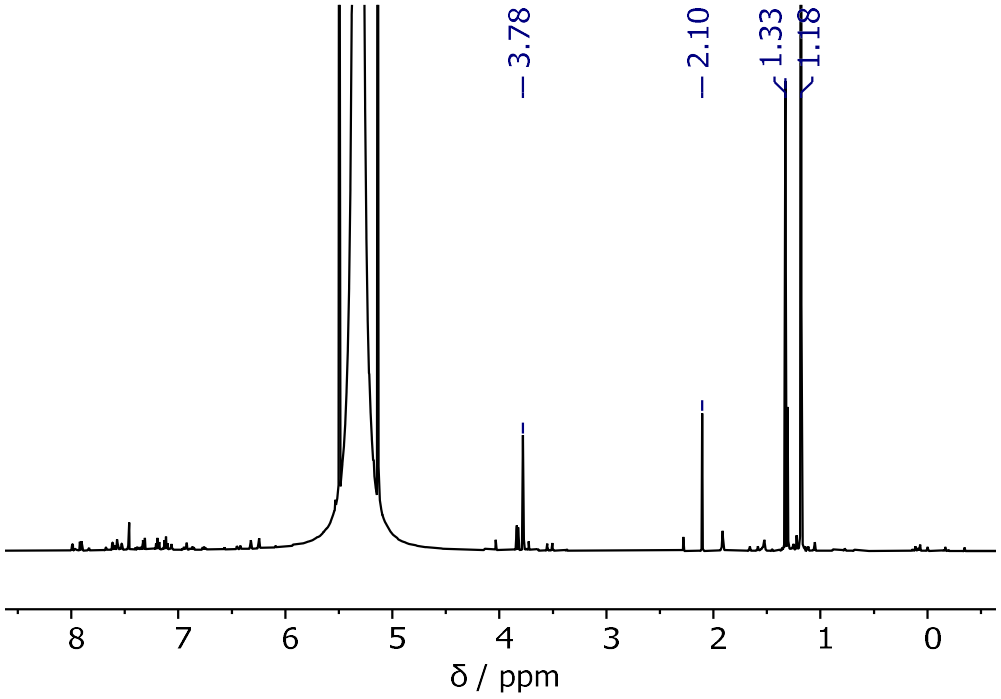

Figure 5.80: ^{1}H NMR (500 MHz, CH_2Cl_2) spectrum of the stepwise reaction of *tri*-bromo *mono*-NTf_2 pyrazabole with DBP and *N*-methyl indole, after pinacol protection.

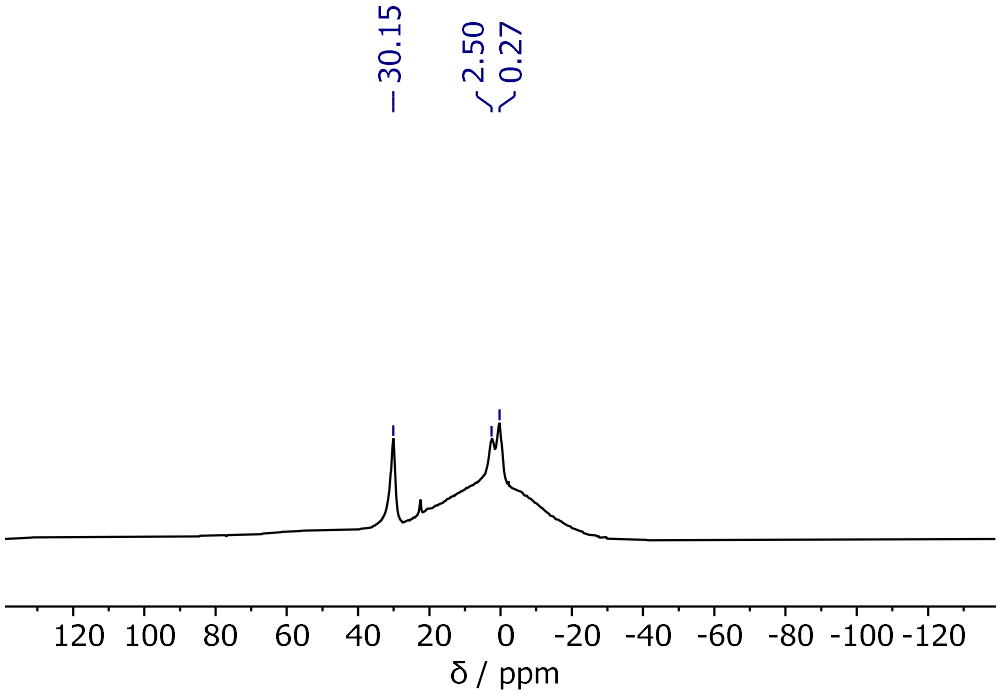

Figure 5.81: ^{11}B NMR (161 MHz, CH_2Cl_2) spectrum of the stepwise reaction of *tri*-bromo *mono*-NTf_2 pyrazabole with DBP and *N*-methyl indole, after pinacol protection.

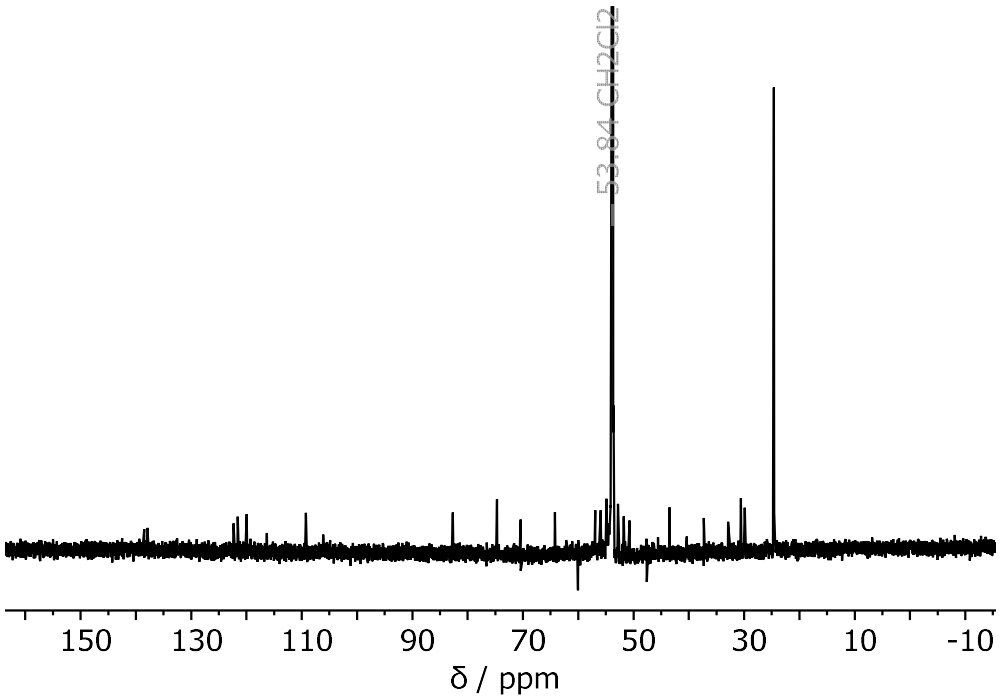

Figure 5.82: $^{13}C\{^{1}H\}$ NMR (126 MHz, CH_2Cl_2) spectrum of the stepwise reaction of *tri*-bromo *mono*-NTf_2 pyrazabole with DBP and *N*-methyl indole, after pinacol protection.

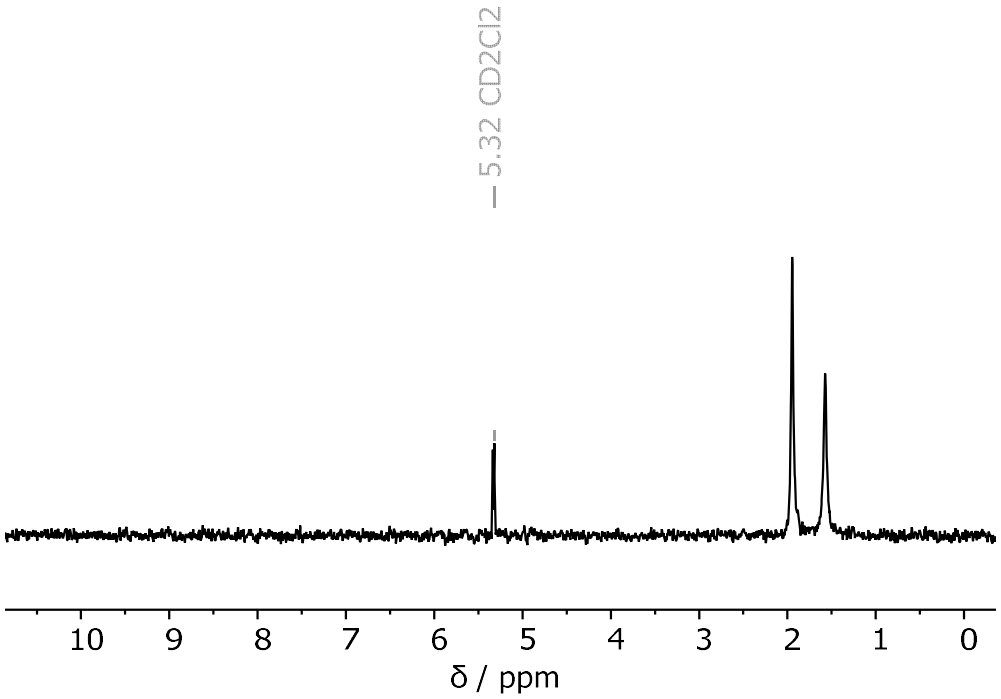

Figure 5.83: ^{2}H NMR (77 MHz, CH_2Cl_2) spectrum of the stepwise reaction of *tri*-bromo *mono*-NTf_2 pyrazabole with DBP and *N*-methyl indole, after pinacol protection.

Synthesis of *Di*-Bromo *Di*-NTf_2 Pyrazabole – 5.4

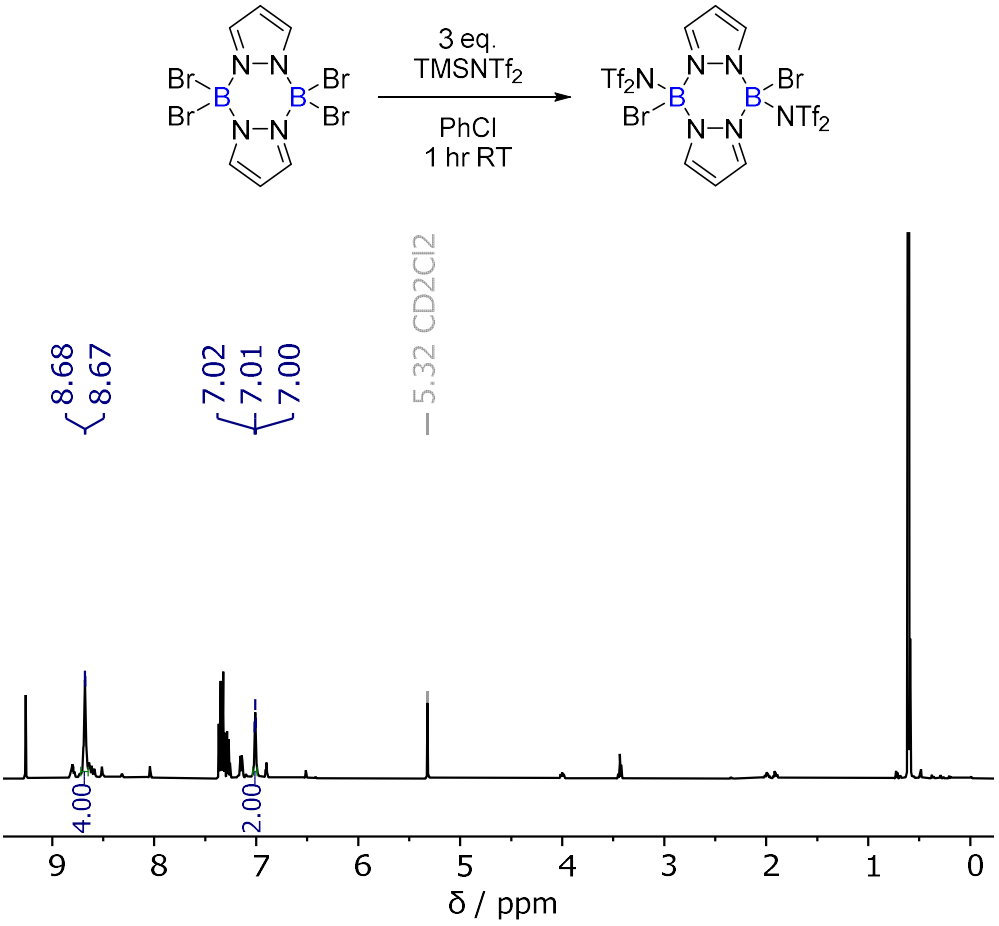

Figure 5.84: ^1H NMR (500 MHz, CD_2Cl_2) spectrum of *in situ* generated *di*-bromo *di*-NTf_2 pyrazabole. *Note: a small amount of residual PhCl and TMSBr is also observed that was not removed in vacou.*

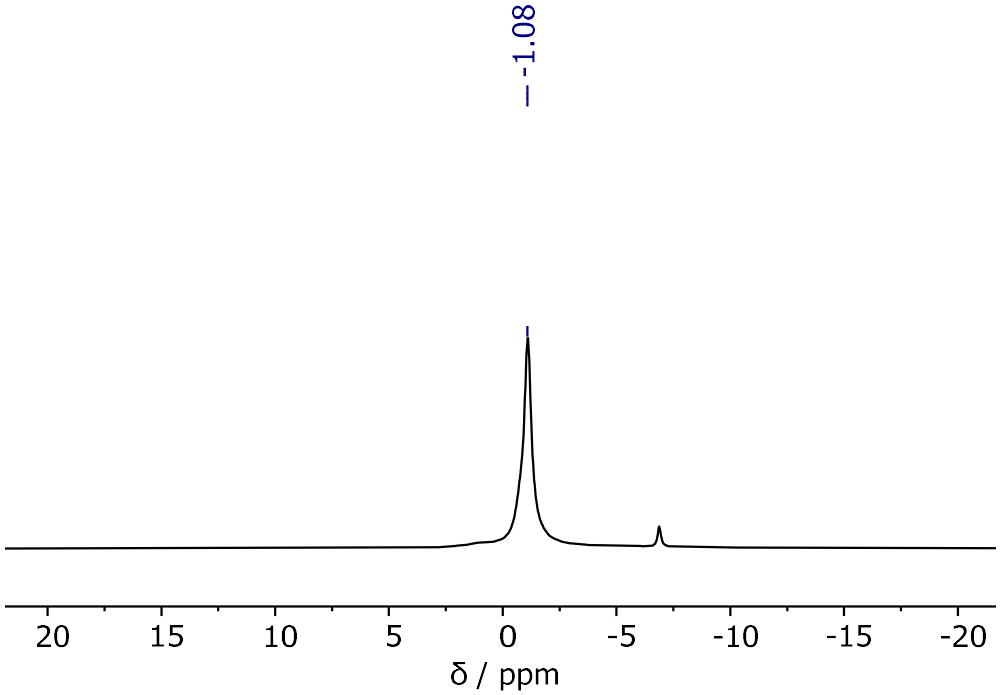

Figure 5.85: ^{11}B NMR (161 MHz, CD_2Cl_2) spectrum of *in situ* generated *di*-bromo *di*-NTf_2 pyrazabole.

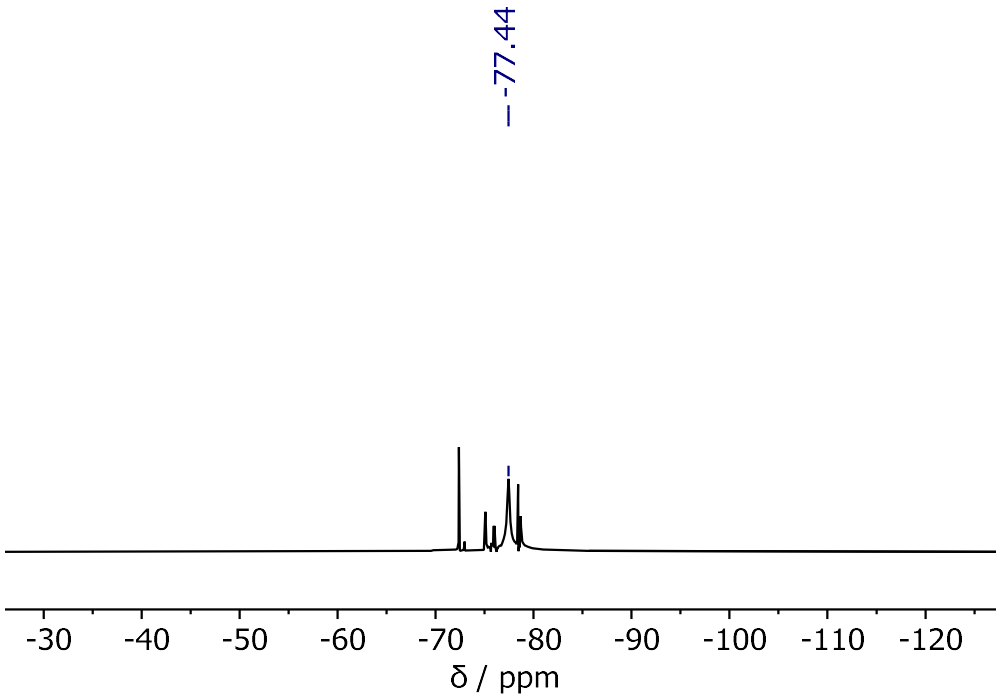

Figure 5.86: ^{19}F NMR (471 MHz, CD_2Cl_2) spectrum of *in situ* generated *di*-bromo *di*-NTf_2 pyrazabole.

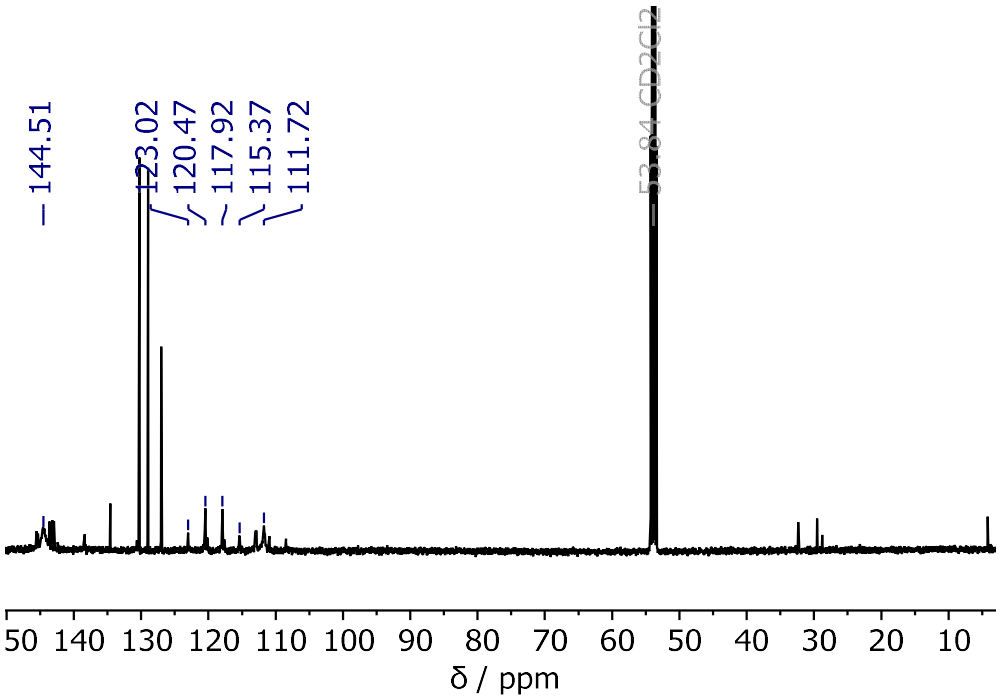

Figure 5.87: $^{13}C\{^{1}H\}$ NMR (126 MHz, CD_2Cl_2) spectrum of *in situ* generated *di*-bromo *di*-NTf_2 pyrazabole. *Note: a small amount of residual PhCl and TMSBr is also observed that was not removed in vacou*.

5.5.6 – Reactivity of *Tetra*-Chloro Pyrazabole with $TMSNTf_2$

Synthesis of *Tri*-Chloro *Mono*-NTf_2 Pyrazabole – 5.11

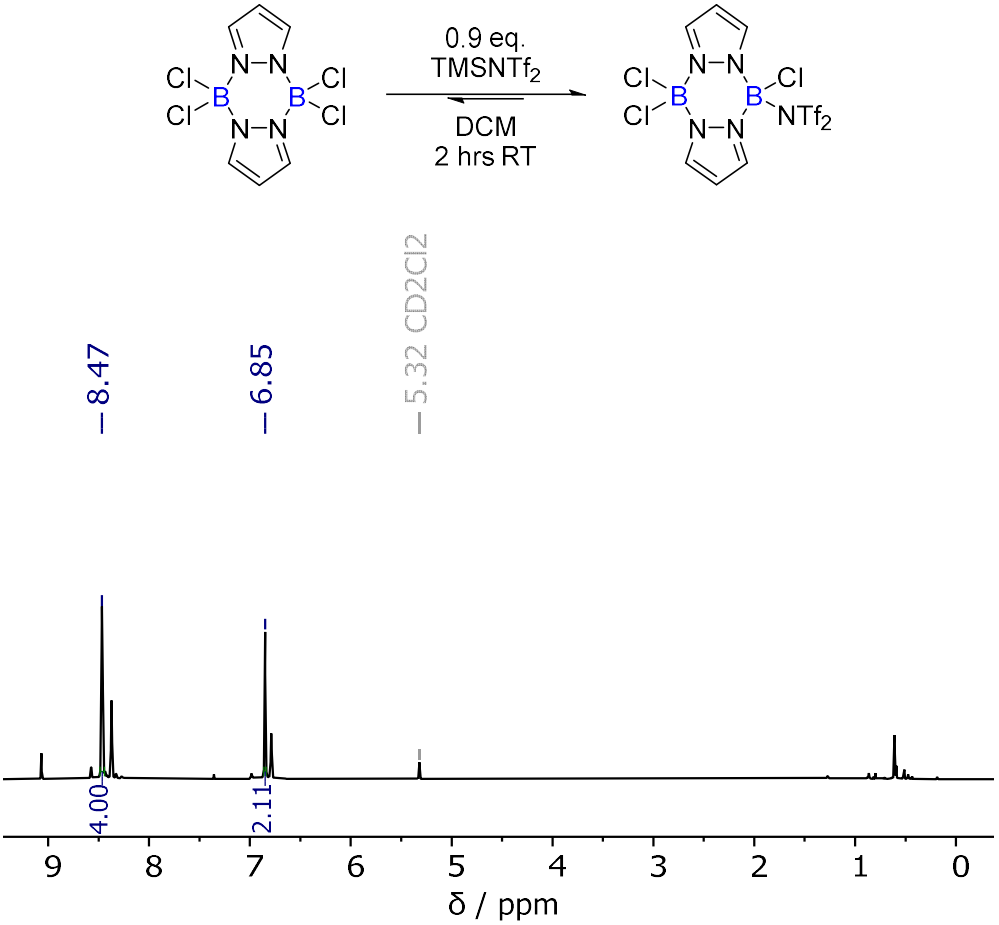

Figure 5.88: ^1H NMR (500 MHz, CD_2Cl_2) spectrum of *in situ* generated *tri*-chloro *mono*-NTf_2 pyrazabole. *Note: a small amount of residual tetra-chloro pyrazabole is also observed, along with minor $HNTf_2$ and TMSCl that was not removed in vacou*.

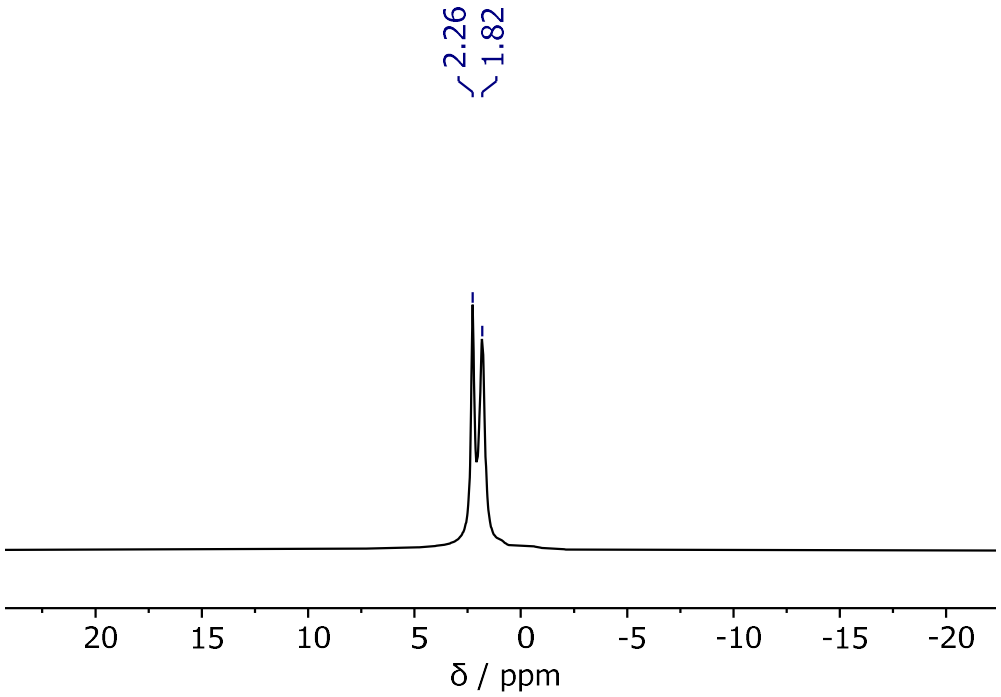

Figure 5.89: ^{11}B NMR (161 MHz, CD_2Cl_2) spectrum of *in situ* generated *tri*-chloro *mono*-NTf_2 pyrazabole. *Note: a small amount of residual tetra-chloro pyrazabole is also observed.*

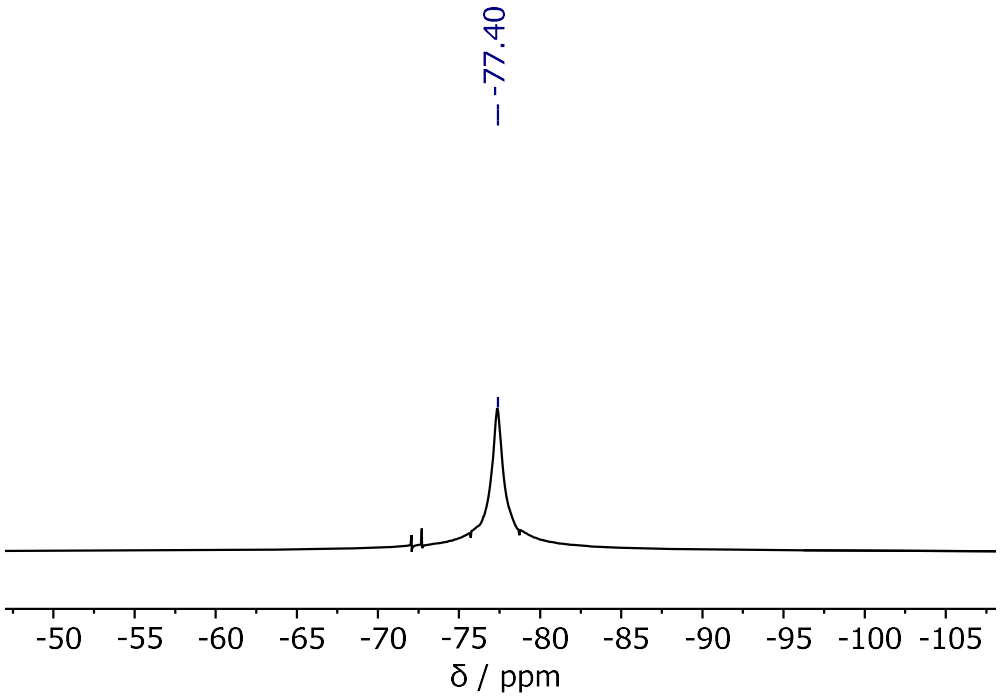

Figure 5.90: ^{19}F NMR (471 MHz, CD_2Cl_2) spectrum of *in situ* generated *tri*-chloro *mono*-NTf_2 pyrazabole.

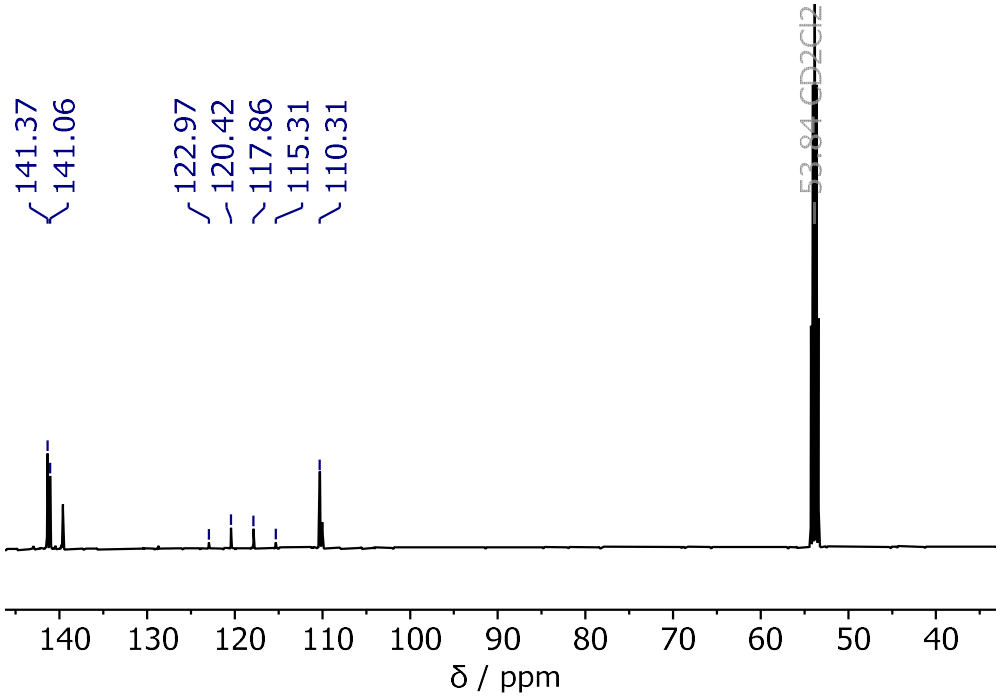

Figure 5.91: $^{13}C\{^{1}H\}$ NMR (126 MHz, CD_2Cl_2) spectrum of *in situ* generated *tri*-chloro *mono*-NTf_2 pyrazabole. *Note: a small amount of residual tetra-chloro pyrazabole is also observed.*

Conversion of 5.11 to the 4-DMAP-Boronium Ion (5.12)

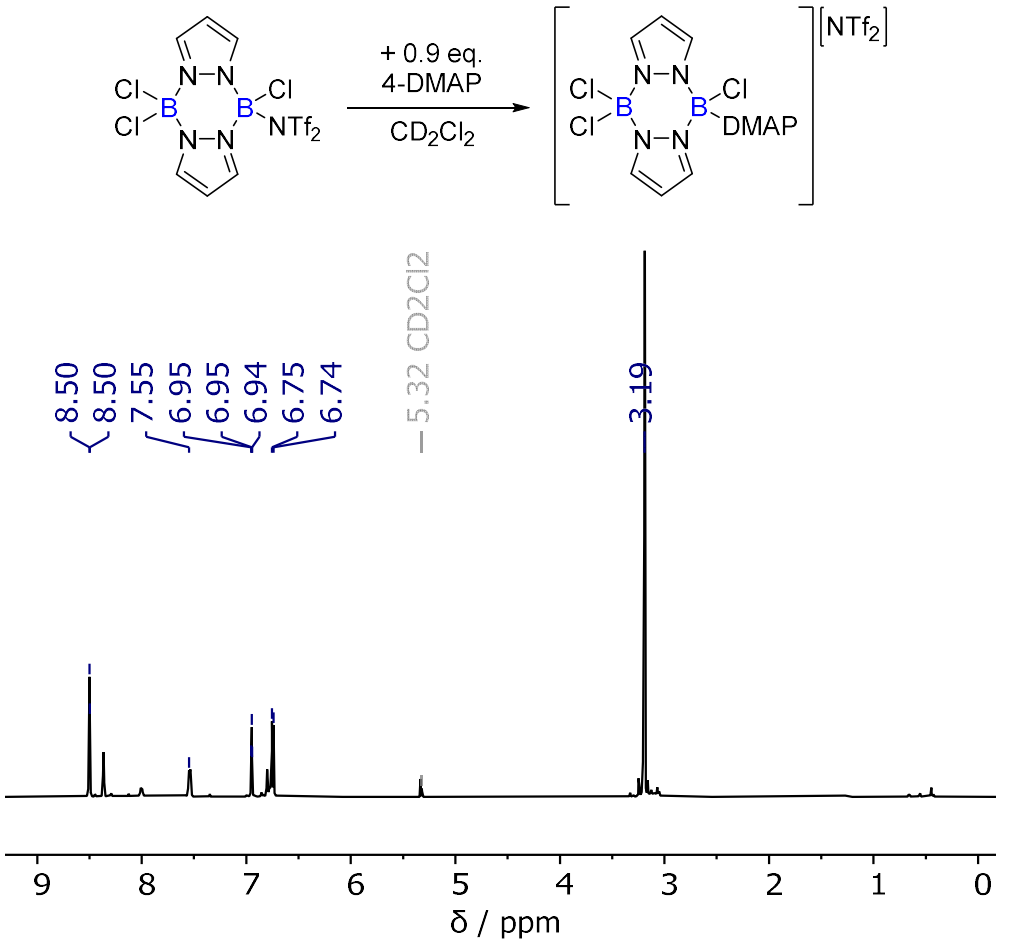

Figure 5.92: ^{1}H NMR (500 MHz, CD_2Cl_2) spectrum of the addition of 4-DMAP to *tri*-chloro *mono*-NTf_2 pyrazabole, forming the respective boronium ion. *Note: a small amount of residual tetra-chloro pyrazabole is also observed, along with minor [4DMAP-H][NTf$_2$].*

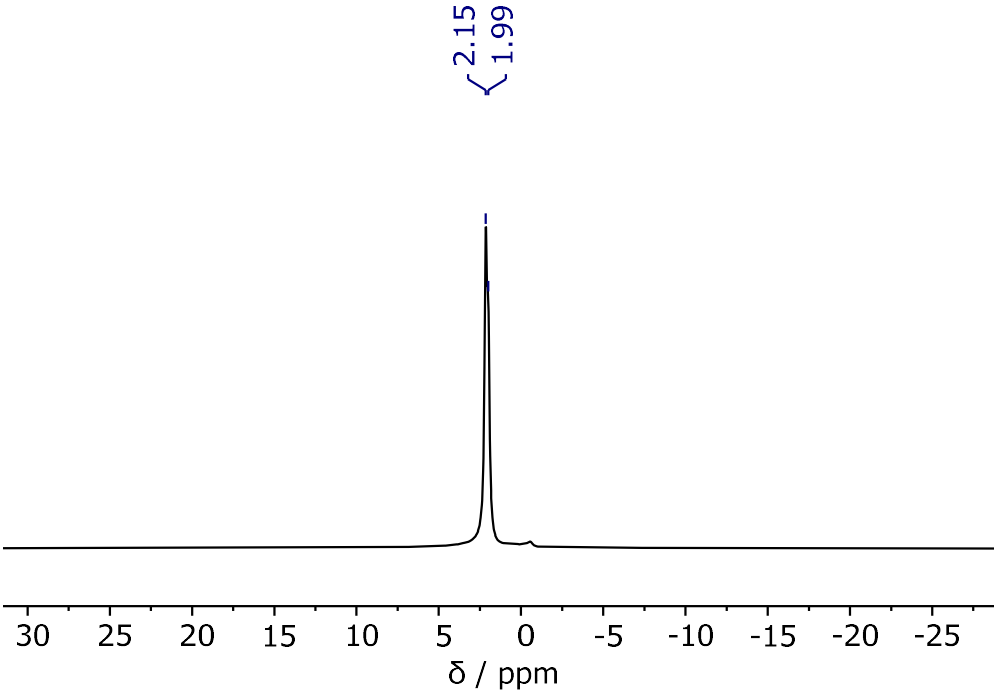

Figure 5.93: ^{11}B NMR (161 MHz, CD_2Cl_2) spectrum of the addition of 4-DMAP to *tri*-chloro *mono*-NTf_2 pyrazabole, forming the respective boronium ion. *Note: a small amount of residual tetra-chloro pyrazabole is also observed.*

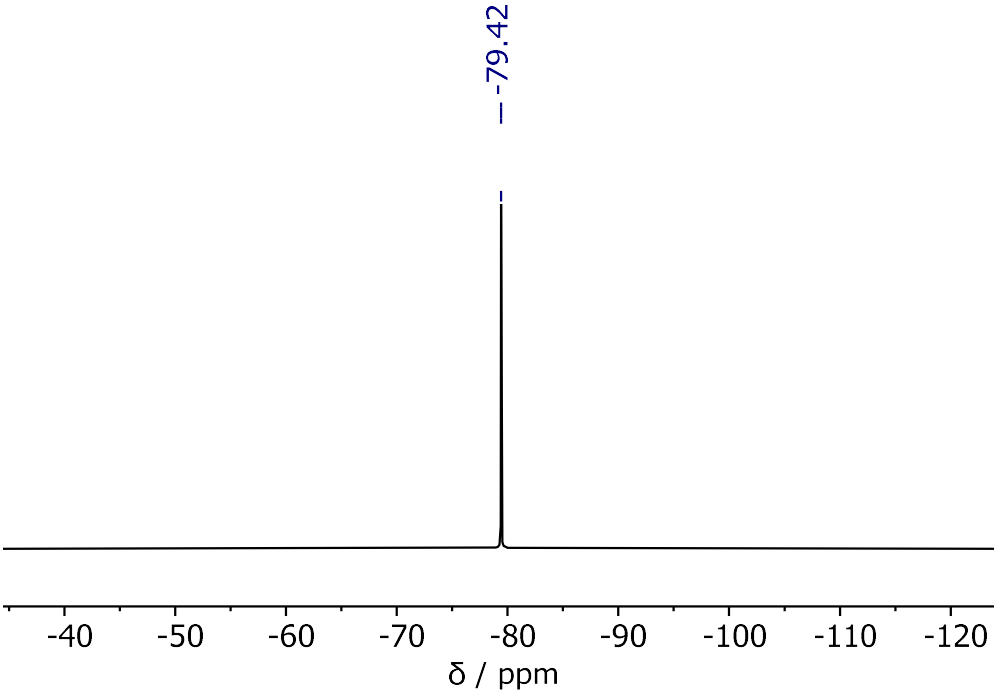

Figure 5.94: ^{19}F NMR (471 MHz, CD_2Cl_2) spectrum of the addition of 4-DMAP to *tri*-chloro *mono*-NTf_2 pyrazabole, forming the respective boronium ion.

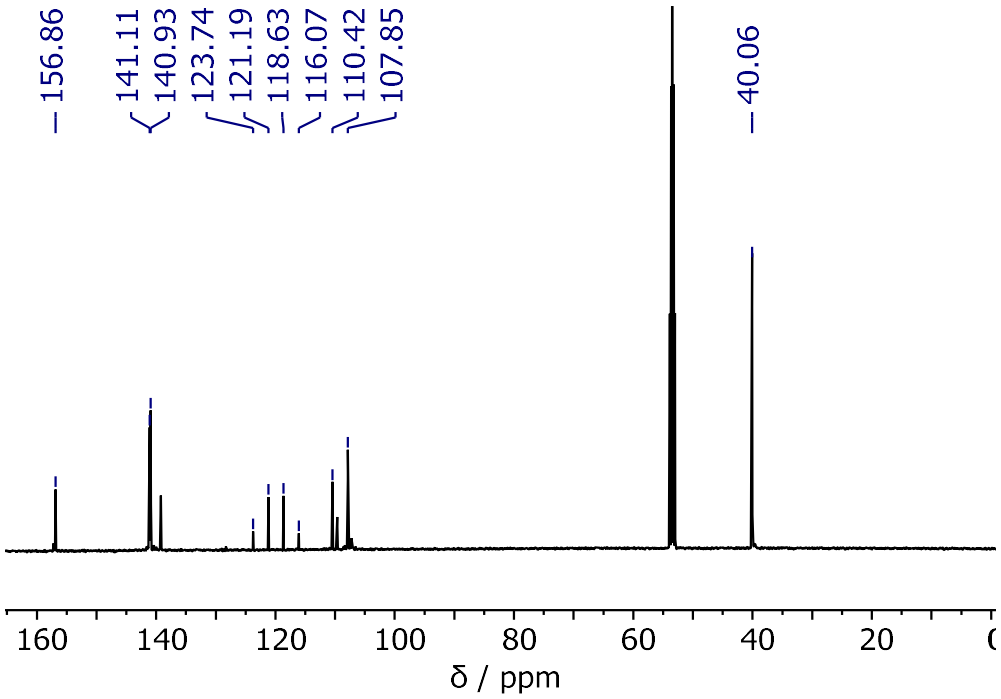

Figure 5.95: $^{13}C\{^{1}H\}$ NMR (126 MHz, CD_2Cl_2) spectrum of the addition of 4-DMAP to *tri*-chloro *mono*-NTf_2 pyrazabole, forming the respective boronium ion. *Note: a small amount of residual tetra-chloro pyrazabole is also observed, along with minor [4DMAP-H][NTf_2].*

Reactivity of *Mono*-Electrophile 5.11 with *N*-Methyl Indole

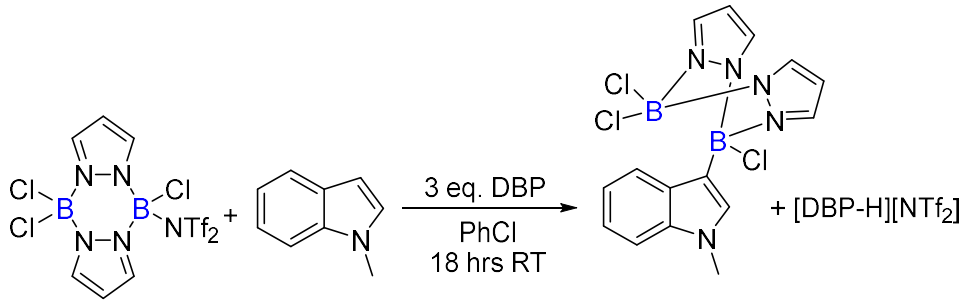

- **NMR spectra after 18 hours RT:**

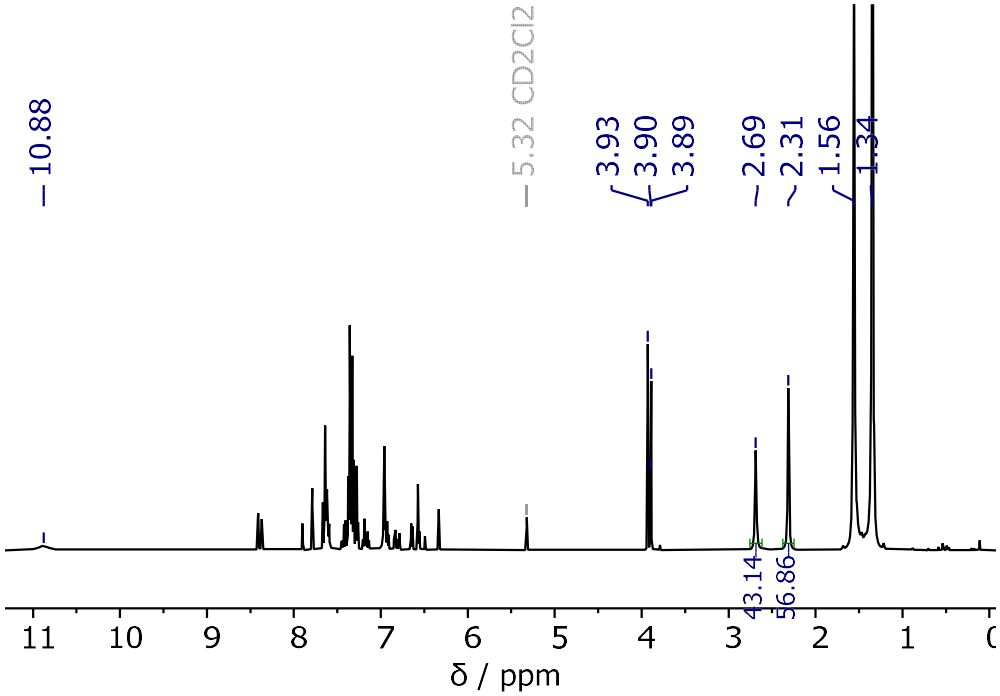

Figure 5.96: ^{1}H NMR (500 MHz, CD_2Cl_2) spectrum of the reaction of *tri*-chloro *mono*-NTf_2 pyrazabole with 3 equiv. DBP and 1 equiv. *N*-methyl indole, after 18 hours at RT.

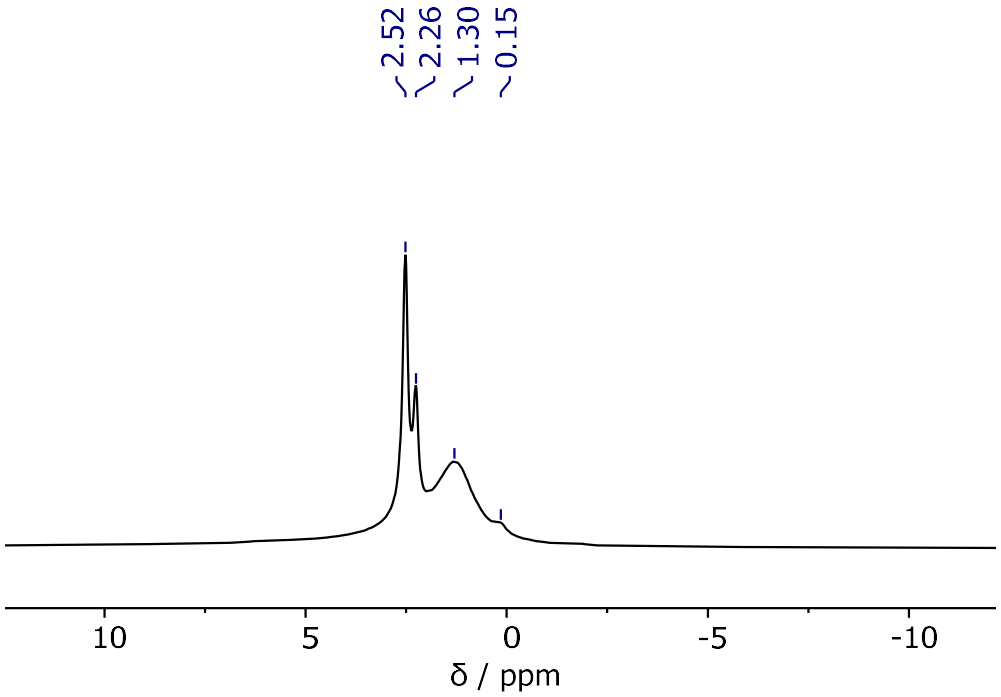

Figure 5.97: ^{11}B NMR (161 MHz, CD_2Cl_2) spectrum of the reaction of *tri*-chloro *mono*-NTf_2 pyrazabole with 3 equiv. DBP and 1 equiv. *N*-methyl indole, after 18 hours at RT.

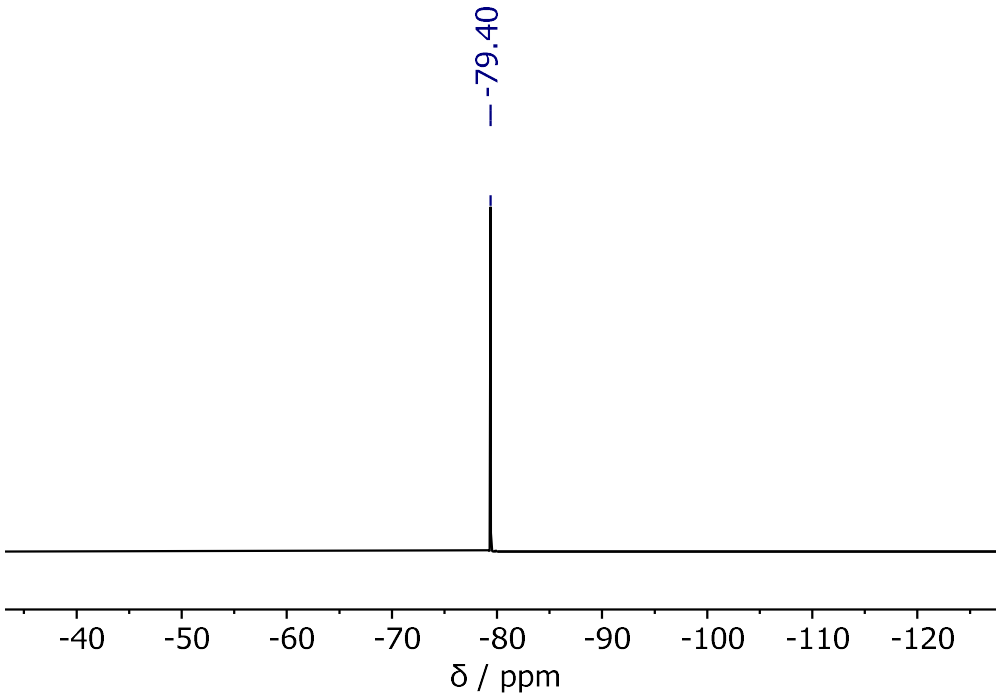

Figure 5.98: ^{19}F NMR (471 MHz, CD_2Cl_2) spectrum of the reaction of *tri*-chloro *mono*-NTf_2 pyrazabole with 3 equiv. DBP and 1 equiv. *N*-methyl indole, after 18 hours at RT.

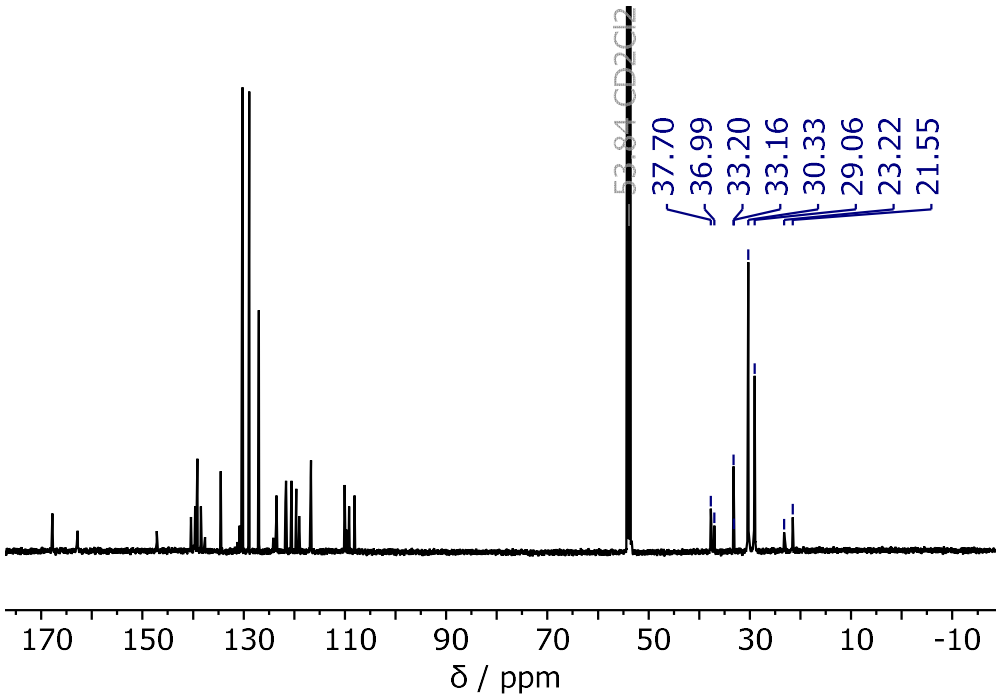

Figure 5.99: $^{13}C\{^{1}H\}$ NMR (126 MHz, CD_2Cl_2) spectrum of the reaction of *tri*-chloro *mono*-NTf_2 pyrazabole with 3 equiv. DBP and 1 equiv. *N*-methyl indole, after 18 hours RT.

- **NMR spectra after pinacol protection in D_2O/CD_2Cl_2:**

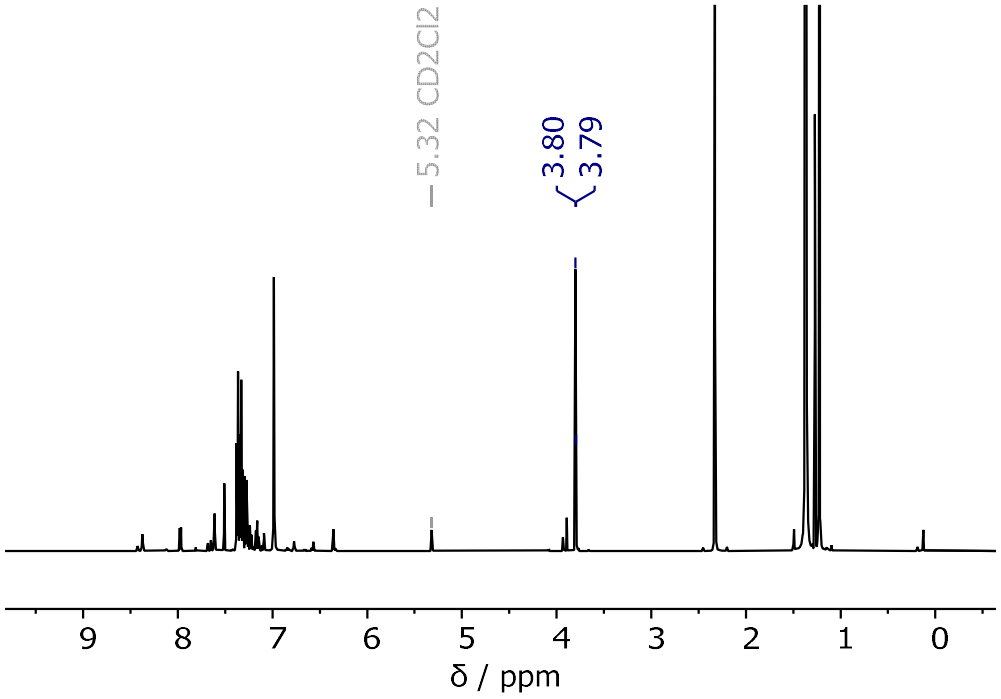

Figure 5.100: ^{1}H NMR (500 MHz, CD_2Cl_2) spectrum of the reaction of *tri*-chloro *mono*-NTf_2 pyrazabole with 3 equiv. DBP and 1 equiv. *N*-methyl indole, after pinacol protection.

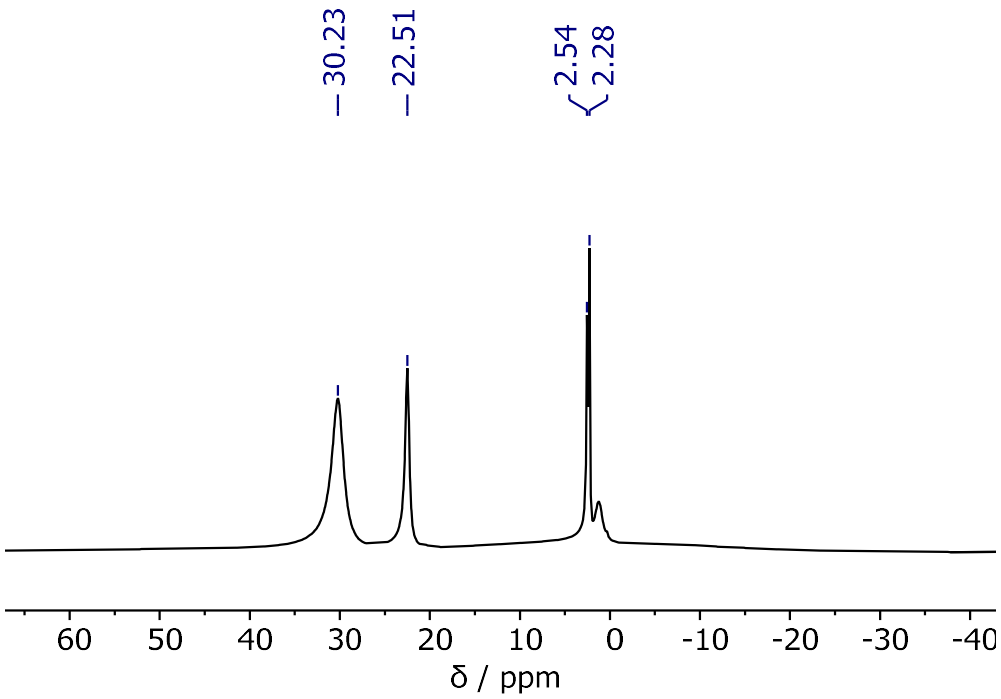

Figure 5.101: ^{11}B NMR (161 MHz, CD_2Cl_2) spectrum of the reaction of *tri*-chloro *mono*-NTf_2 pyrazabole with 3 equiv. DBP and 1 equiv. *N*-methyl indole, after pinacol protection.

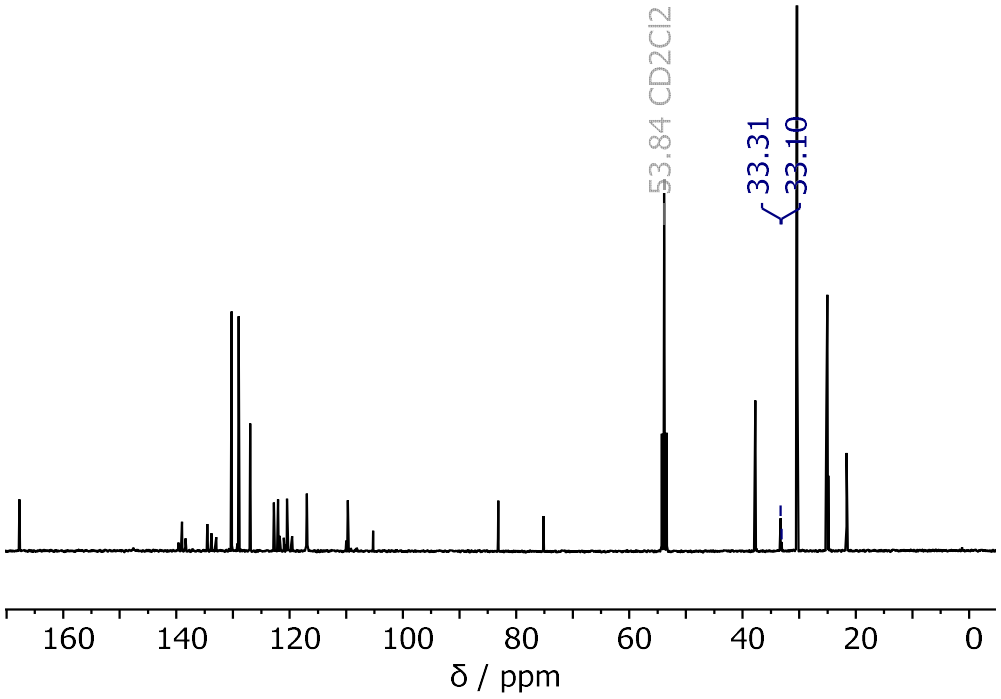

Figure 5.102: $^{13}C\{^1H\}$ NMR (126 MHz, CD_2Cl_2) spectrum of the reaction of *tri*-chloro *mono*-NTf_2 pyrazabole with 3 equiv. DBP and 1 equiv. *N*-methyl indole, after pinacol protection.

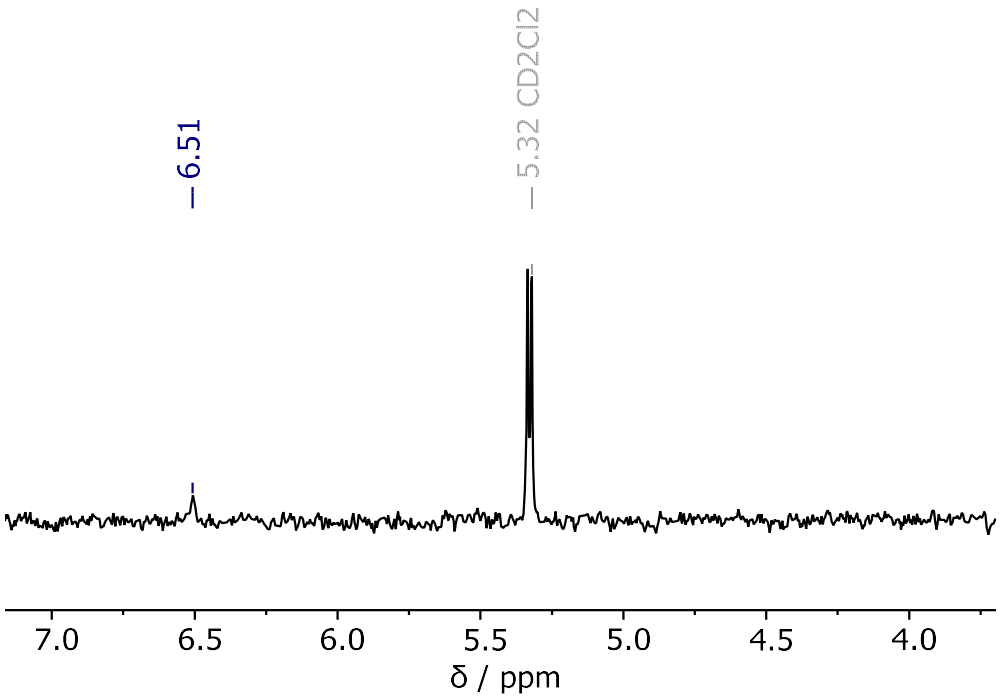

Figure 5.103: ^{2}H NMR (77 MHz, CH_2Cl_2) spectrum of the reaction of *tri*-chloro *mono*-NTf_2 pyrazabole with 3 equiv. DBP and 1 equiv. *N*-methyl indole, after pinacol protection.

Synthesis of *Di*-Chloro *Di*-NTf_2 Pyrazabole – 5.7

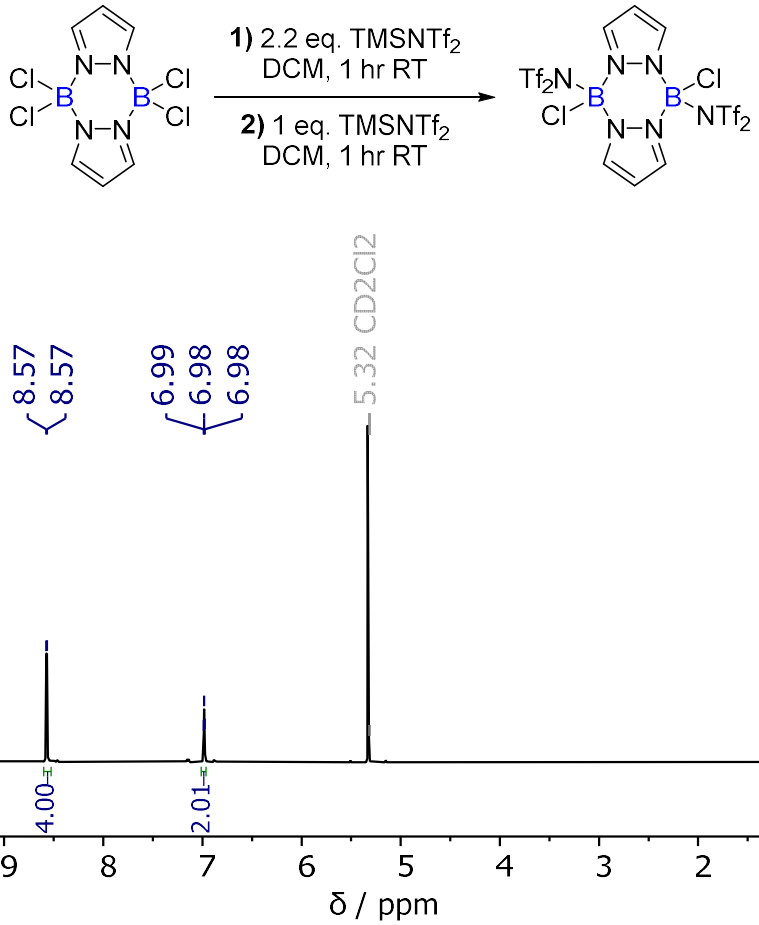

Figure 5.104: ^{1}H NMR (500 MHz, CD_2Cl_2) spectrum of *in situ* generated *di*-chloro *di*-NTf_2 pyrazabole. *Note: a small amount of residual $HNTf_2$ and TMSCl is also observed that was not removed in vacou*.

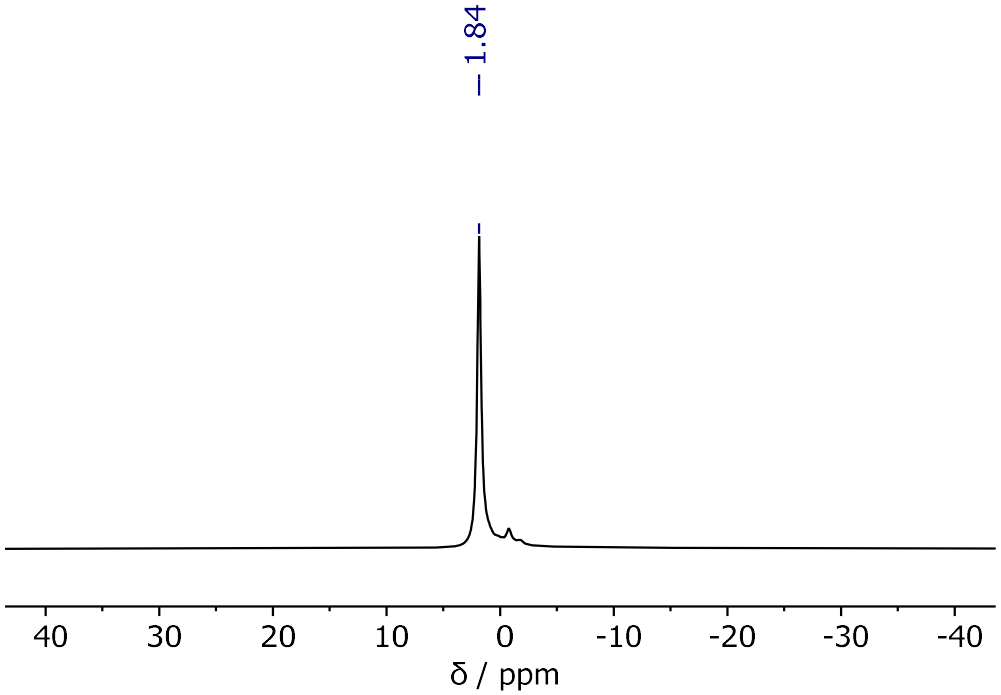

Figure 5.105: ^{11}B NMR (161 MHz, CD_2Cl_2) spectrum of *in situ* generated *di*-chloro *di*-NTf_2 pyrazabole.

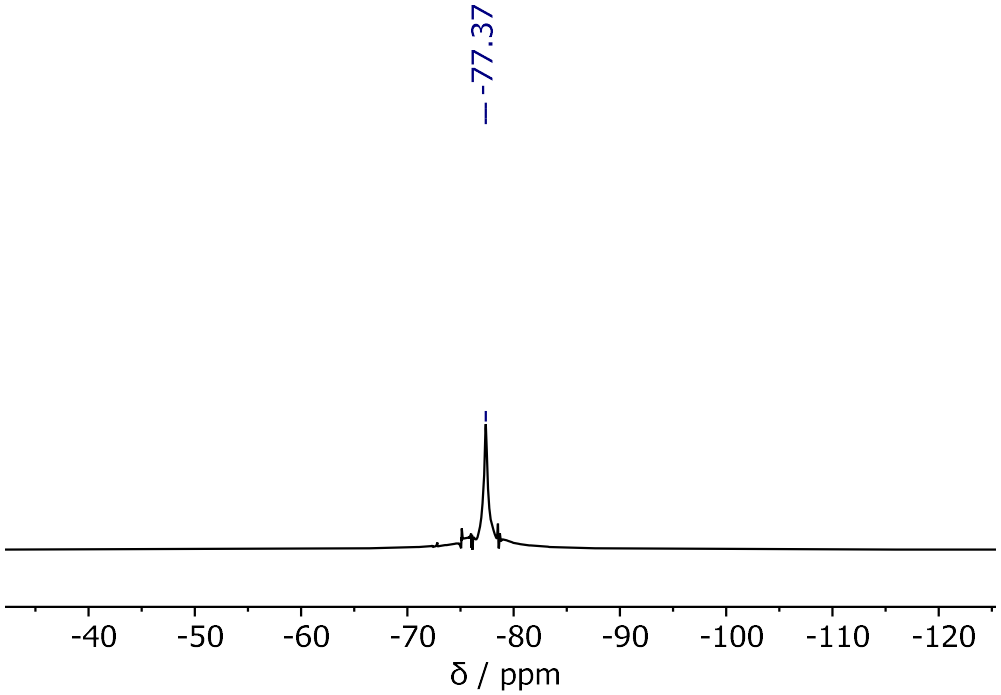

Figure 5.106: ^{19}F NMR (471 MHz, CD_2Cl_2) spectrum of *in situ* generated *di*-chloro *di*-NTf_2 pyrazabole.

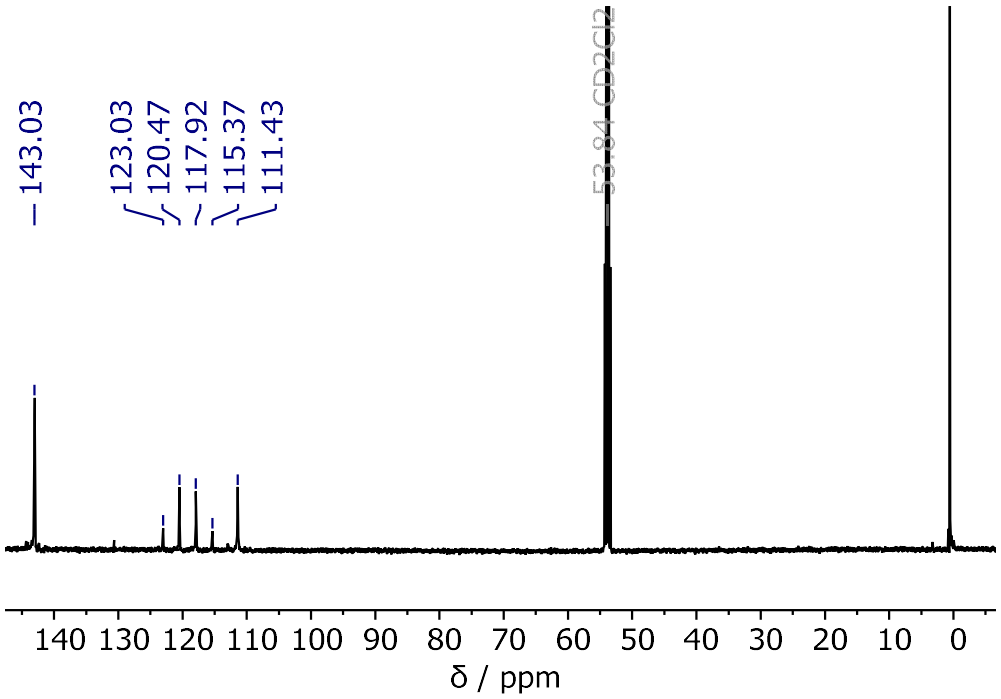

Figure 5.107: $^{13}C\{^{1}H\}$ NMR (126 MHz, CD_2Cl_2) spectrum of *in situ* generated *di*-chloro *di*-NTf_2 pyrazabole. *Note: a small amount of residual TMSCl is also observed that was not removed in vacou*.